MAGNETIC AND GEOCHEMICAL STUDIES OF HEAVY METAL POLLUTION IN SOILS AROUND METAL-SMELTING PLANTS IN OGIJO AND OTA AREAS, SOUTHWESTERN NIGERIA

BY

PAULINE TAIWO ALE

B.Sc. (HONS.) Geology (ABU), M.Sc. Applied Geophysics (Ibadan)

Matric. No.: 130713

A Thesis in the Department of Geology

Submitted to the Faculty of Science

in partial fulfilment of the requirements for the Degree of

DOCTOR OF PHILOSOPHY

of the

UNIVERSITY OF IBADAN

February, 2021

Abstract

Metal recycling, smelting and mining activities are potential contributors of heavy metal in soils, as the soil is the recipient of stockpiled scraps and discharged effluents from the activities. Metal recycling and smelting plants have been established in several parts of the country to meet the need for steel required for industrialisation without adequate safeguards for environmental concerns. The effects of these industries on their immediate environment in Nigeria are under investigated due to very limited available documents on the subject. Therefore, this study was aimed at assessing the level of heavy metals in soils around metal smelting industries in Ogijo and Ota, south western Nigeria.

Soil samples were purposively collected between October and December 2016 at 0cm, 10cm, 20cm and 30cm depths from 105 and 32 locations in Ogijo and Ota, respectively. The soils were dried, disaggregated and divided into two portions; one part retained as whole soil samples, and the other parts were sieved to 180μm, 125μm, 90μm and 65μm fractions. A total of 420 whole soil and 1680 fraction-sized samples were collected from Ogijo, while 128 whole soils and 512 fraction-sized samples were collected from Ota. Each sample was subjected to magnetic susceptibility (χ) analysis in the high and low frequency modes using the Bartington MS2B suite. Samples with high, medium and low magnetic values were selected and subjected to magnetic versus temperature analysis to determine the class of the magnetic elements. Geochemical analysis to ascertain the constituents' metals and their concentrations was also undertaken using the inductively coupled plasma mass spectrometry. Data were evaluated using geochemical method and descriptive statistics.

The magnetic susceptibility readings for whole soils samples at depths 0, 10, 20 and 30 cm were from 51 to 6159.3, 19.2 to 4240.1, 12.1 to 3961.5 and 33.4 to 3870.2, respectively indicating a decrease in magnetic susceptibility with depths. In terms of grain-fractions, the 65μm fractions had the highest (92.6-7541.6) magnetic susceptibility. Magnetic susceptibility versus temperature analysis of the soil samples revealed mostly super-paramagnetic signatures, indicating that the magnetism of constituent materials increased with temperature. Geochemical concentrations (ppm) of copper, lead and Zinc for Ogijo and Ota were from 16 to 834 and 1to 1308; 29 to 2381 and 30 to 161 and, 54 to 10000 and 29 to1400, respectively; as compared to NESREA limits of 72, 164 and 421 respectively. A comparison of the metal concentrations with

their crustal abundances revealed elevated concentrations in most of the soil samples. Calculated index of geo-accumulation for copper, lead and zinc in Ogijo and Ota were: 1.44 and 1.22; 4.80 and 3.10 and, 4.44 and 2.17, respectively. This suggested enrichment of metals in the soils in addition to geogenic sourcing. High and low magnetic susceptibility (χ) correlated with high and low metal concentrations in soils at both Ogijo and Ota, respectively.

Soil around metal recycling and smelting industries in Ogijo and Ota are polluted with copper, lead and zinc and these are especially concentrated in the finest soil fractions. Similar study on vegetation, water and air is recommended.

Keywords: Metal recycling and smelting plants, Magnetic susceptibility, Heavy metal pollution, Super-paramagnetic,

Word count: 500

Certification

I hereby certify that this research work was carried out by Pauline Taiwo ALE under my supervision in the Department of Geology, Faculty of Science, University of Ibadan Nigeria.

---------- ----------

(Supervisor) **Date**

Dr. M. A. Oladunjoye

B.Sc. (Ado-Ekiti), M.Sc. Ph.D. (Ibadan)

Dedication

This research is dedicated to God Almighty and to my beloved ones; My husband and children.

Acknowledgements

I thank God for his mercies and outstretched hand which have sustained me thus far.

I would like to express my sincere gratitude to my supervisor Dr Oladunjoye Michael Adeyinka for his guidance throughout the research and writing period. You made learning and research easy and friendly, thank you sir. An adage says “It takes a whole village to bring up a child” I will say, it takes all in the department to bring up a life time professional.

Thank you:

Prof Olayinka A. I., Prof Adeyemi G. O., Prof Ehinola O. A., Prof Okunola O.A., Prof Tijani M. N., Prof Nton M. E., Prof Elueze A. A. (late), Dr Oyediran I. A., Dr Olatunji A. S., Dr Bolarinwa A. T., Dr Osinowo O. O., Dr Boboye O. A., Dr Adeleye M. A., Dr Omitogun A., Dr Akaigbobi M. I. (late), Dr Adeigbe O. C., Dr Ajayi F., Mr Jaiyeoba, Mr Aladejana J., and all non-teaching staff for your time, advice and sincere comments which have broadened the relevance of this research work.

Also, I thank Prof. Adetola S. O. and Mr. Jacob of Modibbo Adama University of Technology Yola, for granting me access to the geophysics laboratory. In particular, I am grateful to Dr M. O. Kanu of Taraba State University for enlightening me on how to use the Bartington equipment for the research and also, Miss Juliet Ebukam for her assistance during the analysis. I also appreciate Mr Gabriel Olawuyi for being of tremendous help during this research. I am grateful to Dr Robert Otuomagie, the Director of Studies, Nubian Nigeria Limited for the permissions granted me to attend to school demands.

Finally, I would like to thank my family: my late father that had longed to see this day, my mother, children, brothers and sisters for supporting me. My husband for always being there for me; thank you for believing in me and the encouragements. God bless you all.

Table of Contents

List of Tables

List of Figures

CHAPTER ONE

INTRODUCTION

1.1 Background Information

The environment which comprises of the land, water, air and biological systems, plays the most integral part in man survival on earth, but the activities of man however, is constantly introducing harmful substances into the natural environment. These harmful substances overtime gradually degrade the quality of the environment from life sustaining to life destroying. The discharge of materials in any physical state, that is dangerous to the environment or human health is referred to as environmental pollution. Soil, water and air pollution have increased rapidly lately due to increased generation of waste from accelerated industrialisation and urbanisation; the ultimate consequence of this trend is the destruction of life itself which they were meant to support.

According to the European environment integration research news alert of September 1st 2013, soil contamination or pollution among all the other forms of pollution, is classified among those considered to be major threats to environmental quality and the wellbeing of humans. Soil contaminants, amongst others, includes; heavy metals which are by-products from metal smelting companies and mining sites, crude oil, industrial chemicals and production waste. However, pollution from heavy metals is considered to have the most devastating effect to life.

Rachwał *et al*. (2017), defined a heavy metal as an element with density above 6 g/cm^3. The United State Environmental Protection Agency (EPA) more clearly defined a heavy metal as any metallic element with high atomic weight which can be accumulated in food chains and can cause damage to living things even at a very low concentration. These heavy metals include lead, mercury, cadmium and chromium. Less commonly, heavy metals include iron, copper, zinc, aluminium, beryllium, cobalt, manganese and arsenic. Furthermore, the World Health Organisation (WHO) in 2011 listed some of these elements which were classified as heavy metals as carcinogenic, that is, capable of causing cancer in man or toxic to specific body organs. These heavy metals and their target organs are; mercury, lead, arsenic, which affects the central nervous system, mercury, lead, cadmium, copper affecting the kidneys, liver or skin, and nickel, cadmium, copper, chromium; affecting the bones and teeth.

The world has recently seen a rapid increase in industrialization especially in the aspect of metal recycling. Scrap metals yet to be recycled are stockpiled in junk yards polluting the land. During production in these recycling industries there are obvious release of after-production waste products into the land, water and air (which eventually settle on the land), this has also brought along with it increase in the tendency for heavy metals absorption by man. These risks have also informed why industries that use materials that contain heavy metals as their raw materials are adequately located in industrial layouts far away from residential quarters. However, increase in population and migration to urban cities have resulted in residential houses increasingly encroaching these industrial layouts as observed in the sites of this study.

Heavy metal elements, like any other element have a known abundance in the earth, for example mercury (Hg) has an abundance of 8.5×10^{-2} ppm in the earth crust. Also, heavy metals have magnetic properties and therefore, can form magnetic minerals. These magnetic minerals consist of magnetic metal elements with known elemental weight and abundance in the earth crust; hence the molecular weights can be ascertained. It's a known fact that magnetic minerals, especially the iron compounds, are present everywhere, iron being one of the elements with the highest molecular abundance in the earth crust (Zhang *et al*., 2011). During metal recycling, some of the existing molecular compounds of the metals are disintegrated into individual metal elements and released into the environment as heavy metal elements.

An important feature of magnetic metal elements is the grain size effect. When pollutant heavy metal elements are released into the environment, they will either be integrated by absorption into the atomic lattice or be attached to the surface of the naturally occurring magnetic metal elements as shown in Figure 1.1.

These attached elements therefore increase the weight of the natural occurring element. When the abundance in weight increases above the known weight in the earth crust, it signifies an introduction of extra elements from an external source (pollution) and becomes a basis of identifying areas of pollution.

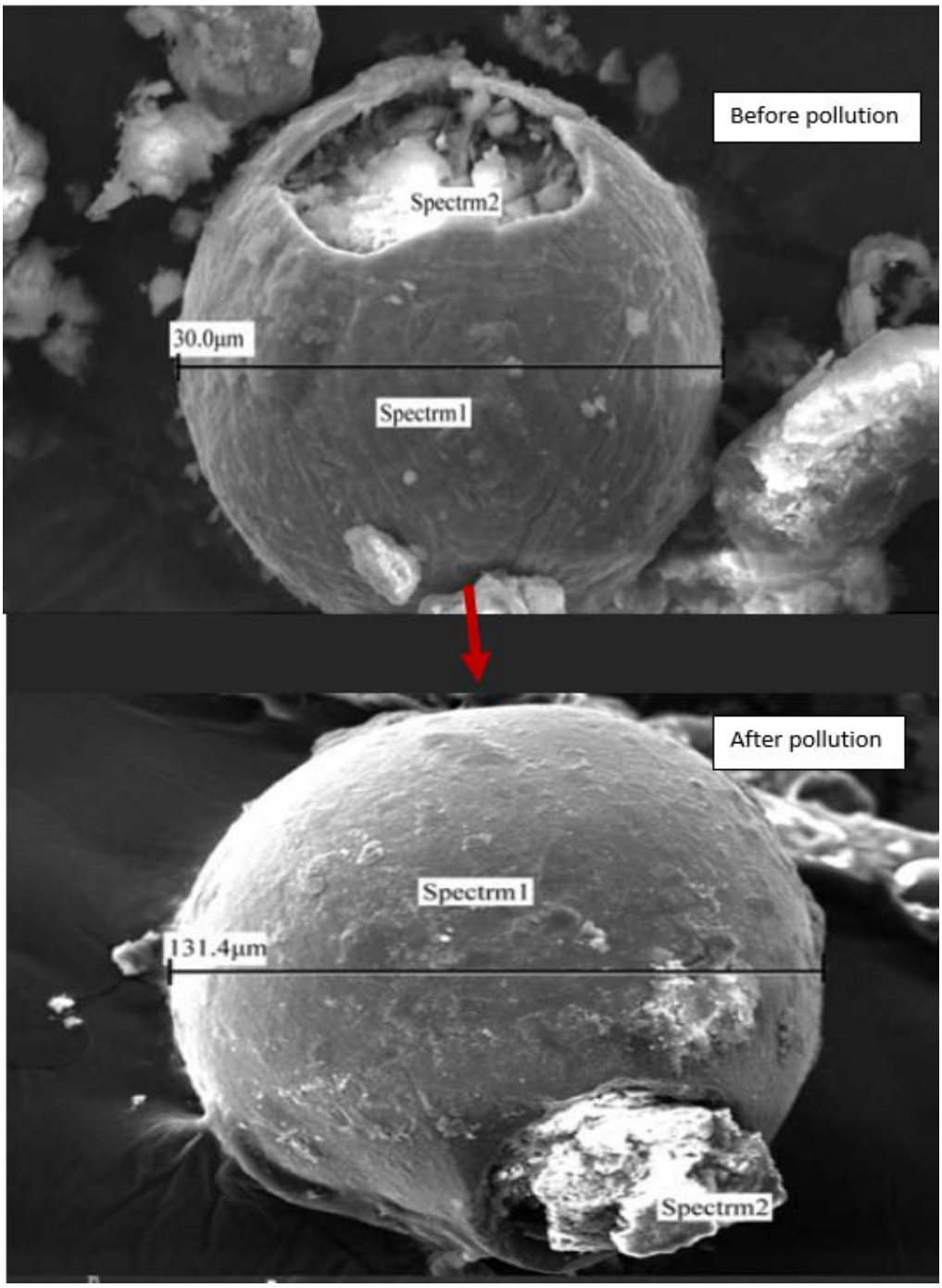

Figure 1.1: Scanning Electron Microscopy (SEM) image showing pollutant incorporated into the atomic lattice of a naturally occurring element thereby increasing the size of the atom from 30 to 131.4 µm (After Zhang *et al.*, 2011)

The conventional method of ascertaining the presence of pollutants is by carrying out geochemical analysis which reveals the weight of each element present in the sample. The use of geochemical analysis in the study of soil pollution has been utilized extensively. This analysis includes various techniques such as the sequential extraction techniques of heavy metal extraction.

Very recently, the magnetic parameters of these elements are now used as a proxy for detecting soil environmental changes (Shendi *et al*., 2013). Among many magnetic parameters used in environmental study, one of utmost importance is the magnetic susceptibility. The magnetic susceptibility of a substance is a measure of its ability to become magnetized by an external magnetic field.

In the natural environment, the measure of the magnetisability of an element distinguishes that element from other elements found in the crust. The mass or weight in abundance of every magnetic element in nature is known; also known is its magnetic susceptibility. Magnetic susceptibility measurement of the soil is directly proportional to the mass of those elements present in it. This implies that the higher the concentration of the metal element present in a soil sample, the higher the magnetic susceptibility. Therefore, a variation from the known weight abundance in nature and magnetic susceptibility of a magnetic metal element reflects the level of pollution.

1.2 Statement of Problem / Research Justification

The centrepiece of today circular economy worldwide is to focus on recycling; which is a pathway of restoring non-biological materials like metals into the economy after use of which metals can be recycled infinitely. Used metals are now raw materials for metal recycling industries. Increase in population and urbanisation has brought about increased in the presence of metal recycling industries due to the readily available raw material and end users.

However, the metal recycling industries has brought along with it, obvious land pollution as can be seen in the increase in junk yards of metals that are yet to be recycled (Figs. 1.2). At the yards, loading and offloading of scrap metals cause an impact of the metals on one another thereby, disintegrating minute particles of metals which become incorporated into the soil and pollute the environment.

During production in these metal smelting industries, major metal elements such as Iron and Aluminium are usually extracted while heavy metals such as lead, chromium and manganese that are considered as waste by-products of production are released as dense fumes and water effluent in to the environment. The pollutants released into the air, eventually settle on the land, water sources and vegetation thereby polluting them (Fig. 1.3).

The heavy metals that are waste products from metal smelting activities have been listed by WHO as life threatening.

The metal smelting industries which were adequately located in layouts at outskirts of towns are now encroached by residential quarters which are next door neighbours to the industries and their dump yards (Figs.1.4 and 1.5). The presence of industrial pollution is heavily obvious in the metal smelting industrial layouts (Figs.1.2, 1.3, 1.4 and 1.5), and the effects of these industries on their immediate environment in Nigeria are under investigated hence, very limited documents are available on the subject to correctly articulate and substantiate the extent of damage these metal industries cause their immediate environment.

Figure 1.2: Junk yard side view of the scrap dump of African steel industry

Figure 1.3: Gaseous waste from chimneys of Monarch steel company in Ogijo industrial layout

Figure 1.4: A satellite view of Ota industrial housing layout showing residential buildings within the environs of the industries. (Source; Google Map)

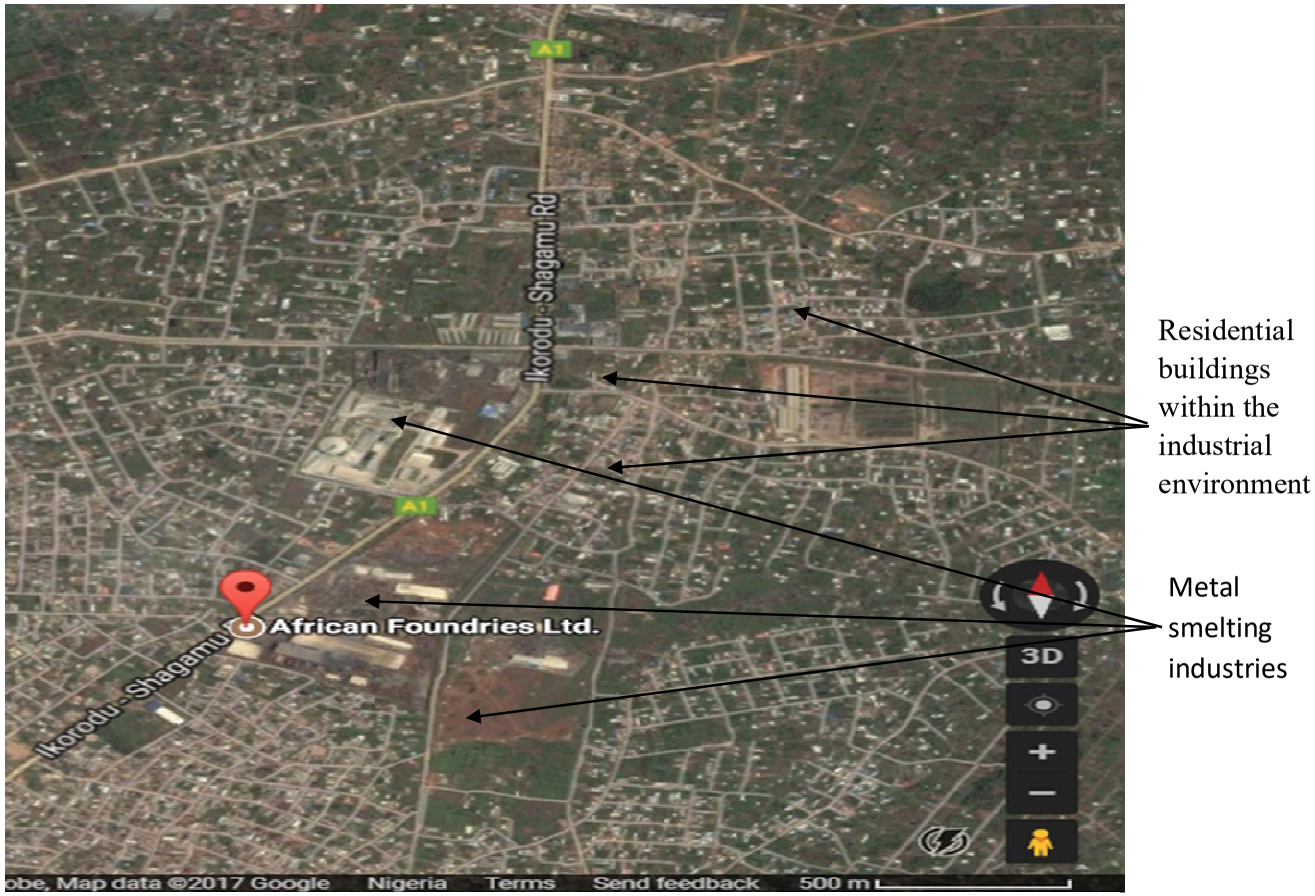

Figure 1.5: A satellite view of Ogijo industrial layout showing residential buildings within the environs of the industries. (Source: Google Map)

1.3 Aim and Objectives of Study

The aim of this research was to determine the level of heavy metal concentration in soils around the iron smelting plants in Ogijo and Ota industrial layouts.

Specific objectives include:

1. To ascertain the type and concentration of heavy metal pollutants in the soils around the iron smelting plants.
2. To determine the grain size concentration of the pollutants with depth.
3. To determine the spatial concentration of pollutants within the study areas.

1.4 Scope and Organisation of Thesis

The scope and methodology of the research work included:

1. Literature review of previous work done on similar research study in other to obtain better insight of the research and identify knowledge gap.
2. Sample collection from two industrial layouts: Ogijo and Ota industrial layouts. Both locations are within Ogun state at a distance of 52.9 km apart by road and 35 km from a straight traverse. Both layouts are located close to the boundaries between Ogun and Lagos state. The sampling was done based on accessibility.
3. Sample Preparation which included drying, crushing, sieving and weighing
4. Laboratory Analysis: The samples where subjected to a frequency dependence Magnetic Susceptibility analysis which exposed them to an external magnetic field of known frequencies in other to obtain their magnetic susceptibilities by using the Bartington Magnetic Susceptibility MS2B dual frequency sensor and the Multisus software.
5. Temperature analysis to measure the temperature dependent magnetic susceptibilities of metals by using the Bartington Geolabsoft software and magnetic susceptibility MS2B equipment.

6. Geochemical analysis of the samples using the inductively coupled plasma mass spectrometry to ascertain the types of magnetic minerals causing the pollution in the vicinities.
7. Descriptive statistical analysis such as box plots, histograms, correlation matrix and density maps.
8. Data Analysis of Geochemical data to ascertain the pollutant heavy metal and the concentration in the site
9. Interpretation of results, deductions and recommendations.
10. Thesis writing.

Field Development Plan

The above scope is presented in an organization chart (Fig. 1.6) detailing actions to be done in each step of the research. Key performance indicators to effectively measure performance are noted and milestone presentations after certain indicators have been achieved were indicated in the chart.

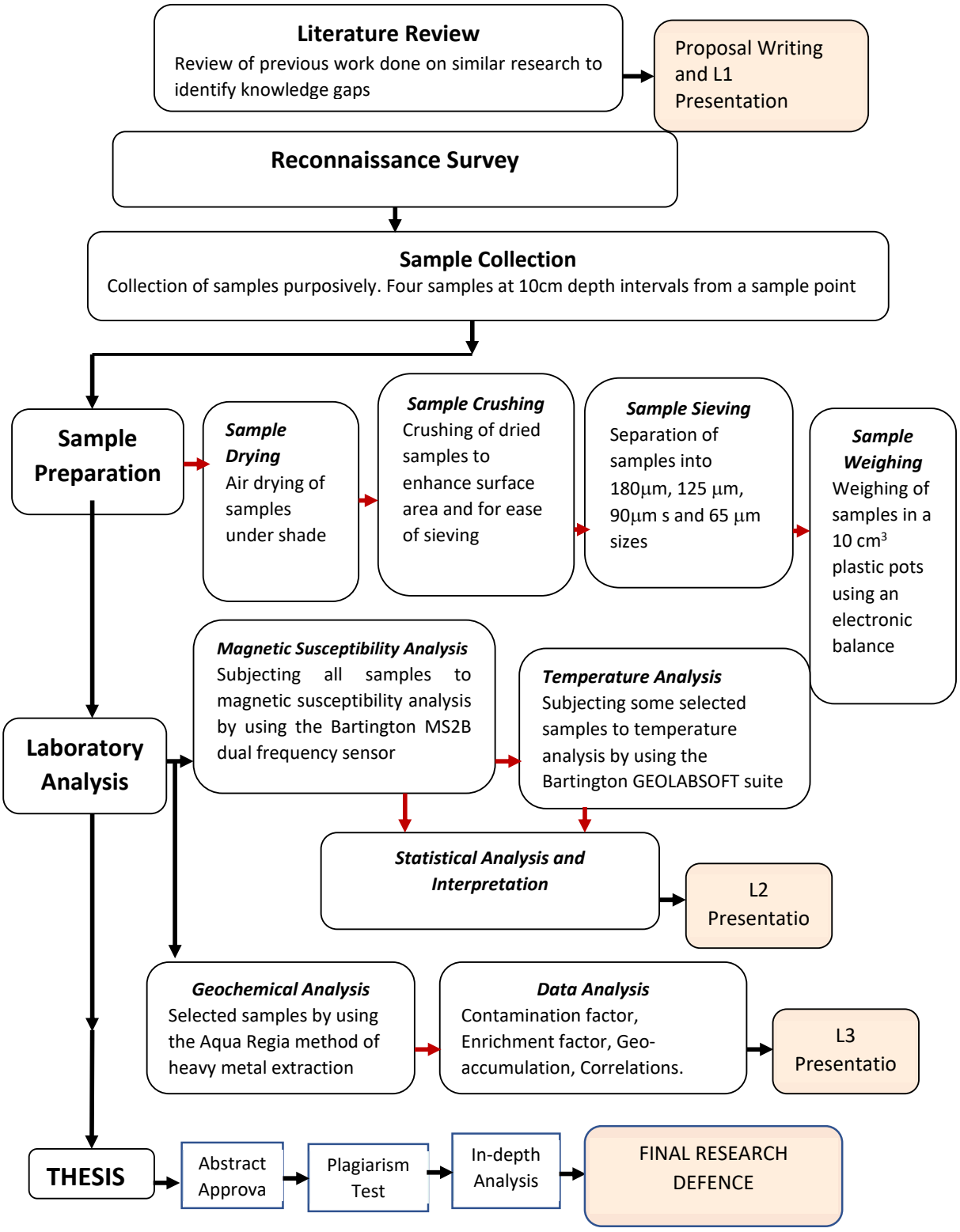

Figure 1.6: Schematic representation of the scope and methodology of the research

1.5 Literature Review

Iron is the fourth most abundant element in the earth crust (Zhang *et al*., 2011), as such, iron compounds (magnetic minerals) are found everywhere but in varying abundance from places to places. In the past years, there had been several theories about the mechanism by which soils are enriched with fine-grained magnetic minerals. For example, Kletetschka and Banerjee (1995) stated that thermal means such as forest fires or bush burning can transform weak magnetic iron oxides and hydroxides into fine grained ferromagnetic, magnetite or maghemite minerals. Singer and Fine (1989), stated that fine grained magnetic minerals accumulate due to long period of weathering and pedogenesis. Also, Thompson and Oldfield (1986), from a different perspective stated that fine grained magnetic minerals are accumulated from coarse airborne magnetic particles that are released mainly from pollution sources. Although the theories are different, there is a general consensus that the magnetic minerals occur as fine grain in their host environment.

Dearing *et al*. (1996) in the bid to evaluate these conflicting theories on a regional scale, analysed top soils; sampled across the whole of England, having localised and distinct environmental units such as farm lands, forest, industrial layouts etc and cutting across different geological terrains. Sampling was done at every interval of 1.5 cm to the depth of 15 cm at each sample point. In order to obtain fine grain samples in accordance to the different theories, Dearing *et al*. (1996) sieved the samples with a 2 mm sieve. Some of the soil samples were geochemically analysed using the aqua regia digestion, while the other part was subjected to magnetic susceptibility measurements in both the low and high frequencies (X_{lf} and X_{lh}).

Analysing the geochemical results and the mass specific frequencies (X_{fd}) of the magnetic susceptibility results, Dearing *et al*. (1996) recorded detectable concentration of superparamagnetic minerals in about 80% of the samples (X_{fd}>2), this value exceeded most published values for palaeosols. The magnetic readings from the free draining arable cultivated soils with history of bush burning were either nil or very low which was an indication that burning is not a major control on soil susceptibility. They also observed that strong magnetic soils occurred in sedimentary and low-grade metamorphic areas located close to places of industrial activities. These sedimentary areas made of chalk, slate and oolitic lime stones that naturally should have negligible concentration

of magnetic minerals, showed high readings indicating the presence of magnetic minerals. They observed that the samples here contained significant proportion of coarse multidomain MD) and stable single domain (SSD) (X_{fd} >14) grains of iron oxides which were evidence of heavy metal pollution from atmospheric emission. The results from the sedimentary terrain exceeded that recorded from the igneous outcrops that showed natural readings obtainable from such environment. Very high magnetic susceptibility readings but low X_{fd} < 2 were associated with some of the industrial areas. The low X_{fd} < 2 is an indication of the dominant pollutants being ferrimagnetic in nature.

Dearing and his team concluded that on a regional scale, variation in soil magnetic susceptibility which is a function of the accumulation of fine-grained magnetic minerals are, as a result of geology and soil formation rather than on land uses such as burning or pollution which are localised factors. It was further explained that localised anomaly is either due to accumulation of fine grain magnetic minerals in moderately well-drained soils that were developed from easily weathered rocks rich in SP and ferrimagnetic minerals or accumulation could also occur in soils not geologically rich in magnetic minerals but whose environment were characterized by the presence of heavy industrial activities.

Similar results were recorded by Bouhsane and Bouhlassa (2018) who assessed the variation in magnetic susceptibility in top soil samples from different occupational locations but having same underlying bedrock, with the aim of understanding how land use by man impacts on the magnetic susceptibility of the soils, hence identifying areas with heavy metal pollution. A total of 62 samples from dense and residual forest, pasture land and cultivated land were assessed using the Bartington magnetic susceptibility meter in both the low and high frequencies. The percentage frequency dependant susceptibility which was calculated from the result showed an average value of 107.087 $\times 10^{-8}$ m^3kg^{-1}, 42.69 $\times$ 10^{-8} m^3kg^{-1} and 57.33 $\times$ 10^{-8} m^3kg^{-1} for the reforested, cultivated and pasture lands respectively. The high values were an indication of high concentration of ferimagnetic minerals (Wojas, 2017) whose origin could be pedogenic, inherited from substratum, or allochthonous that is, from atmospheric pollution. The mass specific frequency X_{fd} indicated the absence of SP grains in the cultivated land while the pasture had a mixture of SP and MD grains. They concluded that paedogenesis is responsible for the high susceptibility that was preserved in the reforested land void of human

interference. The averagely high but reduced values that were observed in the pasture and cultivated land were attributed to human activities.

Zhu *et al*. (2018), used geochemical approach like other researchers to assess heavy metal contamination in soils (Geochemical studies are one of the most widely used approaches to distinguish different geochemical associations of many heavy metals and to obtain their elemental concentrations).

Zhu *et al*. (2018), in assessing the level of heavy metal contamination and their spatial distribution in surface sediments of the Caofeidian, collected surface soil samples from 22 sampling points. The soil samples which were separated into three grain sizes of clay (< 4 μm), silt (4 – 63 μm) and sand (> 63 μm) were subjected to chemical analysis. The concentrations of the heavy metals such as Fe and Mn were measured by Inductively Coupled Plasma Atomic Emission Spectrometer (ICP-AES), and those of Cd, Cr, Cu, Ni, Pb, and Zn were detected by an Inductively Coupled Plasma Mass Spectroscopy (ICP-MS). They reported the silt grain size as having the highest concentration of pollutant among the clay, silt and sand grain sizes. They also observed that the concentration of heavy metals within the 22 soil samples were generally high as compared to others reported from other bays in China which was dependent on the composition of the gain sizes in each sample point. However, it was concluded that hydrodynamic conditions were the major factors affecting the distribution of the grain sizes mix, and hence the heavy metals at the site that constitute more of silt grain size.

Researchers are now combining magnetic susceptibility studies with geochemical analysis in the bid to better ascertain the type of contaminant and their spatial distribution in the environment.

Wojas (2017), assessed the soils in Krakow for heavy metal pollution by carrying out insitu magnetic susceptibility analysis at 112 locations with the Bartington MS2D and MS2H meters, taking readings up to 100 cm depth. 112 soil samples were also taken from the same locations within a depth range of 0 to 10 cm. The samples were subjected to both volume magnetic susceptibility in the low and high frequencies and geochemical analysis. The range of magnetic susceptibility values obtained were 11.8 – 434.6 x 10^{-5} [SI] having average value of 53.0 x 10^{-5}, which according to Wojas (2017), signified the influence of anthropogenic factors on the top layer soil as compared to readings from an unpolluted region of Carpathians that had average values below 30.0 x 10^{-5}. High

readings recorded in the forest area of Krakow was attributed to uninterrupted accumulation of wind deposits of magnetic particles from industrial plants located not too far from the forest. Generally, the values from the volume magnetic susceptibility analysis coincided with the maps from the insitu measurements that identified three major magnetic susceptibility anomalies which coincided with areas in the vicinities of steel works. The geochemical analysis recorded increase in concentration of six heavy metals (Pb, Zn, Cu, Cd, Ni and Fe) which was identified as the major pollutants responsible for the magnetic anomalies. Wojas (2017), concluded that due to the strong positive correlation observed between magnetic parameters and heavy metal contents in the samples, the magnetic susceptibility tool can be used for the assessment of heavy metal pollution.

Few studies have also attempted applying a comparative methodology of magnetic susceptibility, geochemical analysis and pollution index analysis to assess ecological risk in very limited areas with obvious indication of heavy metal pollution.

Shendi *et al.* (2013) in assessing the level of heavy metal contamination in top soil samples from urbanized and industrialized city of Port Said, collected 25 soil samples at 0 – 15 cm depth from three sites of high magnetic susceptibility anomalies where magnetic susceptibility survey has previously been carried out. Two of the sites A and B were located close in the same industrialized environment while the third site C was located away from A and B. The samples were pulverized and screened through a 2 mm sieve. 5 g of each samples were mixed to have a complete mixing of the samples while 1g of each sample were digested geochemically to obtain the total concentration of heavy metal present in each sample. The geochemical results were assessed using the pollution index CF and I_{geo}. Although, the geochemical analysis revealed the presence of heavy metal in all the samples, the results obtained from the pollution index assessment revealed highly contamination with Cd, Pb and Zn and considerable contamination with Mo, V and Fe in sites A and B while site C had minimal contamination. Shendi *et al.* (2013) concluded the heavy metal contamination was as a result of the industrialization especially the iron processing industries present in Port Said

Gabrielyan *et al*. (2018) in assessing the impact of mining activities on the Voghji river and its distributaries located between two mining districts, analysed sediment and water

samples from 8 sampling locations by using Inductively Coupled Plasma Mass Spectrometer (ICPMS) to determine the concentrations of Ti, Fe, Mn, V, Cr, Co, Ni, Cu, Zn, As, Se, Mo, Cd, Sb, and Pb in the sediment and water samples collected within a 3 years period. The analysis showed that the mean concentration of the analysed heavy metals in the samples were close. The results were further subjected to descriptive statistical analysis which revealed that the pollution pattern from the sample points for both the sediments and water samples were similar. Gabrielyan *et al*. (2017) concluded that the two mining districts: Zangezur that mines copper-molybdenum combine and the Kapan district that mines Polymetal were the source of heavy metal pollution in the Voghji River.

Kolawole *et al*. (2018), assessed the impact of industrialization on the mineralogical content of soil in an industrial area by determining the concentration and distribution of some heavy metals in soils and sediments of the study area. Soil samples were collected along the Alaro River before entering, and after draining the industrial estate on its path. The samples were subjected to the aqua regia digestion process and the elemental content was analysed using the inductively coupled plasma mass spectrometry. The result revealed that the heavy metals with their average concentration (mg kg^{-1}) are magnesium (Mn) 324.3, chromium (Cr) 79.9, lead (Pb) 66.1, copper (Cu) 40.7, cadmium (Cd) 14.3, cobalt (Co) 9.1, and nickel (Ni) 6.8 in the following order of decrease in concentration Mn > Cr > Pb > Cu > Cd > Co > Ni.

The results were subjected to Ecological risk assessment using the Single element; CF, EF and I_{geo} and the multi-elemental (contamination degree pollution index and modified pollution index) pollution indices to evaluate the level of contamination by the metals.

The single element assessment revealed a very high contamination of Pb, Cd and Cu in all the samples which was confirmed by the multi-elemental assessment that demonstrated a strong potential ecological risk for Cd, Pb and Cu. The spatial variation of the heavy metals in the sediments showed a lower value in sediments before the river entered the industrial area, an increased value in the industrial area and maximum value at leaving the area. This signified the industrial effluents are discharged into the river. Kolwole *et al.* (2018) concluded that the industrial activities in the study site has significantly enriched the soil with Cd, Pb and Cu.

Orosun *et al*. (2020), carried out magnetic susceptibility investigation on 26 samples from an automobile station to assess the possibility of heavy metal pollution. The samples which were randomly collected were subjected to magnetic susceptibility analysis in both the high and low frequencies using the Bartington magnetic susceptibility meter and geochemical analysis using the Aqua Regia method for the digestion of trace metals. The magnetic susceptibility result obtained showed a significant enhancement as compared to the result obtained from 5 samples that were taken from a control site where there was no chance of pollution. The result obtained from the magnetic susceptibility analysis was confirmed by the geochemical analysis which revealed a high concentration of heavy metals Fe > Cr > As > Mg > Pb > Cu > Zn > Cd > Mn > Ag arranged in decreasing concentration. He then concluded that the pollution was of anthropogenic origin linked to the activities within the automobile station such as vehicular emissions, welding, poor disposal of damaged spare parts.

1.6. Description of the Study Area

Two study locations were used in this research work, namely: Ogijo and Ota industrial layouts. Both sites are located in Ogun state and are government earmarked industrial layouts exclusively for the metal smelting industries. Ota and Ogijo industrial layouts are separated by a distance of 35 km on a straight traverse and 52.7 km by road. Both sites are situated close to the political boundary between Ogun and Lagos state hence the population boom that saw the rise of residential quarters encroaching the industrial layouts.

1.6.1. Ogijo Industrial Layout

The site extends from Ogijo industrial layout in Ogijo town, to Sagamu Steel Plant in Ogun state, south western Nigeria (Fig. 1.7) and situated within the Ewekoro depression in the Eastern Dahomey embayment.

It lies approximately between Latitudes N6^{o} 49' 23.8" and N6^{o} 43' 02.0" and Longitudes E3^{o} 37' 38.8" and E3^{o} 31' 10.6" covering an estimated area of about 10 km sq. It is bounded in the south by Ikorodu, a suburb in Lagos State, at the north by Sagamu town, at the east by Fakale and at the west by Ibafo towns. It has a gentle sloping topography with maximum elevation of about 102 m above mean sea level and minimum elevation of about 26 m above mean sea level.

The mean annual rainfall that forms the major source of groundwater recharge in the area is greater than 1800 mm (Olusola *et al*., 2016). The major sources of water are boreholes and hand dug wells.

The top soil in the area consists of sediments of clay, unconsolidated sands, mud overlying lateritic soil, with a varying proportion of vegetation. Industrialization activities are obvious in this site due to the presence of seven (7) different metal smelting companies, two (2) foundries, a technical outfit and a cement manufacturing company

1.6.2. The Ota Industrial Layout

The Ota industrial layout is located within Ota town, a suburb in Ogun state, south western Nigeria and situated within the Eastern Dahomey embayment. It lies approximately between Latitudes N6^{o} 40' 39.0" and N6^{o} 40' 10.0" and Longitudes E3^{o} 12' 15.0" and E3^{o} 12' 05.0". (Fig. 1.8). It has a gentle sloping low lying topography with maximum elevation of about 7 m above mean sea level and minimum elevation of about 3 m above mean sea level.

The tropical climate of Ota is typical of the climate of the south western Nigeria, which is characterized by two seasons namely the dry and wet (rainy) seasons. The wet season peaks twice annually between June to July and September to October with a break usually in August. The mean annual rainfall that forms the major source of groundwater recharge in the area ranges from 1500 mm to about 3000 mm (Faleyimu *et al*., 2013). The temperature range is between 21^{o} C to 34^{o} C.

The industrial layout is the home to six (6) different metal companies.

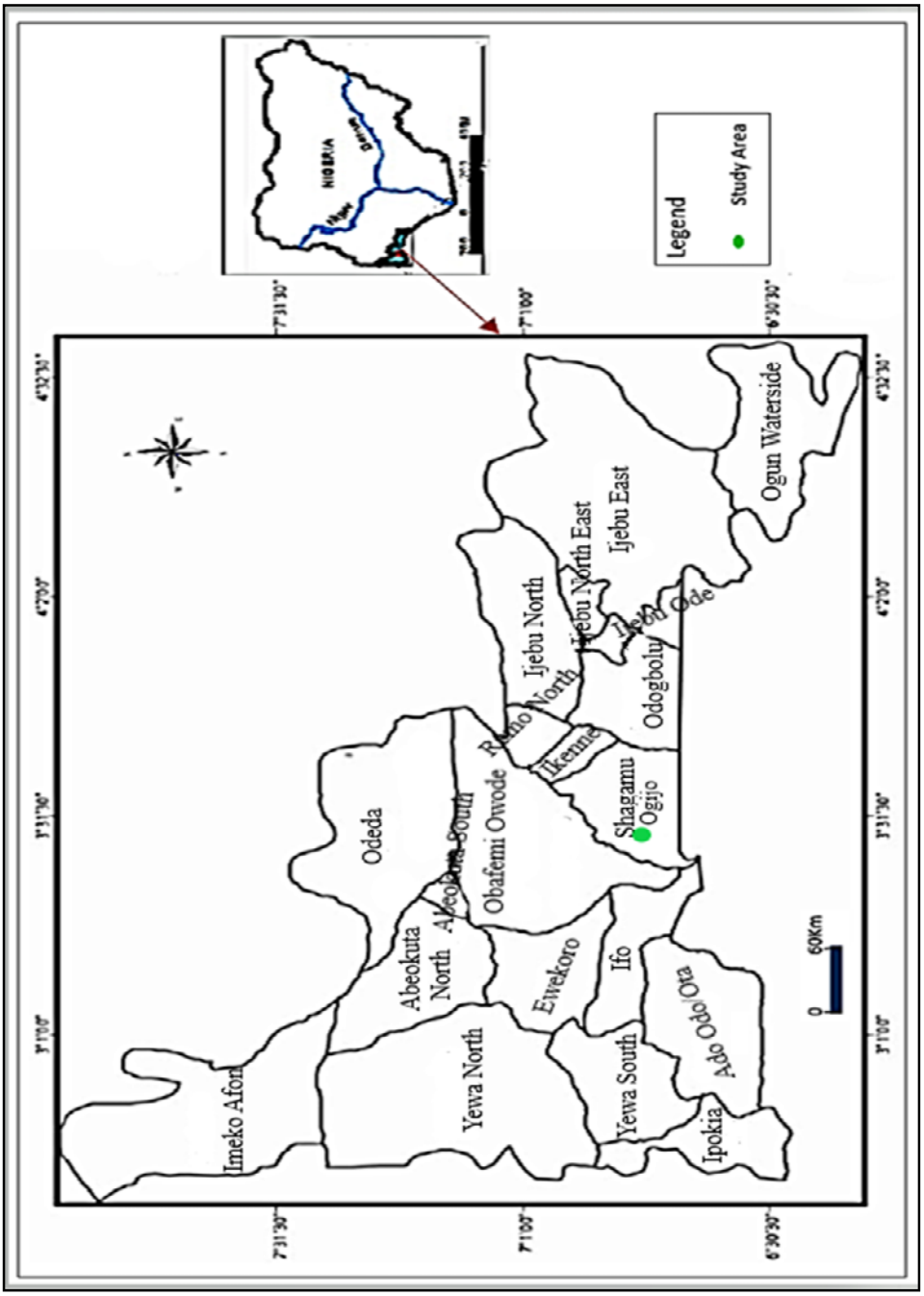

Figure 1.7: Location of Ogijo industrial layout in Ogun state

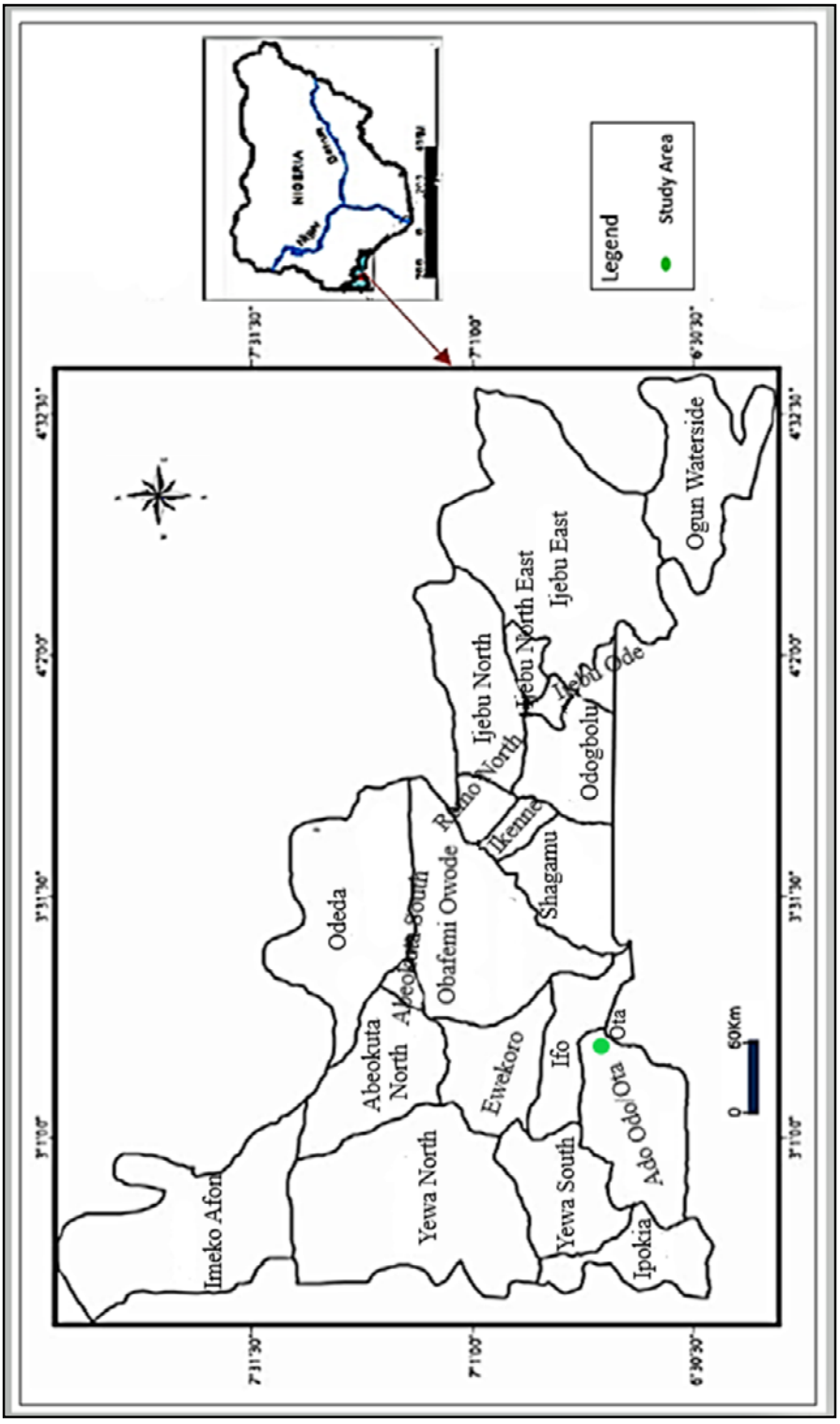

Figure 1.8: Location of Ota industrial layout in Ogun state

CHAPTER TWO

GEOLOGICAL SETTING AND THEORY OF METHODS

2.1 Geological Setting

Ogijo and Ota are both located within the eastern Dahomey basin. The Dahomey Basin is an arcuate coastal basin, and one of the West African margin basins that were formed during the rifting of the continents in late Jurassic to early Cretaceous. (Omatsola and Adegoke, 1981).

The basin is laterally extensive; covering the south eastern parts of Ghana through to the southern Togo and the Republic of Benin to the south western part of Nigeria. It is bounded at the north by the continental inlands and in the south by the Gulf of Guinea. In the eastern part, it is separated from the Niger Delta by the Benin Hinge Line and the subsurface basement high called the Okitipupa Ridge which marks the continental extension of the chain fracture zone (Onuoha, 1999). It is bounded on the west by the Ghana Ridge, also referred to as the Romanche fracture zone.

In the onshore, the basin attains its maximum width of about 13 km along the Nigerian and the Republic of Benin boundary axes. This distance tapers both westwards and eastwards to about 5 km (Olabode, 2015).

Dip wise, the thickness of the strata is about 200 m in the onshore, this progressively increases towards the offshore where thickness reaches about 1,000 m (Olabode and Mohammed, 2016) (Fig. 2.1).

Detailed geology, evolution, and stratigraphy of the basin have been described by Omatsola and Adegoke (1981) and Okosun (1990) to mention a few. These authors have dated the basin to be of pre-Albian to Maastrichian of age (Table 2.1).

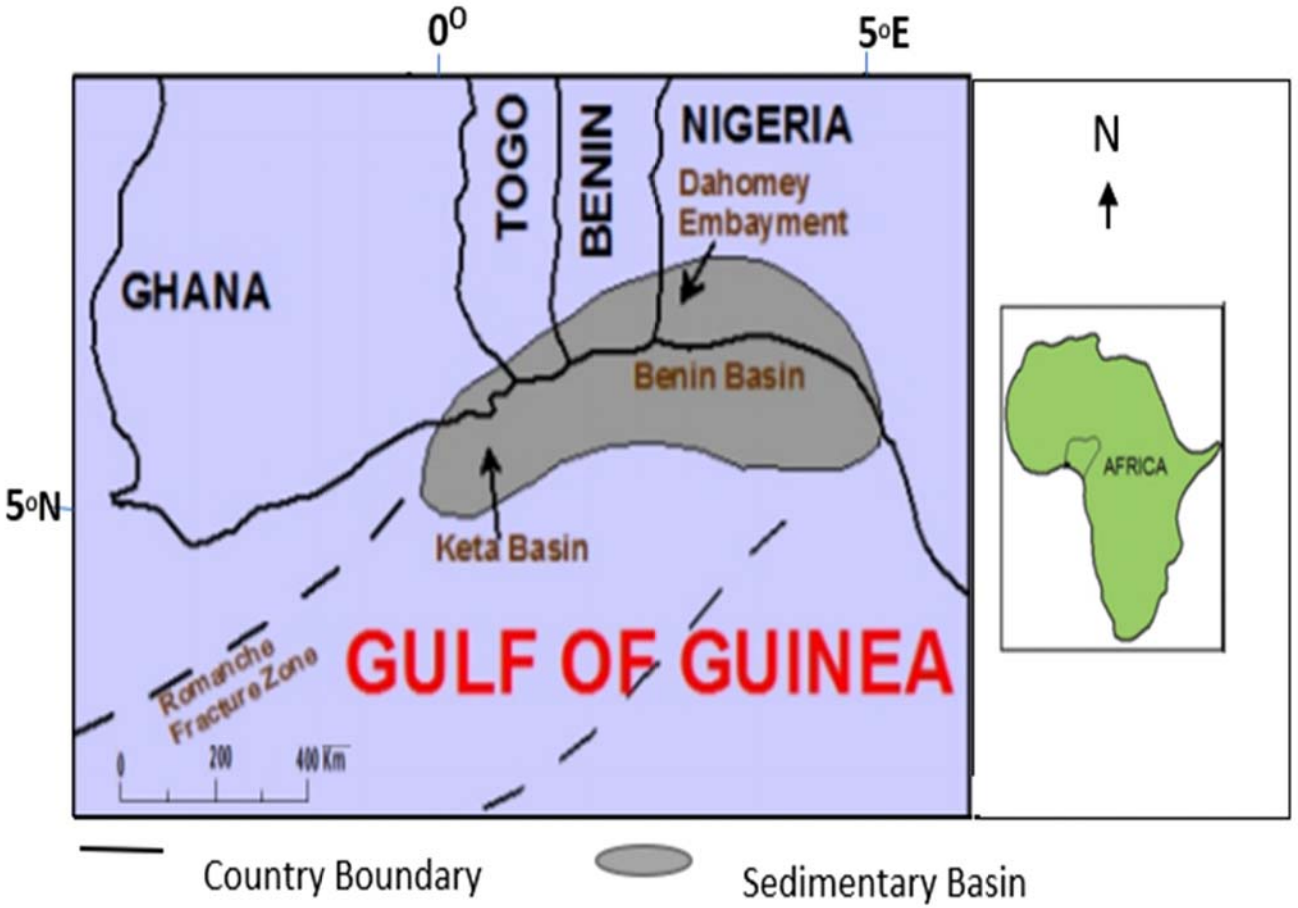

Figure 2. 1: Map showing the Dahomey basin and its boundary across Nigeria, Benin, Togo and Ghana (After Brownfield and Chapentier, 2006)

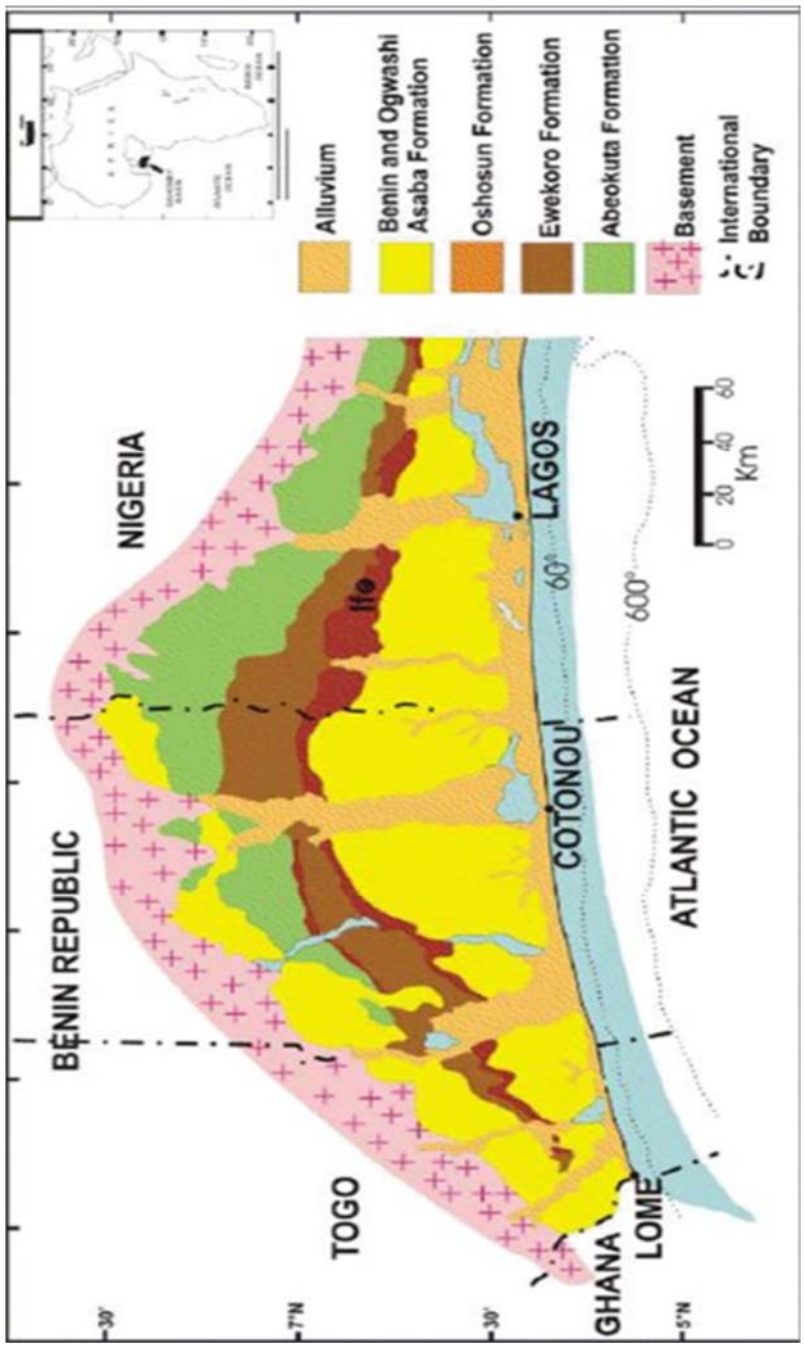

Figure 2.2: Stratigraphic depositions in the Dahomey Basin (Source: Bankole *et al.*, 2006)

Among the several hypotheses that have tried explaining the evolution of the Dahomey Basin, the rift hypothesis is the most popular among scientists. It postulated that a single mega continent called the Gondwanaland was rifted into several parts which drifted apart. In the Lower Jurassic to Early Cretaceous, there was basement fracturing which led to the separation of the African plate from that of the South American plate. The consequent block faulting and subsidence resulted in the formation of several marginal basins (Ojeda, 1982; Omatsola and Adegoke, 1981). There were trans-current movements on the oceanic fracture systems that led to the development of the South Atlantic Ocean. Prior to the opening of the South Atlantic Ocean, there have being several episodes of tectonism and transgressions accompanied by subsidence which brought about several depositions across the entire basin that have resulted in the Formations that make up the Dahomey Basin (Fig. 2.2).

Adediran and Adegoke (1987) proffer a four-stage evolutionary prototype for the Gulf of Guinea basin (Dahomey Basin inclusive); as follows: Stage 1 – The deposition of thick clastic sediments that are mainly non-rounded sandstones with intercalations of fresh water shales in the intracratonic basin. Stage 2 – Deposition sands and silts with intercalations of shales of fluviatile – lacustrine origin within the grabens during the tectonic activity, this was followed by intense erosion, deposition of weathered sediments and sedimentation. Stage 3 – Deposition of paralic order in the northern basins and evaporitic deposits in the southern basins. These activities indicated the beginning of marine interpenetration into the basin after the separation of South America from Africa. Stage 4 – This is the last stage in the development of the Gulf of Guinea and it includes the deposition of marine sediments that are rich in fauna and flora.

The Dahomey basin is primarily made of a combination of inland (onshore) which also, is the north of the basin and the marine parts (offshore), is the south of the basin. In the onshore, Cretaceous strata of non-fossiliferous basal sand sequence made of unconsolidated sands, grits, silts, clays and shales, with thickness of about 200 m (Okosun, 1990) are deposited on the Precambrian basement rocks during the Maastrichtian. This is laid on by horizons of clay beds with lignite and shale intercalations that are fossil bearing; the uppermost are almost entirely argillaceous.

Table 2. 1: Stratigraphic successions in the Dahomey Basin as dated by various researchers (After Okosun, 1990)

Reyment (1965) Adegoke (1969)		**Billman (1992)**		**Omatsola and Adegoke (1981)**		**Okosun (1990)**	
Maastrichtian	Araromi Shale (Informal)	Maastr.	Nkporo Shale	Maastrichtian	Araromi Formation	Maastrichtian	Araromi Formation
		Senonian	Awgu Shale				
		Turonian	Abeokuta Formation	Turonian	Afowo Formation		
		Albian	Unnamed Albian Sands				
	Abeokuta Formation	Pre-Albian	Unnamed Older Folded Sediments	Neocomian - Albian	Ise Formation	Upper Albian - Senonian	Abeokuta Formation

Separating the two sequences is the transitional white to grey sandy and kaolinitic clays conglomerate which likely is a product of degradation from the surrounding Precambrian rocks while, on the offshore, the deposits consist of about 1,000 m thick sequence of sandstones overlaid by black fossiliferous shales (Nuhu, 2009).

In the southern zone, which is coastal and offshore, the oldest sediments consist mainly of loose sand, grits, sandstones and clay with shale intercalations which progressively grade into shale. They are late Albian and possibly Neocomian in age (Omatsola and Adegoke, 1981) (Fig. 2.2 and Table 2.1).

Naming the stratigraphic sequences in the Dahomey basin has posed a major challenge, as many workers have tried naming, correlating and establishing the age of the formations in Nigeria with other countries in the Dahomey basin.

In 1964, Jones and Hockey established the age and lithology of the Abeokuta Formation to be Cretaceous and sands, grits, clays and shale respectively in the Nigerian sector. In 1992, Billman when studying the lithological sequences of the offshore in the Republic of Benin, referred to the Pre-Albian and Abian formations as "Unnamed" while the Turonian, Senonian and the Maastrichian he referred to as the Abeokuta Formation, Awgu and Nkporo Shale, respectively.

Reyment (1965) reported the occurrence of the Ajali Sandstone and the Nsukka Formation close to the basin margin around Ijebu-Ode and the occurrence of Nkporo Shale in the subsurface of the basin.

Jan du Chene *et al*. (1979), from a study of a coastal borehole (Ojo-1), reported the occurrence of strata of Albian to Maastrichtian age. Omatsola and Adegoke (1981) established three new, lithostratigraphic units, the Ise, and Afowo that was dated as Neocomian (Valanginian) and Albian-Turonian as the Araromi Formations. The Ise and the Afowo Formations corresponded to the unnamed Pre-Albian and Abian formations, while the Araromi Formation was considered equivalent to the Nkporo Shale of Billman (1992) (Table 2.2).

Okosun (1990), while evaluating the lithofacies of the eastern Dahomey Embayment, recognized two lithostratigraphic units named, the Abeokuta and Araromi Formations, which were both deposited in the Cretaceous.

Table 2. 2: Regional stratigraphic setting of the eastern Dahomey Basin (After Idowu *et al*., 1993)

AGE		FORMATION			LITHOLOGY
		Ako *et al*. (1980)	**Omatsola and Adegoke (1981)**		
	Eocene	Ilaro Formation	Ilaro Formation		Sand stone
Tertiary	Paleocene	Oshosun Formation	Oshosun Formation		Shale
		Ewekoro Formation	Ewekoro Formation		Lime stone
	Maastrictian		Abeokuta Group	Araromi Formation	Shale
Cretaceous	Turonian			Afowo Formation	Sand stone/shale
	Berremian			Ise Formation	Sand stone

Recently, several distinguished scholars such as Elueze and Nton (2004), Adebiyi (2015), Akinmosin & Osinowo (2010) and the Ministry of Mines and Steel Development (MMSD, 2010) have worked extensively on the stratigraphy of the eastern Dahomey, they generally agreed on five lithostratigraphic units within the basin deposited within a time window of Cretaceous to Recent but has slight discrepancies in the nomenclature and age assigned to the units.

The stratigraphic units within the Dahomey Basin are:

1 Cretaceous Abeokuta group which includes three Formations namely:

Ise Formation

Afowo Formation

Araromi Formation

2 Paleocene Ewekoro Formation

3 Late Paleocene to early Eocene Akinbo Formation

4 Eocene Oshosun and Ilaro Formations and

5 Pleistocene to Recent Benin Formation

2.1.1 Abeokuta group

The Abeokuta group is made up of the Ise, Afowo and Araromi Formations.

2.1.1.1 Ise Formation

This formation is the oldest of the Abeokuta group. It uncomformably overlies the basement complex rocks. Lithologically, the base of the formation consists of a basal conglomerate that is made of poorly rounded quartz pebbles with a silicified and ferruginous sandstone matrix or a soft gritty white clay matrix. This is overlain by poorly sorted coarse to medium grained loose sands, sandstones and kaolinitic clays.

In the offshore the Ise Formation consists of conglomerates, sandstones, shale and minor carbonate. The sandstone is white to light grey, medium to coarse, unsorted, conglomeratic, quartzic, containing mica and chlorite, kaolinite and some carbonate cement (d'Almeida *et al*., 2016).

2.1.1.2 Afowo (Abeokuta) Formation

In Southwestern Nigeria, the Afowo Formation overlies the Ise Formation with a base of well sorted, sub-rounded fluviatile sand, mixed with brackish marine sediments. The sediments are believed to have been deposited in a transitional to marginal marine environment. The Formation is the main petroliferous Formation and generally consists of coarse to medium grained sandstones with thick intercalations of shale, siltstones and pyritised clay (d'Almeida *et al*., 2016). The age has been assigned to be of Turonian to Maastrichtian age.

2.1.1.3 Araromi (Nkporo) Formation

The fossil rich Araromi Formation conformably overlies the Afowo Formation. It consists of layers of sandstone at the base, which is overlain by dark to black shales, siltstones with limestone inclusions, marls and lignite. In the offshore, the Araromi Formation comprises of dark laminated carbonaceous shales with abundant pyrite but poorly preserved fossils (d'Almeida *et al*., 2016). Okosun (1990) stated that for proper recognition and distinguishing of the Abeokuta Formation from the Araromi Formation, it should be noted that the Abeokuta Formation comprises predominantly of unconsolidated sands with intercalations of grey shale, mudstone, silt and clay while the Araromi Formation consists of dark grey and black shales with intercalations of sandstone, limestone, marl, and silty and glauconitic shale.

2.1.2 Ewekoro Formation

The Ewekoro Formation overlies the Abeokuta Group and is of a shallow marine origin. The carbonate rich formation consists of large deposits of limestone and overlying glauconite deposits. The carbonate has generally been classified into four microfacies namely: a sandy biomicrosparite, shelly biomicrite, red phosphatic biomicrite and algal biosparite (Adebiyi, 2015). According to d'Almeida *et al*. (2016), the age of the Formation from biostartigraphic data, is Paleocene or older, but definitely not younger.

2.1.3 Akinbo Formation

Uncomformably overlying the Ewekoro Formation is the Akinbo Formation. The Akinbo base consist of glauconite rich limestones and a top of pure grey, gritty sand with little kaolinitic rich clay. Nton *et al*. (2009) has assigned the formation to be Upper Paleocene to Lower Eocene in age.

2.1.4 Oshosun Formation

The Akinbo Formation overlies the Oshosun Formation which is of Lower Eocene-Middle Eocene in age (Adebiyi, 2015). The lithology of the Oshosun Formation (onshore and offshore) is made up of coloured laminated and glauconitic clay, sandstones and shale intercalations. On the offshore, phosphatic clay stones grading into siltstone are present (Adebiyi, 2015).

2.1.5 Ilaro (Ijebu) Formation

After the Oshosun Formation was deposited, it was followed by a marine regression that led to the deposition of the Ilaro Formation. The Ilaro Formation conformably overlies the Oshosun Formation and consists of massive, poorly consolidated and cross-bedded sandstones. Sub-rounded to rounded pure quartz grains dominate the base of the formation. This texture is an indication of a beach or shoreline and near shore environment. The Ilaro Formation was assigned an Eocene-Oligocene age (d'Almeida *et al*., 2016).

2.1.6 Coastal Plain Sands or Benin Formation

The Coastal Plain Sands are the youngest sedimentary unit and ranges in age from the Oligocene to Recent (Akinmosin and Osinowo, 2010). It is lithologically made of poorly sorted unconsolidated pebbly sands with lenses of clays from both continental and marine origin.

2.2 Geology of Studied Areas

2.2.1 Ogijo Industrial Layout

The industrial layout is situated within the Ewekoro depression in the Eastern Dahomey embayment.

Ogijo industrial layout lies within the Ewekoro, Akimbo and Illaro stratigraphic units occurring south of the Abeokuta group. In the north of Ogijo towards Sagamu town, the geology (Fig. 2.3) consists of arkosic sand stones and grits that tend to be carbonaceous towards the base. Southwards of the site, the geology becomes more argillaceous consisting more of sequences of sandstones, shales, limestones and reddish clay. This grade from coarse to fine sands with packs of shales and clays. No river was observed in the site and the source of water are boreholes and shallow hand dug wells.

2.2.2 Ota Industrial Layout

Ota industrial layout lies within the Ewekoro depression in the Eastern Dahomey embayment. The geology of the site consists of the Coastal Plain Sands which are the youngest sedimentary unit in the depression (Akinmosin and Osinowo, 2010). The geology consists of poorly sorted unconsolidated pebbly sands with lenses of clays (Fig. 2.3). No river was observed in the site. The major source of water is through boreholes.

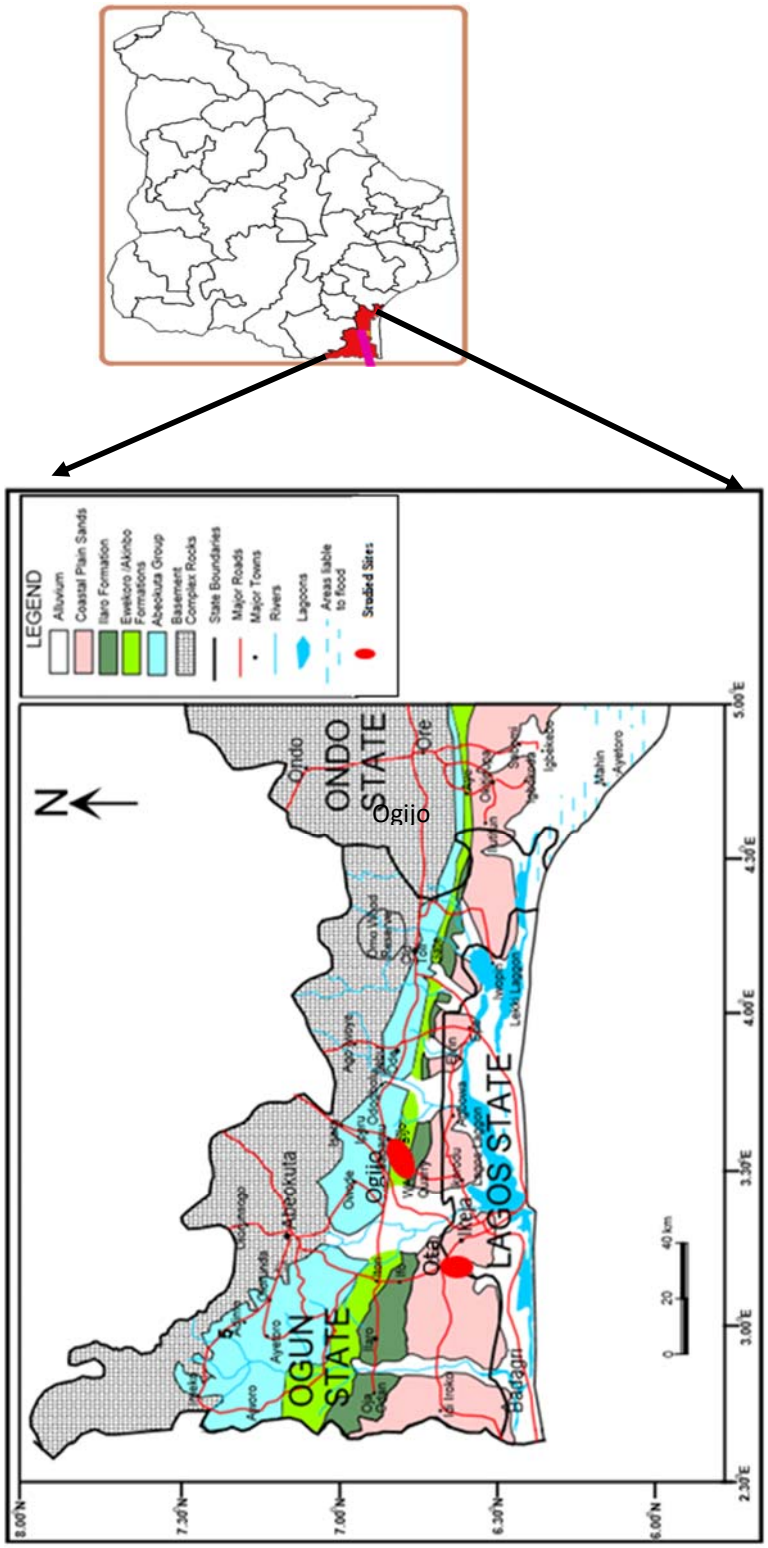

Figure 2.3: Location of Ogijo and Ota industrial layouts on the geological map of Dahomey Basin (Modified after Olabode and Mohammed (2016))

2.3 Theory of Methods

Magnetic Susceptibility

When a material sample is placed in a magnetic field, and the sample is magnetized, the magnetization is described by the magnetization vector M **(**the dipole moment per unit volume). Since the magnetization is induced by the external field B, it is assumed that M is proportional to B. That is,

$$M = XB \qquad (2.1)$$

The proportionality constant χ in equation (1) is known as the magnetic susceptibility of the material. Based on susceptibilities magnitude and temperature dependence, materials are generally classified into five basic classes: diamagnetic, paramagnetic, ferromagnetic, antiferromagnetic and ferrimagnetic (Evans and Heller, 2003).

Diamagnetic materials have weak and negative magnetic susceptibility (Dearing, 1996). Ferrimagnetic materials on the other hand have high magnetic susceptibility these, includes magnetite and other Fe-bearing minerals (Dearing, 1996). In ferrimagnetic materials the saturation magnetization increases with increasing temperature and then drops down. Ferromagnetic materials consist of atoms that are highly ordered and are aligned in the same direction. These results in very high magnetic susceptibility but are rarely found in nature. An example would be pure iron.

Paramagnetic materials have the magnetic moments of their atoms arising mainly from the presence of Manganese (Mn) and Iron (Fe) ions that align only in the presence of a magnetic field resulting in weaker magnetic susceptibility values (Dearing, 1996). Antiferromagnetic materials have small positive susceptibilities at all temperatures.

The Bartington MS2 Magnetic Susceptibility System that was used for the analyses comprises of an MS2 meter that contains some sensors and a Bartsoft control software. The MS2 Magnetic Susceptibility System generates a low frequency AC magnetic field (external field), such that when a sample is placed in this field, there is a change in the field due to induced magnetization from the sample material that is detected by the system. This change is converted into a magnetic susceptibility reading as recorded by

the system. This sensor can generate the AC magnetic field both in the low frequency (0.465 kHz) or high frequency (4.65 kHz). The percentage difference between readings at the two frequencies is called the coefficient of frequency dependence.

The frequency dependent susceptibility was calculated as in equations 2 and 3:

$$X_{fd} = X_{lf} - X_{hf} \quad (2.2)$$

$$X_{fd}\% = 100 * \frac{X_{lf} - X_{hf}}{X_{lf}} \quad (2.3)$$

where:

X_{hf} is the mass-specific susceptibility measured at a high frequency of 4.6 kHz,

X_{lf} is the mass-specific susceptibility measured at a low frequency of 0.46 kHz.

The frequency dependent susceptibility find use in the detection of very fine (ultra-fine) ferromagnetic minerals in soils (Zhu *et al*., 2018) and in the assessment of ultrafine super-paramagnetic magnetite grains (Dearing *et al*., 1996). It can also reflect the concentration of ferrimagnetic minerals in soil, their grain size and types (Zhu *et al*., 2018). Frequency-dependent susceptibility (X_{fd}) can indicate the presence of grains lying at the stable single domain-super-paramagnetic (SSD-SP) boundary, around 0.02 μm for isodiametric grains.

Relatively high X_{fd}% indicates the concentration of SP grains in soil, and if it is less than 4%, MD (multi-domain) and PSD (pseudo single domain) or SSD grains dominate (Zhu *et al*., 2018).

Inductively Coupled Plasma Mass Spectrometry (ICP-MS)

The geochemical investigation was done by using the inductively coupled plasma mass spectrometry which has the capacity of detecting metals. This method involves generating a state of matter referred to as plasma: where orbital electrons from samples are easily removed and become free in the presence of a strong electromagnetic field. The ions based on their mass to charge ratios are detected by the mass spectrometer and recorded.

According to Mahesh *et al*. (2012), the ICP-MS is considered to be a very powerful technique in the determination of elements. Warra *et al*. (2011) concluded the techniques becomes most relevant due to its ability to generate very accurate results up to a level of one part in trillion.

Ecological Risk Analysis Pollution indices

Pollution indices are powerful tools for ecological geochemical assessment and are widely considered as being very useful for the comprehensive evaluation of potential ecological risk from heavy metal pollution. According to Kowalska *et al*. (2018), many researchers have combined several relevant pollution indices tools and have recorded more accurate results. The tools are broadly divided into two groups; the single elemental factor and multi-elemental factor pollution indices.

For this study, the single elemental factor pollution indices will be used to assess heavy metal pollution in the soil samples. These include:

Contamination Factor (CF)

Enrichment Factor (EF)

Index of Geoaccumulation (I_{geo})

CF and I_{geo} will be used to assess individual level of metal pollution while EF will be used to assess the source (anthropogenic or geogenic) of the heavy metal in the soil.

Contamination factor is a measure of the likely impact of anthropogenic activities on the concentration of heavy metals in soil by comparing the concentration of each element to its average crustal concentration. The result will reflect the multiple times the concentration has exceeded its crustal value.

The I_{geo} is also a single metal quantitative tool that quantify the concentration of the toxic heavy metal to a multiple of a constant value of 1.5 by which it is greater than their average crustal values.

The EF tool helps to ascertain the source of the heavy metal pollutants. That is, if the pollutant is from external source or it is naturally occurring.

CHAPTER THREE

MATERIALS AND METHODS

3.1 Research Methodology

3.1.1 Sample Collection

Soil samples were collected based on accessibility (due to infrastructural barriers and restrictions to residential quarters) between October and December 2016; which was after the rainy season from both locations of study. At each sampling points, four soil samples were collected at 0 cm, 10 cm, 20 cm and 30 cm depths from 105 sample points in Ogijo and 32 sample points from Ota. A total of 420 and 128 whole samples were collected from Ogijo and Ota, respectively, in plastic bags and carefully labelled.

The location of each sample points was recorded by a Garmin GPS receiver with a precision of ±10 m enabling future re-visiting if, and when necessary (Figs. 3.1 and 3. 2).

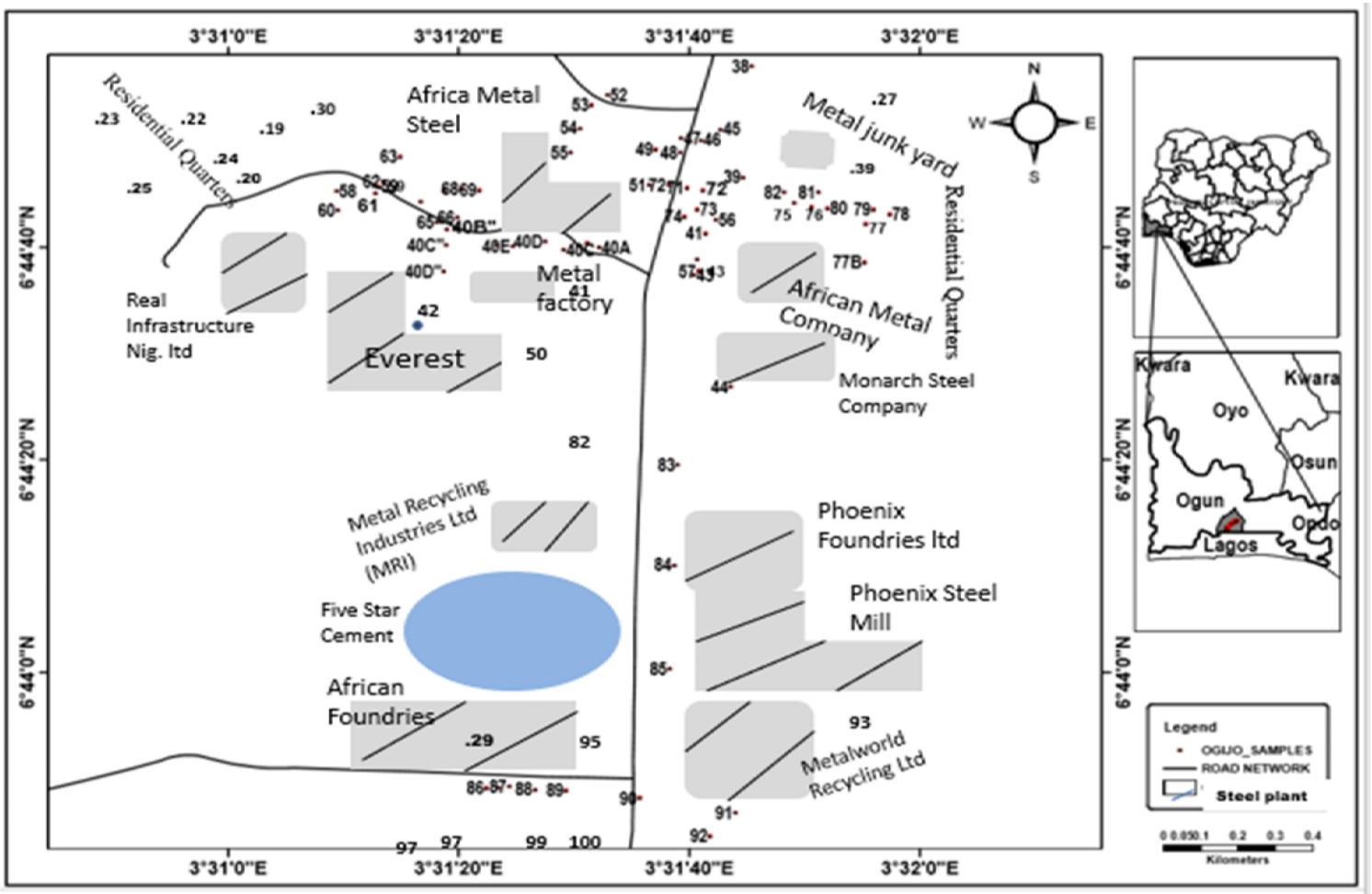

Figure 3.1: Location map of Ogijo industrial layout showing sample points

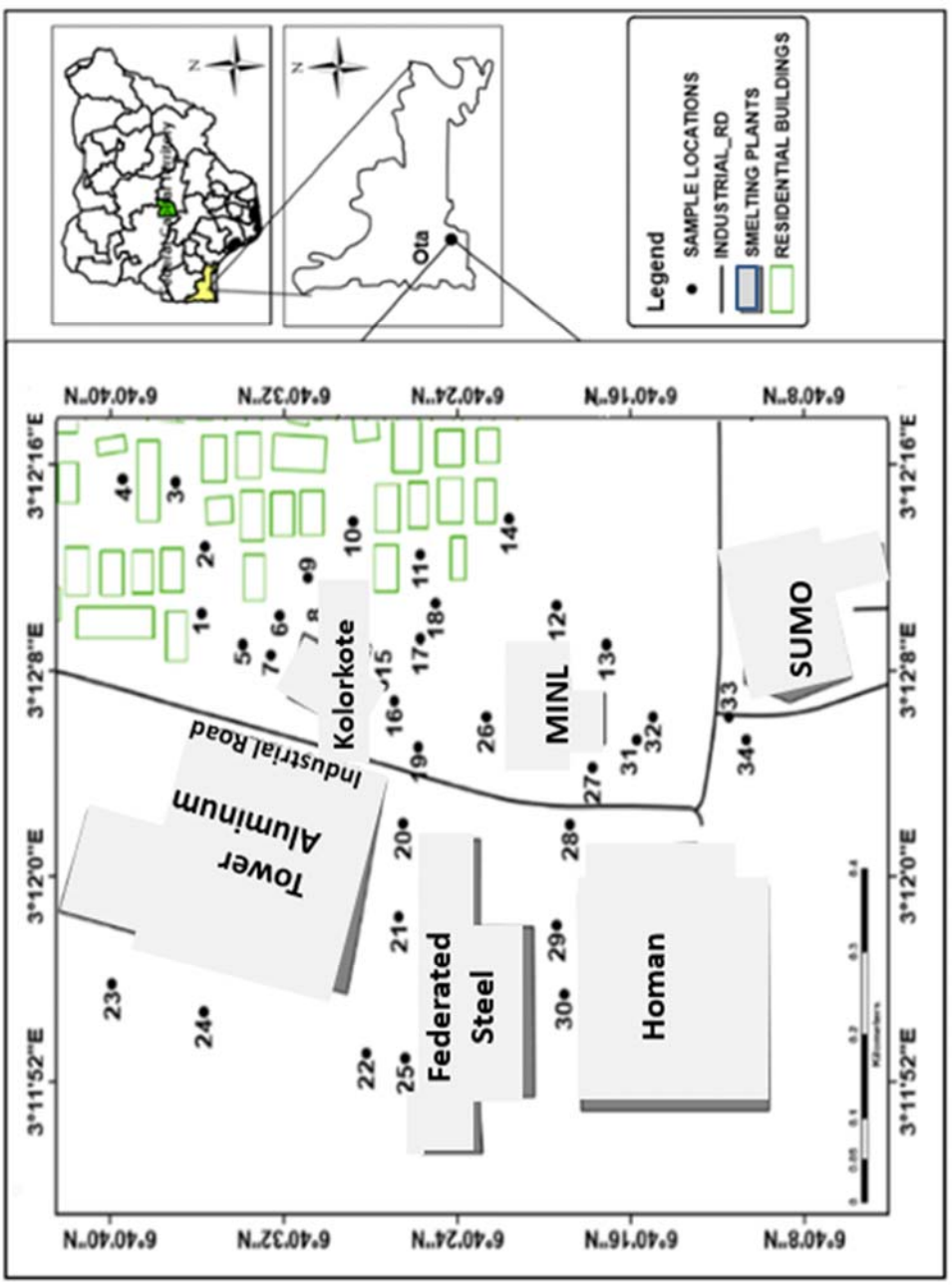

Figure 3. 2: Location map of Ota industrial layout showing sample points

The sample collection was done during the dry season in October thereby reducing moisture problem (Maier *et al*., 2006). Slags were cleared from the top soil at some sample points before sampling.

Sample plastic bags were labelled with a permanent marker and additional paper labels placed inside each plastic bag for each depth. All four samples from a single sample point were then placed in a bigger plastic bag and labelled accordingly for each point location.

3.1.2 Sample Preparation

Each sample was air dried for two days, disaggregated and divided into two portions; one part retained as whole soil samples, and the other parts were sieved to 180 μm, 125 μm, 90 μm and 65 μm grain fractions. A total of 420 whole soil and 1680 fraction-sized samples were collected from Ogijo, while 128 whole soils and 512 fraction-sized samples were collected from Ota. The samples were carefully labelled with permanent maker and packaged in plastic containers.

Precaution: The samples were air dried under a shade (Appendix 3.1) for about two days and in an environment void of any industrial activities, this is necessary to avoid any form of contamination from external source (Kolawole *et al.,* 2018).

3.1.3 Laboratory Analysis

The laboratory analysis was carried out in three phases namely;

- Sample preparation,
- Magnetic susceptibility analysis using:
    - Bartington Multisus-MS2B Dual Frequency susceptibility system,
    - Temperature analysis using the GeoLabsoft / Bartington Instruments susceptibility versus temperature system (MS2 κ/T) and
- Geochemical analysis using the Aqua Regia digestion procedure.

3.1.3.1 Samples Preparation

The Bartington Multisus-MS2B Dual Frequency susceptibility system came with about a hundred standard 10 ml sample container or plastic pots that will contain the samples during analysis. The plastic pots were thoroughly washed and dried. By using an

electronic balance having an accuracy of 0.1mg (Appendix 3.2), the weight of an empty plastic pot was weighed and recorded in the system for weight correction, then, the plastic pots were filled with the samples and labelled appropriately after which each sample in the sampling pots was weighed and the readings were recorded.

3.1.3.2 Magnetic Susceptibility Analysis

Magnetic susceptibility analysis was carried out on all the samples by using the Bartington MS2B dual frequency sensor suite which includes a MULTISUS software, window installed computer, MS2 meter and the MS2 sensor (Appendix 3.3).

The default setting of the meter used for the analysis is presented in Table 3.1. The measured weight for each sample was imputed into the system and the sample placed in the MS2 sensor. The magnetic susceptibility was measured by the MS2 meter and the resultant readings appeared on the screen of the computer and saved as a MLTISUS file. The process was repeated for each sample both in the LF at 0.465 kHz and HF at 4.65 kHz mode. Several readings were taken at each mode and the average calculated by the system. The dual frequency measurements exploit the phenomenon of superparamagnetism. A LF measurement allows the Super-paramagnetic (SP) crystals close to the boundary with Stable Single Domain (SSD) grains (crystals grown by the solute diffusion (SSD) method) to contribute fully to the susceptibility measured, while the HF measurement does not.

The difference in the values of the two measurements based on an in-built algorithm is called the percentage frequency dependence $X_{fd}\%$ which the software automatically calculates. When $X_{fd}\%$ was plotted against the low frequency magnetic susceptibility (X_{lf} cm^3kg^{-1}) (X_{lf} mass specific), an estimate of the SP minerals concentration in the site can be obtained (Dearing, 1994). The range of the cross plot will be used to classify the magnetic grains and to ascertain the presence of external sources. According to Dearing et al, 1996, if $X_{fd}\% > 14$, it signifies the presence of metallic pollutants that are yet to be incorporated into the atomic lattice of the host element, $14 < X_{fd}\% > 10$ are the SP grains, $10 < X_{fd}\% > 2$ indicates the presence of a mixture of SP and non-SP grains and when $X_{fd}\% < 2$ shows the presence of paramagnetic grains.

Table 3.1: Bartington instruments Multisus file showing the default settings used for the analysis

MS2B DEFAULT SETTINGS	UNIT
Range	1
Units	SI
Frequency	LF or HF
Drift Limit	5
Weight Correction	1
Container weight	3.2
Container Correction	1
Container sus SI	-0.3
Container sus CGS	-0.2389

3.1.3.3 Magnetic Susceptibility - Temperature Analysis

The Bartington Temperature Analysis suite (MS2 κ/T) was used for the temperature analysis. The suite comprises of a GEOLABSOFT software that is installed in a windows computer, an MS2W sensor, MS2 meter, MS2WF furnace, MS2WFP power supply and water source (Appendix 3.4).

Eight (8) samples from Ogijo industrial layout and five (5) samples from Ota industrial layout were selected from those with high, low and average magnetic susceptibility readings and were subjected to the temperature analysis.

Each sample was placed and heated in the furnace; MS2WF. The MS2W sensor which was connected to the MS2 meter measured the temperature as it rose at intervals which were initialized in the GEOLABSOFT software. The MS2 meter measured the corresponding magnetic susceptibility at each temperature interval.

The recordings from the MS2W sensor and the MS2 meter were automatically tabulated and plotted on graphs by the GEOLABSOFT which was displayed on the screen of the computer. The MS2WF was connected to the MS2WF that powered the furnace. The MS2W sensor was connected to the cooling system through pipes that ensured the temperature of the sensor was controlled.

A plot of the magnetic susceptibility readings against the temperature values, when compared to the Schematic curves of different magnetic minerals and temperature domains in the Bartington manual (Dearing, 1994), was used as a guide in the classification of the metals present in each sample.

3.1.3.4 Geochemical Analysis

To ascertain the concentration and constituent heavy metal elements responsible for the magnetic susceptibility readings that were recorded, 21 and 10 soil samples from grain fraction sizes of 180, 125, 90 and 65 μm, and ranging from high, medium and low magnetic susceptibility readings, were selected from different depths from Ogijo and Ota respectively and sent to the Acme lab (BUREAU VERITAS MINERAL LABORATORIES) in Canada for geochemical analysis. The thirty-one samples were subjected to the Aqua Regia method of heavy metal extraction by using the inductively coupled plasma mass spectrometry. A total of 33 major and trace heavy metal elements were analysed in the samples and these includes: Copper (Cu), Lead (Pb), Zinc (Zn),

Chromium (Cr), Nickel (Ni), Boron (B), Beryllium (Ba), Cadmium (Cd), Arsenic (As), Mercury (Hg), Molybdenum (Mo), Silver (Ag), Cobalt (Co), manganese (Mn), Iron (Fe), Thorium (Th), Strontium (Sr), Antimony (Sb), Bismuth (Bi), Vanadium (V), Calcium (Ca), Phosphorus (P), Lanthanum (La), Magnesium (Mg), Titanium (Ti), Aluminium (Al), Sodium (Na), Potassium (K), Tungsten (W), Sulphur (S), Thallium (Tl), Gallium (Ga), and Scandium (Sc).

Ecological Risk Analysis

The results of the geochemical analysis were evaluated for metal pollution by using different techniques for environmental assessment. These techniques were:

Contamination Factor: This tool assesses the level of contamination by each metal element. The concentration of each element in the study site was compared to its average crustal concentration. The ratio indicated the number of times the measured concentration has increased relative to its natural concentration in the crust. This is called the contamination factor of that element of interest. Contamination Factor is an indication of the extent of contamination in the site.

$$CF = \frac{C_{0-1}}{C_n} \tag{3.1}$$

Where:

CF = Contamination factor of element of interest

$C_{0\text{-}1}$ = Concentration of the element sample

C_n = Crustal average of element

According to Taylor and Meclenan, 1985 interpretation,

CF < 1 low contamination,

CF = 1-3 Moderate contamination,

CF = 3-6 Considerable contamination,

CF > 6 Very high contamination.

Enrichment factor: This tool distinguishes between anthropogenic and naturally occurring sources of heavy metal pollutants. The EF of metal was defined using Iron as a reference element.

The EF for each element was calculated by using Chen *et al*. (2007) method. It was used to assess the level of contamination by each element and the possible impact of anthropogenic activities in the environment.

$$EF = \frac{{}^{M}/_{F(Sample)}}{{}^{M}/_{F(Background)}} \qquad (3.2)$$

Where:

M / F(Sample): Ratio of the concentration of metal and iron in the sample

M / F(Background): Ratio of average concentration of metal and iron in the crust

According to Chen *et al*. (2007)

EF < 1 indicates no enrichment,

EF = 1–3 indicates minor enrichment,

EF = 3–5 indicates moderate enrichment,

EF = 5–10 moderately to severe enrichment,

EF = 10–25 severe enrichment,

EF = 25–50 very severe enrichment,

EF > 50 extremely severe enrichment

Index of Geo Accumulation: This is a single metal quantitative method which calculates or quantify metal pollution in sediments by comparing the concentration of the toxic heavy metal to a constant value of 1.5 or more times greater than their lithogenic background values, that is, variations occurring in background data due to difference in the lithology of the sediments

This method was proposed by Müller (1969) as referenced by Ebru Yeşim Özkan (2012).

$$I_{geo} = Log^2 \frac{C_n}{1.5B_n} \quad (3.3)$$

Where:

C_n is the measured concentration of metal in the sample,

B_n is the background value,

Factor 1.5 was used because of possible variations of the background data due to litho logical variations.

$I_{geo} \leq 0$ Uncontaminated $0 < I_{geo} < 1$ Uncontaminated/moderately contaminated

$1 < I_{geo} < 2$ moderately contaminated $2 < I_{geo} < 3$ Moderately/strongly contaminated

$3 < I_{geo} < 4$ Strongly contaminated $4 < I_{geo} < 5$ Strongly/extremely contaminated

$5 < I_{geo}$ Extremely contaminated

3.1.3.5 Descriptive Statistical Analysis

Descriptive statistic which is an important tool in analysing numerical data and presenting findings in the form of graphs, histograms, box plots, pie charts and maps are a better way to understand the spatial distribution of pollutant heavy metals in soil samples (Gabrielyan *et al.,* 2018) and possible source of the metals.

Statistical Analysis

The magnetic susceptibility values from the whole samples, grain samples and geochemical analysis were subjected to statistical analysis.

Histograms: To better understand the impact of the smelting plants on the soils of the two industrial layouts, the magnetic susceptibility values of whole soil samples which are a representative of the soil in situ of these environments were analysed. Histogram plots showing the maximum and minimum magnetic susceptibility values of all whole samples with respect to depth were generated. Sample points with high magnetic susceptibility values were easily identified. The histogram plots with depth were useful in understanding the influence of the general geology to the accumulation of the heavy

metals. Histograms of all the magnetic susceptibility values obtained from the grain soil samples were also plotted with respect to the grain sizes of 65, 90, 125 and 180 μm, this gives a better understanding on the variation in concentration of the heavy metals in each grain sizes and with respect to depth.

Density Maps: The magnetic susceptibility values for all the surface samples at 0 cm depth from the whole soil samples and the concentrations of lead from the geochemical analysis were plotted to generate concentration density maps for each site. The aims were to identify areas on the layouts with high magnetic susceptibility anomalies, spatial distribution of lead, the intensity and spatial distribution of pollutants away from the smelting plants and the impact of each smelting plant on the environment.

Box Plots: The box plots showing magnetic susceptibility variation in the different grain sizes at each sample point and at each depth were also generated. The length of the box represents the interquartile range, which contains 50% of the values, and the heavy horizontal line inside the box indicates the median. The "whiskers" are lines that extend from the box to the highest and lowest values.

Geochemical Elemental Concentration: The elemental concentrations of the heavy metals which were recorded from the geochemical analysis were analysed by calculating the mean, minimum, maximum and standard deviations for each element and compared with their respective crustal average. This gives a first-hand knowledge of the specific metal that have a concentration higher than its crustal value, thus, the basis for separating the elements into major and trace metals. Spatial distribution of each major elements in the samples analysed were represented with histograms. Also, histograms of all the major and minor elements concentrations were plotted to identify the elements with the highest concentration in each group.

The Pearson Correlation: The Pearson correlation method was used to generate a correlation matrix of the major and some significant trace elements in both industrial layouts. The matrix was used to ascertain if there were any linear association between the heavy metal elements. Based on the value of correlation coefficient obtained from the matrix, the correlation between two heavy metals can either be positive or negative. According to Orosun *et al.* (2020), positive correlation between two elements signifies the elements are from the same source.

CHAPTER FOUR

RESULTS AND DISCUSSION

4.1 Concentration of Heavy Metal Pollutants in the Soils around Iron Smelting Plants in Ogijo and Ota industrial Layouts

4.1.1 Heavy Metal Pollution in Ogijo

The mass specific magnetic susceptibility values in both the low and high frequencies of all whole samples randomly and purposively collected from Ogijo and the geochemical results were statistically analysed. The charts are, as presented in appendix 4.1. The X_{lf} is more robust and representative of the magnetic regimes in any sample because it accounts for all ferrimagnetic minerals in the samples (Dearing *et al*., 1996). The X_{lf} will be used for most deductions.

4.1.1.1 Pollutants in Whole Soil Samples from Ogijo

Both the X_{hf} and X_{lf} of the whole samples obtained from Ogijo recorded very high values in about 80% of the samples. Sixteen sample points on the surface, seven sample points both at 10 cm and 20 cm, and nine sample points at 30 cm depths all had magnetic susceptibility values above 1000 (Fig. 4.1; Appendix 4.1; Table 4.1); while the control site had a maximum recorded value of 51.5 at the surface, 19.2 at 10 cm, 23.8 at 20 cm and 33.4 at 30 cm depth. When the results from Ogijo are compared to that obtained from the control site, it signified that the values from Ogijo are very high. According to Bouhsane and Bouhlassa (2018), high magnetic susceptibility values is an indication of high concentration of ferrimagnetic minerals whose origin could either be pedogenic, inherited from substratum, or allochthonous, that is, from atmospheric pollution fallout (e.g., polluted dust). Ogijo industrial layout lies within the Ewekoro, Akimbo and Illaro stratigraphic units occurring south of the Abeokuta group. In the north of Ogijo towards Sagamu town, the geology (Fig. 2.3) consists of arkosic sand stones and grits that tend to be carbonaceous towards the base Nton *et al*. (2009). Southwards of the site, the Akimbo and Illaro stratigraphic units becomes dominant and the geology becomes more argillaceous consisting of sequences of poorly consolidated sandstones, shales, limestones and reddish clay that graded from coarse to fine sands with packs of shales and clays (d'Almeida *et al*., 2016). Dearing (1996), in his extensive work in the whole of England stated that sedimentary areas made of chalk, slate and oolitic limestomes etc. naturally should have negligible concentration of magnetic minerals, therefore the

geology couldn't possibly have contributed to the high magnetic susceptibility recorded in the site. A possible source of pollution could be from river effluents; Kolawole *et al*. (2018) recorded high concentration of heavy magnetic elements in soils located downstream of the Alaro river that has been polluted by effluents from industrialization. In the vicinity of Ogijo industrial layout, no river was observed in the site and therefore no possibility of effluent discharge from external source outside the industrial layout could have contributed to the high magnetic presence in the soil of the site.

The X_{lf} readings showed relatively high values; at the 0 cm depth, the range of the values were 7.9 – 6159.3 with mean value of 629.18, at 10 cm depth it ranged between 5.3 – 4240.1 and the mean value was 410.14, at 20 cm depth the range was 5.5 – 3961.5 with a mean value of 424.66 and at 30 cm depth, the value was 5.4 – 3870.2 with a mean value of 447.29. These averages when compared to Wojas (2017), which stated that the average value of X_{lf} in the unpolluted Carpathians was 30 and values above this, signified the influence of anthropogenic factors in the environment. The very high average values measured in Ogijo which was between 629.18 and 410.14 then signified extreme influence of anthropogenic activity in the environment.

The X_{lf} values in all the samples were higher than the X_{hf} values recorded. The dual frequency measurements exploit the phenomenon of superparamagnetism. A low frequency measurement allows the Super-paramagnetic (SP) crystals close to the boundary with Stable Single Domain (SSD) grains (crystals grown by the solute diffusion (SSD) method) to contribute fully to the susceptibility measured, which, while in the high frequency are magnetically blocked because they have relaxation time shorter than the measured time and therefore do not contribute to the measured readings. The difference in values between X_{lf} and X_{hf} at each sample point is presented as a percentage (X_{fd}%) called frequency dependence percentage (Dearing, 1994). This signified the percentage of the ferromagnetic minerals at each sample points. At Ogijo, the mean X_{fd}% calculated for 0 cm depth was 6.04%. This implies that 6.04% of the heavy metals on the surface samples are ferromagnetic minerals. Similarly, at 10 cm depth, the X_{fd}% value was 8.12%, at 20 cm it was 9.44% and 10.30% at 30 cm depth.

From the statistical analysis of the data, it was obvious that the readings show a typical stepladder like distribution with depth, with 44.01% of the sample points having the highest magnetic susceptibility values at the zero depth. This implied that 44.01% of the

sample points have the highest concentration of pollutants at the surface. Also, 12.88% of the sample points showed highest magnetic susceptibility readings at 10 cm depth, 11% and 32.11% of the sample points had their highest magnetic susceptibility values at 20 and 30 cm depths respectively. The result reflects that the surface soils are most polluted. The concentration of the pollutants decreases with depth but showed an appreciable level of enhancement at 30 cm depth. Duan *et al*. (2010), observed similar stepladder variation in the distribution of heavy metal pollutants with depth in soils around steel companies in Nanjing. He recorded an enhancement in the readings at 20 cm depth below which the magnetic values became low and averagely constant.

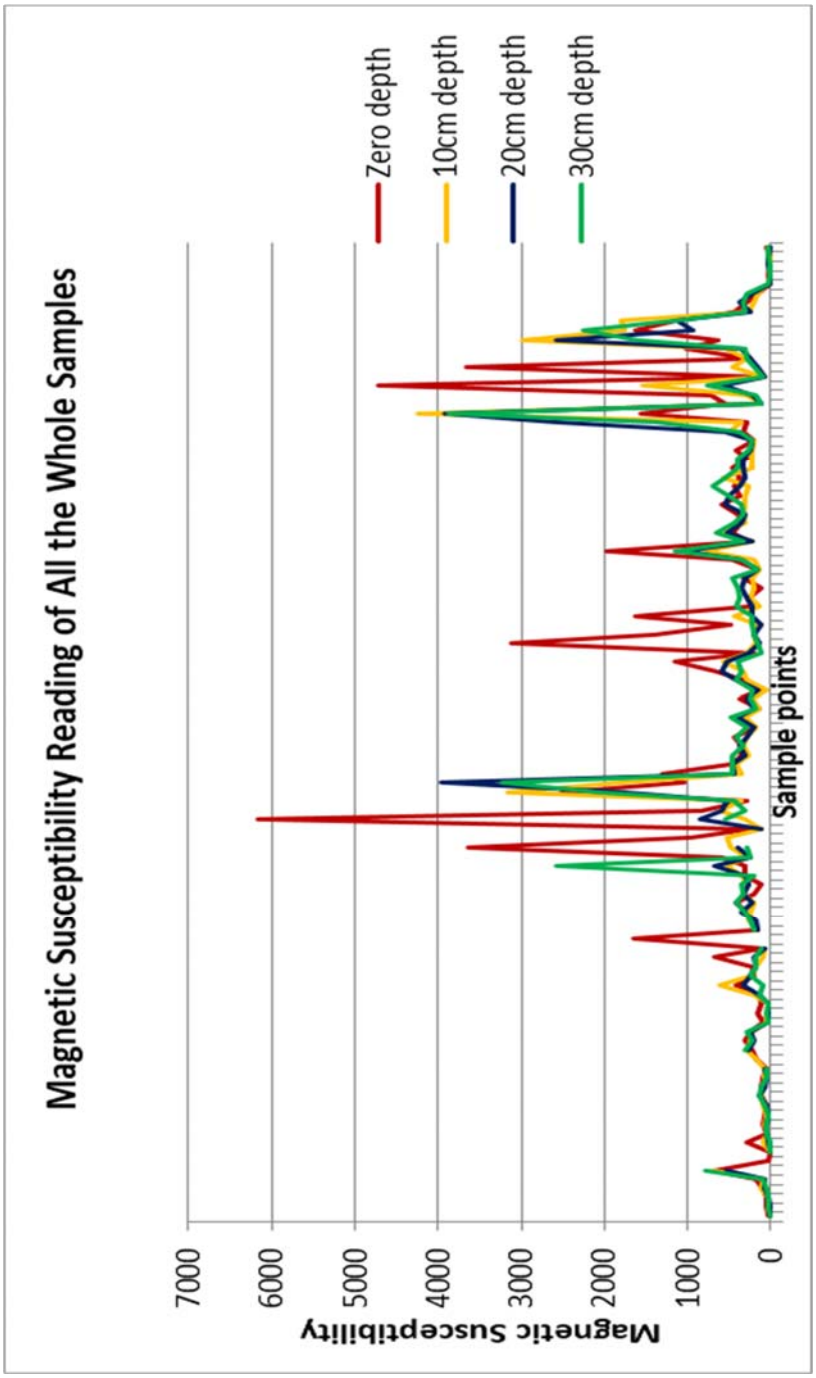

Figure 4.1: Charts showing variations in magnetic susceptibility at 0 cm, 10 cm, 20 cm and 30 cm

Table 4.1 Variation in X_{lf} readings and X_{fd}% with depth

Variation in values in Ogijo, Ota Industrial Layouts and the Control Site					
		Low Frequency Magnetic Susceptibility			
	Depth (cm)	Minimum	Maximum	Total Average	X_{fd}%
Ogijo Industrial Layout	0	7.9	6159.3	629.18	6.04
	10	5.3	4240.1	410.14	8.12
	20	5.5	3961.5	424.66	9.44
	30	5.4	3870.2	447.29	10.30
Ota Industrial Layout	0	30.3	2645	490.44	7.26
	10	23	1257	368.33	6.04
	20	14.4	6343.9	596.14	7.70
	30	8.2	1333.3	270.97	9.59
Control Site	0	11.2	51.5	23.4	4.3
	10	10.3	14.6	14.6	7.3
	20	8	16.58	16.58	10
	30	11.6	21.7	21.7	13.2

4.1.1.2 Type and Elemental Concentration of Pollutants in Soil Samples from Ogijo

Thirty-three heavy metal elements were identified from the geochemical analysis performed on soil samples from Ogijo, the results are presented in Appendix 4. The identified metals have been classified into major elements based on their concentrations.

Major Heavy Metals: The major heavy metals evaluated are zinc (Zn), manganese (Mn), lead (Pb), copper (Cu), barium (Ba), chromium (Cr), and boron (B). The concentrations of these metals showed a wide range in their values in the soil samples. The range of values and their mean were: Zn (54 - >10000: mean 2285.05), Mn (295 - >10000: mean 1950.15), Pd (29 – 2381: mean 525.5), Cu (16 – 834: mean 204.3550), Ba (18 - 749 mean 176.4), Cr (24 – 416 mean 140.2) and B (25 – 334: mean 96.67) Appendix 4.6 and figure 4.2. Presented in the order of decreasing concentration Zn > Mn > Pb > Cu > B > Cr >B.

The major metals, Mn, Zn, Pb and Cu had the highest concentration when compared to their crustal averages. The concentration of Pb in all the samples analysed exceeded the elements crustal average value of 12.5 (Appendix 4.6.1). Copper with an average crustal value of 50, had 66% of the samples having values above the crustal average. Similarly, 95% of the samples had values of Zn above its crustal value of 20. Boron and Cr had 57% and 47% of the samples having values above their respective crustal averages. The least was Ba with 4.7% of the samples having concentrations greater than its average crustal value of 500. (Appendix 4.6). These metals with very high concentrations are responsible for the high magnetic susceptibility readings recorded in the layout.

Among the major and trace heavy metal elements were some that were listed by the World Health Organization (2011) as toxic heavy metals and these includes Hg, As, Cd, Cu, Ni, Cr and Pb. All these elements have values that exceeded the National Environmental Standard and Regulations Enforcement Agency (NESREA) allowable limits in soils (Table 4.2).

Table 4.2: Major elements in Ogijo industrial layout

ELEMENT	SUM	MIN	MAX	MEAN	Crustal Ave	*NESREA limits	SDEV
Cu	4116	16	834	204.35	50	72	204.3673
Pb	12891	29	2381	525.5	12.5	164	634.0814
Zn	46505	54	10000	2285.05	70	421	2633.103
Mn	39731	295	10000	1950.15	1000	-	2137.654
Cr	2830	24	416	140.2	100	100	105.421
Ba	3563	18	749	176.4	500	-	183.443
B	1184	25	334	98.67	10	-	99.27495

*NESREA limits (2011)

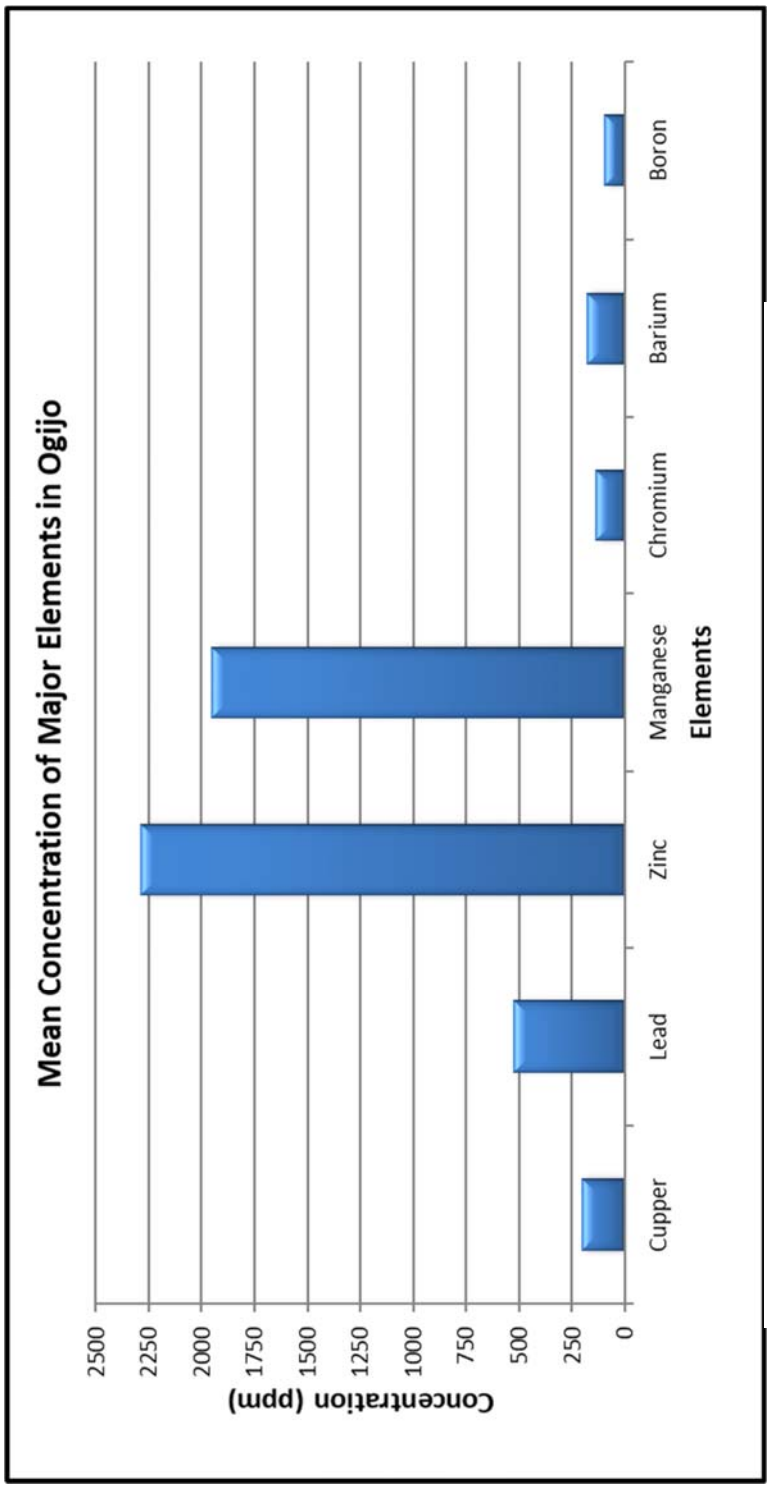

Figure 4. 2: Mean concentration (ppm) of major elements in Ogijo industrial layout

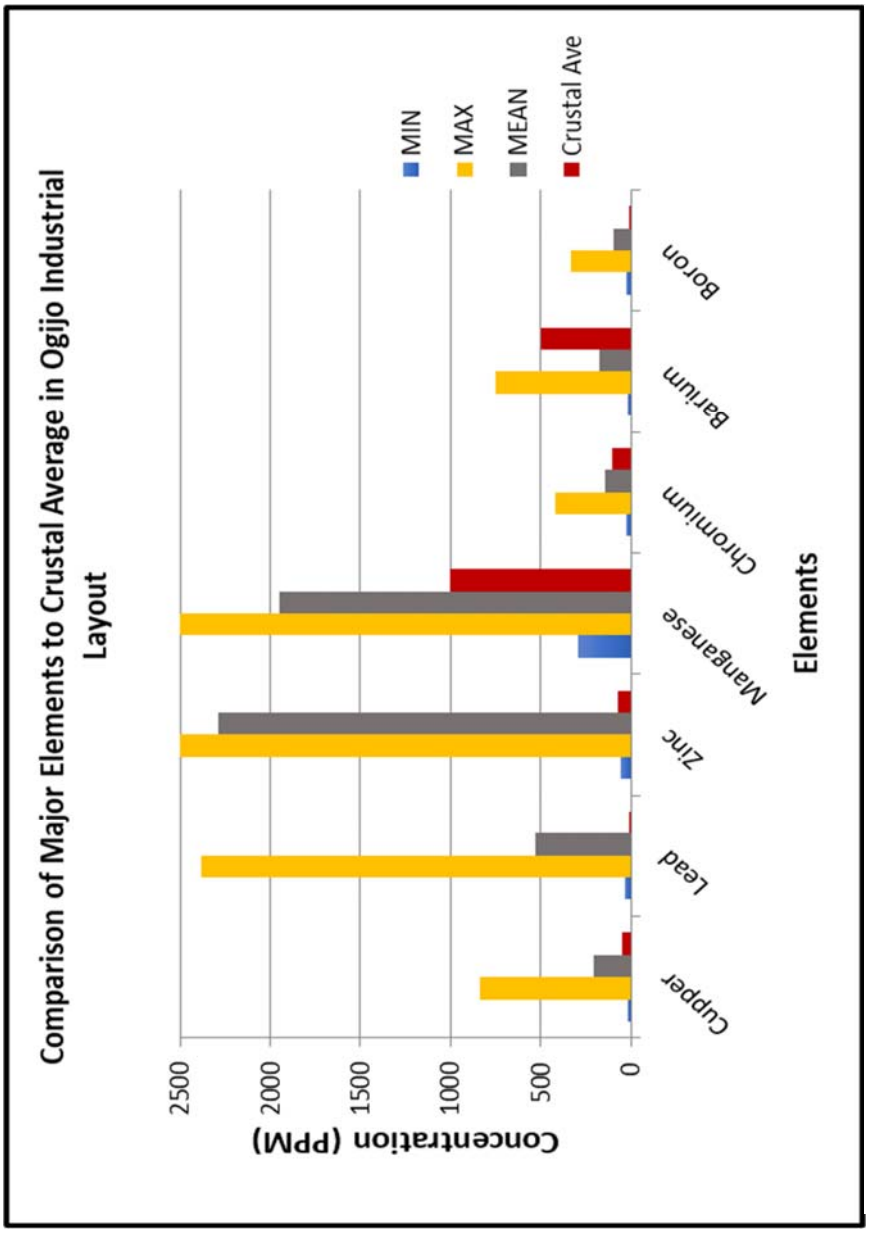

Figure 4.3: Major elements in Ogijo industrial layout as compared to the crustal average

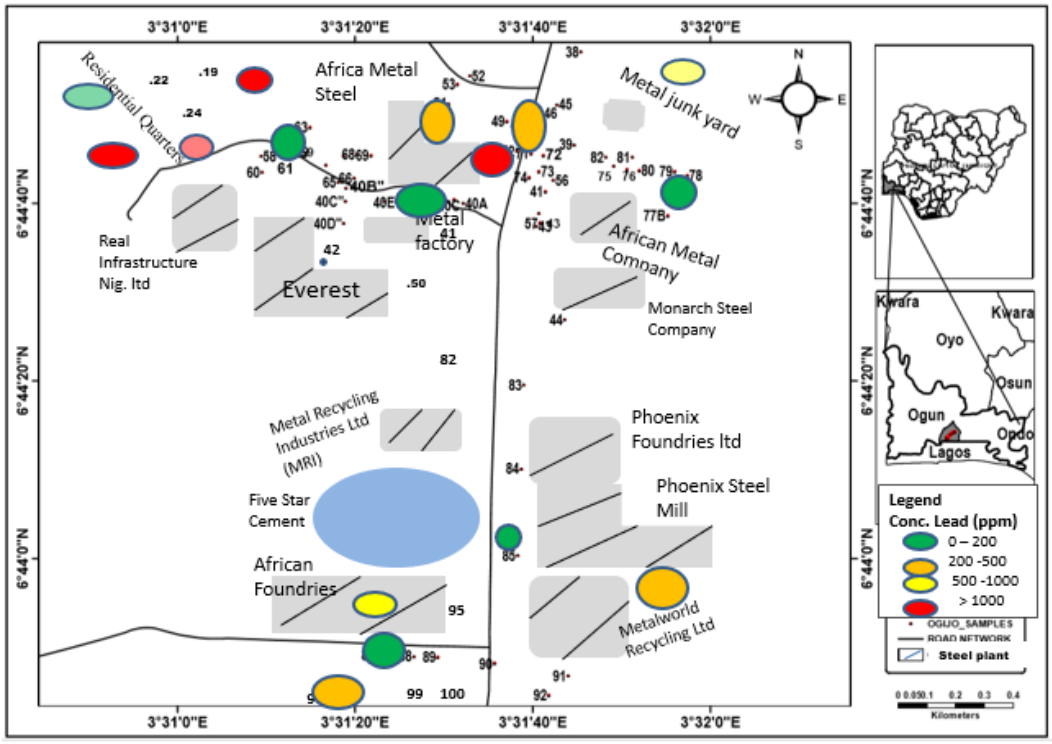

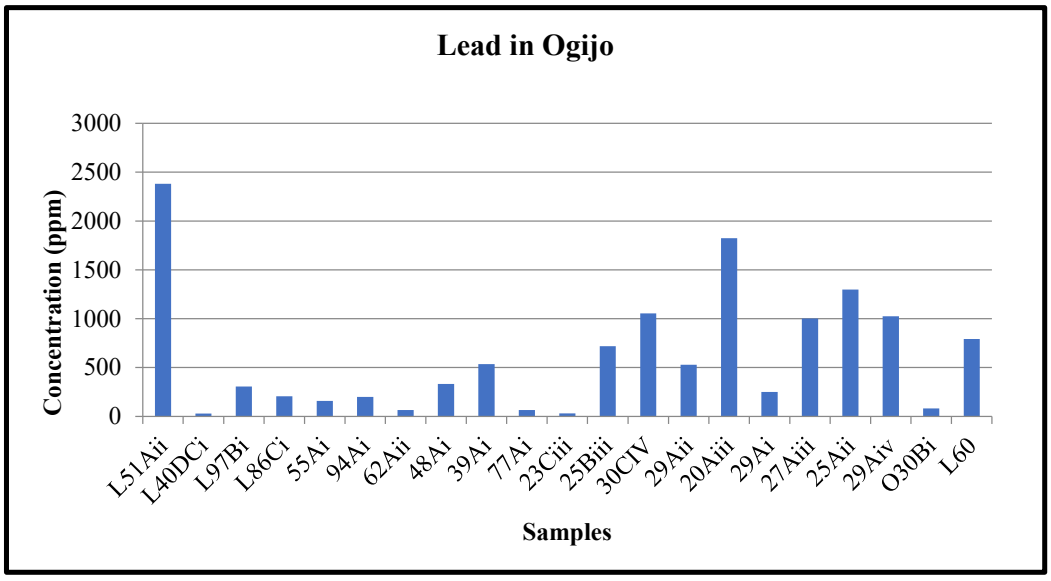

Figure 4. 4: Variation in concentration of lead in Ogijo industrial layout

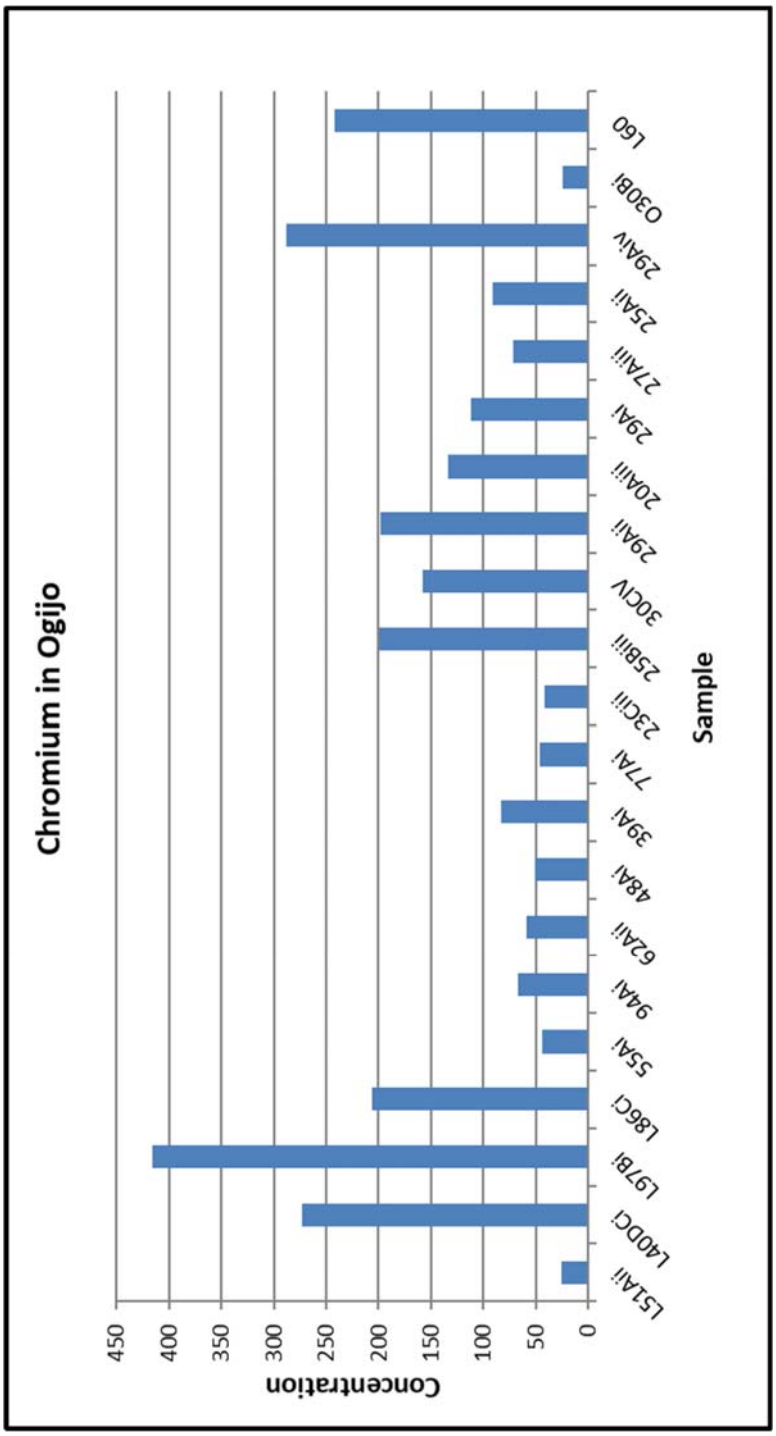

Figure 4.5: Variation in concentration of chromium in each of the samples from Ogijo

(Others are shown in appendix 4.6)

Minor Heavy Metals: The trace heavy metals with their minimum and maximum concentrations in ppm (Table 4.6 and Figure 4.18) were; Ni (5 -171), Sr (7 - 187), As (1 - 12), Co (2 - 96), Fe (4.74 - 28.81), Th (3 - 18), Cd (0.8 - 1438), Ag (0.3 - 1.1), Mo (1 - 59), Bi (3 - 7), V (18 -103), Ca (0.16 - 1.3), P (0.013 - 0.068), La (3 - 35), Mg (002 - 0.33), Ti (0.019 - 0.108), Al (0.39 - 3.58), Na (0.01 – 0.1), K (0.01 - 0.08), W (2 - 6), S (0.05 - 0.13), Ga (5 - 7), Sc (5 - 12) and Hg (Not traceable in all the samples) (Tables 4.3: Appendix 4.5).

Nickel, strontium and vanadium were the significant trace metals in the site with highest recorded values of 171, 187 and 103 ppm, respectively. Generally, the values recorded for each of the trace elements in the samples were extreme when compared to their crustal averages as indicated in Tables 4.3 and Figure 4.6. Some of the trace metals such as molybdenum, nickel, strontium, vanadium, and lanthanum had average values above 10 ppm, while some metals such as mercury, thallium, gallium and scandium were mostly below detection limits in all the samples (Appendix 4.5).

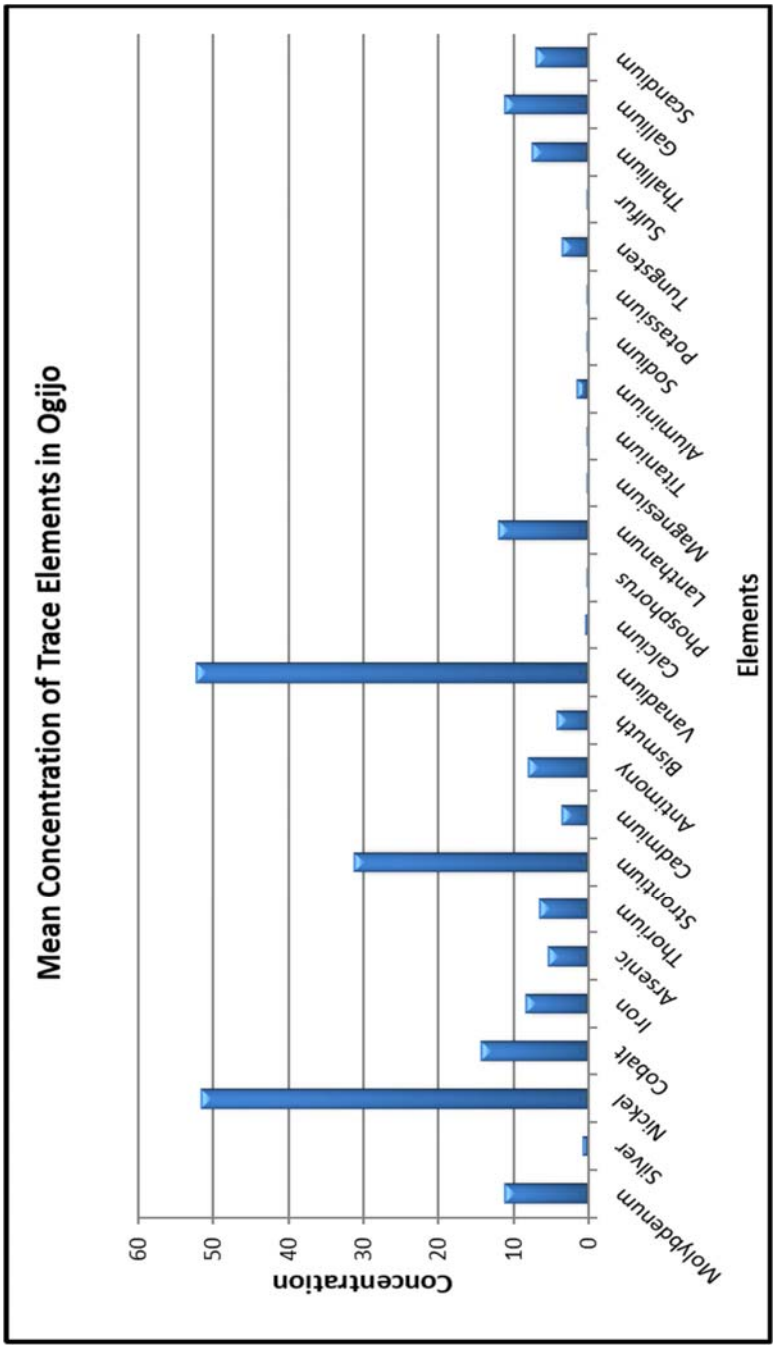

Figure 4.6: Mean concentration of trace heavy metal elements in Ogijo industrial layout

Table 4. 3: Trace elements in Ogijo industrial layout

ELEMENT		SUM	MIN	MAX	MEAN	Crustal Ave	SDEV
Molybdenum	Mo	190	1	59	11.17647	1.2	14.14318
Silver	Ag	9	0.3	1.9	0.818182	0.075	0.48748
Nickel	Ni	1043	5	171	51.65	84	47.89085
Cobalt	Co	293	2	96	14.4	25	20.27678
Iron	Fe	167.85	1.08	28.81	8.29	56300	7.007946
Arsenic	As	108	1	12	5.3	1.8	3.511207
Thorium	Th	109	2	18	6.5625	9.6	4.514682
Strontium	Sr	633	7	187	31.15	370	40.45156
Cadmium	Cd	36.6	0.8	14.3	3.58	0.15	4.199784
Antimony	Sb	121	3	24	8.071429	0.2	5.351457
Bismuth	Bi	38	3	7	4.25	0.025	1.481366
Vanadium	V	1083	18	124	52.35	120	31.14253
Calcium	Ca	9.13	0.16	1.31	0.446	41500	0.32093
Phosphorus	P	1.016	0.013	0.113	0.04925	1050	0.033178
Lanthanum	La	256	3	35	12.05	39	8.611731
Magnesium	Mg	3.34	0.02	0.41	0.1645	23300	0.118106
Titanium	Ti	0.786	0.011	0.108	0.0381	5600	0.021881
Aluminium	Al	30.96	0.39	3.58	1.49	82300	0.93162
Sodium	Na	0.39	0	0.1	0.0325	23600	0.028959
Potassium	K	1.06	0.01	0.17	0.0515	20.9	0.034997
Tungsten	W	35	2	6	3.5	1.25	1.433721
Sulphur	S	0.65	0.05	0.22	0.108333	350	0.062102
Thallium	Tl	38	5	11	7.6	0.85	2.302173
Gallium	Ga	85	5	20	11.14286	19	4.533605
Scandium	Sc	35	5	12	7	22	2.828427

4.1.1.3 Ecological Risk Analysis of Ogijo Industrial Layout

The results from the geochemical analysis were evaluated for heavy metal pollution by subjecting them to environmental assessment using the single elemental factor pollution indices. The results from the assessment are presented below:

Contamination Factor

This tool was used to assess the level of contamination by each of the elements recorded in the site by comparing the values to its average crustal concentrations and the level of contamination were classified according to Taylor and Meclenan (1985) interpretation. The values obtained from the assessment are presented in Table 4.4. The assessment revealed that the soil in Ogijo industrial layout is very highly contaminated with lead and zinc having contamination factor of 42.04 and 32.6 respectively. The layout is considerably contaminated with copper whose value was 4.087 and moderately contaminated with arsenic (Table 4.4). Very high contaminations were recorded for antimony, thallium, bismuth, boron, cadmium and silver but they were not considered as an adequate representation of the contamination level of those metals in the site because only few of the sample points had values above detection limits (Appendix 4.5). For example, cadmium only had detectable values in eleven sample points, and below detectable values in ten sample points. These metal elements can only represent local contaminations around the sample points.

Extremely low values were recorded for Ca, P, Mg, Ti, Al, Na, Ni, Co, Ba, Ga, Sc and Fe (Table 4.4). Although, iron compounds have the highest abundance in the earth crust, the absence of iron contamination in this metal recycling layout is because iron is completely removed from recycled scraps to produce iron rods which is the major products in the layout. The industrial layout was most polluted by lead which had the highest contamination factor with the value of 42.04 (Table 4.4). The level of contamination by the major elements in decreasing order was: Pb > Zn > B > Cu > Mn > Cr > Ba.

Table 4. 4: Contamination Factor of elements found in Ogijo industrial layout

Element	MEAN	Crustal Average	CF	Element	MEAN	Crustal Average	CF
Cu	204.35	50	4.087	Mg	0.1645	23300	7.06E-06
Pb	525.5	12.5	42.04	Ti	0.0381	5600	6.8E-06
Zn	2285.05	70	32.64357	Al	1.49	82300	1.81E-05
Mn	1950.15	1000	1.95015	Na	0.0325	23600	1.38E-06
Cr	140.2	100	1.402	K	0.0515	20.9	0.002464
Ba	176.4	500	0.3528	W	3.5	1.25	2.8
B	98.67	10	9.867	S	0.108333	350	0.00031
Mo	11.17647	1.2	9.313725	Tl	7.6	0.85	8.941176
Ag	0.818182	0.075	10.90909	Ga	11.14286	19	0.586466
Ni	51.65	84	0.614881	Sc	7	22	0.318182
Co	14.4	25	0.576	Sb	8.071429	0.2	40.35715
Fe	8.29	56300	0.000147	Bi	4.25	0.025	170
As	5.3	1.8	2.944444	V	52.35	120	0.43625
Th	6.5625	9.6	0.683594	Ca	0.446	41500	1.07E-05
Sr	31.15	370	0.084189	P	0.04925	1050	4.69E-05
Cd	3.58	0.15	23.86667	La	12.05	39	0.308974

Enrichment Factor

This tool was used to determine the source of each of the identified heavy metal in the site by distinguishing between the metals that have been enriched from anthropogenic source from those that are still in their natural concentration. The classification was based on Chen *et al*. (2007) method of determining if an element has been enriched in an environment from external sources. According to Chen *et al*. (2007), values of EF greater than 50 indicates extremely severe enrichment from anthropogenic sources. The results obtained from the EF analysis are presented in Table 4.5 and they indicated that all the heavy metal elements in Ogijo industrial layout except for calcium, phosphorus, magnesium, titanium, aluminium, sulphur and sodium had been very severely to extremely enriched from anthropogenic source.

Lead, copper, zinc, vanadium and arsenic showed they have been extremely enriched from anthropogenic sources. All the major elements showed that they have been extremely and severely-enriched in the layout in the decreasing order of: Pb > Zn > B > Cu > Mn > Cr > Ba. Also, extreme enrichment was observed in antimony, thallium, bismuth, boron, cadmium, molybdenum, chromium, barium, thorium, and tungsten which have obviously been enriched from anthropogenic sources (Table 4.5), the values will be considered as local enrichment around sample points rather than a representation of the layout due to the non-detection of these metals in some sample points (Appendix 4.5).

This extremely severe enrichment of most of the metals is as a result of continuous release of pollution dust into the environment over long period of activities by the smelting industries in the layout. The geology of Ogijo consists of arkosic sand stones and grits that tend to be carbonaceous towards the base in the north (Nton *et al*., 2009) and more of sequences of poorly consolidated sandstones, shales, limestones and reddish clay that grade from coarse to fine sands with packs of shales and clays in the south (d'Almeida *et al*., 2016). Although the unconsolidated sandstones will allow easy drainage, the clay and shale lenses will inhibit the drainage during the raining season hence, the accumulation of the pollutants at surface samples and samples at 30cm depth as was observed from the stepladder distribution of the pollutants from the magnetic readings. Dearing (1996) recorded similar findings in sedimentary environments with geology that naturally should have low readings showing high readings.

Table 4. 5: Enrichment Factor of elements found in Ogijo industrial layout

Element	Mean	Crustal Ave.	EF	Element	Mean	Crustal Ave.	EF
Cu	204.35	50	27756.10	Bi	4.25	0.025	1154523.52
Pb	525.5	12.5	285506.87	V	52.35	120	2962.71
Zn	2285.05	70	221692.77	Ca	0.446	41500	0.07
Mn	1950.15	1000	13244.08	P	0.05	1050	0.31
Cr	140.2	100	9521.42	La	12.05	39	2098.34
Ba	176.4	500	2395.97	Mg	0.16	23300	0.04
B	98.67	10	67009.90	Ti	0.04	5600	0.04
Mo	11.17	1.2	63252.43	Al	1.49	82300	0.12
Ag	0.81	0.075	74087.08	Na	0.03	23600	0.009
Ni	51.65	84	4175.85	P	0.05	20.9	16.73
Co	14.4	25	3911.79	W	3.5	1.25	19015.68
As	5.3	1.8	19996.64	S	0.11	350	2.10
Th	6.56	9.6	4642.50	Tl	7.6	0.85	60722.34
Sr	31.15	370	571.75	Ga	11.14	19	3982.87
Cd	3.58	0.15	162086.04	Sc	7	22	2160.87
Sb	8.07	0.2	274078.07	Fe	8.29	56300	-

Index of Geo-accumulation

To further quantify elemental contamination, the I_{geo} as proposed by Müller (1969) (as referenced by Ebru Yeşim Özkan (2012)) was carried out on the geochemical results.

Geo-accumulation index is the quantitative single metal approach to quantify metal pollution in sediments when the concentration of toxic heavy metal is 1.5 or more times greater than their lithogenic background values. Any value greater than 5 signifies extreme contamination. The results obtained from this analysis are presented in Table 4.6, which revealed that the soil samples from Ogijo are extremely contaminated with bismuth whose index of geo-accumulation is 6.82. The layout showed strongly/extreme contamination of lead (4.80), zinc (4.44), and antimony (4.75). This analysis indicated that the concentration of bismuth has been increased by 6.82 times in the industrial layout. Similarly, the concentrations of lead, zinc and antimony has been increased by 4.80, 4.44 and 4.75 times in the layout (Table 4.6).

Cadmium (3.99) strongly contaminated the layout, while boron (2.17), molybdenum (2.63), silver (2.86), and thallium (2.57) have moderately contaminated the industrial layout. The contamination by antimony, thallium, boron, molybdenum and cadmium are considered localised since not all the samples showed the presence of these heavy metals in the geochemical analysis; that is, the metals could not be detected in some of the samples (Appendix 4.5).

The order of contamination of the major heavy metals as indicated by this pollution index was Pb > Zn > B > Cu > Mn > Cr > Ba.

Table 4. 6: Index of Geoaccumulation of heavy metal elements in Ogijo industrial layout

Element	Mean	Crustal Ave	I_{geo}	Element	Mean	Crustal Ave	I_{geo}
Cu	204.35	50	1.44	Sr	31.15	370	-4.15
Tl	7.6	0.85	-13.31	Cd	3.58	0.15	3.99
Pb	525.5	12.5	4.80	Sb	8.071429	0.2	4.74
Zn	2285.05	70	4.44	Bi	4.25	0.025	6.82
Mn	1950.15	1000	0.37	V	52.35	120	-1.78
Cr	140.2	100	-0.09	Ca	0.446	41500	-17.09
Ba	176.4	500	-2.08	P	0.04925	1050	-14.96
B	98.67	10	2.71	La	12.05	39	-2.27
Mo	11.1764	1.2	2.63	Mg	0.1645	23300	-17.69
Ag	0.81818	0.075	2.86	Ti	0.0381	5600	-17.75
Ni	51.65	84	-1.28	Al	1.49	82300	-16.33
Co	14.4	25	-1.38	Na	0.0325	23600	-20.05
Iron	8.29	56300	-13.31	K	0.0515	20.9	-9.24
As	5.3	1.8	0.97	W	3.5	1.25	0.90
Th	6.5625	9.6	-1.13	S	0.108333	350	-12.24
Ga	11.14287	19	-1.35	Tl	7.6	0.85	2.57
Sc	7	22	-2.23				

The summaries from the ecological risk analysis are:

Contamination factor:

CF < 1 low contamination, CF = 1-3 Moderate contamination, CF = 3-6 Considerable contamination, and CF > 6 Very high contamination. Results for the heavy metals are: Pb = 42.0, Zn = 32.6, B = 9.8, Cu = 4.0, Mn = 1.9, Cr = 1.4, Ba = 0.3. In the order of decrease in contamination: Pb > Zn > B > Cu > Mn > Cr > Ba.

Enrichment Factor:

EF < 1 indicates no enrichment, EF = 1–3 indicates minor enrichment,
EF = 3–5 indicates moderate enrichment, EF = 5–10 moderately to severe enrichment,
EF = 10–25 severe enrichment, EF = 25–50 very severe enrichment,
EF > 50 extremely severe enrichment

Pb = 285506.87, Zn = 221692.77, B = 67009.90, Cu = 27756.10, Mn = 13244.08, Cr = 9521.42, Ba = 2395.97. In the order of decrease in enrichment: Pb > Zn > B > Cu > Mn > Cr > Ba.

Index of Geo-accumulation

$I_{geo} \leq 0$ Uncontaminated $0 < I_{geo} < 1$ Uncontaminated/moderately contaminated
$1 < I_{geo} < 2$ moderately contaminated $2 < I_{geo} < 3$ Moderately/strongly contaminated
$3 < I_{geo} < 4$ Strongly contaminated $4 < I_{geo} < 5$ Strongly/extremely contaminated
$5 < I_{geo}$ Extremely contaminated

Pb = 4.8, Zn = 4.4, B = 2.7, Cu =1.4, Mn = 0.3, Cr = -0.09, Ba = -2.08.
In the order of decrease in contamination: Pb > Zn > B > C u > Mn > Cr > Ba.

All three analyses signified the same order of increase. Chromium and Barium were listed as uncontaminated or low contamination in the index of geoaccumulation and contamination factor analysis. Boron had minimal ecological risk. Therefore, in Ogijo industrial layout the heavy metal elements with the highest concentration and ecological risk are Pb > Zn > C u > Mn in order of decreasing concentration.

Correlation Matrix of the Major and Some Trace Elements in Ogijo

The correlation matrix was generated for the major and significant trace elements from Ogijo. The elements with high positive and linear correlation of 0.5000 and above indicated the metals were from the same source. The Zn and Ba showed a strong positive correlation with Cu while Mn, B and Cr had significant positive correlation with Ba. Lead showed negative correlation with most of the metals and only significant positive correlation with zinc. The correlation matrix indicates that Cu, Mn, B, and Cr are from the same source material, while Zn and Ba were from the same source. Pb seems to be of a different source. The trace elements also showed some correlation, for instance, B and Ga showed a high and positive correlation value of 1.00, while Cu has a positive correlation of 0.753 with nickel. Similar relationship exists between manganese and Cr whose linear correlation value is 0.885. Negative linear correlation which is an indication of elements from different sources (Orosun *et al.,* 2020), was observed between some of the metals such as between Pb and Ga (-0.605), Cu and Ga (-0.222) and Zn and Ga (-0.127) (Table 4.7).

Table 4.7: Correlation Matrix of major and some trace elements in Ogijo industrial layout

	Mo	*Cu*	*Pb*	*Zn*	*Ba*	*Ni*	*B*	*Mn*	*Sr*	*Cr*	*Sb*	*Ga*	*V*	*La*
Mo	1.000													
Cu	0.944	1.000												
Pb	0.064	0.108	1.000											
Zn	0.399	0.604	0.412	1.000										
Ba	0.500	0.695	-0.032	0.469	1.000									
Ni	0.590	0.753	0.177	0.680	0.532	1.000								
B	-0.082	0.155	-0.049	0.244	0.807	0.079	1.000							
Mn	0.214	0.385	-0.119	0.110	0.828	0.383	0.683	1.000						
Sr	0.111	0.302	-0.189	0.107	0.872	0.210	0.851	0.889	1.000					
Cr	0.240	0.451	-0.032	0.342	0.765	0.609	0.504	0.885	0.739	1.000				
Sb	0.608	0.765	0.390	0.823	0.530	0.727	0.280	0.131	0.131	0.249	1.000			
Ga	-0.237	-0.222	-0.605	-0.127	-0.177	-0.156	1.000	0.006	-0.132	-0.225	-0.313	1.000		
V	0.032	0.133	0.381	0.490	0.130	0.370	0.027	0.144	-0.017	0.302	0.153	0.664	1.000	
La	0.188	0.212	0.363	0.221	0.027	0.445	-0.195	0.156	-0.115	0.239	0.147	0.951	0.776	1

4.1.2 **Heavy Metal Pollution in Ota Soils**

The magnetic susceptibility readings in both high and low frequencies from samples that were obtained from Ota industrial layout, were statistically presented as histograms showing the variations in concentration of magnetic susceptibility at each sampling depth. The histograms are presented in. Appendix 4.8.

4.1.2.1 **Pollutants in Whole Soil Samples from Ota**

About 60% of all recorded magnetic susceptibility values in the high and low frequencies from samples gotten from Ota, showed high readings when compared to the control readings. From the 34 sampling points in Ota, 8 sample points at 0cm, 6 sample points at 10 cm depth, 4 sample points at 20 cm depth and two sample points at 30 cm depths all had magnetic susceptibility values above 500 with the highest magnetic susceptibility value recorded at the site being 6343.9 (Fig. 4.7; Appendix 4.8). These high magnetic susceptibility values are an indication of magnetic minerals which could have originated from the source rock in the environment or introduced from an external source. Bouhsane and Bouhlassa (2018), observed similar results from the assessment of soil samples from different occupational background. The possibility of the source rock in Ota enhancing the magnetic susceptibility is farfetched; this is because, according to Akinmosin and Osinowo (2010), the geology of Ota consists of the Coastal Plain Sands which are characterised by poorly sorted unconsolidated pebbly sands with lenses of clays. This geology has no magnetic characteristic and hence cannot be a contributing factor. Similarly, no river was observed in the vicinity of the industrial layout in Ota and therefore no discharges from an external effluent could have contributed to the high magnetic susceptibility recorded in the site.

At the surface (zero depth), the range of the X_{lf} values obtained were 30.3 to 2645, 23 to 1257 was recorded at 10 cm, 14.4 to 6343.9 at 20 cm depth, and the range of the low frequency magnetic susceptibility values obtained at 30 cm was 8.2 to 1333.3. The mean values of the readings been 480, 377, 579 and 270 respectively. This high magnetic susceptibility anomaly is an indication of strong contamination by heavy metals which far exceeded values of 30 magnetic susceptibility that was considered as unpolluted (Wojas, 2017).

Also, the X_{lf} values in all the samples were relatively higher than the values of the X_{hf}. The mean X_{fd}% calculated for each depth at Ota industrial layout are 7.26%, 6.04%,

7.7% and 9.5% at 0, 10, 20 and 30cm depths respectively. These are the percentage of the heavy metal pollutants in the soil that are ferromagnetic.

The statistical analysis of the data obtained also revealed a defined step ladder like progression with depth within each sampling point as was observed from the statistical result of the whole samples from Ogijo. The statistical analysis revealed that 54.55% of the sample points in Ota had the highest magnetic susceptibility readings or highest concentration of pollutants at the surface (0 cm depth). This value exceeded the 44.01% that was observed from the surface samples from Ogijo. Also, 9.09% of the highest magnetic susceptibility readings were recorded at 10 cm, 21.21% at 20 cm and 15.15% at 30 cm depth. Unlike the concentration distribution observed in Ogijo where there was a progressive reduction with depth and an enhancement at depth 30 cm, in Ota industrial layout, there was a massive reduction in concentration at 10 cm depth (9.09%) when compared to the 54.55% observed at 0 cm. At 20 cm there was an appreciable enhancement and a reduction at 30 cm depth. Zhang *et al*. (2013), observed similar enhancement in magnetic susceptibility readings at 0 – 20 cm depth when he assessed farmlands irrigated with water near a steel plant. They attributed the high magnetic susceptibility readings to the activities of the steel plant in the vicinity.

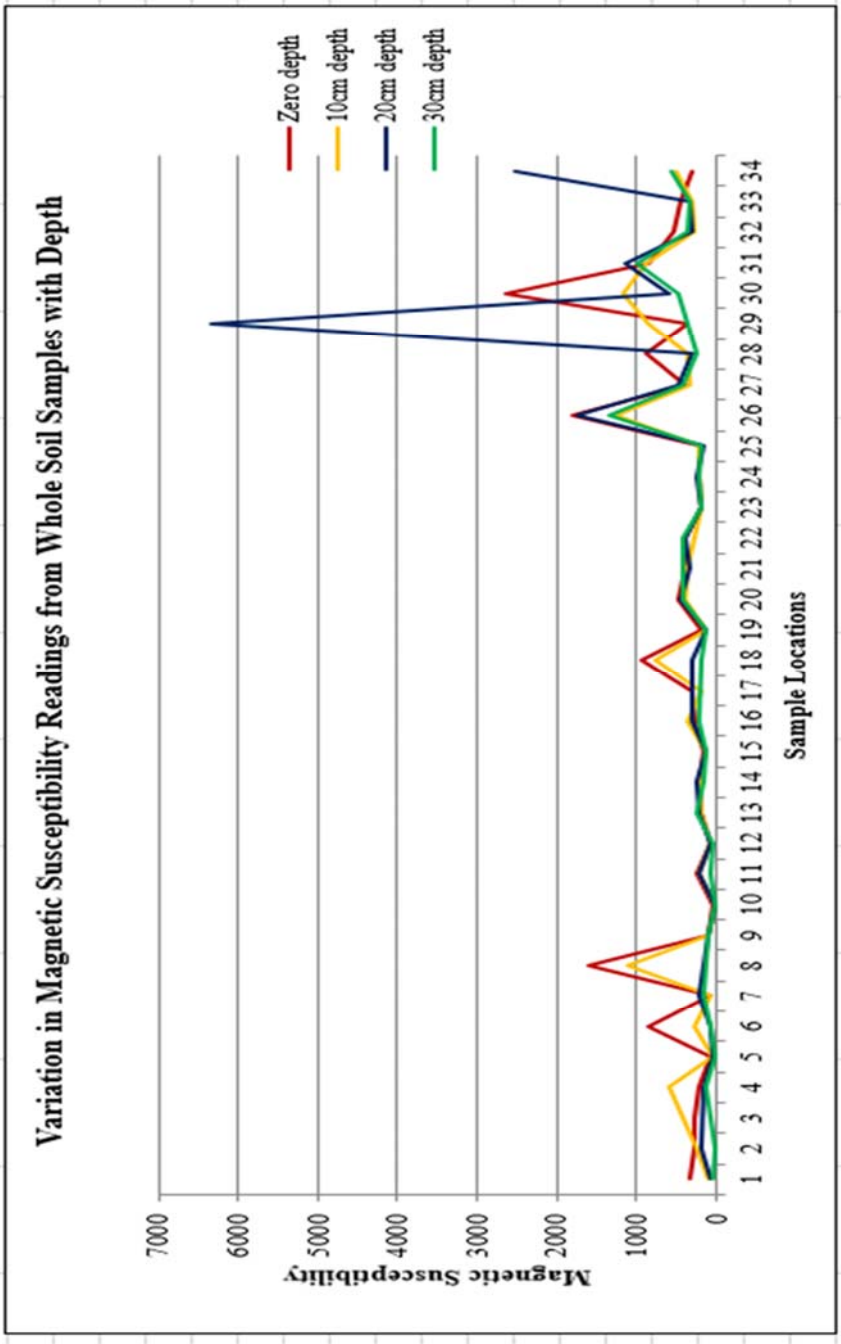

Figure 4. 7: Charts showing variations in magnetic susceptibility at 0 cm,10 cm, 20 cm and 30 cm for all whole samples in Ota industrial layout

4.1.2.2 Type and Elemental Concentration of Pollutants in Soil Samples from Ota

A total of thirty-three heavy metal elements with their concentrations were recorded from the geochemical analysis of soil samples from Ota industrial layout. The results are tabulated in table 4.8. Based on the elemental concentrations of the metals, they are grouped into Major Heavy Metals and Trace Heavy Metals. All unit of concentration is in ppm.

The metal elements classified as major elements include Zinc, Manganese, Lead, Copper, Barium, Chromium, and Vanadium (Table 4.8 and fig. 4.7). The individual element showed a wide range of values between their minimum and maximum values of concentration. The ranges and the mean values are Zn (29 – 1400; 473.8), Mn (163 – 1346; 547.9), Pb (30 – 501;161.3), Cu (7 – 1308; 175.3), Ba (9 – 194; 50.1), Cr (15 – 107; 62.3), and V (11 – 63;39.5) with an order of decreasing mean concentration: Mn > Zn > Cu > Pb > V > Cr > Ba.

The major elements showed whole site distribution and were all detected in all the samples analysed. Lead has concentration values that ranged between 30 and 501 with only about 60% of the sample points showing concentration of lead below 100 (Table 4.8). These 60% samples had values that are below the NASRAE safety limit of 100 for lead allowed in soils. However, 40% of the samples have values that are in the extremes of averagely 400. Chromium was also detected in all the samples with 90% of the samples having values below the NASRAE allowable limit (Fig. 4.9). Vanadium was detected in all the samples ranging in value between 11 and 63 as seen in figure 4.40. There was a fairly average distribution of about 35 in the site.

The trace heavy metals include, Ni (4 - 45), Sr (5 - 14), As (1- 9), Co (<1 - 9), Fe (0.51 - 12.3), Th (3 - 9), Mo (1 - 6), Bi (4 - 5), Ca (0.144 - 0.31), P (0.01 - 0.043), La (5 - 16), Mg (0.02 - 0.15), Ti (0.01 - 0.069), Al (0.89 - 3.36), Na (0.01 - 0.04), K (0.01 - 0.08), W (2 - 3), Ga (6 - 11), (Table 4.8 and Fig. 4.9). Silver, Cadmium, Mercury and Scandium were below detection limits (Table 4.8).

Table 4.8: Results from Aqua Regia method of geochemical analysis of some samples from Ota industrial layout

Element	14Ai	27Ai	5DDi	9Di	28Ai	34Cii	22Bi	8Di	28Di	24Di
Mo	1	2	<1	<1	6	2	<1	<1	4	<1
Cu	27	132	21	7	159	36	23	20	1308	20
Pb	448	501	45	20	230	46	43	62	188	30
Zn	1248	1196	84	29	315	211	119	76	1400	60
Ag	<0.3	<0.3	<0.3	<0.3	<0.3	<0.3	<0.3	<0.3	0.5	<0.3
Ni	6	23	8	4	45	22	7	6	39	8
Co	8	5	3	<1	9	6	5	4	9	4
Mn	492	456	320	163	732	551	573	477	1346	369
Fe	1.54	4.75	1.86	0.51	12.33	6.72	1.75	1.5	9.03	2.12
As	2	5	1	1	7	3	2	2	9	1
Th	5	4	9	3	6	6	4	5	6	8
Sr	11	6	5	5	14	5	7	6	14	6
Cd	<0.5	0.7	<0.5	<0.5	<0.5	<0.5	<0.5	<0.5	0.6	<0.5
Sb	6	<3	<3	<3	4	<3	<3	<3	5	<3
Bi	<3	<3	<3	<3	<3	5	4	<3	<3	<3
V	25	43	39	11	55	49	35	33	63	42
Ca	0.23	0.12	0.06	0.07	0.31	0.11	0.11	0.1	0.2	0.13
P	0.027	0.038	0.015	0.01	0.025	0.018	0.022	0.018	0.043	0.022
La	9	9	15	5	16	11	10	9	11	13
Cr	47	72	46	15	86	72	76	44	107	58
Mg	0.05	0.07	0.03	0.02	0.15	0.02	0.03	0.03	0.07	0.04
Ba	26	53	13	9	194	12	19	23	131	21
Ti	0.017	0.025	0.018	0.01	0.069	0.024	0.019	0.016	0.029	0.028
B	<20	<20	<20	<20	21	<20	<20	<20	75	<20
Al	0.9	1.16	2.1	0.89	3.36	1.44	1.12	1.33	2.11	1.45
Na	<0.01	<0.01	<0.01	<0.01	0.03	<0.01	<0.01	<0.01	0.04	0.01
K	0.07	0.04	0.03	0.01	0.08	0.02	0.02	0.03	0.03	0.05
W	<2	3	<2	<2	<2	<2	<2	<2	2	<2
S	<0.05	<0.05	<0.05	<0.05	<0.05	<0.05	<0.05	<0.05	<0.05	<0.05
Hg	<1	<1	<1	<1	<1	<1	<1	<1	<1	<1

Tl	<5	<5	<5	<5	6	<5	<5	<5	<5	<5
Ga	<5	7	11	<5	7	9	6	7	9	8
Sc	<5	<5	6	<5	<5	<5	<5	<5	<5	<5

Table 4.9: Major heavy metals in Ota industrial layout

ELEMENT		SUM	MIN	MAX	MEAN	Crustal Ave	*NESREA limits	SDEV
Copper	Cu	1753	7	1308	175.3	50	72	401.402
Lead	Pb	1613	30	501	161.3	12.5	164	179.7857
Zinc	Zn	4738	29	1400	473.8	70	421	565.5121
Manganese	Mn	5479	163	1346	547.9	1000	-	319.7542
Vanadium	V	395	11	63	39.5	110	-	14.85672
Chromium	Cr	623	15	107	62.3	100	100	25.87599
Barium	Ba	501	9	194	50.1	500	-	62.27796
Boron	B	96	21	75	48	10		38.18377

***NESREA limits (2011)**

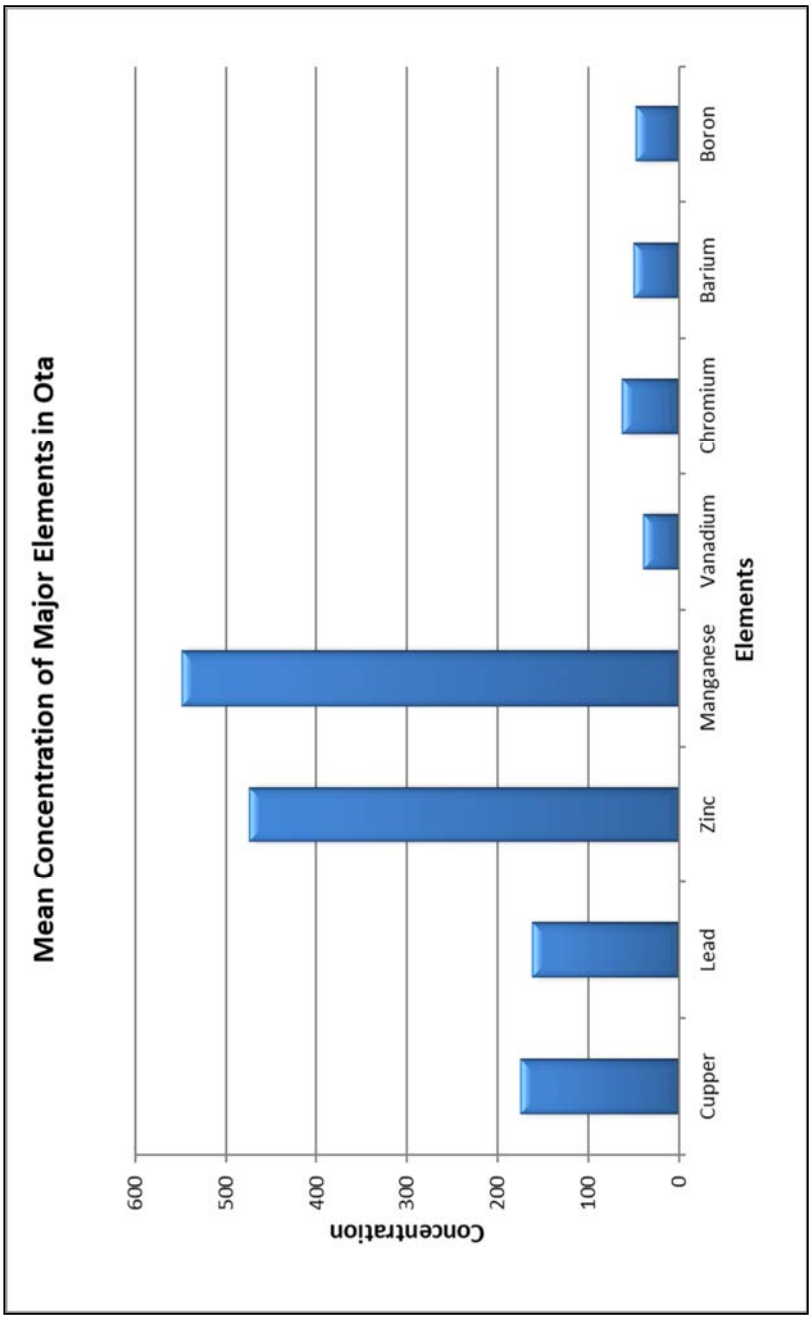

Figure 4.8: Mean concentration (ppm) of major elements in Ota industrial layout

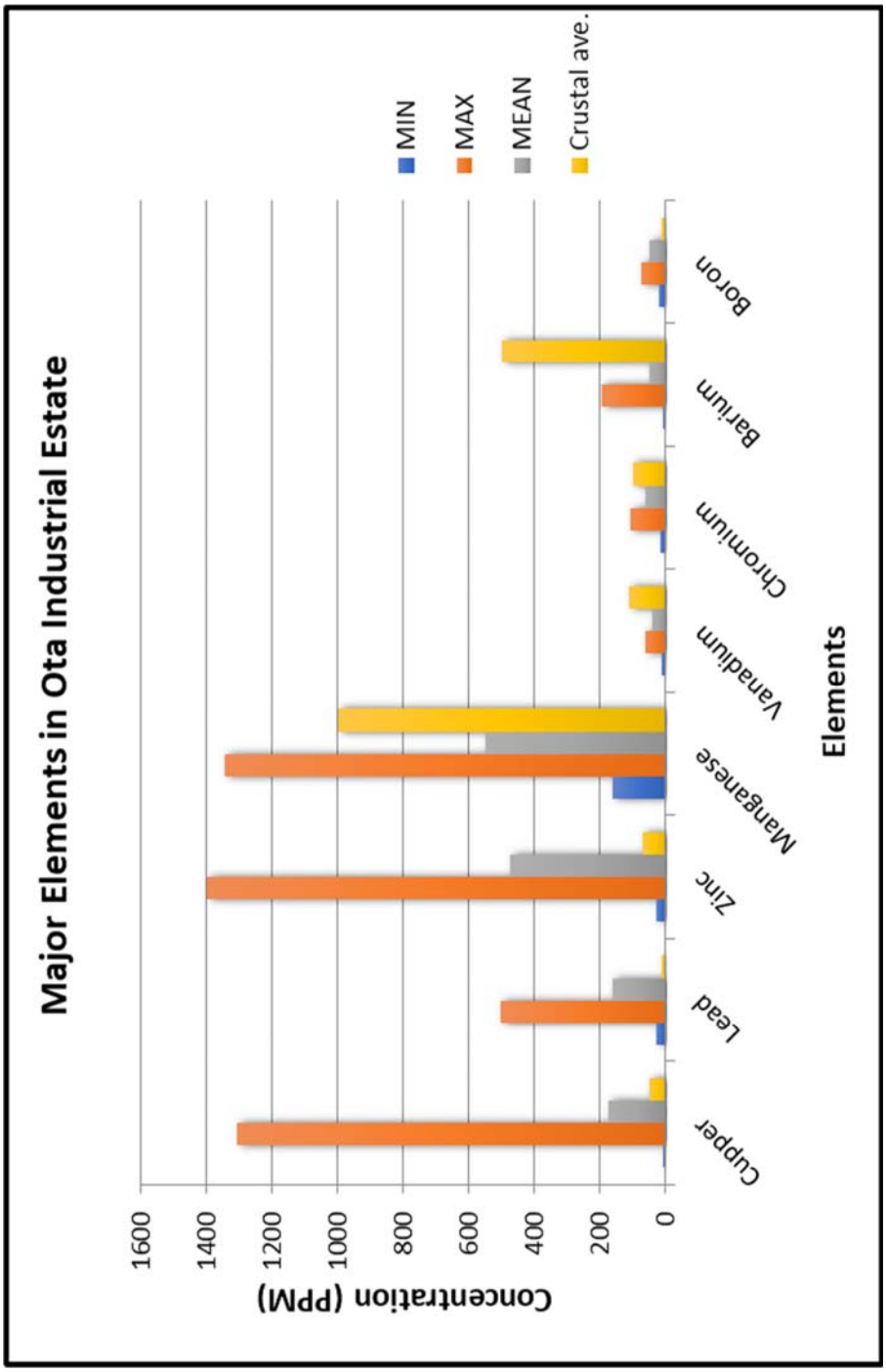

Figure 4.9: Major elements in Ota industrial layout as compared to the crustal average

Table 4.10: Trace heavy metal elements in Ota industrial layout

Element		SUM	MIN	MAX	MEAN	Crustal Ave.	STD
Molybdenum	Mo	15	1	6	3	1.2	2
Nickel	Ni	168	4	45	16.8	84	14.91308
Cobalt	Co	53	3	9	5.8	25	2.260777
Iron	Fe	42.11	0.51	12.33	4.211	56300	3.942133
Arsenic	As	33	1	9	3.3	1.8	2.790858
Thorium	Th	56	3	9	5.6	9.6	1.837873
Strontium	Sr	79	5	14	7.9	370	3.665151
Cadmium	Cd	1.3	0.7	0.6	0.65	0.15	0.070711
Antimony	Sb	15	4	6	5	0.2	1
Bismuth	Bi	9	4	5	4.5	0.025	0.707107
Calcium	Ca	1.44	0.06	0.31	0.144	41500	0.078627
Phosphorus	P	0.238	0.01	0.043	0.0238	1050	0.01013
Lanthanum	La	108	5	16	10.8	39	3.224903
Magnesium	Mg	0.51	0.02	0.15	0.051	23300	0.039285
Titanium	Ti	0.255	0.01	0.069	0.0255	5600	0.016379
Aluminium	Al	15.86	0.89	3.36	1.586	82300	0.756075
Sodium	Na	0.08	0.01	0.04	0.026667	23600	0.015275
Potassium	K	0.38	0.01	0.08	0.038	20.9	0.022509

Table 4.11: Trace heavy metal elements in Ota industrial layout continued

Element		SUM	MIN	MAX	MEAN	Crustal Ave.	STD
Tungsten	W	5	2	3	2.5	1.25	0.707107
Thallium	Tl	6	6	6	6	0.85	
Gallium	Ga	64	6	11	8	19	1.603567
Scandium	Sc	6	6	6	6	22	

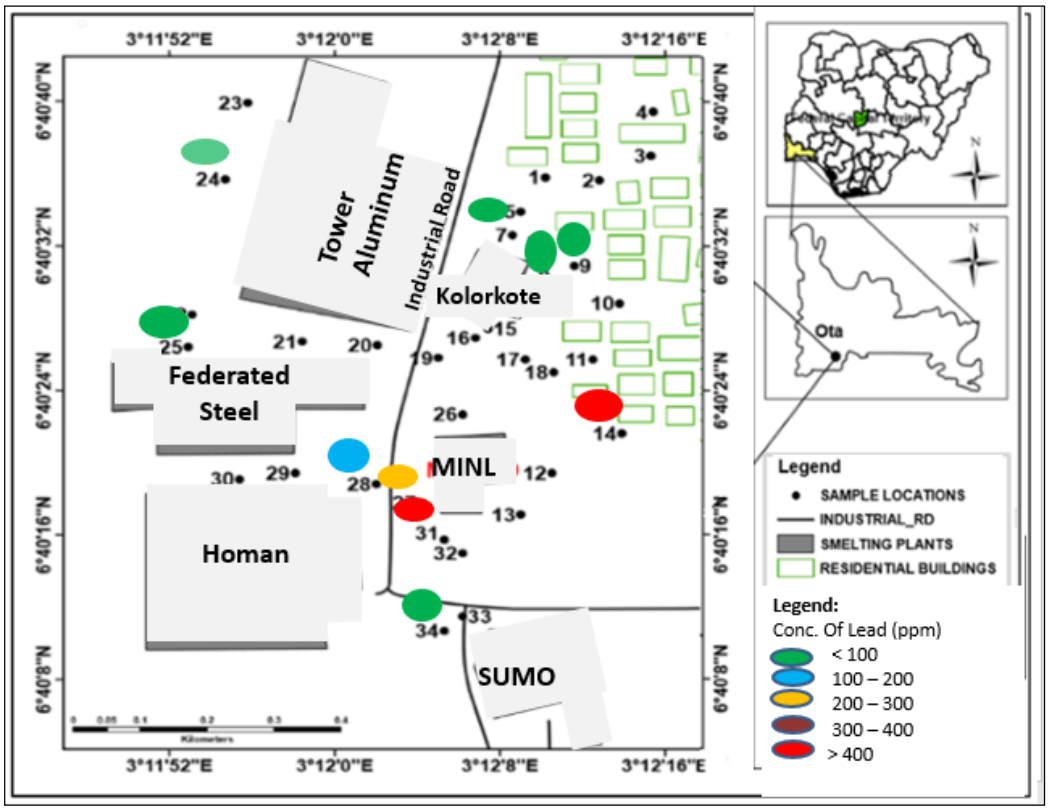

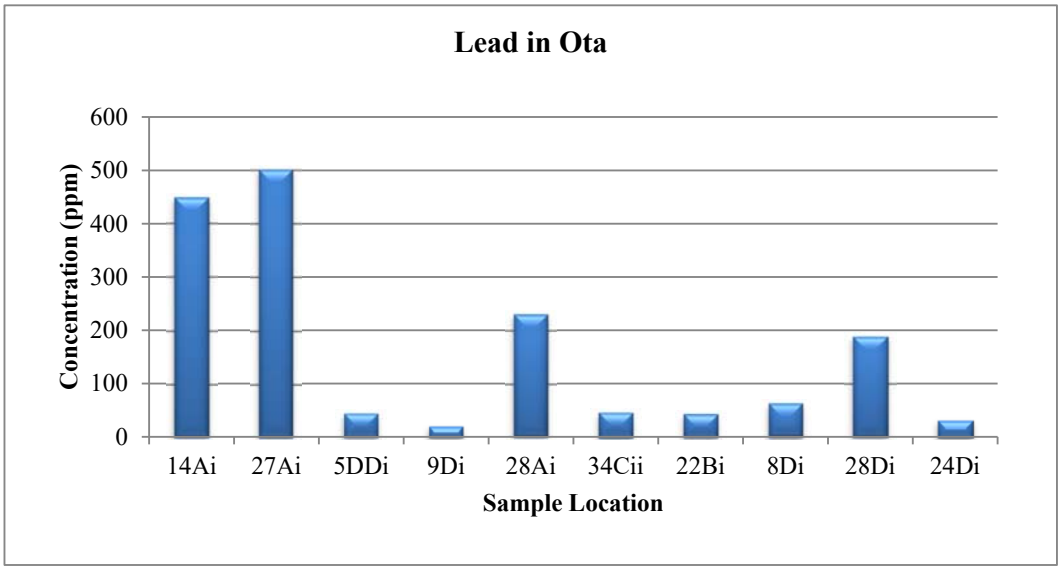

Figure 4.10: Variation in concentration of lead in each of the samples from Ota (Appendix 4.13)

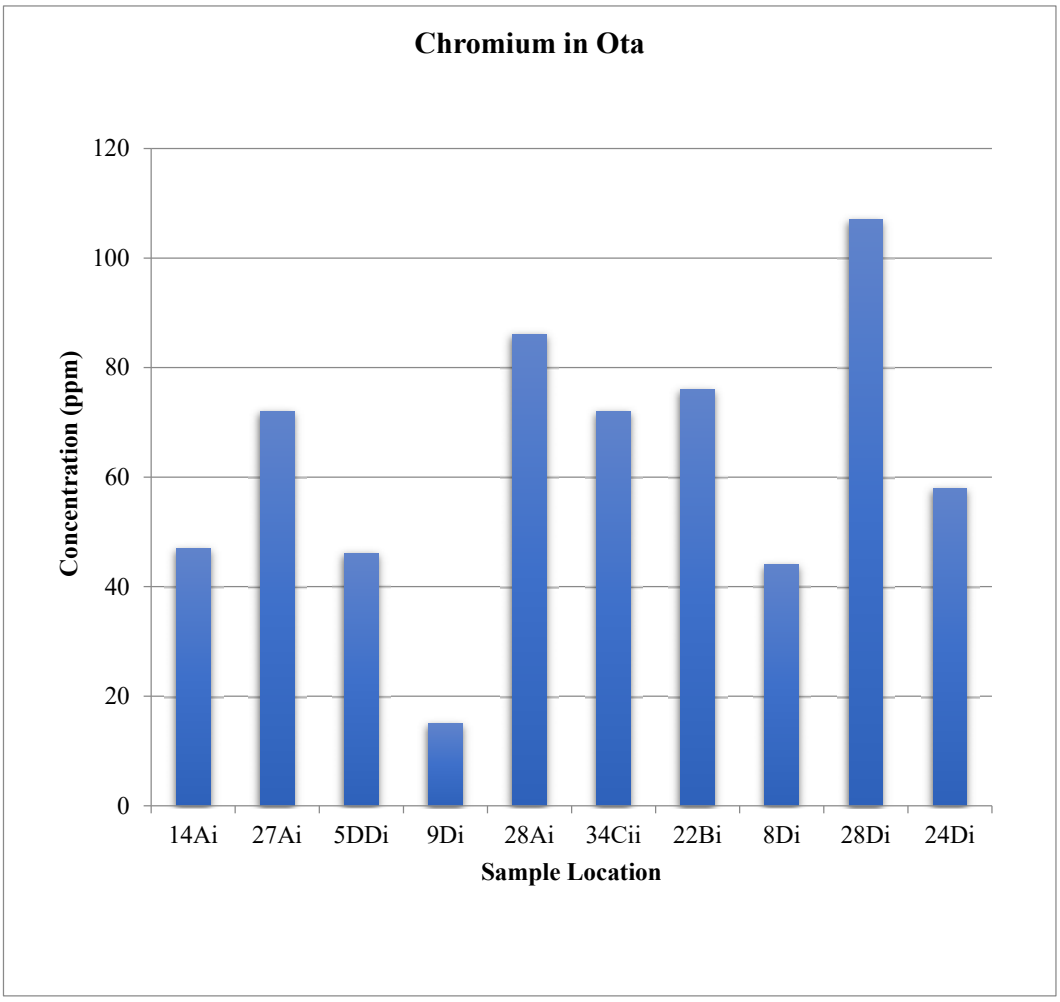

Figure 4.11: Variation in concentration of chromium in each of the samples from Ota (Appendix4.18)

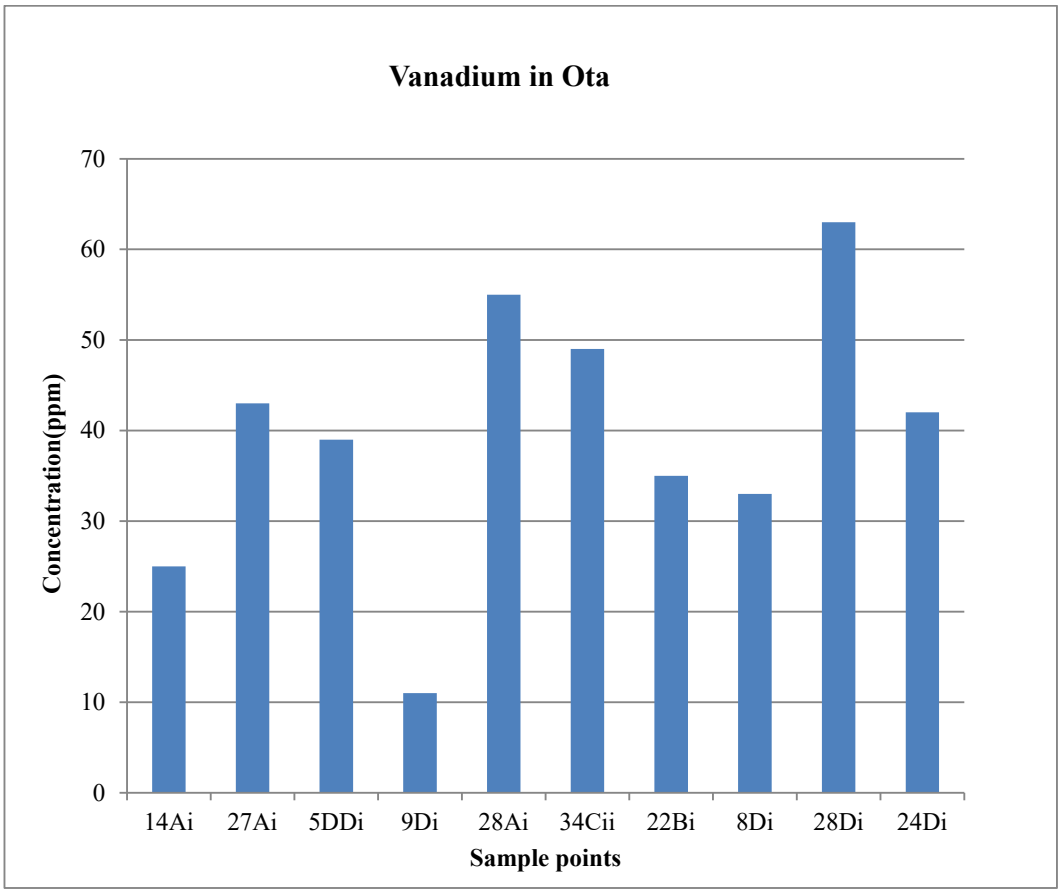

Figure 4.12: Variation in concentration of vanadium in each of the samples from Ota (Appendix 4.18)

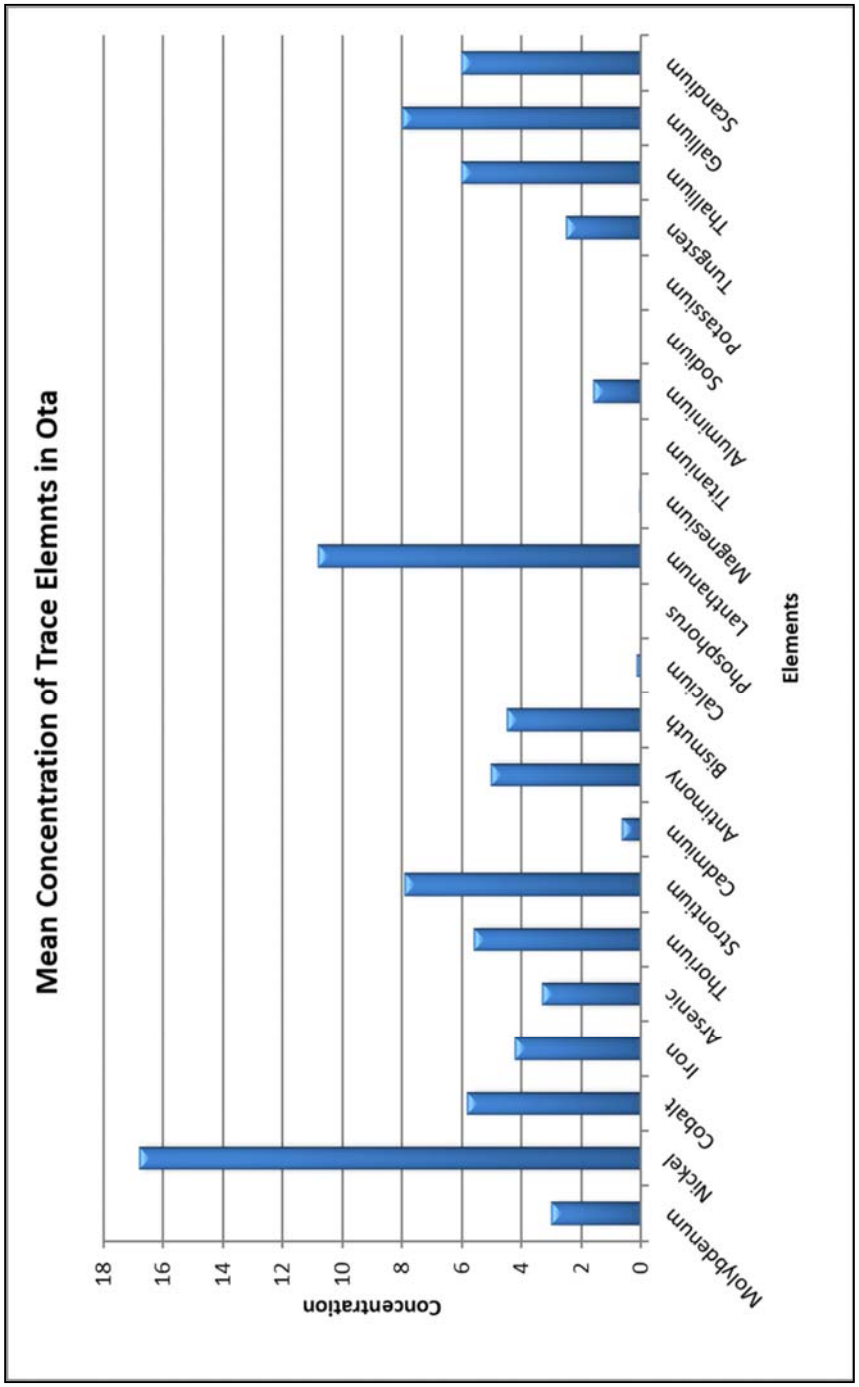

Figure 4.13: Mean concentration in ppm of trace elements in Ota industrial layout

4.1.2.3 Ecological Risk Analysis of Ota Industrial Layout

Single elemental Pollution Indices were used to assess the ecological risk of each heavy metal as obtained from the geochemical results soil samples from Ota.

Contamination Factor

The results of the assessment are presented in Table 4.12. The analysis revealed that Ota industrial layout is very highly contaminated with lead and zinc having contamination factors of 12.9 and 6.8 respectively. The site is considerably contaminated with copper (CF = 3.5) and moderately contamination with arsenic (CF=1.8) (Table 4.12). Although, Sb, Tl, Bi, B, Cd and W showed very high to considerable contaminations, they were not considered because only few of the sample points had values above detection limits (Appendix 4.12). For example, Cd only had values from two sample points, at the other sample points they were below detection limits. These two values can only represent the two sample points but will not adequately be a good representation of the element in the entire industrial layout.

Also, there was no contamination of Ca, P, Mg, Ti, Al, Na and Fe. The absence of Fe and Al contamination in this metal recycling layout, though being among the elements with the highest molecular abundance in the earth crust, shows that Fe and Al are completely sucked out from recycled scraps to produce aluminium sheets and iron rods.

Among the major heavy metals, Pb had the highest level of contamination in the value of 12.9 (Table 4.12). The level of contamination of the major elements in decreasing order was: Pb > Zn > Cu

Table 4.12: Contamination Factor of elements found in Ota industrial layout

ELEMENT	CF	ELEMENT	CF
Cu	3.5	Sb	25
Pb	12.9	Bi	180
Zn	6.8	Ca	3.47E-06
Mn	0.6	P	2.27E-05
V	0.4	La	0.3
Cr	0.6	Mg	2.19E-06
Ba	0.1	Ti	4.55E-06
B	4.8	Al	1.93E-05
Mo	2.5	Na	1.13E-06
Ni	0.2	K	0.002
Co	0.2	W	2
Cd	4.3	Tl	7.1
As	1.8	Ga	0.4
Th	0.6	Sc	0.3
Sr	0.02	Fe	7.48E-05

Enrichment factor (EF)

This tool helps to distinguish the source of the heavy metals in the site thereby, distinguishing between anthropogenic and naturally occurring sources of the heavy metal pollutants.

The result in Table 4.13 indicated that all the heavy metal elements in Ota industrial layout except calcium, phosphorus, magnesium, titanium, aluminium, iron and sodium shows very severe to extreme enrichment from anthropogenic source.

Lead, copper, zinc and arsenic showed extreme enrichment from anthropogenic source. In spite of the high indication that, antimony, thallium, bismuth, boron, cadmium, molybdenum and tungsten have been enriched from anthropogenic sources (Table 4.13), the values will not be considered because the results from the Aqua Regia method of geochemical analysis indicated only few sample points showed values that could be detected; the metals were below detection limits (Table 4.8) and will be considered as been localized to few sample points.

All the major elements showed that they have been extremely and severely-enriched in the layout in the decreasing order Pb > Zn > Ba > Cu > Mn > Cr >V.

Table 4.13: Enrichment Factor of elements found in Ota industrial layout

ELEMENT	MEAN	Crustal Ave	EF	ELEMENT	MEAN	Crustal Ave	EF
Cu	175.3	50	46874.33	Sb	5	0.2	334243.6
Pb	161.3	12.5	172523.2	Bi	4.5	0.025	2406554
Zn	473.8	70	90494.08	Ca	0.144	41500	0.05
Mn	547.9	1000	7325.284	P	0.0238	1050	0.30
V	39.5	110	4800.954	La	10.8	39	3702.39
Cr	62.3	100	8329.352	Mg	0.051	23300	0.02
Ba	50.1	500	1339.649	Ti	0.0255	5600	0.06
B	48	10	64174.78	Al	1.586	82300	0.25
Mo	3	1.2	33424.36	Na	0.026667	23600	0.02
Ni	16.8	84	2673.949	K	0.038	20.9	24.30
Co	5.8	25	3101.781	W	2.5	1.25	26739.49
As	3.3	1.8	24511.2	Tl	6	0.85	94374.68
Th	5.6	9.6	7799.018	Ga	8	19	5629.36
Sr	7.9	370	285.4621	Sc	6	22	3646.29
Cd	0.65	0.15	57935.57	Fe	4.211	56300	-

Index of Geo-Accumulation

To quantify elemental contamination, the I_{geo} as proposed by Müller (1969) was also carried out on the geochemical results from Ota industrial layout.

Geo-accumulation index is the quantitative single metal approach to quantify metal pollution in sediments when the concentration of toxic heavy metal is 1.5 or more times greater than their lithogenic background values

In Ota industrial layout, the analysis reveals that bismuth has a value of 6.90 which indicates extreme contamination from bismuth. Antimony has a value of 4.05 which is an indication of the site being strongly and at the verge of extreme contamination by antimony. Lead has a value of 3.10; which shows the site is strongly contaminated by it while copper with a value of 1.22 shows moderate contamination within the site (Table 4.14).

The pollution by bismuth, antimony, thallium, boron and cadmium are very localised since only few samples showed the presence of these heavy metals in the geochemical analysis. The metals could not be detected in most of the samples as seen in the Aqua Regia Method of geochemical analysis result (Table 4.8). Lead, zinc and copper were present in all the samples. The analysis reveals that the concentration of lead has been increased by 3.10 times in the industrial layout. Similarly, the concentrations of copper and zinc have been increased by 1.22 and 2.17 times respectively in the layout (Table 4.14).

The order of contamination of these three major heavy metals as indicated by this pollution index is Pb > Zn > Cu.

Table 4.14: Index of Geo-accumulation values for heavy metal elements in Ota

ELEMENT	**MEAN**	**Crustal Ave**	**I_{geo}**	**ELEMENT**	**MEAN**	**Crustal Ave**	**I_{geo}**
Cu	175.3	50	1.22	Co	5.8	25	-2.69
Pb	161.3	12.5	3.10	As	3.3	1.8	0.289
Zn	473.8	70	2.17	Th	5.6	9.6	-1.36
Mn	547.9	1000	-1.45	Sr	7.9	370	-6.13
V	39.5	110	-2.06	Cd	0.65	0.15	1.53
Cr	62.3	100	-1.26	Sb	5	0.2	4.05
Ba	50.1	500	-3.90	Bi	4.5	0.025	6.90
B	48	10	1.67	Ca	0.144	41500	-18.72
Mo	3	1.2	0.73	P	0.0238	1050	-16.01
Ni	16.8	84	-2.90	La	10.8	39	-2.43
Mg	0.051	23300	-19.38	W	2.5	1.25	0.41
Ti	0.0255	5600	-18.32	Tl	6	0.85	2.23
Al	1.586	82300	-16.24	Ga	8	19	-1.83
Na	0.0267	23600	-20.34	Sc	6	22	-2.45
Fe	4.211	56300	-14.29				

Correlation Matrix of the major and some trace elements in Ota industrial layout

To distinguish the pollution sources, the major and significant trace heavy metal elements from Ota industrial layout were analysed through Pearson's correlation (Table 4.15). The elements with high positive and linear correlations were shaded, which could be an indication of same source with the corresponding element. For example, copper has a high and positive correlation with manganese (0.9070). Similar relationship exists between lead and zinc (0.8255). Negative correlations were observed between some of the elements such as between nickel and gallium (-0.0174) and zinc and lanthanum (-0.1434) Table 4.15.

The comparison of the magnetic susceptibility and elemental concentrations from ten samples selected from high, medium and low magnetic susceptibility readings, shows there is a direct relationship between the concentrations of the elements as obtained from the geochemical analysis to that of the magnetic susceptibility readings. Each heavy metal element has a known weight or abundance in the earth crust and a known magnetic susceptibility (Table 4.17), both properties have a direct relationship. The higher the concentration of an element in a sample, the higher its contribution to the magnetic susceptibility of that sample. Because, each heavy metal element in the sample uniquely contributes to the magnetic susceptibility reading that was recorded, the dominant elements in a sample determine the magnetic susceptibility value. For example, sample 5Di of 180 μm grain size that was taken at zero depth has a magnetic susceptibility reading of 69.7. From the geochemical analysis of this sample, Pb (45 ppm), Zn (84 ppm), Cu (21 ppm), Ni (8ppm), Th (9 ppm), Sr (5 ppm), V (39 ppm), La (15 ppm), Cr (46 ppm), Ba (13 ppm), Ga (11 ppm), Sc (6 ppm) and Mn (320 ppm) were elements in it (Appendix 4.13).

Table 4.15: Correlation Matrix of major and some trace heavy metal elements in Ota industrial layout

	Cu	Pb	Zn	Ga	Ni	Ba	Mn	Sr	V	La	Cr
Cu	1.0000										
Pb	0.1286	1.0000									
Zn	0.6154	0.8255	1.0000								
Ga	0.2101	-0.2787	0.0062	1.0000							
Ni	0.6189	0.2967	0.4133	-0.0174	1.0000						
Ba	0.5518	0.3059	0.3537	-0.1657	0.9140	1.0000					
Mn	0.9070	0.1832	0.5855	0.0126	0.7453	0.6843	1.0000				
Sr	0.6419	0.4133	0.5764	-0.1394	0.7233	0.8582	0.7787	1.0000			
V	0.6190	0.1066	0.3191	0.2438	0.8265	0.6680	0.7745	0.5193	1.0000		
La	0.0727	-0.0905	-0.1434	0.4355	0.4750	0.4908	0.2557	0.3271	0.6749	1.0000	
Cr	0.6701	0.2377	0.4696	-0.1575	0.8024	0.6755	0.8643	0.6307	0.9158	0.4828	1.0000

4.2 Grain Size Concentration of Pollutants in Ogijo and Ota Industrial Layouts

4.2.1 Grain Size Magnetic Susceptibility Analysis Readings from Ogijo Industrial Layout

The magnetic susceptibility readings from the gain samples were statistically analysed. Histograms showing the variation in magnetic susceptibility in each grain size with depth as well as box plots were generated for each sample points. Two box plots were plotted for readings from each sample point showing the average magnetic susceptibility at each depth and the other showing the average magnetic susceptibility within the same grain size at each sample point.

Statistical analysis using histograms and box plots revealed distinct stepladder patterns of magnetic susceptibility distribution when the magnetic susceptibility of different grain sizes were plotted at same depth. At each depth of each sample point, the magnetic susceptibility readings from the different grains of same depth revealed that 15% of the highest magnetic susceptibility values were from samples of grain size 180 μm, 2% of the highest magnetic susceptibility values were from samples of grain size 125 μm, 10% of the highest magnetic susceptibility values were from samples of grain size 90 μm while a 73% of the highest magnetic susceptibility values within the same depth were from samples of grain size 65 μm, This findings implies that, at depths 0, 10, 20 and 30cm, the 65 μm grain size at each of these depths had the highest magnetic susceptibility reading recorded (Table 4.16 and Appendix 4.10). Since magnetic susceptibility measurement recorded for a soil is directly proportional to the total mass of the different metal elements present in it, it then implies from the above result, that most of the pollutants are found within the 65 μm grain sizes at the four different depths. Zhu *et al.* (2018), recorded similar findings when he compared magnetic susceptibility readings obtained from sediments of the Caofeidian and the central Bohai Bay with that from Laolongou and the cape of Caofeidian. They concluded that concentrations of heavy metals in sediments increase with decreasing particle size because the fine-grained sediments tend to adsorb much more heavy metals due to their high specific surface area.

Charts and density maps showing variation in magnetic susceptibility readings within grains sizes 180 μm, 125 μm, 90 μm, and 65 μm at depths of 0 cm, 10 cm, 20 cm and 30 cm for all samples across the site in Ogijo are presented in Appendices 4.5 and 46.

Comparative study of the 65 μm grains from the different depths showed that the soil grain samples at zero depth had the highest magnetic values representing 44.8% of the values from the same sample points. 65 μm at 10 and 20 cm depths represents 12.6% and 17.2% respectively while 65 μm grains from 30 cm depth represents 24.1%. All these percentages reflect the pollutants in the same grain sizes at different depths. The result reveal that the 65 μm grains at 0 cm are the most polluted, and a progressive enhancement in the percentage of pollutants occurred at both 20 and 30 cm after a distinct reduction at 10 cm depth. This trend is also reflected in the different density maps showing magnetic susceptibility values of 65 μm at the four different depths. (Appendices 4.5 to 4.7).

A plot of X_{fd}% against the X_{lf} cm^3kg^{-1} (X_{lf} mass specific) readings showed that the pollutants in Ogijo are Superparamagnetic metals as represented by X_{fd}% values between 14 and 2 (Fig. 4.14). Also present in the site are some minute metallic substances that are yet to be absorbed into the atomic lattice of the host elements; these were represented by X_{fd}% values greater than 14, values of X_{fd}% below 2 indicates pollutants that are paramagnetic elements (Fig. 4.14). Similar findings were observed from the analysis of the whole grain samples from Ogijo.

Table 4. 16: Total percentage of pollutants in soils of different grain sizes

Grain Size (μm)	Percentage Pollution (%) in Ogijo	Percentage Pollution (%) in Ota
180	15	17.6
125	2	2.9
90	10	5.8
65	73	73.5

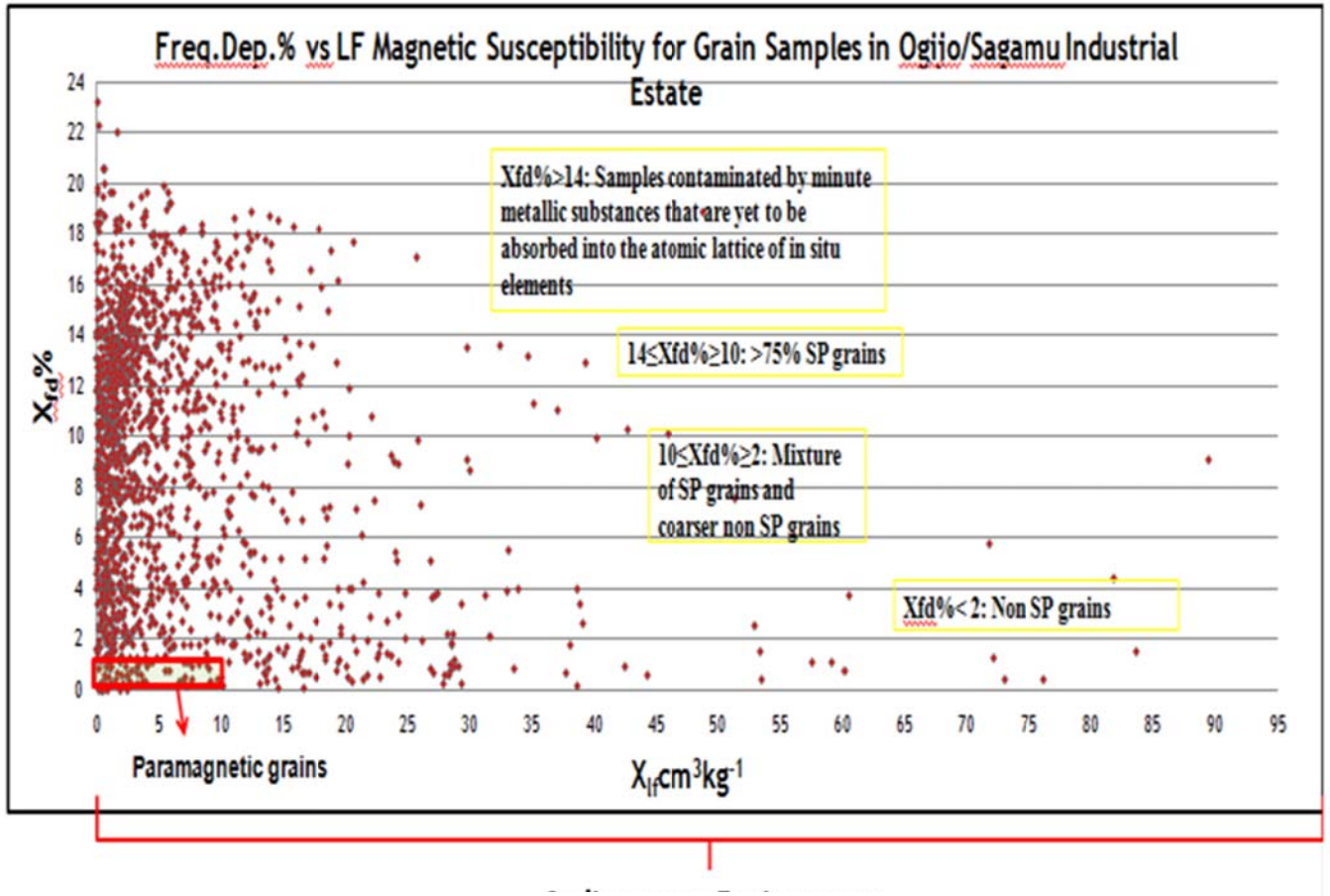

Figure 4.14: Chart showing estimate of Superparamagnetic minerals in all the grain samples

4.2.2 Temperature Analysis Results from Ogijo Industrial Layout

Metals magnetic behave when subjected to varying degrees of temperature is specific to certain magnetic minerals. To further confirm the types of heavy metals present in the samples, some grain samples were subjected to the analysis. The result from the Magnetic Susceptibility – Temperature analysis was presented as a measure of magnetic susceptibility of each sample as the temperature varies. The values of the magnetic susceptibility and corresponding temperatures obtained were plotted to produces a curve which reflects the type of mineral present in the sample and the domain that it exists (Fig. 4.15).

A general schematic trend of different minerals and domains (Fig. 4.16) in high temperature as given by Dearing (1994) in the magnetic susceptibility hand book was used as a guide in understanding the curves.

The high temperature domain is particularly complex in interpreting because of the irreversible change and several diagnostic transitions that occurs. It should be noted that temperature versus magnetic susceptibility analysis is qualitative and some of the shapes of the curves are still ambiguous due to the presences of different minerals or mixture of minerals in the sample, for example, ferrimagnetic minerals tends to dominate the temperature vs. magnetic susceptibility curve even when other minerals are present in a considerable amount. According to Dearing (1994) in the Bartington manual, a mixture of Stable Single Domain (SSD) grains, magnetite and paramagnetic minerals will give rise to an intermediate curve.

The plots obtained from the Magnetic Susceptibility – Temperature analysis reveals that the contaminants are likely SP metals, with the presence of some paramagnetic or canted antiferromagnetic metals (Figs. 4.15 and 4.16). For example, samples 40DCi, 90Ai, 77Ci and 59Ai plots obtained from the magnetic susceptibility - temperature analysis revealed that the samples are dominated by SP metals, while 67Bi is likely dominated by paramagnetic or canted antiferromagnetic (Fig. 4.15; Appendix 4.11 and Fig 4.16).

It was noted that the values of the magnetic susceptibilities measured were not directly proportional in value to that obtained from the Magnetic Susceptibility – Temperature analysis; this is because, according to the result obtained from the plot of X_{fd}% versus X_{lf} cm^3kg^{-1} (Fig. 4.14), the soil samples consist of a mixture of Superparamagnetic grains (which could either be ferromagnetic or/and ferrimagnetic metals), minute metallic

contaminants that are yet to be absorbed into the atomic lattice of the in-situ elements and non Supaparagmatic grains especially of paramagnetic elements. A mixture of minerals in the samples as revealed by the X_{fd}% versus X_{lf} cm^3kg^{-1} plot, according to Dearing (1994), will result to ambiguous curves as were observed in Figure 4.15.

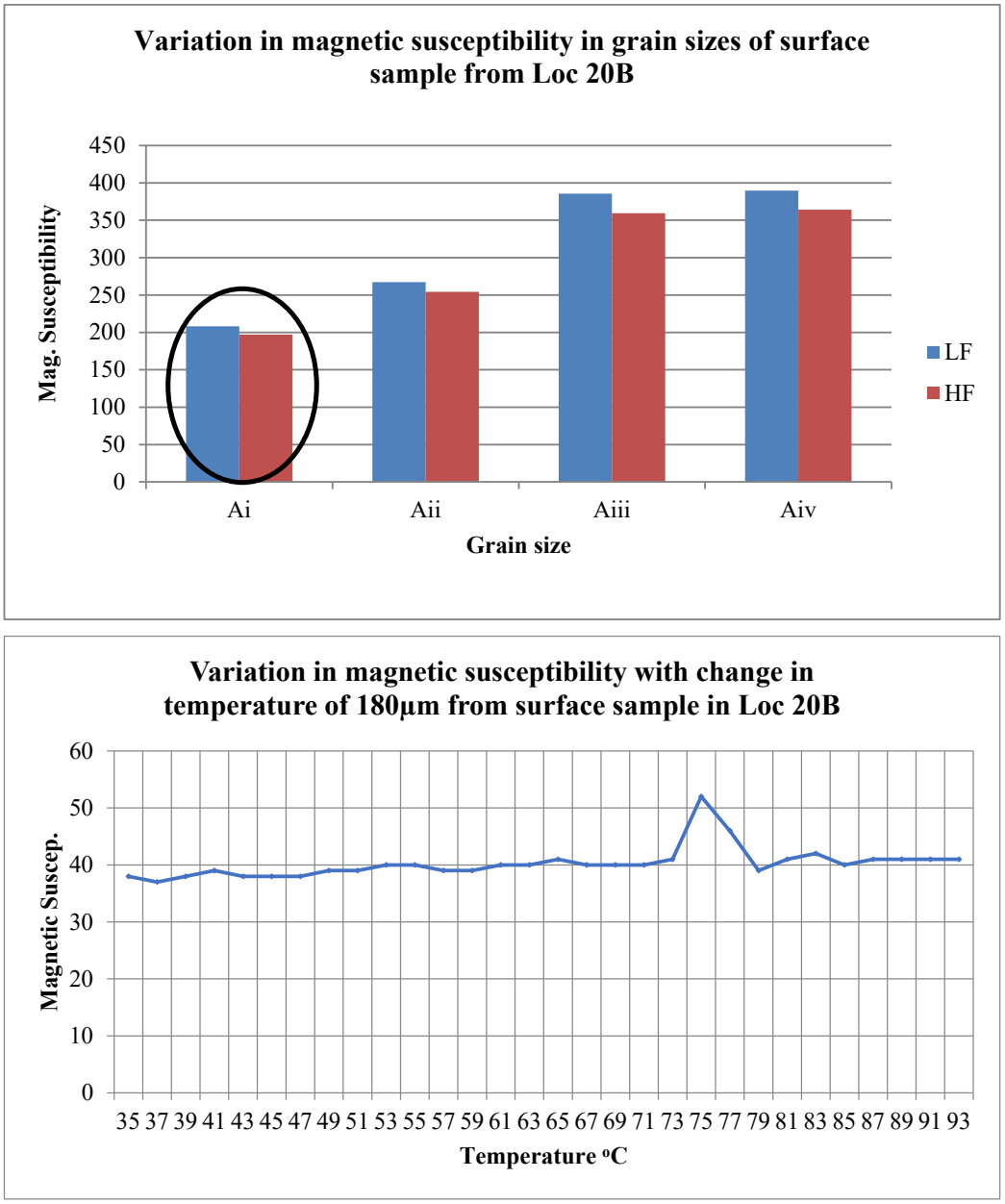

Figure 4.15: Curve showing variations in magnetic susceptibility with change in temperature for sample Ai (180 µm), from location 20B in Ogijo industrial layout (Others are in Appendix 4.4)

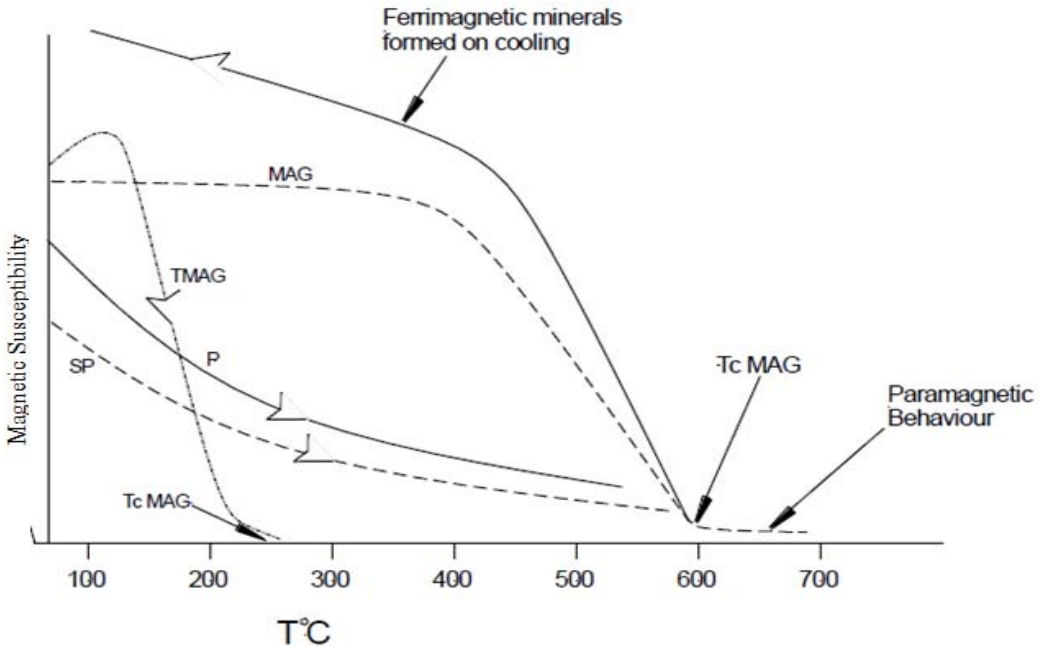

Figure 4.16: Schematic curves of different minerals and domains; super paramagnetic (SP), paramagnetic (P), and magnetite (MAG: TC 580ºC). (Source Dearing, 1994, based on Thompson and Oldfield, 1986)

4.2.3 **Grain Size Magnetic Susceptibility Analysis Readings for Ota Industrial Layout**

The statistical analysis of the magnetic susceptibility readings for the different grain sizes at same depth reveals that 17.6% of the highest magnetic susceptibility values were from samples of grain size 180 µm, 2.9% of the highest magnetic susceptibility values were from samples of grain size 125 µm, 5.8% of the highest magnetic susceptibility values were from samples of grain size 90 µm while a 73.5% of the highest magnetic susceptibility values within the same depth were from samples of grain size 65 µm (Table 4.16 and Appendices 4.13 - 4.17) and this is an indication that the 65 µm samples are the most polluted.

At the different depth of 0, 10, 20 and 30cm, when comparing the variation of magnetic susceptibility of the 65 µm grains from the histograms and box plots, the results showed that the 65µm grains at zero depth had the highest magnetic values representing 48.1% of the values from the same sample points. 65 µm at 10 cm and 20 cm depths represents 18.5% each and 65 µm grains from 30 cm depth represents 14.8%. All these percentages reflect the pollutants in the same grain sizes at different depths. The result reflected a progressive decrease in concentration of magnetic susceptibility with depth. Charts and density maps showing variation in magnetic susceptibility readings within grains sizes 180 µm, 125 µm, 90 µm, and 65 µm at depths of 0 cm, 10 cm, 20 cm and 30 cm for all samples across the site in Ota are presented in Appendices 4.13 - 4.17.

The plot of X_{fd}% agaist X_{lf} cm^3kg^{-1} (Fig. 4.17), classified about 90% of the pollutants as SP minerals which is indicated by X_{fd}% values between 14 and 2. Less than 10% of the pollutants were minute metallic substances that were yet to be incorporated into the atomic lattice of the naturally occurring metal elements (X_{fd}% > 14). The very few points below X_{fd}% < 2 indicated pollutants that were paramagnetic metals.

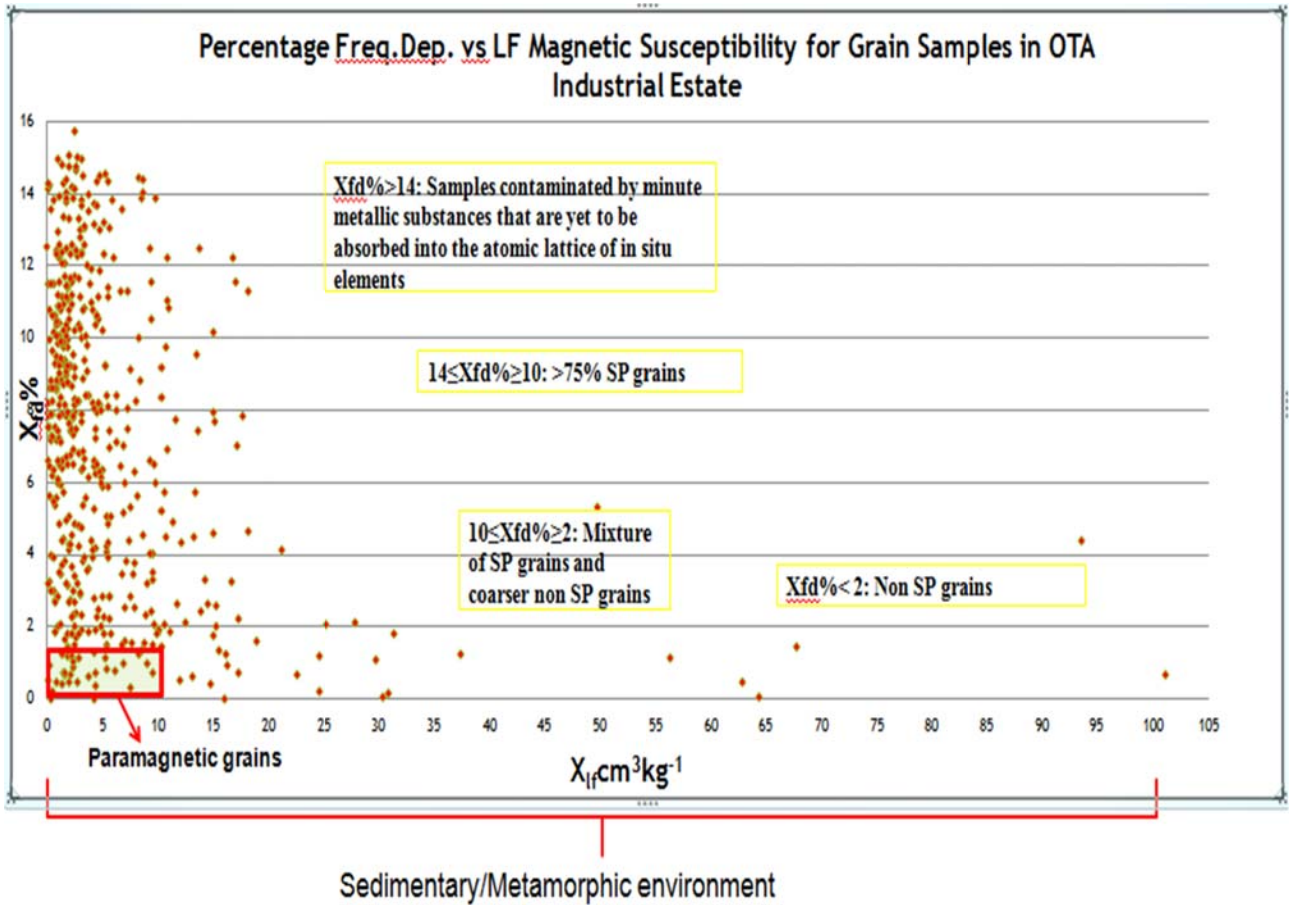

Figure 4.17: Charts showing estimate of super paramagnetic minerals in all the grain samples in Ota industrial layout

4.2.4 Temperature Analysis Results from Ota Industrial Layout

The values of the magnetic susceptibility and corresponding temperatures were plotted to produce a curve which is a reflection of the type of mineral present in the sample and the domain exist (Fig. 4.18).

The results of the analysis were compared to general schematic trend of different minerals and domains (Fig. 4.15) in high temperature as given by Dearing (1994) in the magnetic susceptibility hand book. The schematic trend was used as a guide in interpreting the curves.

The result of the plots obtained from the magnetic susceptibility vs temperature analysis revealed that the contaminants are likely SP metals. Similar finding was earlier observed from the X_{fd}% versus X_{lf} cm^3kg^{-1} plot (Figs. 4.18 and 4.17, Appendix 4.11).

The limitation of this analysis is that no sample contains only one specific metal type. As was revealed in the plot of X_{fd}% versus X_{lf} cm^3kg^{-1} (Fig. 4.17), the minerals in the samples were basically super paramagnetic and paramagnetic. And thus, curves generated would not specifically match the schematic trends used for the interpretation. Dearing (1994), noted that this limitation will result in ambiguous curves as were observed from the results of the analysis.

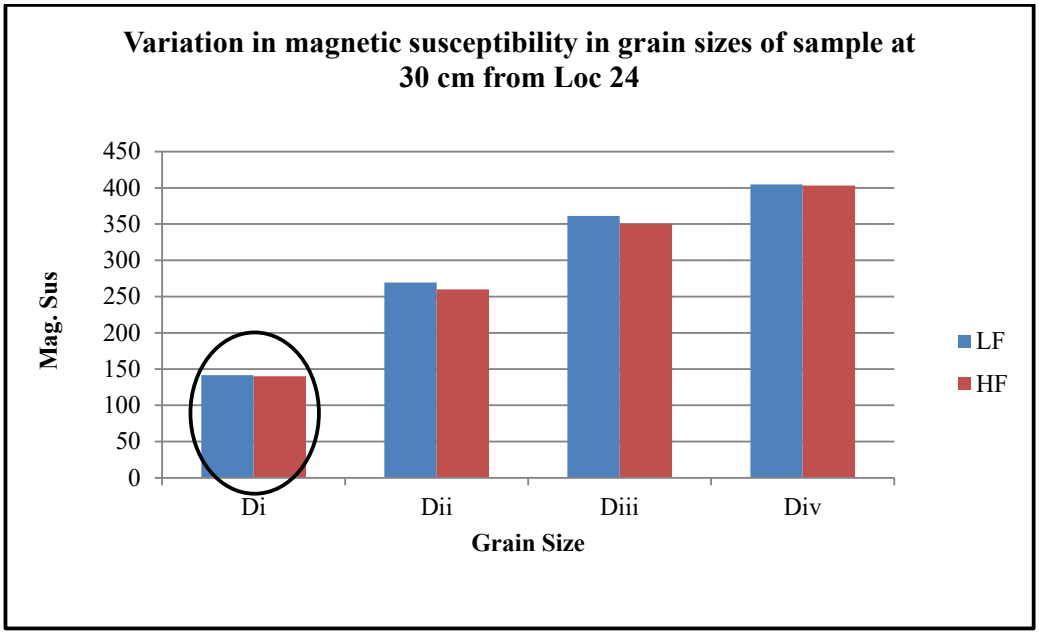

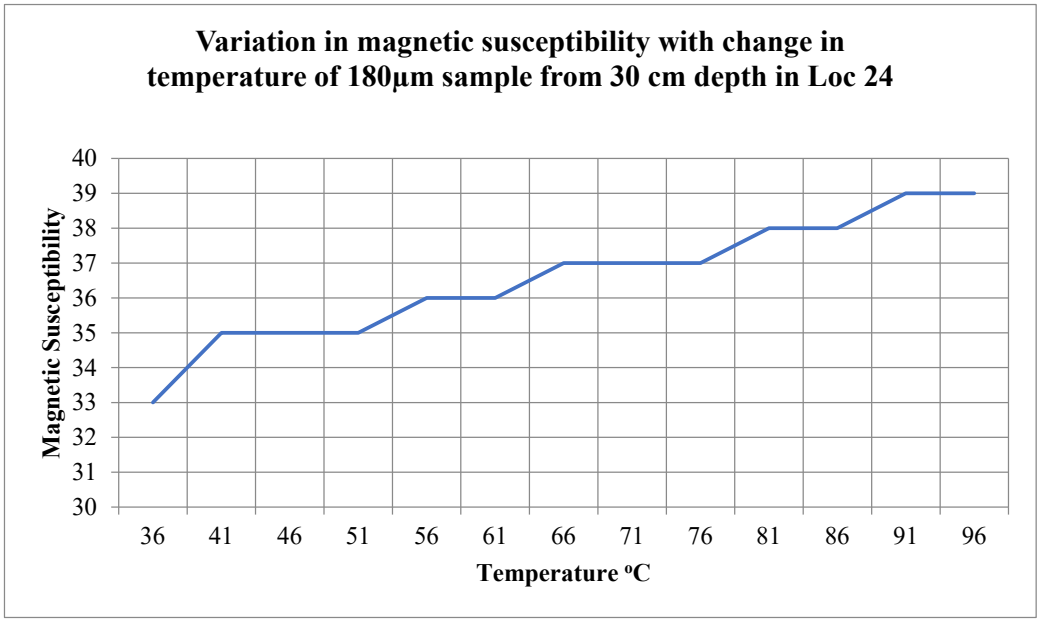

Figure 4.18: Charts showing variations in magnetic susceptibility with temperature in location 24, Ota industrial layout

4.3 Spatial Distribution of Pollutant within the Industrial Layouts

4.3.1 Spatial Distribution of Magnetic Susceptibility Readings across Ogijo Industrial Layout

To determine the spatial concentrations and distribution of heavy metal pollutants across Ogijo, a plot of the range of magnetic susceptibility readings at each sample point for all magnetic susceptibility readings at 0 cm depth from the whole grain samples is presented in Figure 4.19. A magnetic susceptibility concentration density map showing spots of magnetic anomalies in Ogijo industrial layout was generated (Fig. 4.19). Six hot spots were identified from the density maps and these represent sample points with magnetic susceptibility values greater than 2000. These spots are in very close proximity with some of the smelting plants. Figure 4.19 shows the magnetic susceptibility obtained from samples from within or the closest proximity to each smelting plant in Ogijo.

To further understand the spatial variation of the pollution away from the smelting plants, lines of profiles were taken away and between some of the smelting plants. A profile across Real infrastructure and Everest steel limited, showed a heavy presence of the pollutants at the environs of the industries (Fig. 4.21) with an average value greater than 800. The activities of Real infrastructure limited (with magnetic susceptibility values greater than 5085.8), Everest Steel limited (magnetic susceptibility 1143.8) and the small metal factory where fabrication is taking place have negatively impacted the environment with heavy metals. Magnetic values which exceeded 30 as was recommended by Wojas (2017) as an indication of the presence of pollution, were observed in the vicinity of the industries, which is an indication of pollution that was likely from atmospheric dust, rather than from vehicular activities since the road had been damaged and not pliable at time of sampling. At the environs of Sagamu steel, the readings were extremely low. This was because at Sagamu steel there was an obvious evidence of remediation that has been done were the surface soils in the environment had been covered by freshly dug clayey soils.

Similarly, African metal steel (6159.3), Monarch steel company (2517.7), African metal company (2101.3), Phoenix (the foundries section) (4709.5), Metal world recycling (3669) and African foundries limited (1630.4) had negatively impacted the environment

with heavy metals. Metal recycling industries (MRI) (419.2) had the least impact in the industrial layout. (Figs: 4.20 - 4.22).

It can be deduced that the extent of contamination around the industries reflects the frequencies of their industrial activities. Also, the low magnetic susceptibility readings in the range of 100s recorded away from the industries when compared the extremely high values very close to the industries, could be a pointer to the fact that the pollution from the fumes that were released into the atmosphere are of little significance or if the pollutants are of significant values, but because of their atomic weight and effect of gravity, they are deposited or settled on the land as soon as they were released into the atmosphere thereby limiting the area extent to be polluted.

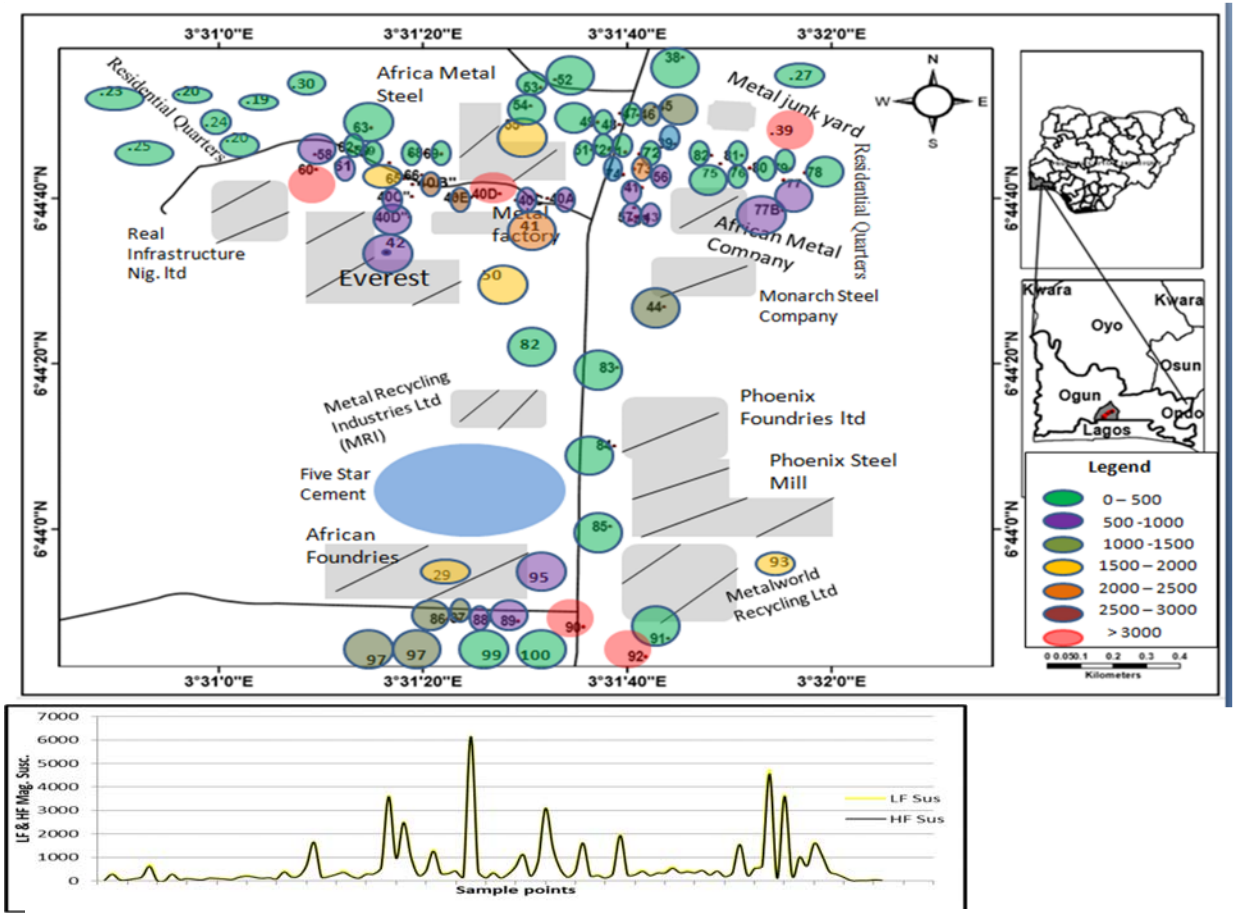

Figure 4.19: Pollution density map showing magnetic susceptibility anomalies in surface soil of Ogijo industrial layout

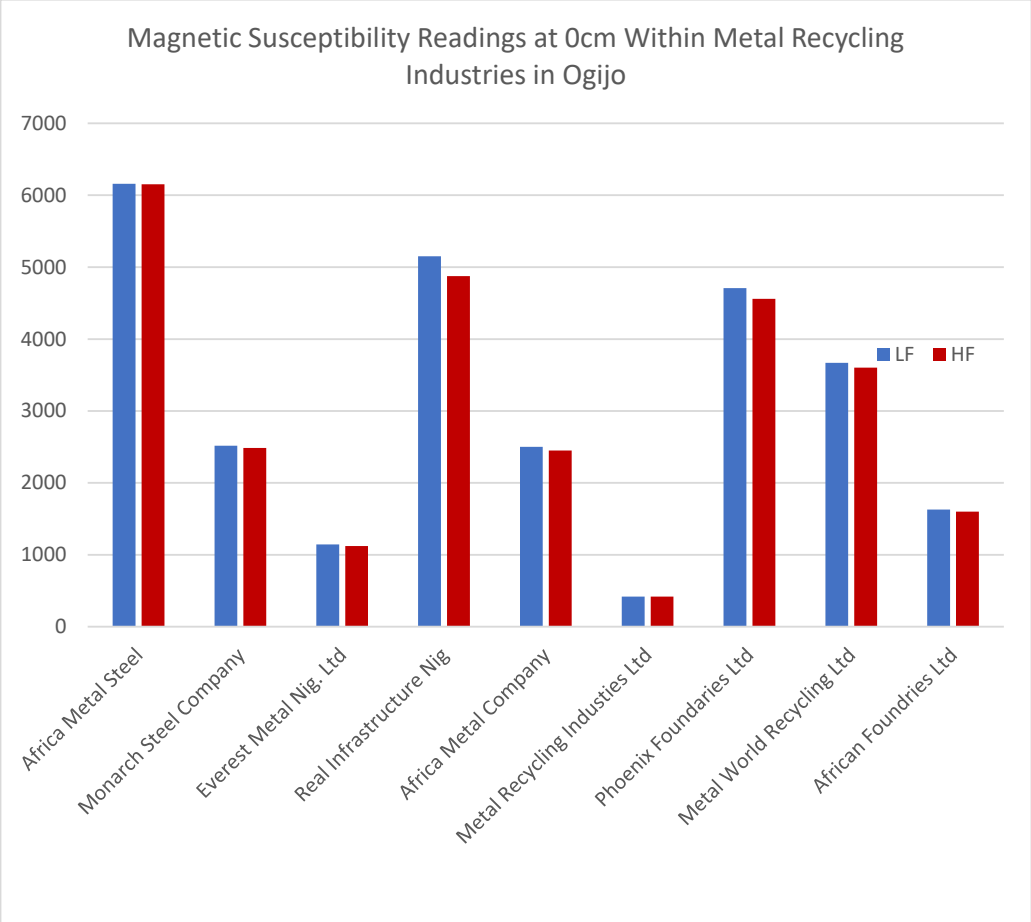

Figure 4.20: Magnetic susceptibility values of surface soil samples at each of the metal recycling industries in Ogijo industrial layout

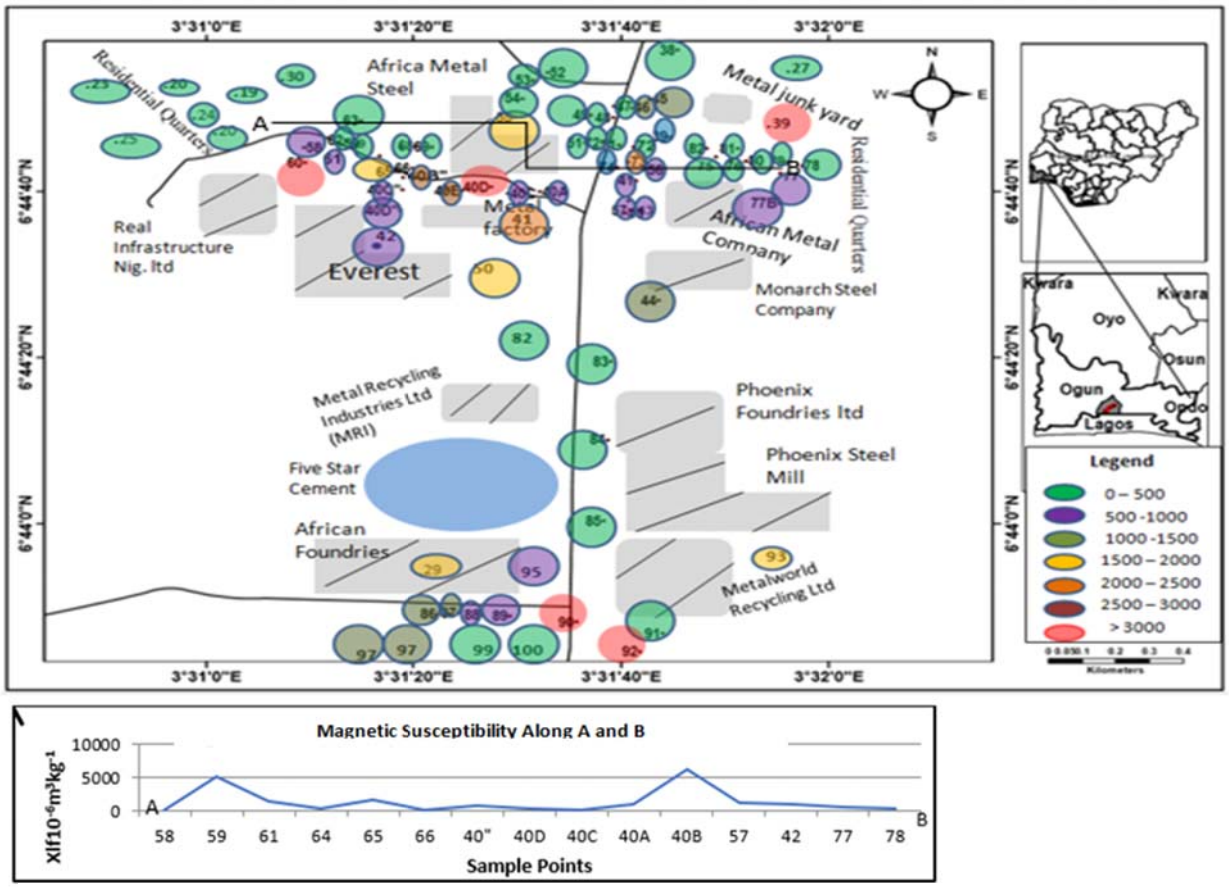

Figure 4.21: Magnetic susceptibility readings from A to B in Ogijo industrial layout

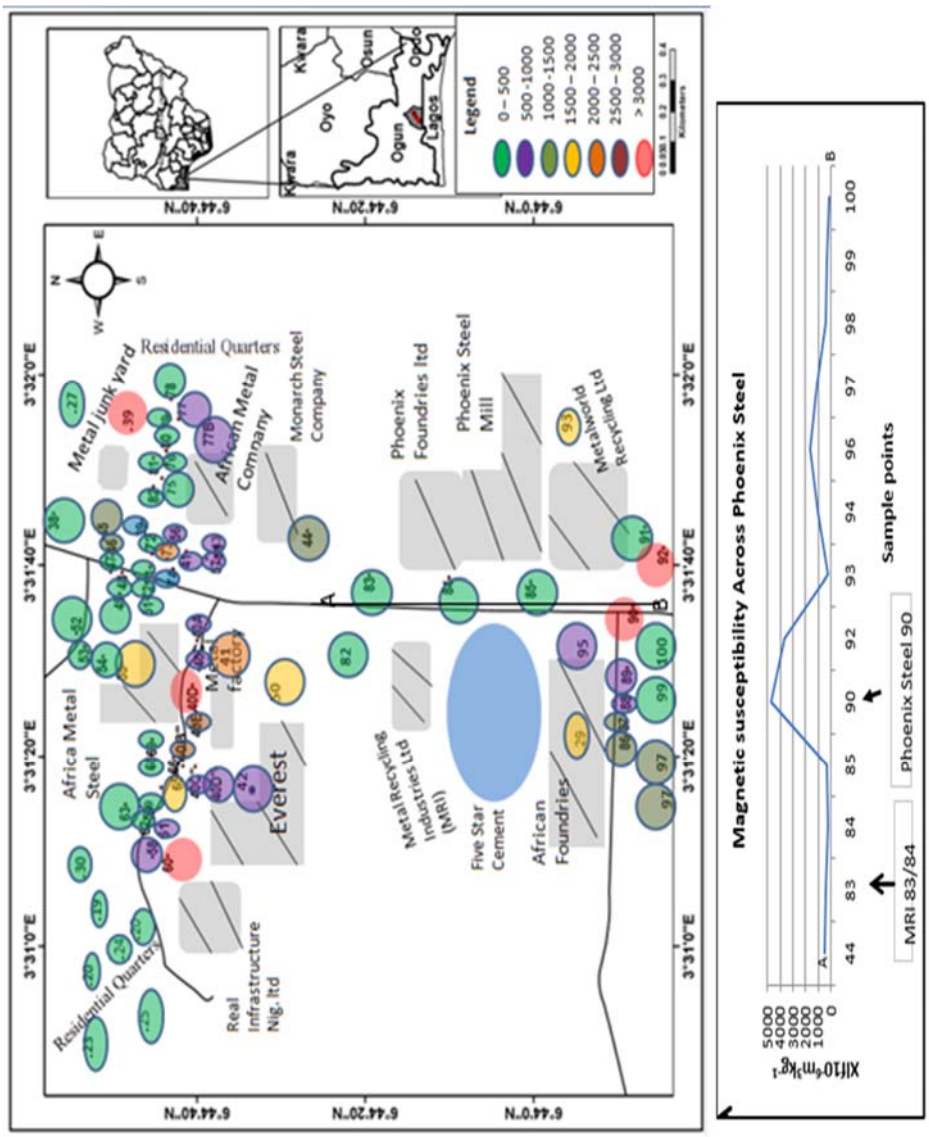

Figure 4.22: Magnetic Susceptibility readings within the range of A to B in Ogijo industrial layout

4.3.2 Pattern of Distribution of Pollution with Depth

Five distinct patterns of distribution of magnetic susceptibility readings with depth were identified: samples where the magnetic susceptibility readings increased with depth represents 15.2% of all the samples, samples which show the magnetic susceptibility reading decreasing with depth represents 33.3%, 10.5% of the samples have magnetic susceptibility readings approximately constant in all the depths, 20% of the samples shows an enhancement in the magnetic susceptibility readings at 20 cm depth in a decrease-increase-decrease pattern while 21% of the samples shows an enhancement of the magnetic susceptibility readings at 30 cm depth; that is, an increase-decrease-increase pattern (Fig 4.23). Similar patterns were also recorded for samples obtained within the metal recycling industries and the difference in the patterns of distribution of the magnetic susceptibility readings could be a reflection of the production activities of the metal industries over a long period. At Africa Metal Steel, Everest Metal Nigeria Limited, Phoenix Foundries, Real Infrastructure and Metal World Recycling, the decreasing with depth pattern was recorded (Fig. 4.23); this is an indication that the industries have being actively recycling metals for some time. A plot of the magnetic susceptibility readings from the samples at zero depth (surface samples) (Appendices 4.17 and 4.18) indicated that, these same industries mentioned above except for Everest Metal Nigeria Limited, have readings greater than 3000, which are the highest values recorded in the site and are the major contributors of the pollutant in the environment of the industrial layout.

The least contributor to the environmental pollution is the Metal Recycling Industries Limited whose highest magnetic susceptibility value was 419.2 as recorded from the surface sample (Figure 4.20).

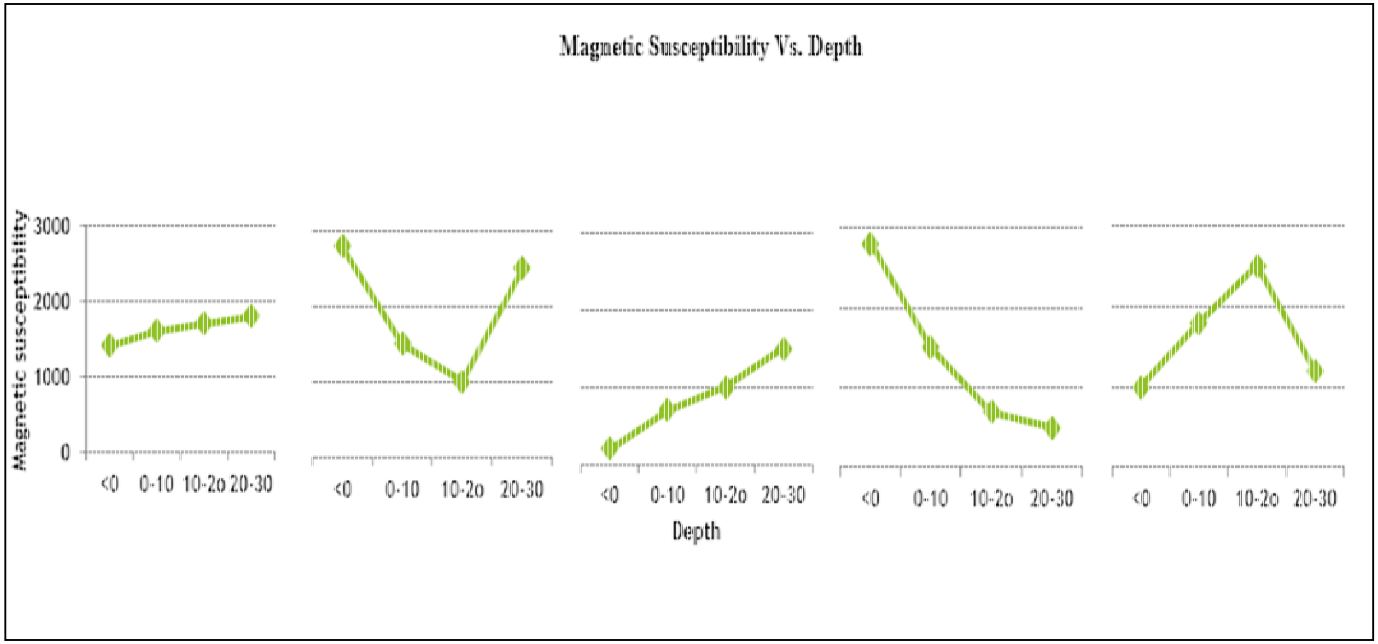

Figure 4.23: Five distinct patterns of distribution of magnetic susceptibility readings of whole samples in Ogijo industrial layout

4.3.3 Comparison of Magnetic Susceptibility Readings with Geochemical Concentration of Heavy Metals

The comparison of the magnetic susceptibility and elemental concentrations from twenty-one samples selected among high, medium and low magnetic susceptibility readings, revealed that there is a direct relationship between the concentrations of the elements as shown from the geochemical analysis to that of the magnetic susceptibility readings (Fig. 4.24). The weight/concentration of an element determines the magnetic susceptibility that is, the higher the concentration of an element, the higher the magnetic susceptibility. Therefore, the sum of all the elements present in a sample, uniquely determine the magnetic susceptibility value of the sample. This is because each element has a unique magnetic susceptibility value (Table 4.17) and each element contributes significantly to the magnetic reading. For example, in sample 40D at depth 20 cm, grain size of 180 μm has a magnetic susceptibility reading of 857.7 and the geochemical analysis reveals that the dominant elements found in the samples are Mn (3237 ppm), Zn (332 ppm) and Cr (273 ppm). However, in sample 97 at 10 cm depth, 180 μm grain size has a magnetic susceptibility reading of 2038.1. The geochemical analysis reveals that the elements in the sample are Mn (>10000 ppm), Zn (1666 ppm), Cr (416 ppm), Cu (303 ppm) and Ba (749 ppm) [Fig. 4.24, and Table 4.17].

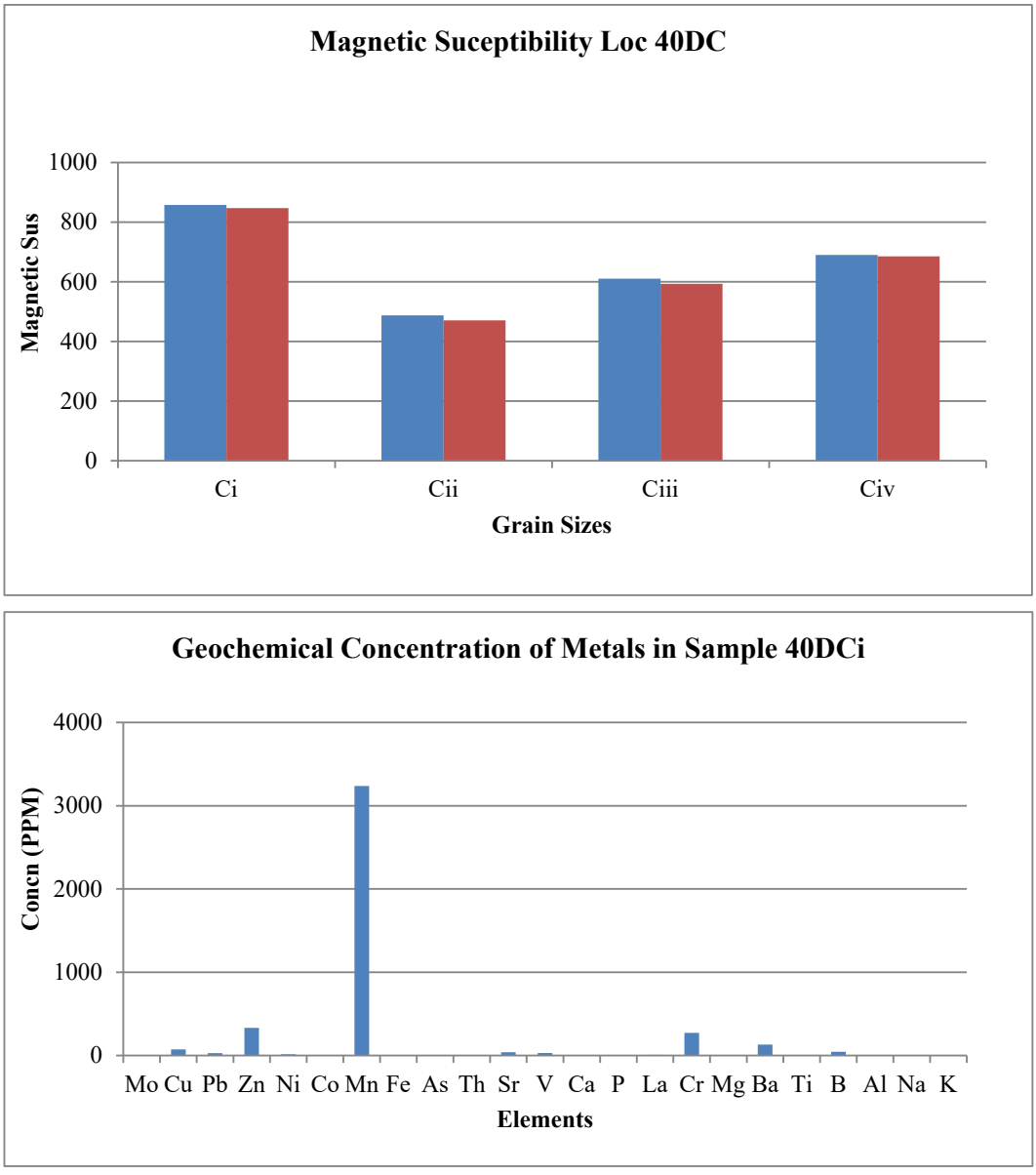

Figure 4.24: Charts showing magnetic susceptibility values for specific grain sizes and their corresponding elemental concentration (Refer to other charts in Appendix 4.7)

Table 4.17: Landolt Börnstein data base of magnetic susceptibility of elements

Element		**Magnetic Susceptibility**	**Element**		**Magnetic Susceptibility**
Manganese	Mn	+511	Magnesium	Mg	+13.1
Molybdenum	Mo	+72	Mercury	Hg	-33.5
Aluminum	Al	+16.5	Potassium	K	+20.8
Antimony	Sb	-99	Silver	Ag	-19.5
Arsenic (gray)	As	-5.6	Arsenic (yellow)	As	-23.2
Barium	Ba	+20.6	Sodium	Na	+16
Bismuth	Bi	-280.1	Tungsten	W	+55
Boron	B	-6.7	Thallium	Tl	+50
Cadmium	Cd	-19.7	Thorium	Th	+97
Calcium	Ca	+40	Zinc	Zn	-9.15
Copper	Cu	-5.46	Vanadium	V	+285
Chromium	Cr	+167	Phosphorus (white)	P	-26.66
Gallium	Ga	-21.6	Phosphorus (Red)	P	-20.77
Lead	Pb	-23	Scandium	Sc	+295.2
Titanium	Ti	+151	Strontium	Sr	+92

4.3.4 Spatial Distribution of Magnetic Susceptibility Readings Across Ota Industrial Layout

The low frequency magnetic susceptibility readings over sample point's location and concentration density map from the magnetic susceptibility readings were generated for Ota industrial layout (Fig.4.25). The maps revealed three areas with high magnetic susceptibility anomalies of which two of the spots had readings greater than 1000. Generally, the maps revealed an enhanced magnetic susceptibility values at sample points between smelting plants. The concentration reduced away from the plants. From the nine samples taken from within the estate, the highest recorded magnetic susceptibility reading was 333.9, six of the samples had readings above 100 and the lowest reading was 30.3. These values exceeded the X_{lf} : 30 limit of Wojas, 2017 that signifies pollution in an environment. Magnetic readings from inside or very close to each smelting plants were: Federated steel company; 2645, Tower Aluminium; 1598.3, Homan; 529.6, MINL; 502, Kolorkote Nigeria limited; 302.6 and SUMO steel; 295 (Fig. 4.26).

Two lines of profiles were taken to study the spatial variation of pollution within the layout; Figure 4.27 shows a profile cutting across Tower Aluminium, Korlokote and Homan industries. The profile revealed a mark increase in magnetic susceptibility readings at the locations of the metal recycling industries but with a wider radius of contamination as observed between Korlokote Nigeria limited and MNL limited. This wider radius of contamination is because of the proximity between them. In the second profile (Fig. 4.28), running beside Federated steel, the magnetic susceptibility readings at sample point 25 was 1817.5 to sample point 10 within the estate having reading of 236.9. Federated steel company stands as the highest source of contamination at the industrial layout as a whole.

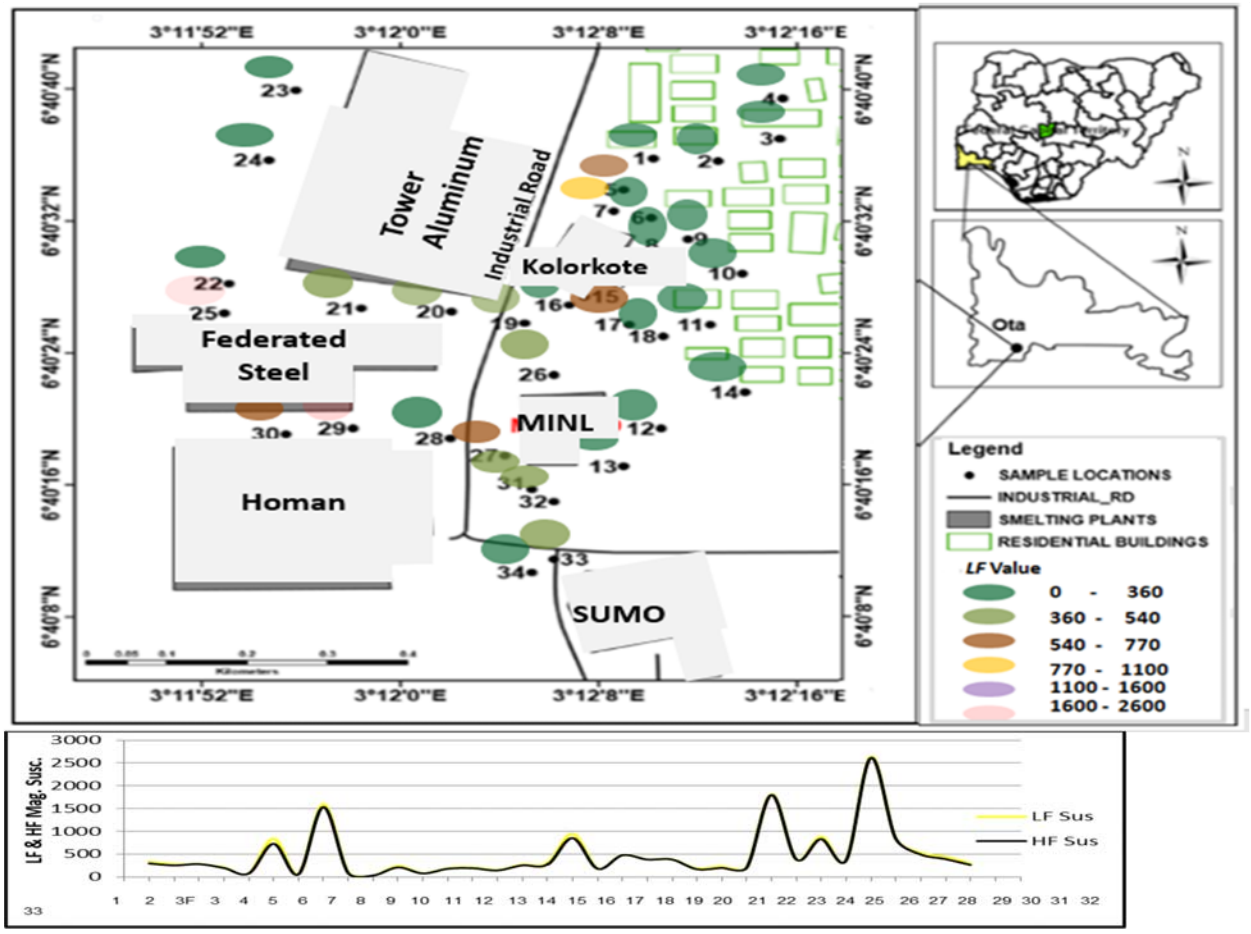

Figure 4.25: Concentration density map showing areas with magnetic susceptibility anomalies in Ota Industrial Layout

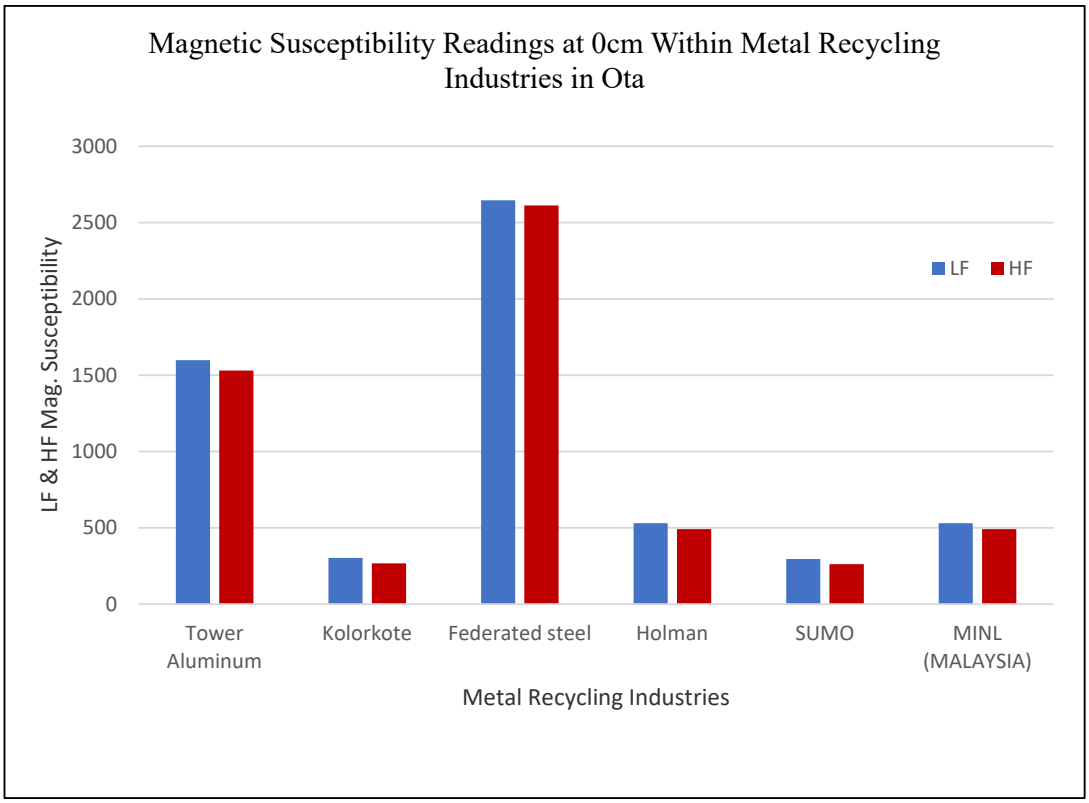

Figure 4.26: Magnetic susceptibility values of surface soil samples at each of the metal recycling industries in Ota industrial layout

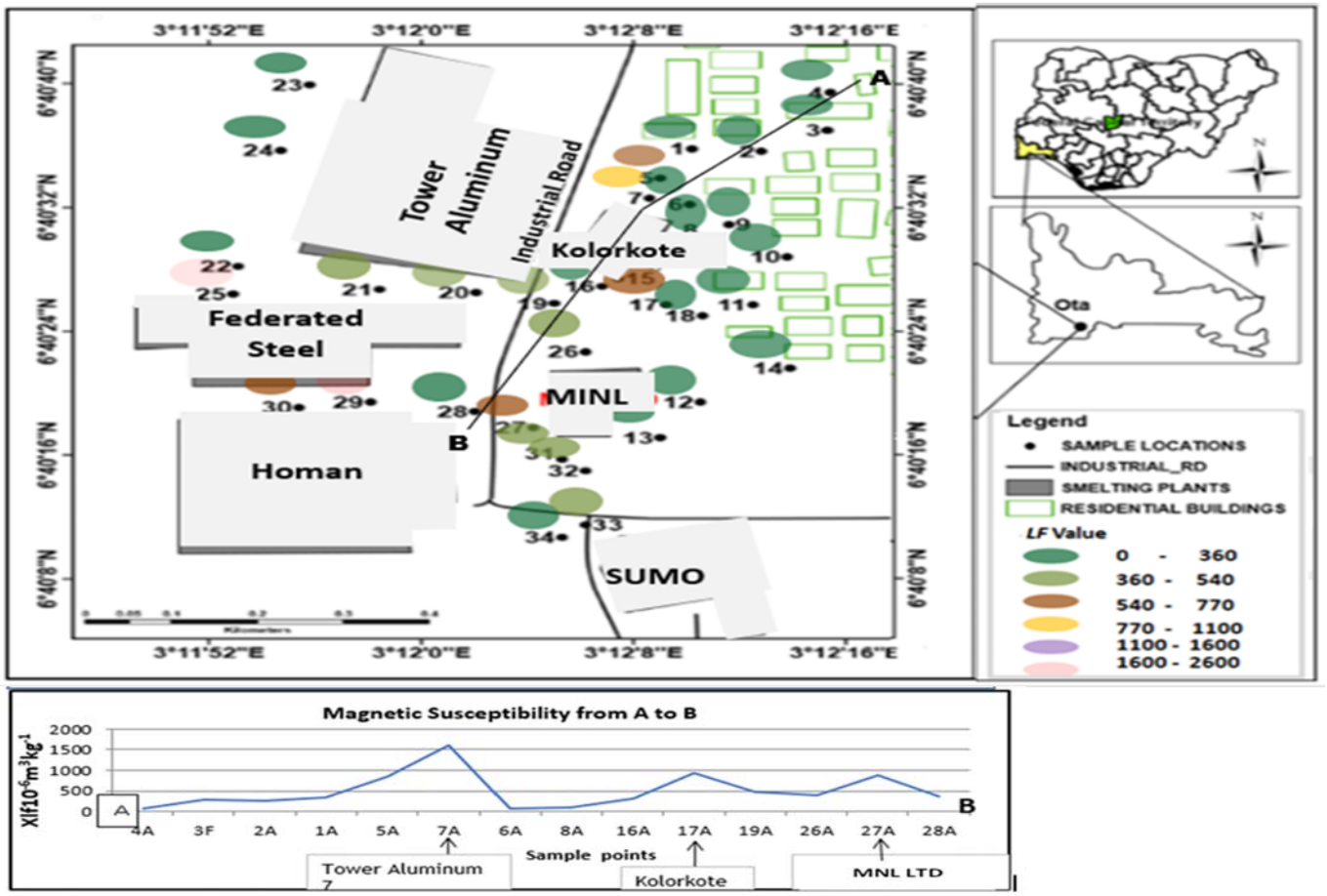

Figure 4.27: Magnetic susceptibility readings from A to B in Ota industrial layout

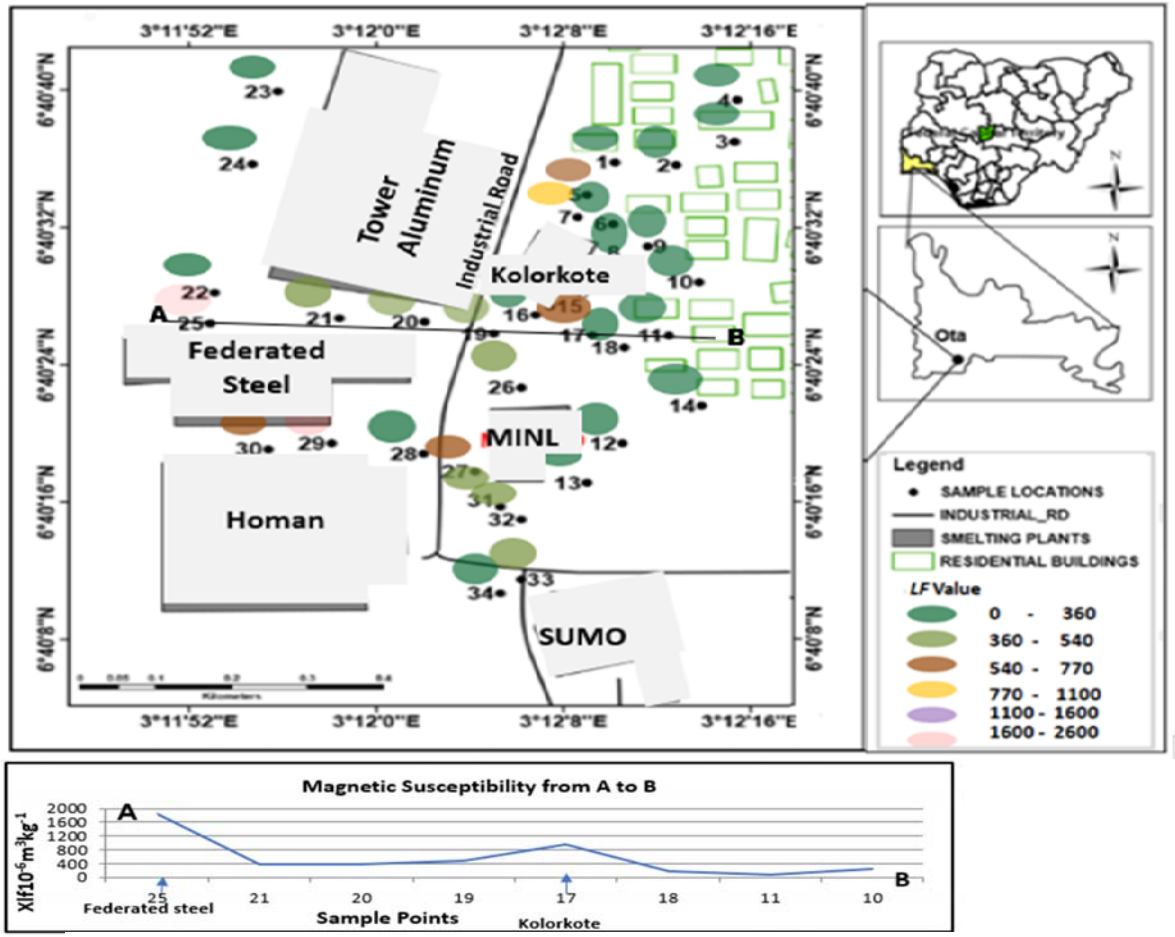

Figure 4.28: Magnetic susceptibility readings across Federated Steel and Kolorkote in Ota industrial layout

4.3.5 Pattern of Distribution of Pollution with Depth

Five distinct patterns of distribution of magnetic susceptibility readings with depth were identified also in Ota industrial layout. These were similar to that identified in Ogijo industrial layout (Fig. 4.23). The patterns includes samples where the magnetic susceptibility readings increased with depth represents which 3.1% of all the samples, samples which shows the magnetic susceptibility reading decreasing with depth representing 37.5%, 15.6% of the samples have magnetic susceptibility readings approximately constant in all the depths, 29.9% of the samples shows an enhancement in the magnetic susceptibility readings at 20 cm depth in a decrease-increase-decrease pattern while 21.9% of the samples shows an enhancement of the magnetic susceptibility readings at 30 cm depth; that is, an increase-decrease-increase pattern. The difference in the patterns of distribution of the magnetic susceptibility readings is likely a reflection of the production activities of the metal industries over a long period of time.

Magnetic susceptibility readings of samples obtained within the metal recycling industries also showed distinct patterns of distribution with depth which could also reflect the production activities of the metal industries over a long period. At kolorkote Nigeria limited, Federated Steel Limited, Tower Aluminium and Holman industries, the decreasing with depth pattern was recorded (Fig. 4.23); this is an indication that the industries have being actively recycling metals for some time. A plot of the magnetic susceptibility readings from surface samples (Fig. 4.26) revealed that, these industries all had readings greater than 200.

The two samples taken from within Federated Steel Limited had the highest values recorded in the site and is the major contributor of the pollutant in the environment of the industrial layout (Figs. 4.26 and 4.29).

The least contributor to heavy metal pollution in the environment of Ota industrial layout is SUMO Industries limited; the recorded magnetic susceptibility value from surface samples within SUMO was 295.2. (Appendix 4.10). The low magnetic susceptibility values around SUMO as compared to the other industries could be due to the fact that the company is fairly new in the environment.

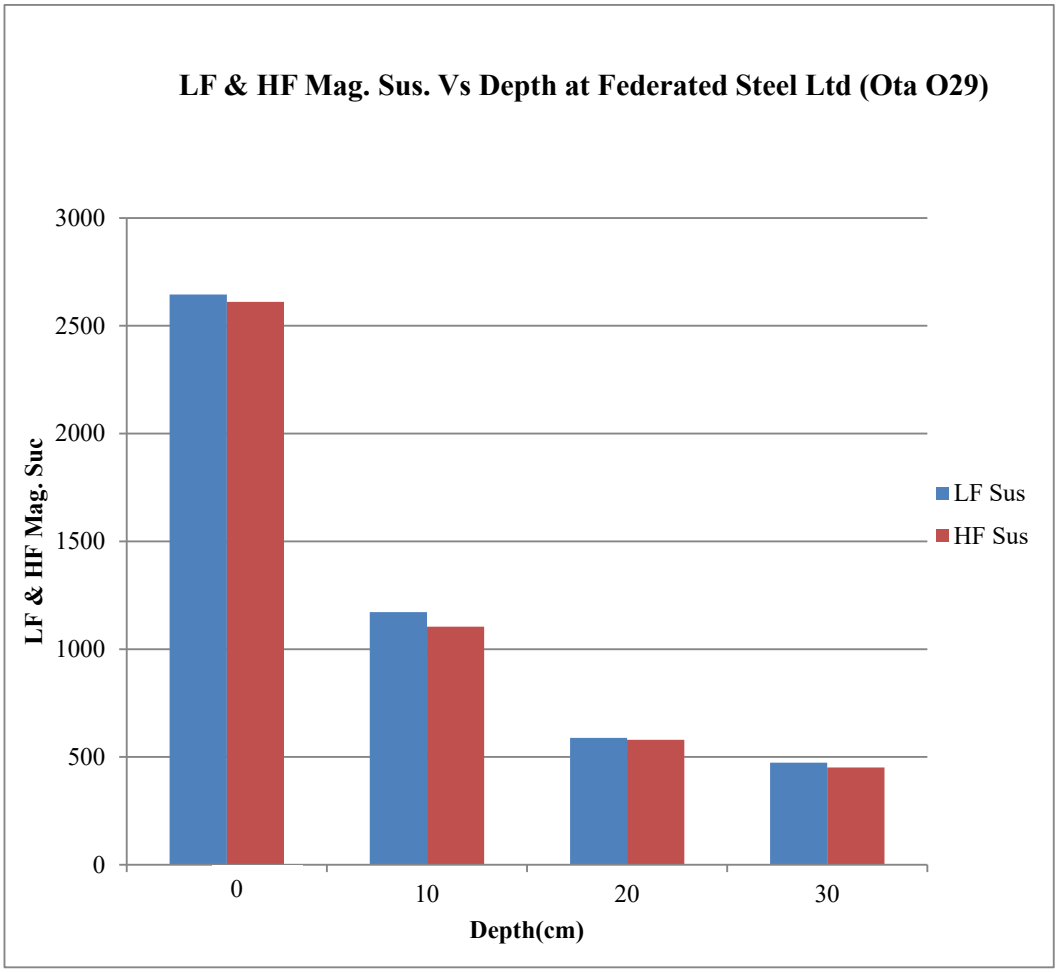

Figure 4.29: Variation in magnetic susceptibility readings from soil samples taken from a metal recycling industry in Ota (Appendix 4.8).

4.4 Comparison of Results from Ogijo and Ota Industrial Layouts

From the results of the similar analysis carried out on soil samples from Ogijo and Ota industrial layouts, the following were deduced:

High X_{lf} readings which exceeded the readings from the control site and the 30-limit indicating pollution as recorded by Wojas 2017, were recorded in both Ogijo and Ota industrial layouts.

The whole samples magnetic susceptibility readings from both sites showed a typical stepladder distribution with depth; with the highest values occurring at the zero depth. At Ogijo industrial layout, 44.01% of the sample points have their highest magnetic susceptibility values at zero depth, while 12.88% was at 10 cm, 11% at 20 cm and 32.11% at 30 cm depth. Similar results were obtained from Ota industrial layout; where 54.55% of the sample points have the highest concentration of pollutants at zero depth, while 9.09% of the samples have the highest values at 10 cm, 21.21% at 20 cm and 15.15% at 30 cm depth (Fig. 4.30).

Five distinct patterns of distribution of pollutants (from magnetic susceptibility readings) with depth in the whole samples were also identified in both industrial layouts, these are; increase in magnetic susceptibility readings as depth increases (Ogijo: 15.2%, Ota: 3.1%), decrease in the readings as the depth increases (Ogijo: 33.3%, Ota: 37.5%) , approximately constant readings with increase in depth (Ogijo: 10.5%, Ota: 15.6%), increase in the readings with depth but with an obvious drop at 30 cm depth (Ogijo: 20%, Ota: 29.9%) and decrease in the readings with increase in depth, but with an enhancement at 30 cm depth (Ogijo: 21%, Ota: 21.9%).

The grain size magnetic analysis also produced similar results from the industrial layouts. In Ogijo industrial layout, 15% of the pollutants are found in grain size 180 μm, while 2%, 10% and 73% of the pollutants are found in the 125 μm, 90 μm and 65 μm respectively. In Ota industrial layout, 73.5% of the pollutants are found in the 65 μm grain size while 17.6%, 2.9%, and 5.8% of the pollutants are found in the 180 μm, 125 μm and 90 μm respectively (Fig.4.31).

The X_{fd}% from both sites shows that the dominant metals present in the sites are superparamagnetic and few paramagnetic. In Ogijo industrial layout however, some

appreciable numbers of the samples are contaminated by minute metallic substances that are yet to be absorbed into the atomic lattice of in-situ elements.

The temperature vs. the magnetic susceptibility analysis of the grain samples from both sites further confirmed the metals present to be more of superparamagnetic and few of paramagnetic in nature.

The geochemical analysis of samples from both sites indicated that copper, lead, zinc, manganese, chromium, barium and boron are the major elements found in both sites. Ota has vanadium as one of its major elements (Fig. 4.32).

The results from the data analysis of the geochemical results of the samples singled out lead, zinc and copper as the dominant heavy metal pollutants within both industrial layouts.

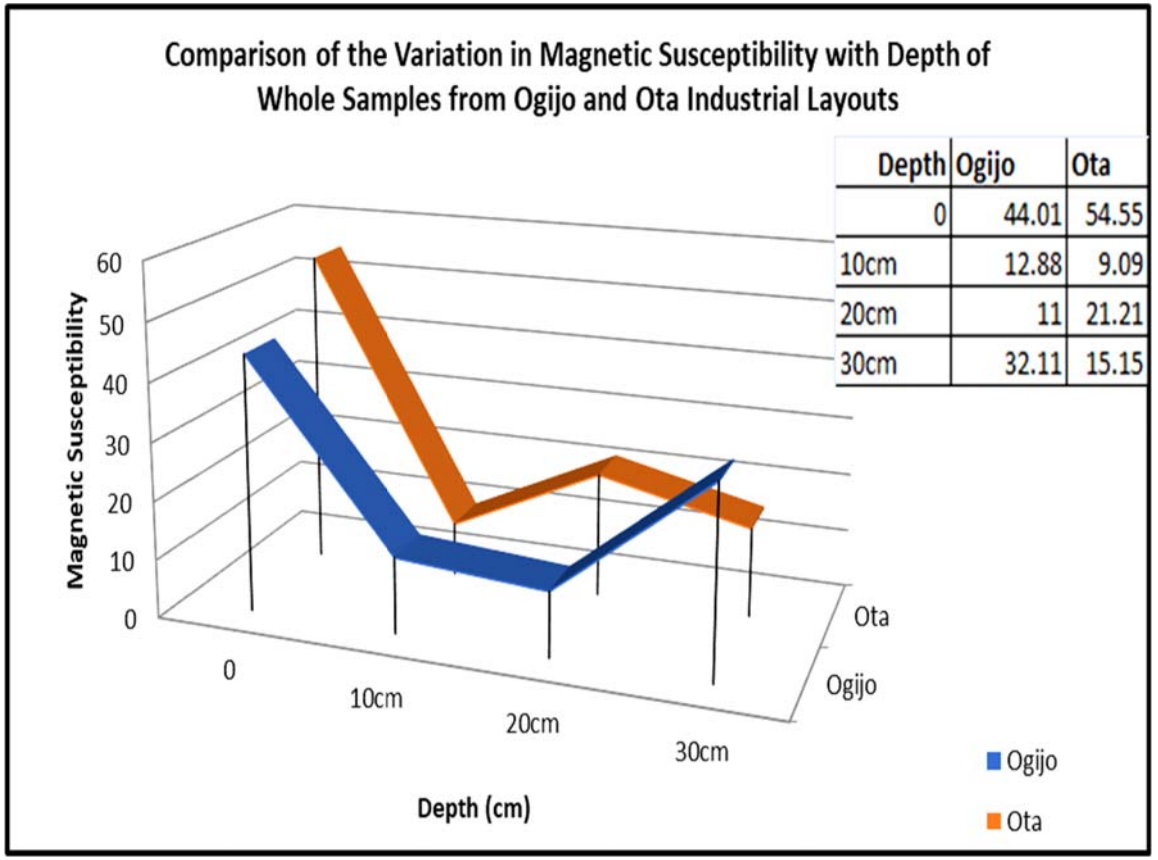

Figure 4.30: Values of magnetic susceptibility of whole samples with depth in Ogijo and Ota industrial layouts

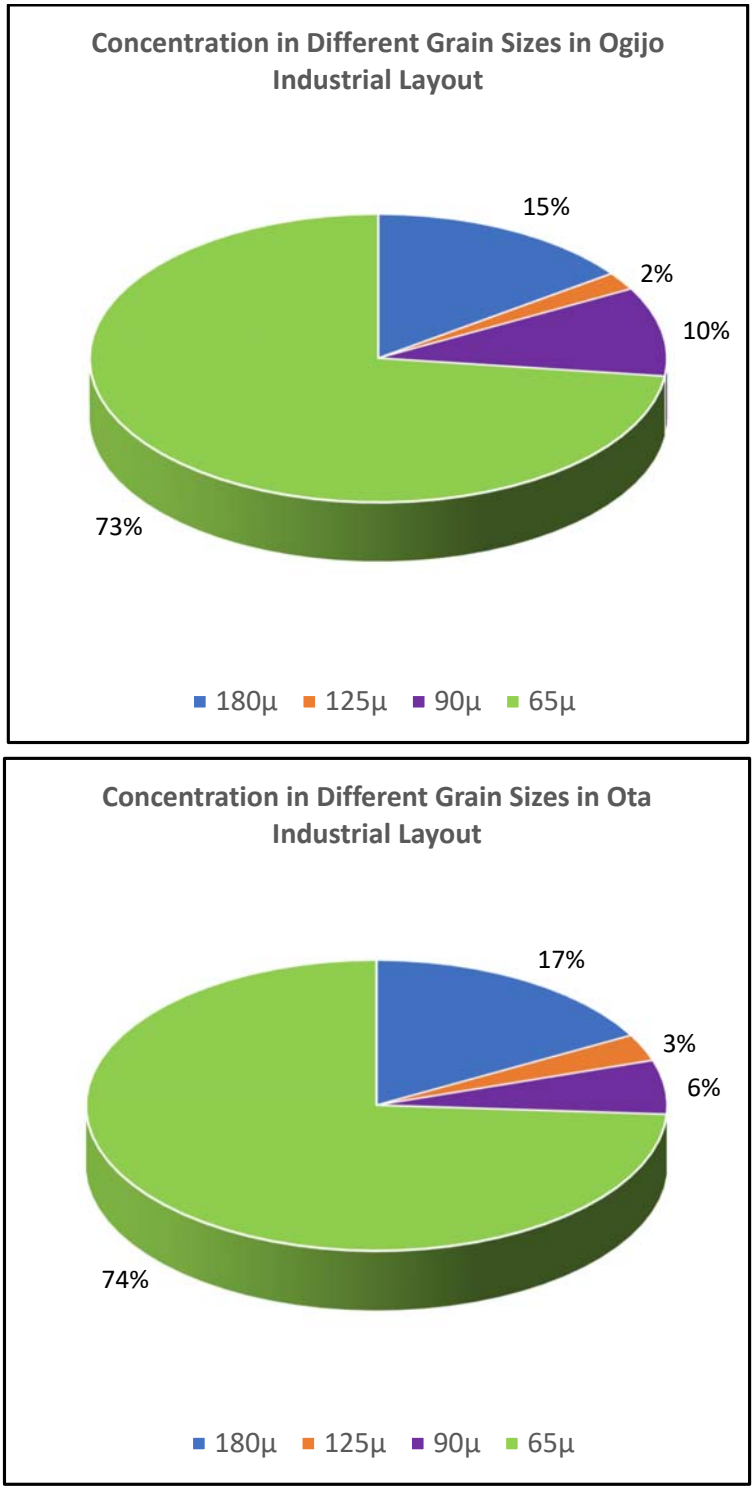

Figure 4.31: Concentration of pollutants in grain sizes in Ogijo and Ota industrial layouts

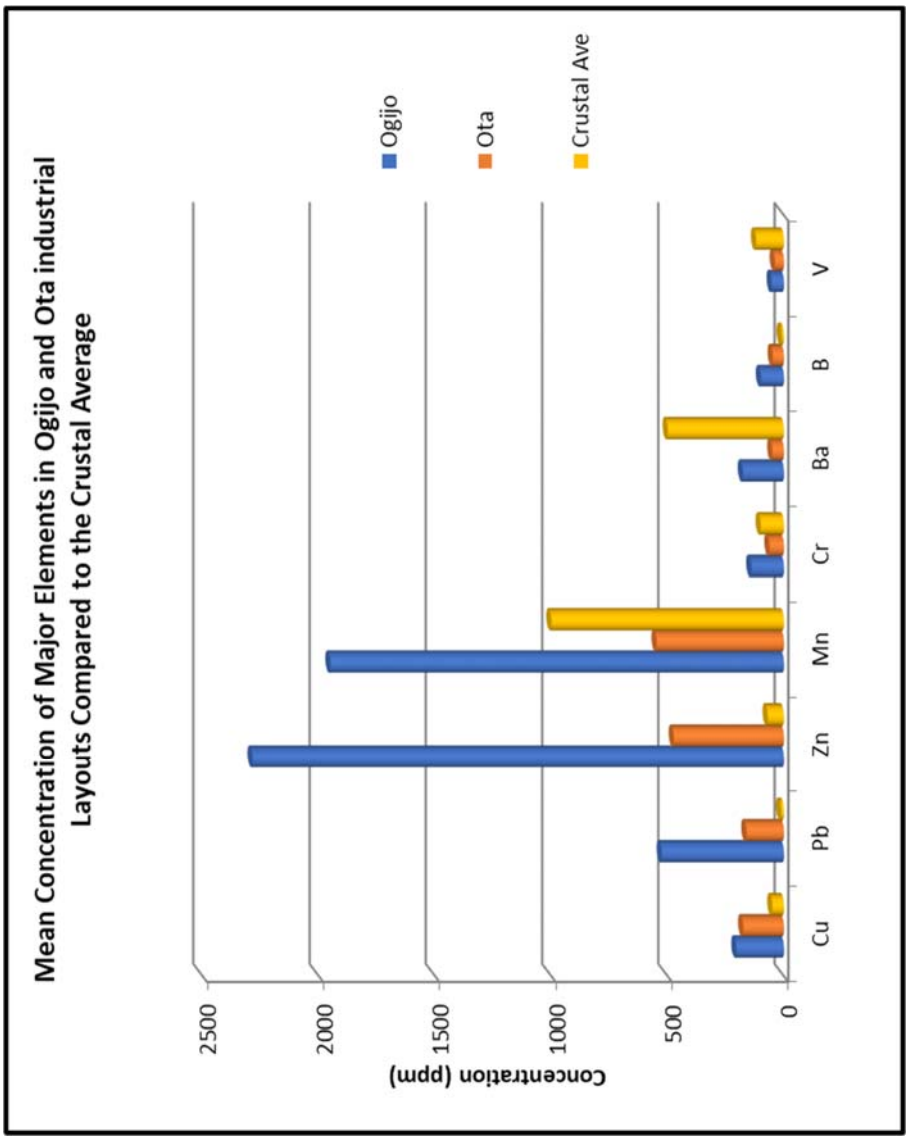

Figure 4.32: Concentration of major elements in Ogijo and Ota industrial layouts

CHAPTER FIVE

CONCLUSIONS AND RECOMMENDATIONS

5.1 Conclusions

Ogijo and Ota, two metal recycling industrial layouts which were originally located at the outskirt of the town have now been encroached into by residential quarters. In other to determine the level of heavy metal concentration in soils around the iron smelting plants in the layouts, the soils were assessed to ascertain the type and concentration of heavy metals in them, the concentration of the heavy metals in the 65, 90, 125 and 180 μm grain sizes of the soils and the spatial distribution of the pollutants in the industrial layouts.

Both the high and low frequency magnetic susceptibility readings of the whole samples from Ogijo and Ota recorded very high values. About 80% of the samples from Ogijo and 60% of the samples from Ota had X_{lf} values greater than the results obtained from the control site. The X_{lf} values were an indication of heavy metal pollution in the layouts.

The frequency dependence percentage which signifies the percentage of ferromagnetic minerals in samples, revealed that 6.04%, 8.12%, 9.44% and 10.30% of the heavy metals at 0, 10, 20 and 30 cm in Ogijo were ferromagnetic while, 7.26%, 6.04%, 7.7% and 9.5% at 0, 10, 20 and 30 cm depths respectively were recorded for Ota.

From both sites also, a typical stepladder like distribution in concentration of the pollutants were observed with depth. In Ogijo, 44.01% of the sample points had the highest magnetic susceptibility values at 0 cm depth which implied 44.01% of the sample points had the highest concentration of pollutants at the surface, while 12.88% of the sample points showed highest magnetic susceptibility readings at 10 cm depth, 11% of the sample points at 20 cm depth and 32.11% of the sample points had their highest values at 30 cm depth. Similar findings were recorded from Ota, where 54.55% of the sample points in Ota had the highest magnetic susceptibility readings or highest concentration of pollutants at the surface (0 cm depth). 9.09% of the highest magnetic susceptibility readings were recorded at 10 cm, 21.21% at 20 cm and 15.15% at 30 cm depth respectively. The results revealed that the surface soils at both industrial layouts were the most polluted.

Magnetic susceptibility and geochemical assessments of the soil samples from these industrial layouts have revealed a high concentration of heavy metal pollution. The plot of X_{fd}% against X_{lf} cm^3kg^{-1} indicated that about 80% of the contaminants were super paramagnetic while about 15% were minute metallic substances that were yet to be absorbed into the atomic lattice of the in-situ elements.

Magnetic susceptibility assessment of the whole samples from both sites showed a typical stepladder distribution with depth which is a reflection of the concentration of pollutants at the different depths of investigation. The variation of magnetic susceptibility with temperature analysis further confirmed that, the dominant pollutants in the sites are mainly the super paramagnetic metals.

The major heavy metals evaluated from both sites were Zinc, Manganese, Lead, Copper, Barium, Chromium, Vanadium and Boron. The concentrations of these metals showed a wide range in their values in the soil samples. In Ogijo, the order of decreasing concentration of the heavy metals were Zn > Mn > Pb > Cu > B > Cr > B. While in Ota it was Mn > Zn > Cu > Pb > V > Cr > Ba.

The ecological risk pollution single elemental pollution indices signified lead, zinc and copper had been severely and extremely enriched in the layouts in the decreasing order of Pb > Zn > Cu. Copper, lead and zinc were wide spread and detected in all the samples with concentrations (ppm) ranging between 16 to 834 and 1 to 1308; 29 to 2381 and 30 to 161 and, 54 to 10000 and 29 to1400, in Ogijo and Ota respectively. The average values of these elements exceeded the NESREA limits of 72, 164 and 421 for copper, lead and zinc respectively.

High geochemical affinity was demonstrated between the elements within the same locations; In Ogijo, Zn and Ba showed a strong positive correlation with Cu while Mn, B and Cr had significant positive correlation with Ba. Lead showed negative correlation with most of the metals and only significant positive correlation with zinc. The correlation matrix indicates that Cu, Mn, B, and Cr are from the same source material, while Zn and Ba were from the same source. Pb seems to be of a different source. In Ota Pb showed a significant correlation with Cu, while Zn with both Pb and Cu; the elements could be from the same source.

The analysis on the grain samples from both layouts revealed a spatial distribution of the pollutants that seems to favour the 65μm grain sizes at 0 cm depth. Soils with grain sizes of 65 μm are most polluted with about 73% and 74% of the pollutants found in this grain size in Ogijo and Ota industrial layouts respectively. The least polluted grain size in both layouts is the 125 μm which recorded 2% and 3% in Ogijo and Ota. Comparative study of the variation in magnetic susceptibility within the 65 μm with depth revealed that the 65 μm at 0 cm is the most polluted with value of 44.8%, while at 10 cm there was a reduction to 12.6% and a progressive enhancement at 20 and 30 cm with values of 17.2% and 24.1% respectively. At Ota the 65 μm grains at 0 cm were the most polluted having value of 48.1%. Same magnetic susceptibility value of 18.5% was recorded at 10 and 20 cm, while at 30 cm the value recorded was 14.8%.

Statistical analysis of the magnetic susceptibility readings of the whole samples revealed a general range of values between 100 and 6000 in Ogijo and in Ota and distinctively showed higher concentrations of the pollutants in and at the proximity of the recycling industries. Africa metal steel and Federated steel in Ogijo and Ota respectively were identified as the major contributors of pollutants in the industrial layouts.

The two sites which are located within sedimentary environments with negligible magnetic properties have no rivers in close vicinity. It is therefore, concluded that the soils in the two industrial layouts have been enriched beyond values that could be generated from geogenic source and are attributed to anthropogenic (metal recycling) activities.

5.2 Recommendations

As a matter of urgency, similar magnetic susceptibility and geochemical analysis should be carried out on the environment of all metal recycling plants within or outside industrial layouts in the nation.

The analysis should not be limited to soil but extended to water, air and vegetation in the environs of such industries.

For academic purposes, more studies should be done to asses heavy metal association with finer grain sizes of soil.

5.3 Contributions to Knowledge

Not many researches on heavy metal pollution have been done worldwide using the magnetic susceptibility as a tool. This research has confirmed that magnetic susceptibility method can be used as a proxy in assessing heavy metal pollution in soil samples.

The results from this research have further proven that heavy metal pollution is associated with heavy metal recycling. Though, metal recycling is economically acceptable worldwide, it has also brought along an inherent danger to life.

The uniqueness of combining magnetic susceptibility, geochemical, pollution indices and magnetic versus temperature analysis in studying heavy metal pollution has made this research a novel work in Nigeria and in the world at large.

And most importantly, this research has revealed that Ogijo and Ota industrial layouts which are both located in Nigeria, are extremely polluted with heavy metals especially lead, zinc and copper.

This research can be used as a justification for carrying out remediation activities on both sites.

REFERENCES

Adebiyi, A.O., 2015. Upper Cretaceous to Paleogene Palynosequence Stratigraphy of H-1 Well Offshore Eastern Dahomey Basin, Southwestern Nigeria: *International Journal of Research and Innovations in Earth Science (IJRIES)*, V. 2, P. 82-88.

Adediran, S.A., and Adegoke, O.S., 1987. Evolution of the Sedimentary Basins of the Gulf of Guinea. In: Matheis and Schandeimeir (eds), *Current Research in Africa Earth Sciences, Balkema, Rotterdam*, P. 283-286

Adegoke, O. S., 1969. Eocene Stratigraphy of Southern Nigeria: *Collogue sur Eocene v. III Bur. Rech. Geol. Min. Mem*., No. 69, P. 23 – 48.

Akinmosin, A., and Osinowo, O.O., 2010. Petrographical Study of Ewekoro Carbonate Rocks, in Ibese, Southwestern Nigeria: *Earth Sciences Research Journal*, V. 14, P. 187-196.

Ako, B.D., O.S. Adegoke and S.W. Peters, 1980. Stratigraphy of Oshosun formation in Southwestern Nigeria. *Journal of Mining Geology*, No. 17, P. 99-106.

Bankole, et al. (2006) Palynostratigraphic Age and Paleoenvironments of the newly exposed section of the Oshosun Formation in the Sagamu Quarry, Dahomey Basin. *Nigerian Association of Petroleum Explorationists Bulletin*. vol. 19, 1 P. 25 – 30

Billman, H.G., 1992. Offshore stratigraphy and paleontology of Dahomey Embayment, West Africa: *Nigerian Association of Petroleum Explorationist Bulletin*. V. 7, No. 2, P. 121-130.

Bouhsane, N., and Bouhlassa, S., 2018. Assessing Magnetic Susceptibility Profiles of Topsoils under Different Occupations: *International Journal of Geophysics,* V. 2018, Article ID 9481405, 8 pages

Brownfield, M.E., and Charpentier, R.R., 2006. Geology and Total Petroleum Systems of the Gulf of Guinea Province of West Africa U.S. *Geological Survey* Bulletin 2207C.

Chen C.W., Kao C. M., Chen C. F., and Dong C.D., 2007. Distribution and Accumulation of Metals in Sediments of Kaoshiung Harbor, Taiwan: *Chemosphere*, V. 66, P. 1431–1440.

Chunxia Z., Erwin A., and Qingqing Q., 2013. Heavy Metal Pollution in Farmland Irrigated with River Water near a Steel Plant – Magnetic and Geochemical Signature: *Geophysical Journal International*, V. 192, P. 963 - 974

Chunxia Z., Qingqing Q., John D.A.P., and Baochun H., 2011. Assessment of Heavy Metal Pollution from a Fe-smelting Plant in Urban River Sediments Using Environmental Magnetic and Geochemical Methods: *Elsevier Environmental Pollution*, V. 159, P. 3057-3070

d'Almeida, G.A.F., Kaki, C., and Adeoye, J.A., 2016. Benin and Western Nigeria Offshore Basins: A Stratigraphic Nomenclature Comparison: *International Journal of Geosciences*, V. **7**, P. 177-188.

Dearing, J. A., 1994. Environmental Magnetic Susceptibility: Using the BartingtonMS2 System: *British Library Cataloguing in Publication Data. Shive*, P. Suggestions for the use of SI Units in Magnetism. EOS, 1986. 6**7**, 25.

Dearing, J.A., Hay, K.L., Baban, S.M.J., Huddleston, A.S., Wellington, E.M.H., and Loveland, P.J., 1996. Magnetic-susceptibility of Soil - an Evaluation of Conflicting Theories Using a National Data Set: *Geophysical Journal International*, V. 127, P. 728–734.

Duan, X.M., Hu, S.Y., Yan, H.T., Blaha, U., Rösler, W., Appel, E., and Sun, W.H., 2010. Relationship Between Magnetic Parameters and Heavy Element Contents of Arable Soil Around a Steel Company: *Nanjing. Science China (Earth Sciences)* V. 53, No. 3, P. 411-418

Elueze A.A., and Nton, M.E., 2004. Organic Geochemical Appraisal of Limestones and Shales in Part of Eastern Dahomey Basin, Southwestern Nigeria: *J. Min. Geology*, V. 40, No. 1, P. 29-40.

European Environment Integration Research News Alert., Sept. 1, 2013. Soil Contamination: Impacts on Human Health: *Science for Environment Policy* Issue, V. 5, P. 6.

Evans, M. F., and Heller, F., 2003. Environmental Magnetism- Principles and Applications of Environmagnetics: *International Geophysics Series, Academic Press, Amsterdam*, V. 86. P. 293.

Faleyimu, O. I., Agbeja, B. O., and Akinyemi, O., 2013. State of Forest Regeneration in Southwest Nigeria: *Afr. J. Agric. Res.* V. 8, P. 3381–3383.

Gabrielyan, A.V., Shahnazaryan, G.A., and Minasyan, S.H., 2018. Distribution and Identification of Sources of Heavy Metals in the Voghji River Basin Impacted by Mining Activities (Armenia): *Journal of Chemistry,* V. 2018, Article ID 7172426, 9 pages

Idowu, J.O., Ajiboye, S.A., Ilesanmi, M.A. and Tanimola, A., 1993. Origin and Significance of Organic Matter of Oshosun Formation, Southwestern Nigeria: *Jour. Min. Geol*. V. 29, P. 9-17.

Jan Du Chene, R.E., and Salami, M.B., 1979. Palynology and Micropaleontology of the Upper Eocene of the Well Nsukka-1 (Niger Delta): *Compte Rendu desSéances de la Société de Physique et d'Histoire Naturelle de Genève*, V. 13, P. 5-9,

Jones, H.A., and Hockey, R.D., 1964. The Geology of South Western Nigeria: *Bulletin, Geological Survey, Nigeria,* V. 31, P. 101

Kletetschka, G., and Banerjee, S. K., 1995. Magnetic Stratigraphy of Chinese Loess as a Record of Natural Fires: *Geophys. Res. Lett*: V. 22, P. 1341-1343.

Kolawole, T.O., Olatunji, A.S., Jimoh, M.T., Fajemila, O.T., 2018. Heavy Metal Contamination and Ecological Risk Assessment in Soils and Sediments of an Industrial Area in Southwestern Nigeria: *Journal of Health & Pollution,* V. 8, No. 19

Kowalska, J.B., Mazurek, R., Siorek, M.G., Zaleski, T., 2018. Pollution indices as useful tools for the comprehensive evaluation of the degree of soil contamination–A review: *Environmental Geochemistry Health,* V. 40, P. 2395–2420

Mahesh, B., Baburao, C., Bhargavi, S., Sreekanth, N. and Sreenu, D., 2012. Inductively Coupled Plasma Mass Spectrometry (ICP-MS): *International Journal of Research in Pharmacy and Chemistry*, V. 2(3), PP. 671 – 680.

Maier, G., Scholger, R., and Schon, J., 2006. The Influence of Soil Moisture on Magnetic Susceptibility Measurements: *Journal of Applied Geophysics*, V. 59, P. 162- 175. http://dx.doi.org/10.1016/j.jappgeo.2005.10.001

Müller, G., 1969. Index of Geoaccumulation in the Sediments of the Rhine River: *Geo journal,* V. 2, P. 108-118.

NESREA (2011) "1st Eleven Gazetted Regulations Federal Republic of Nigeria Official Gazette".

Nton, M.E., Ikhane, P.R., and Tijani, M.N., 2009. Aspect of Rock-Evaluation Studies of the Maastrichtian-Eocene Sediments from Subsurface, in the Eastern Dahomey Basin Southwestern Nigeria: *European Journal of Scientific Research*, V. 25, P. 417-427.

Nuhu, G. O., 2009. Geology and Mineral Resources of Nigeria: *Springer Dordrecht Heidelberg London New York Library of Congress* Control Number: 2009921152 _c Springer-Verlag Berlin Heidelberg.

Ojeda, H. A. O., 1982. Structural Framework, Stratigraphy, and Evolution of Brazilian Marginal Basins: *American Association of Petroleum Geologist Bulletin***,** V.66, No. 6, P. 732 – 749.

Okosun, E.A., 1990. A Review of the Cretaceous Stratigraphy of the Dahomey Embayment, West Africa: *Cretaceous. Research, Elsevier*, V. 11, P. 17-27.

Olabode, S. O., 2015. Subsidence Patterns in the Nigerian Sector of Benin (Dahomey) Basin: Evidence from Three Offshore Wells. *Ife Journal of Science* vol. 17, no. 2.

Olabode, S.O., and Mohammed, M.Z., 2016. Depositional Facies and Sequence Stratigraphic Study in Parts of Benin (Dahomey) Basin SW Nigeria: Implications on the Re-Interpretation of Tertiary Sedimentary Successions: *International Journal of Geosciences*, V. 7, P. 210-228.

Olusola, K., Azegbobor, A., Olusegun, A., Emmanuel, J., and Maxwell, O., 2016. Geochemical Analysis of Domestic Groundwater Sources in a Suburb of Ota, Southwestern Nigeria: *Indian Journal of Science and Technology*, V. 9, No. 22, DOI: 10.17485/ijst/2016/v9i22/87337.

Omatsola, M.E., and Adegoke, O.S., 1981. Tectonic Evolution and Cretaceous Stratigraphy of the Dahomey Basin: *Journal of Mining and Geology*, V. 18, No. 1, P. 130-137.

Onuoha, K.O., 1999. Structural Features of Nigeria's Coastal Margin: An Assessment Based on Age Data from Wells: *Journal of African Earth Sciences*, V. 29, No. 3, P. 485-499.

Orosun, M. M., Oniku, S. A., Peter, A., Orosun, R. O, Salawu, N.B., and Hitler, L., 2020. Magneticsusceptibility Measurement and Heavy Metal Pollution at an Automobile Station in Ilorin, North-Central Nigeria: *Environmental Research Communications*, V. 2 015001.

Rachwał, M., Wawer, M., Magiera, T., and Steinnes, E., 2017. Integration of Soil Magnetometry and Geochemistry for Assessment of Human Health Risk from Metallurgical Slag Dumps: *Environ Sci Pollut Res,* V. 24, P. 26410–26423

Reyment, R.A., 1965. Aspects of the Geology of Nigeria: *Ibadan University Press*, P. 133.

Shendi, E. H., Attia,T. E. and Shehata, M.A., 2013. Magnetic Susceptibility as an Indicator to Heavy Metal Contamination of the Urban Top Soil in Port Said City and Surroundings: *Egypt Journal of Environmental Science, Toxicology and Food Technology*, V. 6, PP. 47-55.

Singer, M.J., and Fine, P., 1989. Pedogenic Factors Affecting Magnetic Susceptibility of Northern Californian Soil: *Soil Sci. SOC.* Am. J., 53, 1119-1127.

Taylor, S.R., and McLennan, S.M., 1985. The Continental Crust: Its Composition and Evolution: Blackwell, Oxford, UK., ISBN-13: 978-0632011483, P. 312.

The Ministry of Mines and Steel Development (MMSD), 2010.

The US Environmental Protection Agency (EPA), 2000.

The World Health Organization (2011).

Thompson, R., and Oldfield, F., (1986). Environmental Magnetism. Allen and Unwin, London, http://dx.doi.org/10.1007/978-94-011-8036-8.

Warra, A.A., and Jimoh, W. L.O., 2011. Overview of an Inductively Coupled Plasma (ICP) System: *International Journal of Chemical Research*, V. 3, No. 2, P. 41–48.

Wojas, A., 2017. The Magnetic Susceptibility of Soils in Krakow, Southern Poland: *Acta Geophysica - Springer*. V. 65, P. 453–463.

Zhu, H., Bing, H., Yi, H., Wu.Y., and Sun, Z., 2018. Spatial Distribution and Contamination Assessment of Heavy Metals in Surface Sediments of the Caofeidian

Adjacent Sea after the Land Reclamation, Bohai Bay: *Journal of Chemistry*, V, 2018, Article ID 2049353, 13 pages.

APPENDICE

Appendix 3.1 Sample Drying Under Shade Before Crushing

Appendix 3.2: Electronic Weighing Balance Used to Weigh the Samples

Appendix 3.3: The Bartington Magnetic Susceptibility Suites Used for Magnetic Susceptibility Analysis

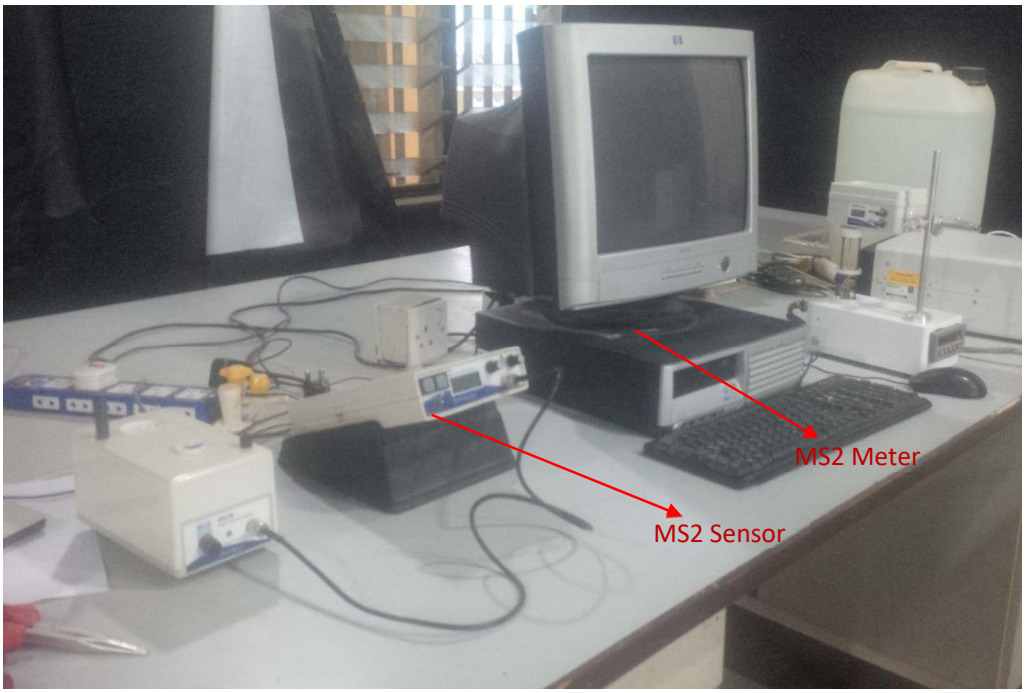

Appendix 3.4: The Bartington Temperature Analysis Suites Used for Temperature Vs Magnetic Susceptibility Analysis

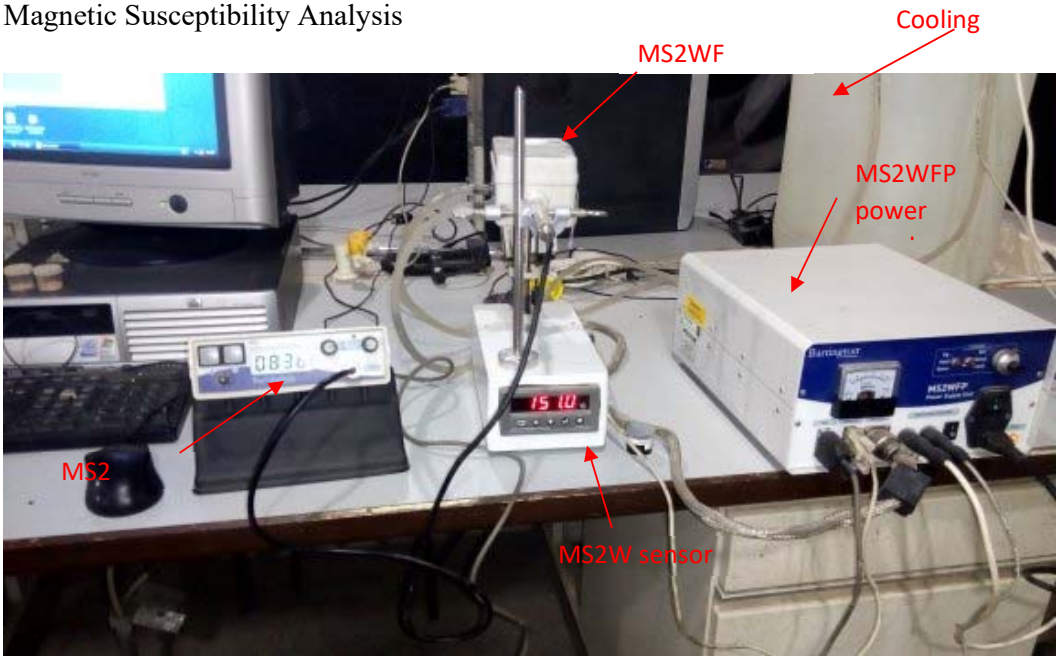

Appendix 4.1: Variation in Low and High Magnetic Susceptibility Readings of Whole Samples with Depth in All the Location in Ogijo Industrial Layout

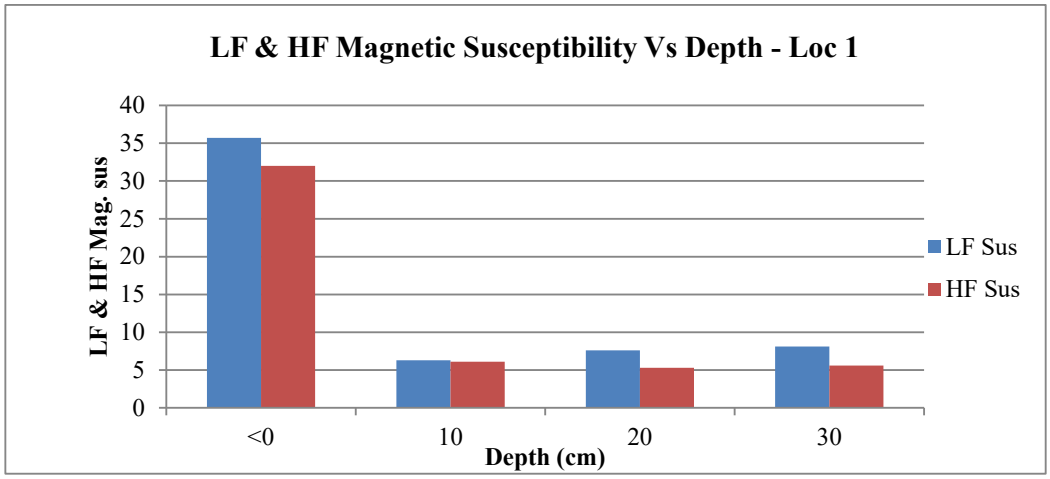

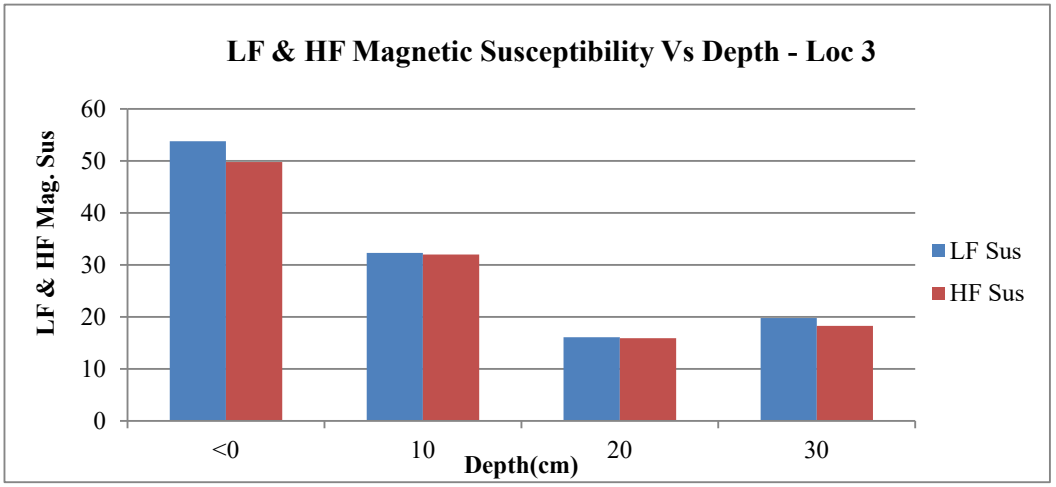

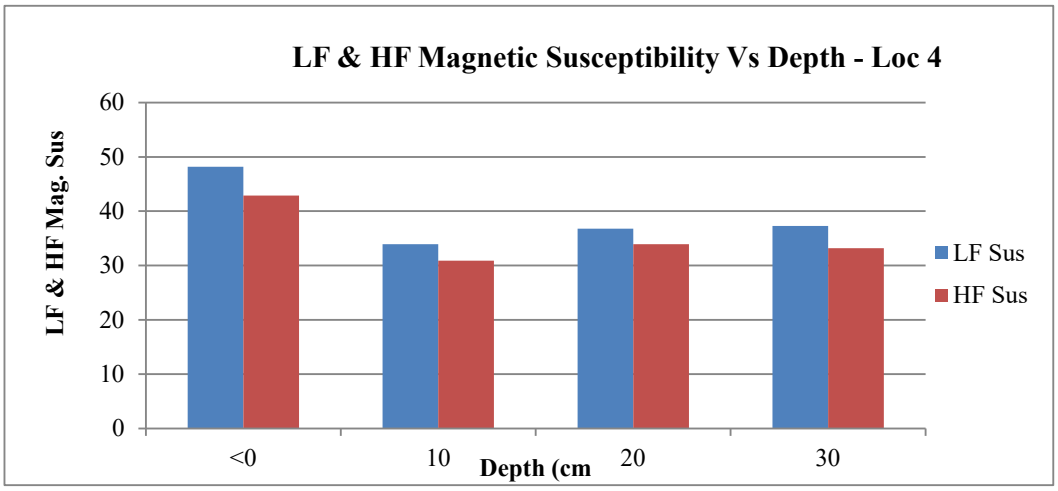

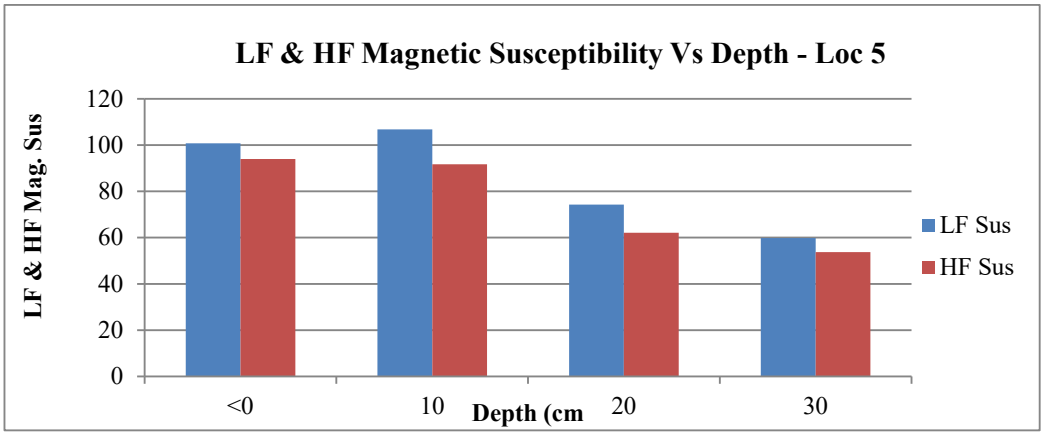
LF & HF Magnetic Susceptibility Vs Depth - Loc 5
LF & HF Mag. Sus
120
100
80
60
40
20
0
<0
10
20
30
Depth (cm
LF Sus
HF Sus

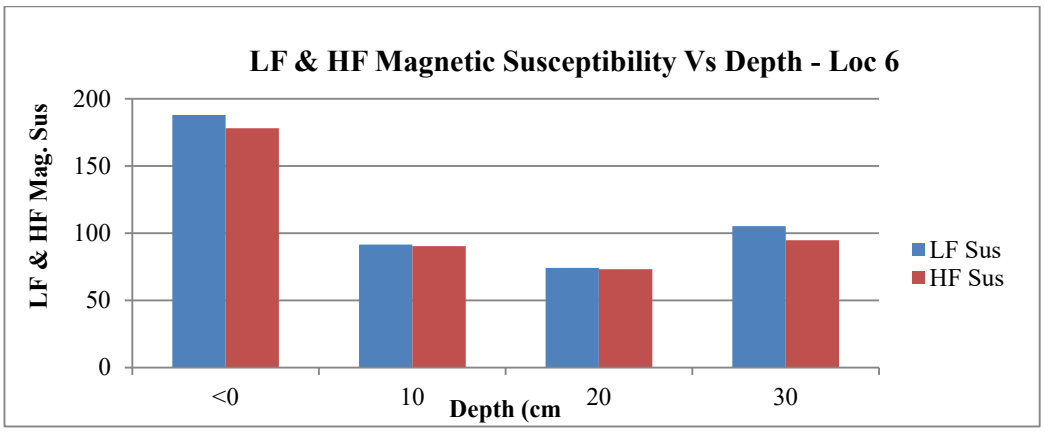
LF & HF Magnetic Susceptibility Vs Depth - Loc 6
LF & HF Mag. Sus
200
150
100
50
0
<0
10
20
30
Depth (cm
LF Sus
HF Sus

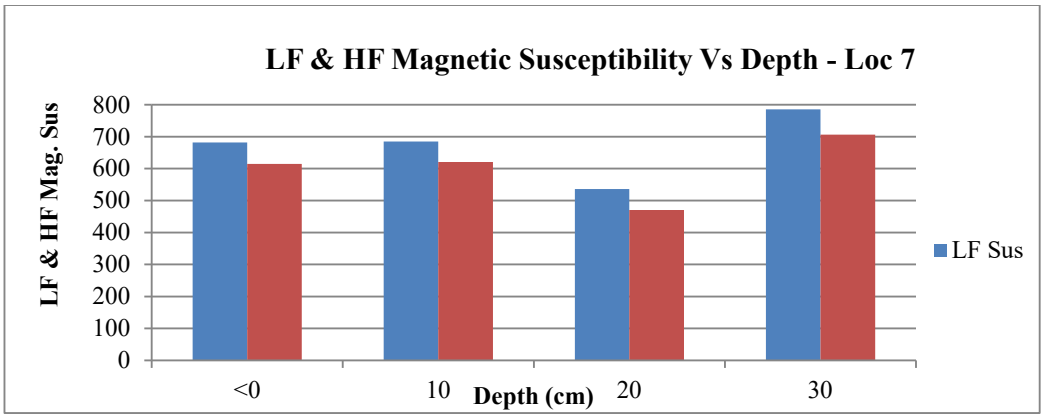
LF & HF Magnetic Susceptibility Vs Depth - Loc 7
LF & HF Mag. Sus
800
700
600
500
400
300
200
100
0
<0
10
20
30
Depth (cm)
LF Sus

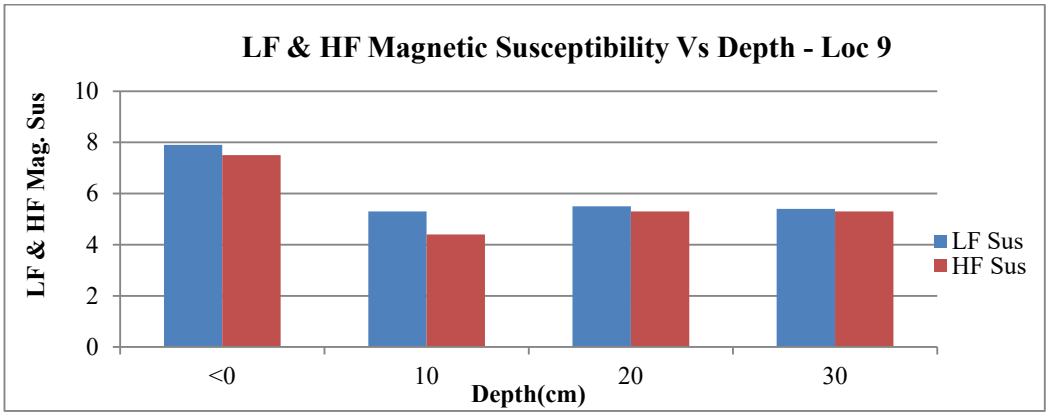
LF & HF Magnetic Susceptibility Vs Depth - Loc 9
LF & HF Mag. Sus
10
8
6
4
2
0
<0
10
20
30
Depth(cm)
LF Sus
HF Sus

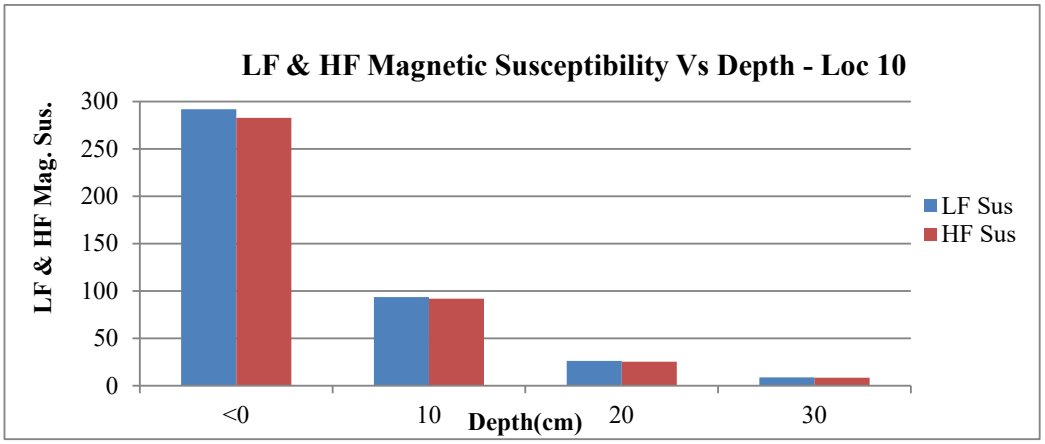
LF & HF Magnetic Susceptibility Vs Depth - Loc 10
LF & HF Mag. Sus.
300
250
200
150
100
50
0
<0
10
20
30
Depth(cm)
LF Sus
HF Sus

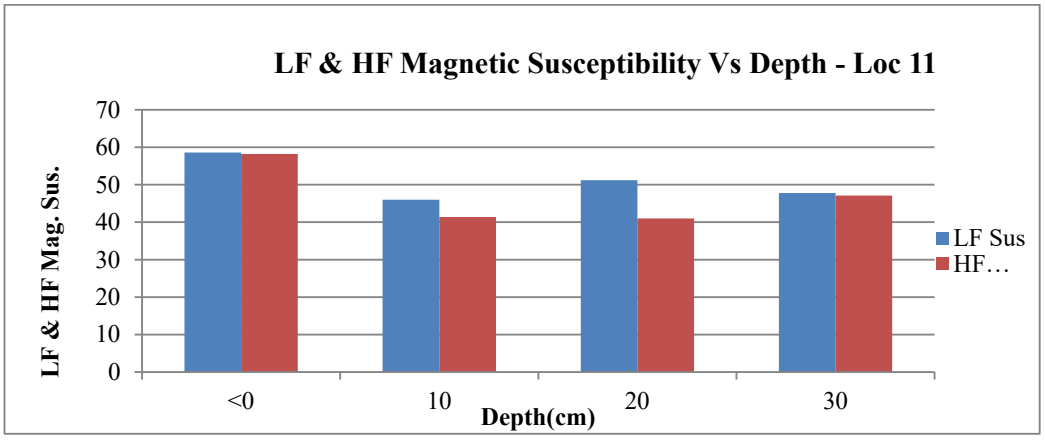
LF & HF Magnetic Susceptibility Vs Depth - Loc 11
LF & HF Mag. Sus.
70
60
50
40
30
20
10
0
<0
10
20
30
Depth(cm)
LF Sus
HF…

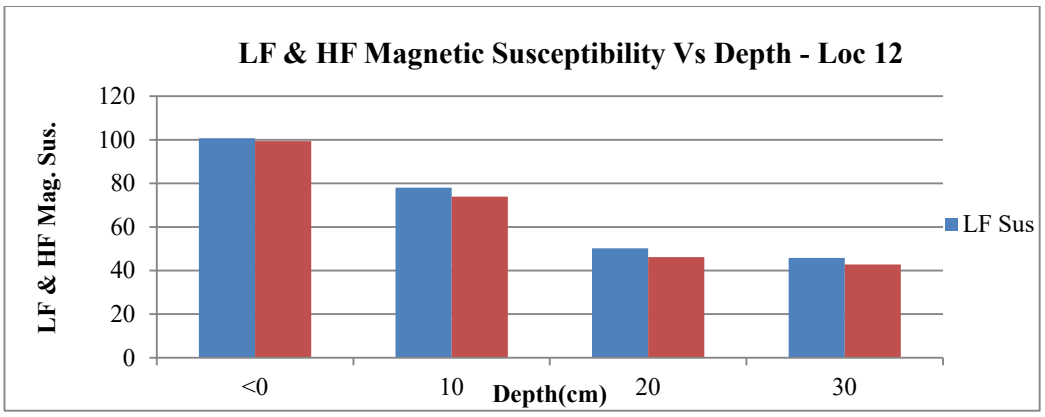
LF & HF Magnetic Susceptibility Vs Depth - Loc 12
LF & HF Mag. Sus.
120
100
80
60
40
20
0
<0
10
20
30
Depth(cm)
LF Sus

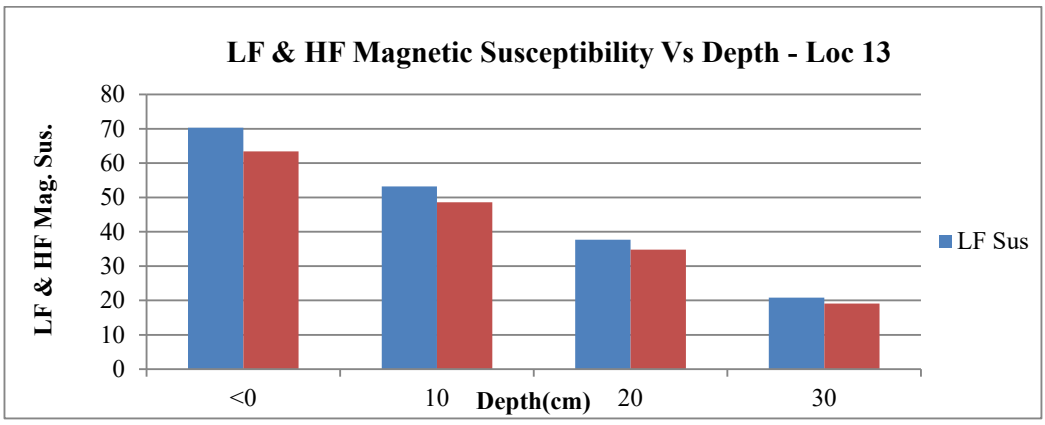
LF & HF Magnetic Susceptibility Vs Depth - Loc 13
LF & HF Mag. Sus.
80
70
60
50
40
30
20
10
0
<0
10
20
30
Depth(cm)
LF Sus

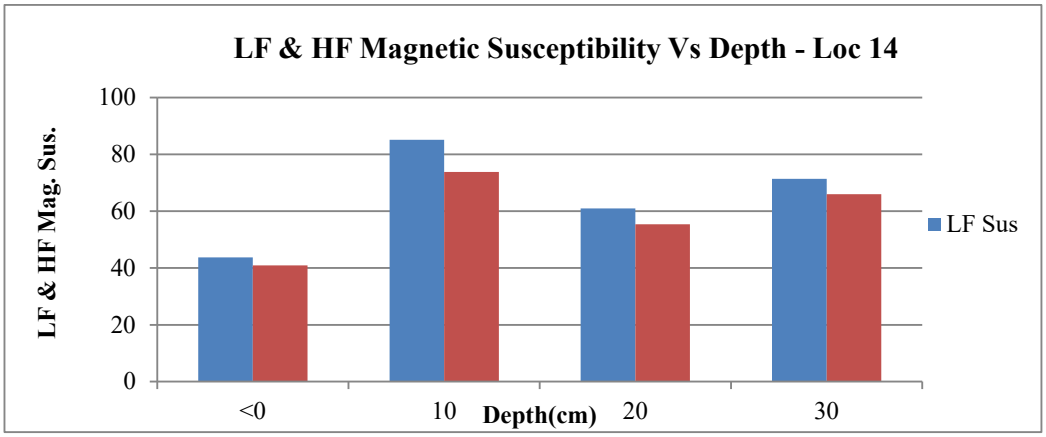
LF & HF Magnetic Susceptibility Vs Depth - Loc 14
LF & HF Mag. Sus.
100
80
60
40
20
0
<0
10
Depth(cm)
20
30
LF Sus

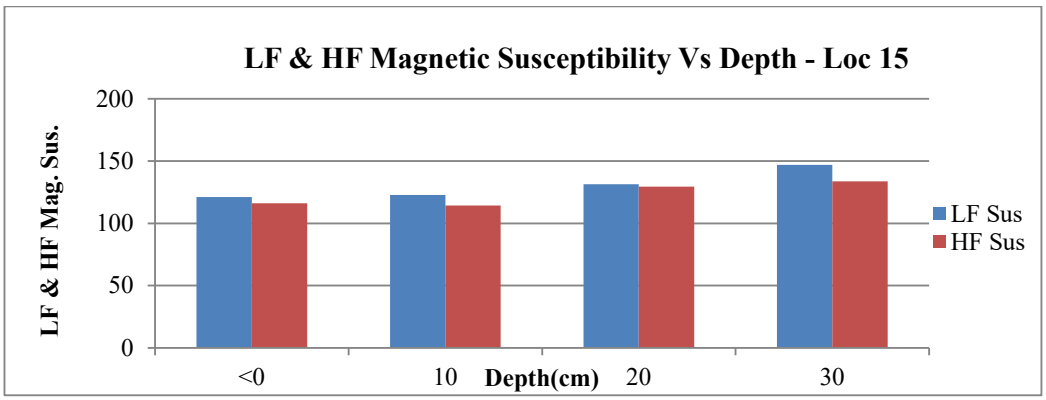
LF & HF Magnetic Susceptibility Vs Depth - Loc 15
LF & HF Mag. Sus.
200
150
100
50
0
<0
10
Depth(cm)
20
30
LF Sus
HF Sus

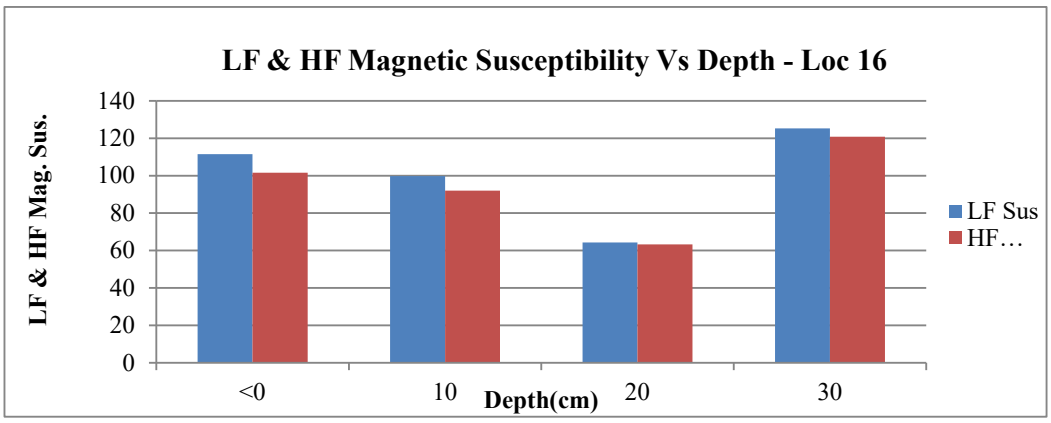
LF & HF Magnetic Susceptibility Vs Depth - Loc 16
LF & HF Mag. Sus.
140
120
100
80
60
40
20
0
<0
10
Depth(cm)
20
30
LF Sus
HF…

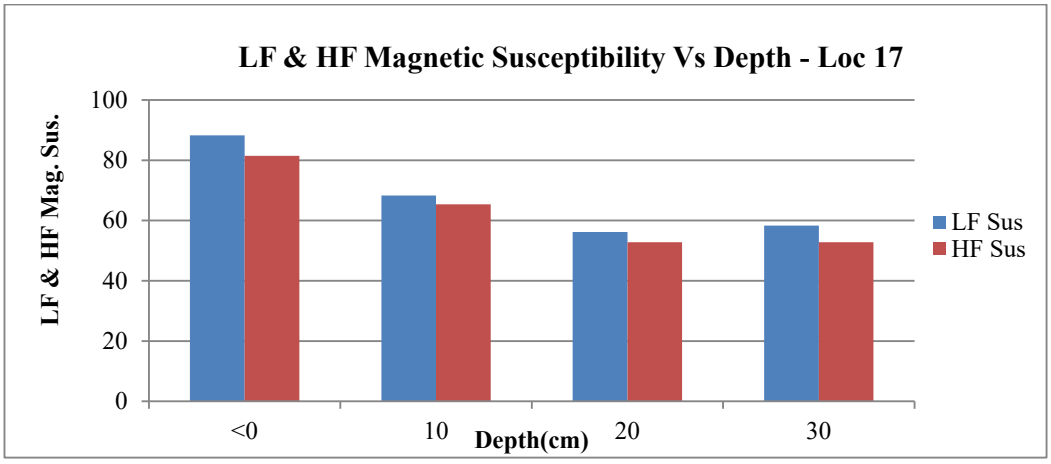
LF & HF Magnetic Susceptibility Vs Depth - Loc 17
LF & HF Mag. Sus.
100
80
60
40
20
0
<0
10
Depth(cm)
20
30
LF Sus
HF Sus

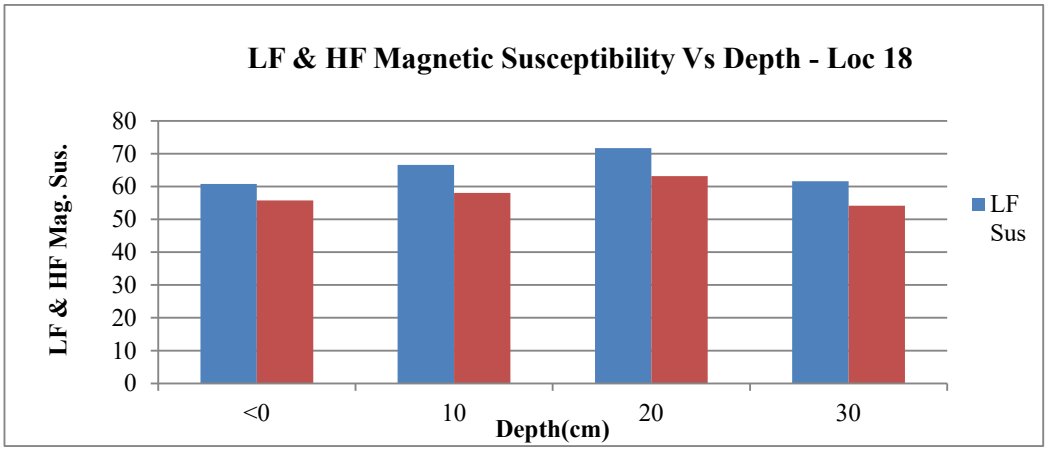
LF & HF Magnetic Susceptibility Vs Depth - Loc 18
LF & HF Mag. Sus.
80
70
60
50
40
30
20
10
0
<0
10
20
30
Depth(cm)
LF Sus

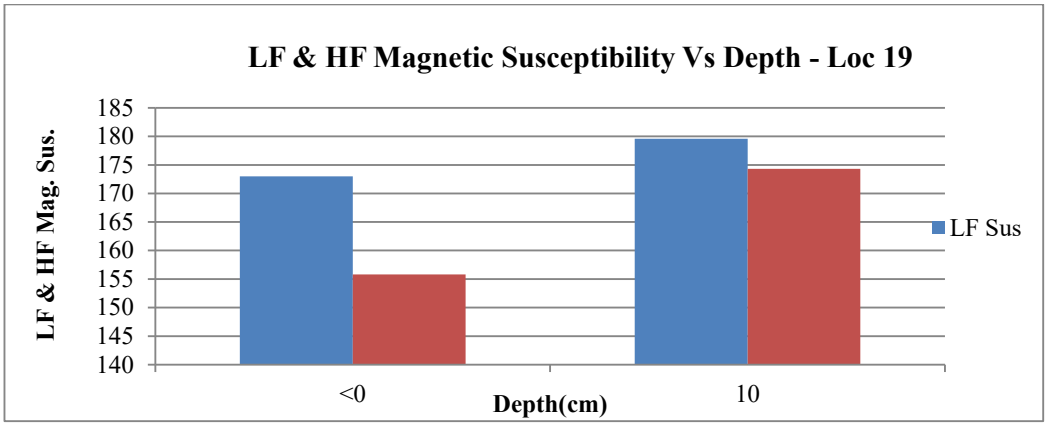
LF & HF Magnetic Susceptibility Vs Depth - Loc 19
LF & HF Mag. Sus.
185
180
175
170
165
160
155
150
145
140
<0
Depth(cm)
10
LF Sus

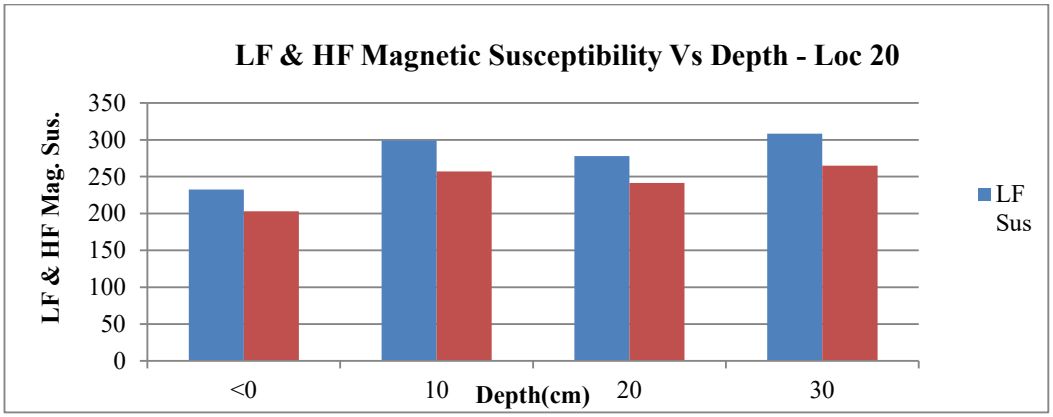
LF & HF Magnetic Susceptibility Vs Depth - Loc 20
LF & HF Mag. Sus.
350
300
250
200
150
100
50
0
<0
10
Depth(cm)
20
30
LF Sus

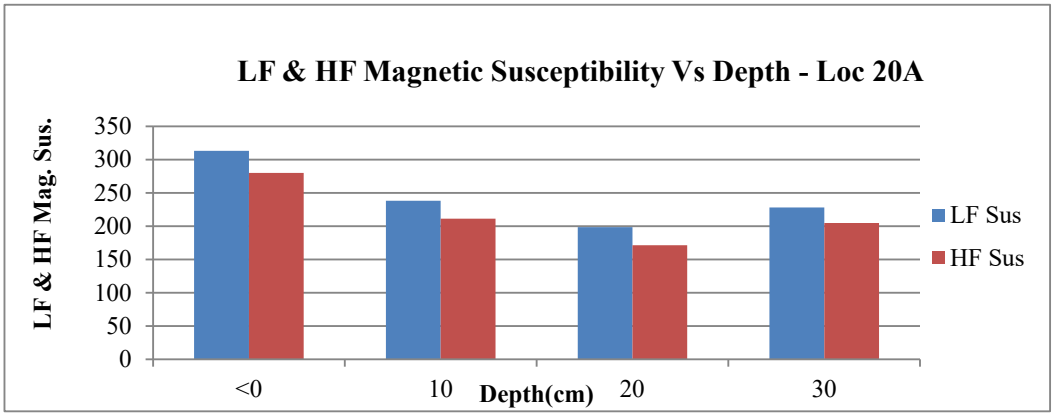
LF & HF Magnetic Susceptibility Vs Depth - Loc 20A
LF & HF Mag. Sus.
350
300
250
200
150
100
50
0
<0
10
Depth(cm)
20
30
LF Sus
HF Sus

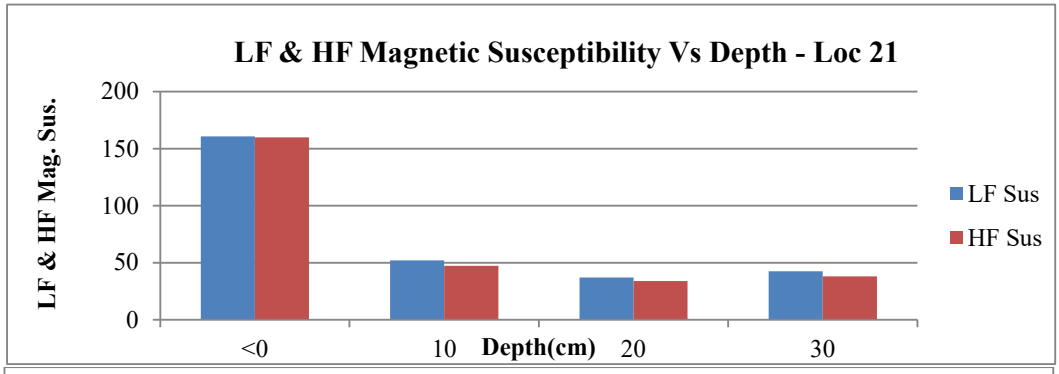
LF & HF Magnetic Susceptibility Vs Depth - Loc 21
LF & HF Mag. Sus.
200
150
100
50
0
<0
10
20
30
Depth(cm)
LF Sus
HF Sus

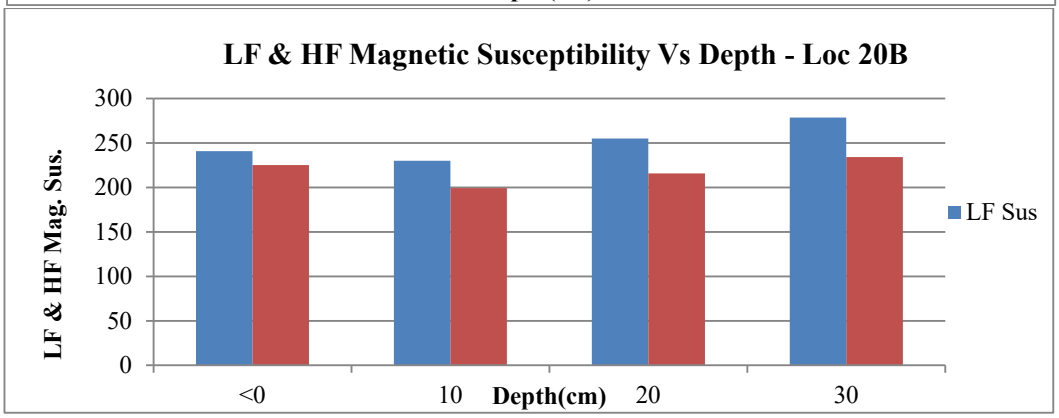
LF & HF Magnetic Susceptibility Vs Depth - Loc 20B
LF & HF Mag. Sus.
300
250
200
150
100
50
0
<0
10
20
30
Depth(cm)
LF Sus

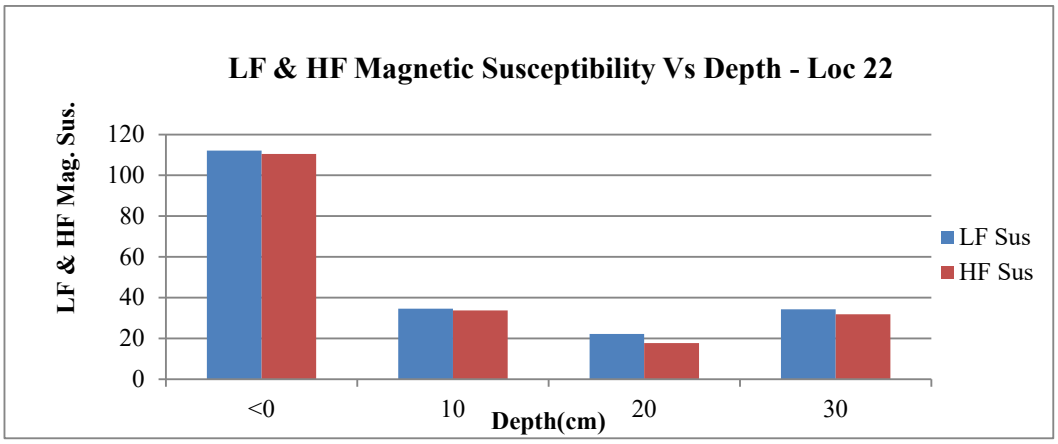
LF & HF Magnetic Susceptibility Vs Depth - Loc 22
LF & HF Mag. Sus.
120
100
80
60
40
20
0
<0
10
20
30
Depth(cm)
LF Sus
HF Sus

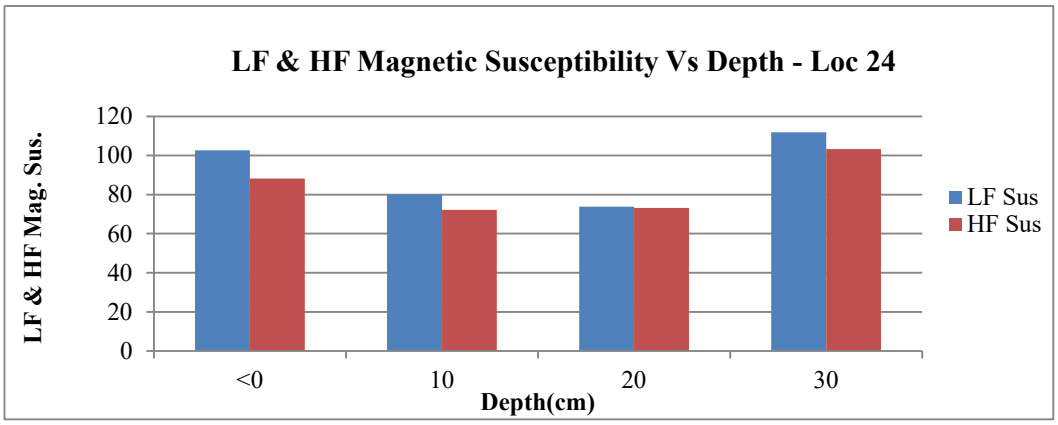
LF & HF Magnetic Susceptibility Vs Depth - Loc 24
LF & HF Mag. Sus.
120
100
80
60
40
20
0
<0
10
20
30
Depth(cm)
LF Sus
HF Sus

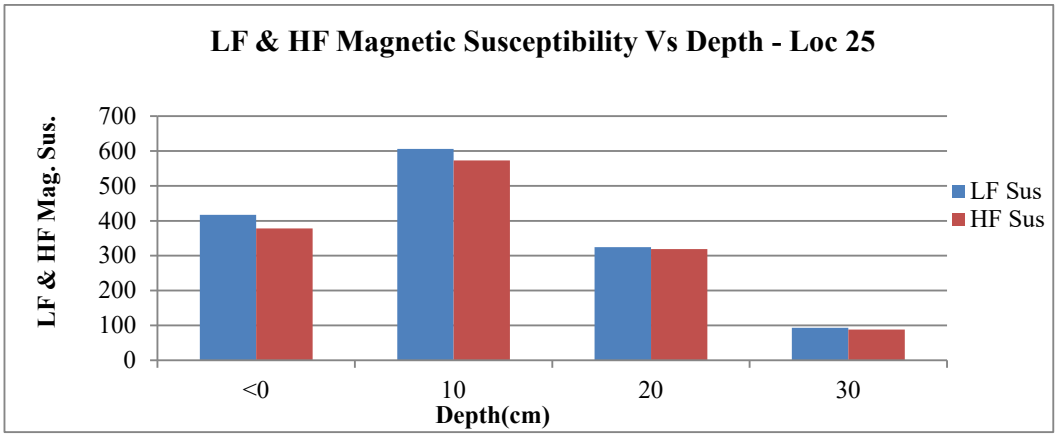
LF & HF Magnetic Susceptibility Vs Depth - Loc 25
LF & HF Mag. Sus.
700
600
500
400
300
200
100
0
<0
10
20
30
Depth(cm)
LF Sus
HF Sus

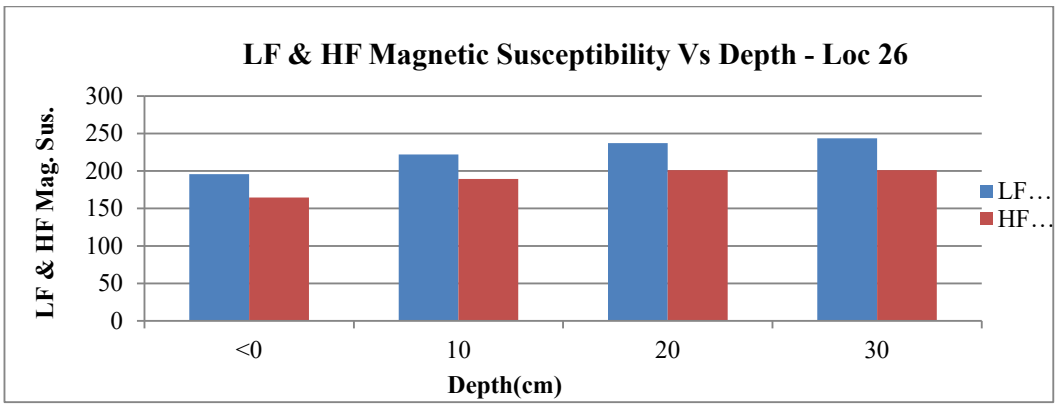
LF & HF Magnetic Susceptibility Vs Depth - Loc 26
LF & HF Mag. Sus.
300
250
200
150
100
50
0
<0
10
20
30
Depth(cm)
LF…
HF…

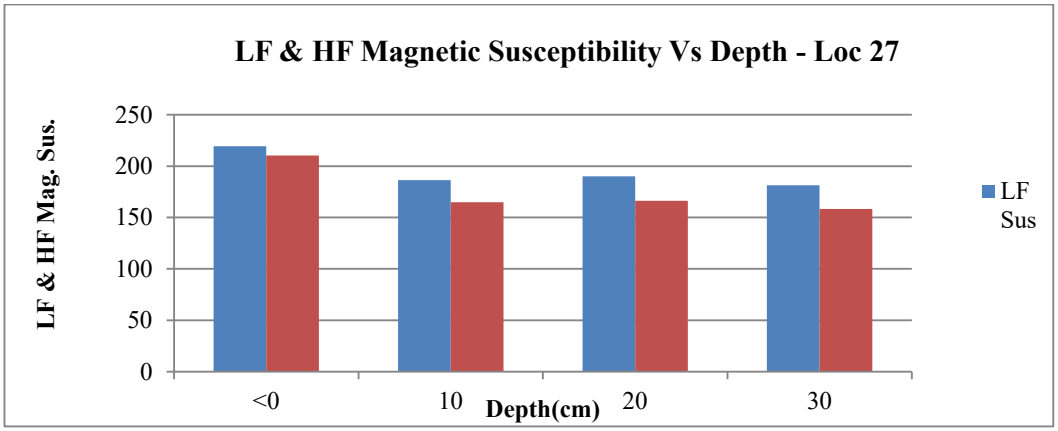
LF & HF Magnetic Susceptibility Vs Depth - Loc 27
LF & HF Mag. Sus.
250
200
150
100
50
0
<0
10
Depth(cm)
20
30
LF
Sus

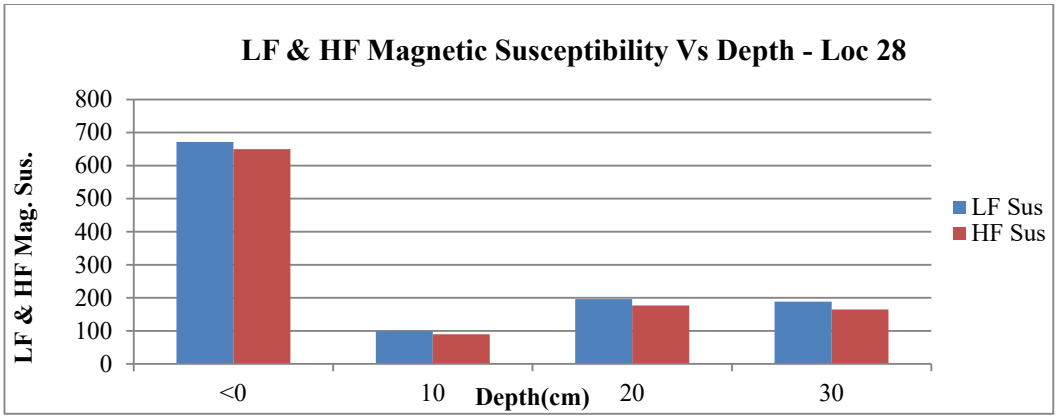
LF & HF Magnetic Susceptibility Vs Depth - Loc 28
LF & HF Mag. Sus.
800
700
600
500
400
300
200
100
0
<0
10
Depth(cm)
20
30
LF Sus
HF Sus

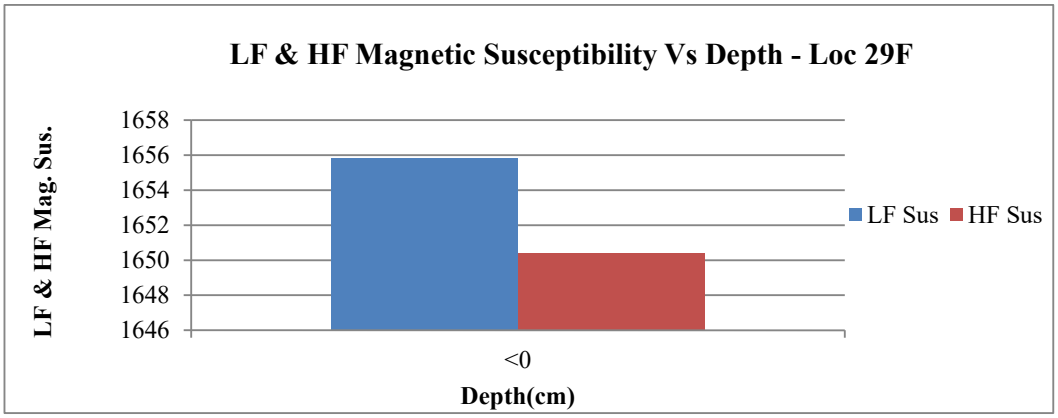
LF & HF Magnetic Susceptibility Vs Depth - Loc 29F
LF & HF Mag. Sus.
1658
1656
1654
1652
1650
1648
1646
<0
Depth(cm)
LF Sus
HF Sus

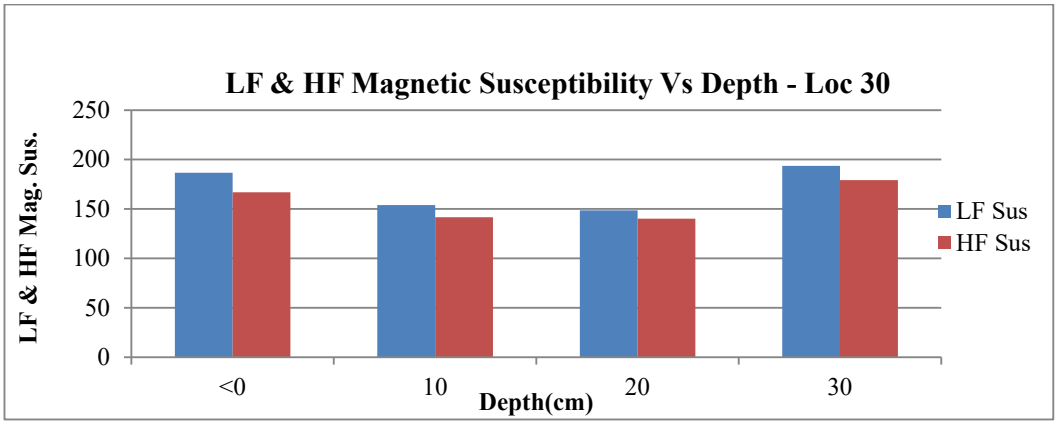
LF & HF Magnetic Susceptibility Vs Depth - Loc 30
LF & HF Mag. Sus.
250
200
150
100
50
0
<0
10
20
30
Depth(cm)
LF Sus
HF Sus

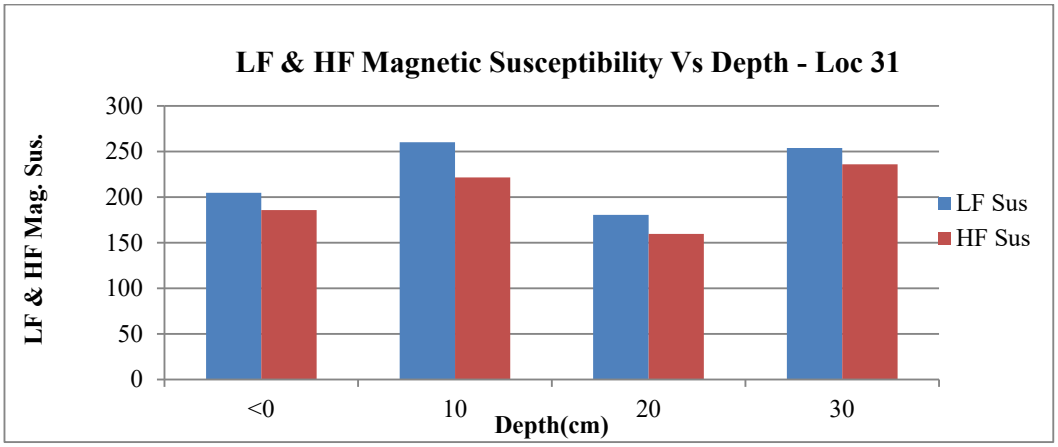
LF & HF Magnetic Susceptibility Vs Depth - Loc 31
LF & HF Mag. Sus.
300
250
200
150
100
50
0
<0
10
20
30
Depth(cm)
LF Sus
HF Sus

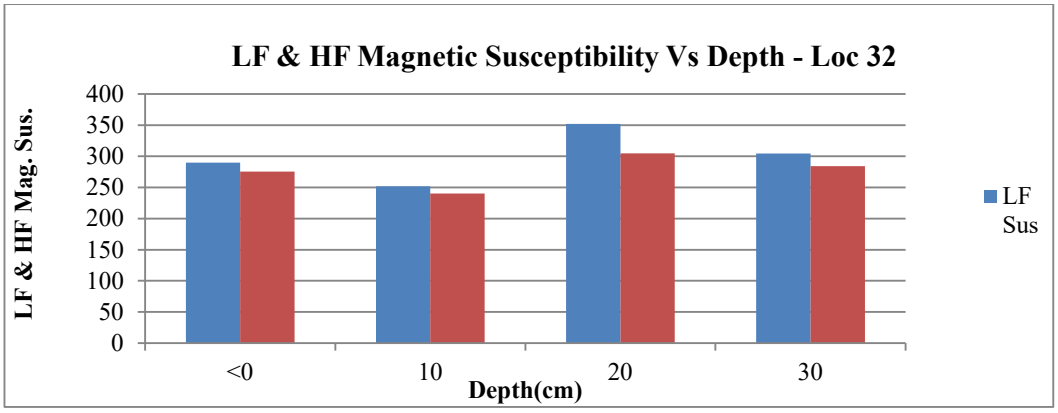
LF & HF Magnetic Susceptibility Vs Depth - Loc 32
LF & HF Mag. Sus.
400
350
300
250
200
150
100
50
0
<0
10
20
30
Depth(cm)
LF Sus

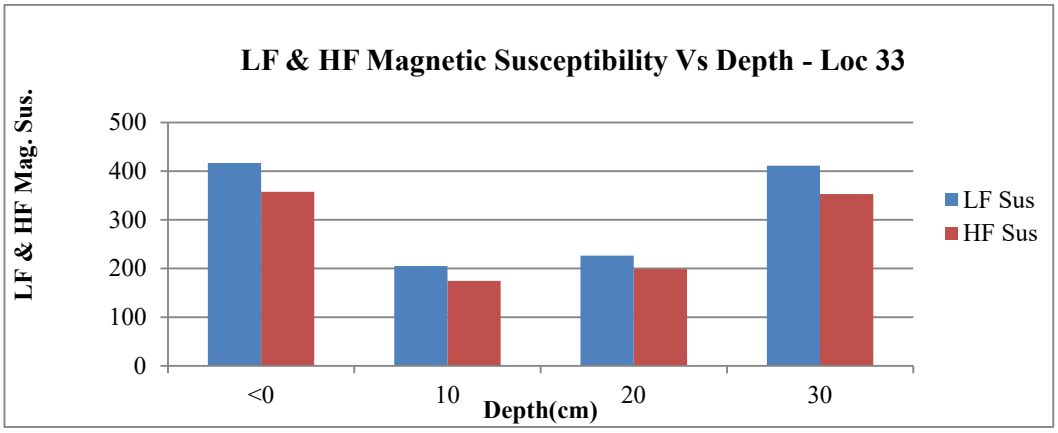
LF & HF Magnetic Susceptibility Vs Depth - Loc 33
LF & HF Mag. Sus.
500
400
300
200
100
0
<0
10
20
30
Depth(cm)
LF Sus
HF Sus

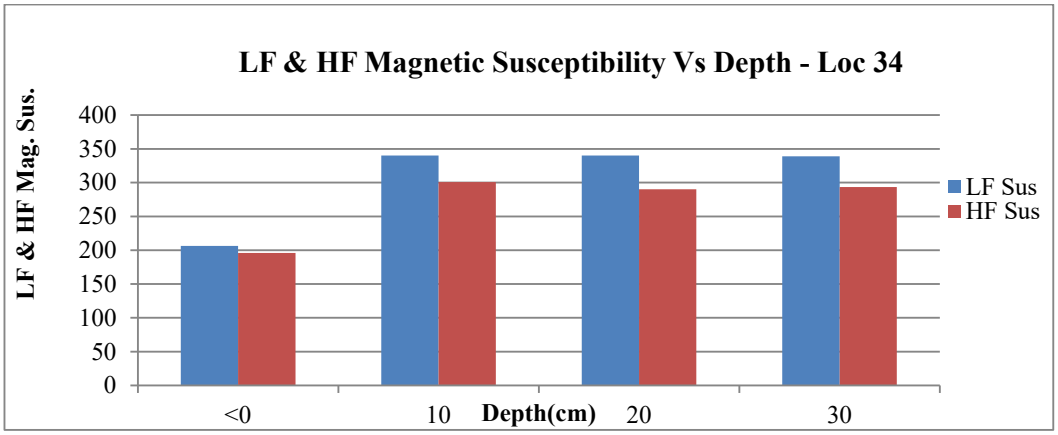
LF & HF Magnetic Susceptibility Vs Depth - Loc 34
LF & HF Mag. Sus.
400
350
300
250
200
150
100
50
0
<0
10
Depth(cm)
20
30
LF Sus
HF Sus

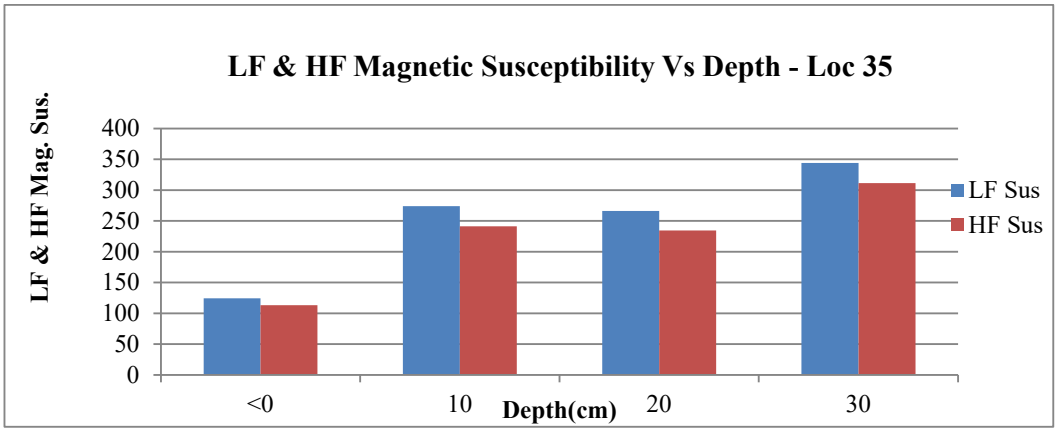
LF & HF Magnetic Susceptibility Vs Depth - Loc 35
LF & HF Mag. Sus.
400
350
300
250
200
150
100
50
0
<0
10
Depth(cm)
20
30
LF Sus
HF Sus

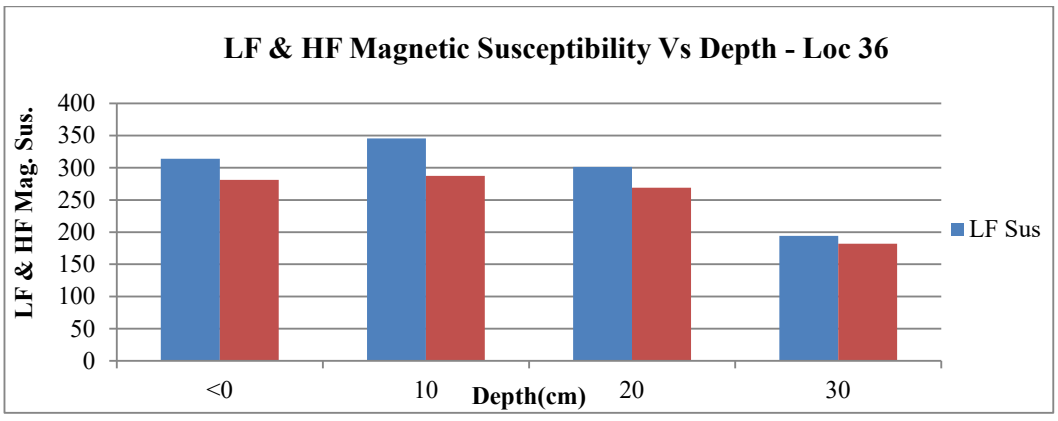
LF & HF Magnetic Susceptibility Vs Depth - Loc 36
LF & HF Mag. Sus.
400
350
300
250
200
150
100
50
0
<0
10
Depth(cm)
20
30
LF Sus

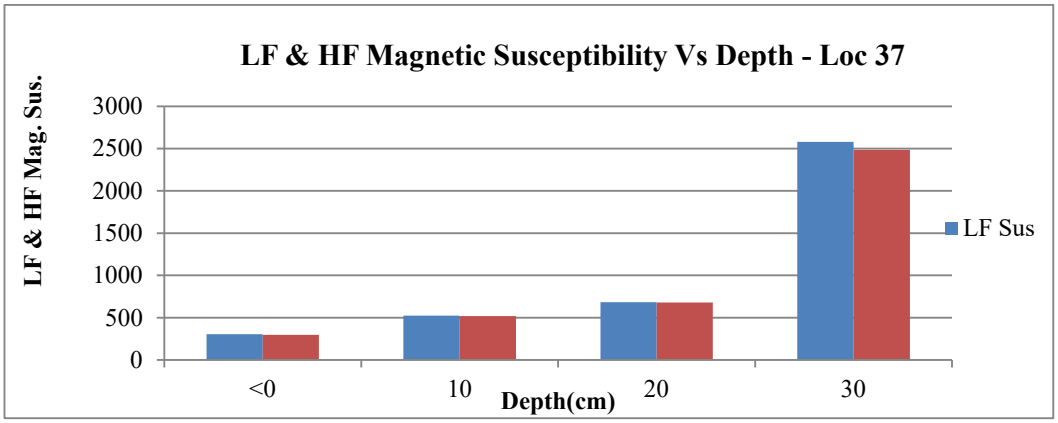
LF & HF Magnetic Susceptibility Vs Depth - Loc 37
LF & HF Mag. Sus.
3000
2500
2000
1500
1000
500
0
<0
10
20
30
Depth(cm)
LF Sus

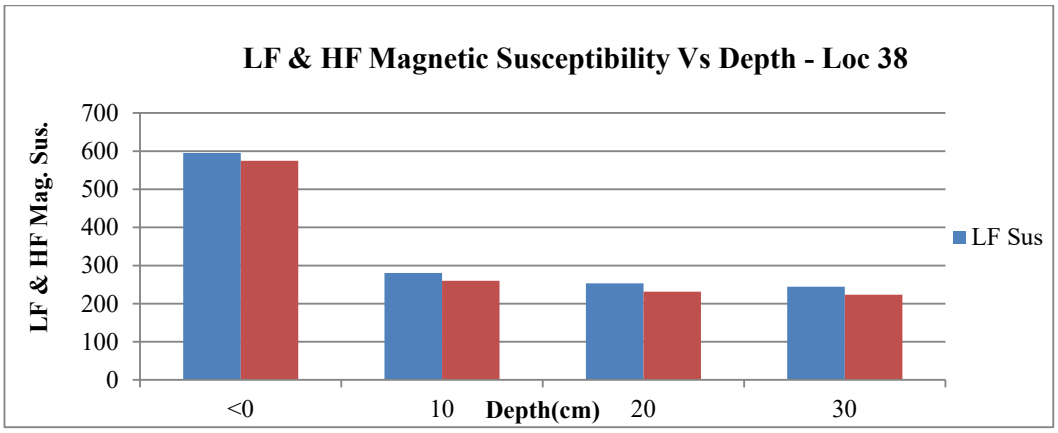
LF & HF Magnetic Susceptibility Vs Depth - Loc 38
LF & HF Mag. Sus.
700
600
500
400
300
200
100
0
<0
10
Depth(cm)
20
30
LF Sus

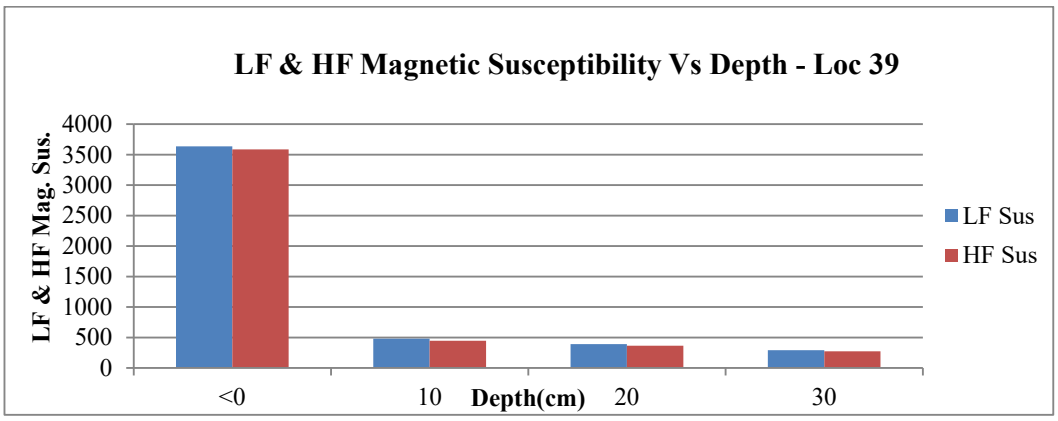
LF & HF Magnetic Susceptibility Vs Depth - Loc 39
LF & HF Mag. Sus.
4000
3500
3000
2500
2000
1500
1000
500
0
<0
10
Depth(cm)
20
30
LF Sus
HF Sus

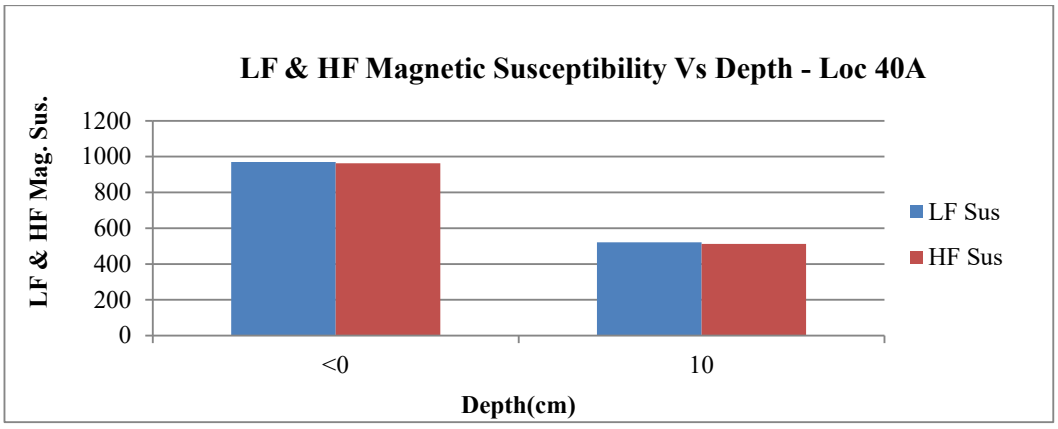
LF & HF Magnetic Susceptibility Vs Depth - Loc 40A
LF & HF Mag. Sus.
1200
1000
800
600
400
200
0
<0
10
Depth(cm)
LF Sus
HF Sus

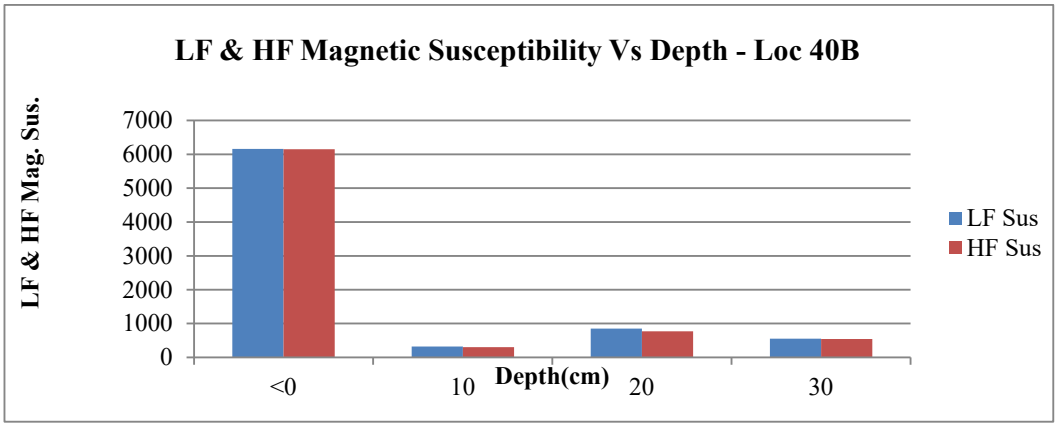
LF & HF Magnetic Susceptibility Vs Depth - Loc 40B
LF & HF Mag. Sus.
7000
6000
5000
4000
3000
2000
1000
0
<0
10
20
30
Depth(cm)
LF Sus
HF Sus

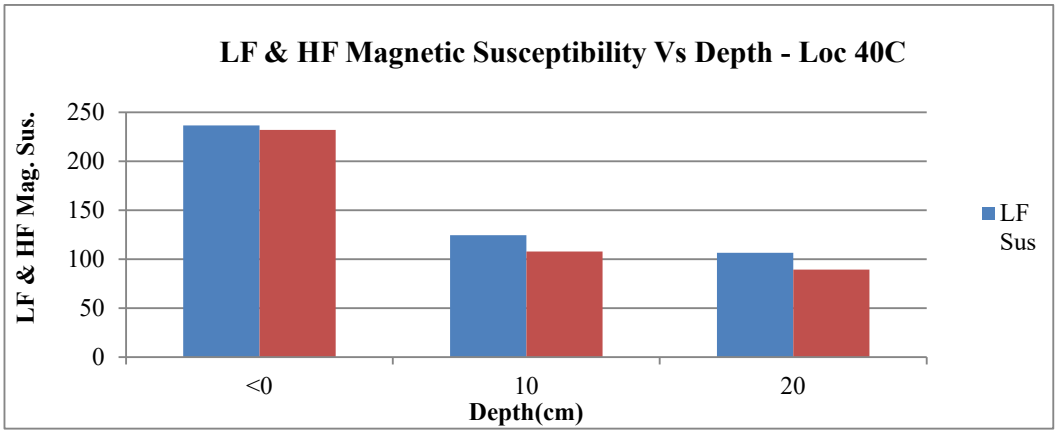
LF & HF Magnetic Susceptibility Vs Depth - Loc 40C
LF & HF Mag. Sus.
250
200
150
100
50
0
<0
10
20
Depth(cm)
LF Sus

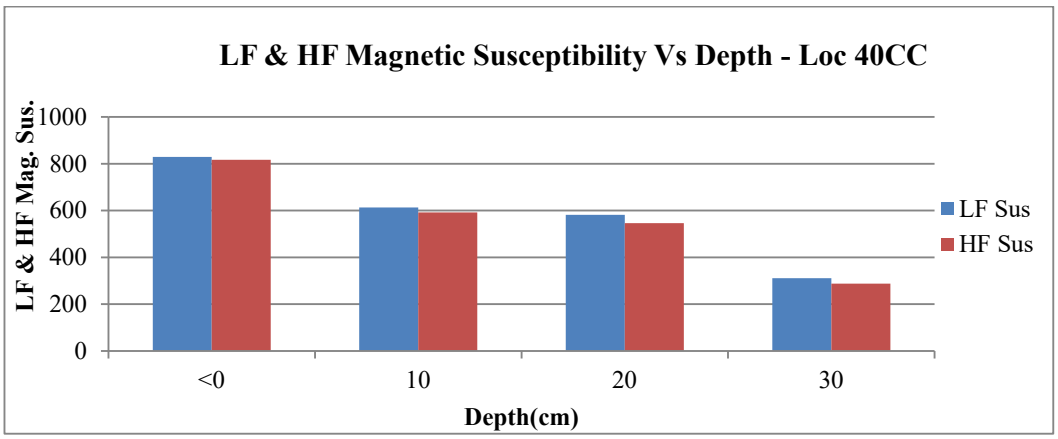
LF & HF Magnetic Susceptibility Vs Depth - Loc 40CC
LF & HF Mag. Sus.
1000
800
600
400
200
0
<0
10
20
30
Depth(cm)
LF Sus
HF Sus

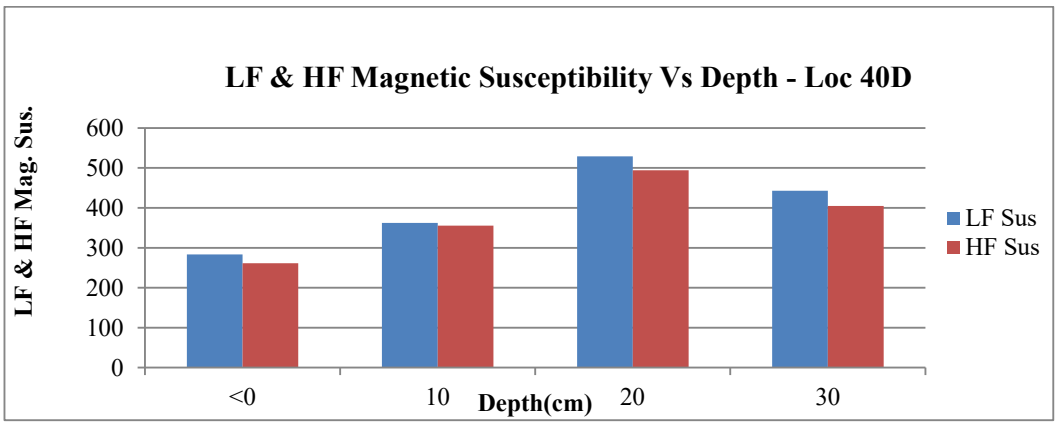
LF & HF Magnetic Susceptibility Vs Depth - Loc 40D
LF & HF Mag. Sus.
600
500
400
300
200
100
0
<0
10
20
30
Depth(cm)
LF Sus
HF Sus

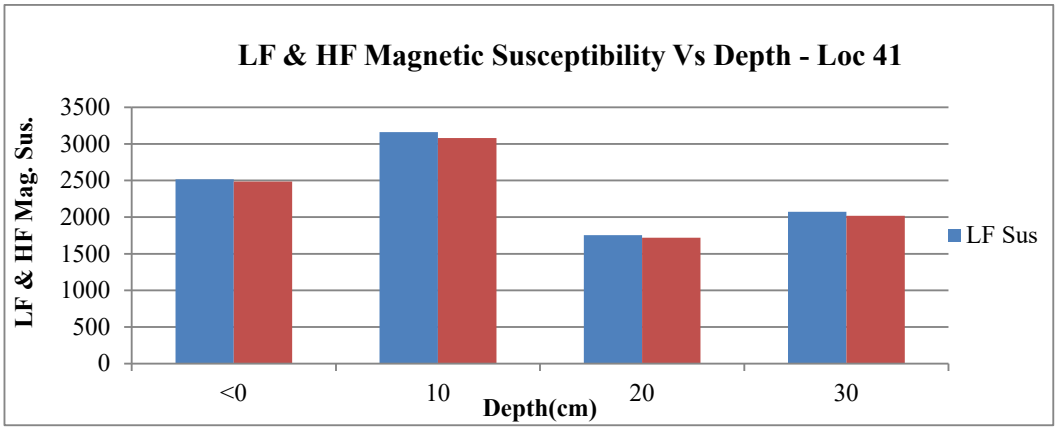
LF & HF Magnetic Susceptibility Vs Depth - Loc 41
LF & HF Mag. Sus.
3500
3000
2500
2000
1500
1000
500
0
<0
10
20
30
Depth(cm)
LF Sus

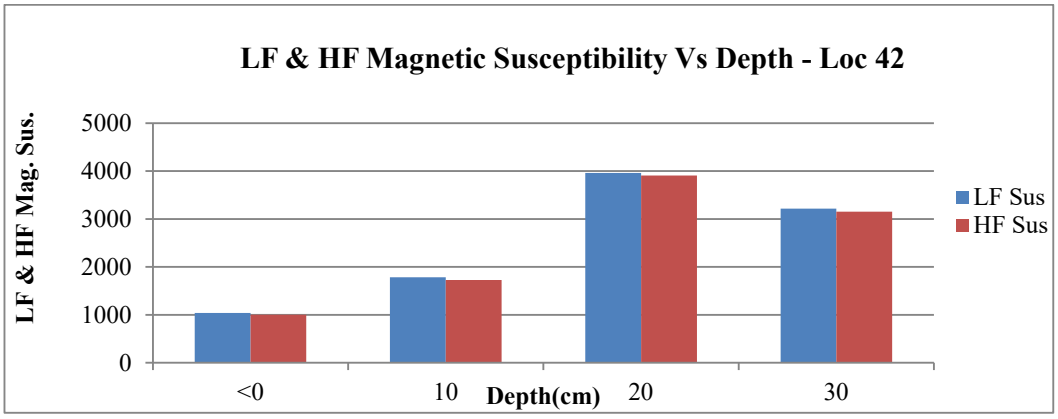
LF & HF Magnetic Susceptibility Vs Depth - Loc 42
LF & HF Mag. Sus.
5000
4000
3000
2000
1000
0
<0
10
Depth(cm)
20
30
LF Sus
HF Sus

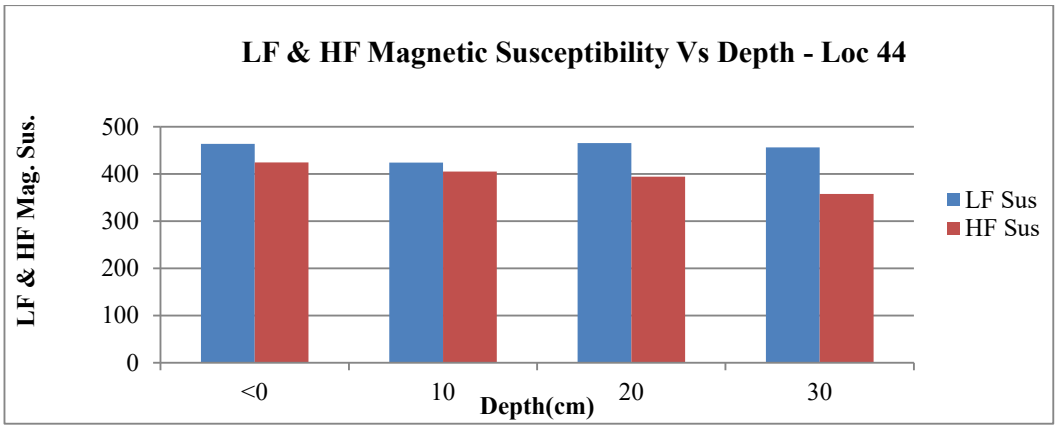
LF & HF Magnetic Susceptibility Vs Depth - Loc 44
LF & HF Mag. Sus.
500
400
300
200
100
0
<0
10
20
30
Depth(cm)
LF Sus
HF Sus

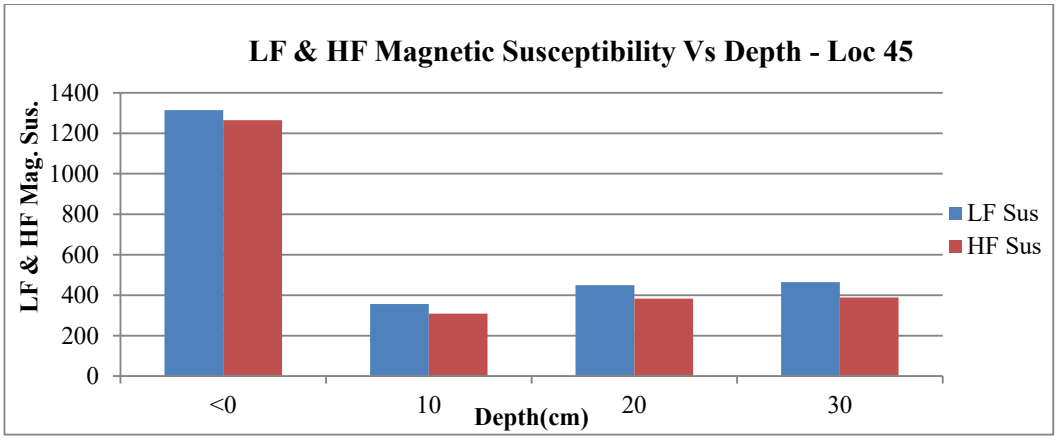
LF & HF Magnetic Susceptibility Vs Depth - Loc 45
LF & HF Mag. Sus.
1400
1200
1000
800
600
400
200
0
<0
10
20
30
Depth(cm)
LF Sus
HF Sus

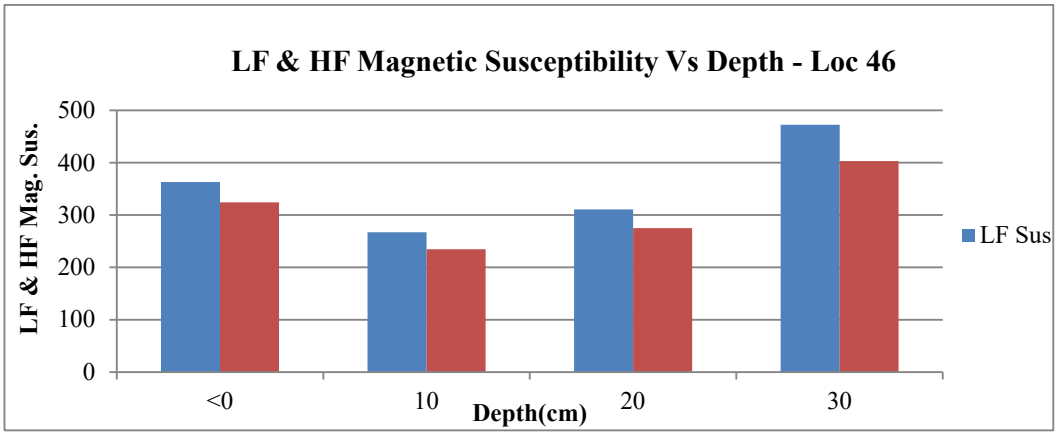
LF & HF Magnetic Susceptibility Vs Depth - Loc 46
LF & HF Mag. Sus.
500
400
300
200
100
0
<0
10
20
30
Depth(cm)
LF Sus

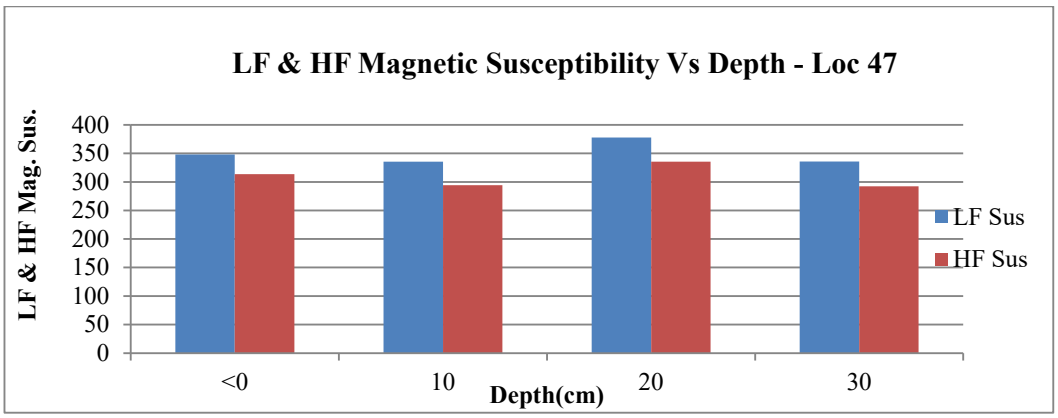
LF & HF Magnetic Susceptibility Vs Depth - Loc 47
LF & HF Mag. Sus.
400
350
300
250
200
150
100
50
0
<0
10
20
30
Depth(cm)
LF Sus
HF Sus

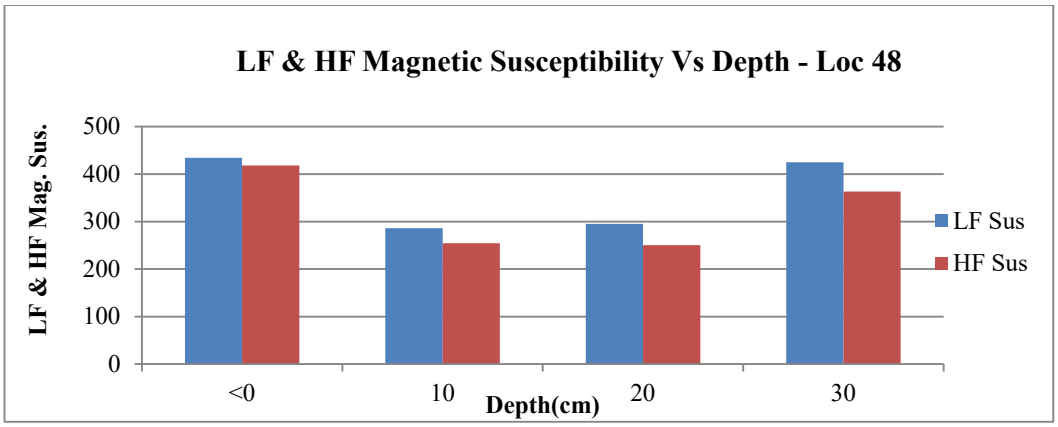
LF & HF Magnetic Susceptibility Vs Depth - Loc 48
LF & HF Mag. Sus.
500
400
300
200
100
0
<0
10
20
30
Depth(cm)
LF Sus
HF Sus

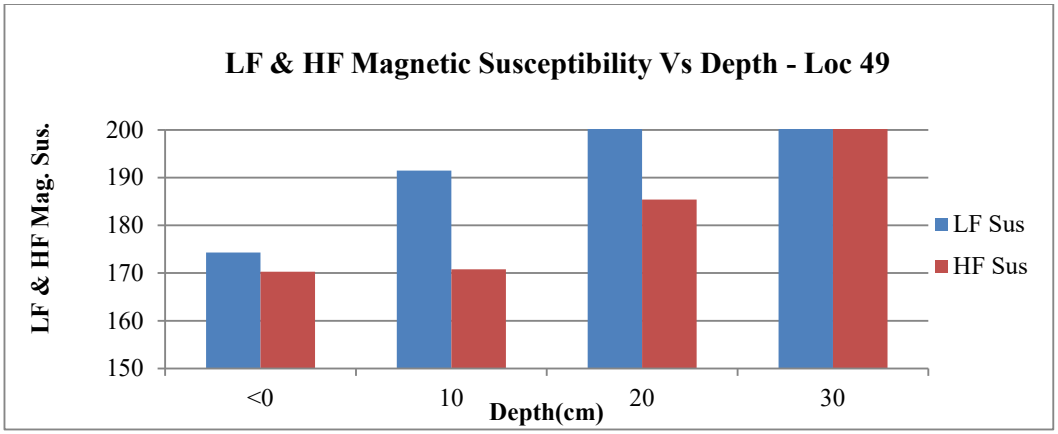
LF & HF Magnetic Susceptibility Vs Depth - Loc 49
LF & HF Mag. Sus.
200
190
180
170
160
150
<0
10
20
30
Depth(cm)
LF Sus
HF Sus

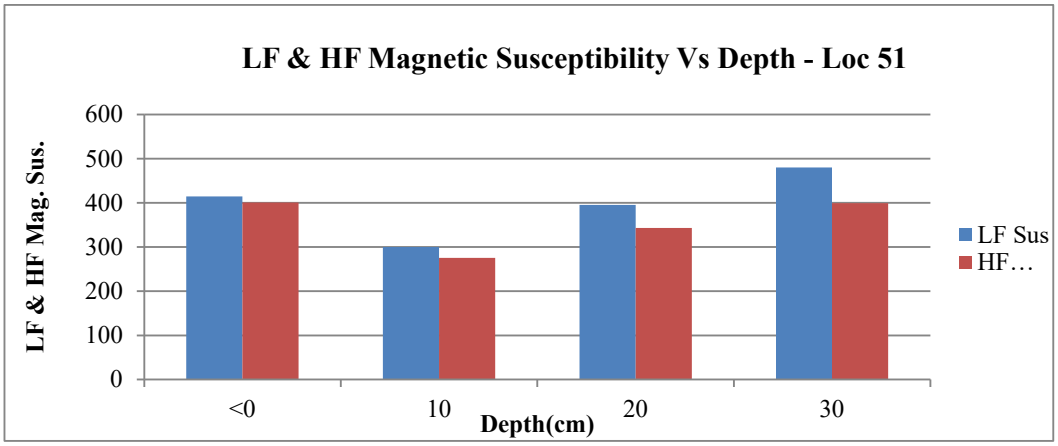
LF & HF Magnetic Susceptibility Vs Depth - Loc 51
LF & HF Mag. Sus.
600
500
400
300
200
100
0
<0
10
20
30
Depth(cm)
LF Sus
HF…

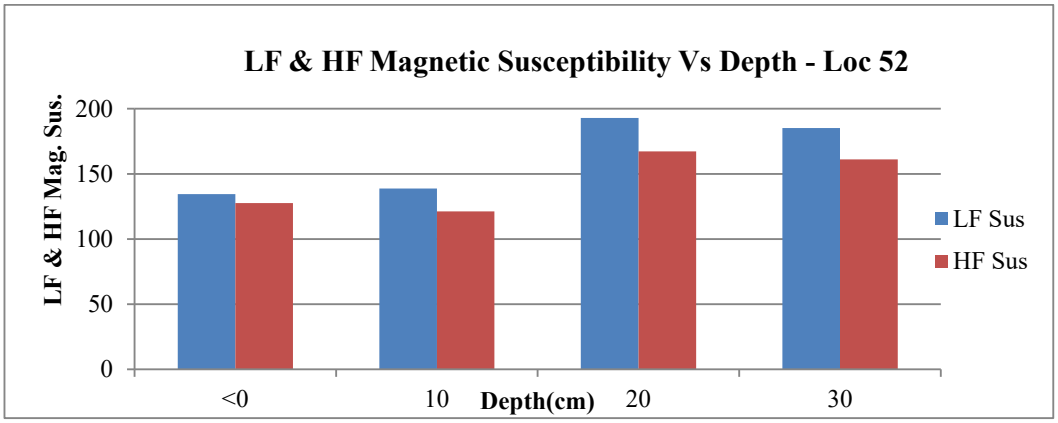
LF & HF Magnetic Susceptibility Vs Depth - Loc 52
LF & HF Mag. Sus.
200
150
100
50
0
<0
10
Depth(cm)
20
30
LF Sus
HF Sus

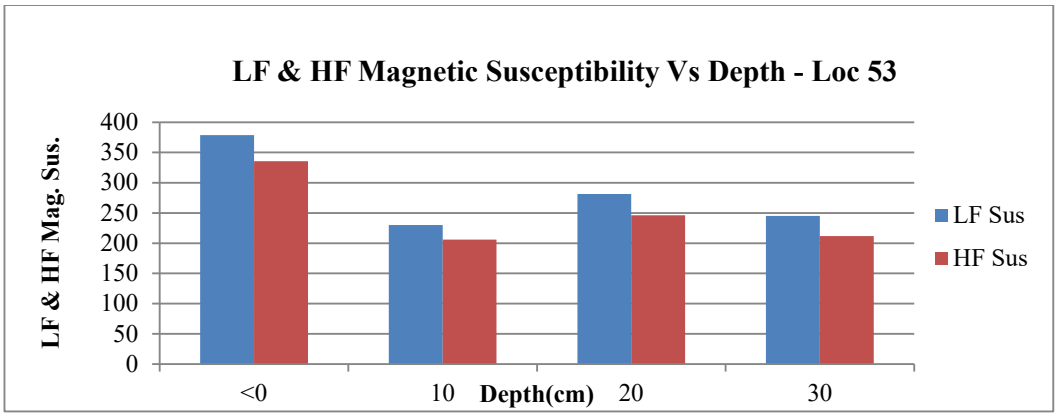
LF & HF Magnetic Susceptibility Vs Depth - Loc 53
LF & HF Mag. Sus.
400
350
300
250
200
150
100
50
0
<0
10
Depth(cm)
20
30
LF Sus
HF Sus

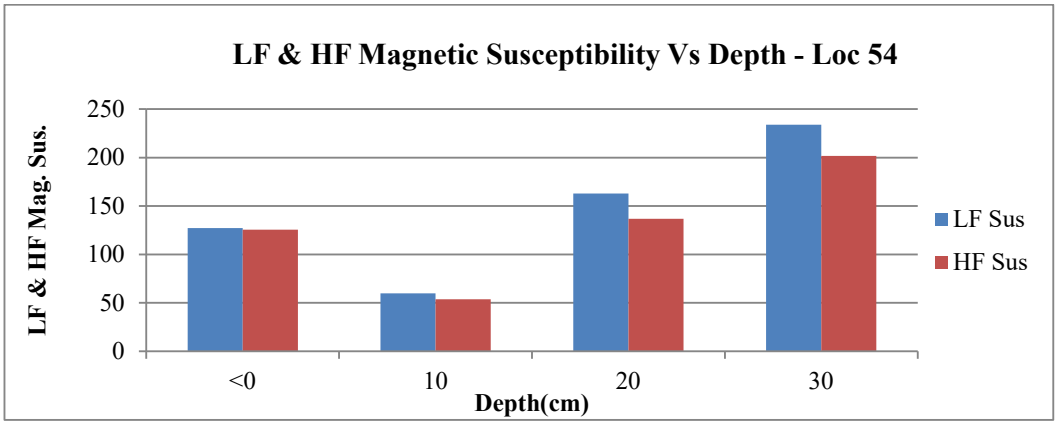
LF & HF Magnetic Susceptibility Vs Depth - Loc 54
LF & HF Mag. Sus.
250
200
150
100
50
0
<0
10
20
30
Depth(cm)
LF Sus
HF Sus

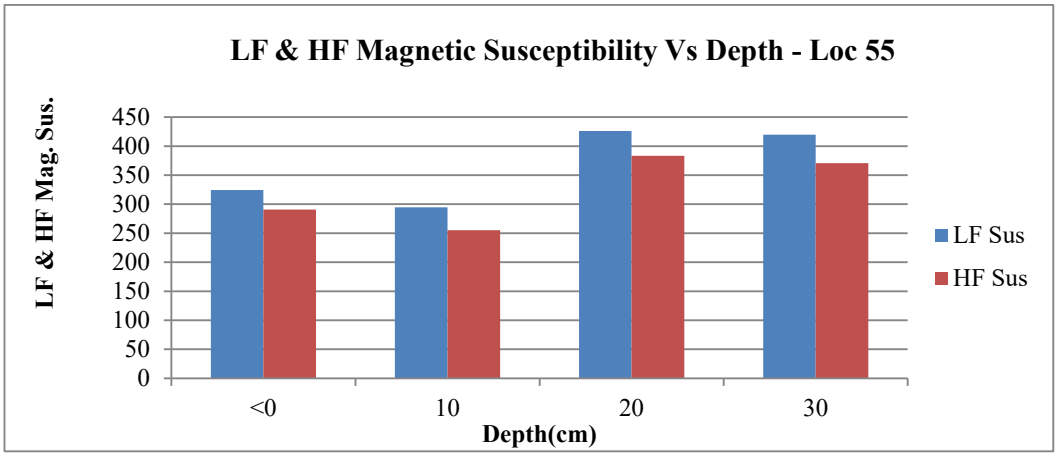
LF & HF Magnetic Susceptibility Vs Depth - Loc 55
LF & HF Mag. Sus.
450
400
350
300
250
200
150
100
50
0
<0
10
20
30
Depth(cm)
LF Sus
HF Sus

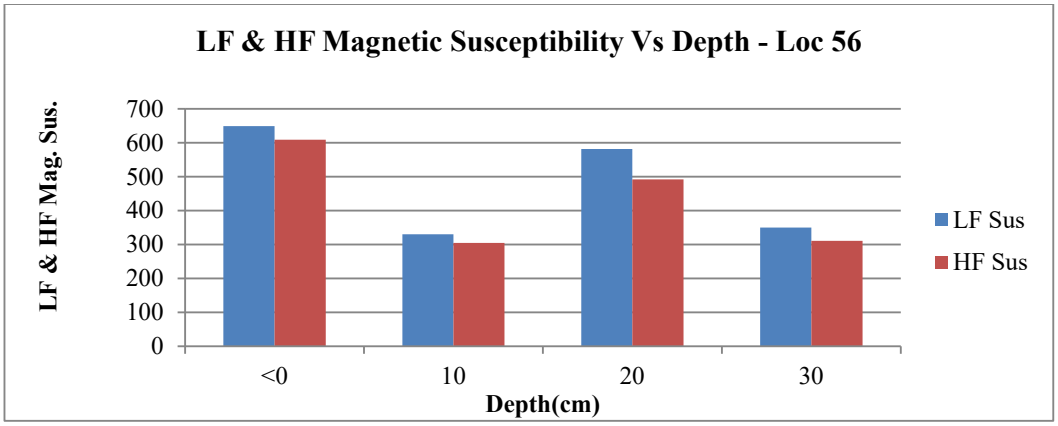
LF & HF Magnetic Susceptibility Vs Depth - Loc 56
LF & HF Mag. Sus.
700
600
500
400
300
200
100
0
<0
10
20
30
Depth(cm)
LF Sus
HF Sus

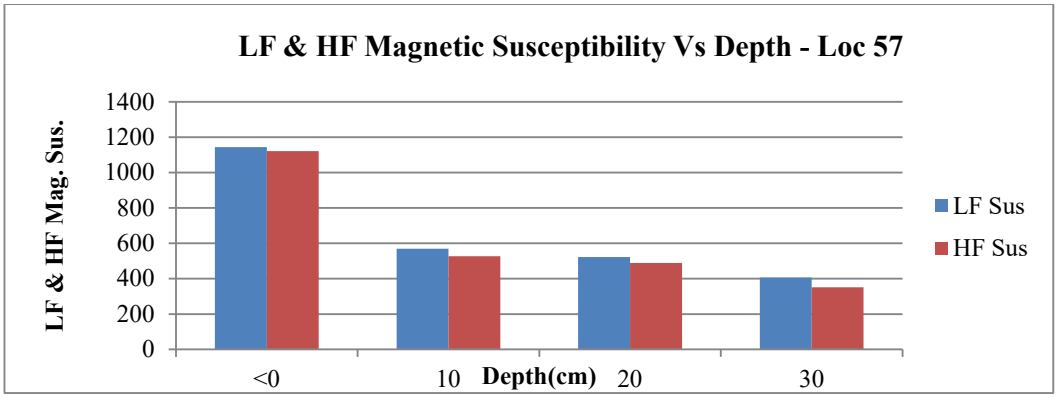
LF & HF Magnetic Susceptibility Vs Depth - Loc 57
LF & HF Mag. Sus.
1400
1200
1000
800
600
400
200
0
<0
10
Depth(cm)
20
30
LF Sus
HF Sus

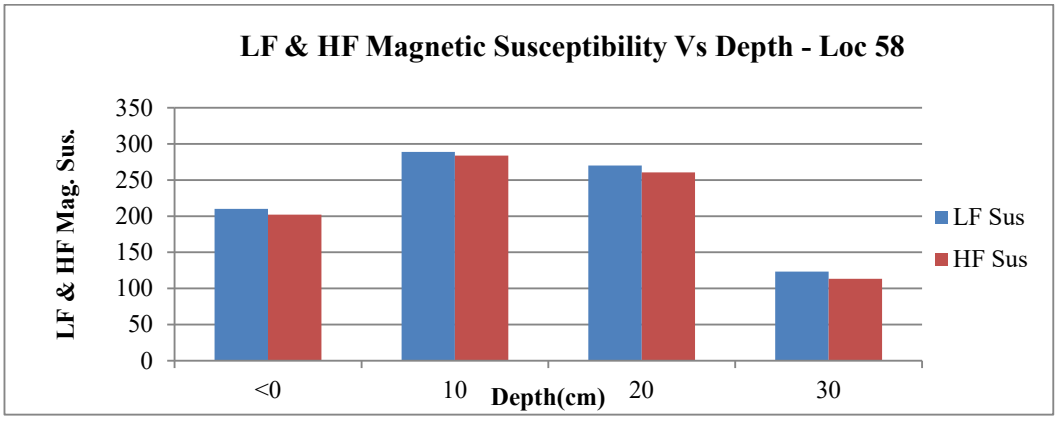
LF & HF Magnetic Susceptibility Vs Depth - Loc 58
LF & HF Mag. Sus.
350
300
250
200
150
100
50
0
<0
10
Depth(cm)
20
30
LF Sus
HF Sus

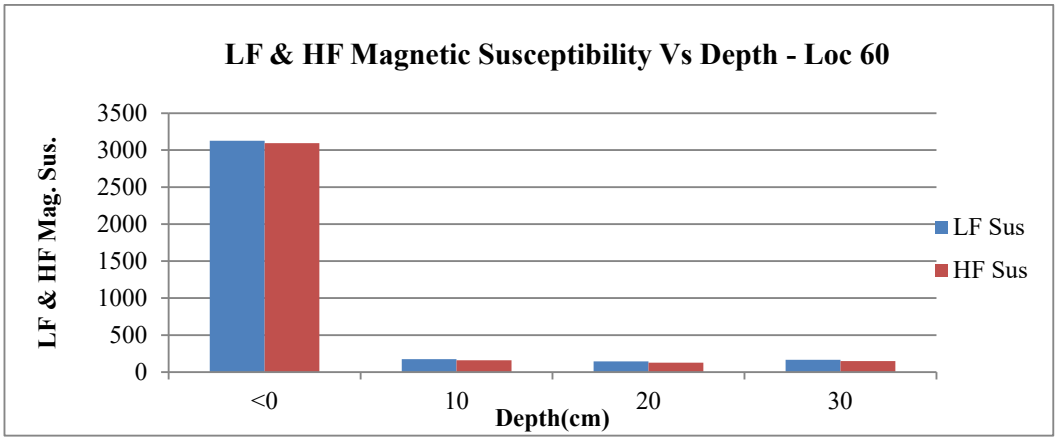
LF & HF Magnetic Susceptibility Vs Depth - Loc 60
LF & HF Mag. Sus.
3500
3000
2500
2000
1500
1000
500
0
<0
10
20
30
Depth(cm)
LF Sus
HF Sus

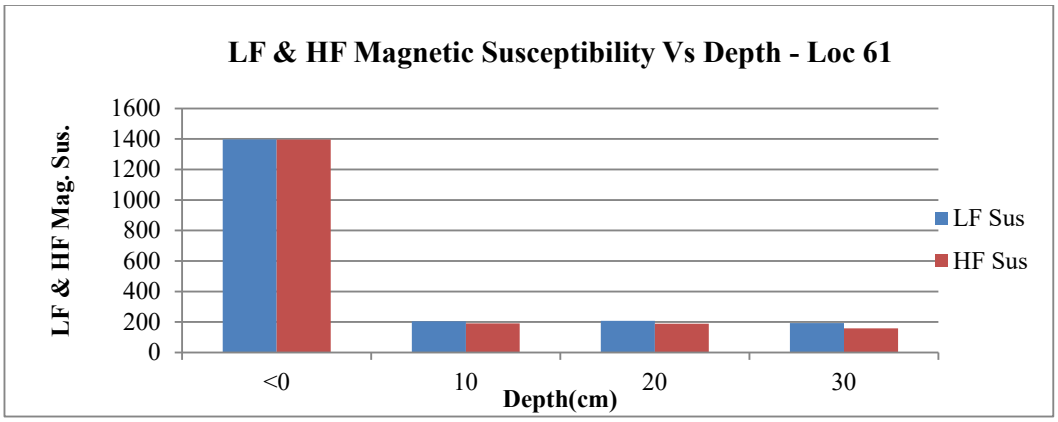
LF & HF Magnetic Susceptibility Vs Depth - Loc 61
LF & HF Mag. Sus.
1600
1400
1200
1000
800
600
400
200
0
<0
10
20
30
Depth(cm)
LF Sus
HF Sus

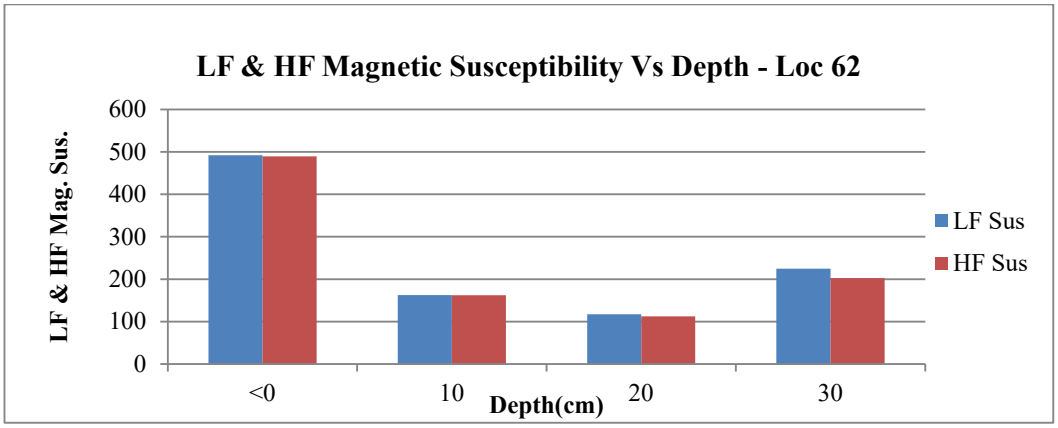
LF & HF Magnetic Susceptibility Vs Depth - Loc 62
LF & HF Mag. Sus.
600
500
400
300
200
100
0
<0
10
20
30
Depth(cm)
LF Sus
HF Sus

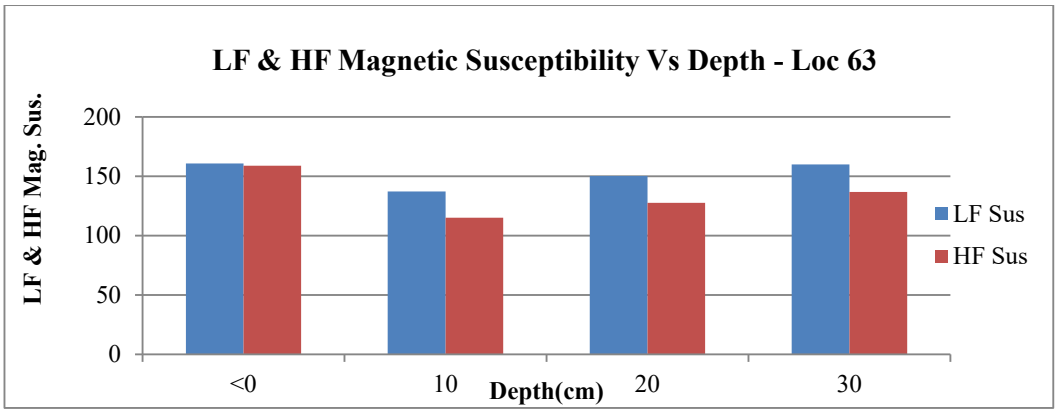
LF & HF Magnetic Susceptibility Vs Depth - Loc 63
LF & HF Mag. Sus.
200
150
100
50
0
<0
10
20
30
Depth(cm)
LF Sus
HF Sus

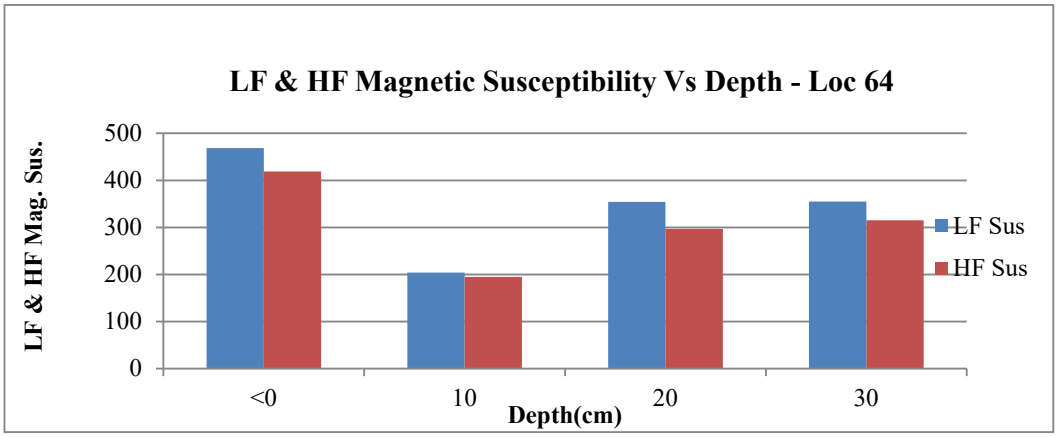
LF & HF Magnetic Susceptibility Vs Depth - Loc 64
LF & HF Mag. Sus.
500
400
300
200
100
0
<0
10
20
30
Depth(cm)
LF Sus
HF Sus

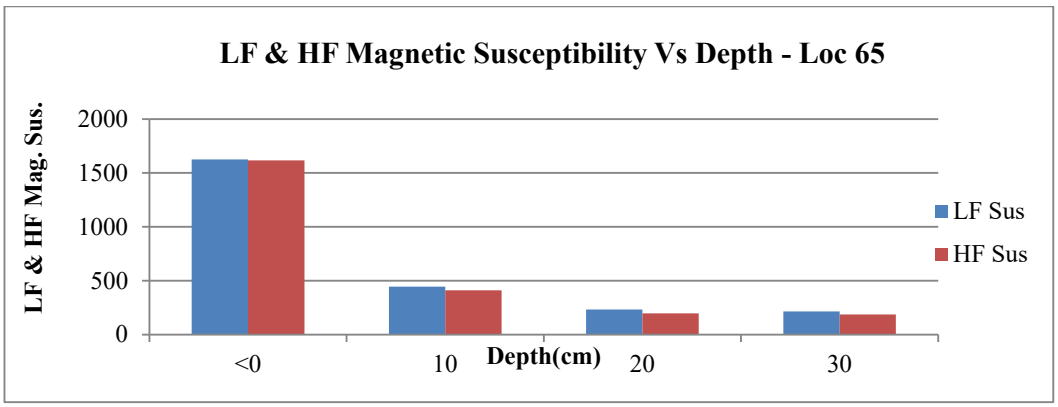
LF & HF Magnetic Susceptibility Vs Depth - Loc 65
LF & HF Mag. Sus.
2000
1500
1000
500
0
<0
10
Depth(cm)
20
30
LF Sus
HF Sus

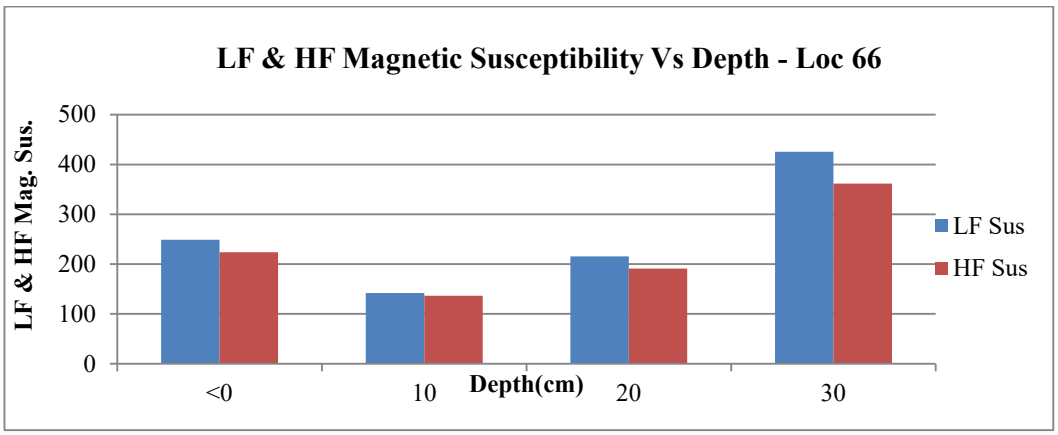
LF & HF Magnetic Susceptibility Vs Depth - Loc 66
LF & HF Mag. Sus.
500
400
300
200
100
0
<0
10
Depth(cm)
20
30
LF Sus
HF Sus

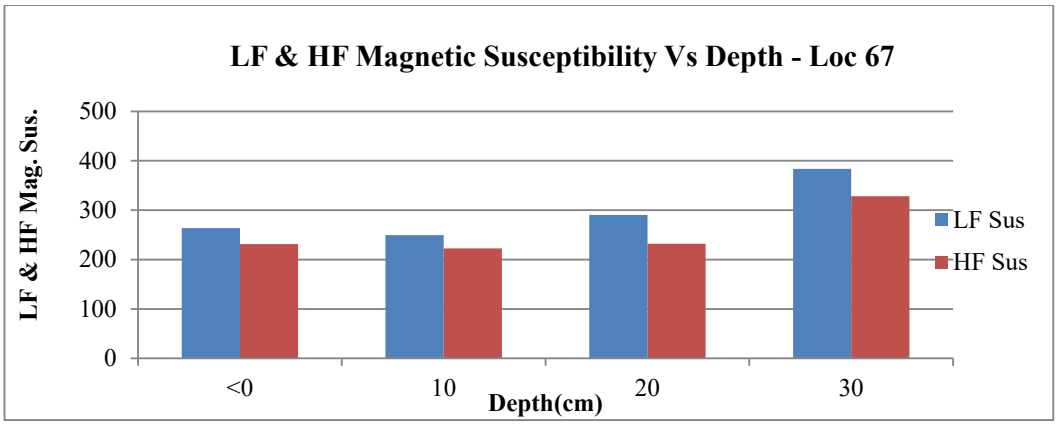
LF & HF Magnetic Susceptibility Vs Depth - Loc 67
LF & HF Mag. Sus.
500
400
300
200
100
0
<0
10
20
30
Depth(cm)
LF Sus
HF Sus

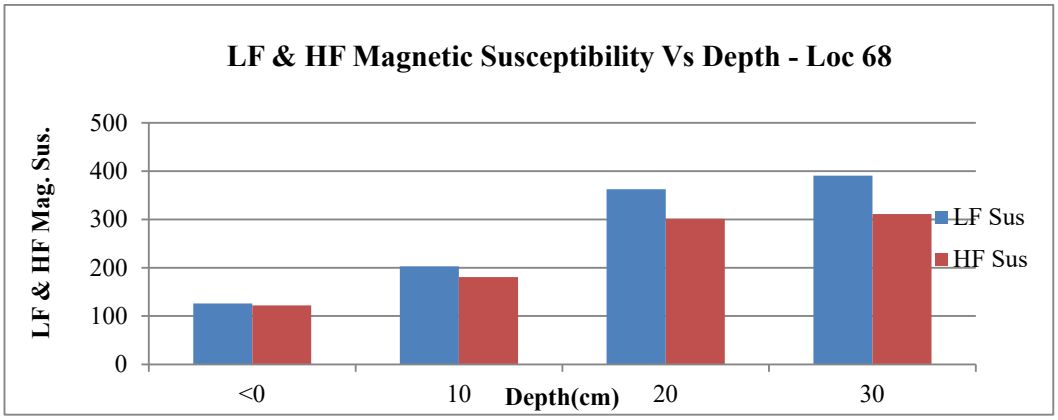
LF & HF Magnetic Susceptibility Vs Depth - Loc 68
LF & HF Mag. Sus.
500
400
300
200
100
0
<0
10
20
30
Depth(cm)
LF Sus
HF Sus

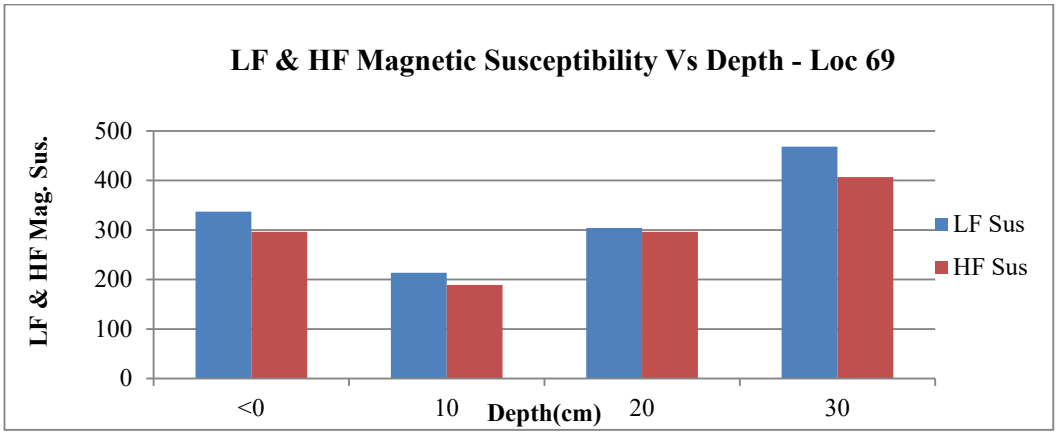
LF & HF Magnetic Susceptibility Vs Depth - Loc 69
LF & HF Mag. Sus.
500
400
300
200
100
0
<0
10
20
30
Depth(cm)
LF Sus
HF Sus

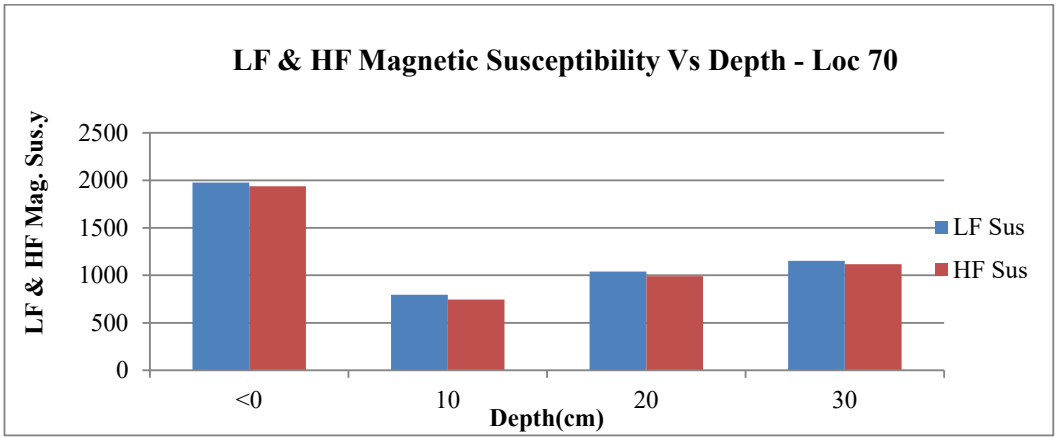
LF & HF Magnetic Susceptibility Vs Depth - Loc 70
LF & HF Mag. Sus.y
2500
2000
1500
1000
500
0
<0
10
20
30
Depth(cm)
LF Sus
HF Sus

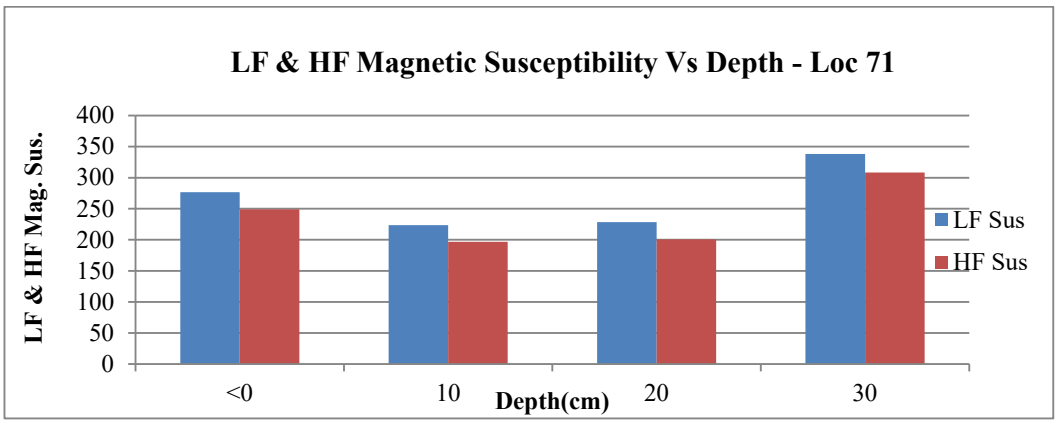
LF & HF Magnetic Susceptibility Vs Depth - Loc 71
LF & HF Mag. Sus.
400
350
300
250
200
150
100
50
0
<0
10
20
30
Depth(cm)
LF Sus
HF Sus

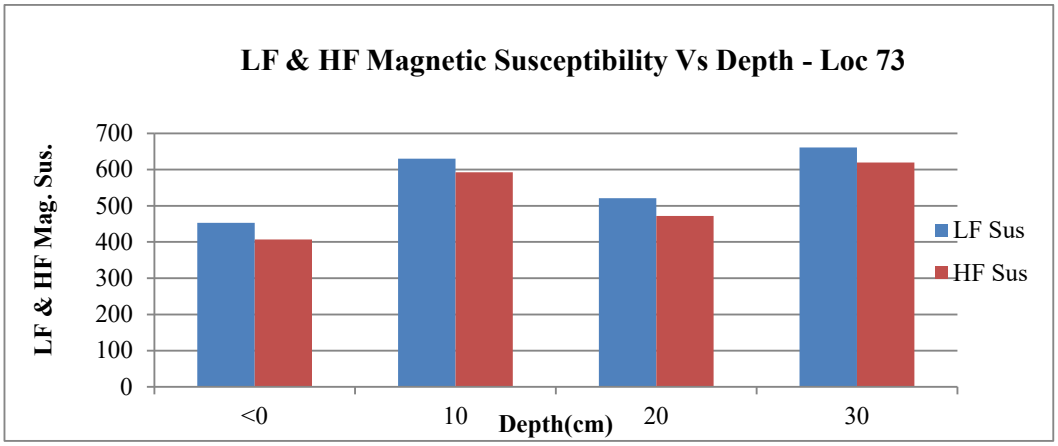
LF & HF Magnetic Susceptibility Vs Depth - Loc 73
LF & HF Mag. Sus.
700
600
500
400
300
200
100
0
<0
10
20
30
Depth(cm)
LF Sus
HF Sus

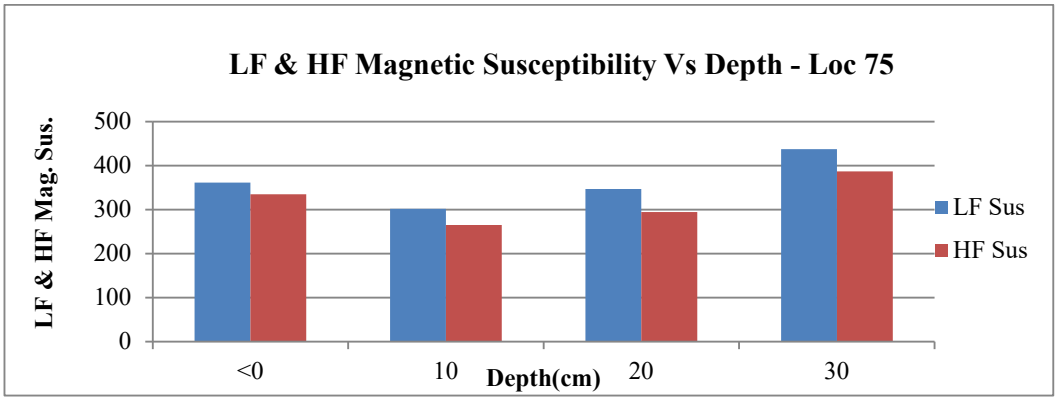
LF & HF Magnetic Susceptibility Vs Depth - Loc 75
LF & HF Mag. Sus.
500
400
300
200
100
0
<0
10
20
30
Depth(cm)
LF Sus
HF Sus

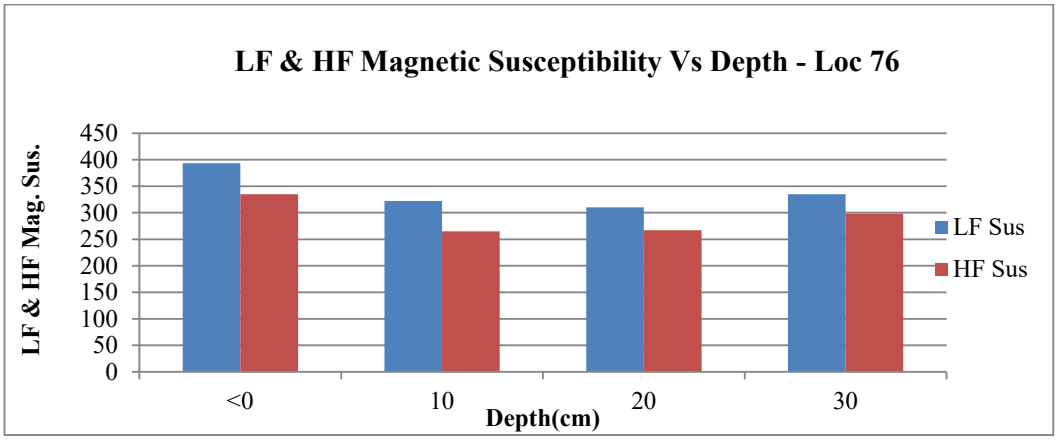
LF & HF Magnetic Susceptibility Vs Depth - Loc 76
LF & HF Mag. Sus.
450
400
350
300
250
200
150
100
50
0
<0
10
20
30
Depth(cm)
LF Sus
HF Sus

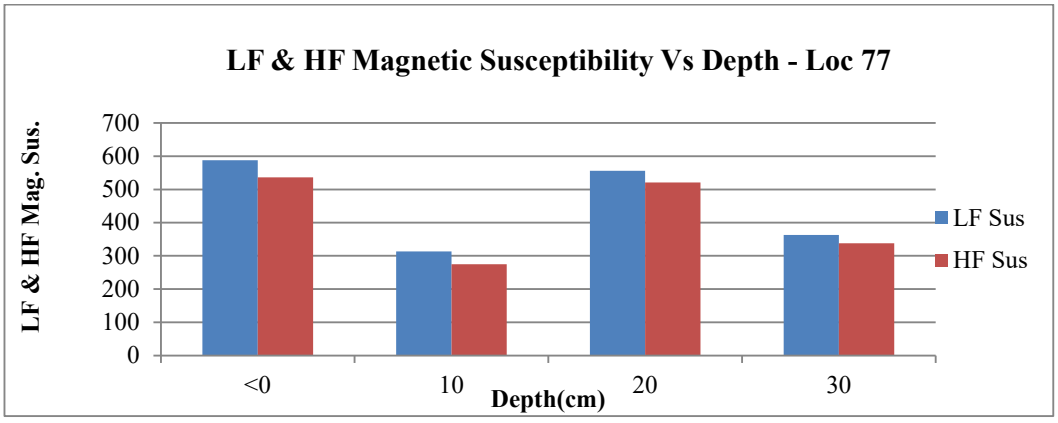
LF & HF Magnetic Susceptibility Vs Depth - Loc 77
LF & HF Mag. Sus.
700
600
500
400
300
200
100
0
<0
10
20
30
Depth(cm)
LF Sus
HF Sus

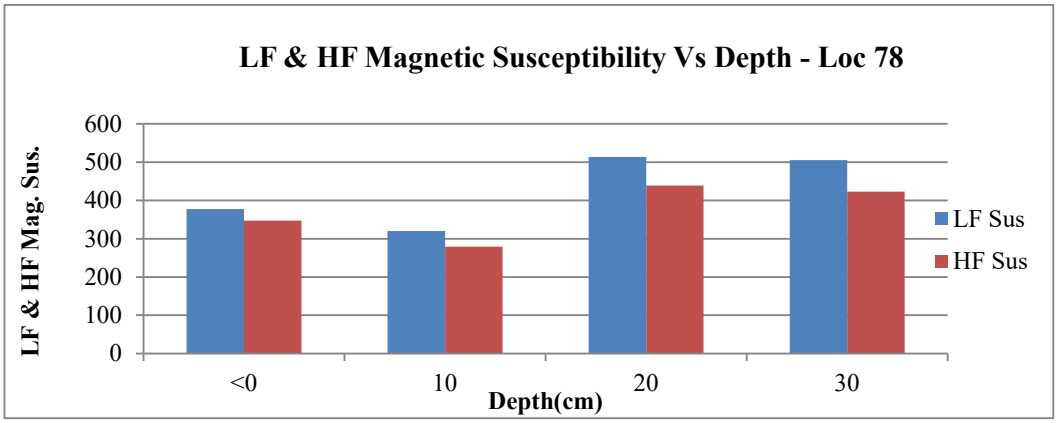
LF & HF Magnetic Susceptibility Vs Depth - Loc 78
LF & HF Mag. Sus.
600
500
400
300
200
100
0
<0
10
20
30
Depth(cm)
LF Sus
HF Sus

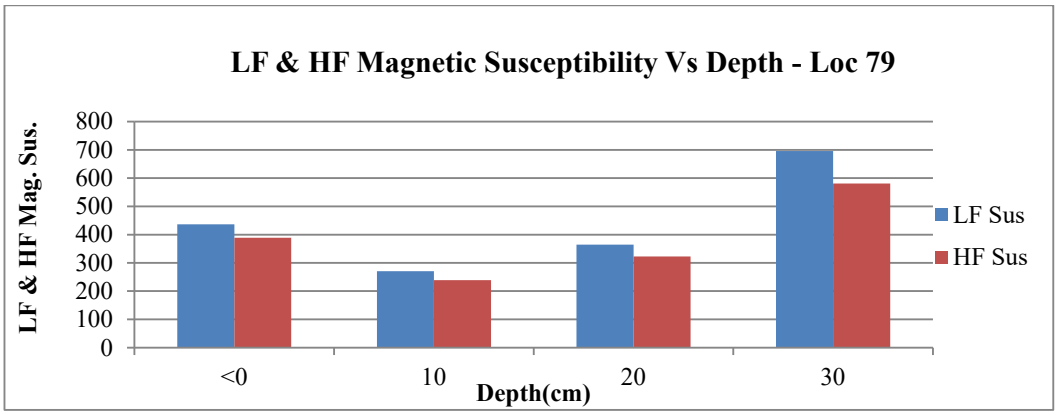
LF & HF Magnetic Susceptibility Vs Depth - Loc 79
LF & HF Mag. Sus.
800
700
600
500
400
300
200
100
0
<0
10
20
30
Depth(cm)
LF Sus
HF Sus

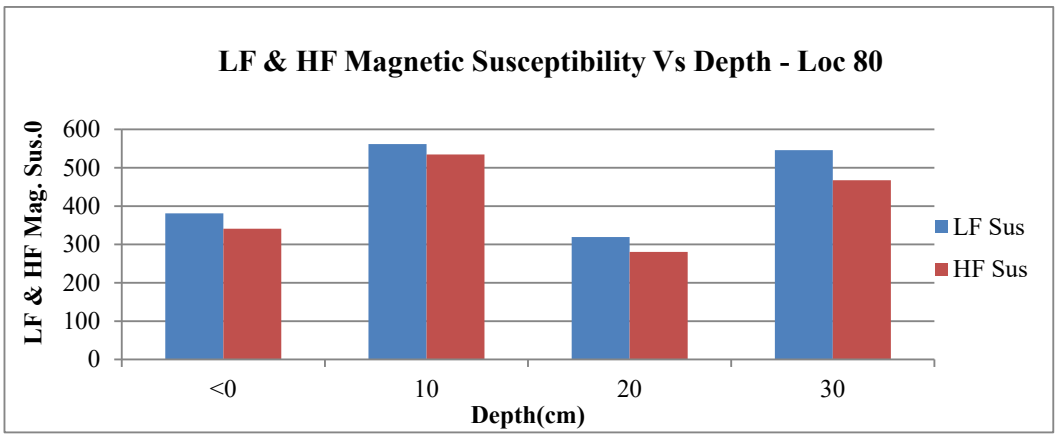
LF & HF Magnetic Susceptibility Vs Depth - Loc 80
LF & HF Mag. Sus.0
600
500
400
300
200
100
0
<0
10
20
30
Depth(cm)
LF Sus
HF Sus

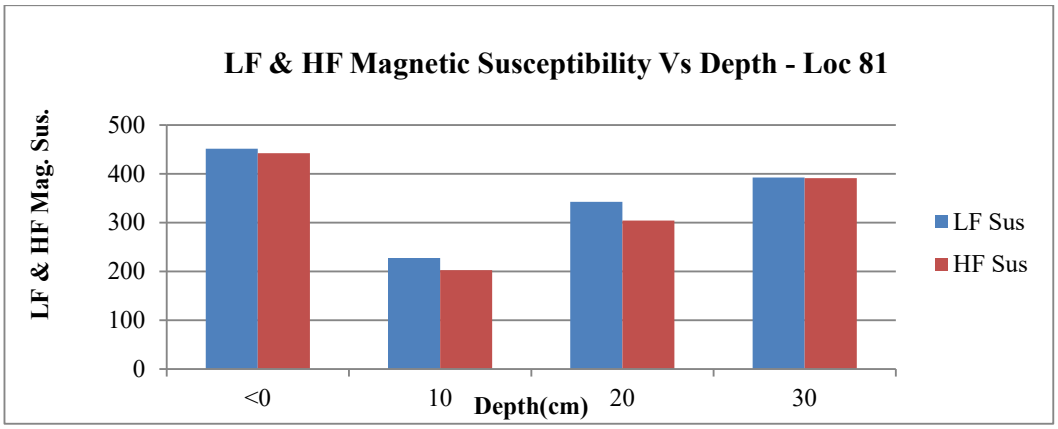
LF & HF Magnetic Susceptibility Vs Depth - Loc 81
LF & HF Mag. Sus.
500
400
300
200
100
0
<0
10
Depth(cm)
20
30
LF Sus
HF Sus

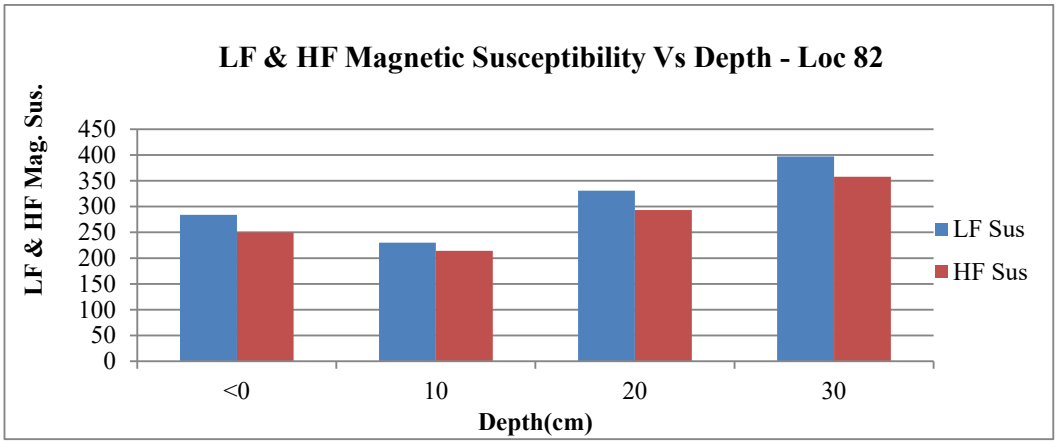
LF & HF Magnetic Susceptibility Vs Depth - Loc 82
LF & HF Mag. Sus.
450
400
350
300
250
200
150
100
50
0
<0
10
20
30
Depth(cm)
LF Sus
HF Sus

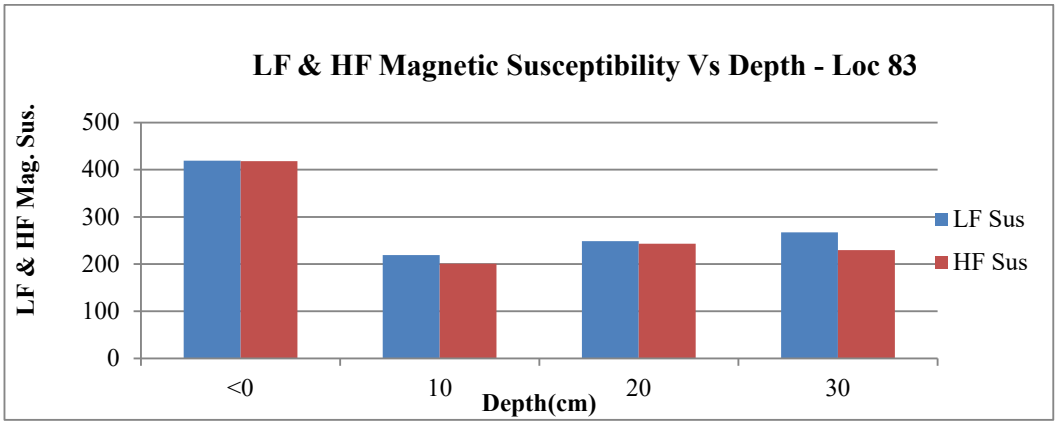
LF & HF Magnetic Susceptibility Vs Depth - Loc 83
LF & HF Mag. Sus.
500
400
300
200
100
0
<0
10
20
30
Depth(cm)
LF Sus
HF Sus

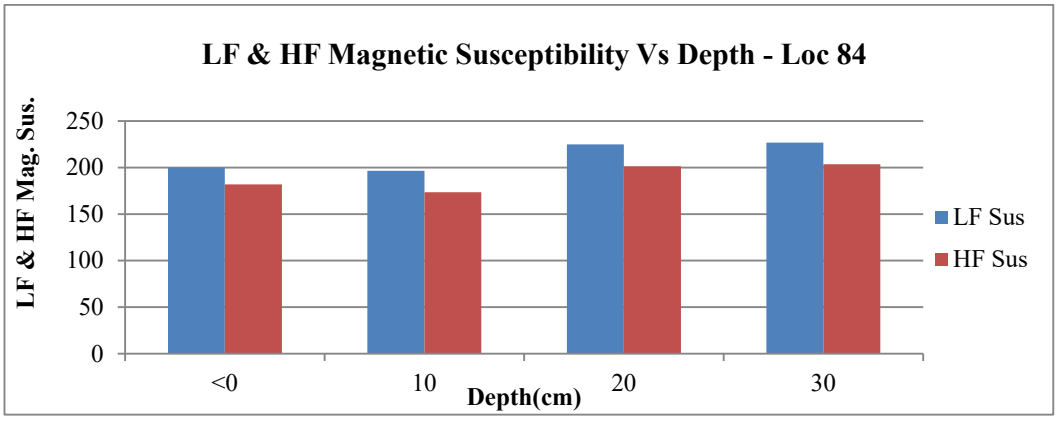
LF & HF Magnetic Susceptibility Vs Depth - Loc 84
LF & HF Mag. Sus.
250
200
150
100
50
0
<0
10
20
30
Depth(cm)
LF Sus
HF Sus

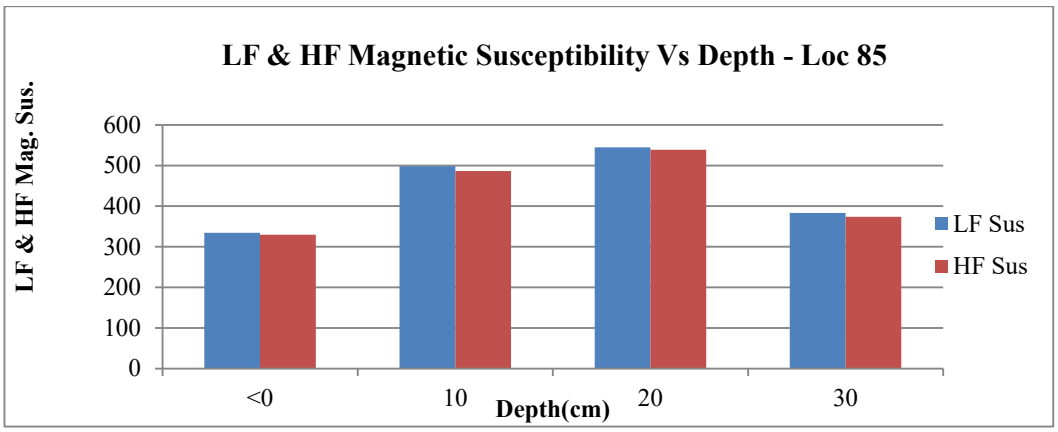
LF & HF Magnetic Susceptibility Vs Depth - Loc 85
LF & HF Mag. Sus.
600
500
400
300
200
100
0
<0
10
20
30
Depth(cm)
LF Sus
HF Sus

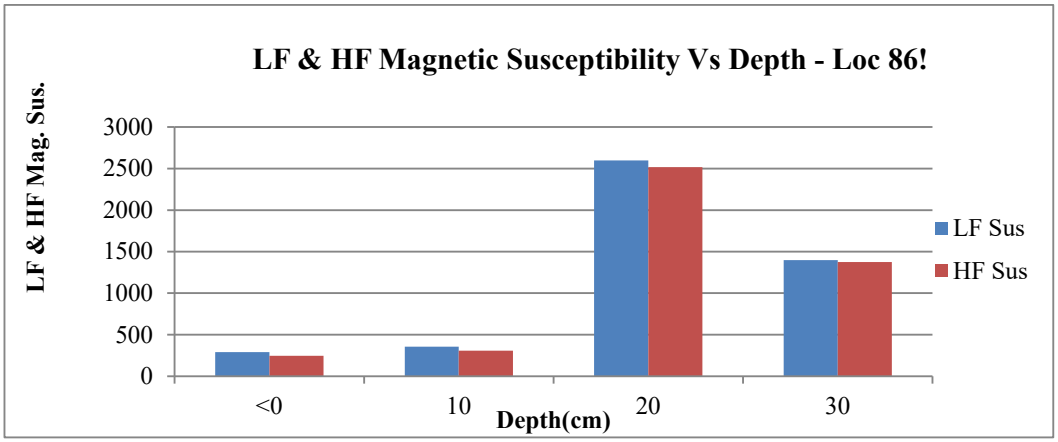
LF & HF Magnetic Susceptibility Vs Depth - Loc 86!
LF & HF Mag. Sus.
3000
2500
2000
1500
1000
500
0
<0
10
20
30
Depth(cm)
LF Sus
HF Sus

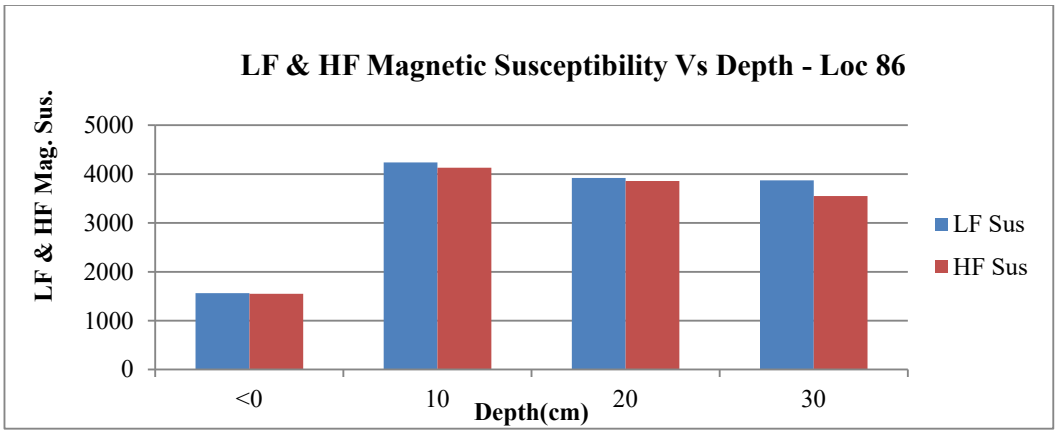
LF & HF Magnetic Susceptibility Vs Depth - Loc 86
LF & HF Mag. Sus.
5000
4000
3000
2000
1000
0
<0
10
20
30
Depth(cm)
LF Sus
HF Sus

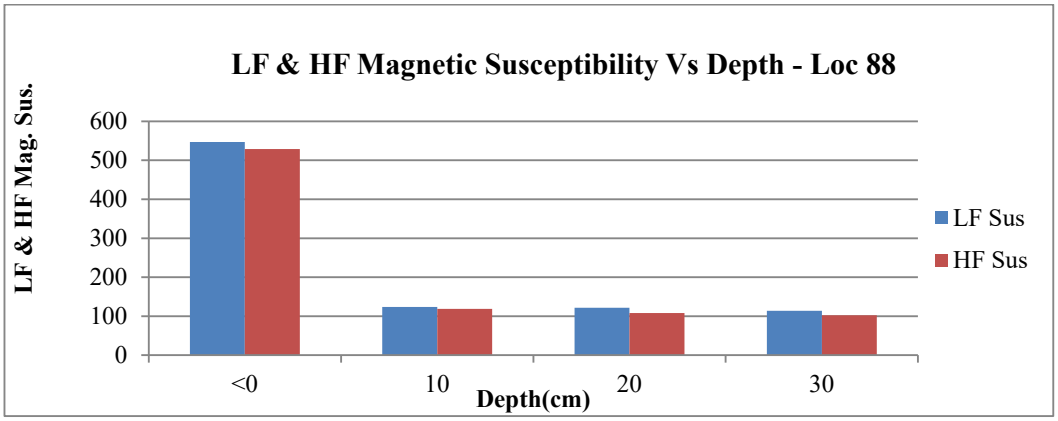
LF & HF Magnetic Susceptibility Vs Depth - Loc 88
LF & HF Mag. Sus.
600
500
400
300
200
100
0
<0
10
20
30
Depth(cm)
LF Sus
HF Sus

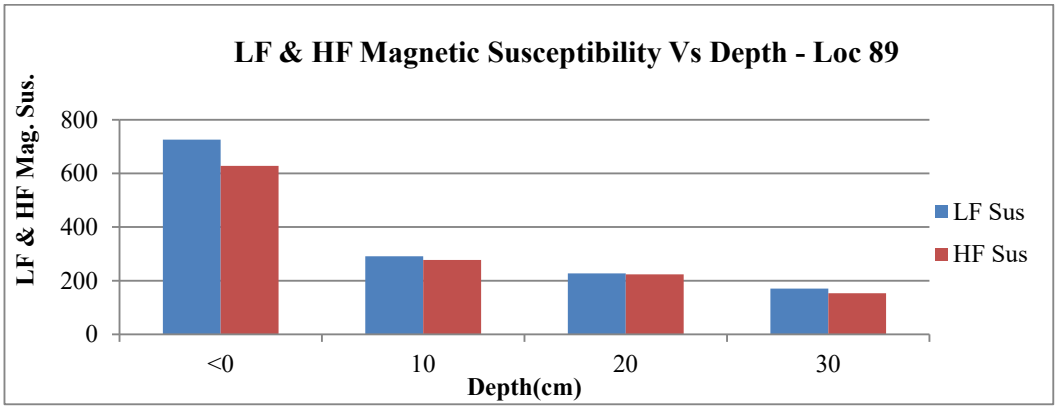
LF & HF Magnetic Susceptibility Vs Depth - Loc 89
LF & HF Mag. Sus.
800
600
400
200
0
<0
10
20
30
Depth(cm)
LF Sus
HF Sus

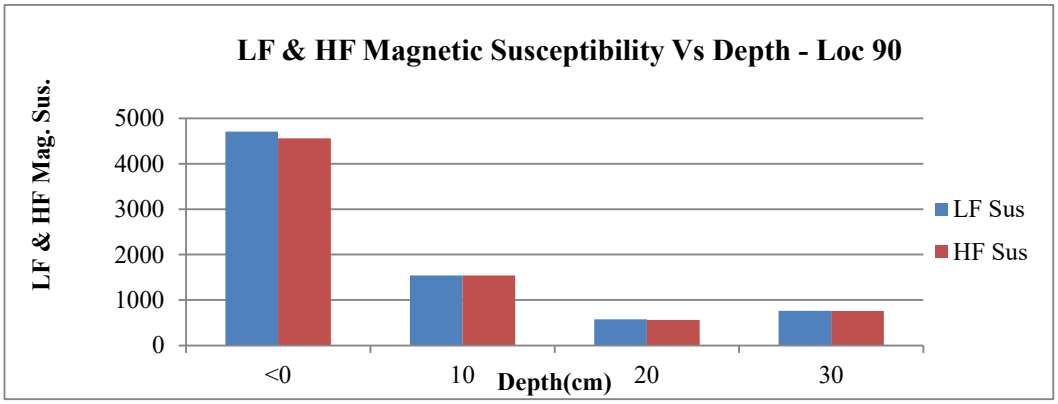
LF & HF Magnetic Susceptibility Vs Depth - Loc 90
LF & HF Mag. Sus.
5000
4000
3000
2000
1000
0
<0
10
20
30
Depth(cm)
LF Sus
HF Sus

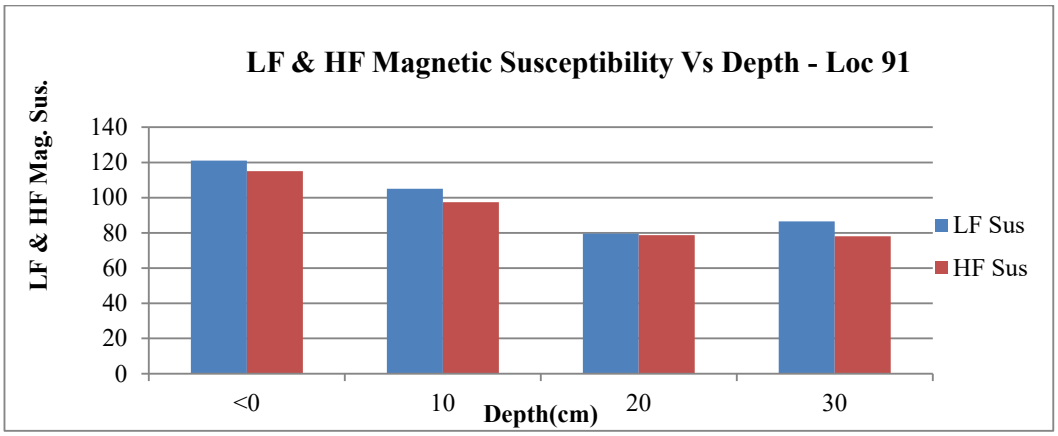
LF & HF Magnetic Susceptibility Vs Depth - Loc 91
LF & HF Mag. Sus.
140
120
100
80
60
40
20
0
<0
10
20
30
Depth(cm)
LF Sus
HF Sus

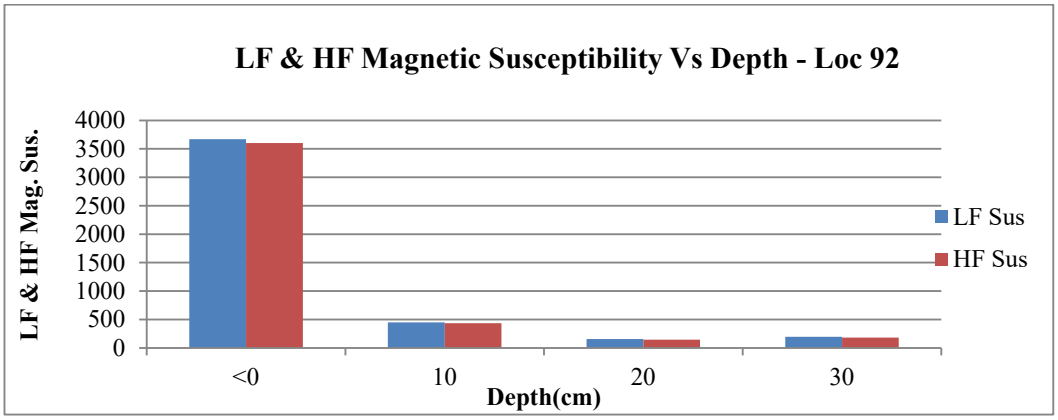
LF & HF Magnetic Susceptibility Vs Depth - Loc 92
LF & HF Mag. Sus.
4000
3500
3000
2500
2000
1500
1000
500
0
<0
10
20
30
Depth(cm)
LF Sus
HF Sus

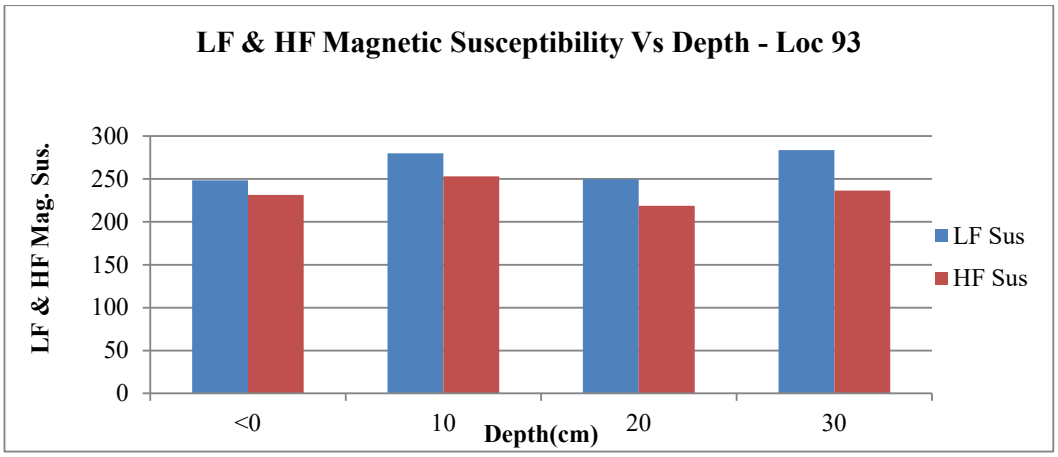
LF & HF Magnetic Susceptibility Vs Depth - Loc 93
LF & HF Mag. Sus.
300
250
200
150
100
50
0
<0
10
20
30
Depth(cm)
LF Sus
HF Sus

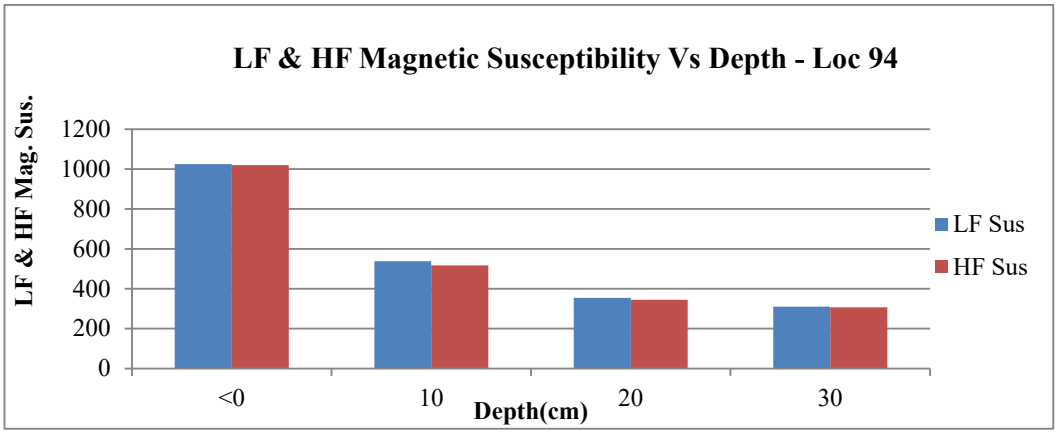
LF & HF Magnetic Susceptibility Vs Depth - Loc 94
LF & HF Mag. Sus.
1200
1000
800
600
400
200
0
<0
10
20
30
Depth(cm)
LF Sus
HF Sus

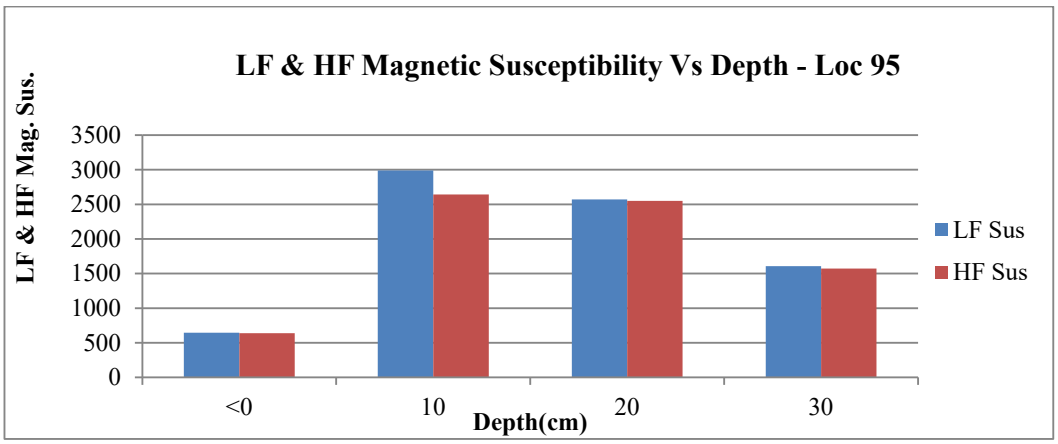
LF & HF Magnetic Susceptibility Vs Depth - Loc 95
LF & HF Mag. Sus.
3500
3000
2500
2000
1500
1000
500
0
<0
10
20
30
Depth(cm)
LF Sus
HF Sus

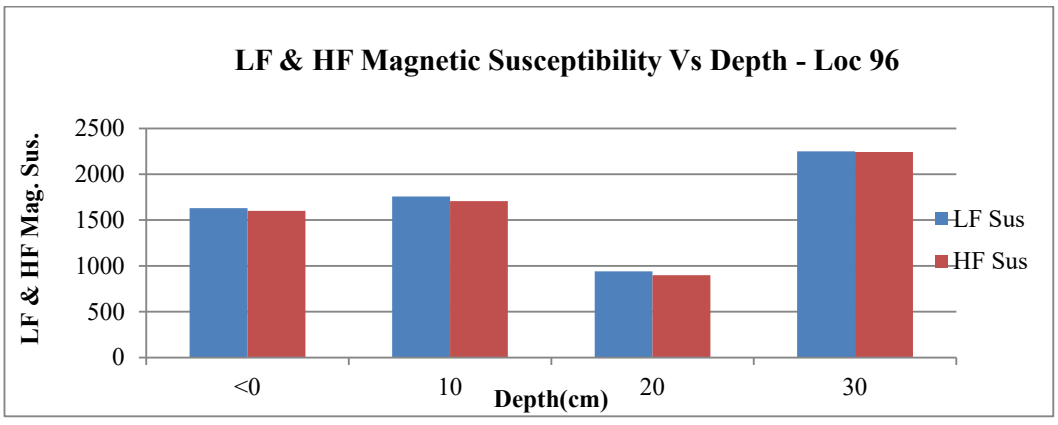
LF & HF Magnetic Susceptibility Vs Depth - Loc 96
LF & HF Mag. Sus.
2500
2000
1500
1000
500
0
<0
10
20
30
Depth(cm)
LF Sus
HF Sus

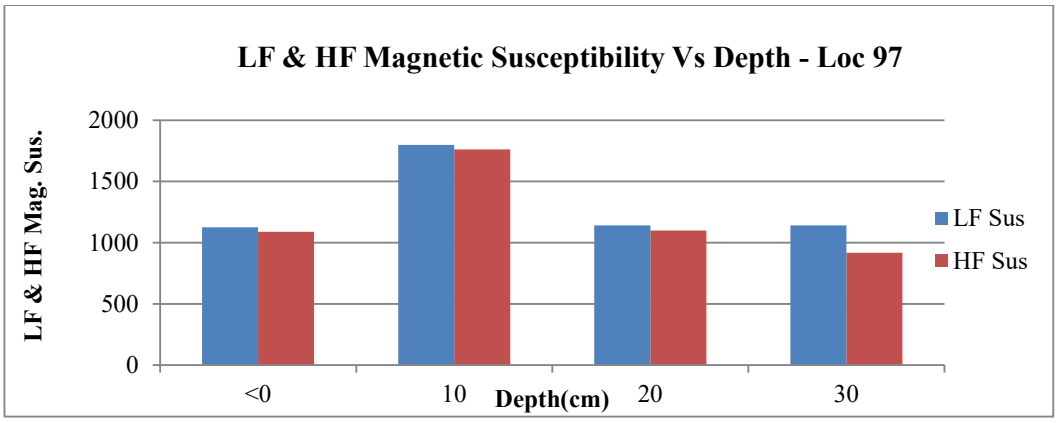
LF & HF Magnetic Susceptibility Vs Depth - Loc 97
LF & HF Mag. Sus.
2000
1500
1000
500
0
<0
10
20
30
Depth(cm)
LF Sus
HF Sus

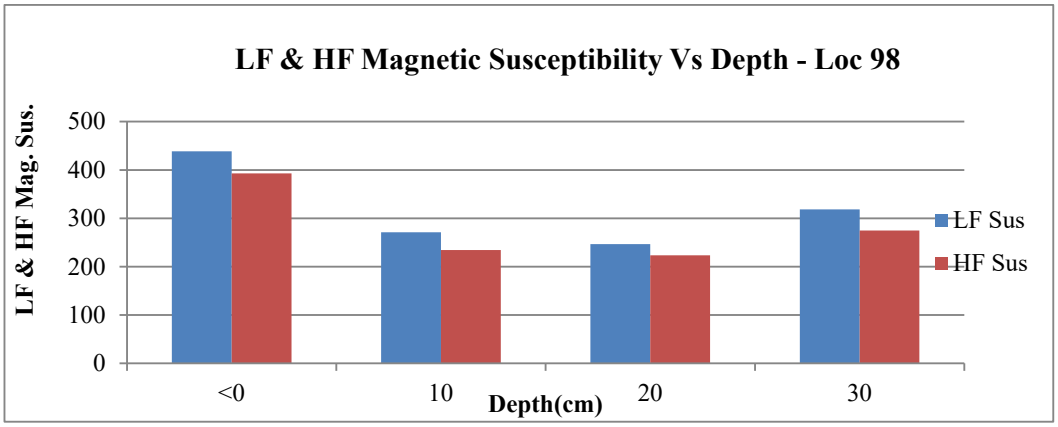
LF & HF Magnetic Susceptibility Vs Depth - Loc 98
LF & HF Mag. Sus.
500
400
300
200
100
0
<0
10
20
30
Depth(cm)
LF Sus
HF Sus

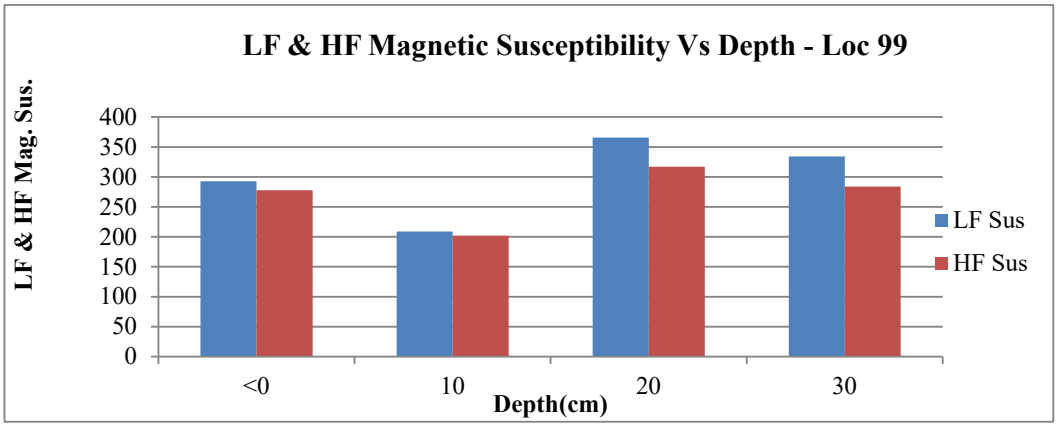
LF & HF Magnetic Susceptibility Vs Depth - Loc 99
LF & HF Mag. Sus.
400
350
300
250
200
150
100
50
0
<0
10
20
30
Depth(cm)
LF Sus
HF Sus

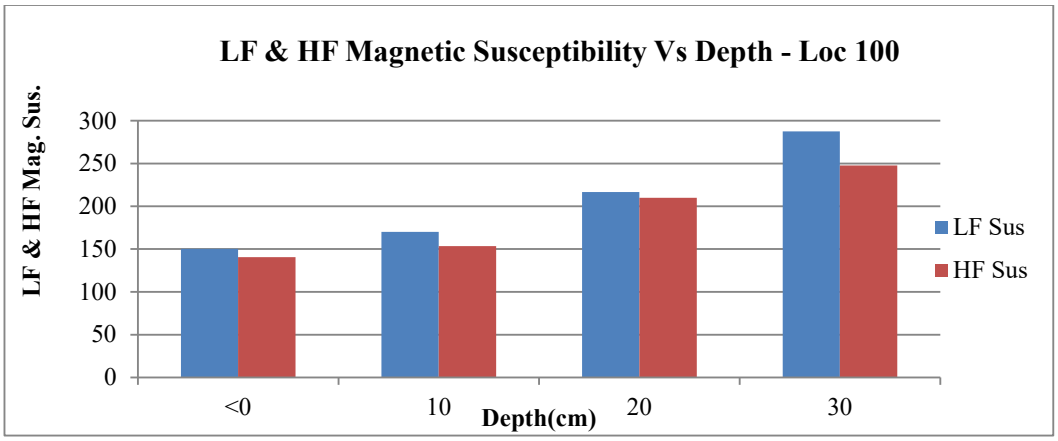
LF & HF Magnetic Susceptibility Vs Depth - Loc 100
LF & HF Mag. Sus.
300
250
200
150
100
50
0
<0
10
20
30
Depth(cm)
LF Sus
HF Sus

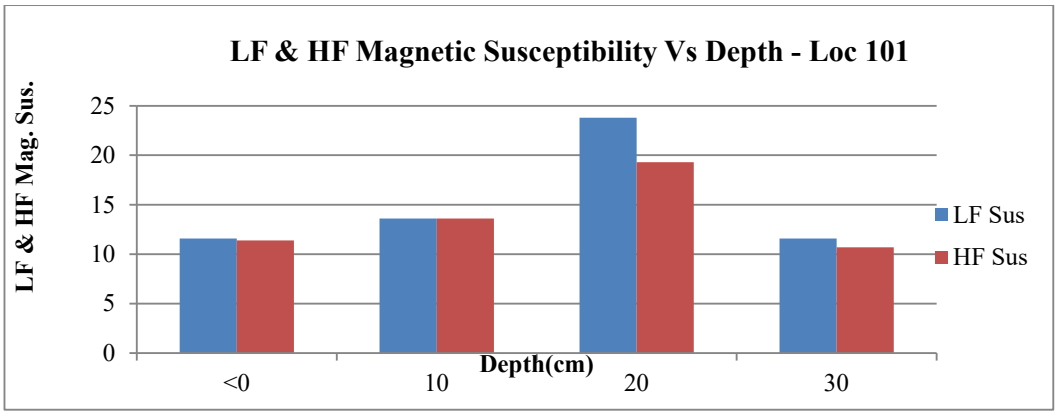
LF & HF Magnetic Susceptibility Vs Depth - Loc 101
LF & HF Mag. Sus.
25
20
15
10
5
0
<0
10
20
30
Depth(cm)
LF Sus
HF Sus

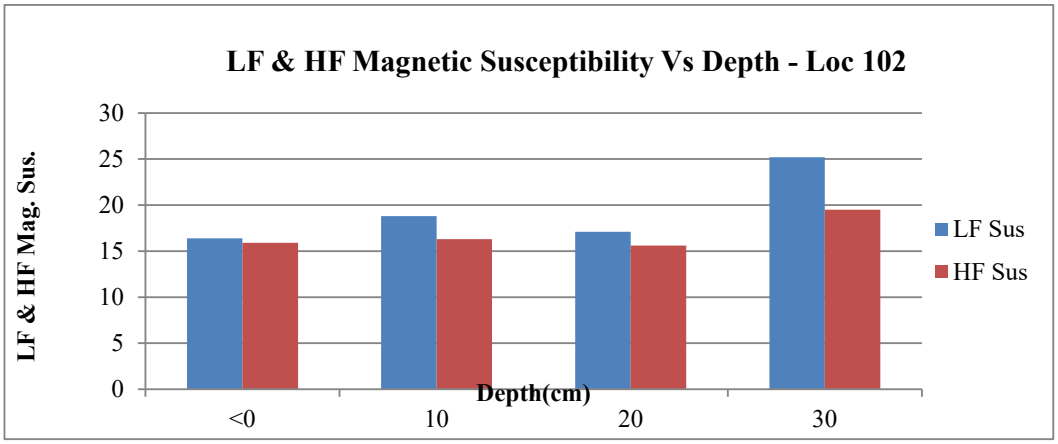
LF & HF Magnetic Susceptibility Vs Depth - Loc 102
LF & HF Mag. Sus.
30
25
20
15
10
5
0
<0
10
20
30
Depth(cm)
LF Sus
HF Sus

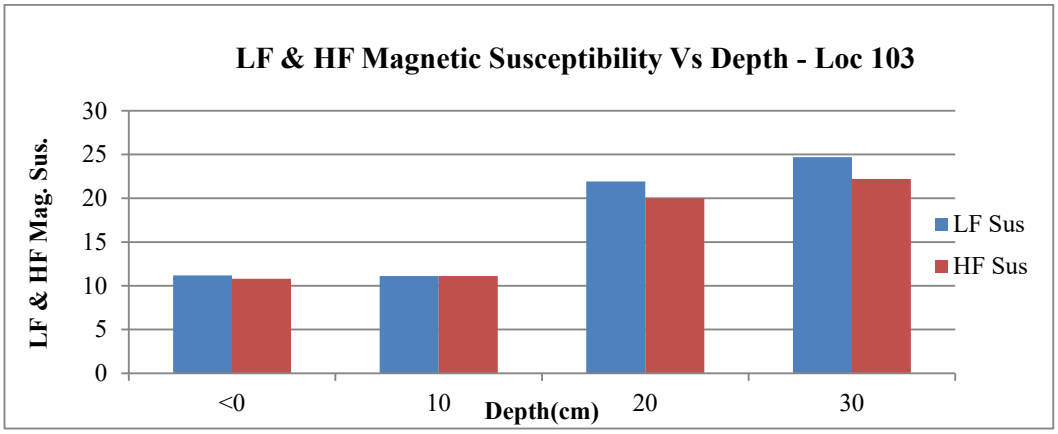
LF & HF Magnetic Susceptibility Vs Depth - Loc 103
LF & HF Mag. Sus.
30
25
20
15
10
5
0
<0
10
Depth(cm)
20
30
LF Sus
HF Sus

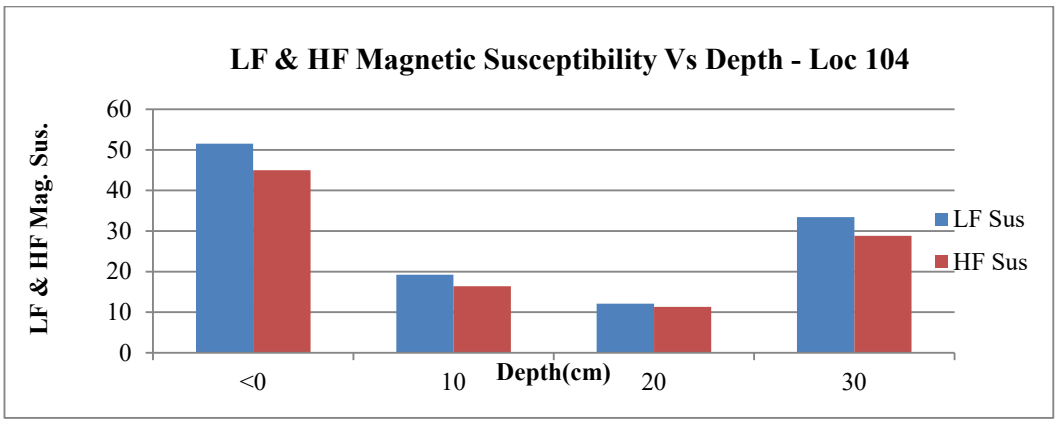
LF & HF Magnetic Susceptibility Vs Depth - Loc 104
LF & HF Mag. Sus.
60
50
40
30
20
10
0
<0
10
Depth(cm)
20
30
LF Sus
HF Sus

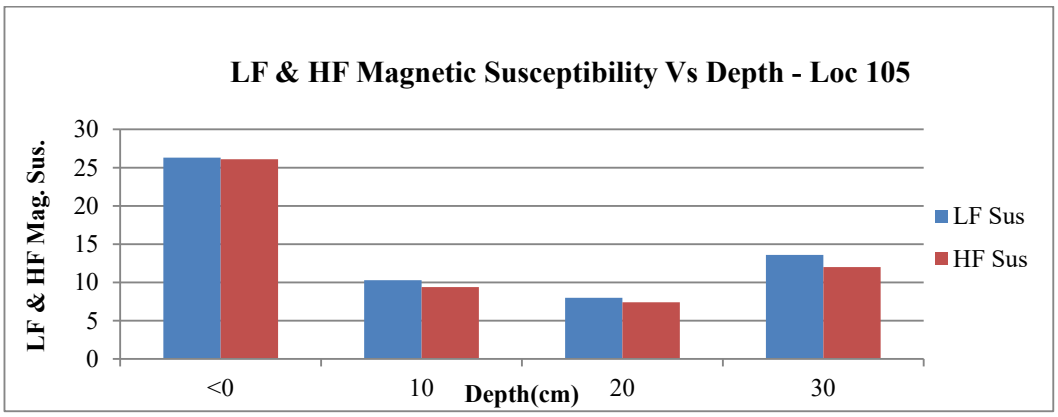
LF & HF Magnetic Susceptibility Vs Depth - Loc 105
LF & HF Mag. Sus.
30
25
20
15
10
5
0
<0
10
Depth(cm)
20
30
LF Sus
HF Sus

Appendix 4.2.: Variation in Magnetic Susceptibility Readings in the Four Grain Sizes (180 µm,125 µm, 90 µm, 65 µm) and Their Associated Weight with Depth for All the

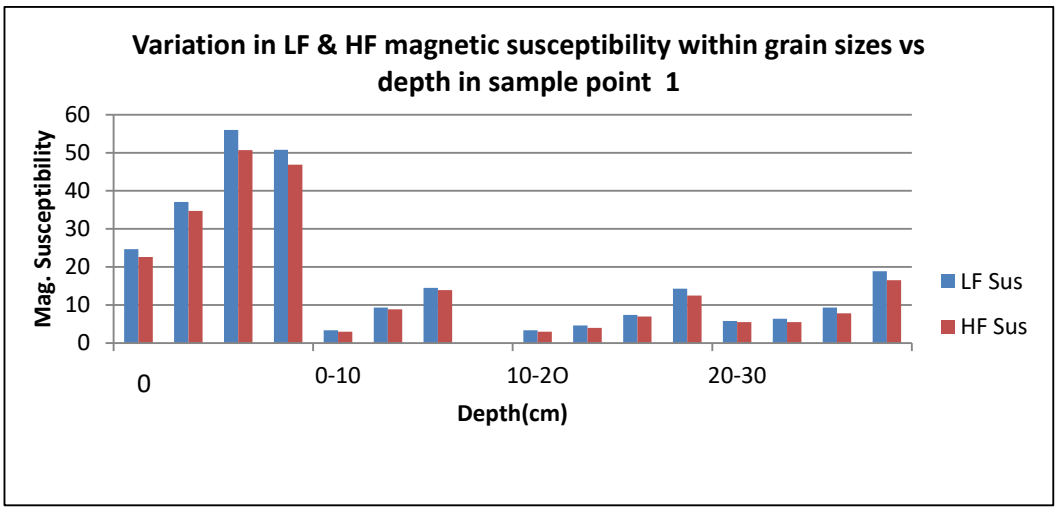

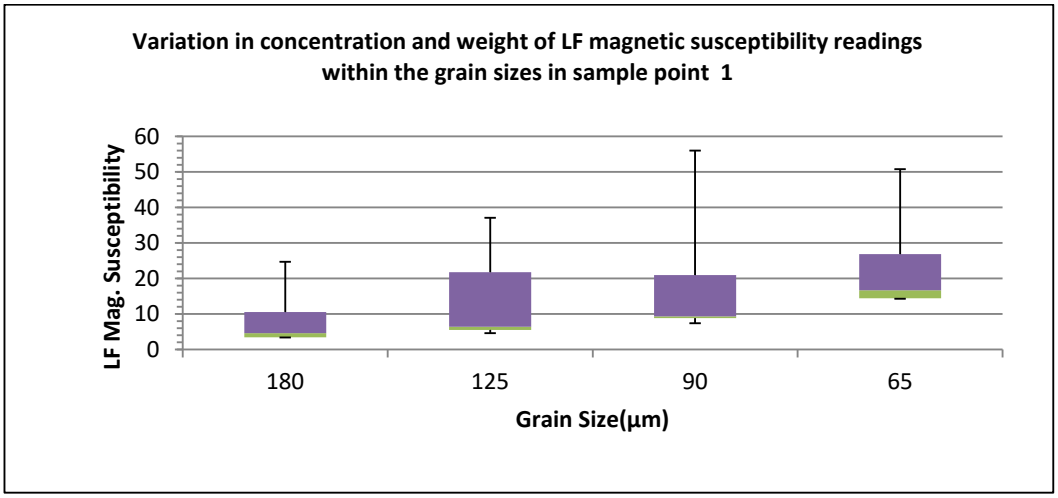

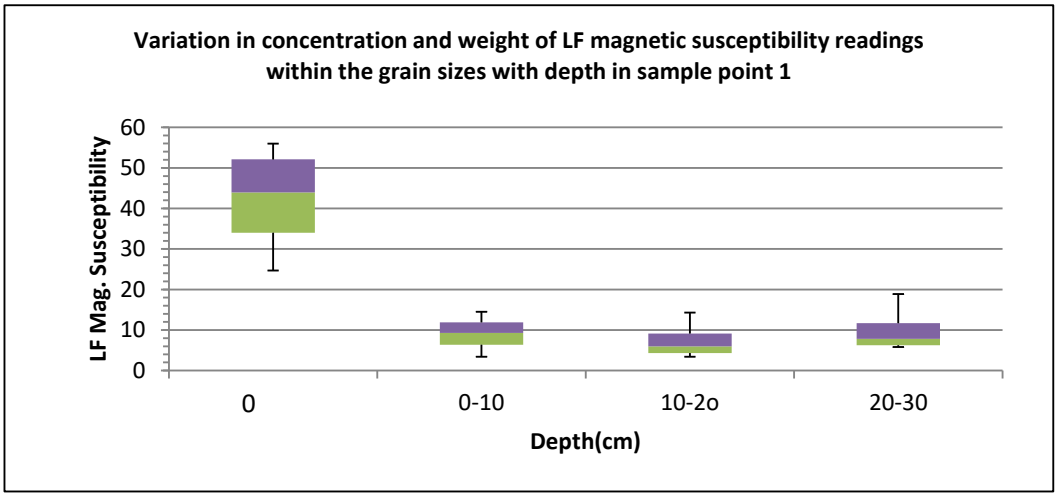

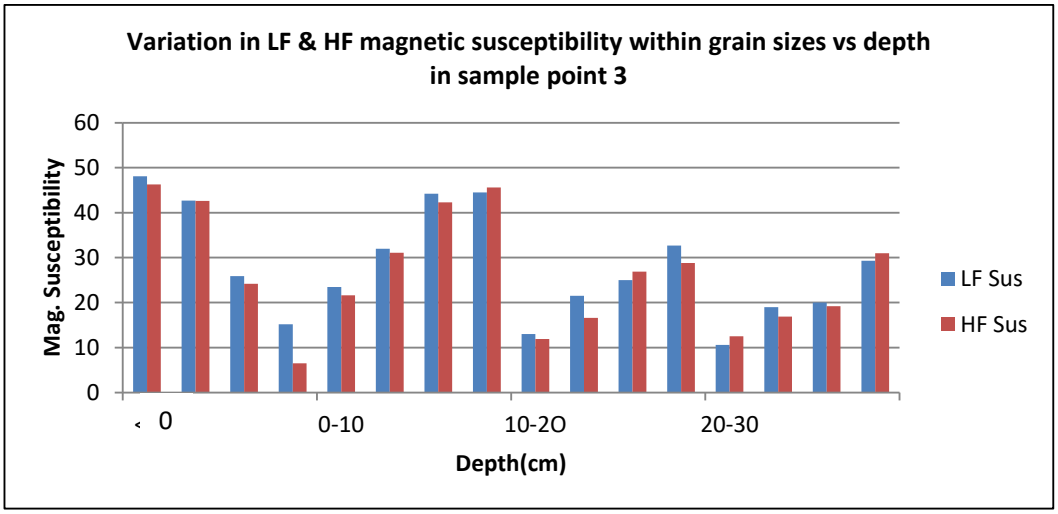
Variation in LF & HF magnetic susceptibility within grain sizes vs depth in sample point 3
Mag. Susceptibility
60
50
40
30
20
10
0
0
0-10
10-2O
20-30
Depth(cm)
LF Sus
HF Sus

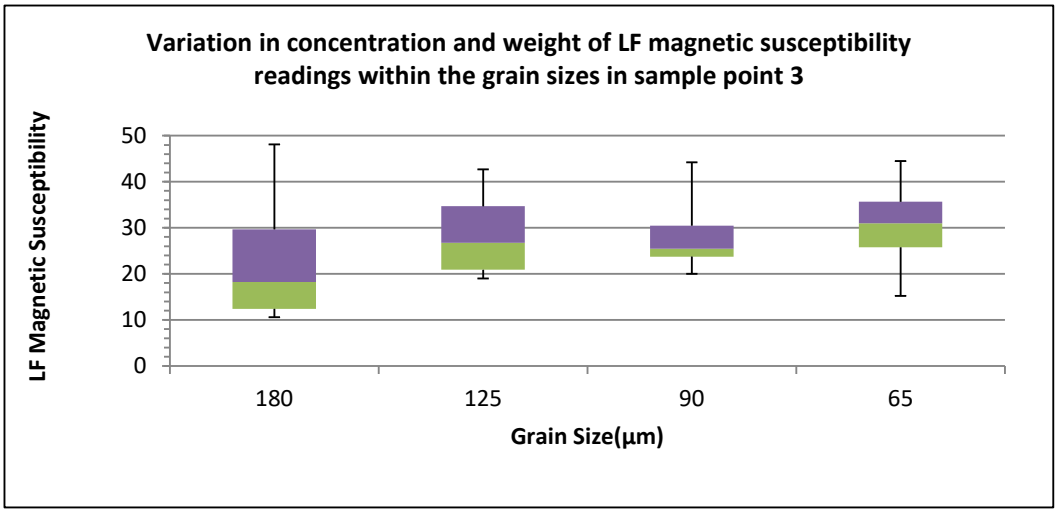
Variation in concentration and weight of LF magnetic susceptibility readings within the grain sizes in sample point 3
LF Magnetic Susceptibility
50
40
30
20
10
0
180
125
90
65
Grain Size(µm)

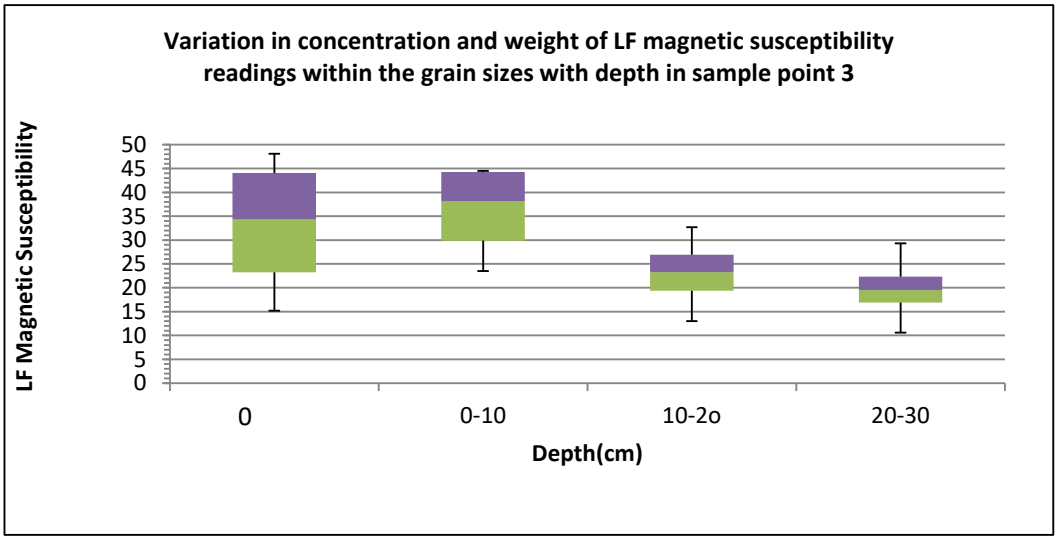
Variation in concentration and weight of LF magnetic susceptibility readings within the grain sizes with depth in sample point 3
LF Magnetic Susceptibility
50
45
40
35
30
25
20
15
10
5
0
0
0-10
10-2o
20-30
Depth(cm)

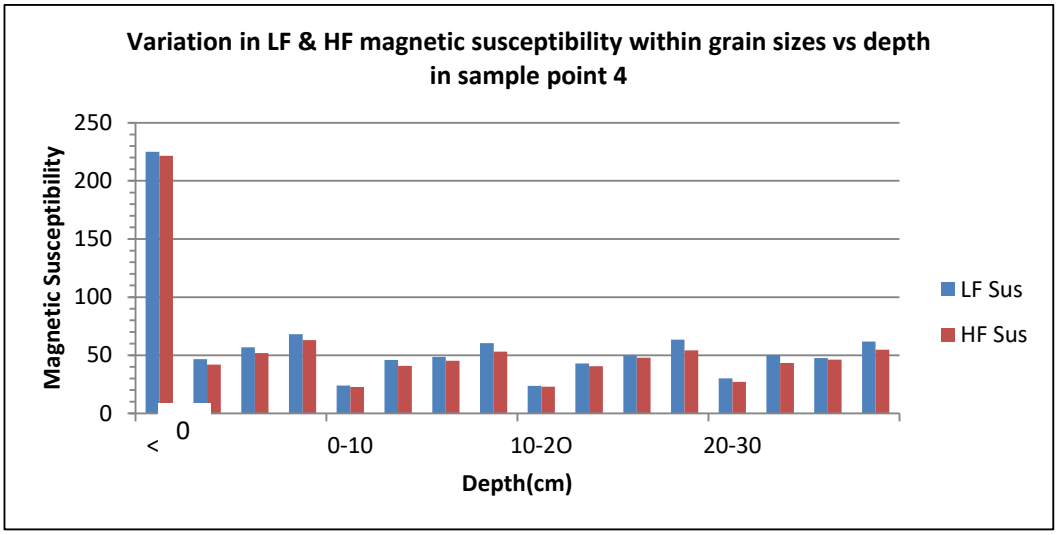
Variation in LF & HF magnetic susceptibility within grain sizes vs depth in sample point 4
Magnetic Susceptibility
250
200
150
100
50
0
< 0
0-10
10-2O
20-30
Depth(cm)
LF Sus
HF Sus

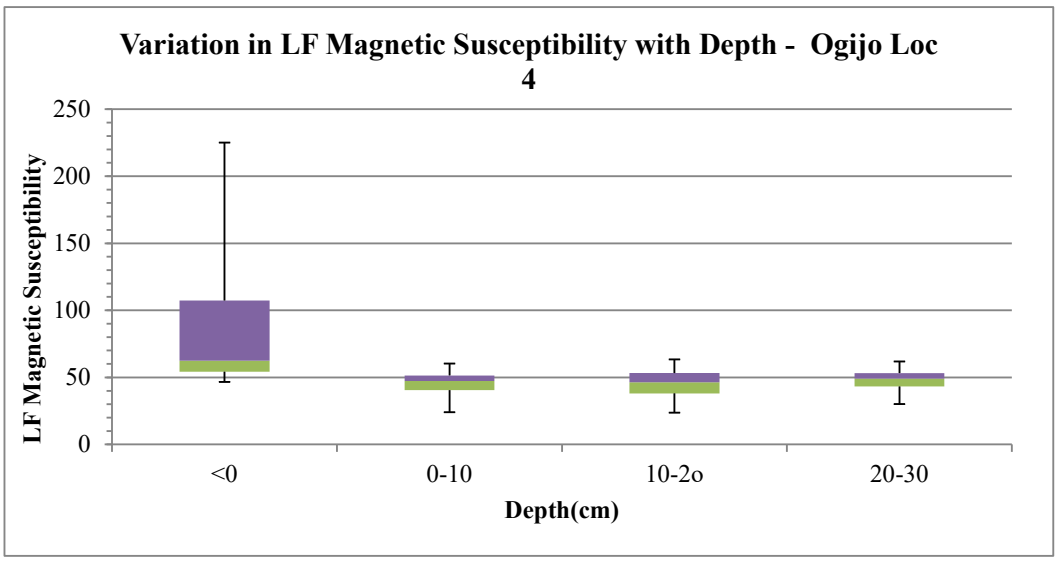
Variation in LF Magnetic Susceptibility with Depth - Ogijo Loc 4
LF Magnetic Susceptibility
250
200
150
100
50
0
<0
0-10
10-2o
20-30
Depth(cm)

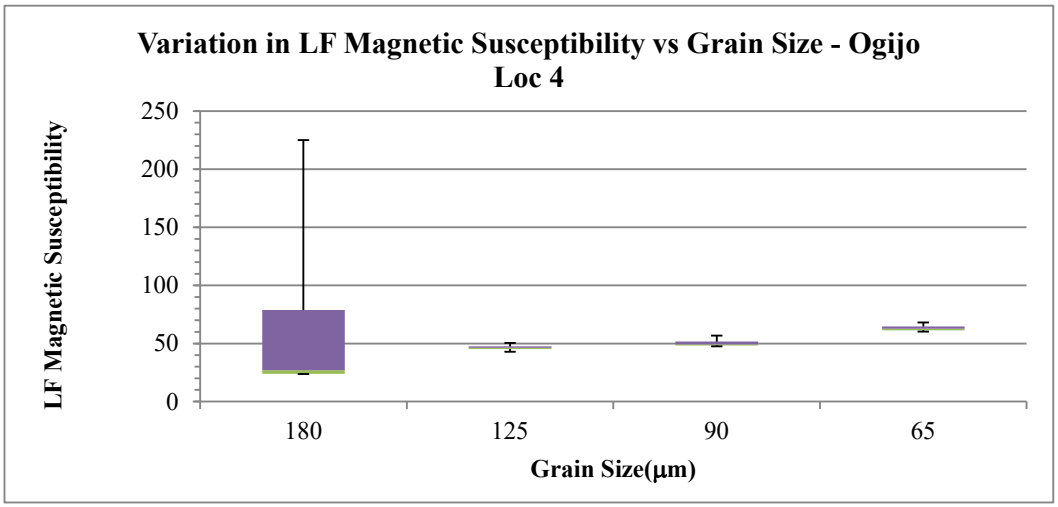
Variation in LF Magnetic Susceptibility vs Grain Size - Ogijo Loc 4
LF Magnetic Susceptibility
250
200
150
100
50
0
180
125
90
65
Grain Size(µm)

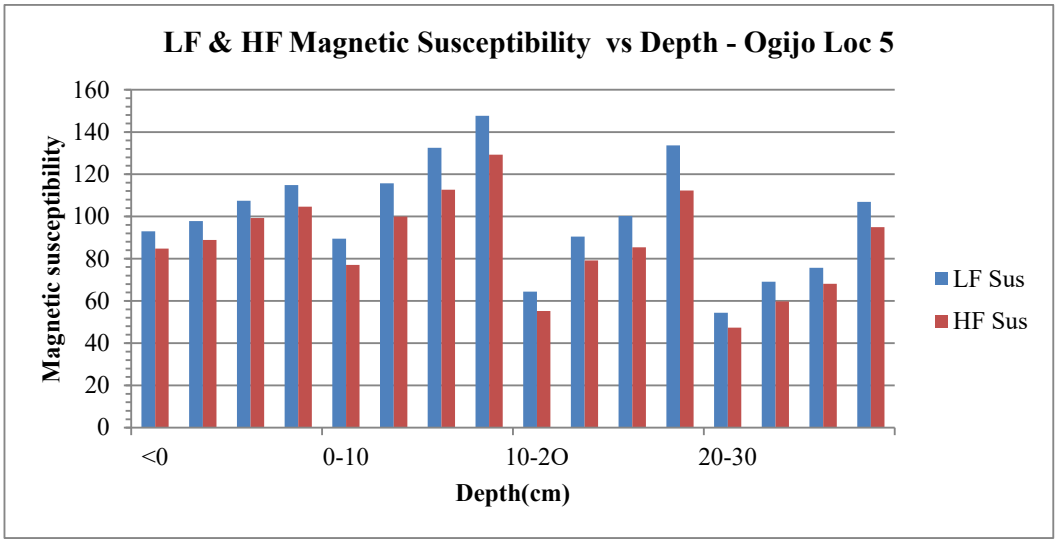
LF & HF Magnetic Susceptibility vs Depth - Ogijo Loc 5
Magnetic susceptibility
160
140
120
100
80
60
40
20
0
<0
0-10
10-2O
20-30
Depth(cm)
LF Sus
HF Sus

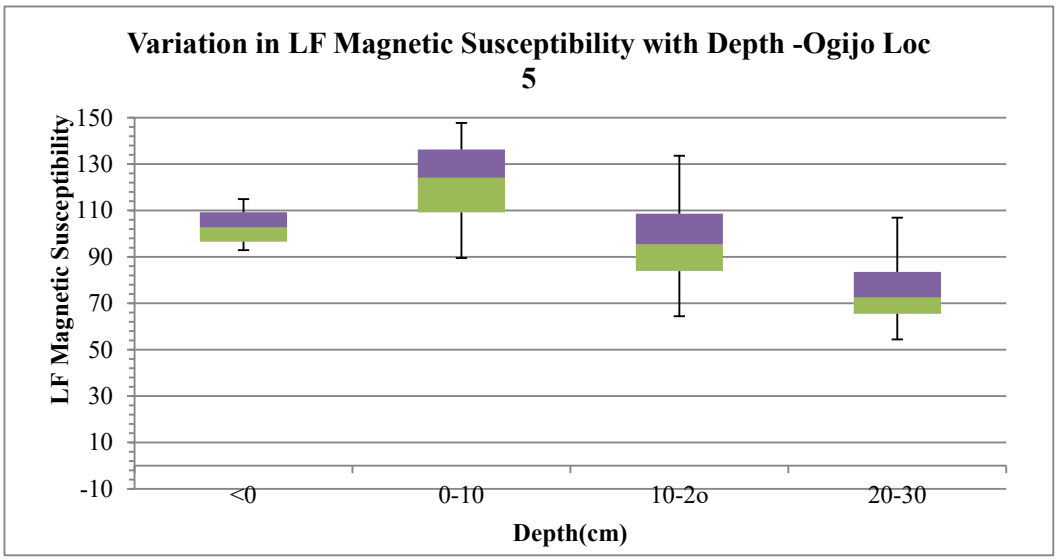
Variation in LF Magnetic Susceptibility with Depth -Ogijo Loc 5
LF Magnetic Susceptibility
150
130
110
90
70
50
30
10
-10
<0
0-10
10-2o
20-30
Depth(cm)

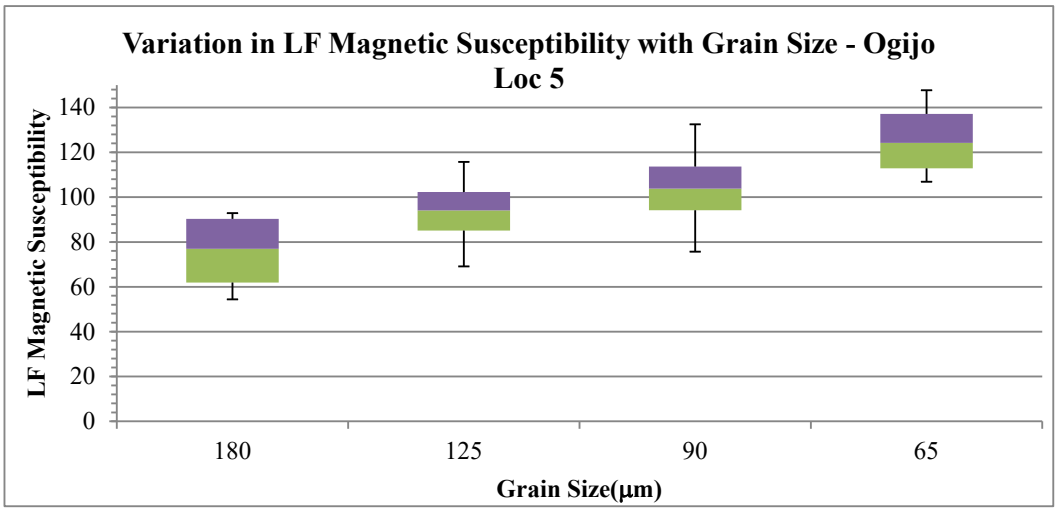
Variation in LF Magnetic Susceptibility with Grain Size - Ogijo Loc 5
LF Magnetic Susceptibility
140
120
100
80
60
40
20
0
180
125
90
65
Grain Size(µm)

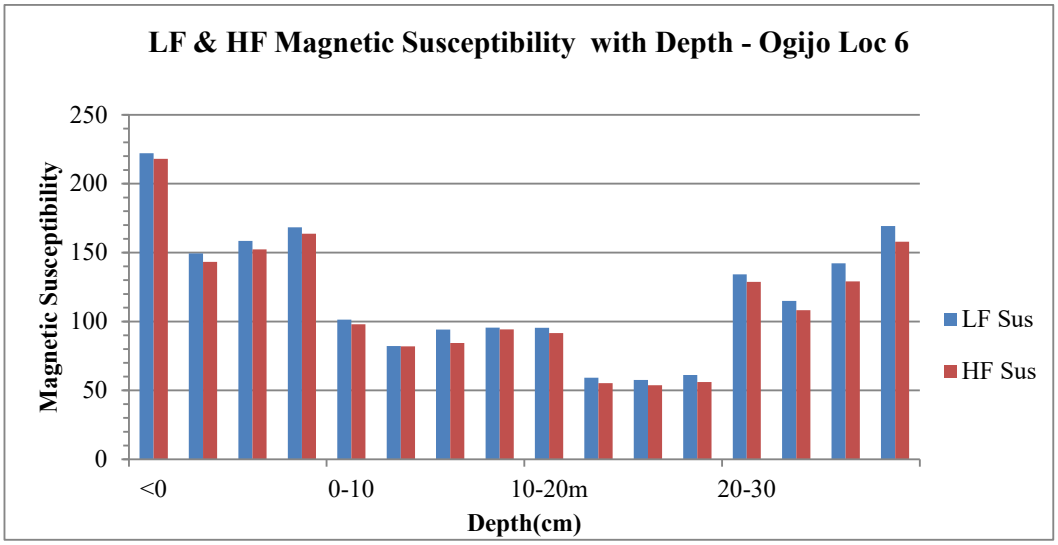
LF & HF Magnetic Susceptibility with Depth - Ogijo Loc 6
Magnetic Susceptibility
250
200
150
100
50
0
<0
0-10
10-20m
20-30
Depth(cm)
LF Sus
HF Sus

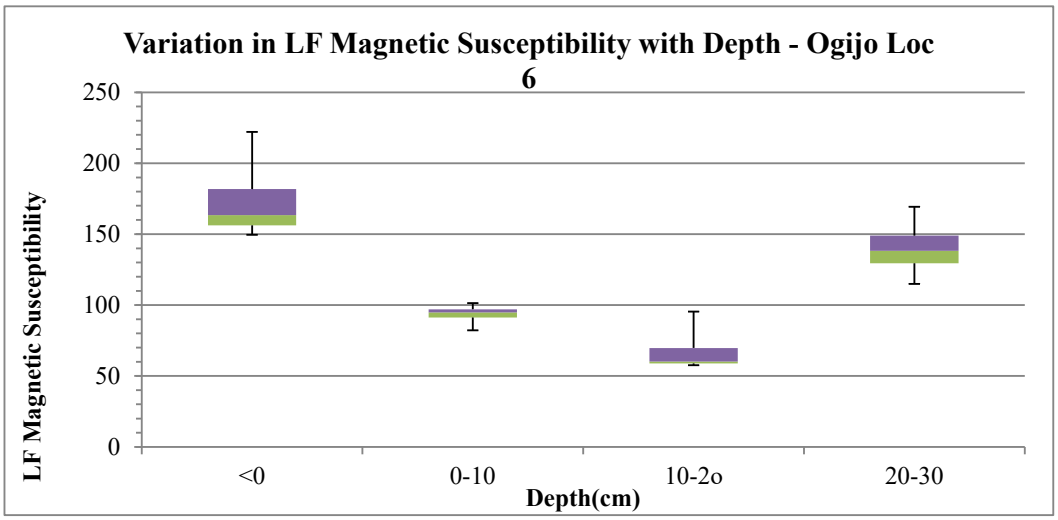
Variation in LF Magnetic Susceptibility with Depth - Ogijo Loc 6
LF Magnetic Susceptibility
250
200
150
100
50
0
<0
0-10
10-2o
20-30
Depth(cm)

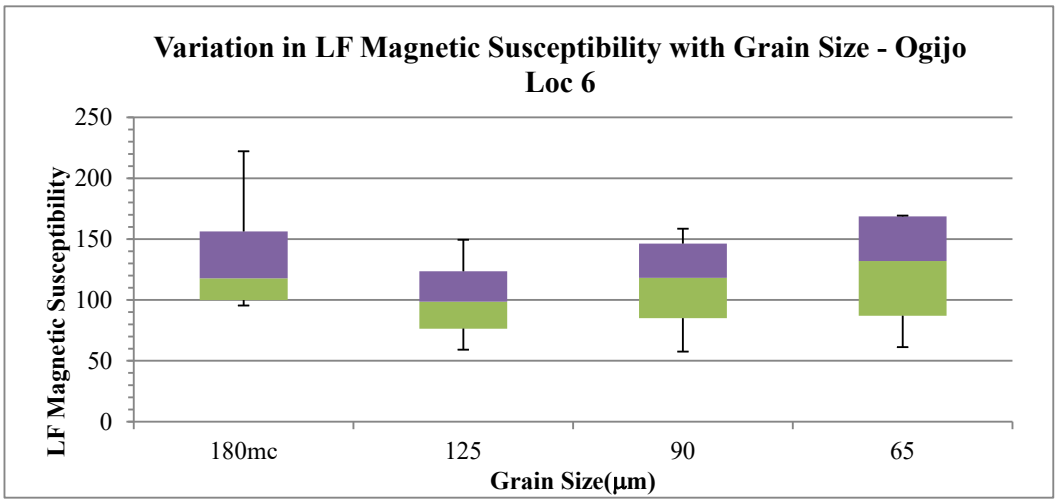
Variation in LF Magnetic Susceptibility with Grain Size - Ogijo Loc 6
LF Magnetic Susceptibility
250
200
150
100
50
0
180mc
125
90
65
Grain Size(μm)

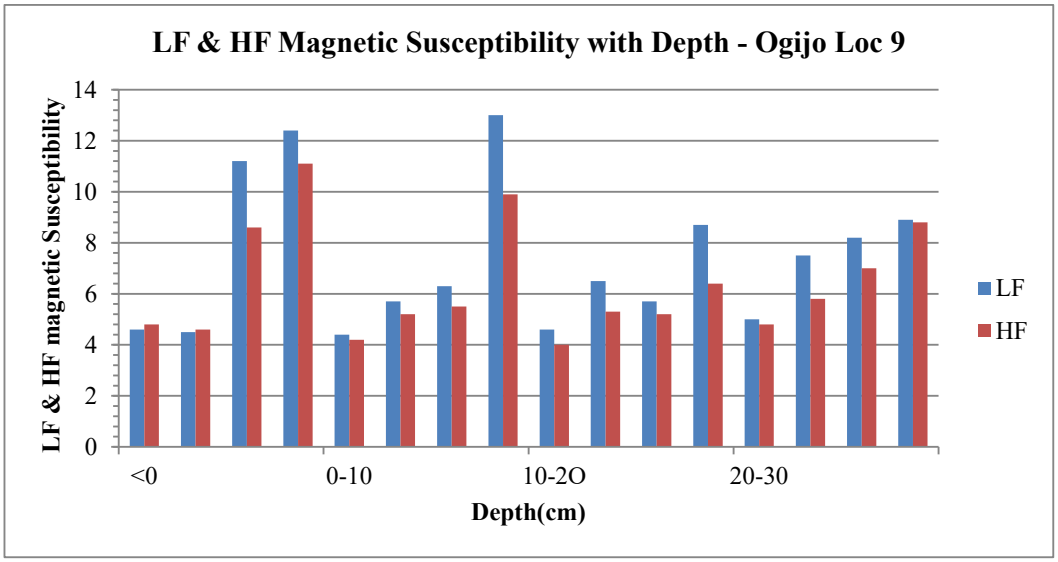
LF & HF Magnetic Susceptibility with Depth - Ogijo Loc 9
LF & HF magnetic Susceptibility
14
12
10
8
6
4
2
0
<0
0-10
10-2O
20-30
Depth(cm)
LF
HF

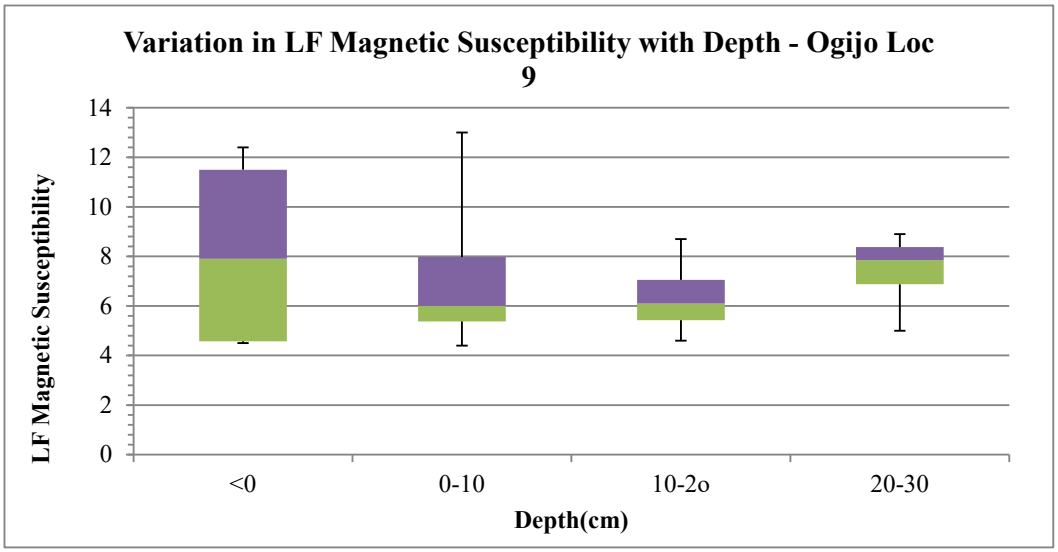
Variation in LF Magnetic Susceptibility with Depth - Ogijo Loc 9
LF Magnetic Susceptibility
14
12
10
8
6
4
2
0
<0
0-10
10-2o
20-30
Depth(cm)

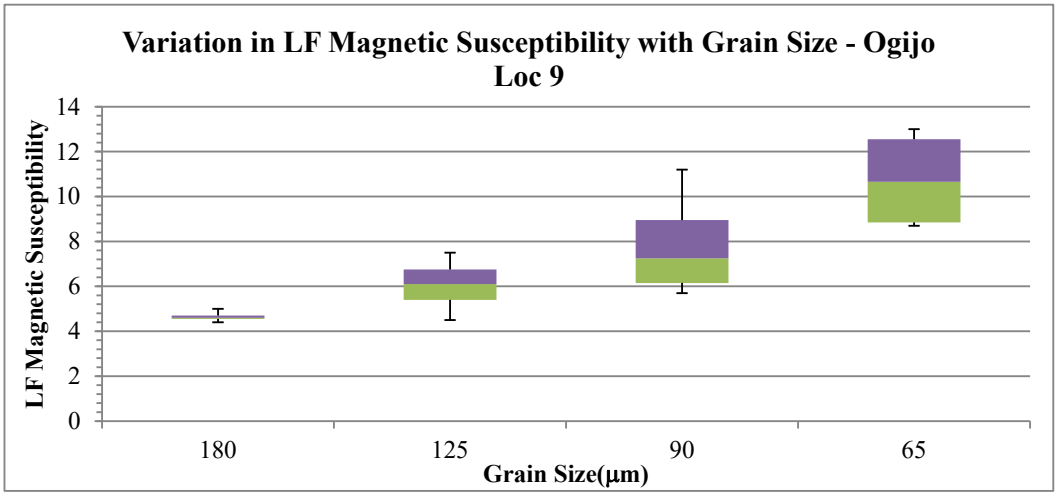
Variation in LF Magnetic Susceptibility with Grain Size - Ogijo Loc 9
LF Magnetic Susceptibility
14
12
10
8
6
4
2
0
180
125
90
65
Grain Size(µm)

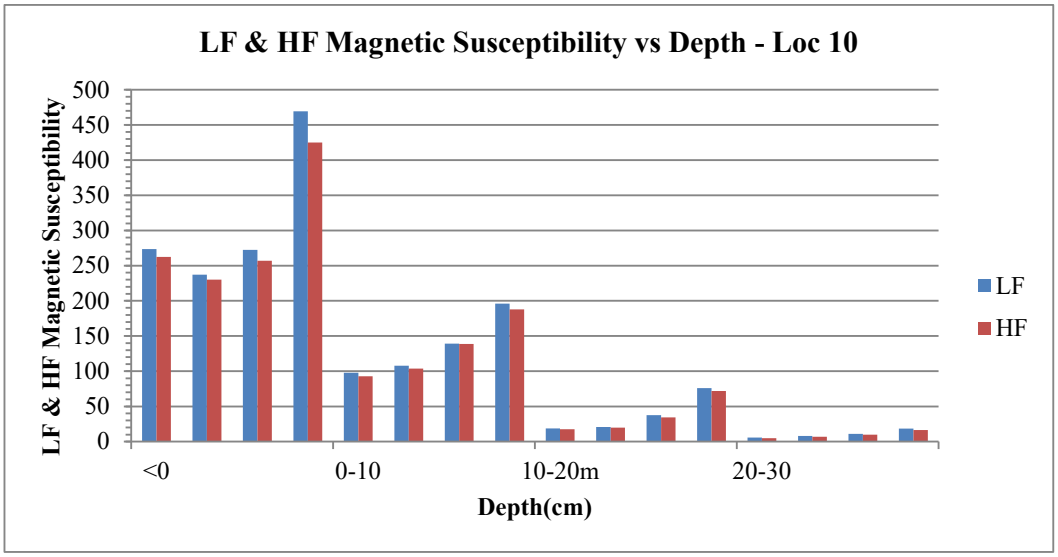
LF & HF Magnetic Susceptibility vs Depth - Loc 10
LF & HF Magnetic Susceptibility
500
450
400
350
300
250
200
150
100
50
0
<0
0-10
10-20m
20-30
Depth(cm)
LF
HF

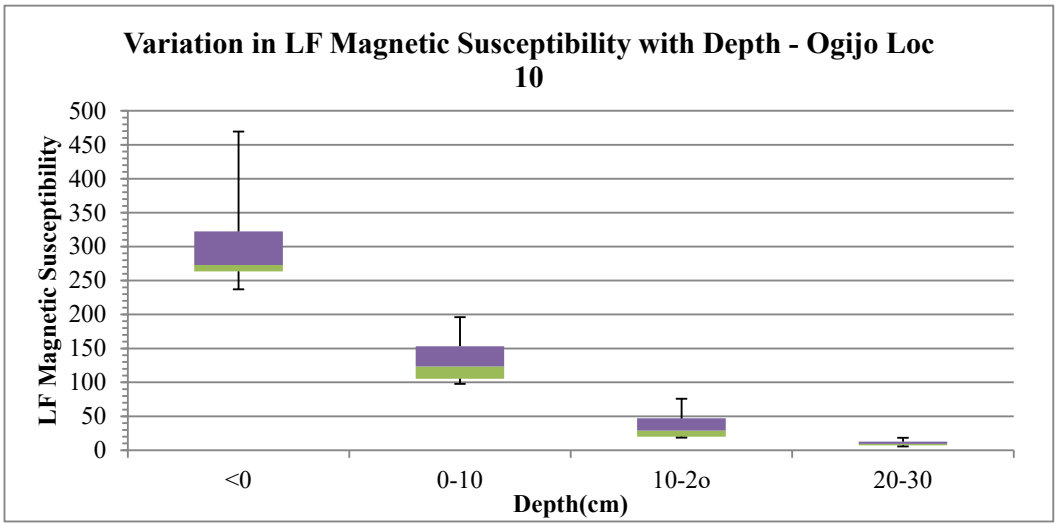
Variation in LF Magnetic Susceptibility with Depth - Ogijo Loc 10
LF Magnetic Susceptibility
500
450
400
350
300
250
200
150
100
50
0
<0
0-10
10-2o
20-30
Depth(cm)

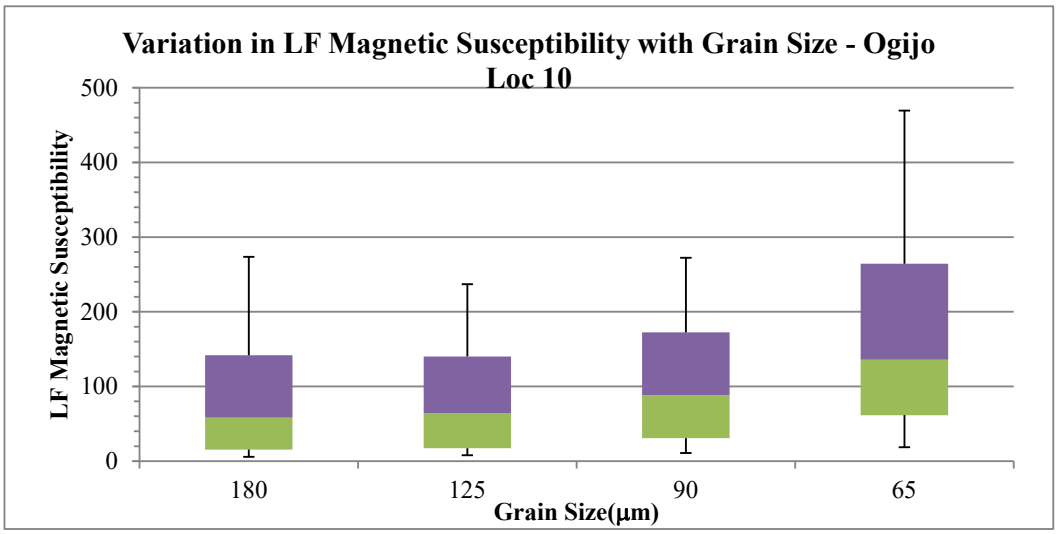
Variation in LF Magnetic Susceptibility with Grain Size - Ogijo Loc 10
LF Magnetic Susceptibility
500
400
300
200
100
0
180
125
90
65
Grain Size(µm)

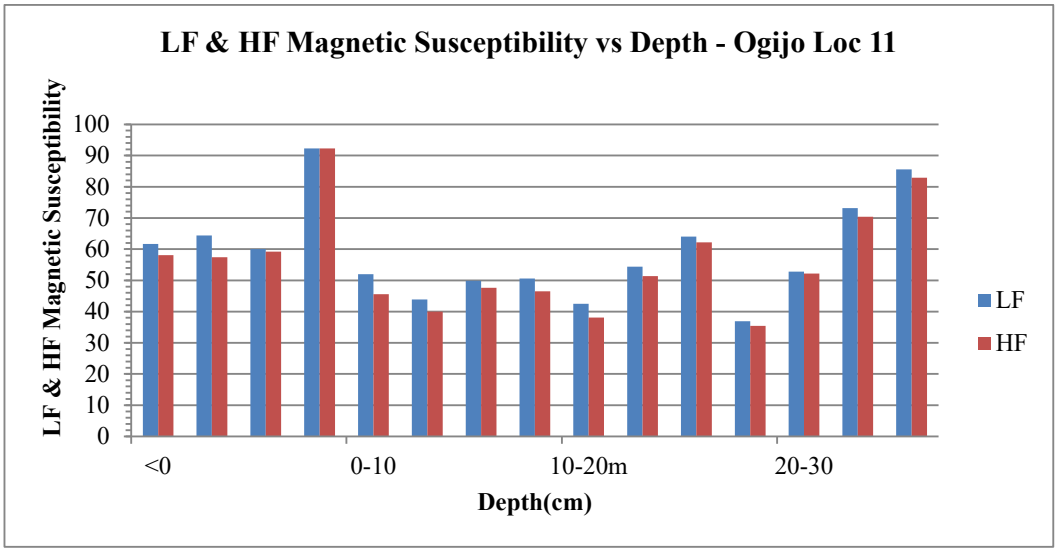
LF & HF Magnetic Susceptibility vs Depth - Ogijo Loc 11
LF & HF Magnetic Susceptibility
100
90
80
70
60
50
40
30
20
10
0
<0
0-10
10-20m
20-30
Depth(cm)
LF
HF

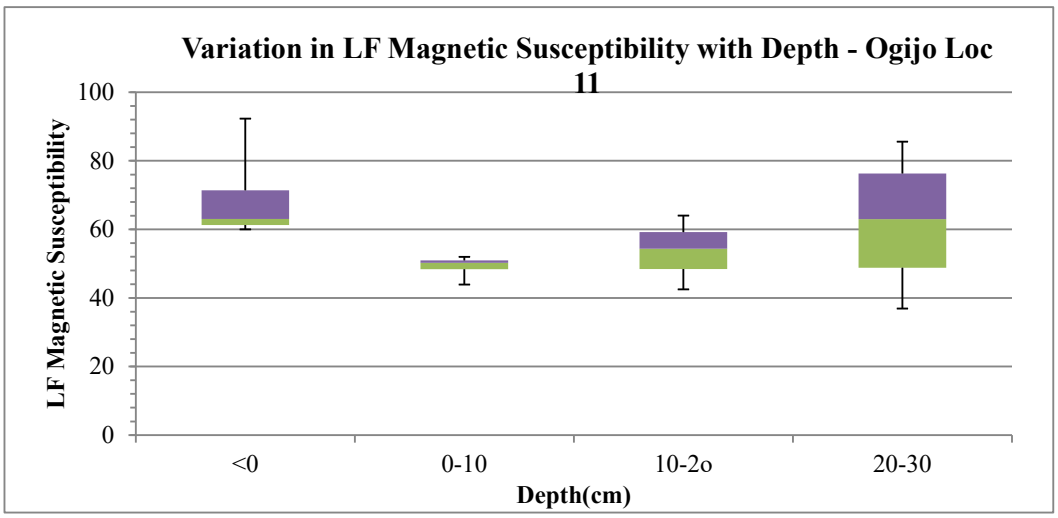
Variation in LF Magnetic Susceptibility with Depth - Ogijo Loc 11
LF Magnetic Susceptibility
100
80
60
40
20
0
<0
0-10
10-2o
20-30
Depth(cm)

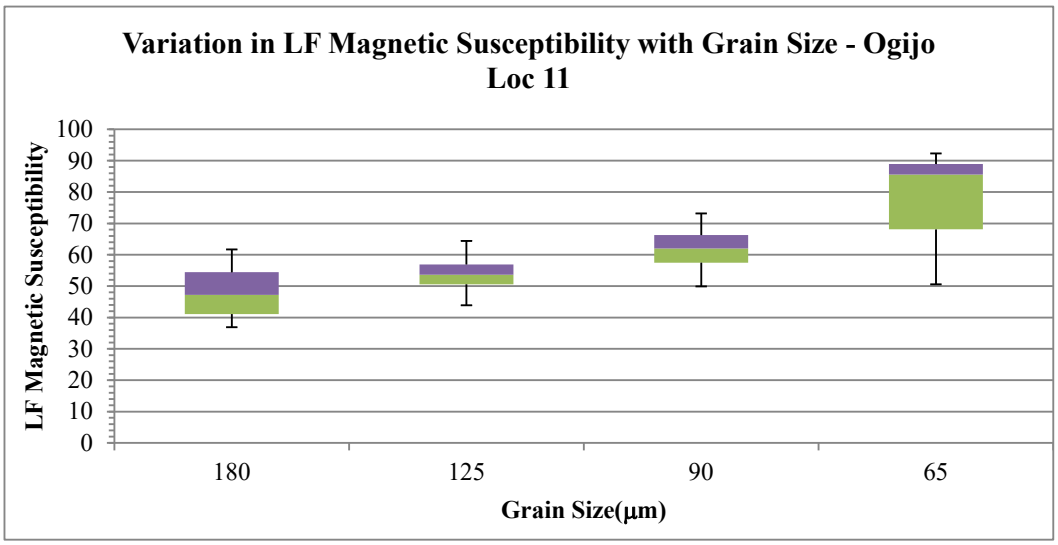
Variation in LF Magnetic Susceptibility with Grain Size - Ogijo Loc 11
LF Magnetic Susceptibility
100
90
80
70
60
50
40
30
20
10
0
180
125
90
65
Grain Size(µm)

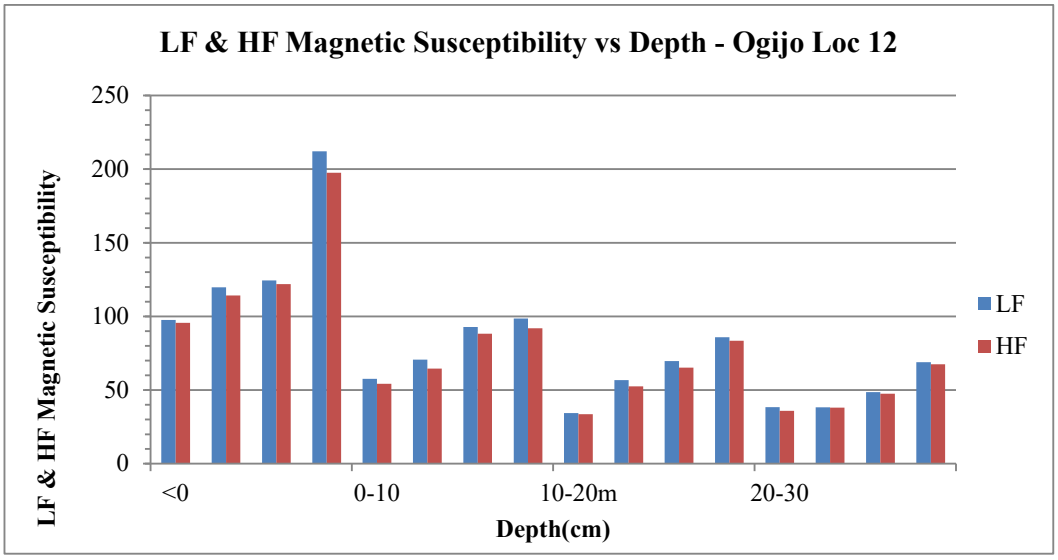
LF & HF Magnetic Susceptibility vs Depth - Ogijo Loc 12
LF & HF Magnetic Susceptibility
250
200
150
100
50
0
<0
0-10
10-20m
20-30
Depth(cm)
LF
HF

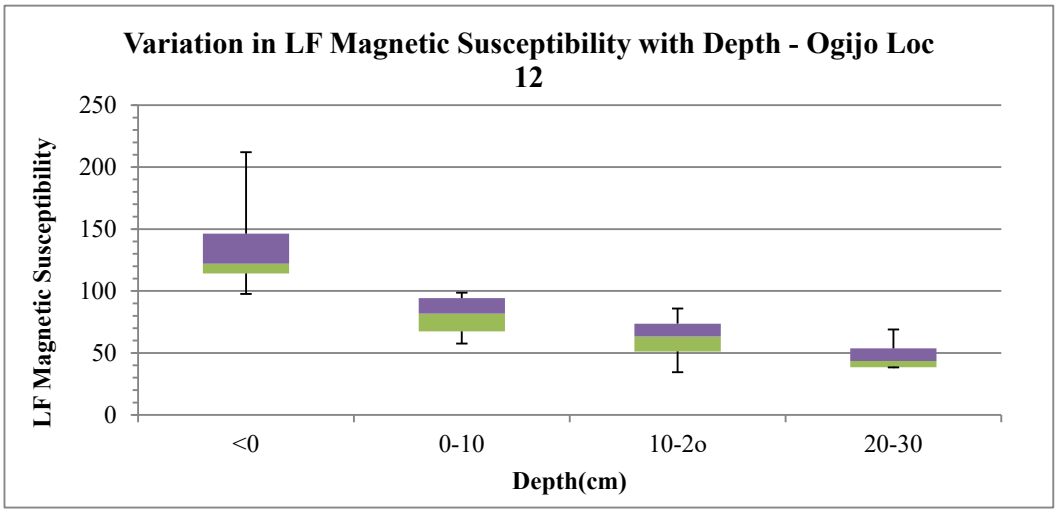
Variation in LF Magnetic Susceptibility with Depth - Ogijo Loc 12
LF Magnetic Susceptibility
250
200
150
100
50
0
<0
0-10
10-2o
20-30
Depth(cm)

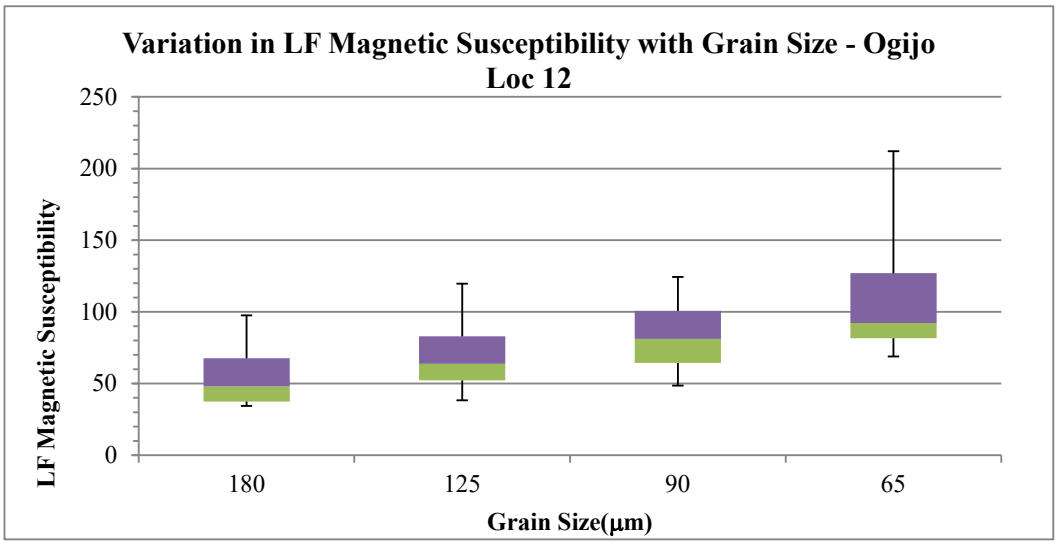
Variation in LF Magnetic Susceptibility with Grain Size - Ogijo Loc 12
LF Magnetic Susceptibility
250
200
150
100
50
0
180
125
90
65
Grain Size(µm)

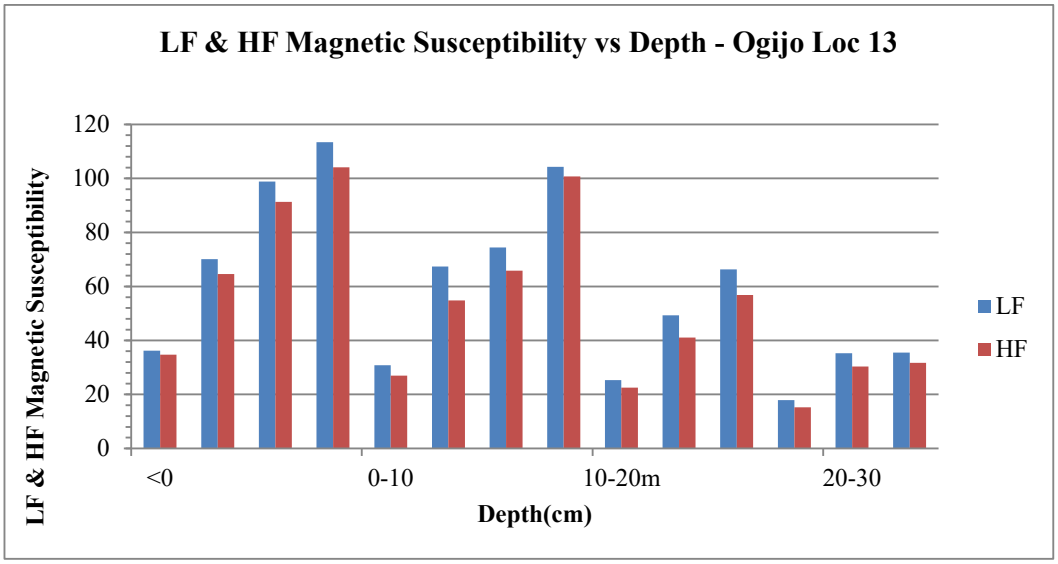
LF & HF Magnetic Susceptibility vs Depth - Ogijo Loc 13
LF & HF Magnetic Susceptibility
120
100
80
60
40
20
0
<0
0-10
10-20m
20-30
Depth(cm)
LF
HF

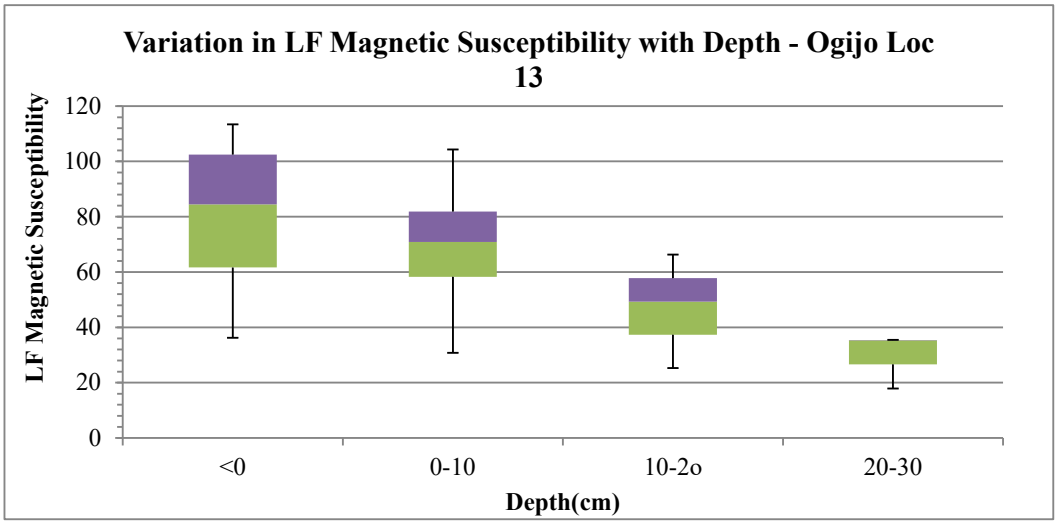
Variation in LF Magnetic Susceptibility with Depth - Ogijo Loc 13
LF Magnetic Susceptibility
120
100
80
60
40
20
0
<0
0-10
10-2o
20-30
Depth(cm)

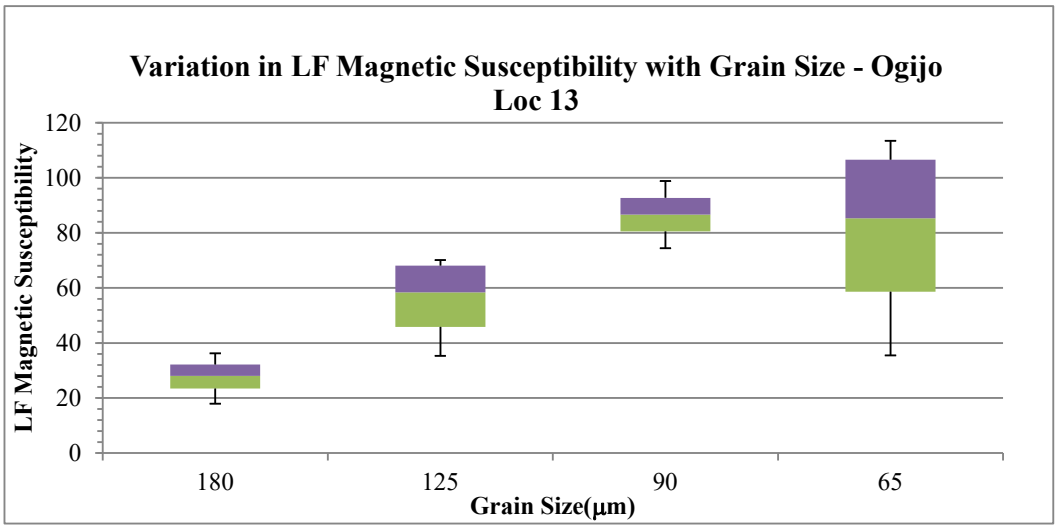
Variation in LF Magnetic Susceptibility with Grain Size - Ogijo Loc 13
LF Magnetic Susceptibility
120
100
80
60
40
20
0
180
125
90
65
Grain Size(µm)

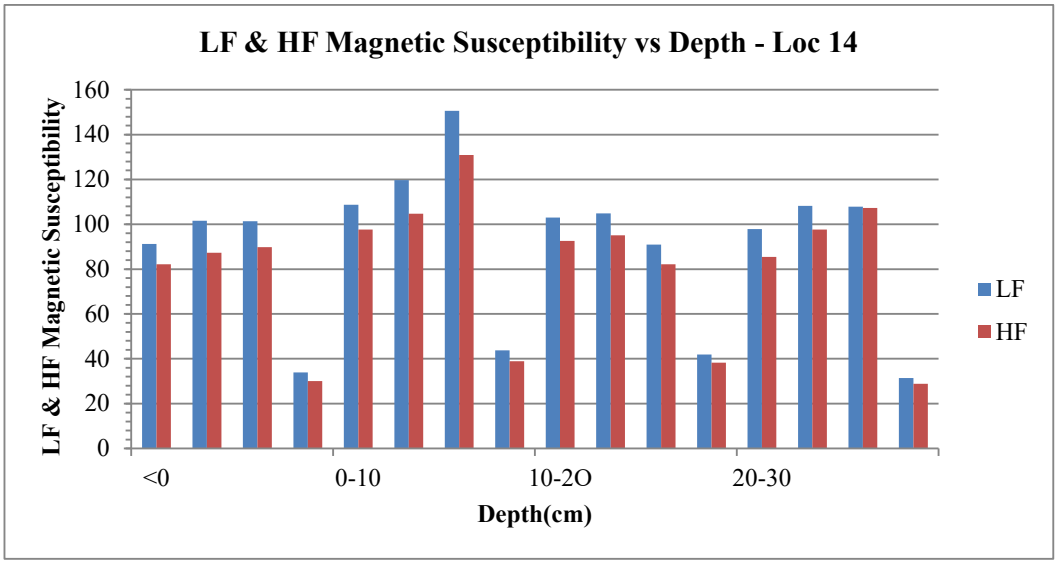
LF & HF Magnetic Susceptibility vs Depth - Loc 14
LF & HF Magnetic Susceptibility
160
140
120
100
80
60
40
20
0
<0
0-10
10-2O
20-30
Depth(cm)
LF
HF

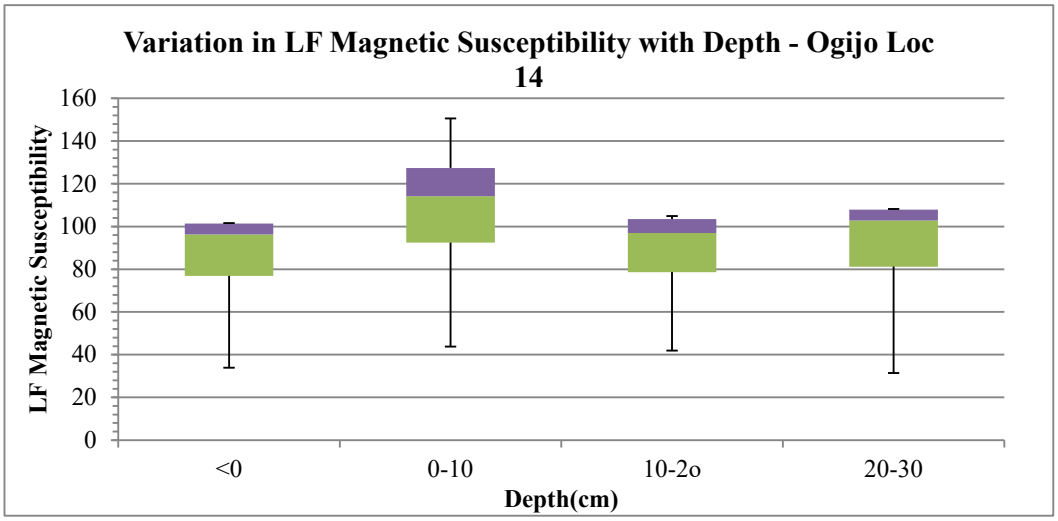
Variation in LF Magnetic Susceptibility with Depth - Ogijo Loc 14
LF Magnetic Susceptibility
160
140
120
100
80
60
40
20
0
<0
0-10
10-2o
20-30
Depth(cm)

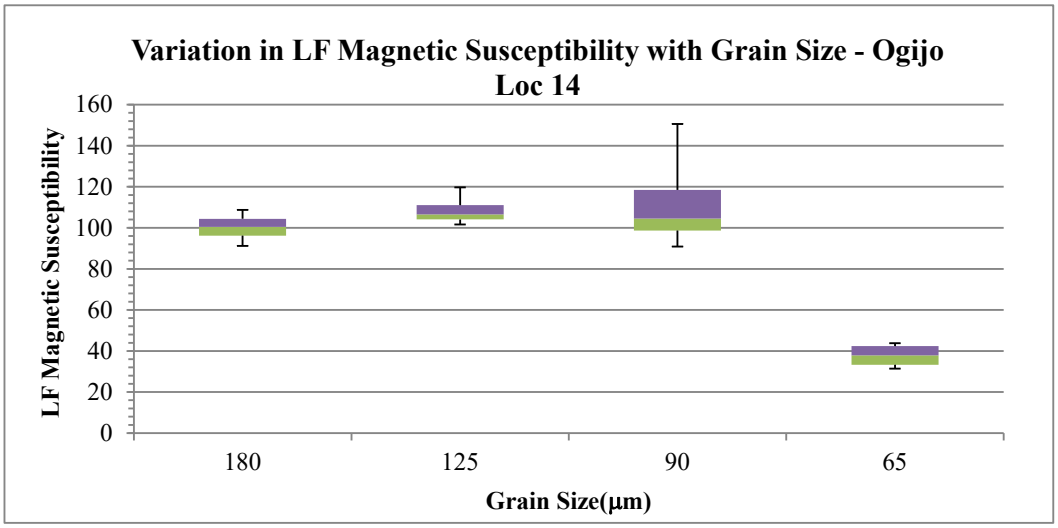
Variation in LF Magnetic Susceptibility with Grain Size - Ogijo Loc 14
LF Magnetic Susceptibility
160
140
120
100
80
60
40
20
0
180
125
90
65
Grain Size(µm)

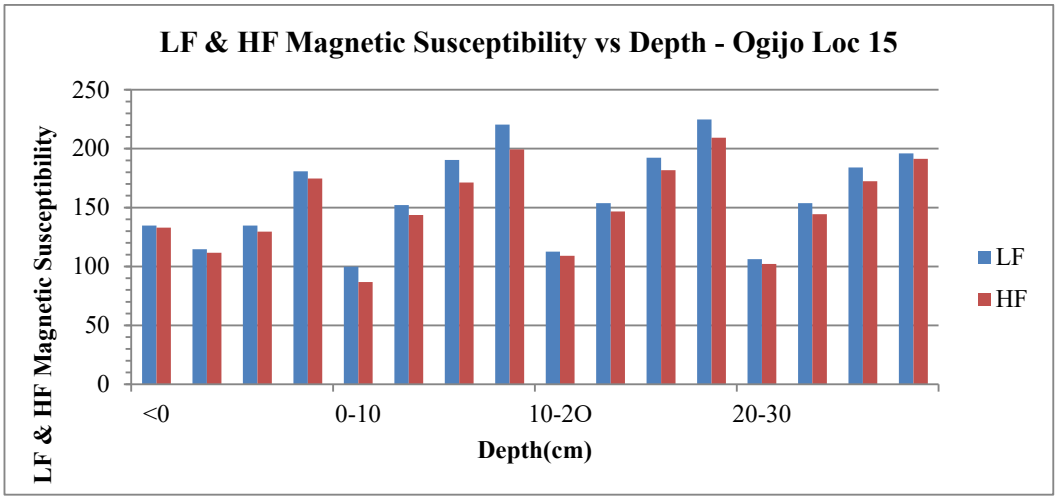
LF & HF Magnetic Susceptibility vs Depth - Ogijo Loc 15
LF & HF Magnetic Susceptibility
250
200
150
100
50
0
<0
0-10
10-2O
20-30
Depth(cm)
LF
HF

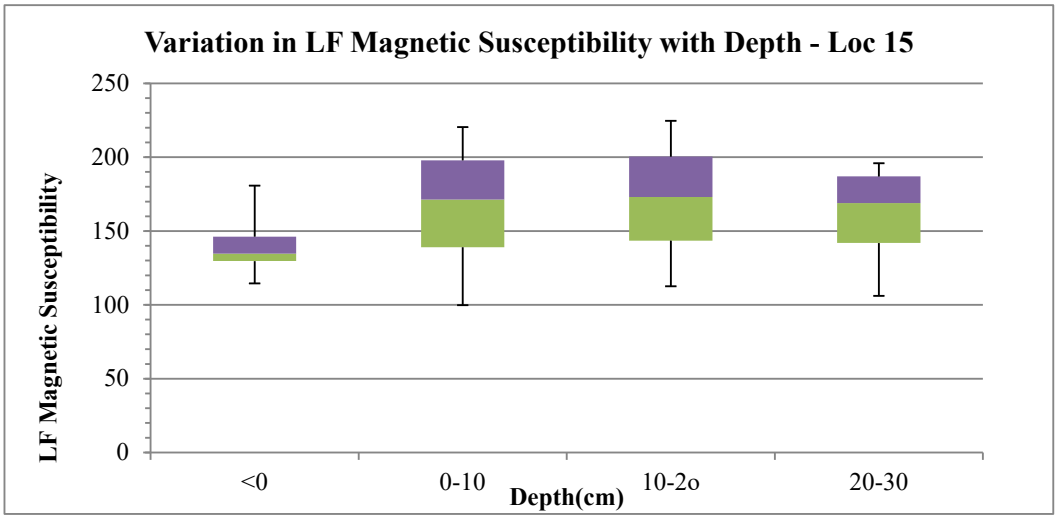
Variation in LF Magnetic Susceptibility with Depth - Loc 15
LF Magnetic Susceptibility
250
200
150
100
50
0
<0
0-10
10-2o
20-30
Depth(cm)

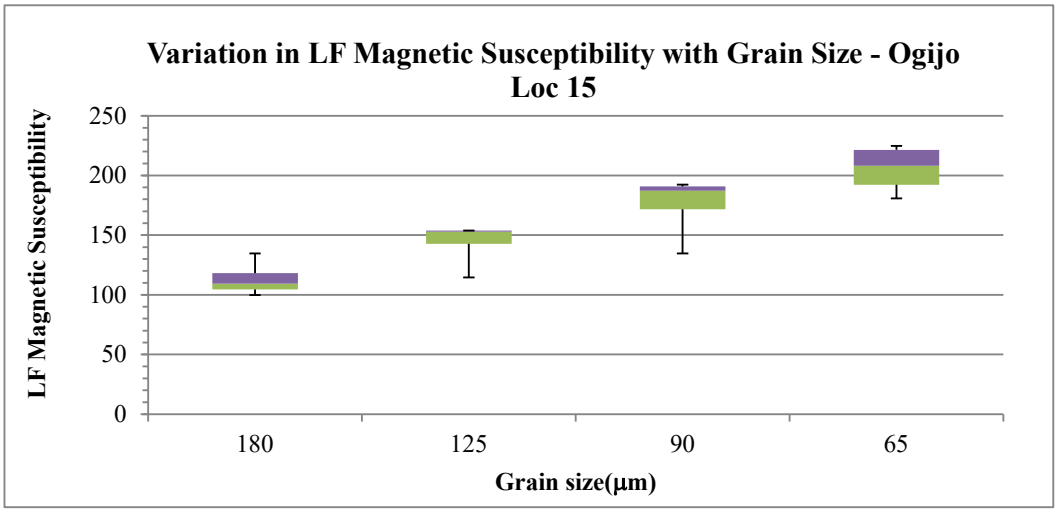
Variation in LF Magnetic Susceptibility with Grain Size - Ogijo Loc 15
LF Magnetic Susceptibility
250
200
150
100
50
0
180
125
90
65
Grain size(µm)

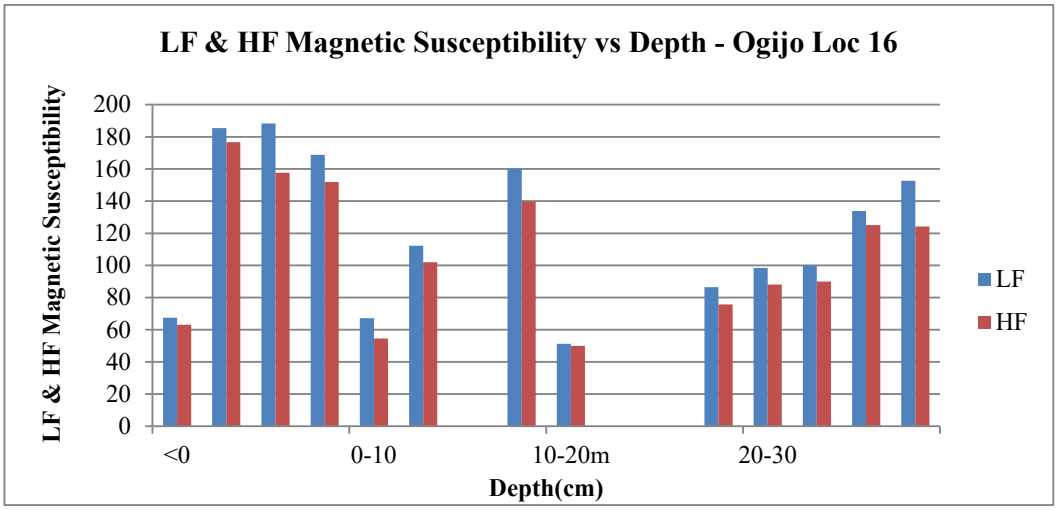
LF & HF Magnetic Susceptibility vs Depth - Ogijo Loc 16
LF & HF Magnetic Susceptibility
200
180
160
140
120
100
80
60
40
20
0
<0
0-10
10-20m
20-30
Depth(cm)
LF
HF

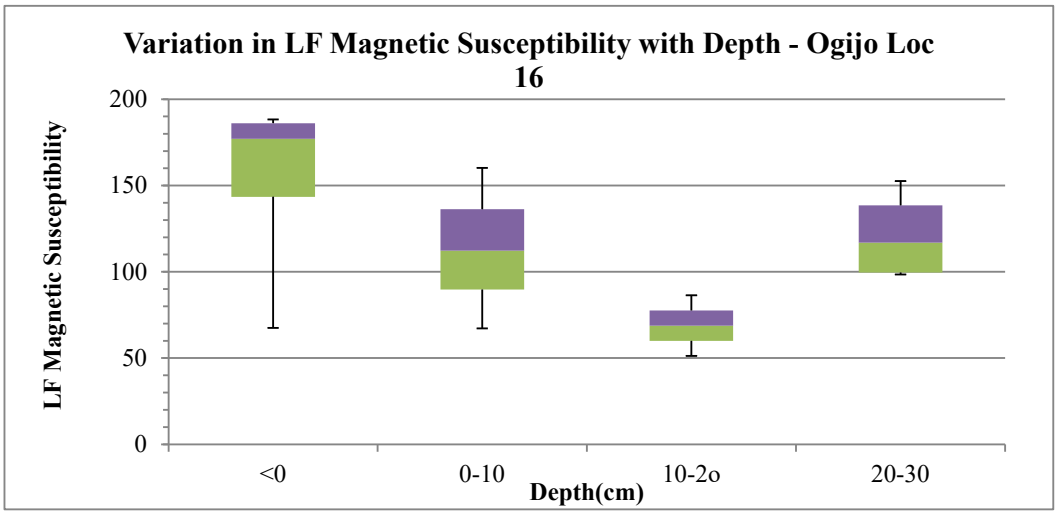
Variation in LF Magnetic Susceptibility with Depth - Ogijo Loc 16
LF Magnetic Susceptibility
200
150
100
50
0
<0
0-10
10-2o
20-30
Depth(cm)

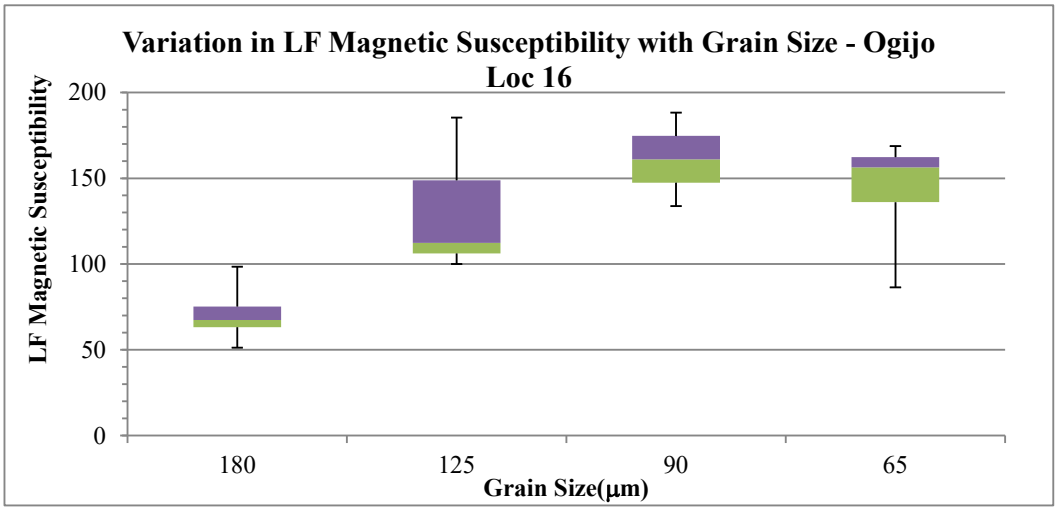
Variation in LF Magnetic Susceptibility with Grain Size - Ogijo Loc 16
LF Magnetic Susceptibility
200
150
100
50
0
180
125
90
65
Grain Size(µm)

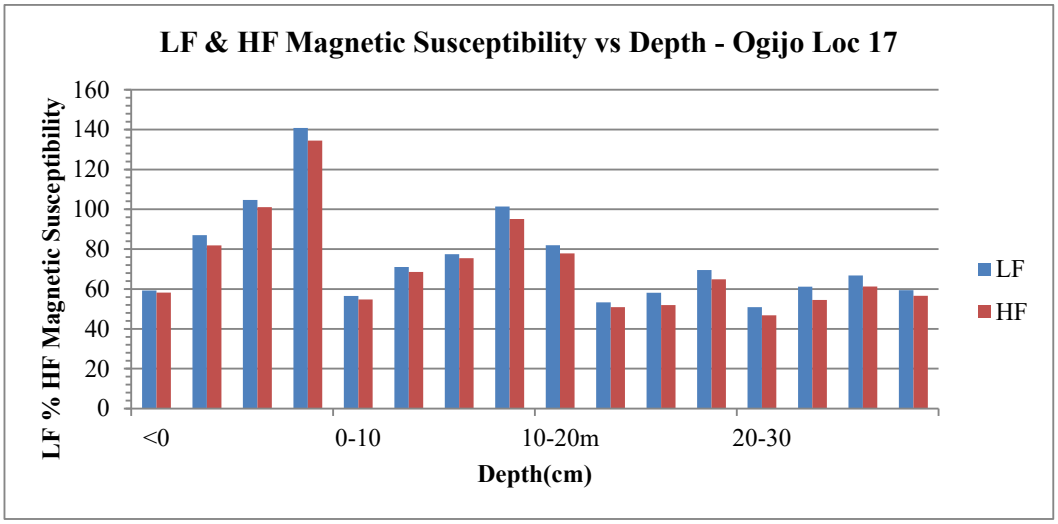
LF & HF Magnetic Susceptibility vs Depth - Ogijo Loc 17
LF % HF Magnetic Susceptibility
160
140
120
100
80
60
40
20
0
<0
0-10
10-20m
20-30
Depth(cm)
LF
HF

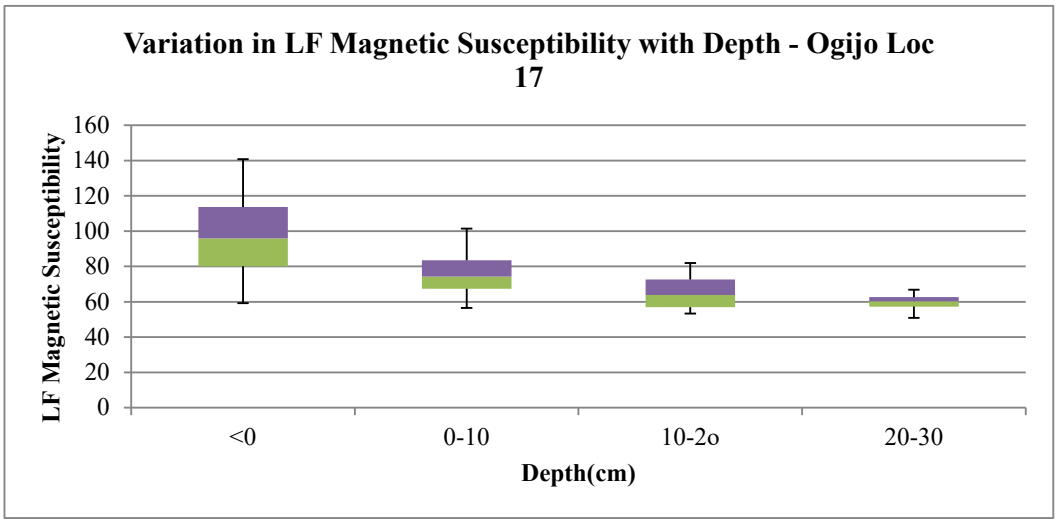
Variation in LF Magnetic Susceptibility with Depth - Ogijo Loc 17
LF Magnetic Susceptibility
160
140
120
100
80
60
40
20
0
<0
0-10
10-2o
20-30
Depth(cm)

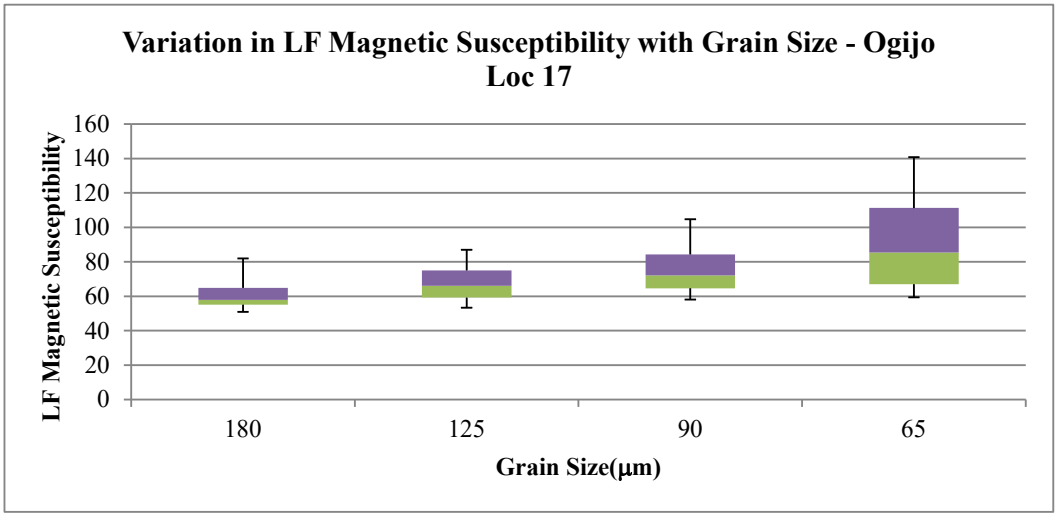
Variation in LF Magnetic Susceptibility with Grain Size - Ogijo Loc 17
LF Magnetic Susceptibility
160
140
120
100
80
60
40
20
0
180
125
90
65
Grain Size(µm)

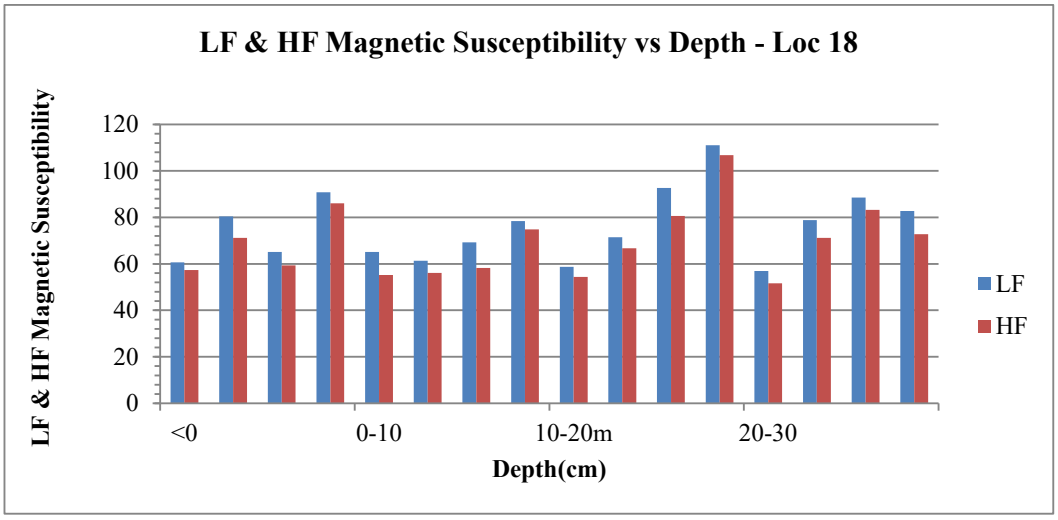
LF & HF Magnetic Susceptibility vs Depth - Loc 18
LF & HF Magnetic Susceptibility
120
100
80
60
40
20
0
<0
0-10
10-20m
20-30
Depth(cm)
LF
HF

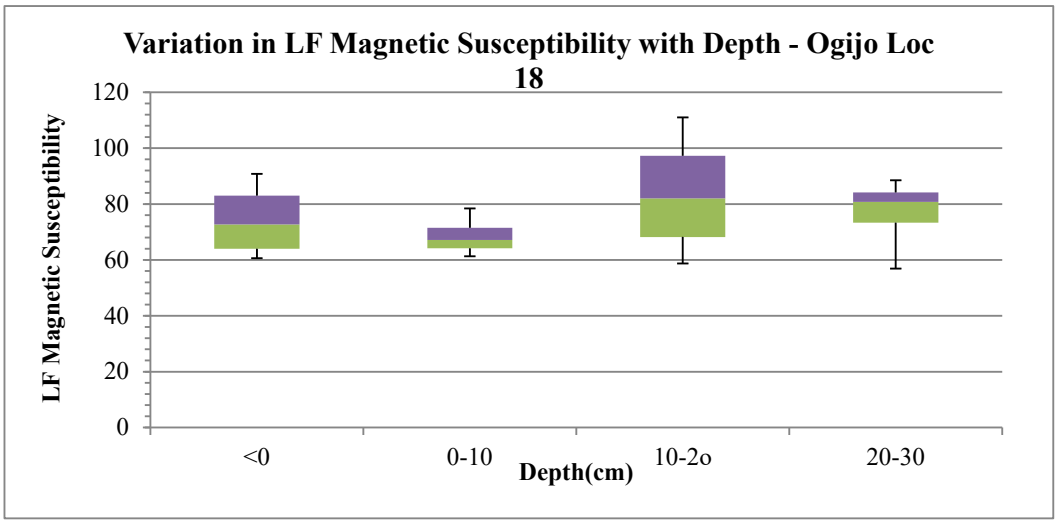
Variation in LF Magnetic Susceptibility with Depth - Ogijo Loc 18
LF Magnetic Susceptibility
120
100
80
60
40
20
0
<0
0-10
10-2o
20-30
Depth(cm)

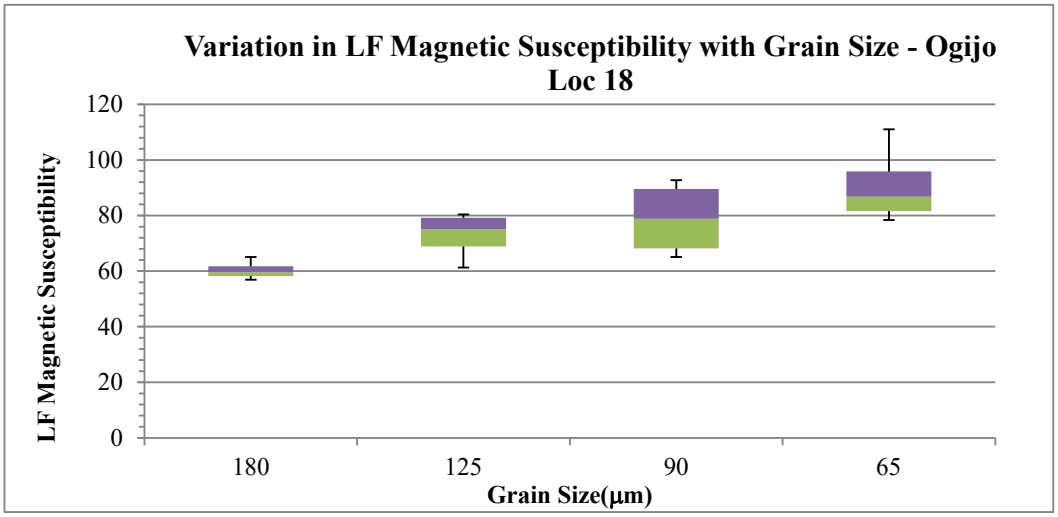
Variation in LF Magnetic Susceptibility with Grain Size - Ogijo Loc 18
LF Magnetic Susceptibility
120
100
80
60
40
20
0
180
125
90
65
Grain Size(µm)

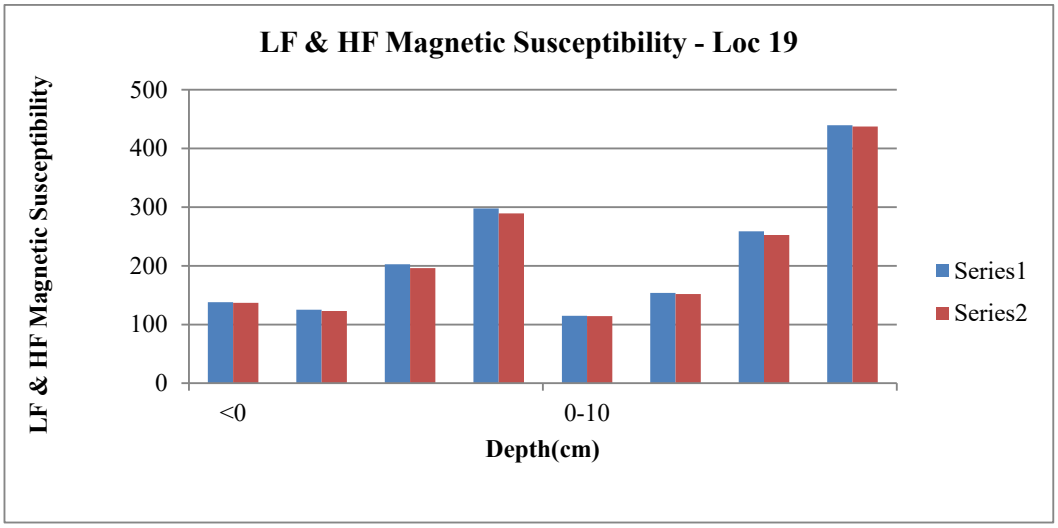
LF & HF Magnetic Susceptibility - Loc 19
LF & HF Magnetic Susceptibility
500
400
300
200
100
0
<0
0-10
Depth(cm)
Series1
Series2

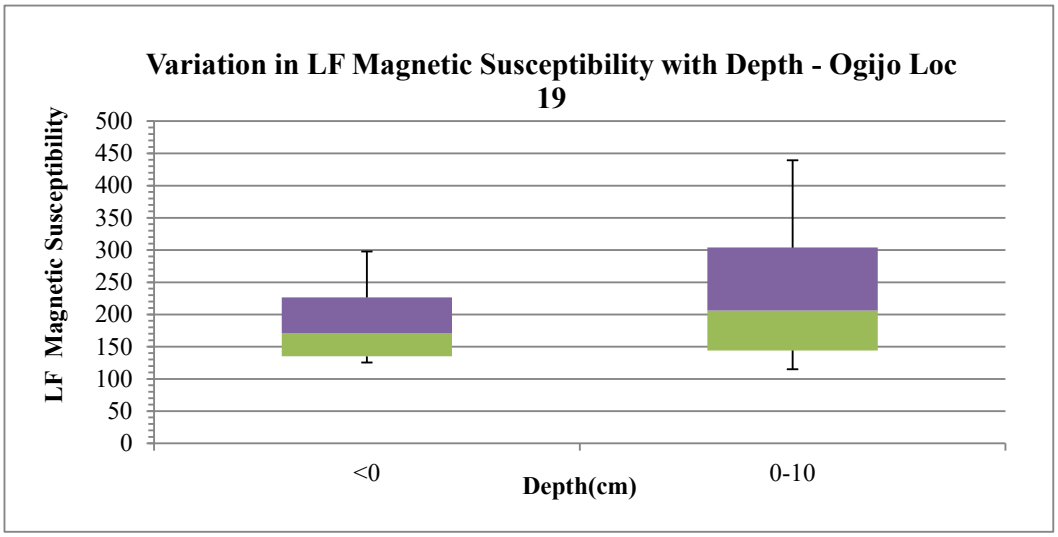
Variation in LF Magnetic Susceptibility with Depth - Ogijo Loc 19
LF Magnetic Susceptibility
500
450
400
350
300
250
200
150
100
50
0
<0
Depth(cm)
0-10

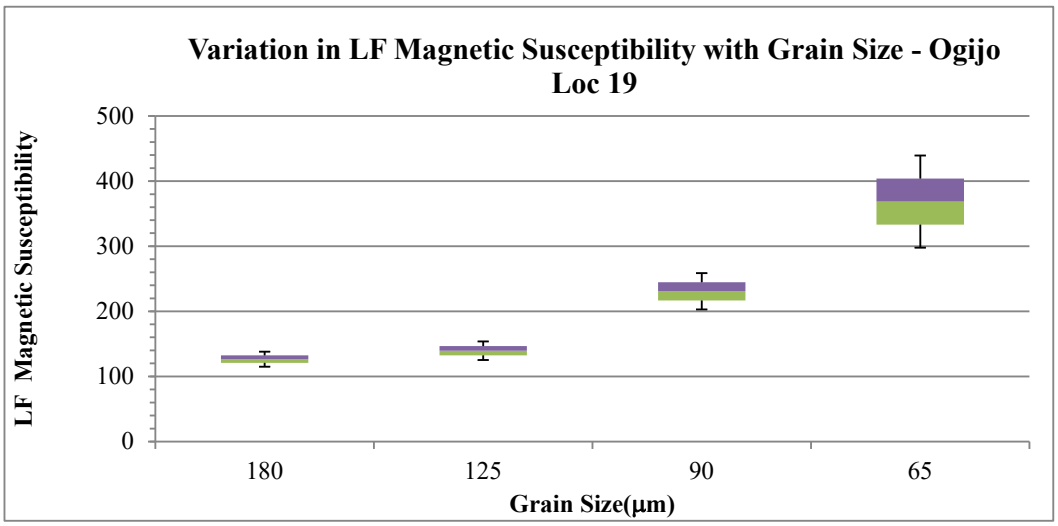
Variation in LF Magnetic Susceptibility with Grain Size - Ogijo Loc 19
LF Magnetic Susceptibility
500
400
300
200
100
0
180
125
90
65
Grain Size(µm)

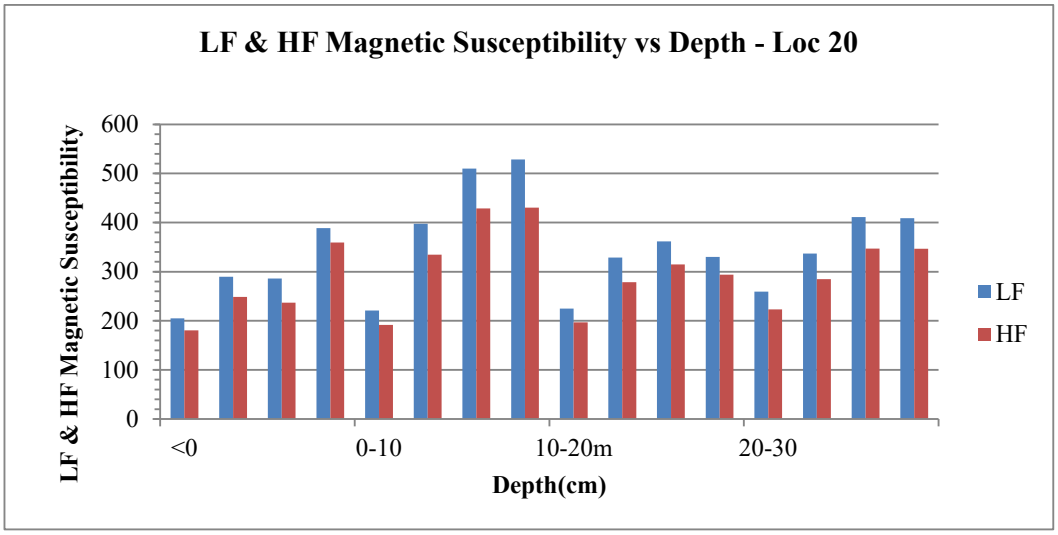
LF & HF Magnetic Susceptibility vs Depth - Loc 20
LF & HF Magnetic Susceptibility
600
500
400
300
200
100
0
<0
0-10
10-20m
20-30
Depth(cm)
LF
HF

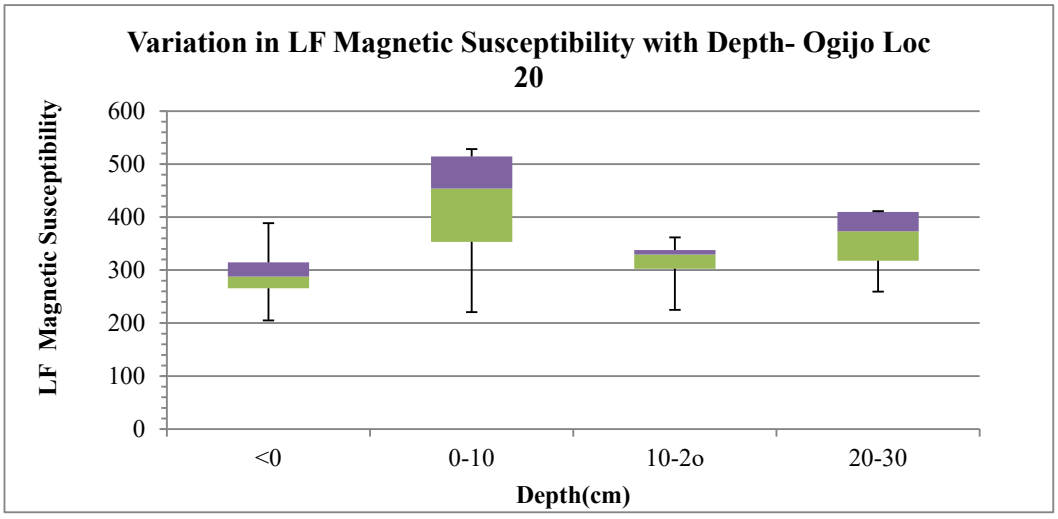
Variation in LF Magnetic Susceptibility with Depth- Ogijo Loc 20
LF Magnetic Susceptibility
600
500
400
300
200
100
0
<0
0-10
10-2o
20-30
Depth(cm)

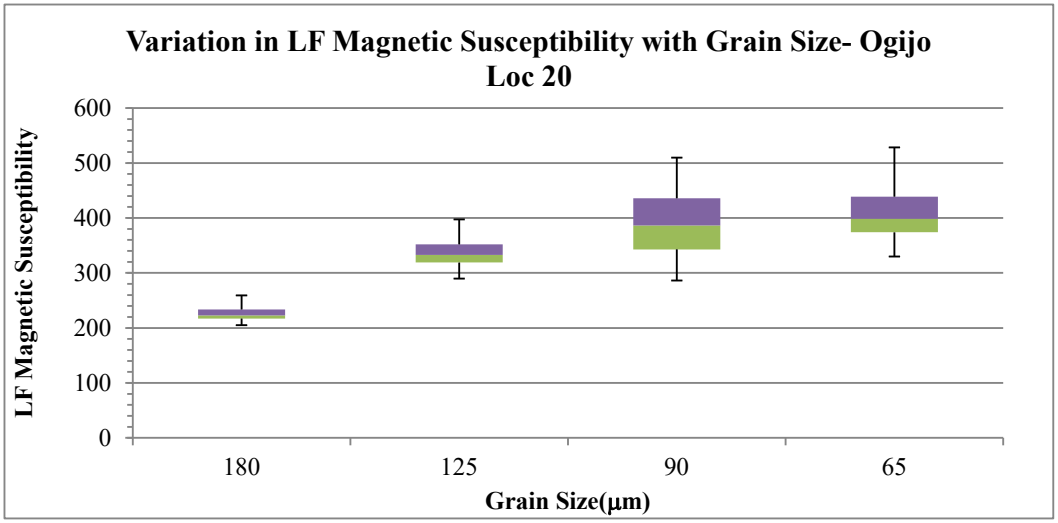
Variation in LF Magnetic Susceptibility with Grain Size- Ogijo Loc 20
LF Magnetic Susceptibility
600
500
400
300
200
100
0
180
125
90
65
Grain Size(µm)

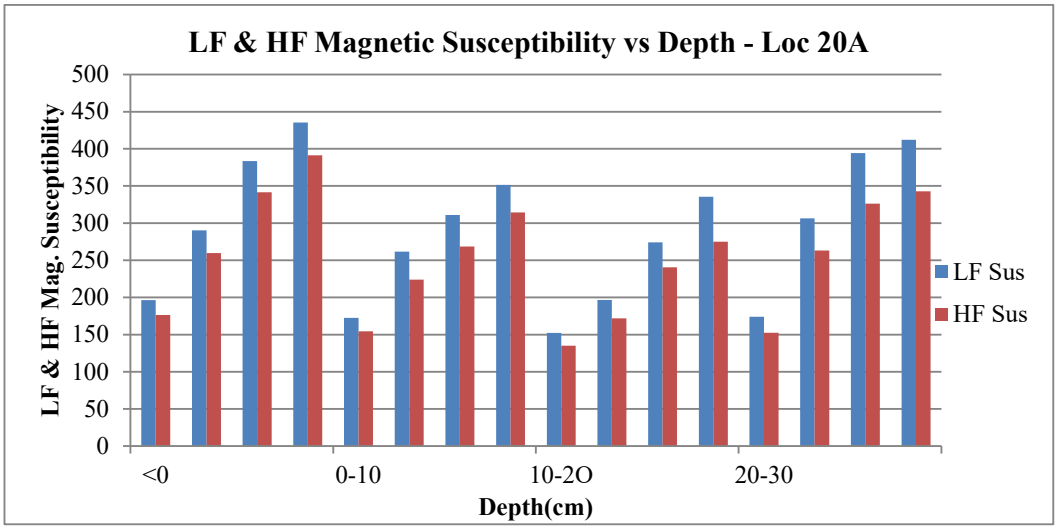
LF & HF Magnetic Susceptibility vs Depth - Loc 20A
LF & HF Mag. Susceptibility
500
450
400
350
300
250
200
150
100
50
0
<0
0-10
10-2O
20-30
Depth(cm)
LF Sus
HF Sus

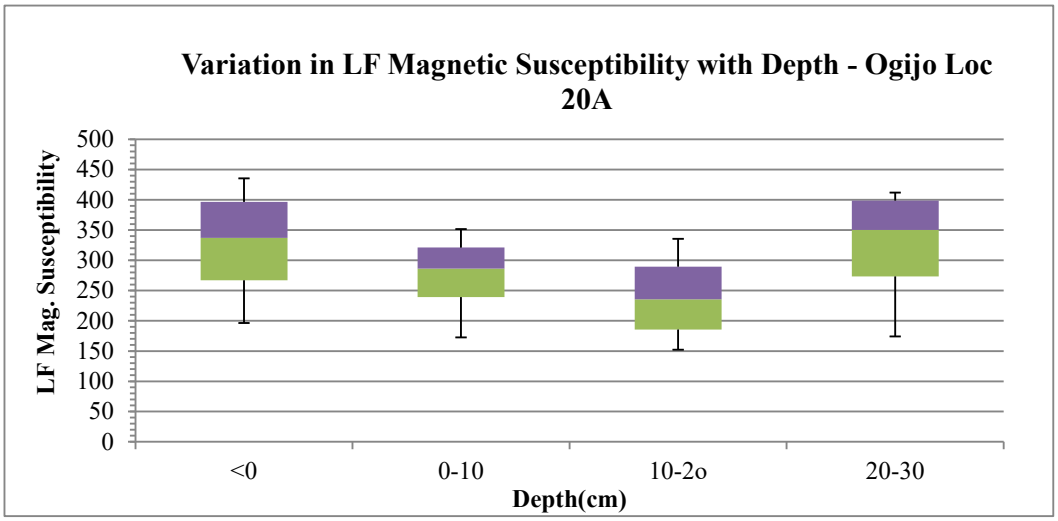
Variation in LF Magnetic Susceptibility with Depth - Ogijo Loc 20A
LF Mag. Susceptibility
500
450
400
350
300
250
200
150
100
50
0
<0
0-10
10-2o
20-30
Depth(cm)

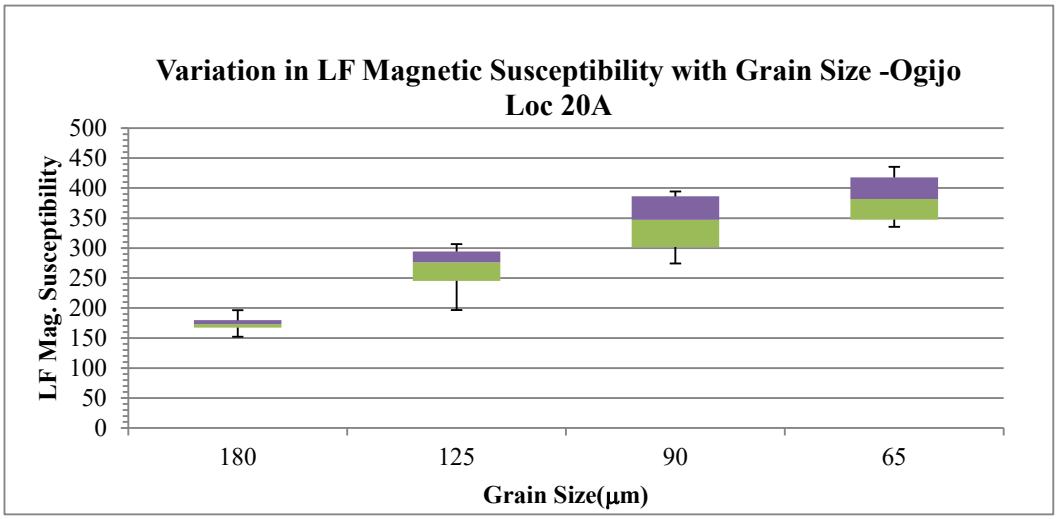
Variation in LF Magnetic Susceptibility with Grain Size -Ogijo Loc 20A
LF Mag. Susceptibility
500
450
400
350
300
250
200
150
100
50
0
180
125
90
65
Grain Size(µm)

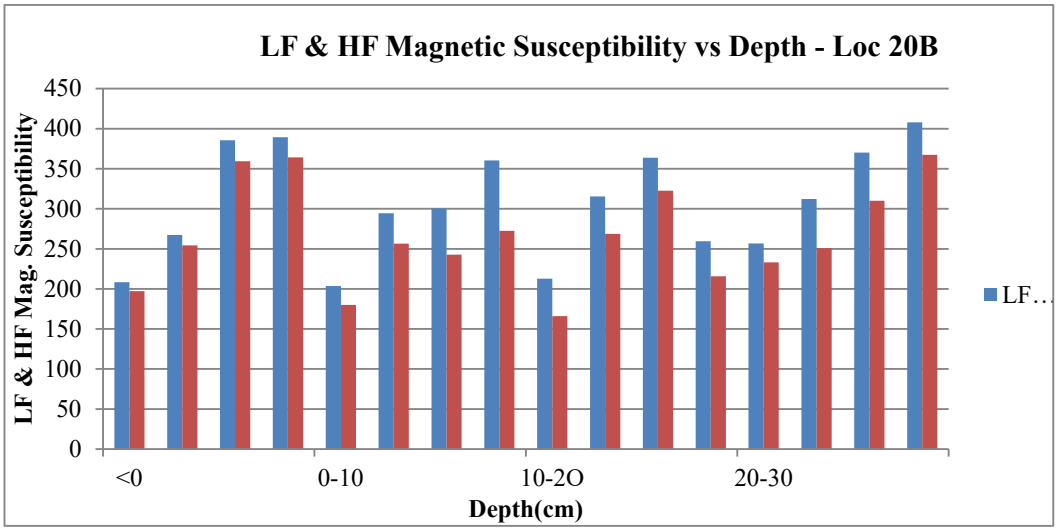
LF & HF Magnetic Susceptibility vs Depth - Loc 20B
LF & HF Mag. Susceptibility
450
400
350
300
250
200
150
100
50
0
<0
0-10
10-2O
20-30
Depth(cm)
LF…

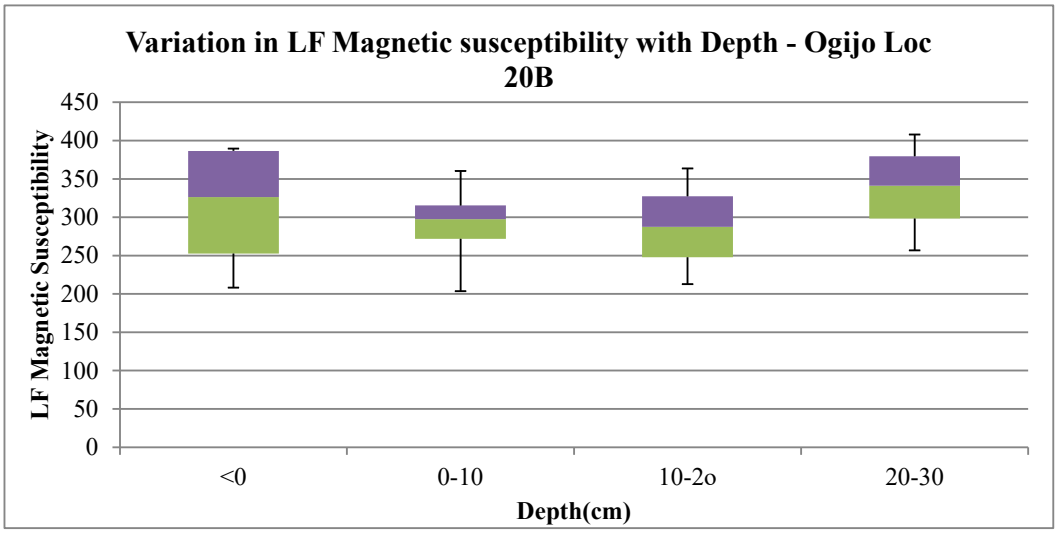
Variation in LF Magnetic susceptibility with Depth - Ogijo Loc 20B
LF Magnetic Susceptibility
450
400
350
300
250
200
150
100
50
0
<0
0-10
10-2o
20-30
Depth(cm)

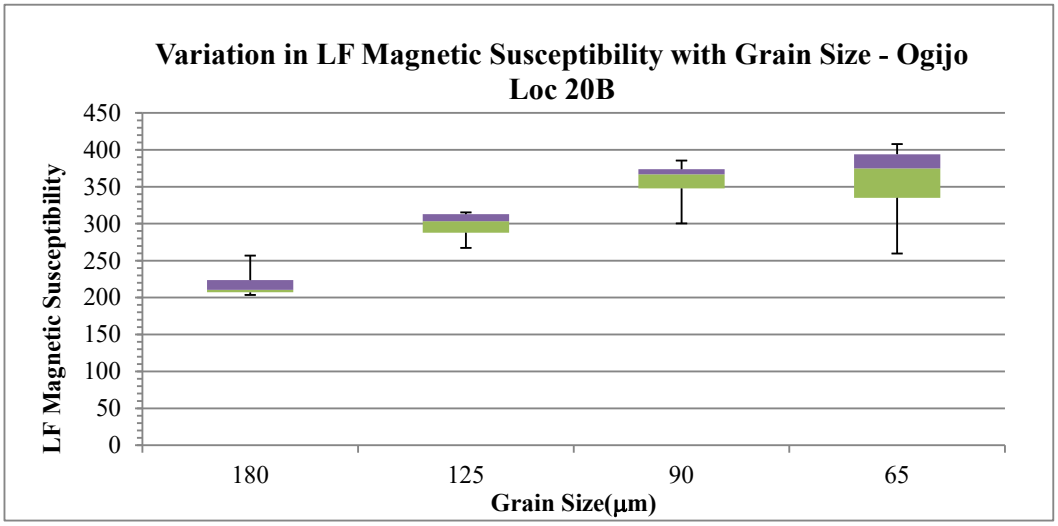
Variation in LF Magnetic Susceptibility with Grain Size - Ogijo Loc 20B
LF Magnetic Susceptibility
450
400
350
300
250
200
150
100
50
0
180
125
90
65
Grain Size(µm)

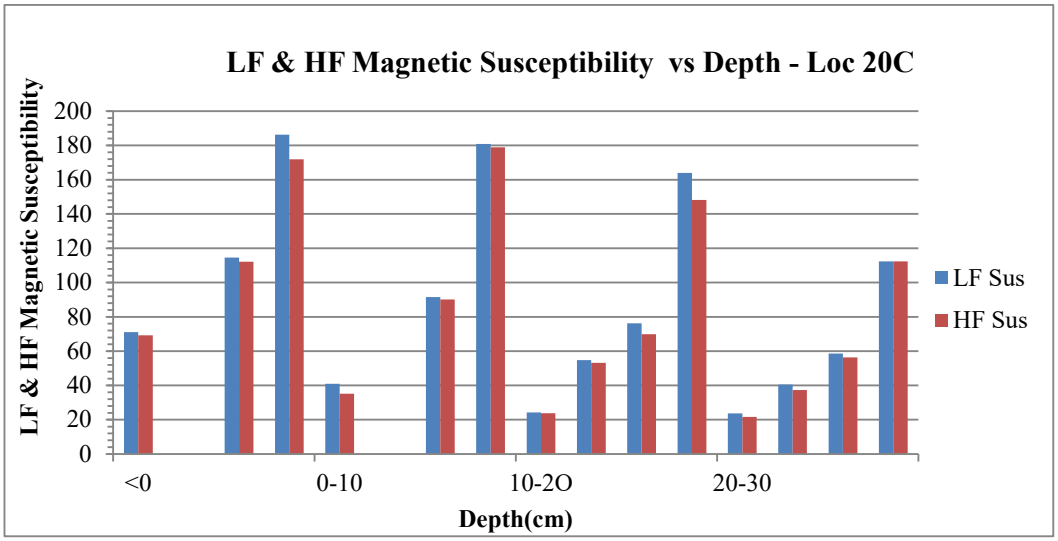
LF & HF Magnetic Susceptibility vs Depth - Loc 20C
LF & HF Magnetic Susceptibility
200
180
160
140
120
100
80
60
40
20
0
<0
0-10
10-2O
20-30
Depth(cm)
LF Sus
HF Sus

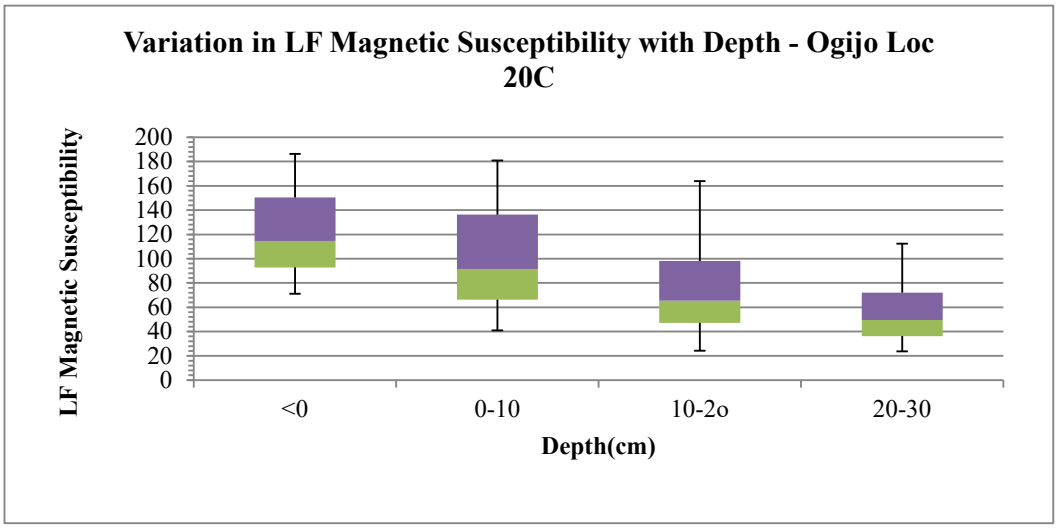
Variation in LF Magnetic Susceptibility with Depth - Ogijo Loc 20C
LF Magnetic Susceptibility
200
180
160
140
120
100
80
60
40
20
0
<0
0-10
10-2o
20-30
Depth(cm)

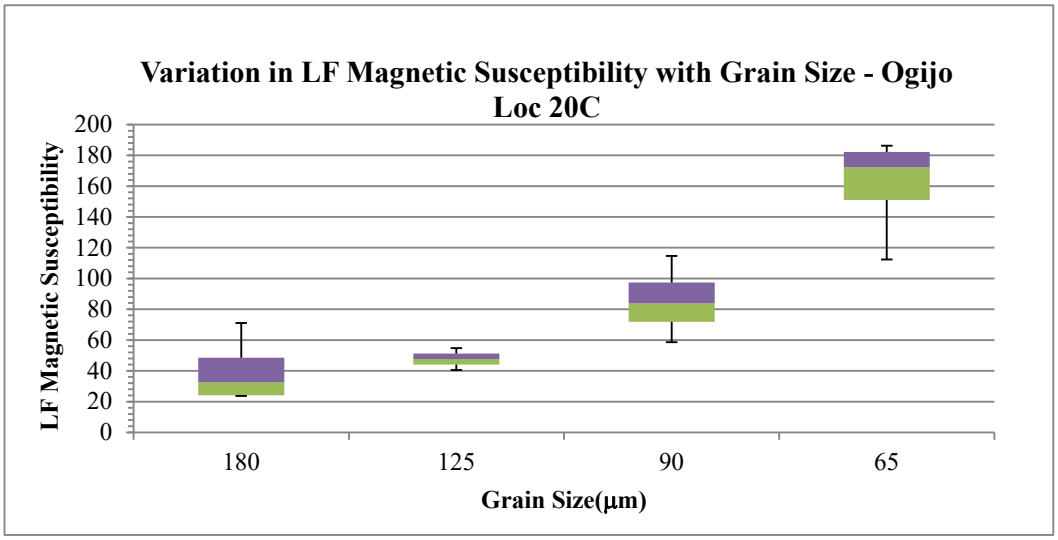
Variation in LF Magnetic Susceptibility with Grain Size - Ogijo Loc 20C
LF Magnetic Susceptibility
200
180
160
140
120
100
80
60
40
20
0
180
125
90
65
Grain Size(µm)

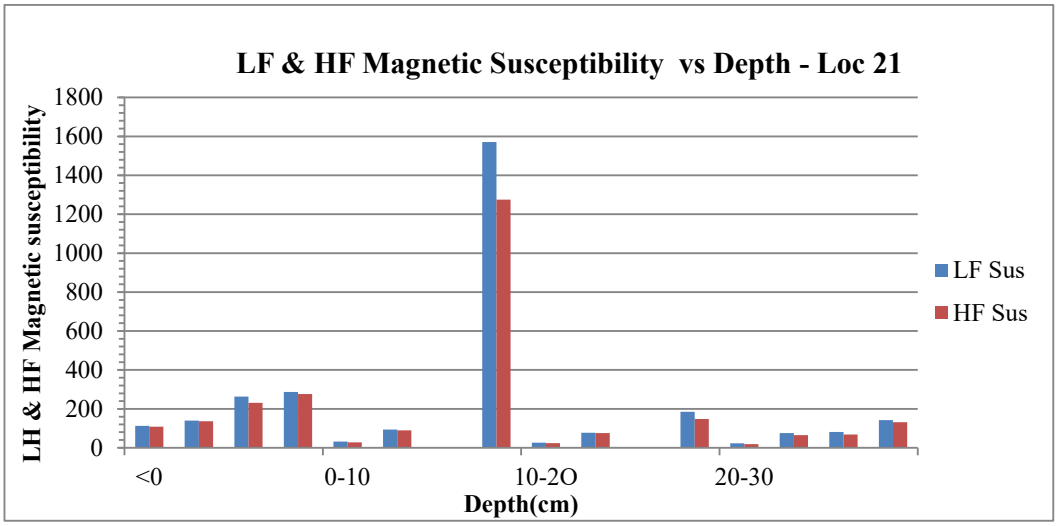
LF & HF Magnetic Susceptibility vs Depth - Loc 21
LH & HF Magnetic susceptibility
1800
1600
1400
1200
1000
800
600
400
200
0
<0
0-10
10-2O
20-30
Depth(cm)
LF Sus
HF Sus

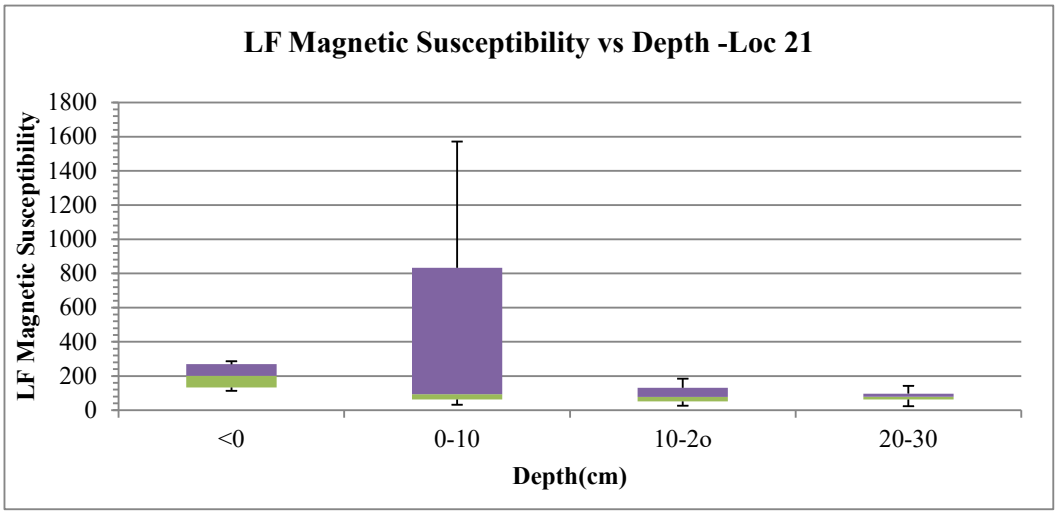
LF Magnetic Susceptibility vs Depth -Loc 21
LF Magnetic Susceptibility
1800
1600
1400
1200
1000
800
600
400
200
0
<0
0-10
10-2o
20-30
Depth(cm)

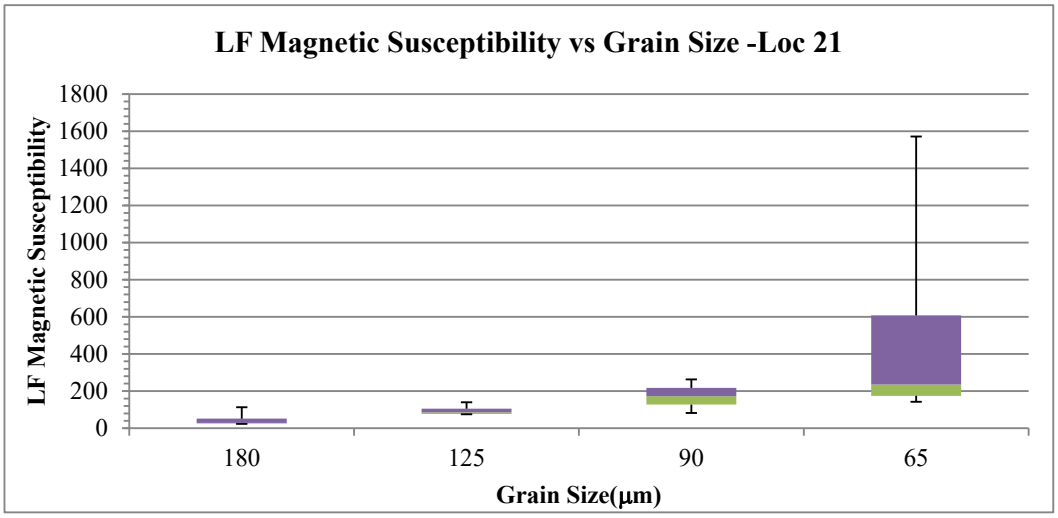
LF Magnetic Susceptibility vs Grain Size -Loc 21
LF Magnetic Susceptibility
1800
1600
1400
1200
1000
800
600
400
200
0
180
125
90
65
Grain Size(µm)

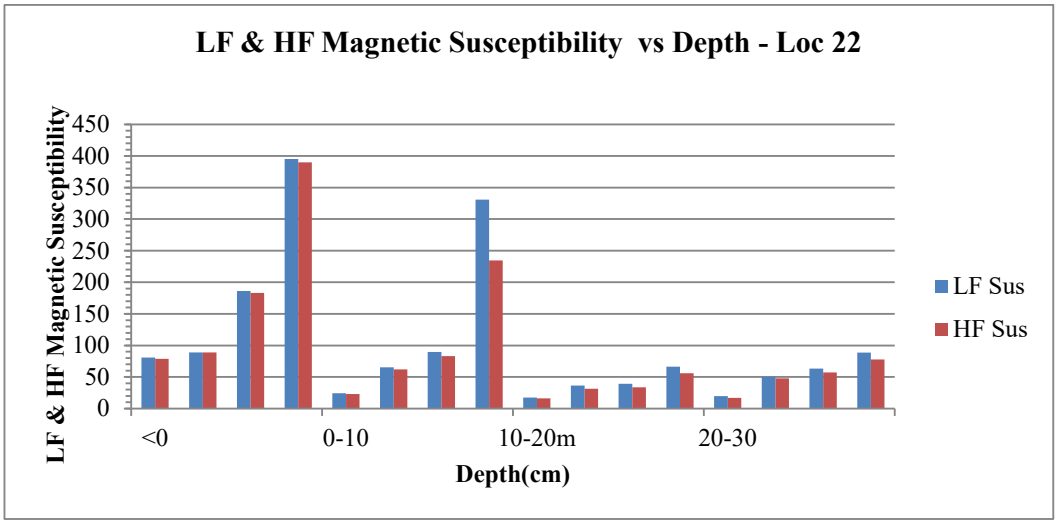
LF & HF Magnetic Susceptibility vs Depth - Loc 22
LF & HF Magnetic Susceptibility
450
400
350
300
250
200
150
100
50
0
<0
0-10
10-20m
20-30
Depth(cm)
LF Sus
HF Sus

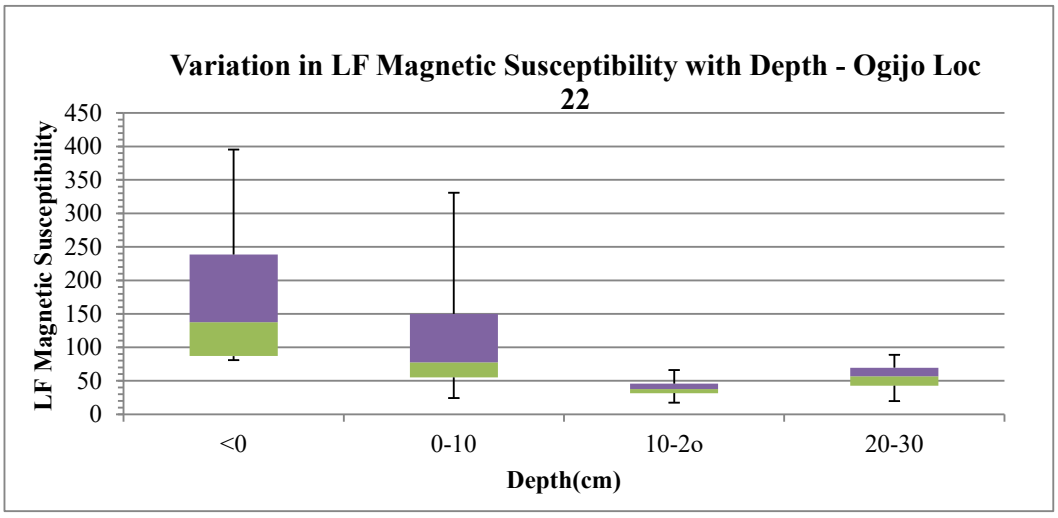
Variation in LF Magnetic Susceptibility with Depth - Ogijo Loc 22
LF Magnetic Susceptibility
450
400
350
300
250
200
150
100
50
0
<0
0-10
10-2o
20-30
Depth(cm)

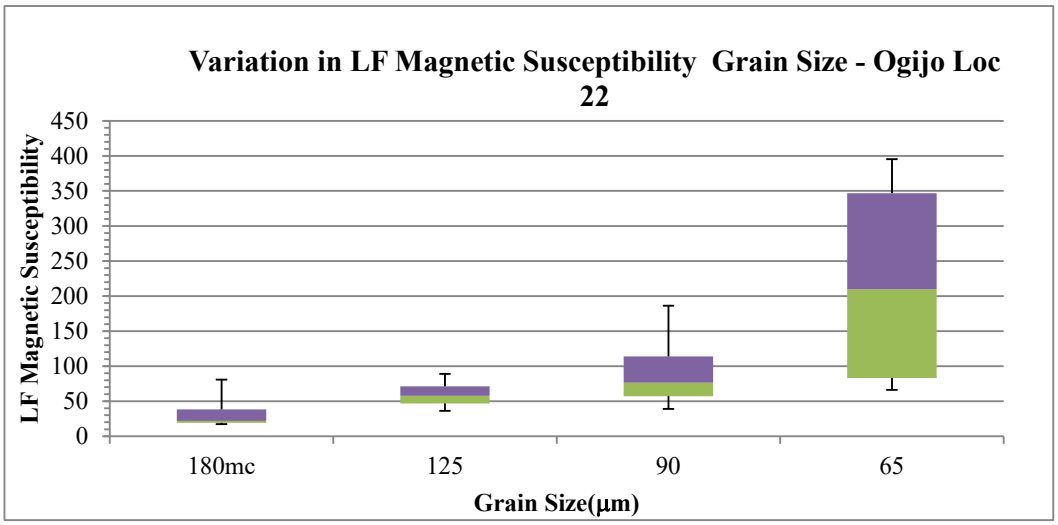
Variation in LF Magnetic Susceptibility Grain Size - Ogijo Loc 22
LF Magnetic Susceptibility
450
400
350
300
250
200
150
100
50
0
180mc
125
90
65
Grain Size(µm)

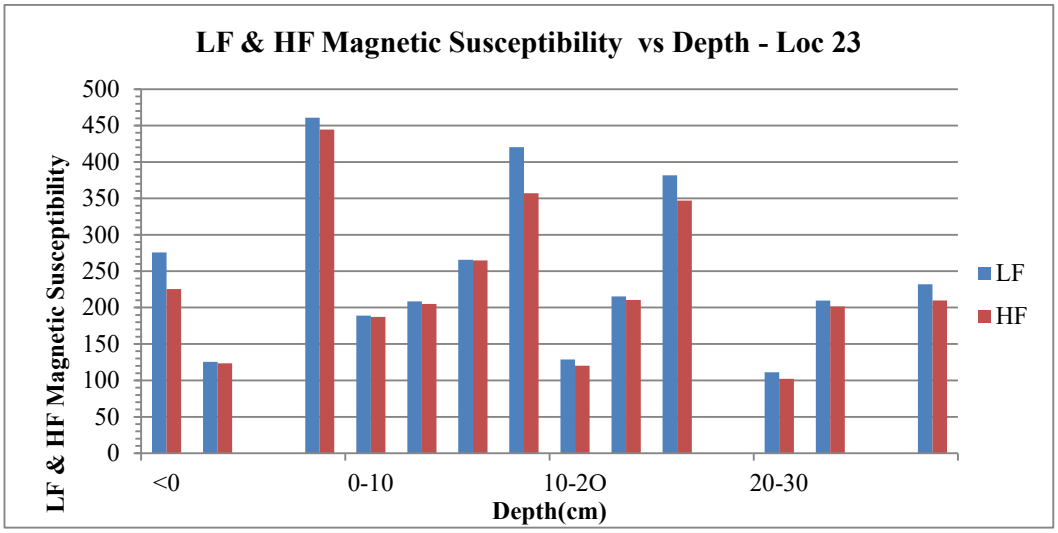
LF & HF Magnetic Susceptibility vs Depth - Loc 23
LF & HF Magnetic Susceptibility
500
450
400
350
300
250
200
150
100
50
0
<0
0-10
10-2O
20-30
Depth(cm)
LF
HF

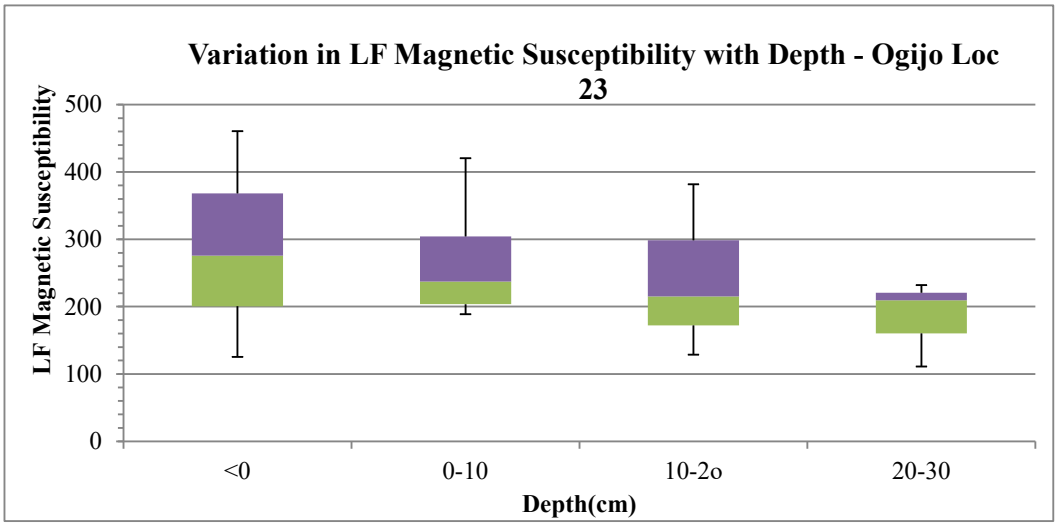
Variation in LF Magnetic Susceptibility with Depth - Ogijo Loc 23
LF Magnetic Susceptibility
500
400
300
200
100
0
<0
0-10
10-2o
20-30
Depth(cm)

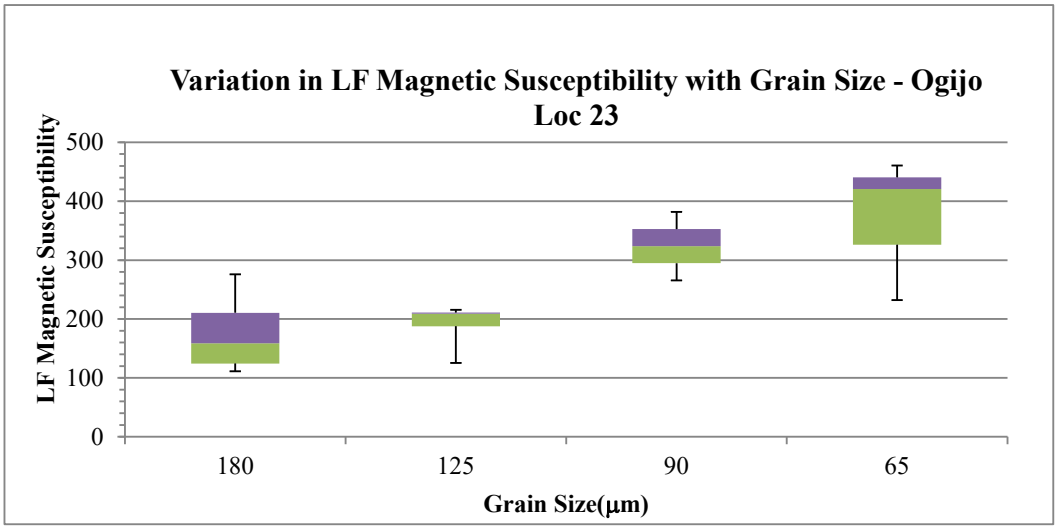
Variation in LF Magnetic Susceptibility with Grain Size - Ogijo Loc 23
LF Magnetic Susceptibility
500
400
300
200
100
0
180
125
90
65
Grain Size(µm)

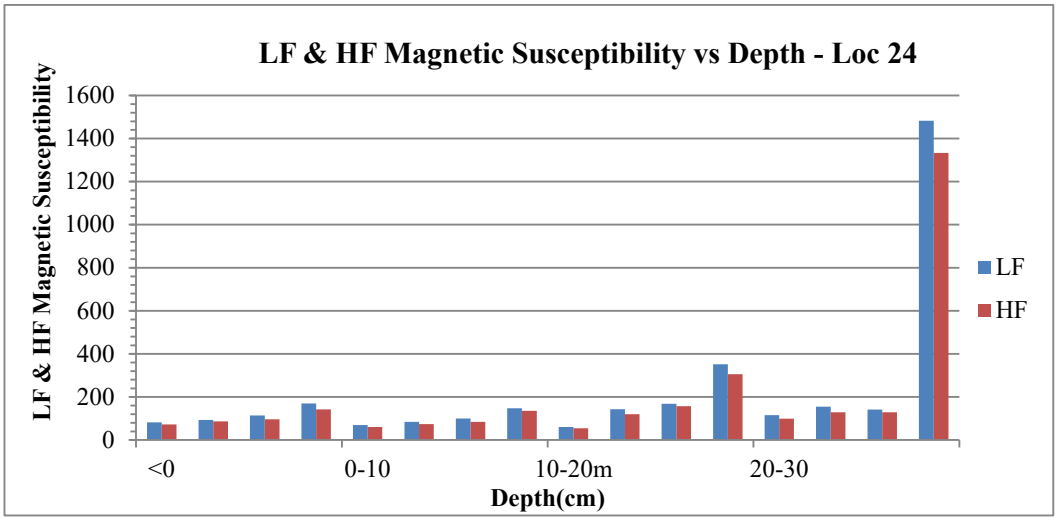
LF & HF Magnetic Susceptibility vs Depth - Loc 24
LF & HF Magnetic Susceptibility
1600
1400
1200
1000
800
600
400
200
0
<0
0-10
10-20m
20-30
Depth(cm)
LF
HF

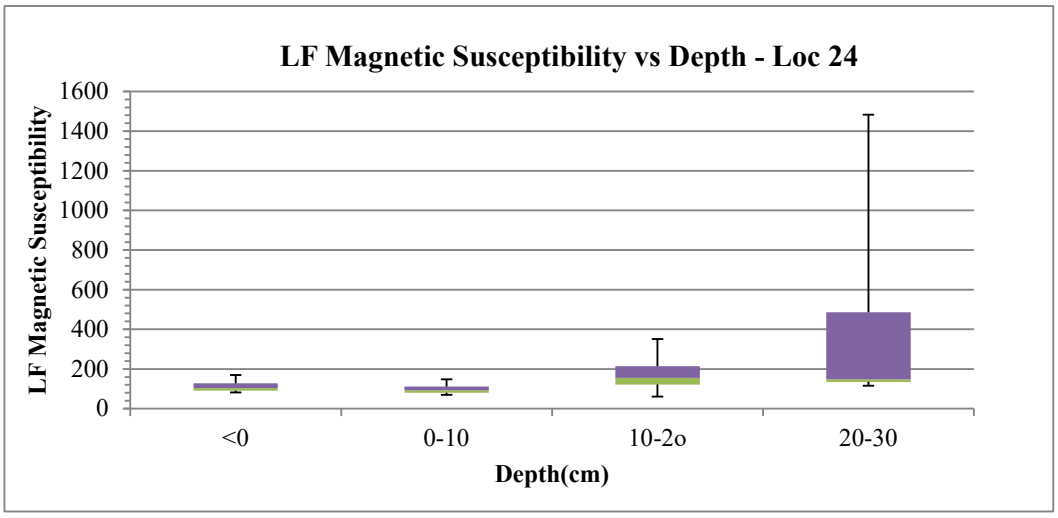
LF Magnetic Susceptibility vs Depth - Loc 24
LF Magnetic Susceptibility
1600
1400
1200
1000
800
600
400
200
0
<0
0-10
10-2o
20-30
Depth(cm)

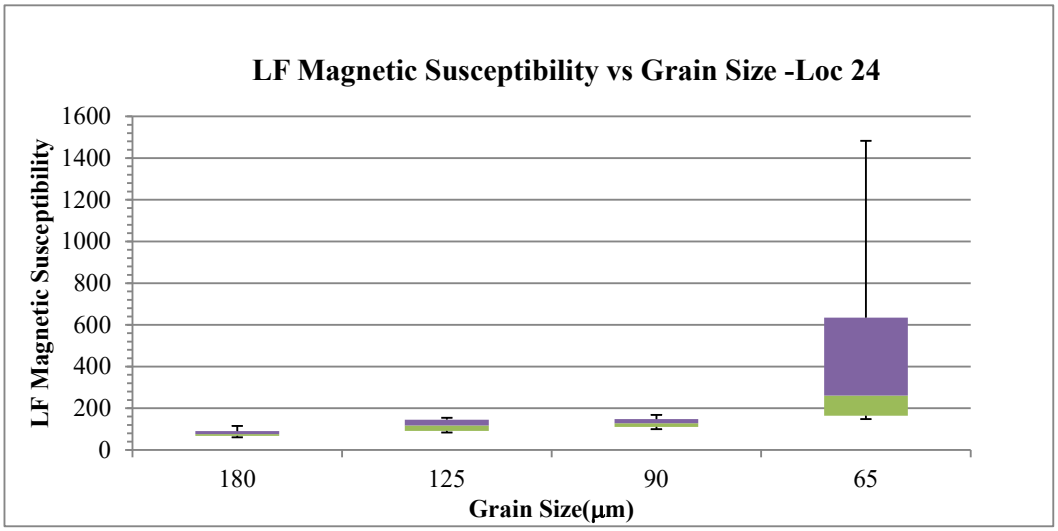
LF Magnetic Susceptibility vs Grain Size -Loc 24
LF Magnetic Susceptibility
1600
1400
1200
1000
800
600
400
200
0
180
125
90
65
Grain Size(µm)

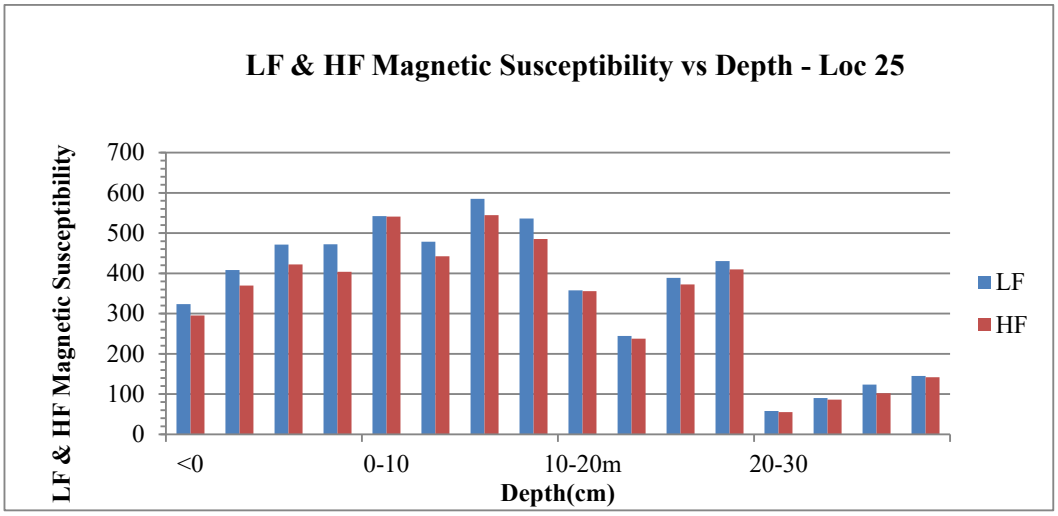
LF & HF Magnetic Susceptibility vs Depth - Loc 25
LF & HF Magnetic Susceptibility
700
600
500
400
300
200
100
0
<0
0-10
10-20m
20-30
Depth(cm)
LF
HF

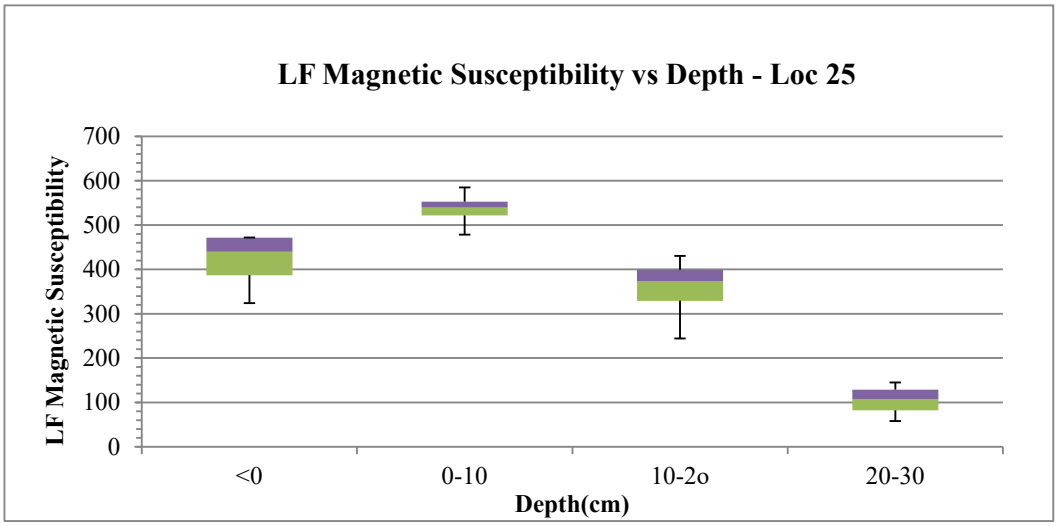
LF Magnetic Susceptibility vs Depth - Loc 25
LF Magnetic Susceptibility
700
600
500
400
300
200
100
0
<0
0-10
10-2o
20-30
Depth(cm)

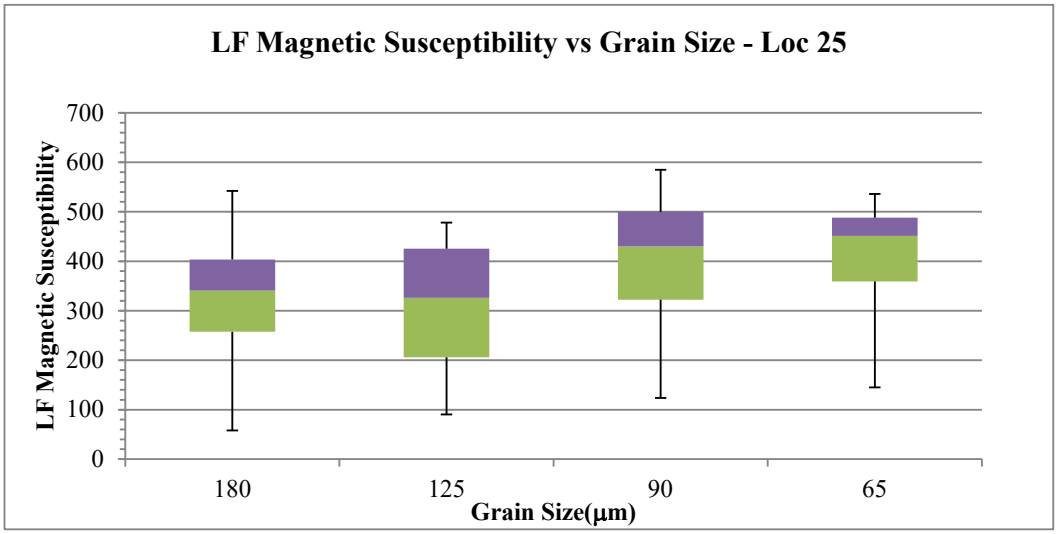
LF Magnetic Susceptibility vs Grain Size - Loc 25
LF Magnetic Susceptibility
700
600
500
400
300
200
100
0
180
125
90
65
Grain Size(µm)

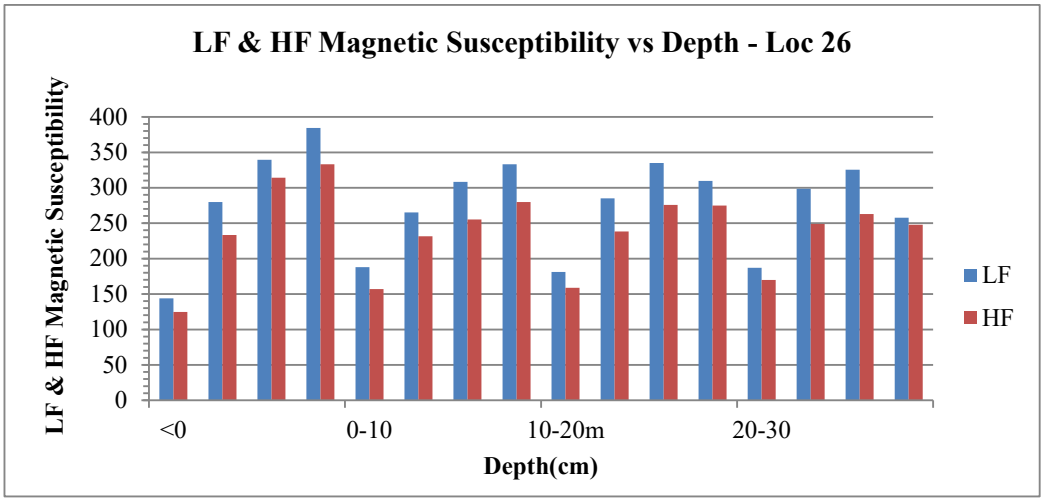
LF & HF Magnetic Susceptibility vs Depth - Loc 26
LF & HF Magnetic Susceptibility
400
350
300
250
200
150
100
50
0
<0
0-10
10-20m
20-30
Depth(cm)
LF
HF

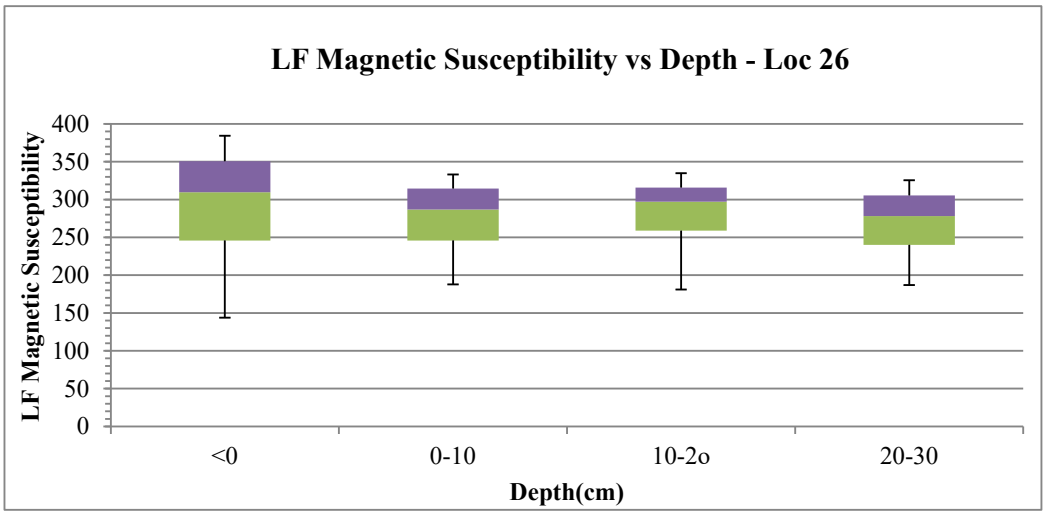
LF Magnetic Susceptibility vs Depth - Loc 26
LF Magnetic Susceptibility
400
350
300
250
200
150
100
50
0
<0
0-10
10-2o
20-30
Depth(cm)

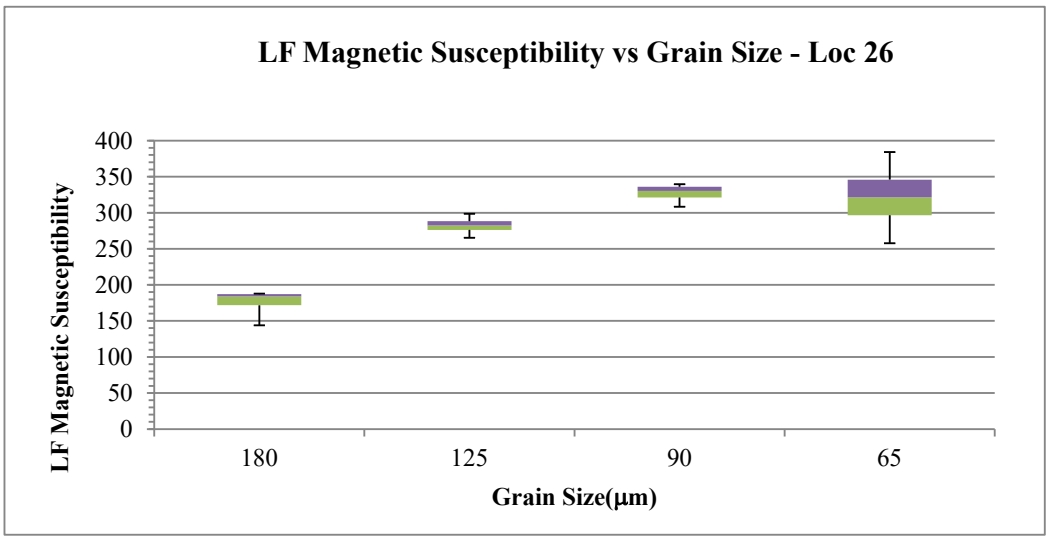
LF Magnetic Susceptibility vs Grain Size - Loc 26
LF Magnetic Susceptibility
400
350
300
250
200
150
100
50
0
180
125
90
65
Grain Size(µm)

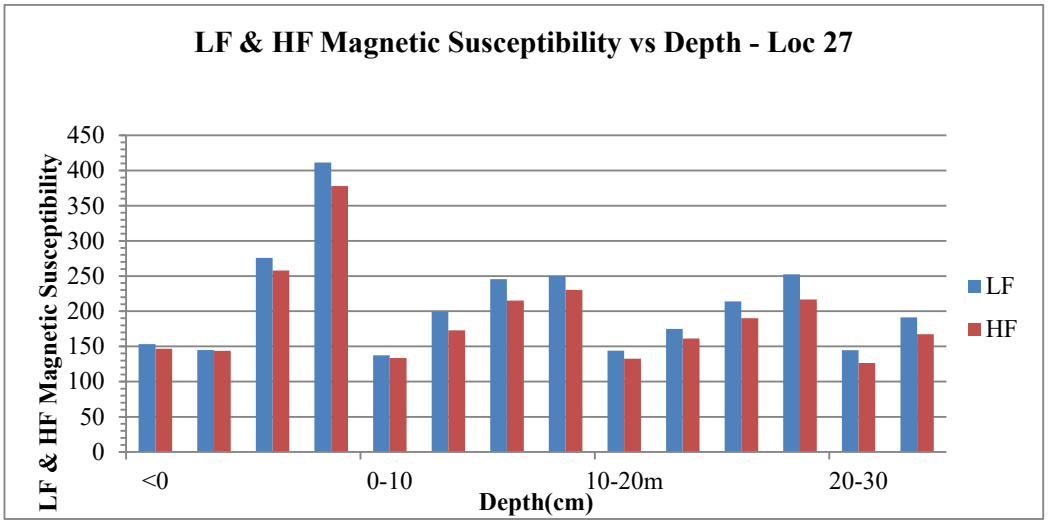
LF & HF Magnetic Susceptibility vs Depth - Loc 27
LF & HF Magnetic Susceptibility
450
400
350
300
250
200
150
100
50
0
<0
0-10
10-20m
20-30
Depth(cm)
LF
HF

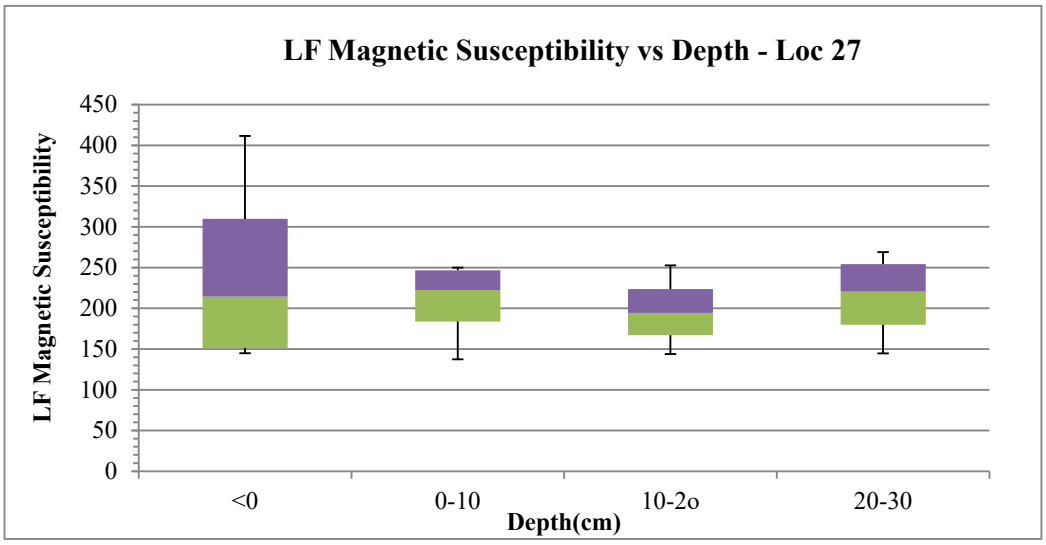
LF Magnetic Susceptibility vs Depth - Loc 27
LF Magnetic Susceptibility
450
400
350
300
250
200
150
100
50
0
<0
0-10
10-2o
20-30
Depth(cm)

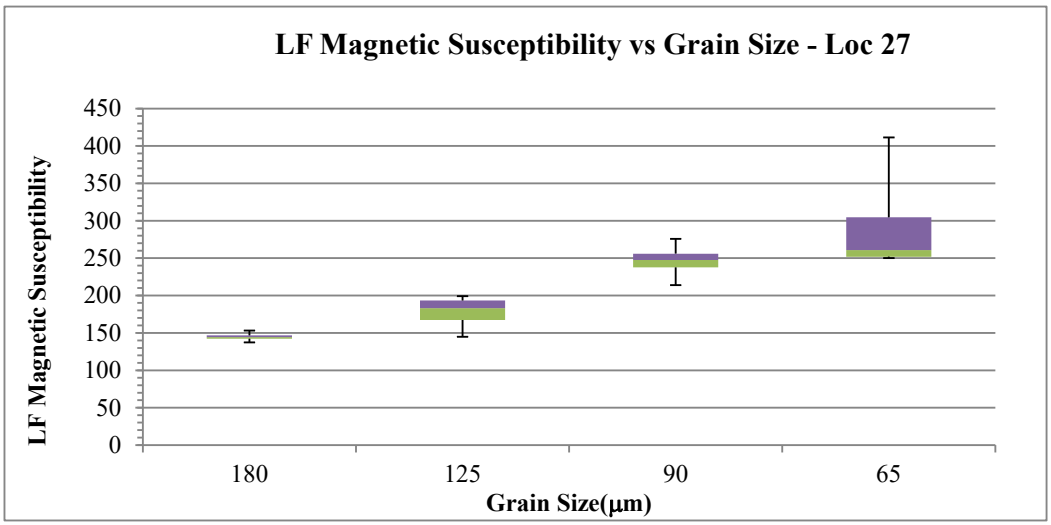
LF Magnetic Susceptibility vs Grain Size - Loc 27
LF Magnetic Susceptibility
450
400
350
300
250
200
150
100
50
0
180
125
90
65
Grain Size(µm)

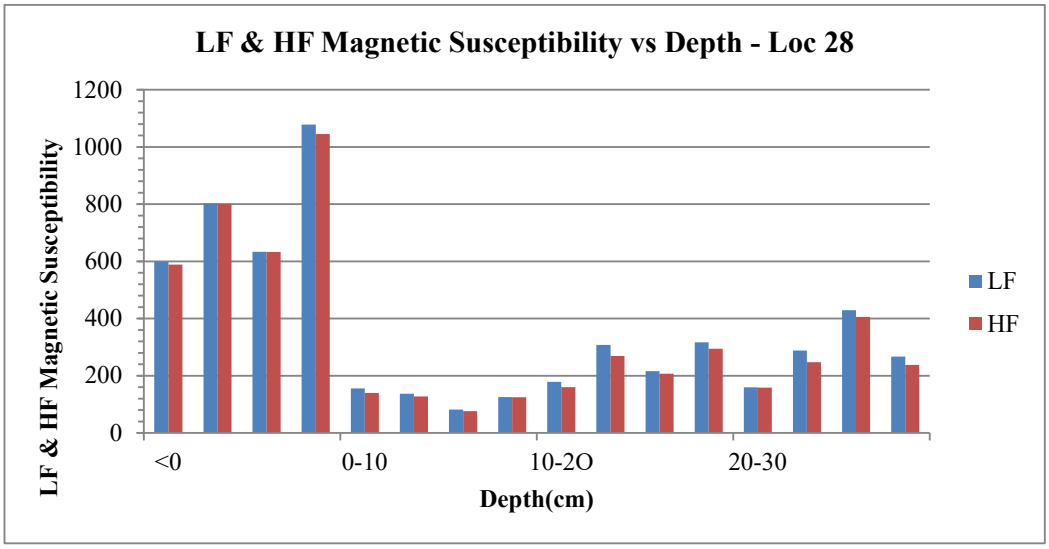
LF & HF Magnetic Susceptibility vs Depth - Loc 28
LF & HF Magnetic Susceptibility
1200
1000
800
600
400
200
0
<0
0-10
10-2O
20-30
Depth(cm)
LF
HF

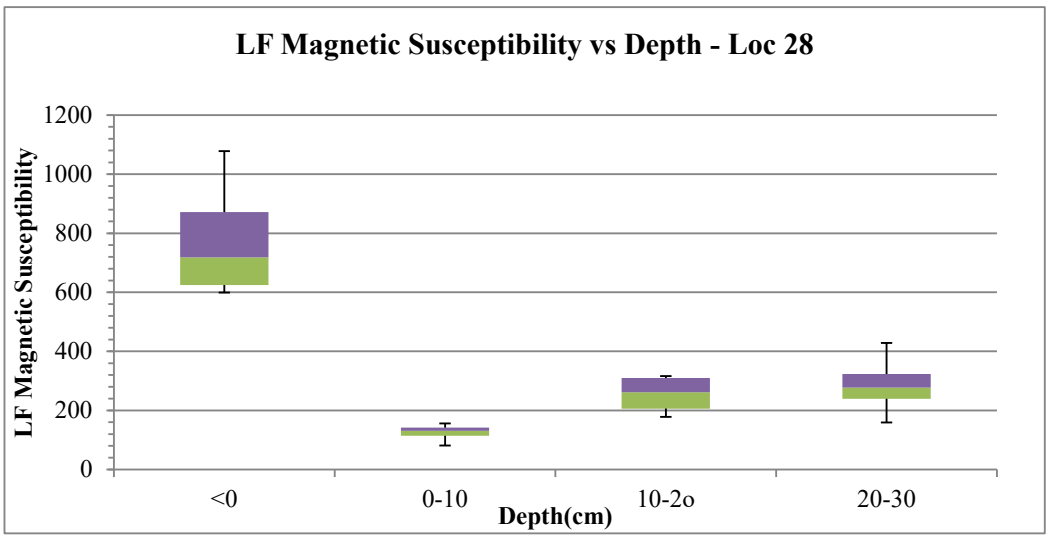
LF Magnetic Susceptibility vs Depth - Loc 28
LF Magnetic Susceptibility
1200
1000
800
600
400
200
0
<0
0-10
10-2o
20-30
Depth(cm)

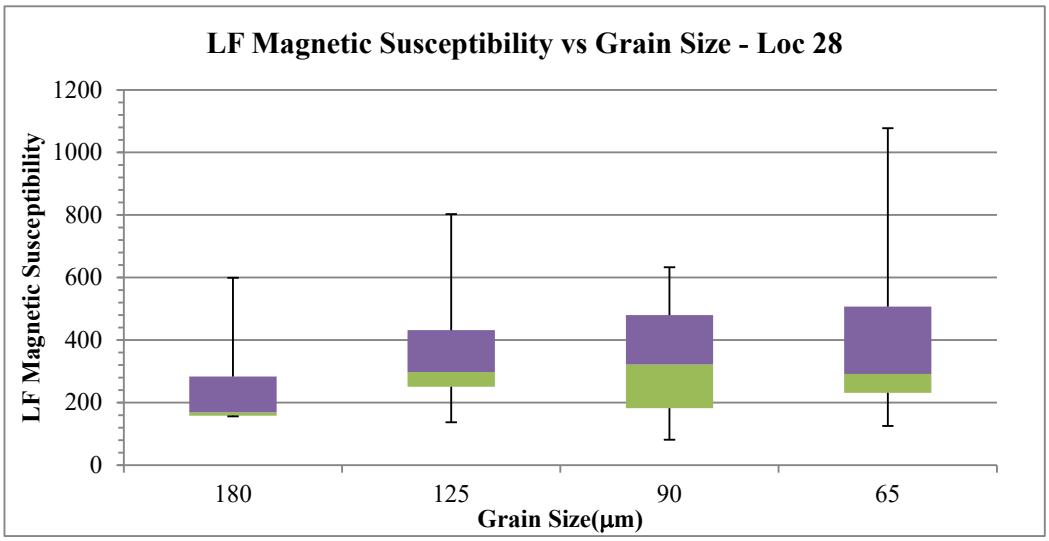
LF Magnetic Susceptibility vs Grain Size - Loc 28
LF Magnetic Susceptibility
1200
1000
800
600
400
200
0
180
125
90
65
Grain Size(µm)

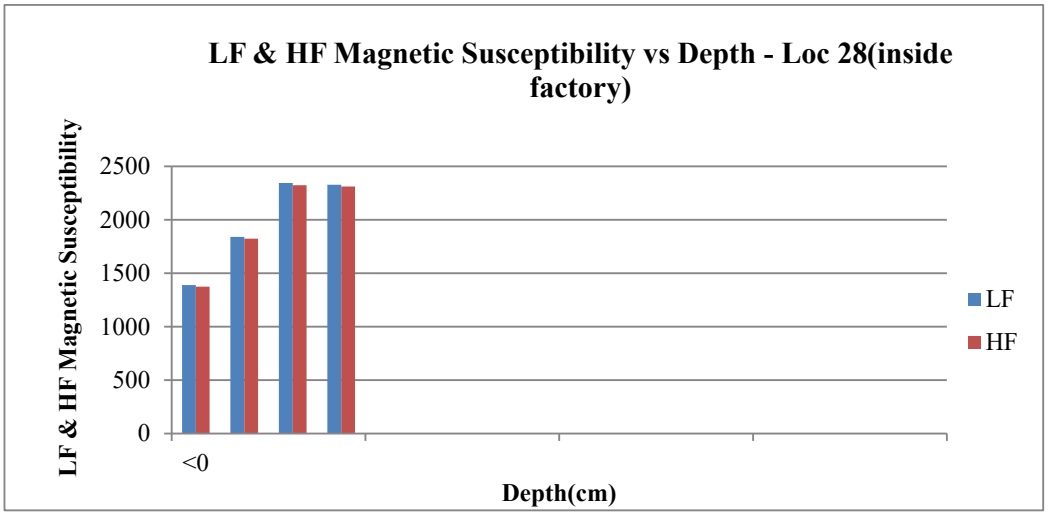
LF & HF Magnetic Susceptibility vs Depth - Loc 28(inside factory)
LF & HF Magnetic Susceptibility
2500
2000
1500
1000
500
0
<0
Depth(cm)
LF
HF

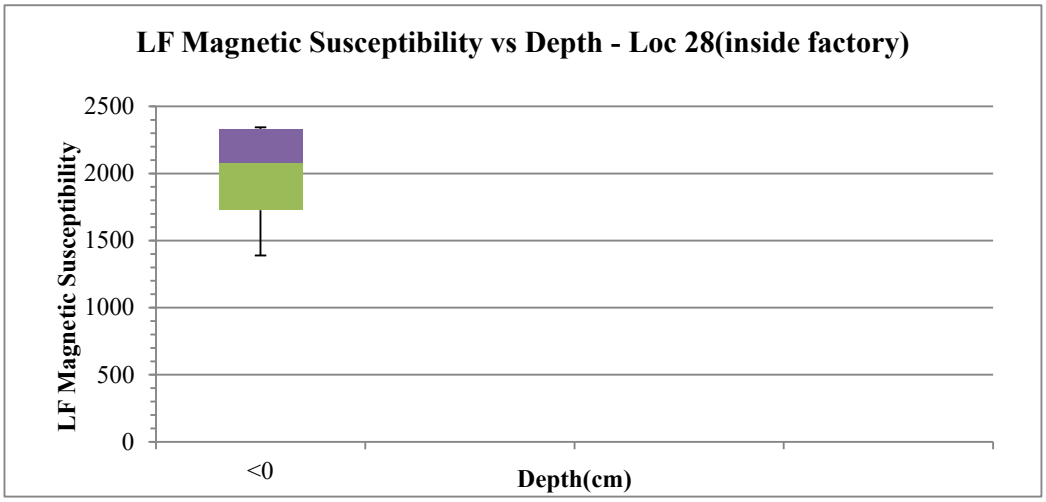
LF Magnetic Susceptibility vs Depth - Loc 28(inside factory)
LF Magnetic Susceptibility
2500
2000
1500
1000
500
0
<0
Depth(cm)

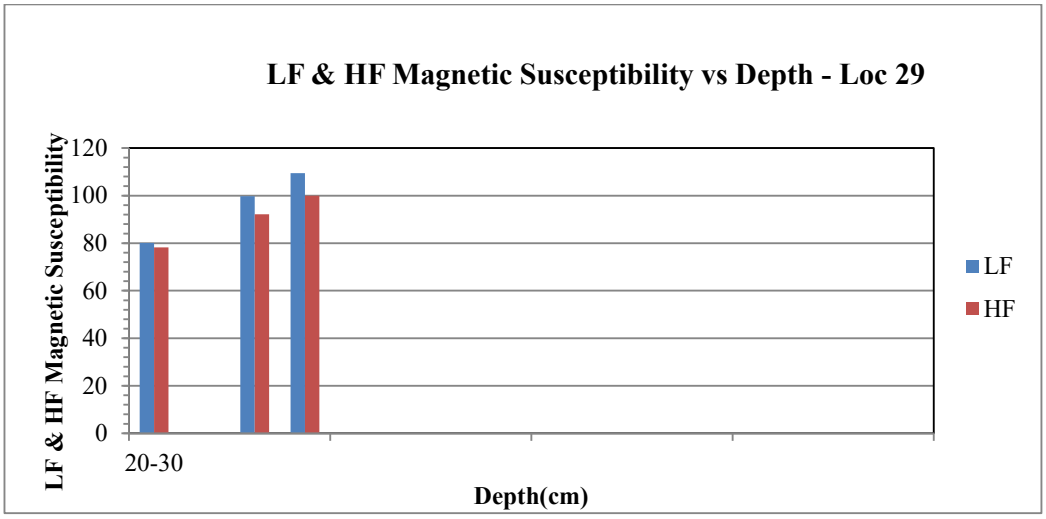
LF & HF Magnetic Susceptibility vs Depth - Loc 29
LF & HF Magnetic Susceptibility
120
100
80
60
40
20
0
20-30
Depth(cm)
LF
HF

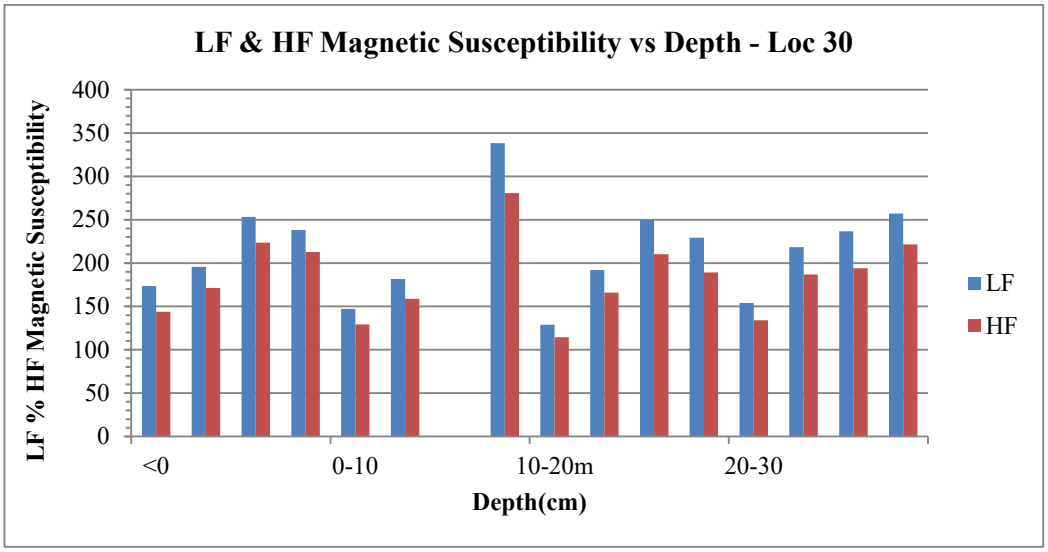
LF & HF Magnetic Susceptibility vs Depth - Loc 30
LF % HF Magnetic Susceptibility
400
350
300
250
200
150
100
50
0
<0
0-10
10-20m
20-30
Depth(cm)
LF
HF

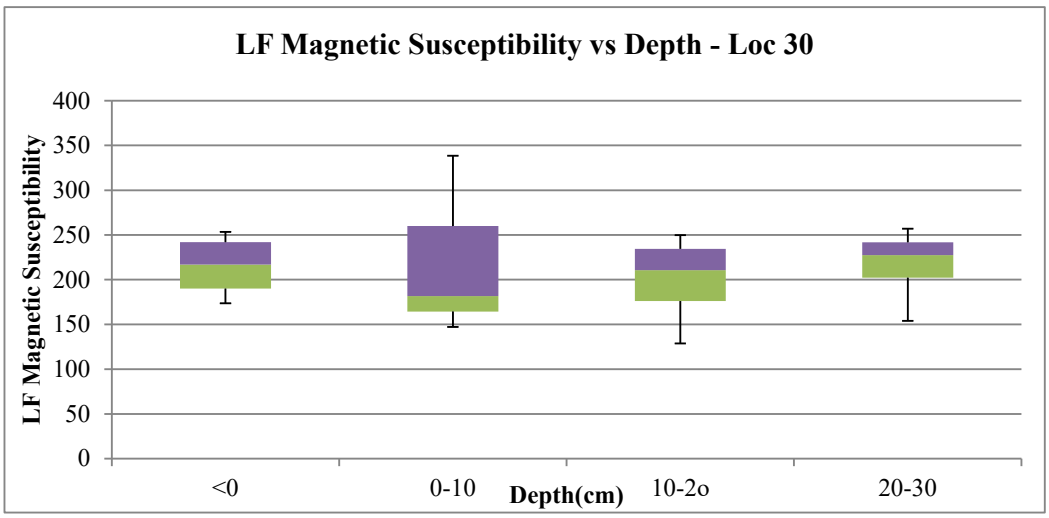
LF Magnetic Susceptibility vs Depth - Loc 30
LF Magnetic Susceptibility
400
350
300
250
200
150
100
50
0
<0
0-10
Depth(cm)
10-2o
20-30

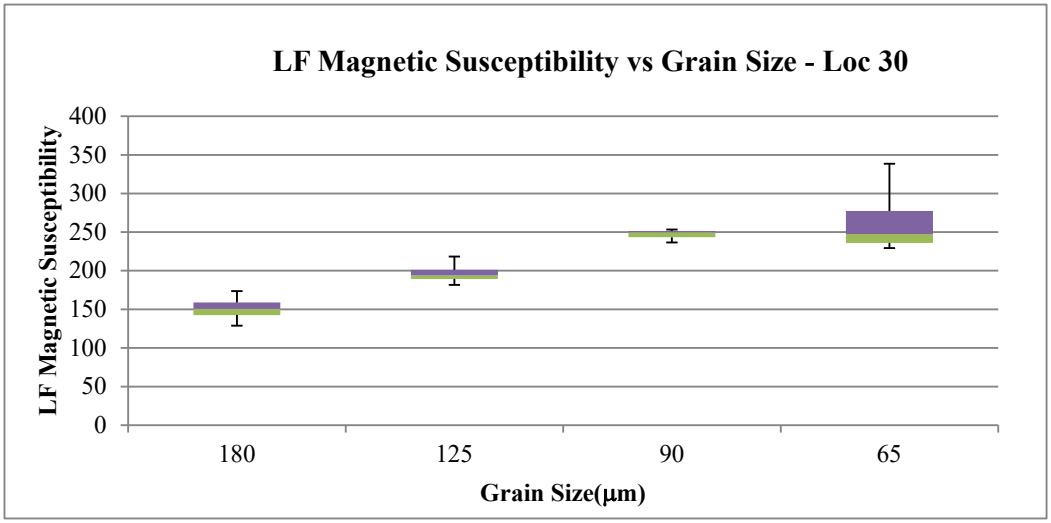
LF Magnetic Susceptibility vs Grain Size - Loc 30
LF Magnetic Susceptibility
400
350
300
250
200
150
100
50
0
180
125
90
65
Grain Size(µm)

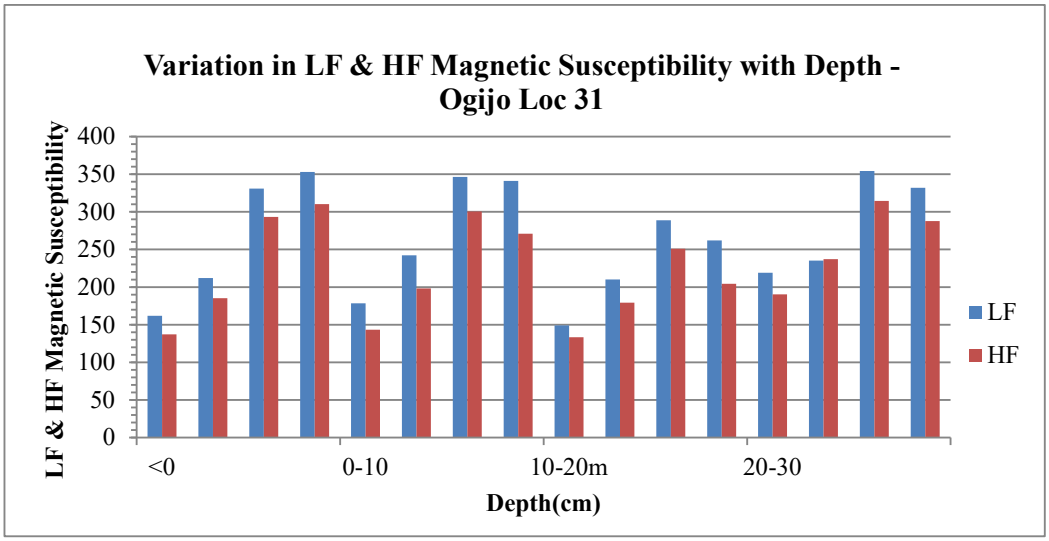
Variation in LF & HF Magnetic Susceptibility with Depth - Ogijo Loc 31
LF & HF Magnetic Susceptibility
400
350
300
250
200
150
100
50
0
<0
0-10
10-20m
20-30
Depth(cm)
LF
HF

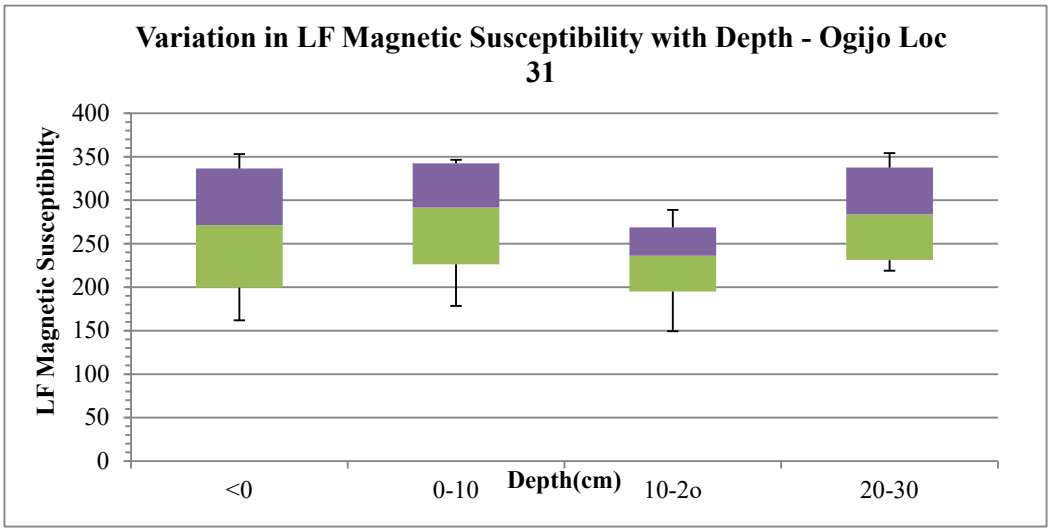
Variation in LF Magnetic Susceptibility with Depth - Ogijo Loc 31
LF Magnetic Susceptibility
400
350
300
250
200
150
100
50
0
<0
0-10
Depth(cm)
10-2o
20-30

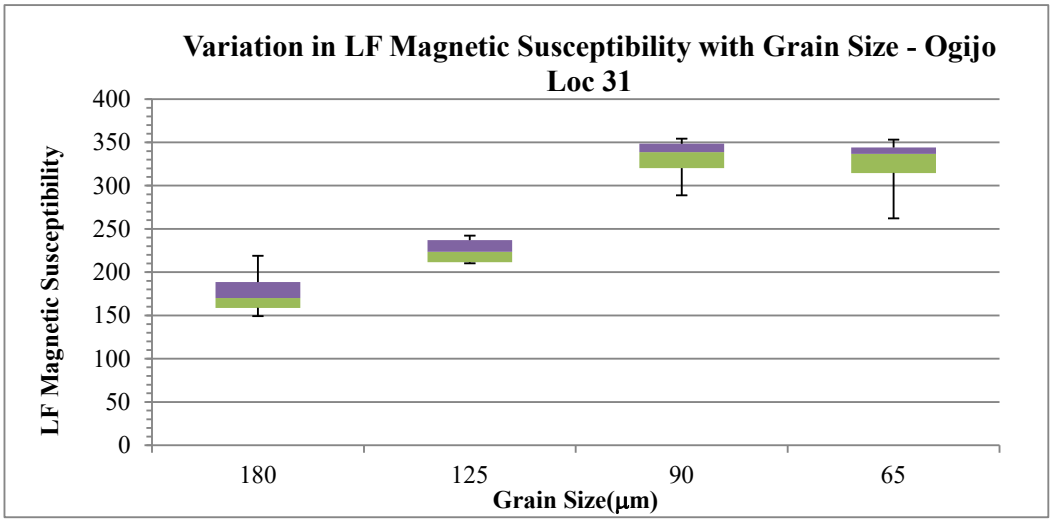
Variation in LF Magnetic Susceptibility with Grain Size - Ogijo Loc 31
LF Magnetic Susceptibility
400
350
300
250
200
150
100
50
0
180
125
90
65
Grain Size(µm)

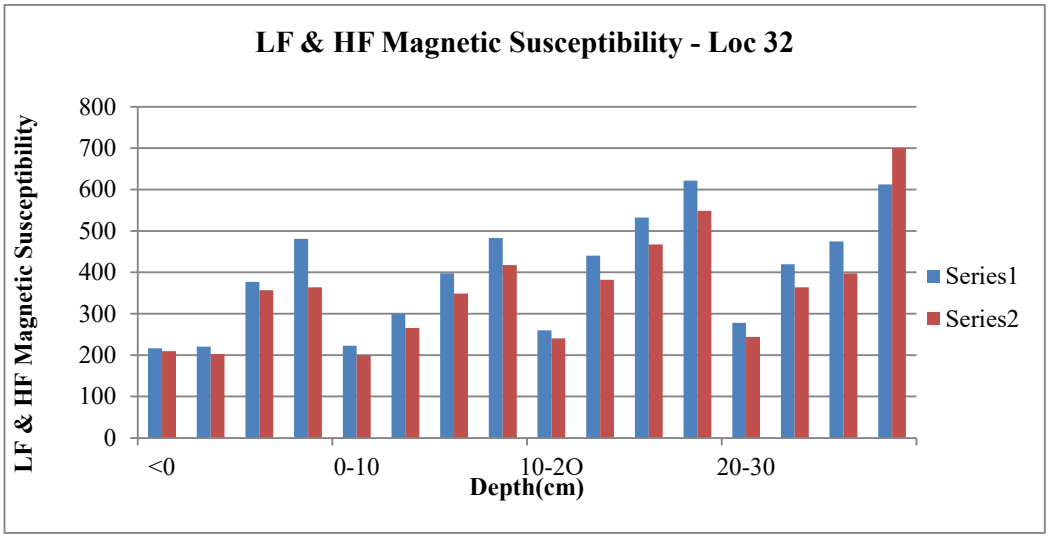
LF & HF Magnetic Susceptibility - Loc 32
LF & HF Magnetic Susceptibility
800
700
600
500
400
300
200
100
0
<0
0-10
10-2O
20-30
Depth(cm)
Series1
Series2

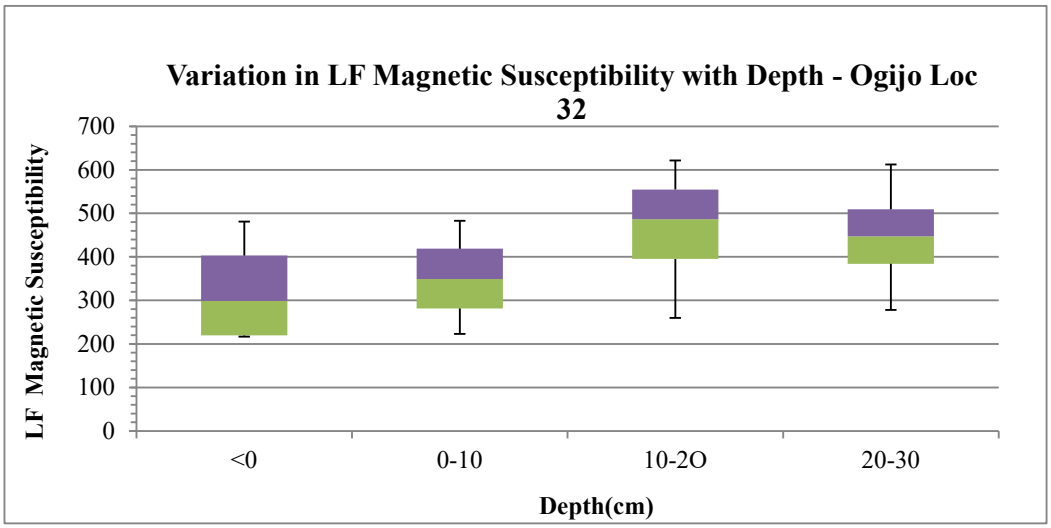
Variation in LF Magnetic Susceptibility with Depth - Ogijo Loc 32
LF Magnetic Susceptibility
700
600
500
400
300
200
100
0
<0
0-10
10-2O
20-30
Depth(cm)

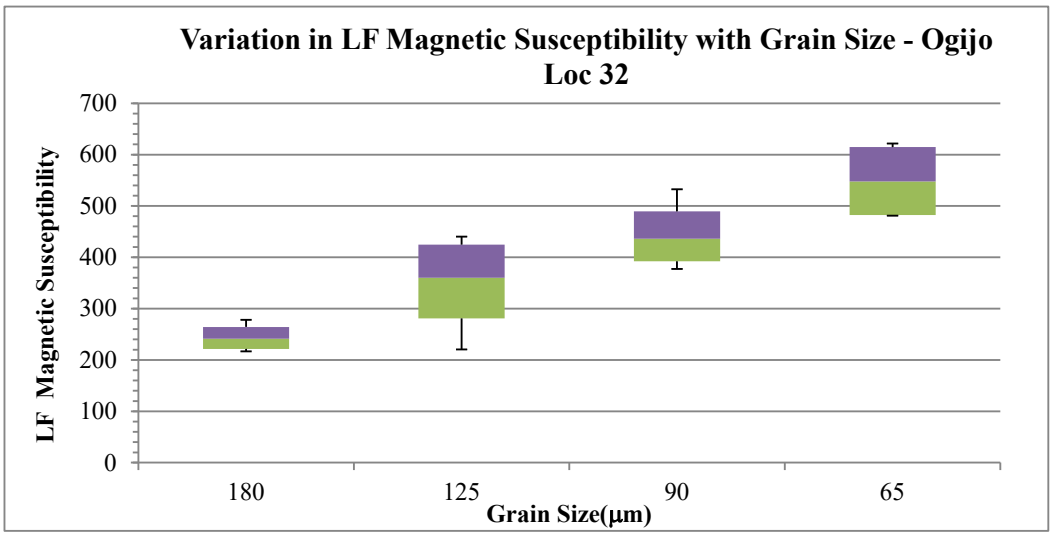
Variation in LF Magnetic Susceptibility with Grain Size - Ogijo Loc 32
LF Magnetic Susceptibility
700
600
500
400
300
200
100
0
180
125
90
65
Grain Size(µm)

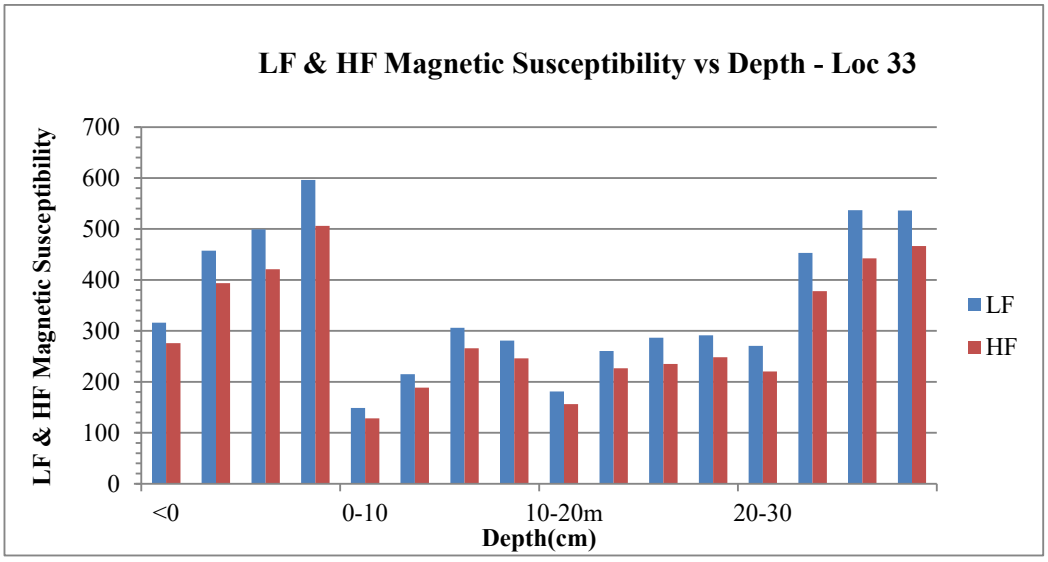
LF & HF Magnetic Susceptibility vs Depth - Loc 33
LF & HF Magnetic Susceptibility
700
600
500
400
300
200
100
0
<0
0-10
10-20m
20-30
Depth(cm)
LF
HF

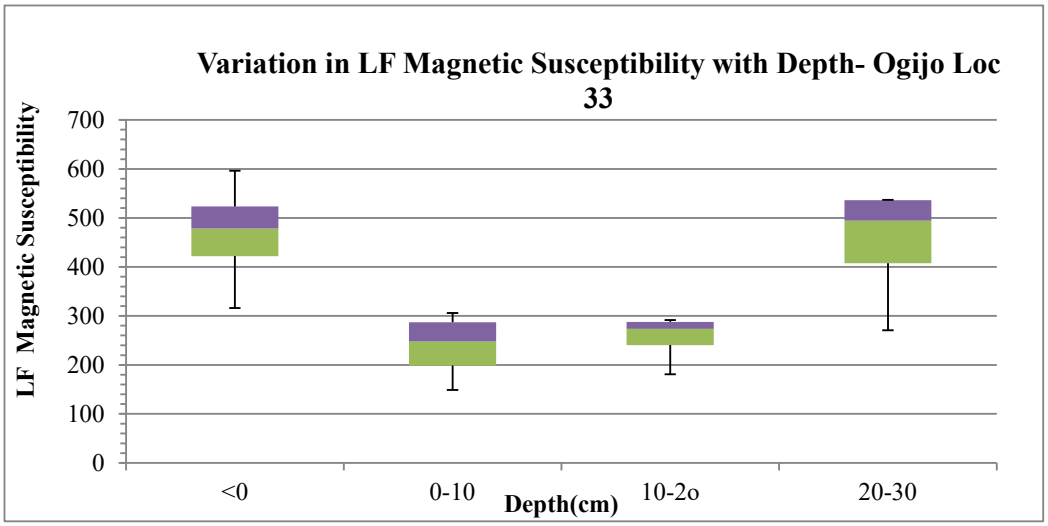
Variation in LF Magnetic Susceptibility with Depth- Ogijo Loc 33
LF Magnetic Susceptibility
700
600
500
400
300
200
100
0
<0
0-10
Depth(cm)
10-2o
20-30

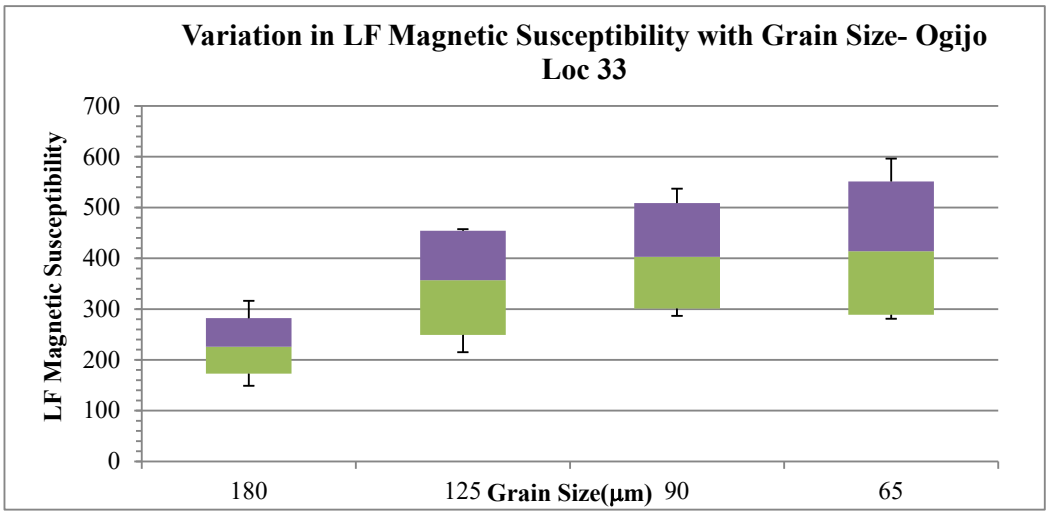
Variation in LF Magnetic Susceptibility with Grain Size- Ogijo Loc 33
LF Magnetic Susceptibility
700
600
500
400
300
200
100
0
180
125
Grain Size(µm)
90
65

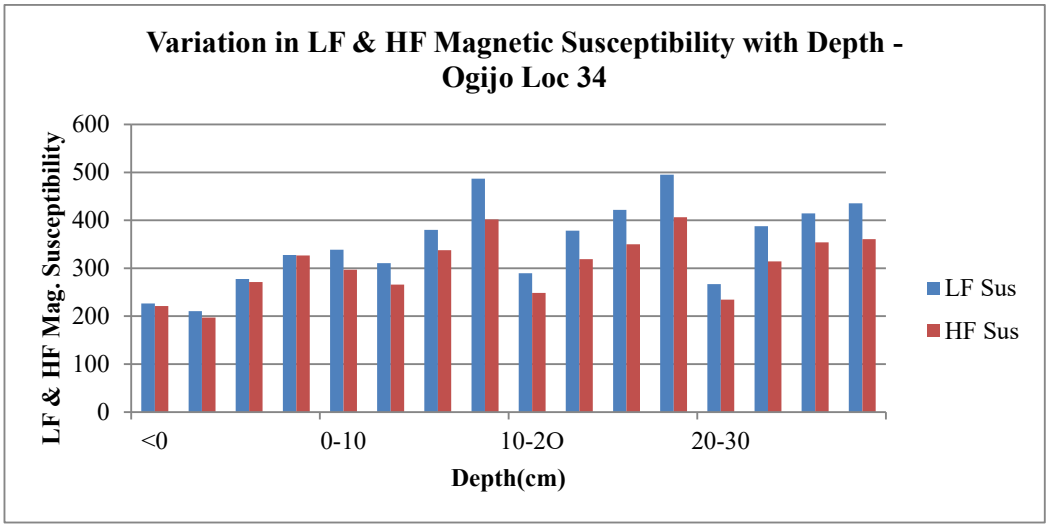
Variation in LF & HF Magnetic Susceptibility with Depth - Ogijo Loc 34
LF & HF Mag. Susceptibility
600
500
400
300
200
100
0
<0
0-10
10-2O
20-30
Depth(cm)
LF Sus
HF Sus

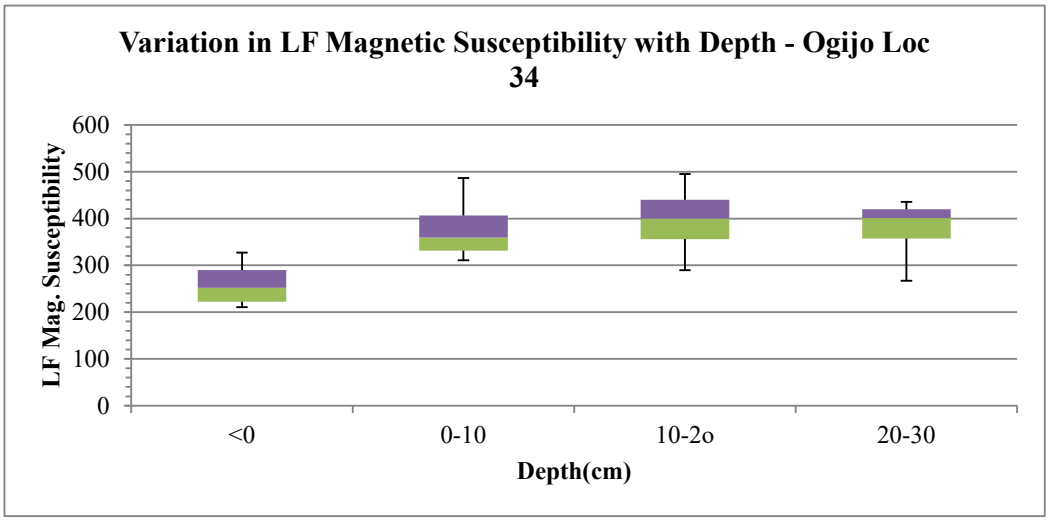
Variation in LF Magnetic Susceptibility with Depth - Ogijo Loc 34
LF Mag. Susceptibility
600
500
400
300
200
100
0
<0
0-10
10-2o
20-30
Depth(cm)

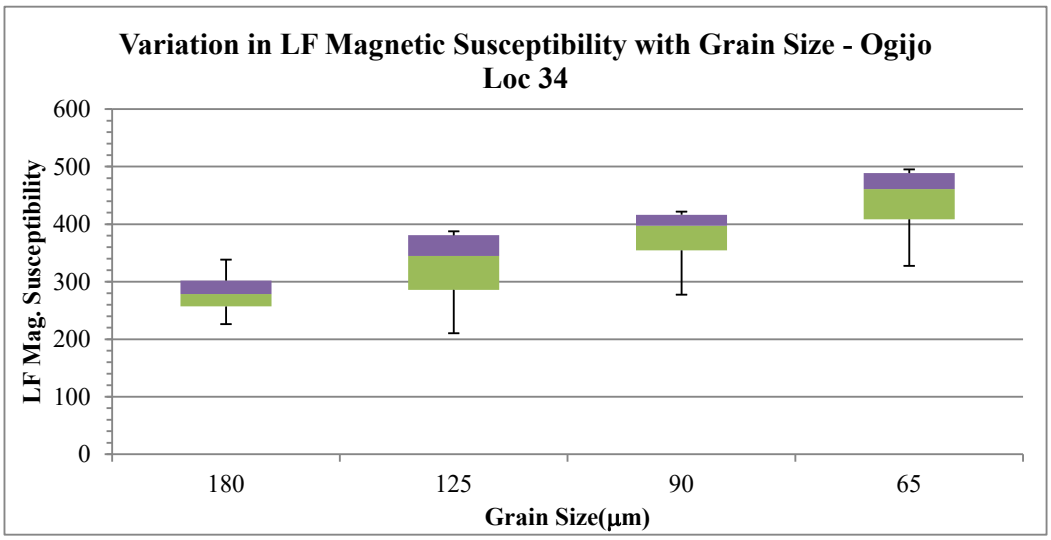
Variation in LF Magnetic Susceptibility with Grain Size - Ogijo Loc 34
LF Mag. Susceptibility
600
500
400
300
200
100
0
180
125
90
65
Grain Size(µm)

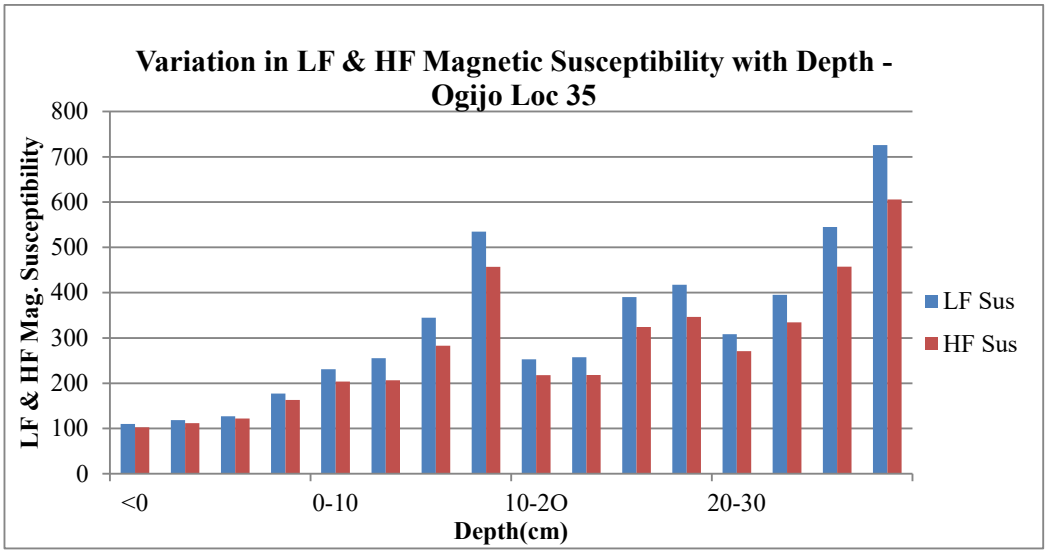
Variation in LF & HF Magnetic Susceptibility with Depth - Ogijo Loc 35
LF & HF Mag. Susceptibility
800
700
600
500
400
300
200
100
0
<0
0-10
10-2O
20-30
Depth(cm)
LF Sus
HF Sus

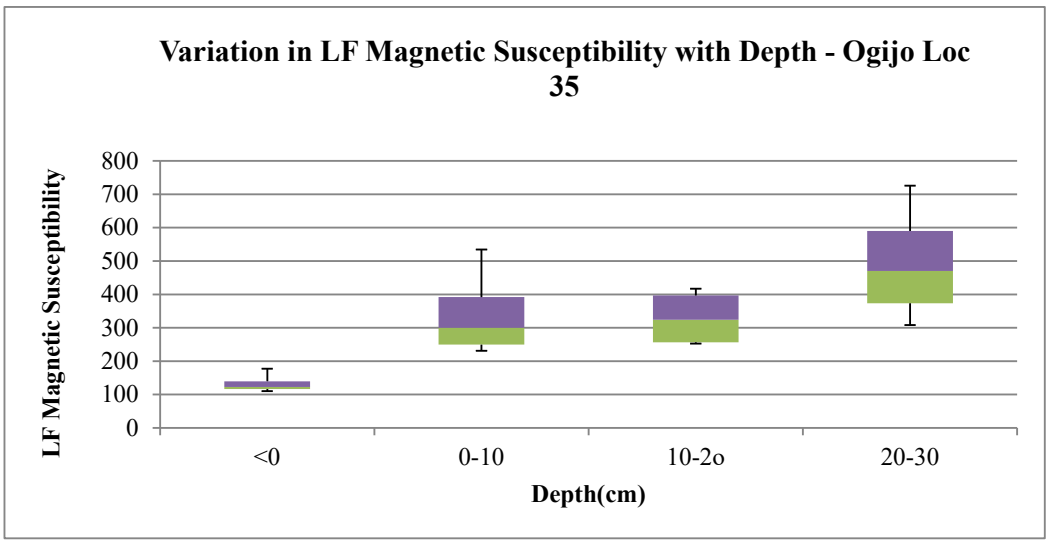
Variation in LF Magnetic Susceptibility with Depth - Ogijo Loc 35
LF Magnetic Susceptibility
800
700
600
500
400
300
200
100
0
<0
0-10
10-2o
20-30
Depth(cm)

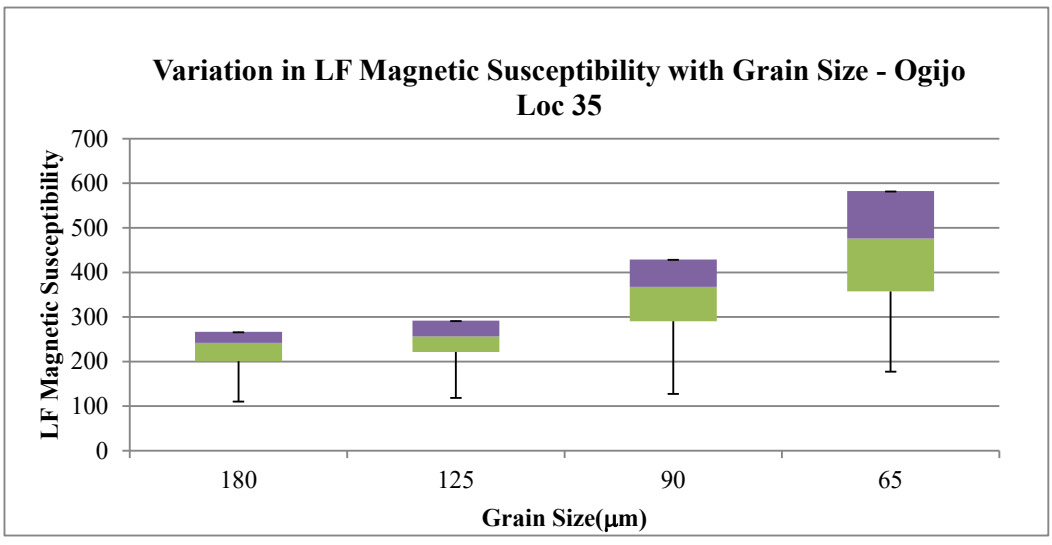
Variation in LF Magnetic Susceptibility with Grain Size - Ogijo Loc 35
LF Magnetic Susceptibility
700
600
500
400
300
200
100
0
180
125
90
65
Grain Size(µm)

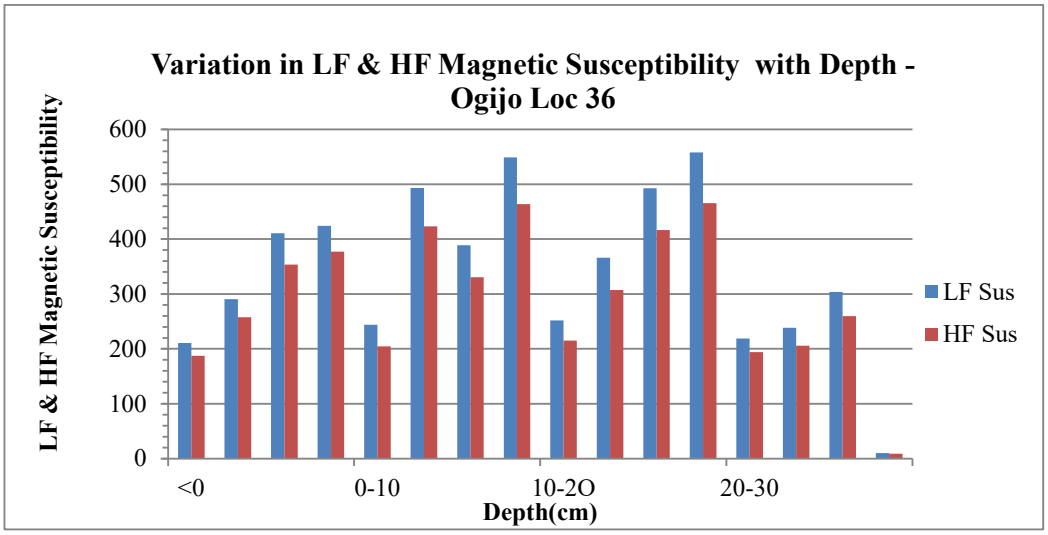
Variation in LF & HF Magnetic Susceptibility with Depth - Ogijo Loc 36
LF & HF Magnetic Susceptibility
600
500
400
300
200
100
0
<0
0-10
10-2O
20-30
Depth(cm)
LF Sus
HF Sus

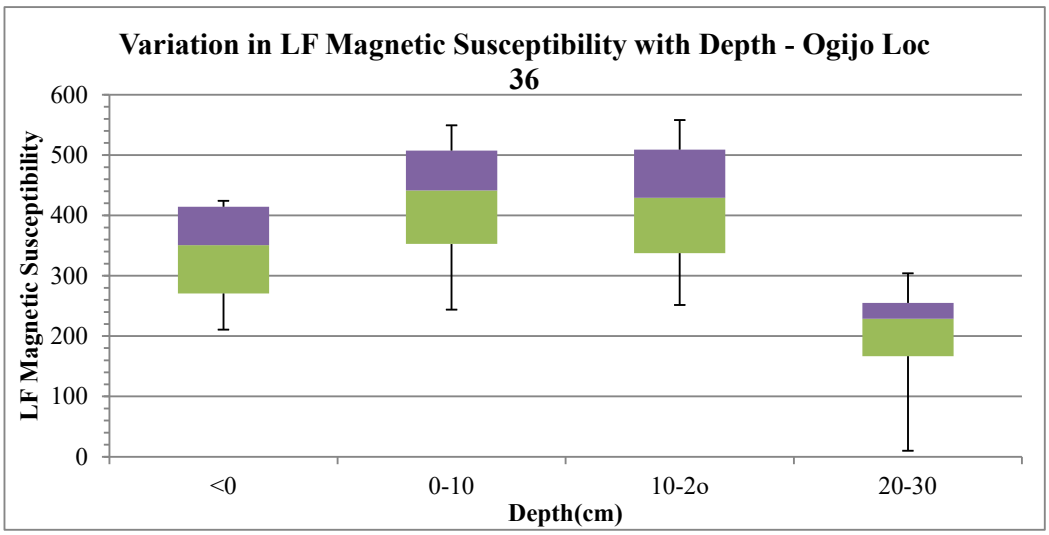
Variation in LF Magnetic Susceptibility with Depth - Ogijo Loc 36
LF Magnetic Susceptibility
600
500
400
300
200
100
0
<0
0-10
10-2o
20-30
Depth(cm)

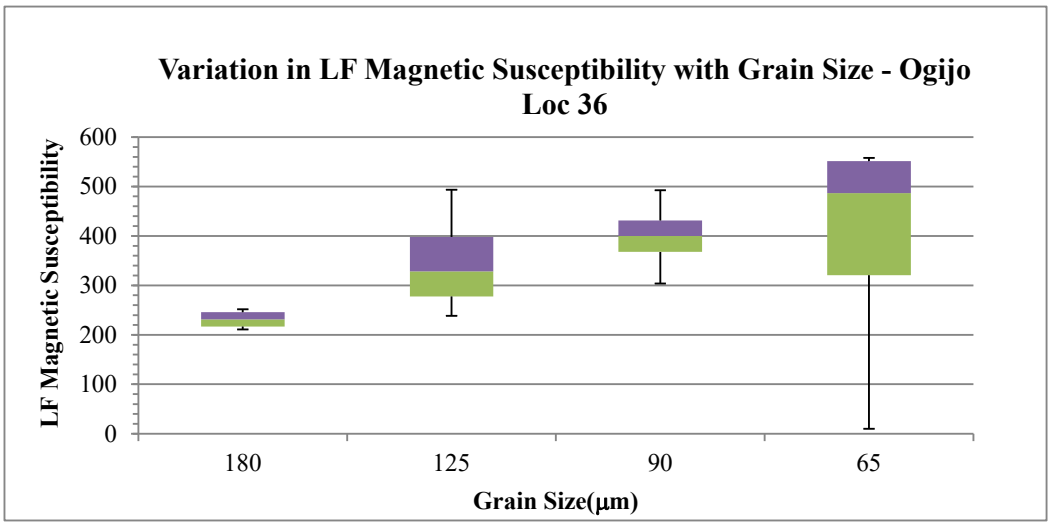
Variation in LF Magnetic Susceptibility with Grain Size - Ogijo Loc 36
LF Magnetic Susceptibility
600
500
400
300
200
100
0
180
125
90
65
Grain Size(µm)

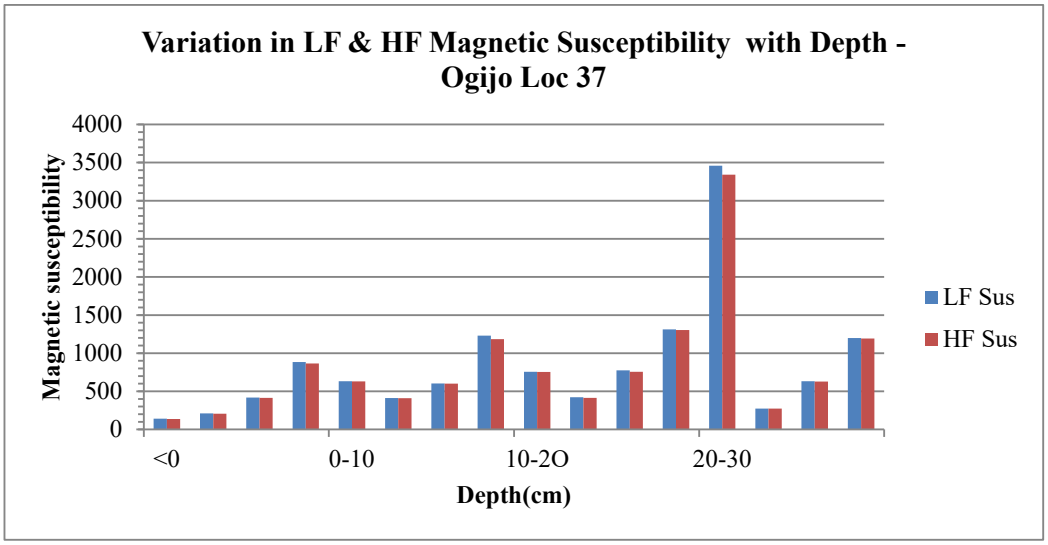
Variation in LF & HF Magnetic Susceptibility with Depth - Ogijo Loc 37
Magnetic susceptibility
4000
3500
3000
2500
2000
1500
1000
500
0
<0
0-10
10-2O
20-30
Depth(cm)
LF Sus
HF Sus

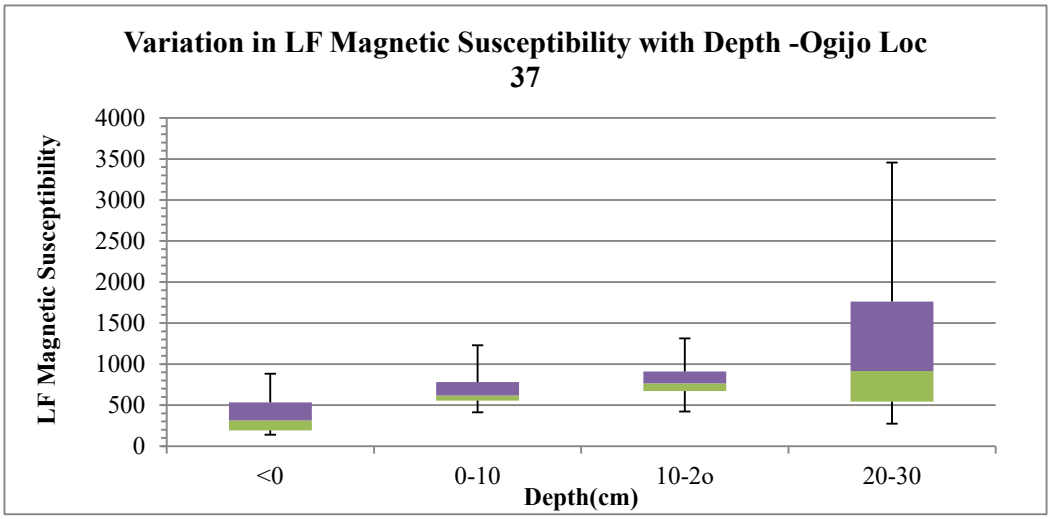
Variation in LF Magnetic Susceptibility with Depth -Ogijo Loc 37
LF Magnetic Susceptibility
4000
3500
3000
2500
2000
1500
1000
500
0
<0
0-10
10-2o
20-30
Depth(cm)

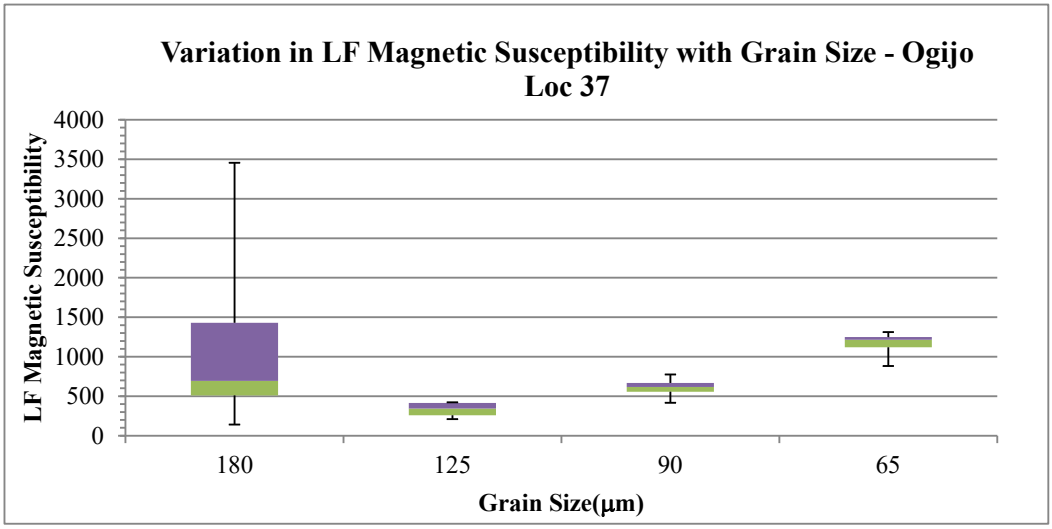
Variation in LF Magnetic Susceptibility with Grain Size - Ogijo Loc 37
LF Magnetic Susceptibility
4000
3500
3000
2500
2000
1500
1000
500
0
180
125
90
65
Grain Size(µm)

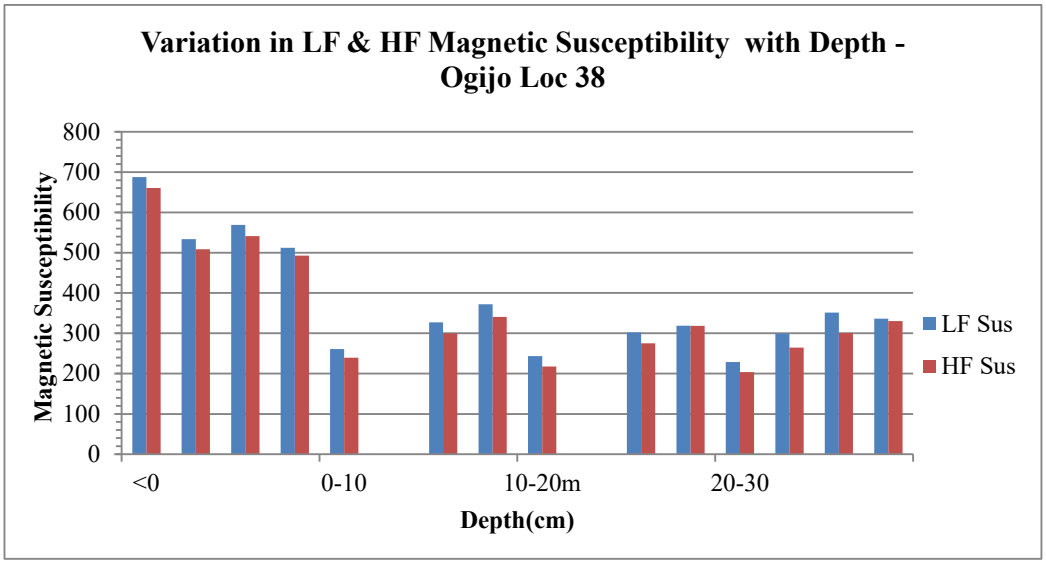
Variation in LF & HF Magnetic Susceptibility with Depth - Ogijo Loc 38
Magnetic Susceptibility
800
700
600
500
400
300
200
100
0
<0
0-10
10-20m
20-30
Depth(cm)
LF Sus
HF Sus

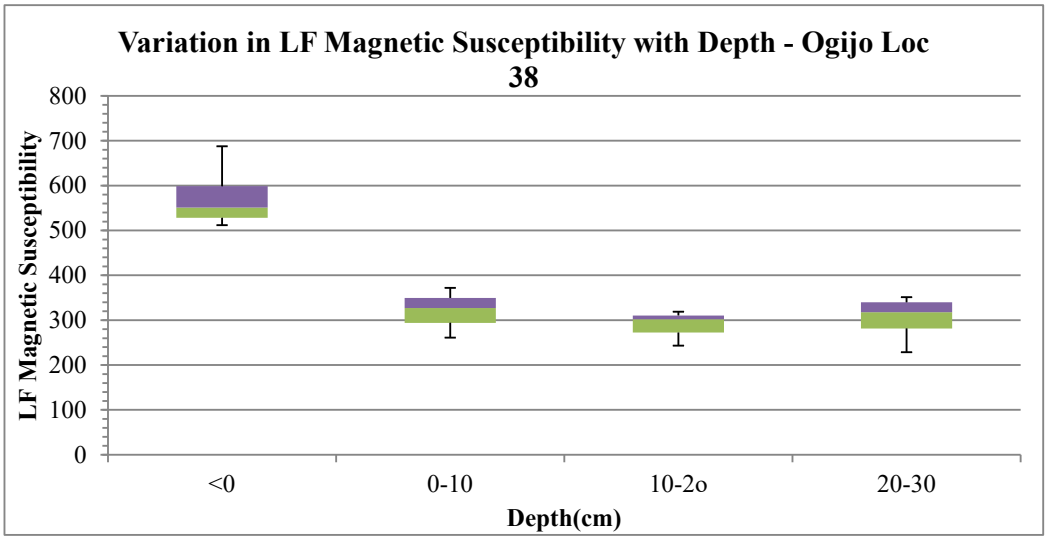
Variation in LF Magnetic Susceptibility with Depth - Ogijo Loc 38
LF Magnetic Susceptibility
800
700
600
500
400
300
200
100
0
<0
0-10
10-2o
20-30
Depth(cm)

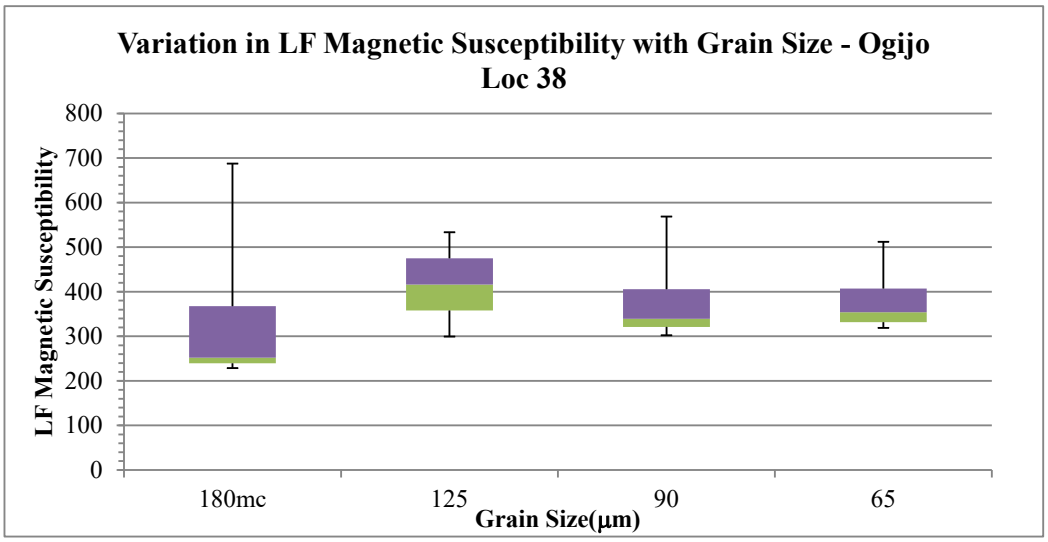
Variation in LF Magnetic Susceptibility with Grain Size - Ogijo Loc 38
LF Magnetic Susceptibility
800
700
600
500
400
300
200
100
0
180mc
125
90
65
Grain Size(µm)

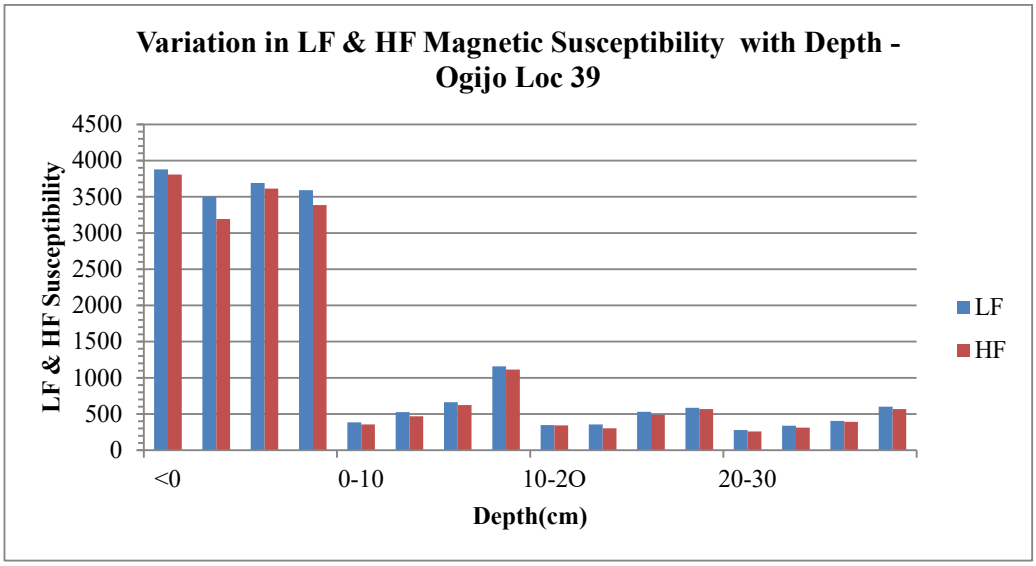
Variation in LF & HF Magnetic Susceptibility with Depth - Ogijo Loc 39
LF & HF Susceptibility
4500
4000
3500
3000
2500
2000
1500
1000
500
0
<0
0-10
10-2O
20-30
Depth(cm)
LF
HF

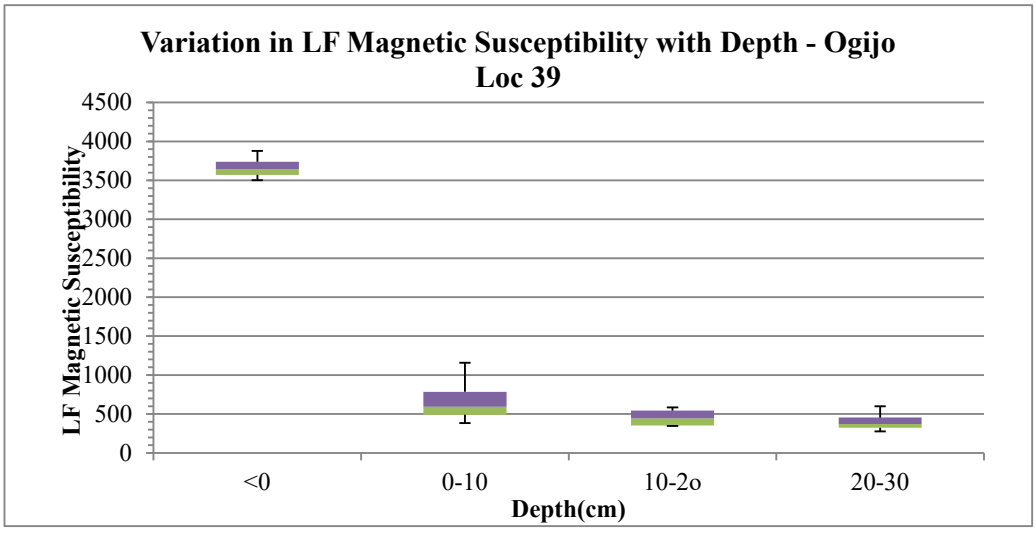
Variation in LF Magnetic Susceptibility with Depth - Ogijo Loc 39
LF Magnetic Susceptibility
4500
4000
3500
3000
2500
2000
1500
1000
500
0
<0
0-10
10-2o
20-30
Depth(cm)

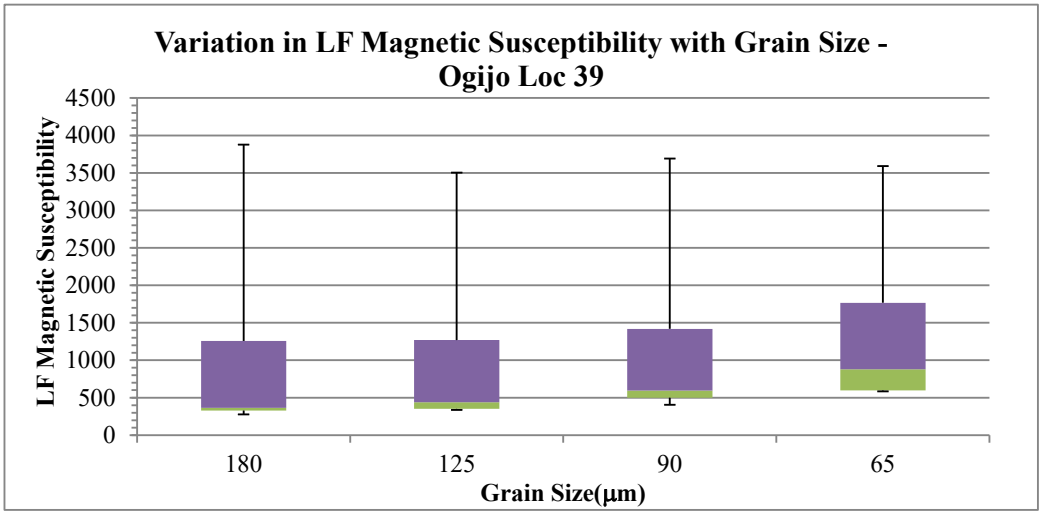
Variation in LF Magnetic Susceptibility with Grain Size - Ogijo Loc 39
LF Magnetic Susceptibility
4500
4000
3500
3000
2500
2000
1500
1000
500
0
180
125
90
65
Grain Size(µm)

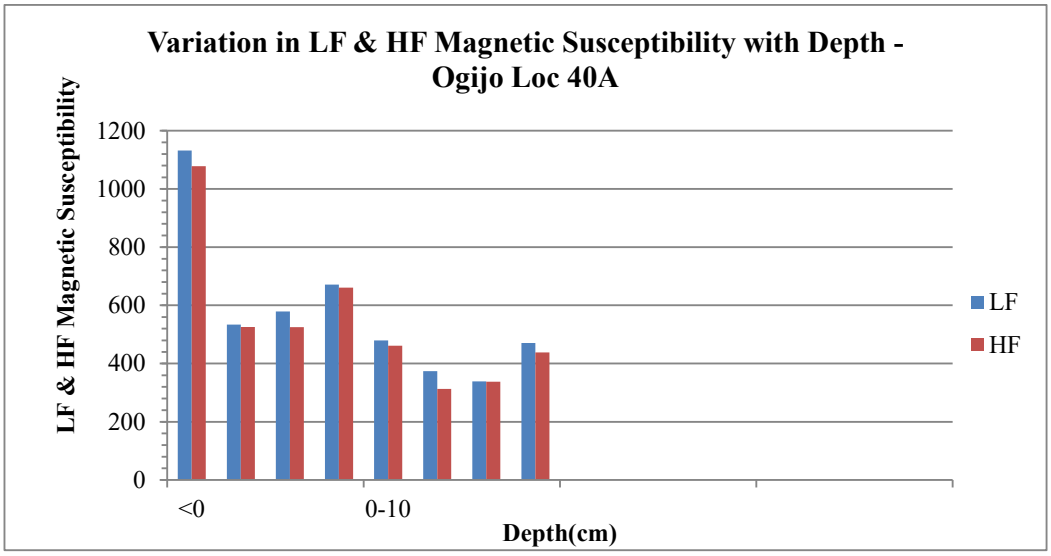
Variation in LF & HF Magnetic Susceptibility with Depth - Ogijo Loc 40A
LF & HF Magnetic Susceptibility
1200
1000
800
600
400
200
0
<0
0-10
Depth(cm)
LF
HF

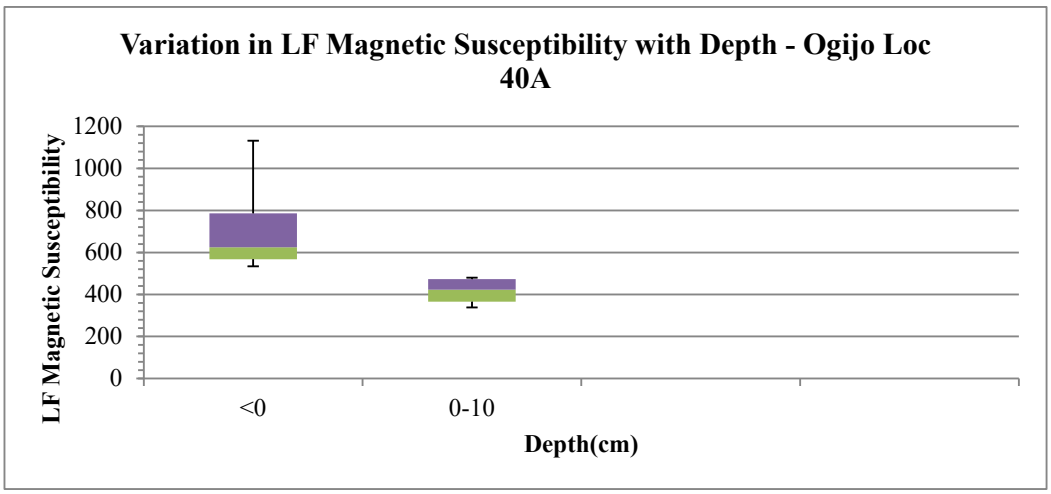
Variation in LF Magnetic Susceptibility with Depth - Ogijo Loc 40A
LF Magnetic Susceptibility
1200
1000
800
600
400
200
0
<0
0-10
Depth(cm)

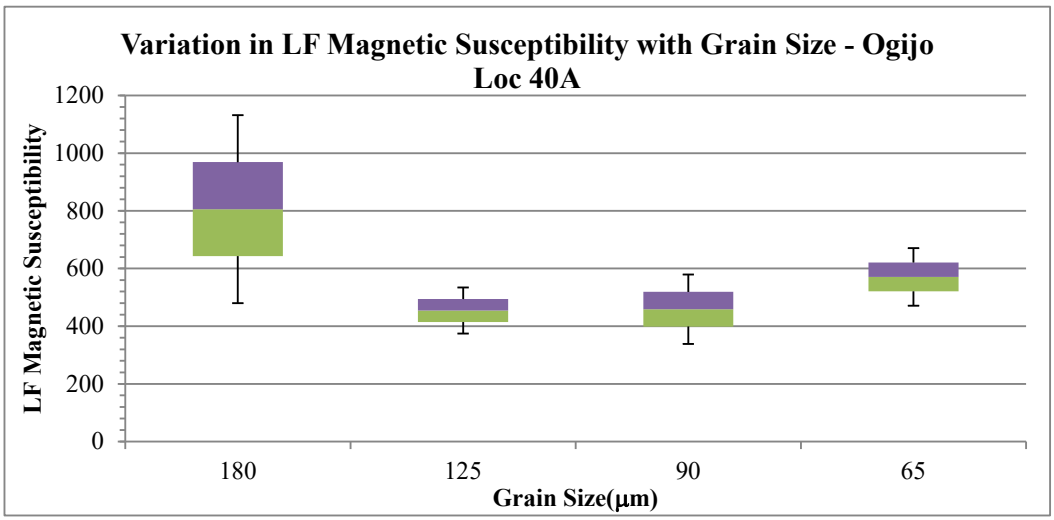
Variation in LF Magnetic Susceptibility with Grain Size - Ogijo Loc 40A
LF Magnetic Susceptibility
1200
1000
800
600
400
200
0
180
125
90
65
Grain Size(µm)

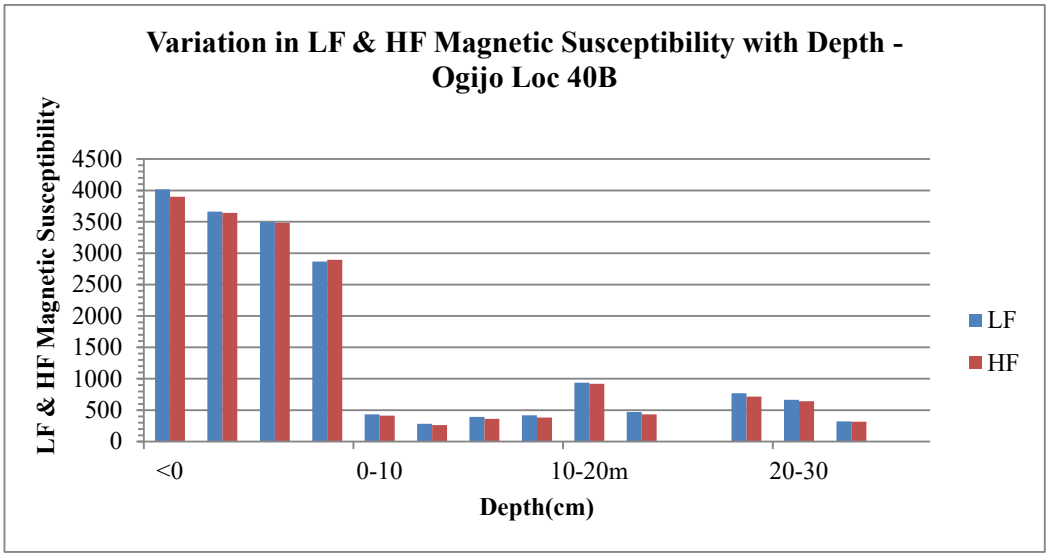
Variation in LF & HF Magnetic Susceptibility with Depth - Ogijo Loc 40B
LF & HF Magnetic Susceptibility
4500
4000
3500
3000
2500
2000
1500
1000
500
0
<0
0-10
10-20m
20-30
Depth(cm)
LF
HF

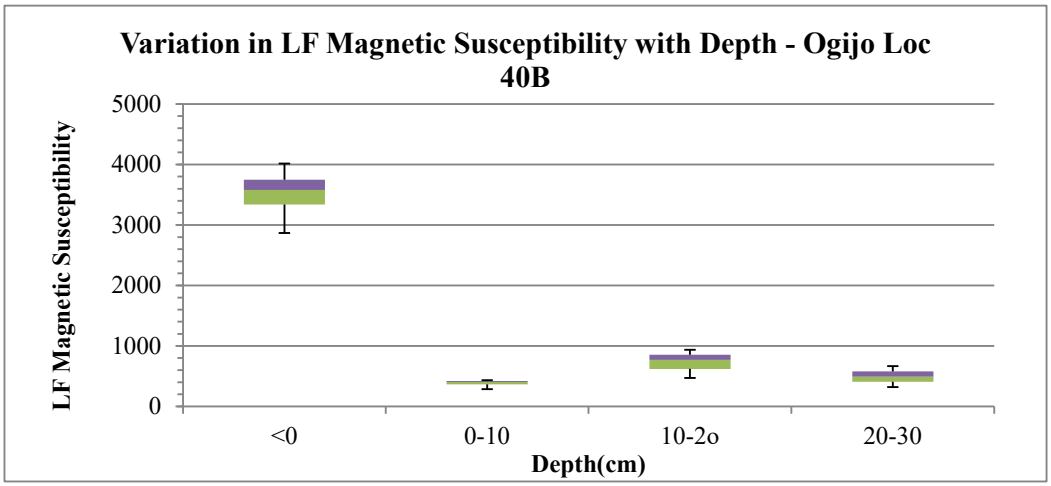
Variation in LF Magnetic Susceptibility with Depth - Ogijo Loc 40B
LF Magnetic Susceptibility
5000
4000
3000
2000
1000
0
<0
0-10
10-2o
20-30
Depth(cm)

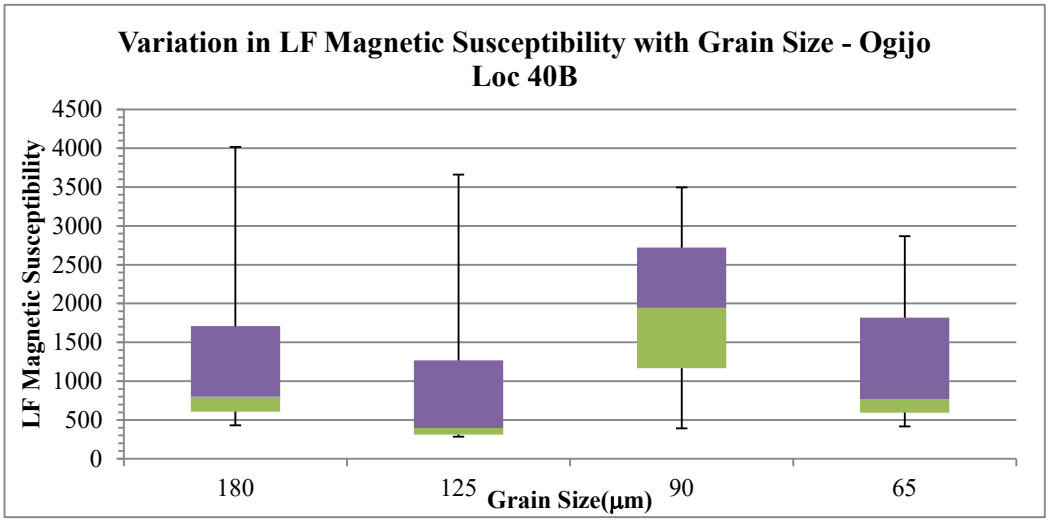
Variation in LF Magnetic Susceptibility with Grain Size - Ogijo Loc 40B
LF Magnetic Susceptibility
4500
4000
3500
3000
2500
2000
1500
1000
500
0
180
125
90
65
Grain Size(µm)

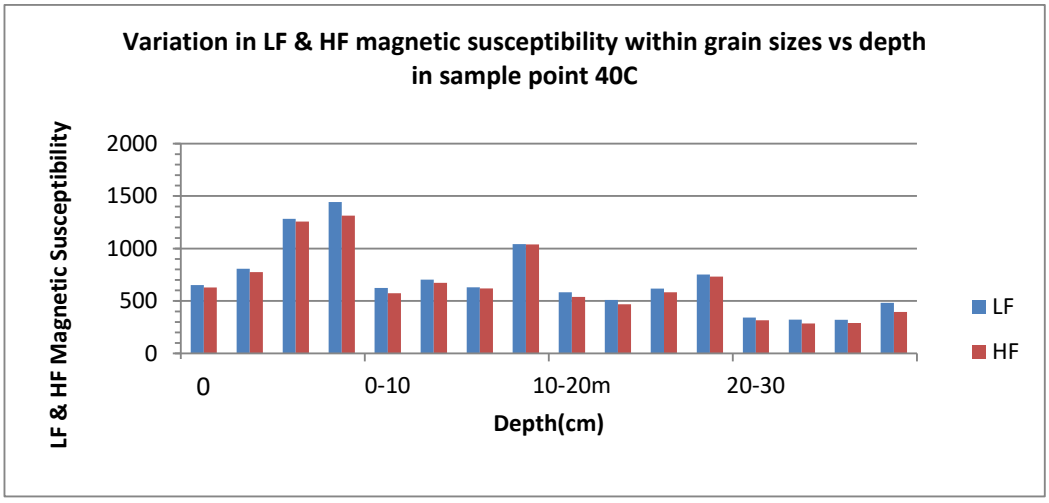
Variation in LF & HF magnetic susceptibility within grain sizes vs depth in sample point 40C
LF & HF Magnetic Susceptibility
2000
1500
1000
500
0
0
0-10
10-20m
20-30
Depth(cm)
LF
HF

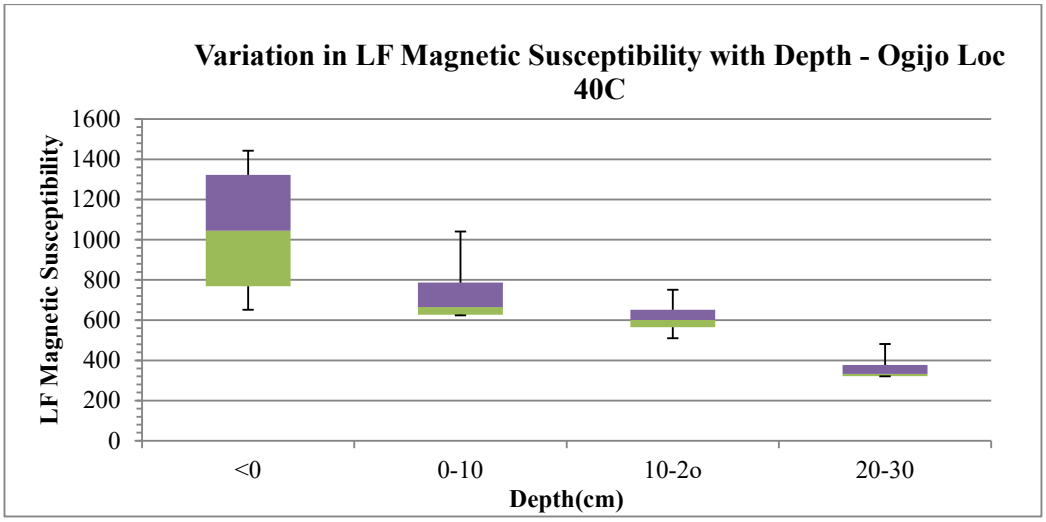
Variation in LF Magnetic Susceptibility with Depth - Ogijo Loc 40C
LF Magnetic Susceptibility
1600
1400
1200
1000
800
600
400
200
0
<0
0-10
10-2o
20-30
Depth(cm)

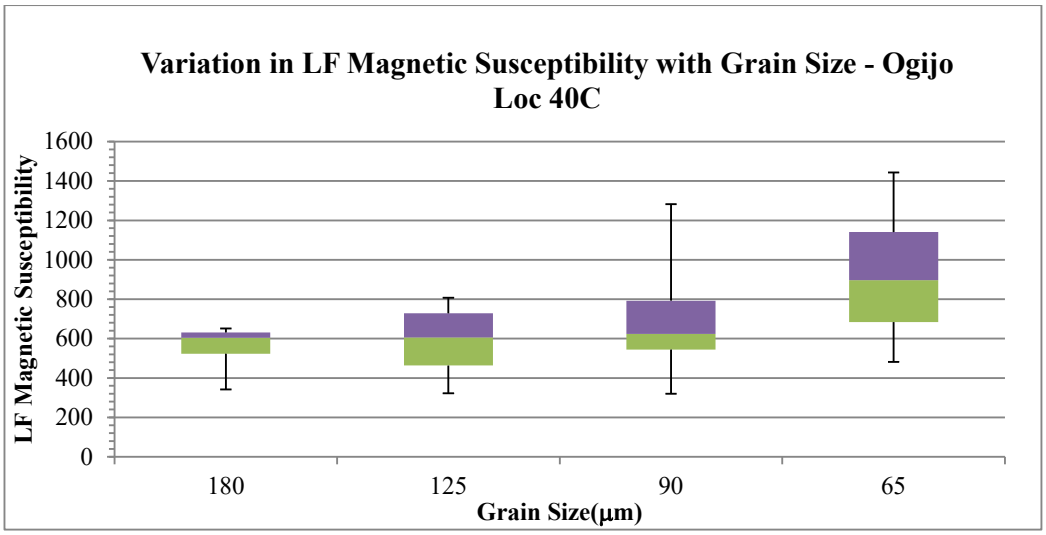
Variation in LF Magnetic Susceptibility with Grain Size - Ogijo Loc 40C
LF Magnetic Susceptibility
1600
1400
1200
1000
800
600
400
200
0
180
125
90
65
Grain Size(µm)

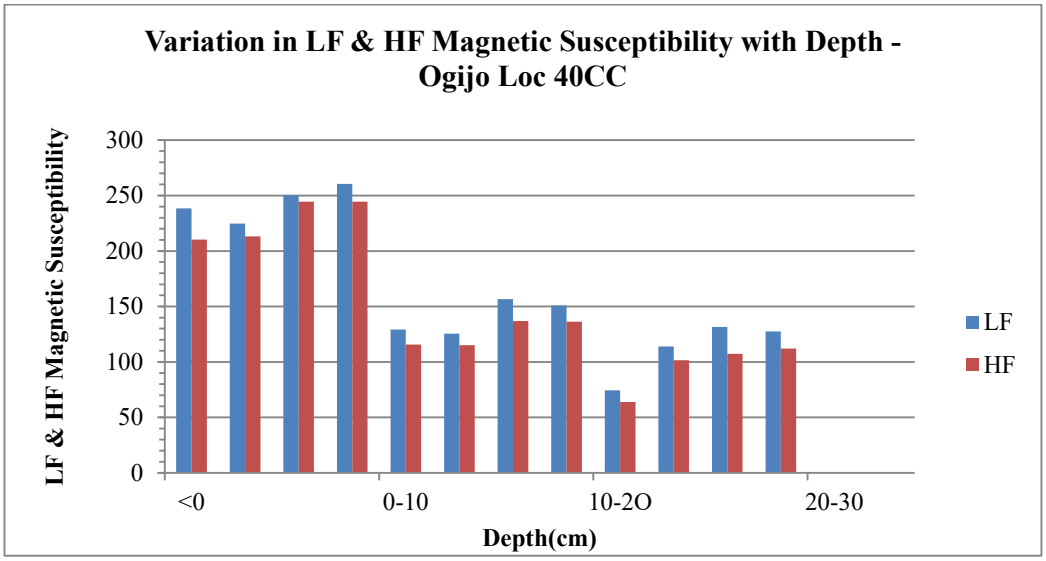
Variation in LF & HF Magnetic Susceptibility with Depth - Ogijo Loc 40CC
LF & HF Magnetic Susceptibility
300
250
200
150
100
50
0
<0
0-10
10-2O
20-30
Depth(cm)
LF
HF

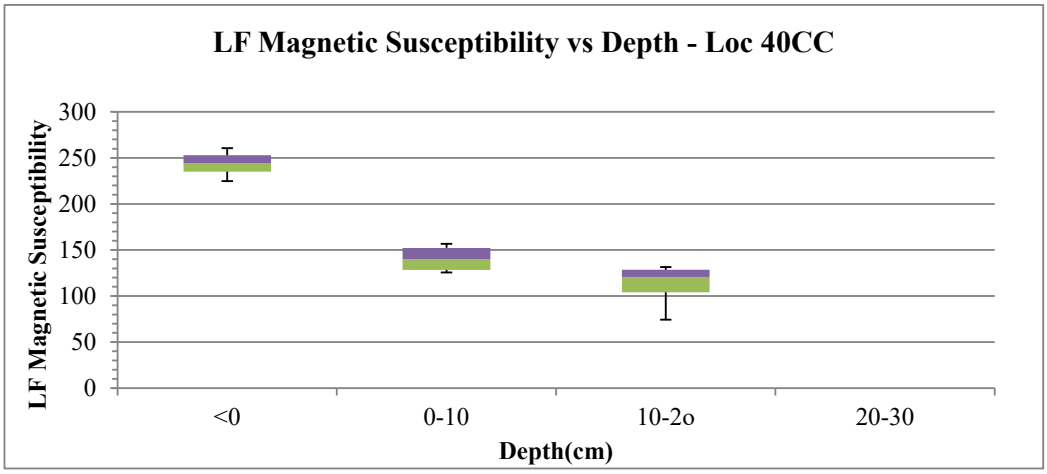
LF Magnetic Susceptibility vs Depth - Loc 40CC
LF Magnetic Susceptibility
300
250
200
150
100
50
0
<0
0-10
10-2o
20-30
Depth(cm)

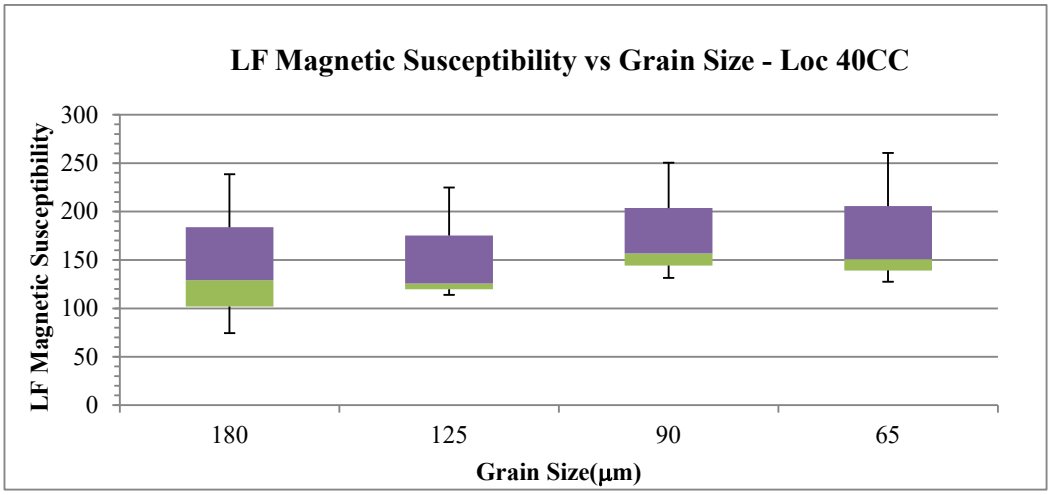
LF Magnetic Susceptibility vs Grain Size - Loc 40CC
LF Magnetic Susceptibility
300
250
200
150
100
50
0
180
125
90
65
Grain Size(µm)

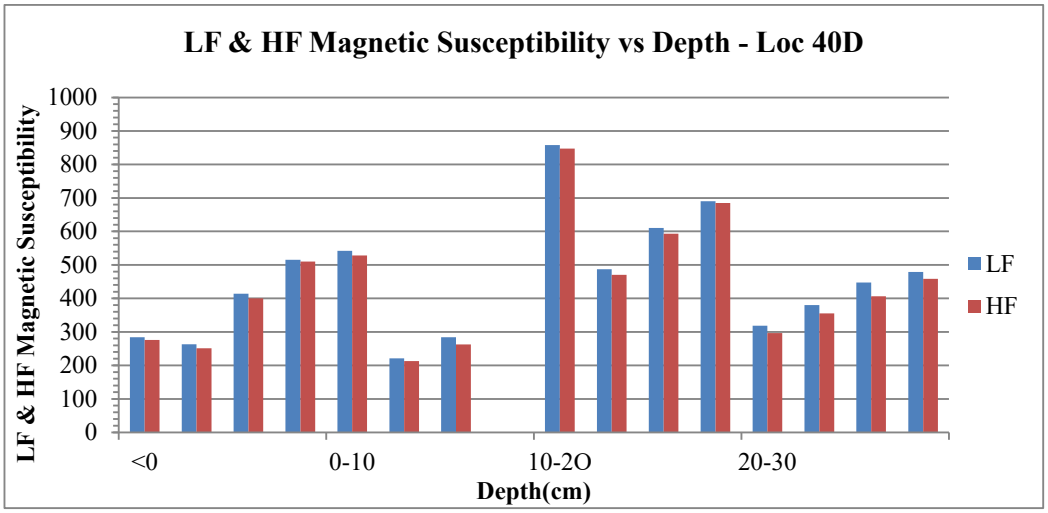
LF & HF Magnetic Susceptibility vs Depth - Loc 40D
LF & HF Magnetic Susceptibility
1000
900
800
700
600
500
400
300
200
100
0
<0
0-10
10-2O
20-30
Depth(cm)
LF
HF

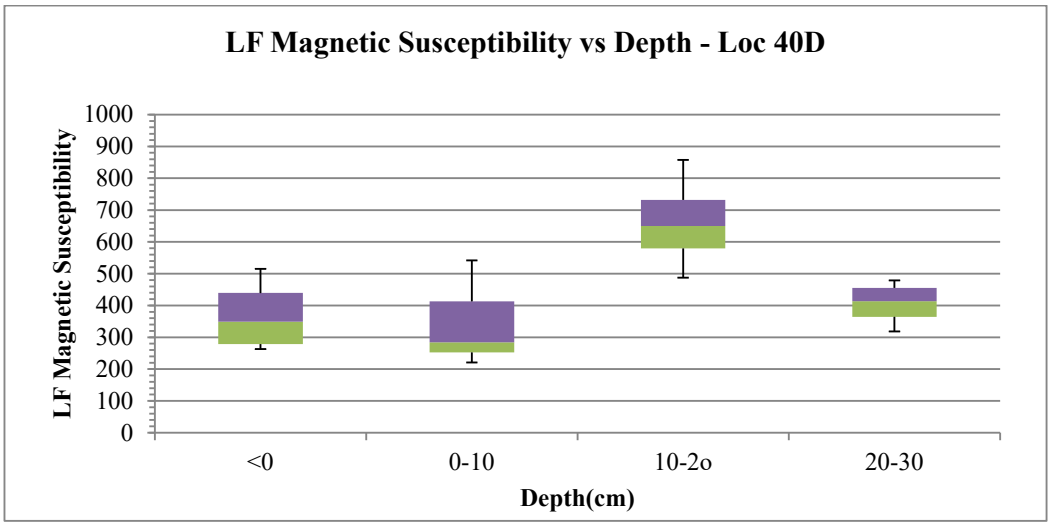
LF Magnetic Susceptibility vs Depth - Loc 40D
LF Magnetic Susceptibility
1000
900
800
700
600
500
400
300
200
100
0
<0
0-10
10-2o
20-30
Depth(cm)

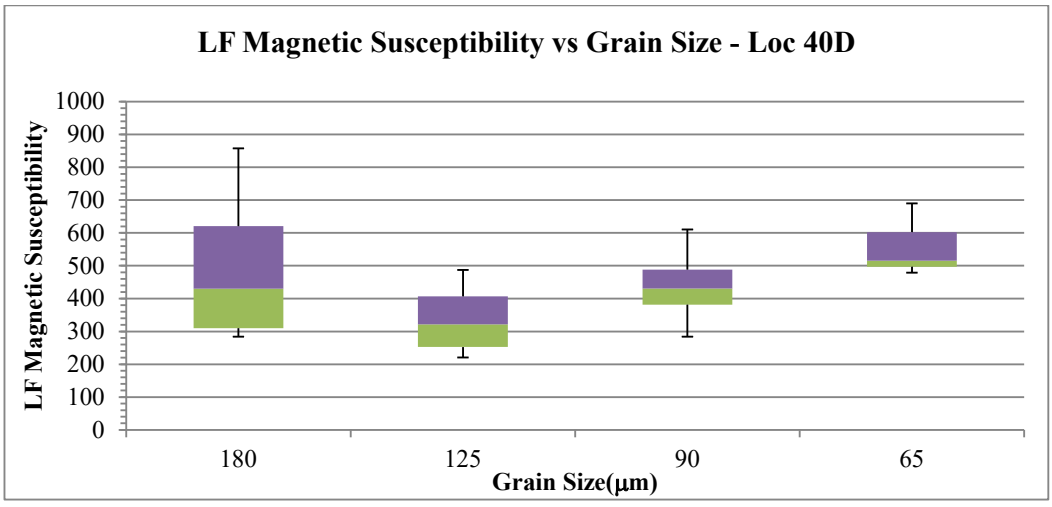
LF Magnetic Susceptibility vs Grain Size - Loc 40D
LF Magnetic Susceptibility
1000
900
800
700
600
500
400
300
200
100
0
180
125
90
65
Grain Size(µm)

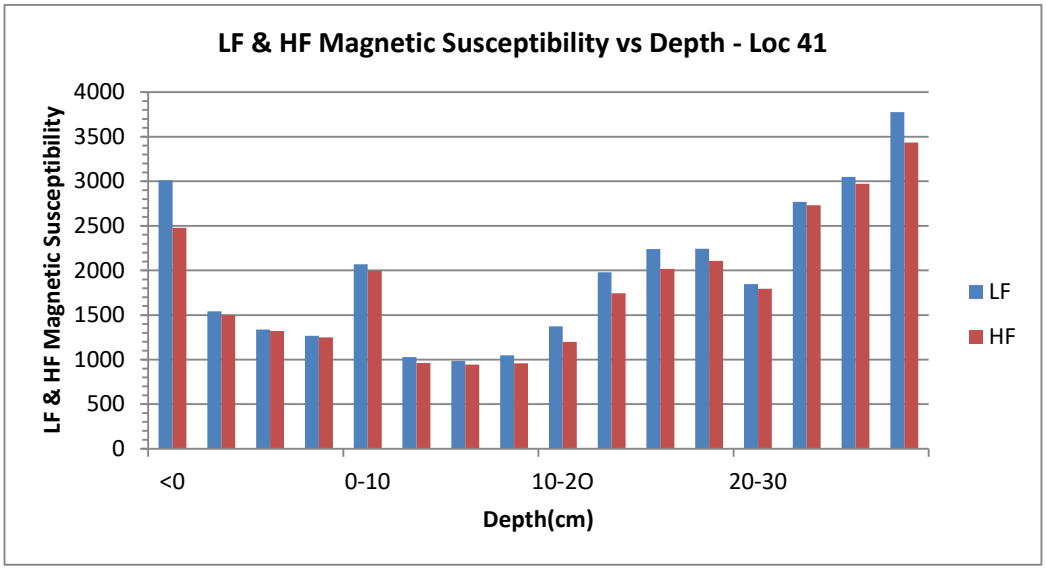
LF & HF Magnetic Susceptibility vs Depth - Loc 41
LF & HF Magnetic Susceptibility
4000
3500
3000
2500
2000
1500
1000
500
0
<0
0-10
10-2O
20-30
Depth(cm)
LF
HF

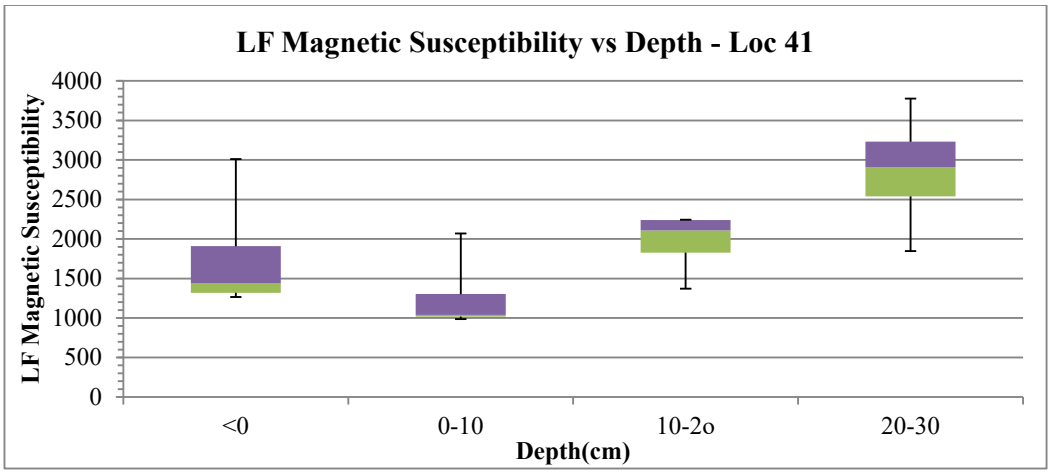
LF Magnetic Susceptibility vs Depth - Loc 41
LF Magnetic Susceptibility
4000
3500
3000
2500
2000
1500
1000
500
0
<0
0-10
10-2o
20-30
Depth(cm)

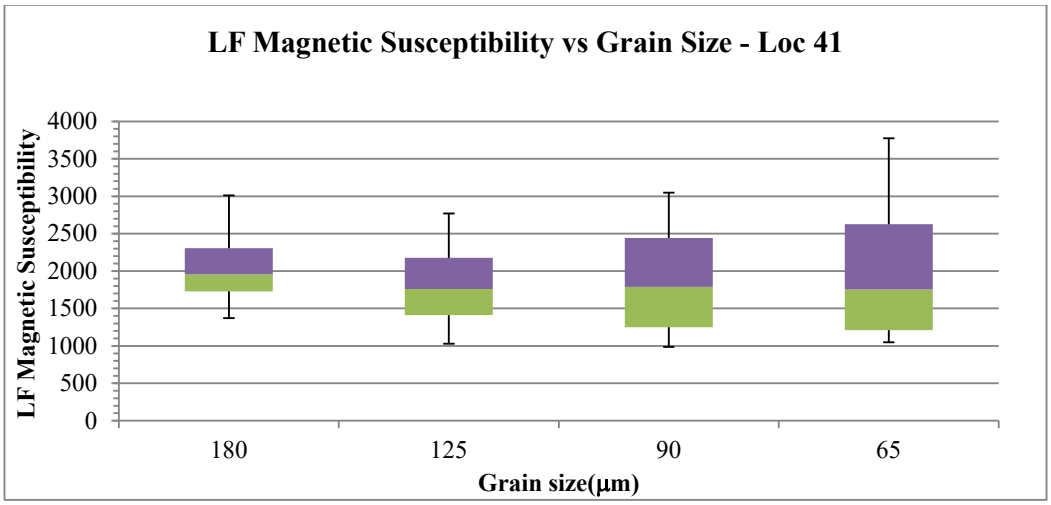
LF Magnetic Susceptibility vs Grain Size - Loc 41
LF Magnetic Susceptibility
4000
3500
3000
2500
2000
1500
1000
500
0
180
125
90
65
Grain size(µm)

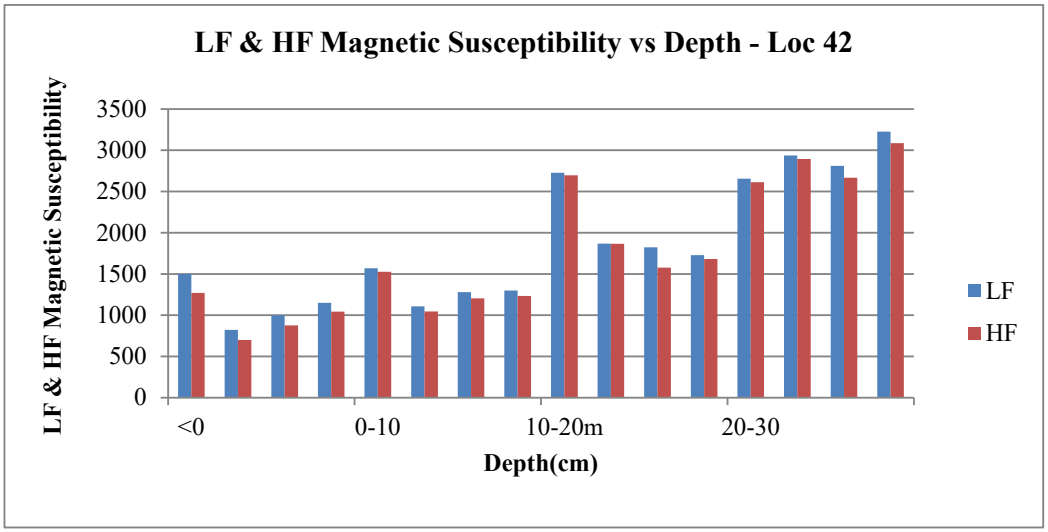
LF & HF Magnetic Susceptibility vs Depth - Loc 42
LF & HF Magnetic Susceptibility
3500
3000
2500
2000
1500
1000
500
0
<0
0-10
10-20m
20-30
Depth(cm)
LF
HF

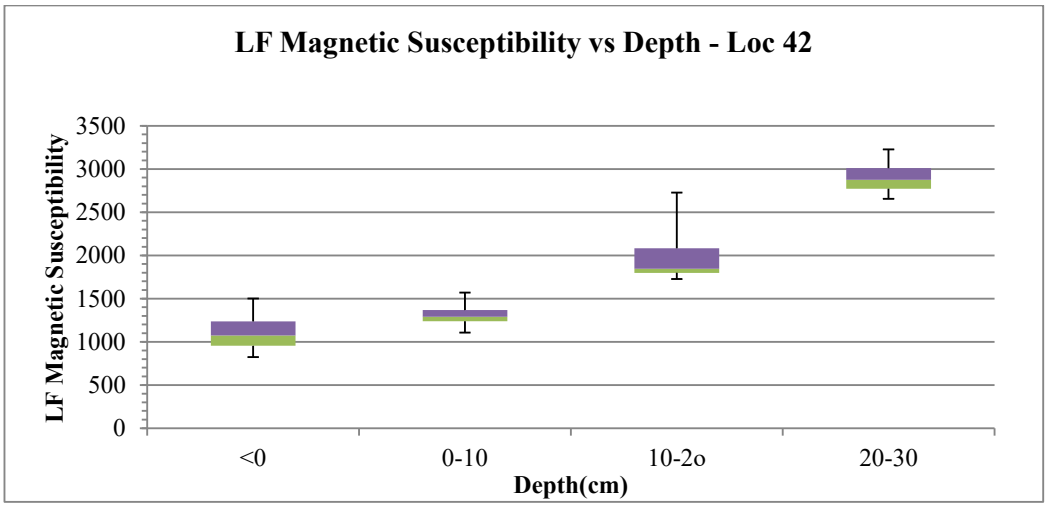
LF Magnetic Susceptibility vs Depth - Loc 42
LF Magnetic Susceptibility
3500
3000
2500
2000
1500
1000
500
0
<0
0-10
10-2o
20-30
Depth(cm)

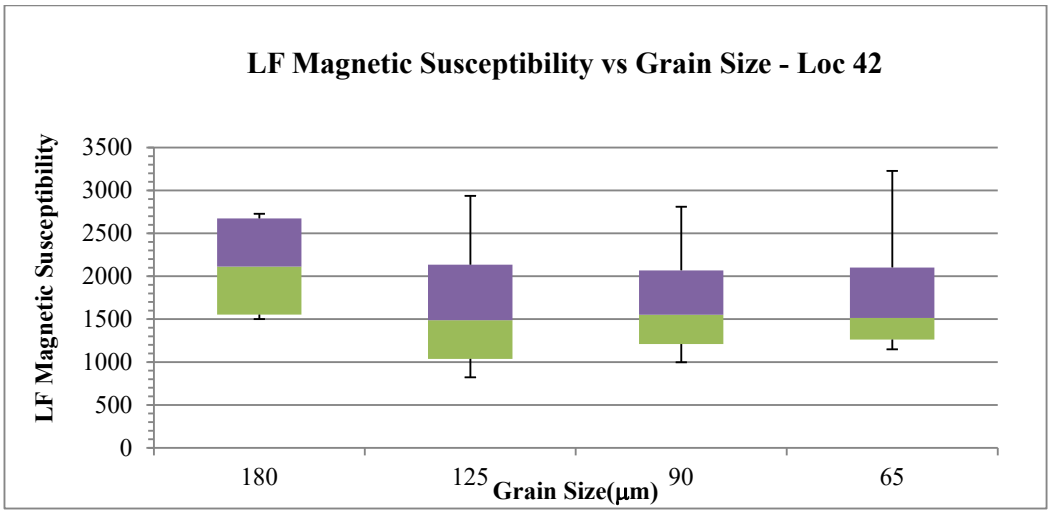
LF Magnetic Susceptibility vs Grain Size - Loc 42
LF Magnetic Susceptibility
3500
3000
2500
2000
1500
1000
500
0
180
125
90
65
Grain Size(µm)

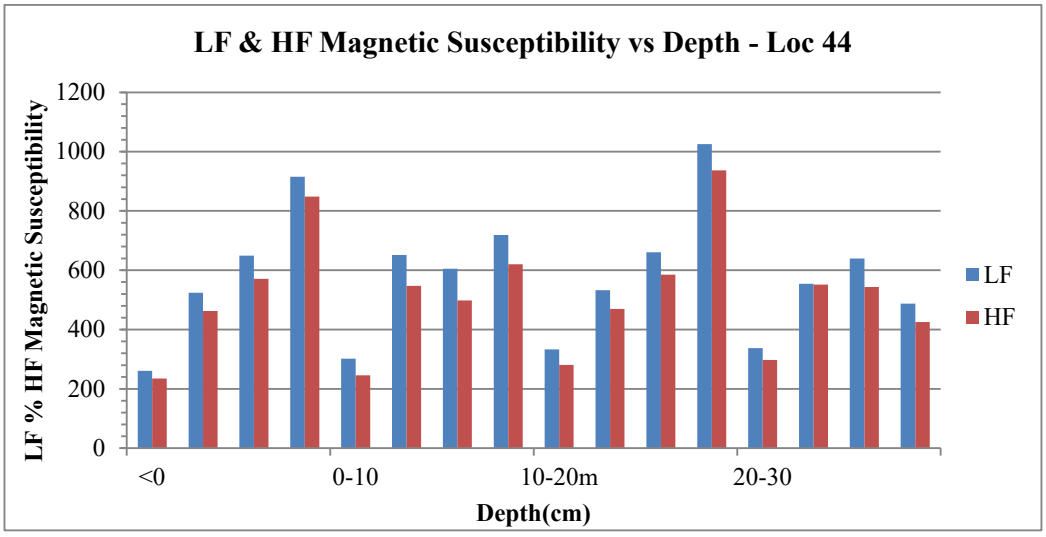
LF & HF Magnetic Susceptibility vs Depth - Loc 44
LF % HF Magnetic Susceptibility
1200
1000
800
600
400
200
0
<0
0-10
10-20m
20-30
Depth(cm)
LF
HF

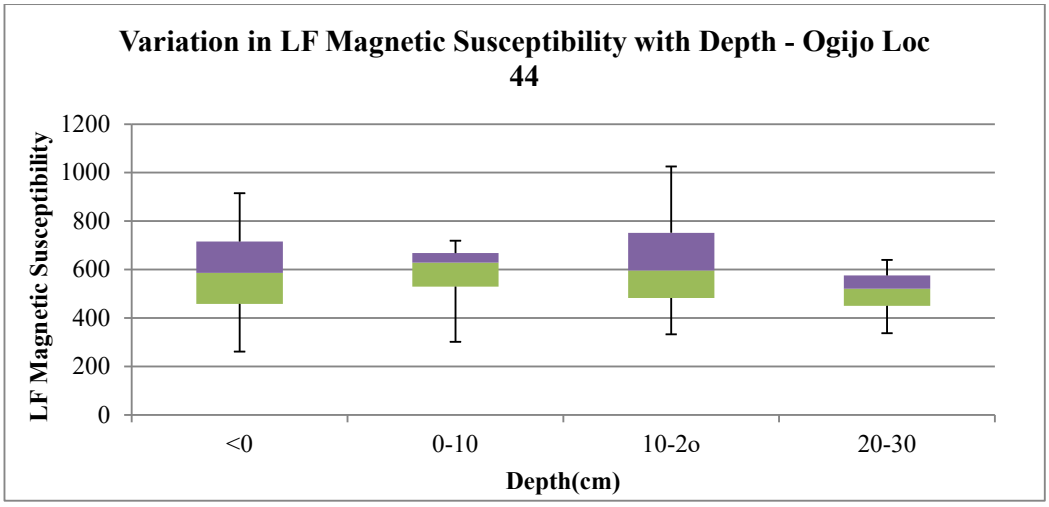
Variation in LF Magnetic Susceptibility with Depth - Ogijo Loc 44
LF Magnetic Susceptibility
1200
1000
800
600
400
200
0
<0
0-10
10-2o
20-30
Depth(cm)

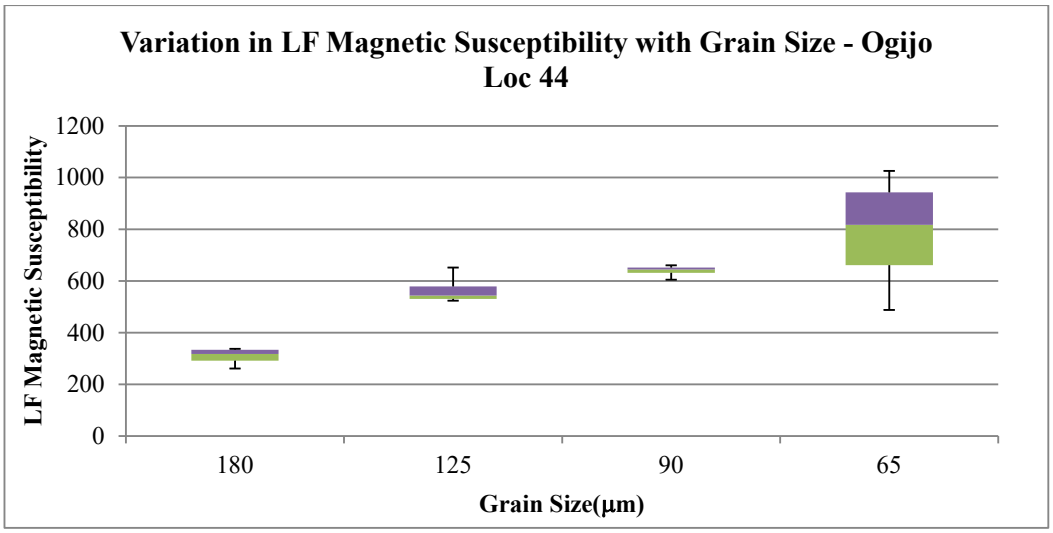
Variation in LF Magnetic Susceptibility with Grain Size - Ogijo Loc 44
LF Magnetic Susceptibility
1200
1000
800
600
400
200
0
180
125
90
65
Grain Size(µm)

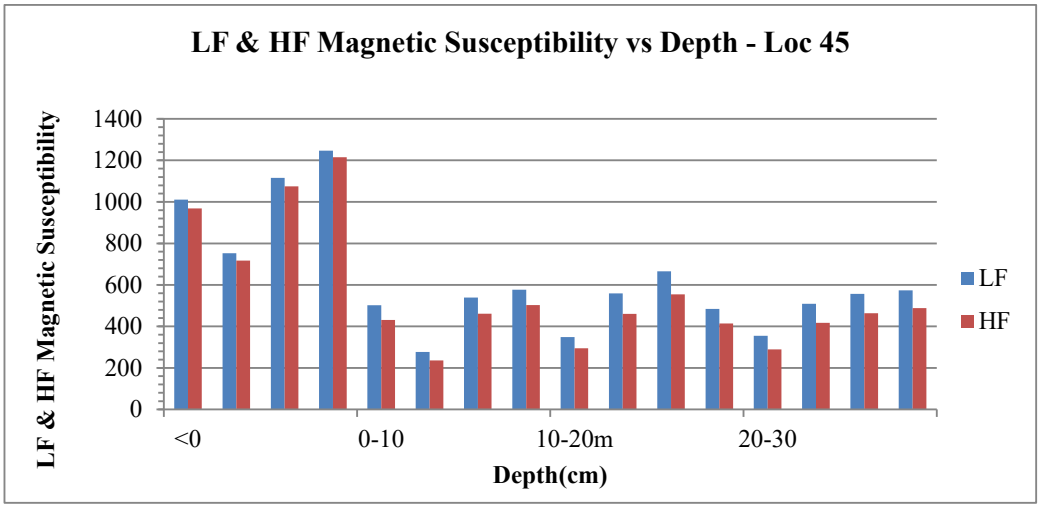
LF & HF Magnetic Susceptibility vs Depth - Loc 45
LF & HF Magnetic Susceptibility
1400
1200
1000
800
600
400
200
0
<0
0-10
10-20m
20-30
Depth(cm)
LF
HF

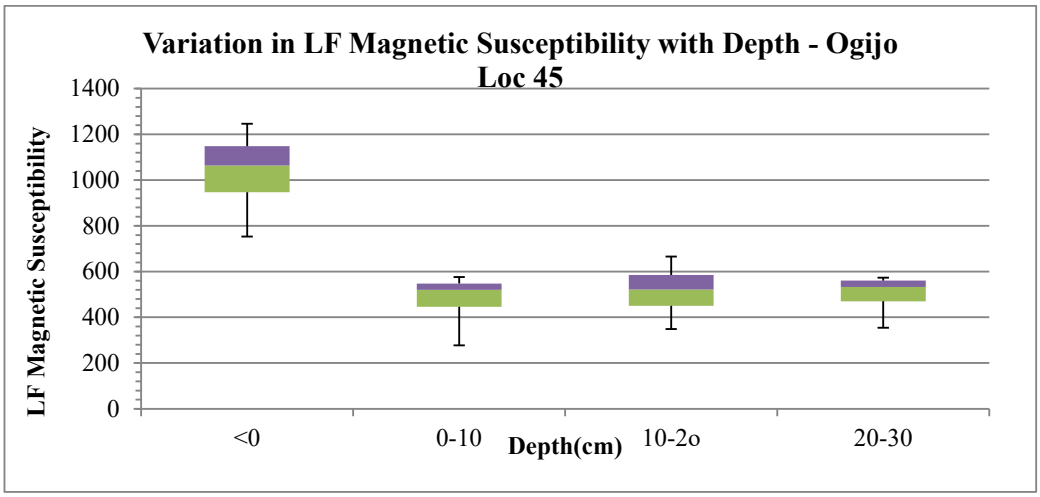
Variation in LF Magnetic Susceptibility with Depth - Ogijo Loc 45
LF Magnetic Susceptibility
1400
1200
1000
800
600
400
200
0
<0
0-10
Depth(cm)
10-2o
20-30

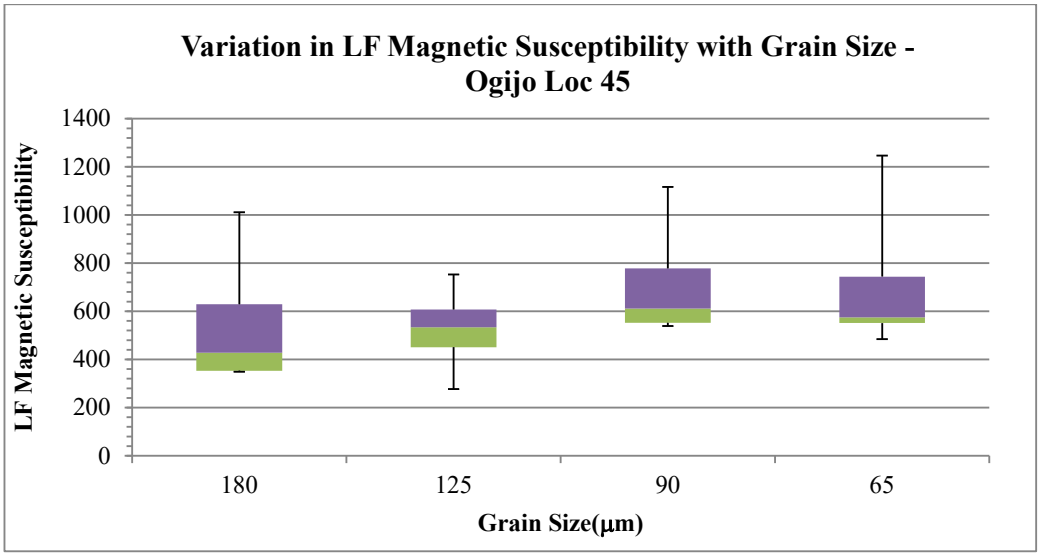
Variation in LF Magnetic Susceptibility with Grain Size - Ogijo Loc 45
LF Magnetic Susceptibility
1400
1200
1000
800
600
400
200
0
180
125
90
65
Grain Size(µm)

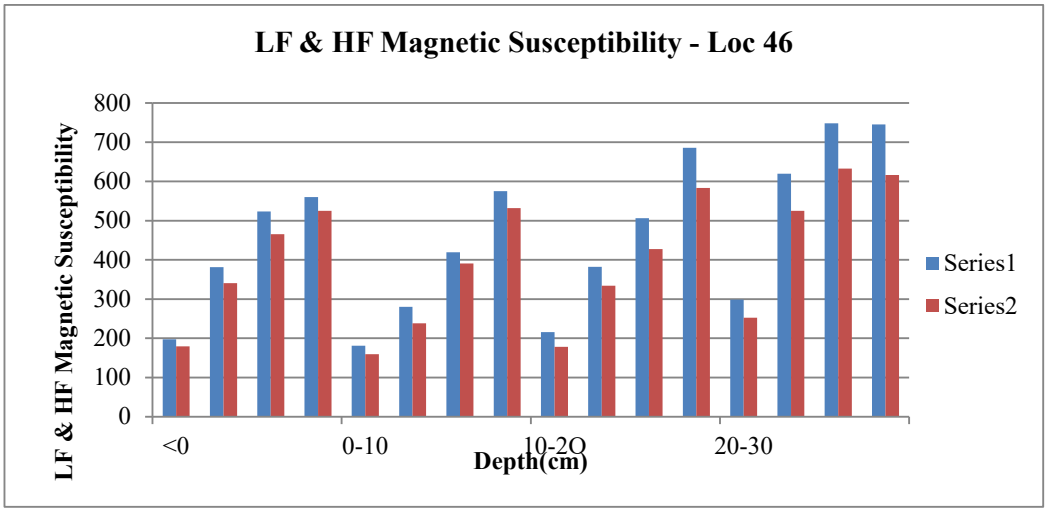
LF & HF Magnetic Susceptibility - Loc 46
LF & HF Magnetic Susceptibility
800
700
600
500
400
300
200
100
0
<0
0-10
10-20
20-30
Depth(cm)
Series1
Series2

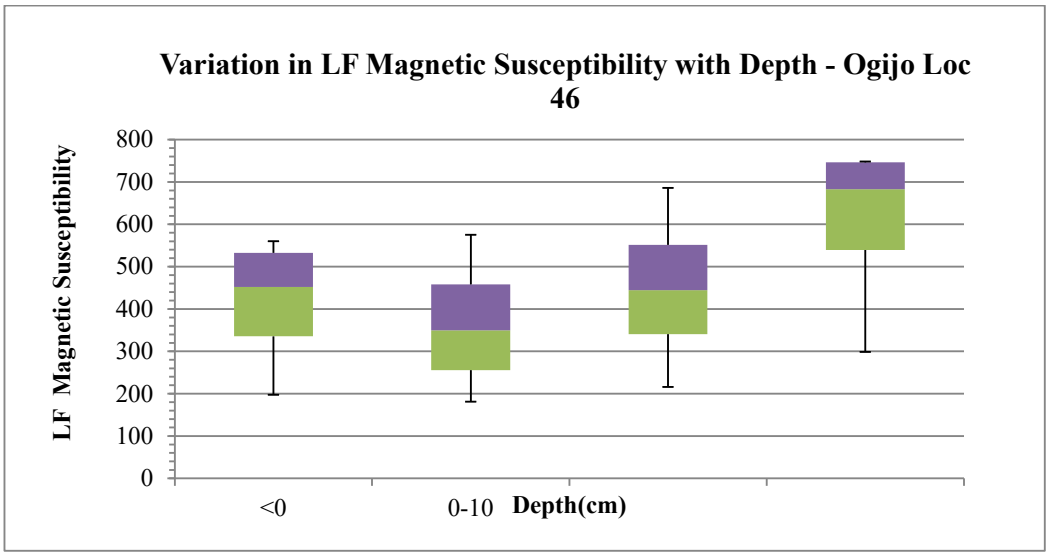
Variation in LF Magnetic Susceptibility with Depth - Ogijo Loc 46
LF Magnetic Susceptibility
800
700
600
500
400
300
200
100
0
<0
0-10
Depth(cm)

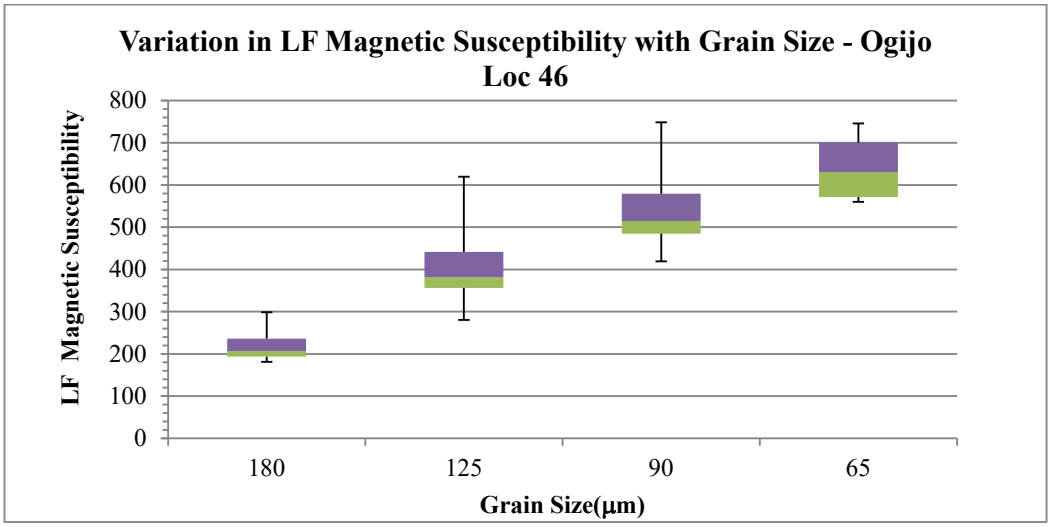
Variation in LF Magnetic Susceptibility with Grain Size - Ogijo Loc 46
LF Magnetic Susceptibility
800
700
600
500
400
300
200
100
0
180
125
90
65
Grain Size(μm)

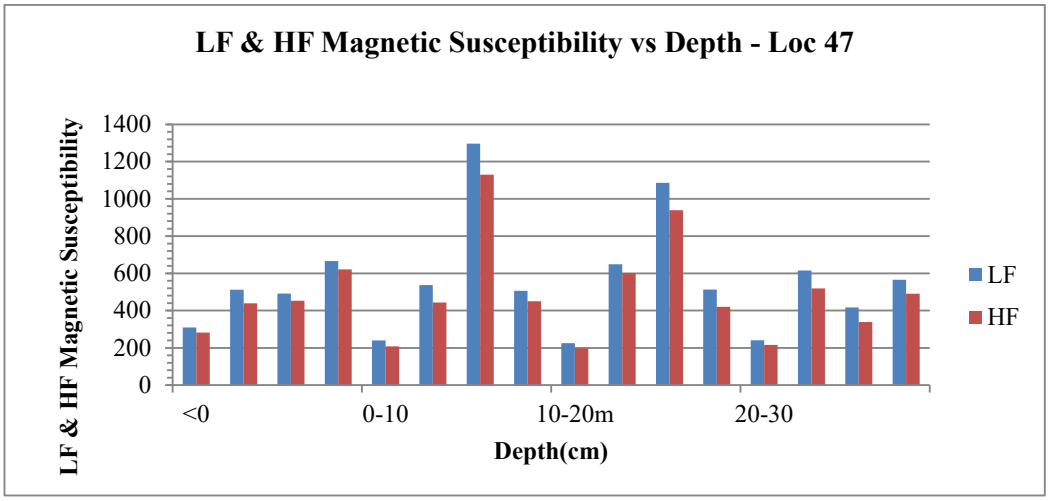
LF & HF Magnetic Susceptibility vs Depth - Loc 47
LF & HF Magnetic Susceptibility
1400
1200
1000
800
600
400
200
0
<0
0-10
10-20m
20-30
Depth(cm)
LF
HF

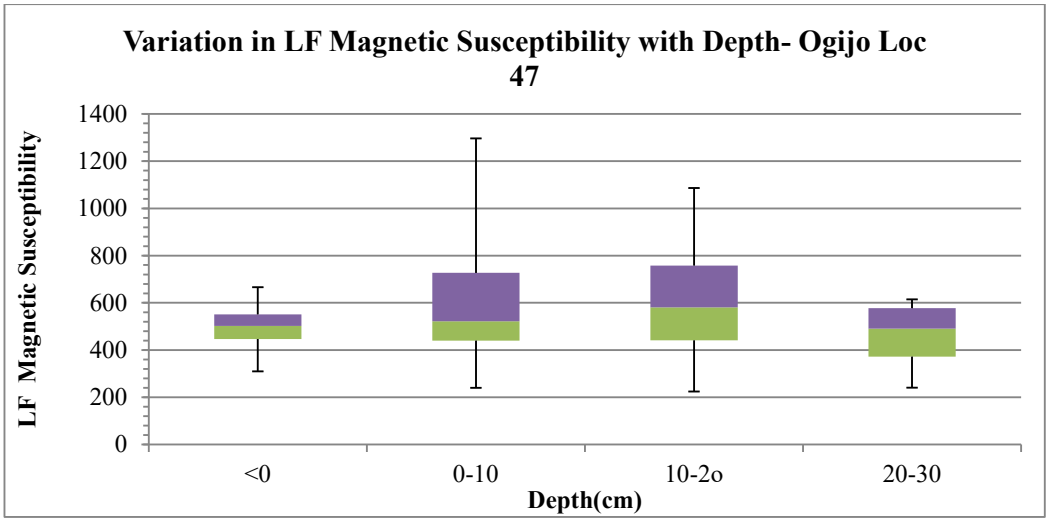
Variation in LF Magnetic Susceptibility with Depth- Ogijo Loc 47
LF Magnetic Susceptibility
1400
1200
1000
800
600
400
200
0
<0
0-10
10-2o
20-30
Depth(cm)

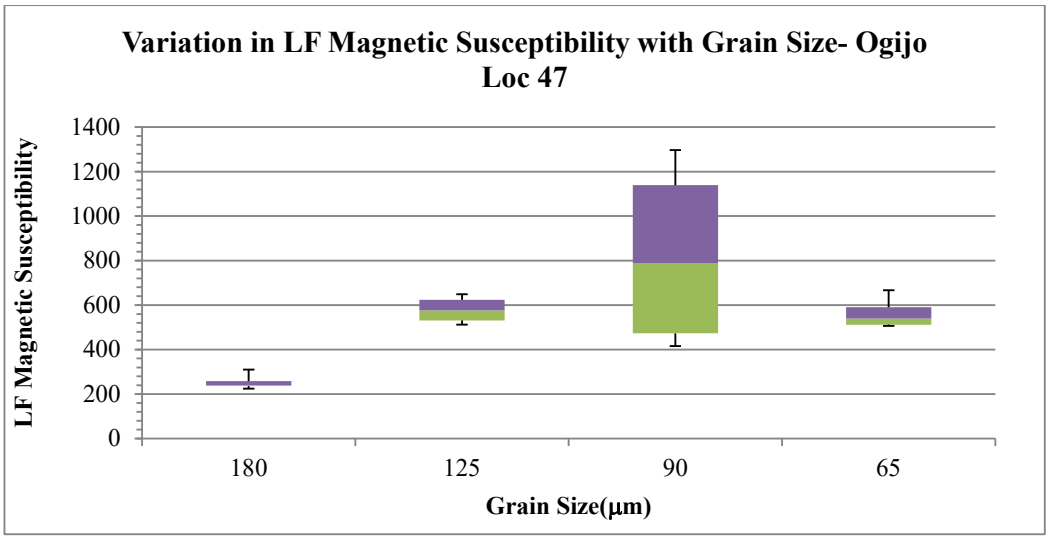
Variation in LF Magnetic Susceptibility with Grain Size- Ogijo Loc 47
LF Magnetic Susceptibility
1400
1200
1000
800
600
400
200
0
180
125
90
65
Grain Size(µm)

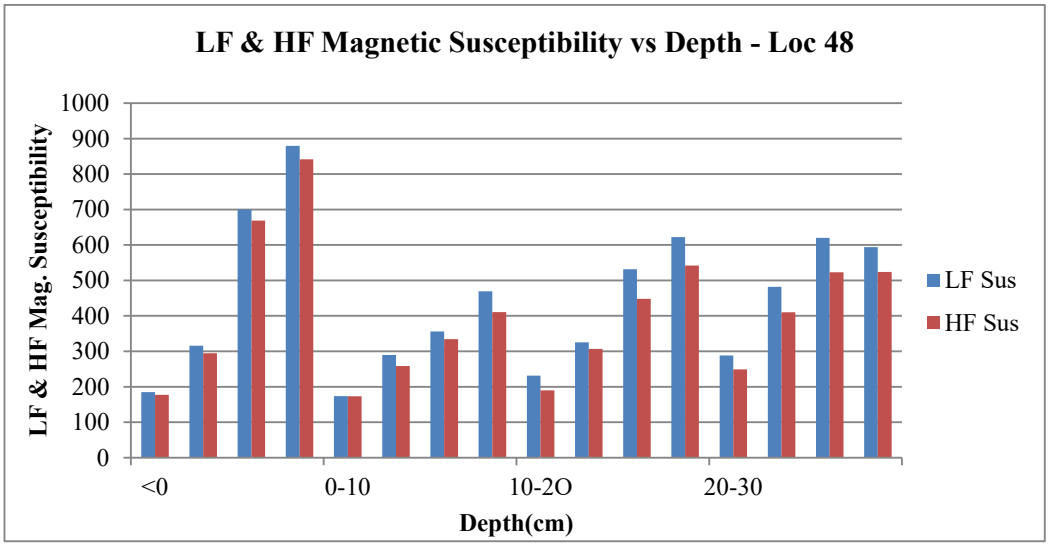
LF & HF Magnetic Susceptibility vs Depth - Loc 48
LF & HF Mag. Susceptibility
1000
900
800
700
600
500
400
300
200
100
0
<0
0-10
10-2O
20-30
Depth(cm)
LF Sus
HF Sus

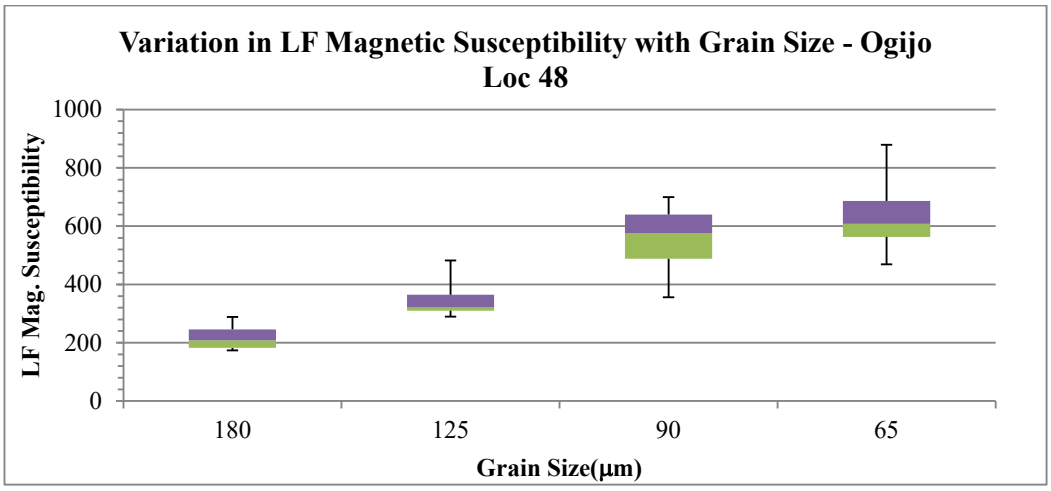
Variation in LF Magnetic Susceptibility with Grain Size - Ogijo Loc 48
LF Mag. Susceptibility
1000
800
600
400
200
0
180
125
90
65
Grain Size(µm)

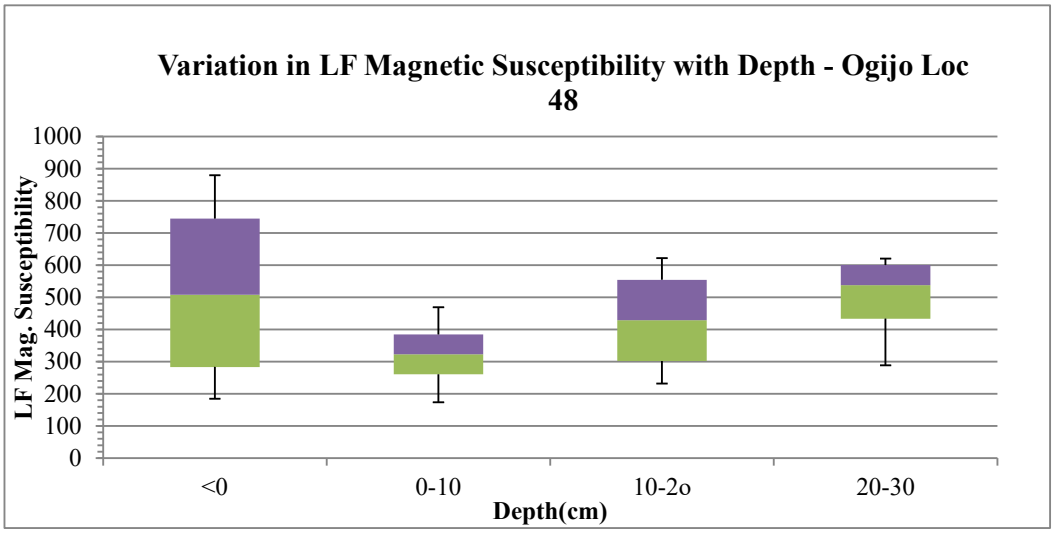
Variation in LF Magnetic Susceptibility with Depth - Ogijo Loc 48
LF Mag. Susceptibility
1000
900
800
700
600
500
400
300
200
100
0
<0
0-10
10-2o
20-30
Depth(cm)

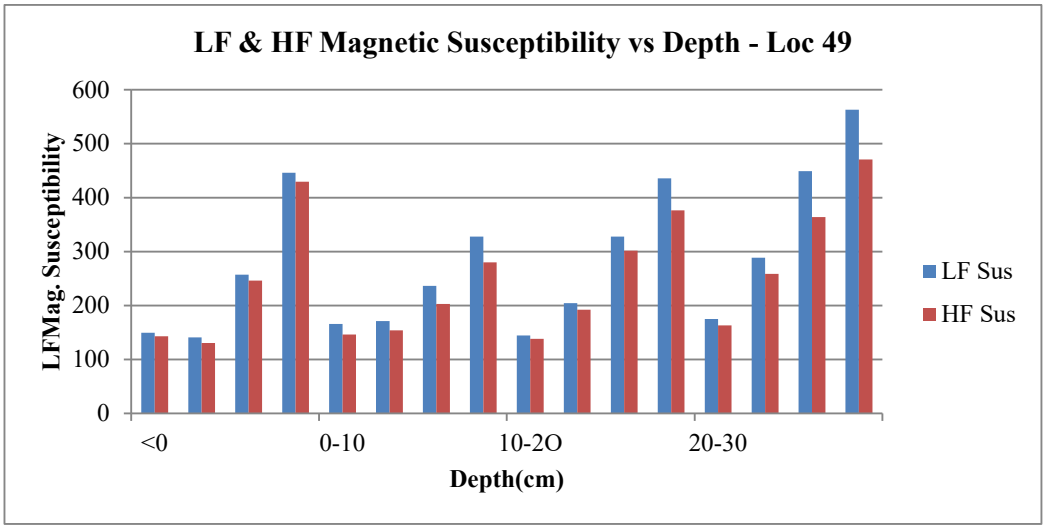
LF & HF Magnetic Susceptibility vs Depth - Loc 49
LFMag. Susceptibility
600
500
400
300
200
100
0
<0
0-10
10-2O
20-30
Depth(cm)
LF Sus
HF Sus

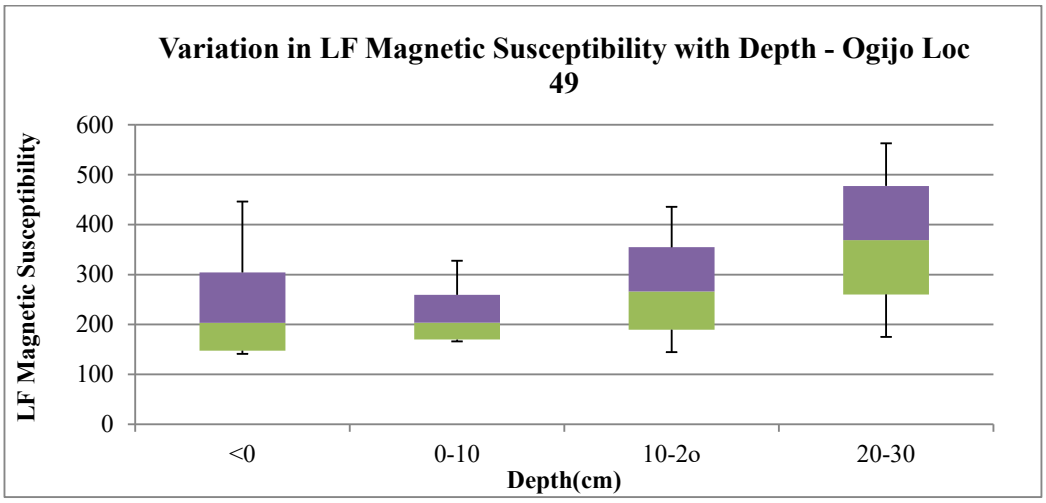
Variation in LF Magnetic Susceptibility with Depth - Ogijo Loc 49
LF Magnetic Susceptibility
600
500
400
300
200
100
0
<0
0-10
10-2o
20-30
Depth(cm)

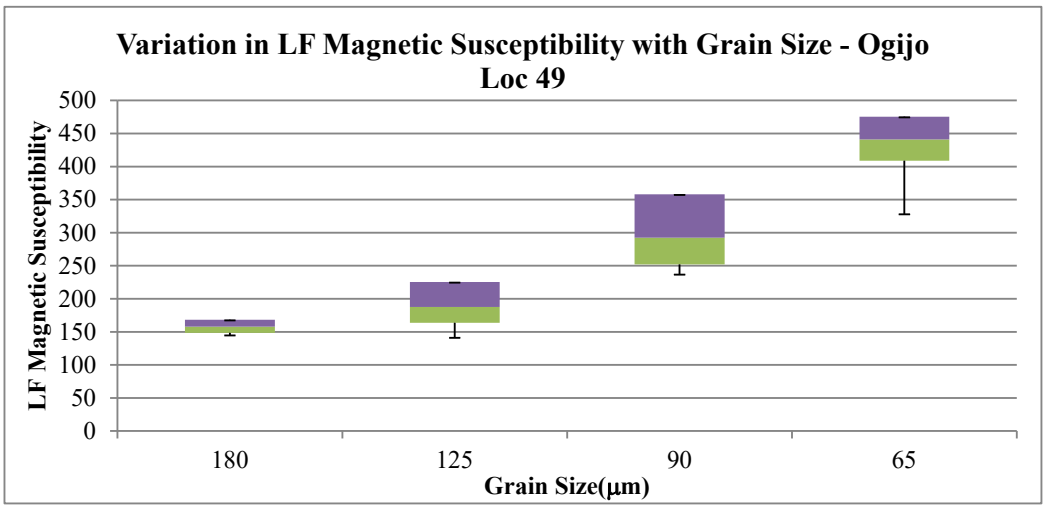
Variation in LF Magnetic Susceptibility with Grain Size - Ogijo Loc 49
LF Magnetic Susceptibility
500
450
400
350
300
250
200
150
100
50
0
180
125
90
65
Grain Size(µm)

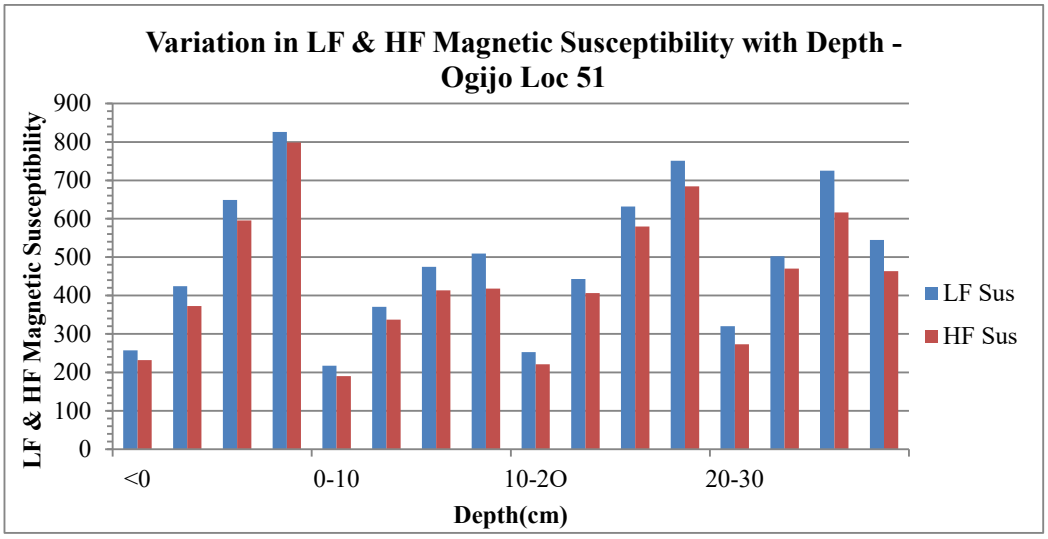
Variation in LF & HF Magnetic Susceptibility with Depth - Ogijo Loc 51
LF & HF Magnetic Susceptibility
900
800
700
600
500
400
300
200
100
0
<0
0-10
10-2O
20-30
Depth(cm)
LF Sus
HF Sus

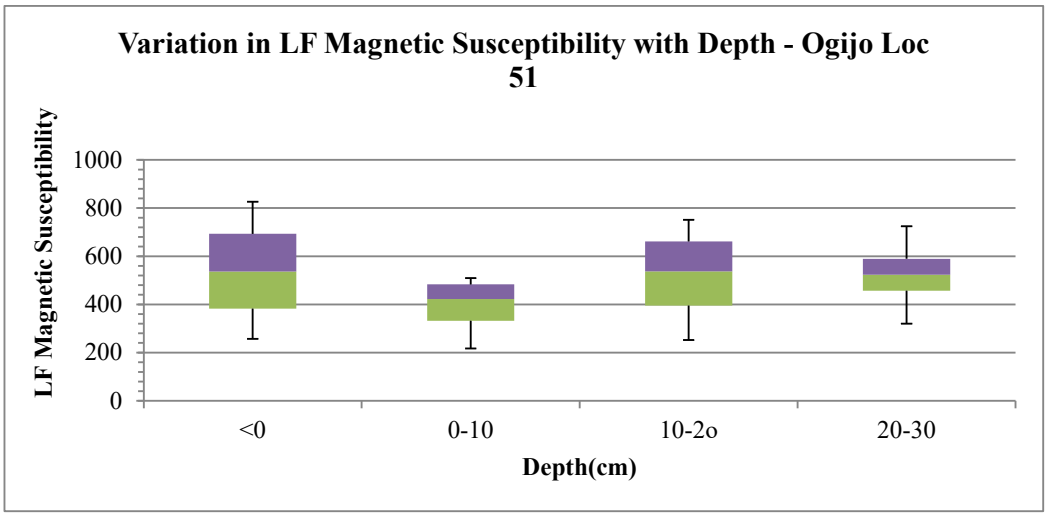
Variation in LF Magnetic Susceptibility with Depth - Ogijo Loc 51
LF Magnetic Susceptibility
1000
800
600
400
200
0
<0
0-10
10-2o
20-30
Depth(cm)

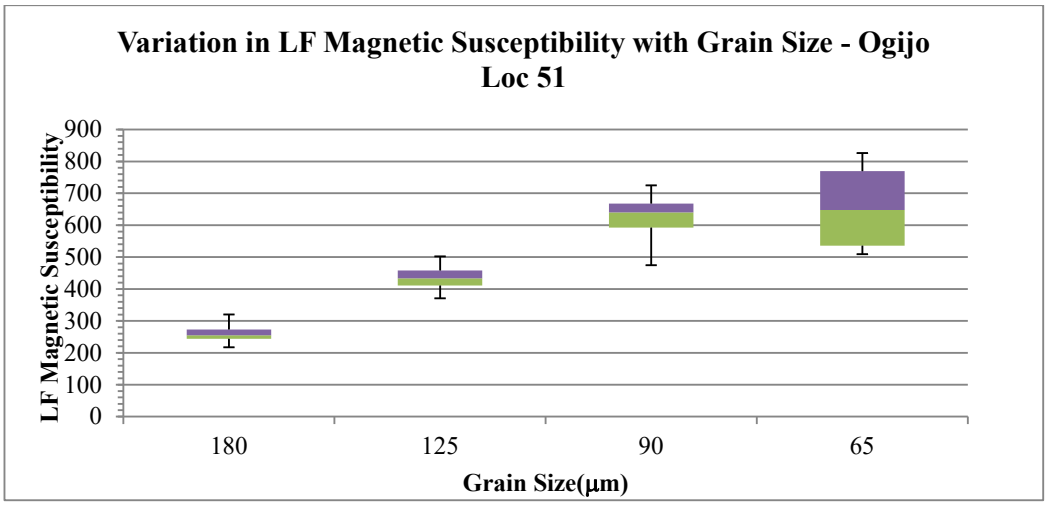
Variation in LF Magnetic Susceptibility with Grain Size - Ogijo Loc 51
LF Magnetic Susceptibility
900
800
700
600
500
400
300
200
100
0
180
125
90
65
Grain Size(µm)

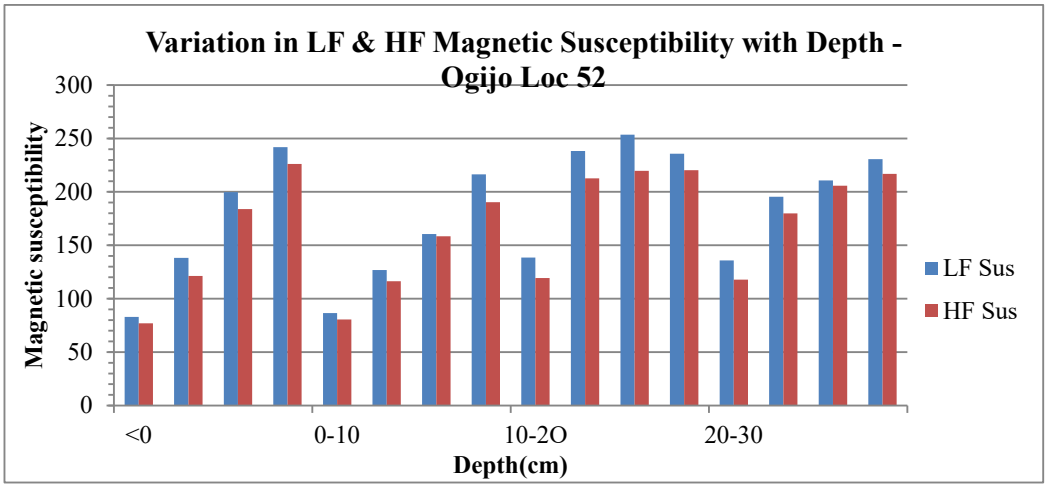
Variation in LF & HF Magnetic Susceptibility with Depth - Ogijo Loc 52
Magnetic susceptibility
300
250
200
150
100
50
0
<0
0-10
10-2O
20-30
Depth(cm)
LF Sus
HF Sus

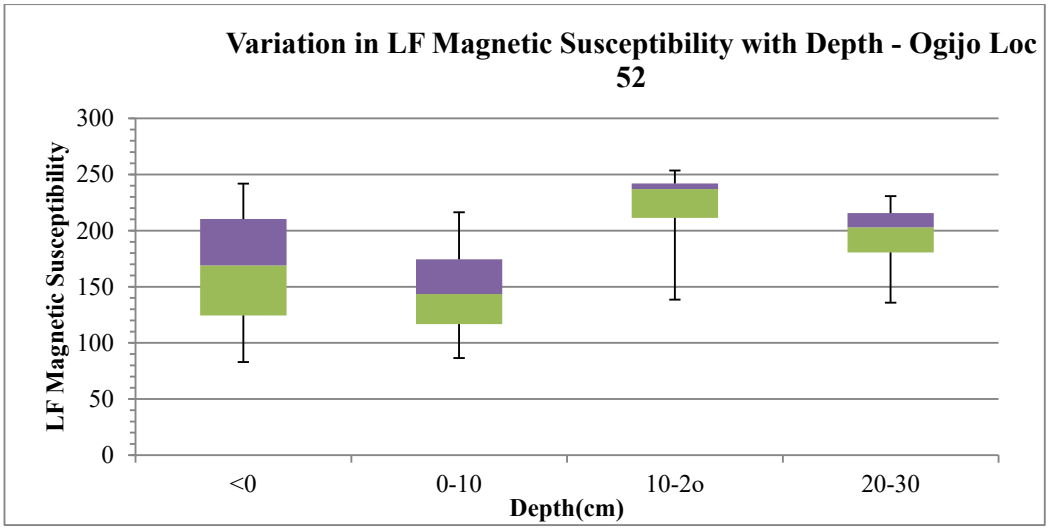
Variation in LF Magnetic Susceptibility with Depth - Ogijo Loc 52
LF Magnetic Susceptibility
300
250
200
150
100
50
0
<0
0-10
10-2o
20-30
Depth(cm)

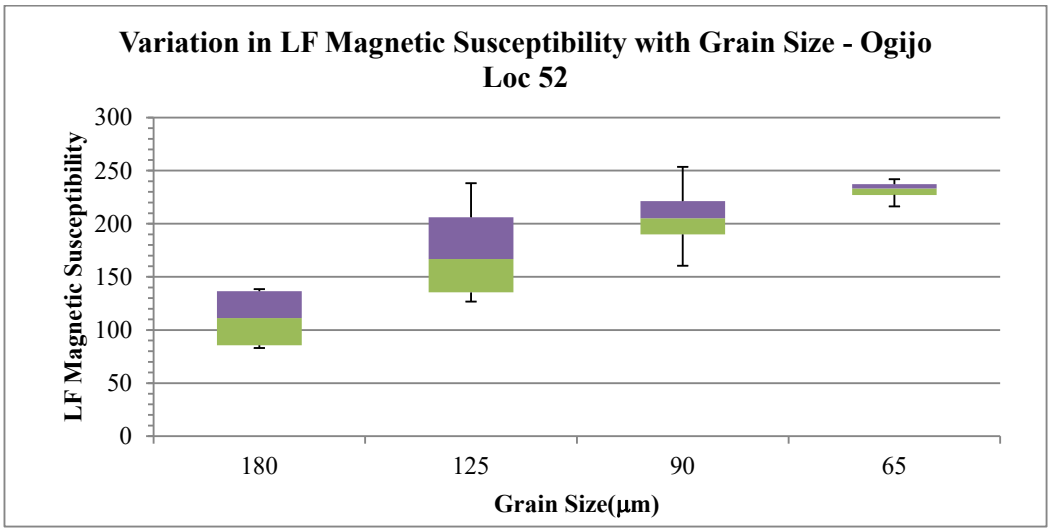
Variation in LF Magnetic Susceptibility with Grain Size - Ogijo Loc 52
LF Magnetic Susceptibility
300
250
200
150
100
50
0
180
125
90
65
Grain Size(µm)

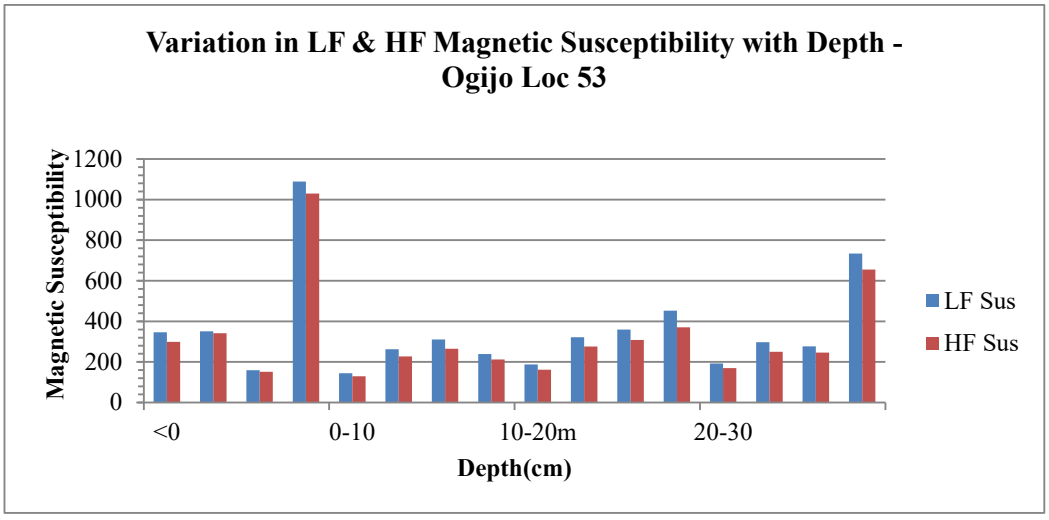
Variation in LF & HF Magnetic Susceptibility with Depth - Ogijo Loc 53
Magnetic Susceptibility
1200
1000
800
600
400
200
0
<0
0-10
10-20m
20-30
Depth(cm)
LF Sus
HF Sus

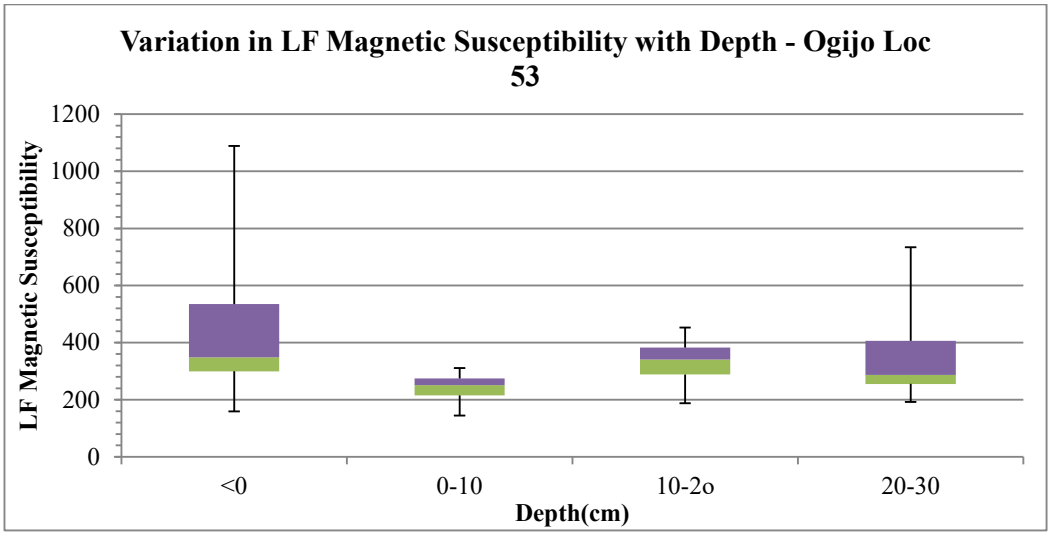
Variation in LF Magnetic Susceptibility with Depth - Ogijo Loc 53
LF Magnetic Susceptibility
1200
1000
800
600
400
200
0
<0
0-10
10-2o
20-30
Depth(cm)

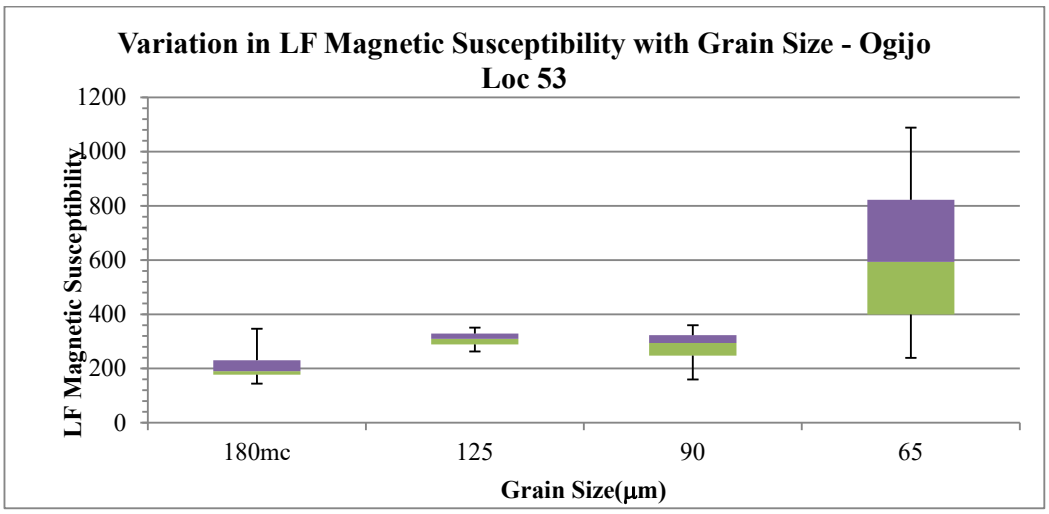
Variation in LF Magnetic Susceptibility with Grain Size - Ogijo Loc 53
LF Magnetic Susceptibility
1200
1000
800
600
400
200
0
180mc
125
90
65
Grain Size(µm)

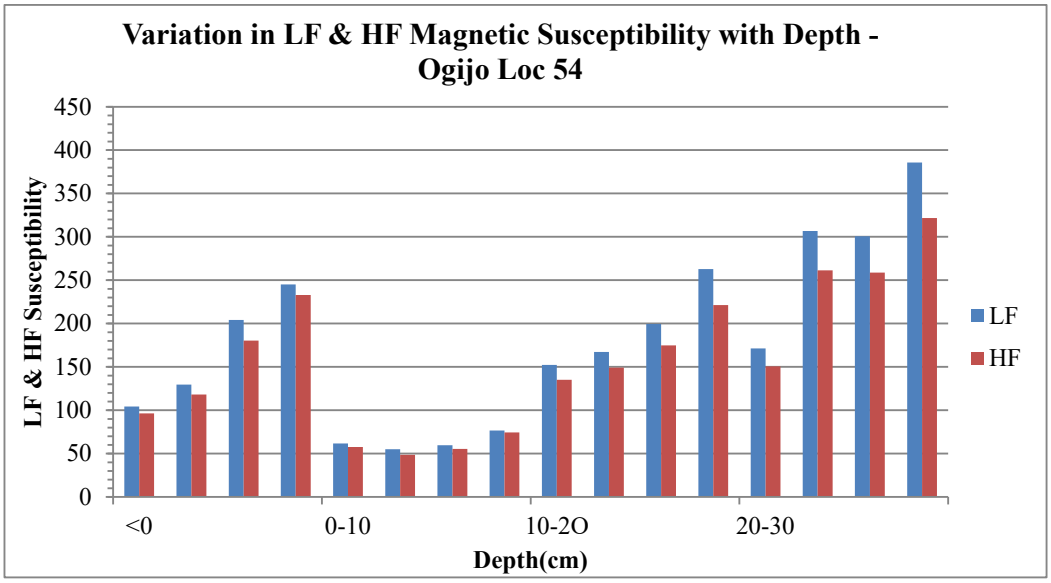
Variation in LF & HF Magnetic Susceptibility with Depth - Ogijo Loc 54
LF & HF Susceptibility
450
400
350
300
250
200
150
100
50
0
<0
0-10
10-2O
20-30
Depth(cm)
LF
HF

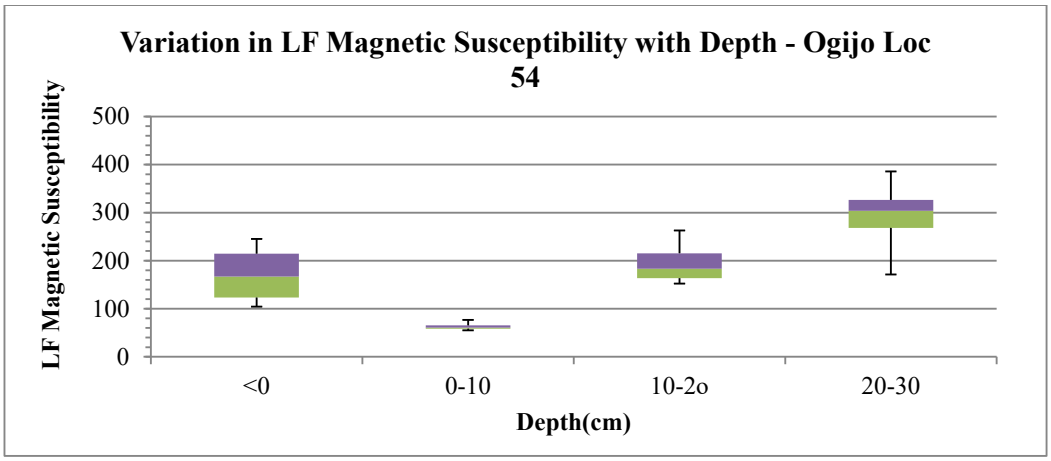
Variation in LF Magnetic Susceptibility with Depth - Ogijo Loc 54
LF Magnetic Susceptibility
500
400
300
200
100
0
<0
0-10
10-2o
20-30
Depth(cm)

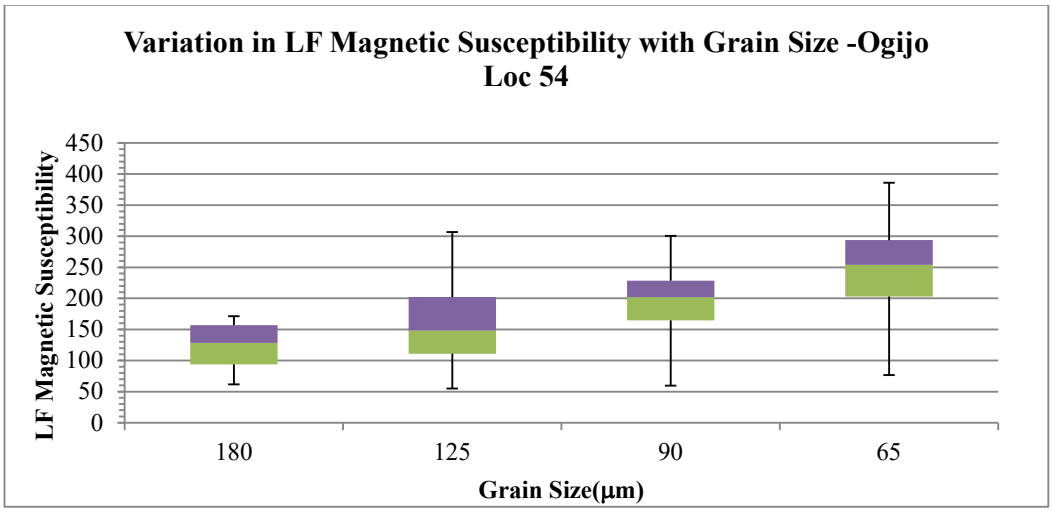
Variation in LF Magnetic Susceptibility with Grain Size -Ogijo Loc 54
LF Magnetic Susceptibility
450
400
350
300
250
200
150
100
50
0
180
125
90
65
Grain Size(µm)

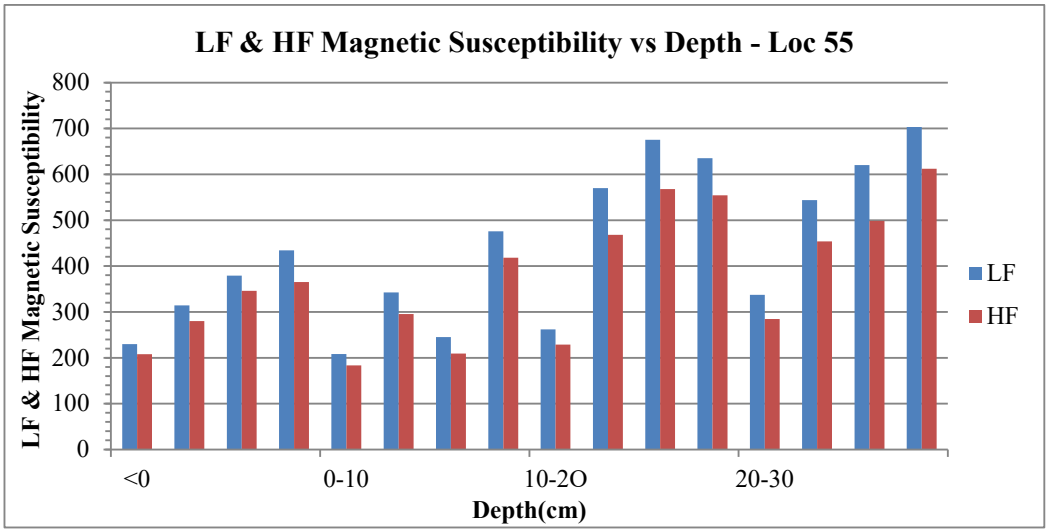
LF & HF Magnetic Susceptibility vs Depth - Loc 55
LF & HF Magnetic Susceptibility
800
700
600
500
400
300
200
100
0
<0
0-10
10-2O
20-30
Depth(cm)
LF
HF

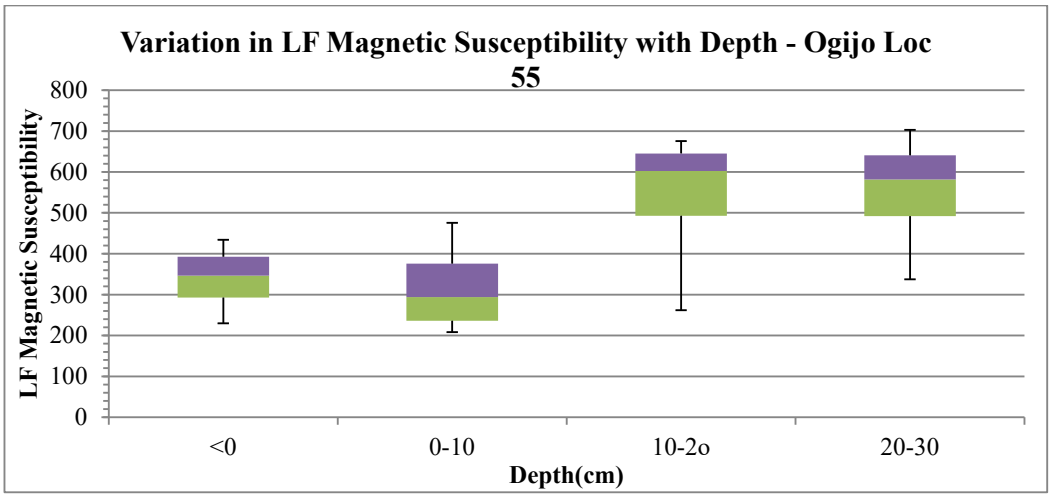
Variation in LF Magnetic Susceptibility with Depth - Ogijo Loc 55
LF Magnetic Susceptibility
800
700
600
500
400
300
200
100
0
<0
0-10
10-2o
20-30
Depth(cm)

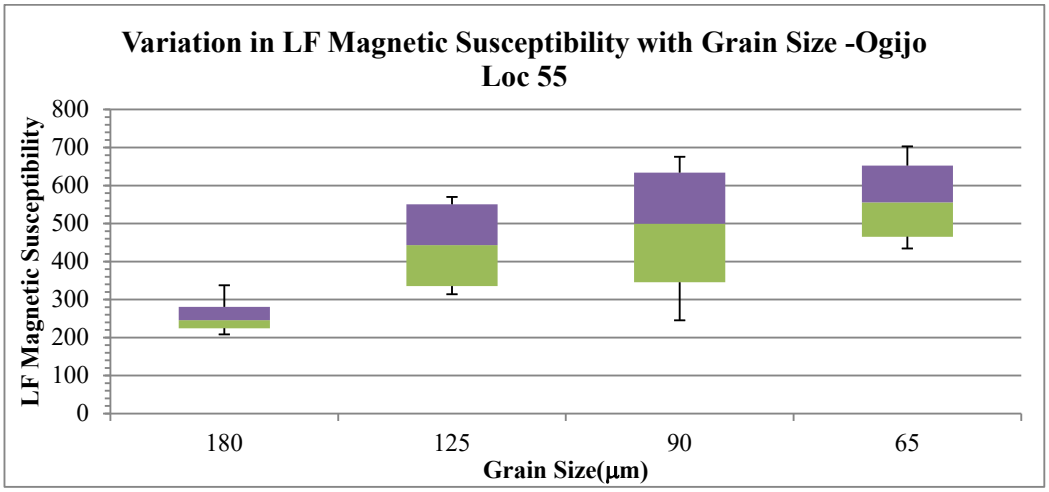
Variation in LF Magnetic Susceptibility with Grain Size -Ogijo Loc 55
LF Magnetic Susceptibility
800
700
600
500
400
300
200
100
0
180
125
90
65
Grain Size(µm)

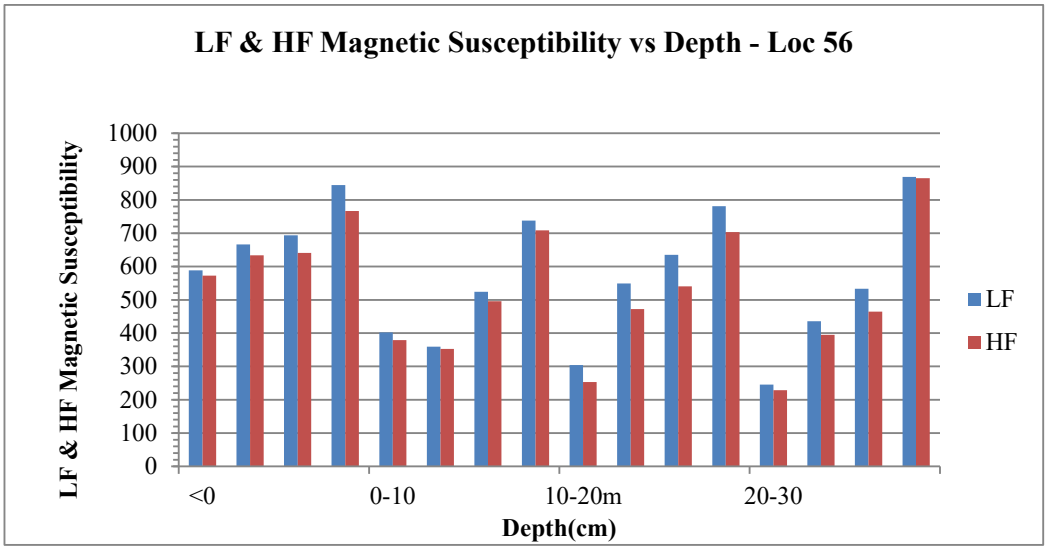
LF & HF Magnetic Susceptibility vs Depth - Loc 56
LF & HF Magnetic Susceptibility
1000
900
800
700
600
500
400
300
200
100
0
<0
0-10
10-20m
20-30
Depth(cm)
LF
HF

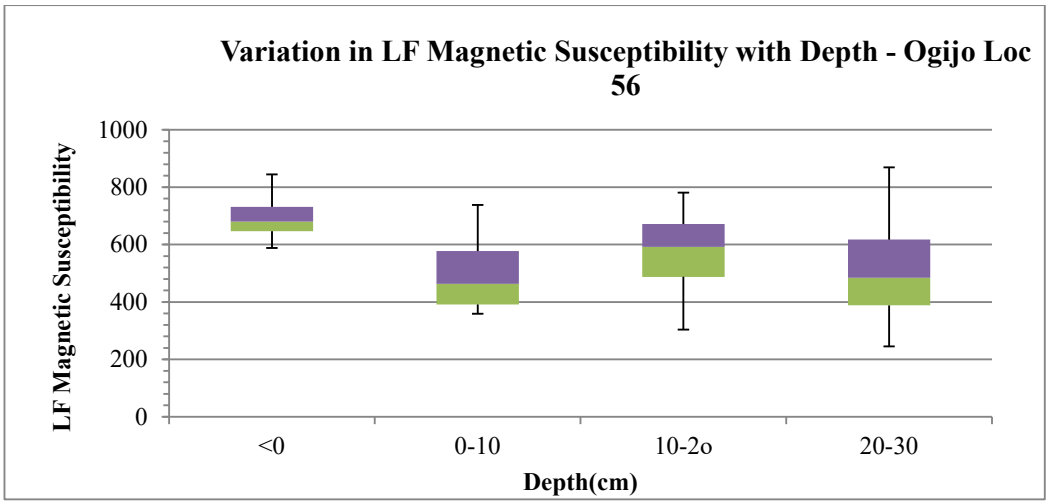
Variation in LF Magnetic Susceptibility with Depth - Ogijo Loc 56
LF Magnetic Susceptibility
1000
800
600
400
200
0
<0
0-10
10-2o
20-30
Depth(cm)

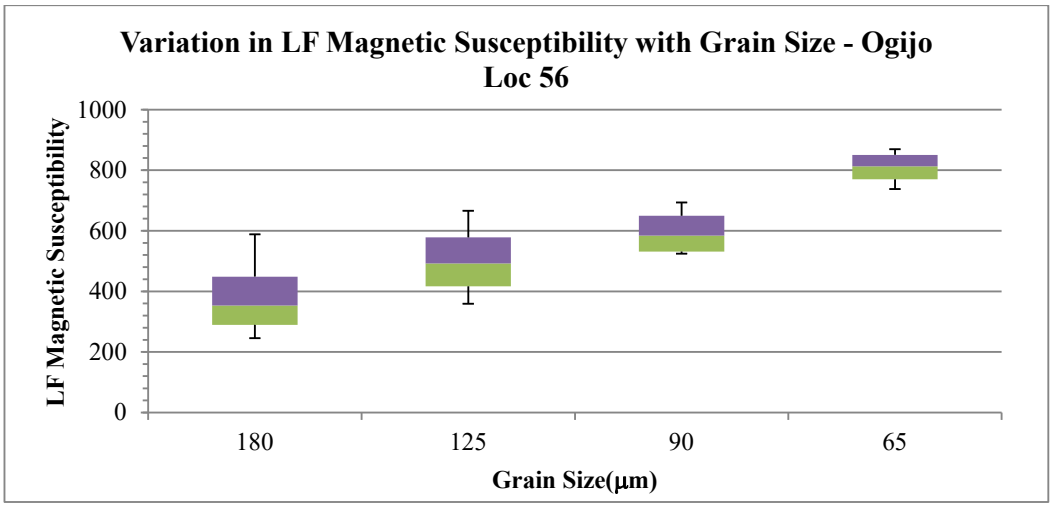
Variation in LF Magnetic Susceptibility with Grain Size - Ogijo Loc 56
LF Magnetic Susceptibility
1000
800
600
400
200
0
180
125
90
65
Grain Size(µm)

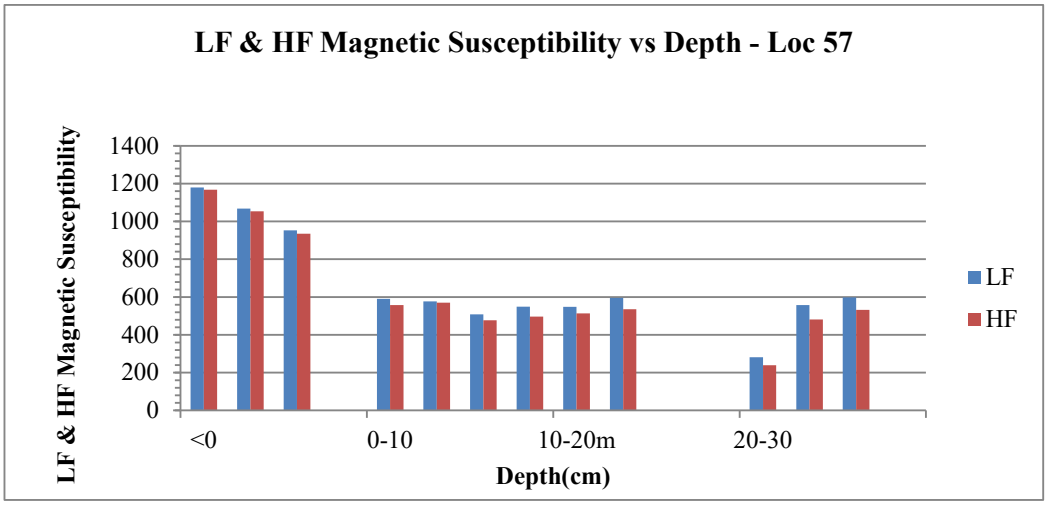
LF & HF Magnetic Susceptibility vs Depth - Loc 57
LF & HF Magnetic Susceptibility
1400
1200
1000
800
600
400
200
0
<0
0-10
10-20m
20-30
Depth(cm)
LF
HF

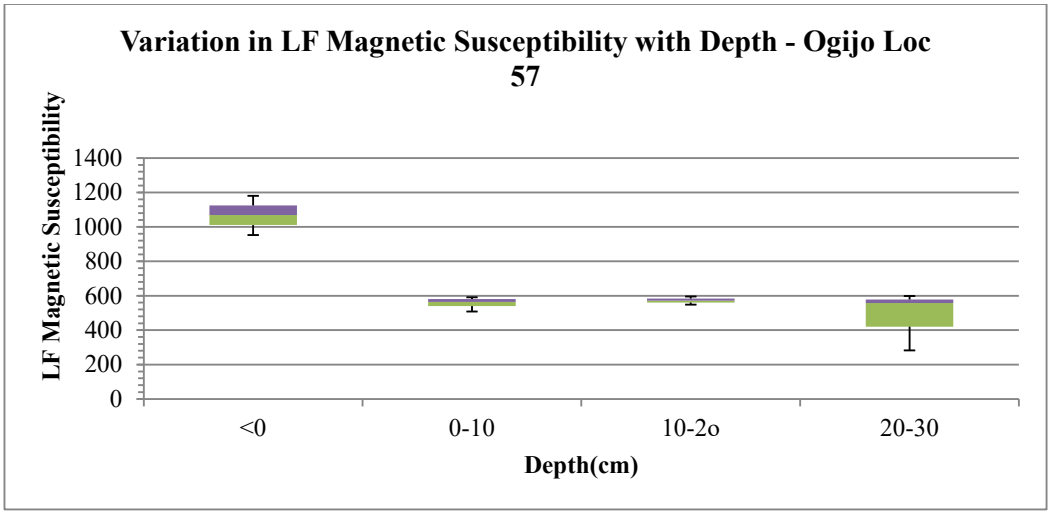
Variation in LF Magnetic Susceptibility with Depth - Ogijo Loc 57
LF Magnetic Susceptibility
1400
1200
1000
800
600
400
200
0
<0
0-10
10-2o
20-30
Depth(cm)

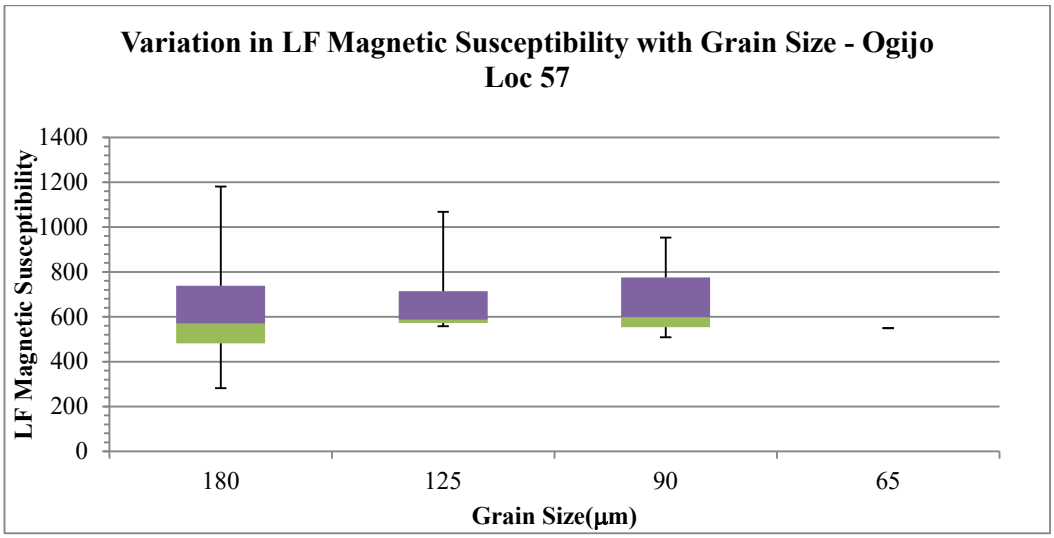
Variation in LF Magnetic Susceptibility with Grain Size - Ogijo Loc 57
LF Magnetic Susceptibility
1400
1200
1000
800
600
400
200
0
180
125
90
65
Grain Size(µm)

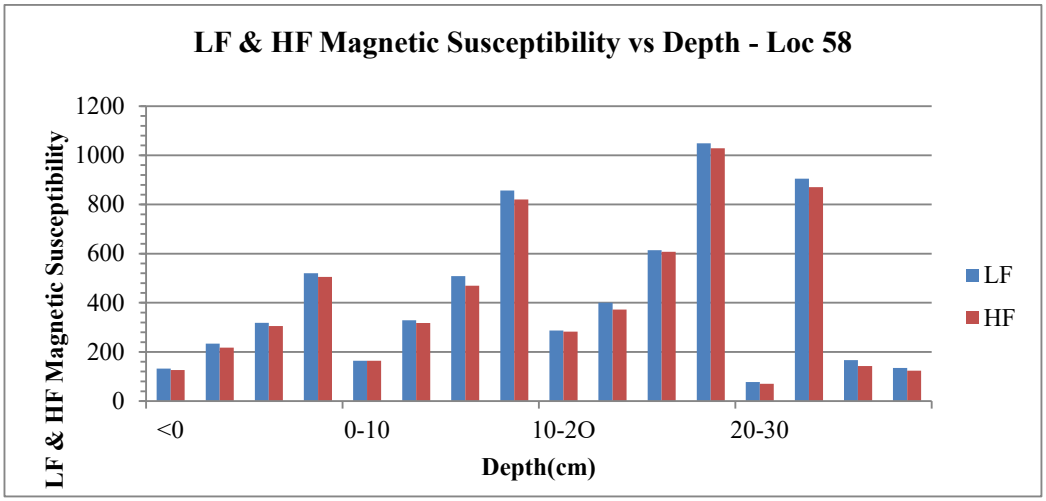
LF & HF Magnetic Susceptibility vs Depth - Loc 58
LF & HF Magnetic Susceptibility
1200
1000
800
600
400
200
0
<0
0-10
10-2O
20-30
Depth(cm)
LF
HF

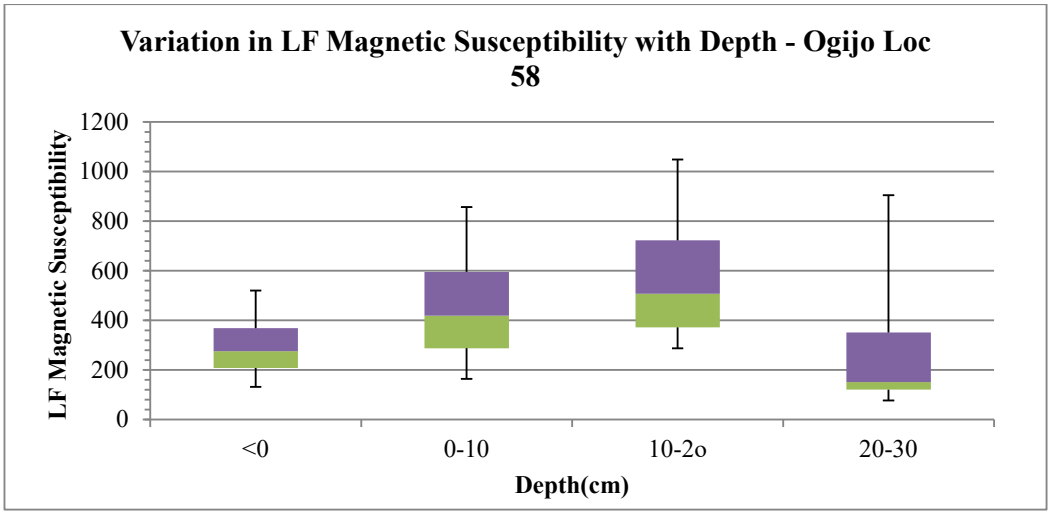
Variation in LF Magnetic Susceptibility with Depth - Ogijo Loc 58
LF Magnetic Susceptibility
1200
1000
800
600
400
200
0
<0
0-10
10-2o
20-30
Depth(cm)

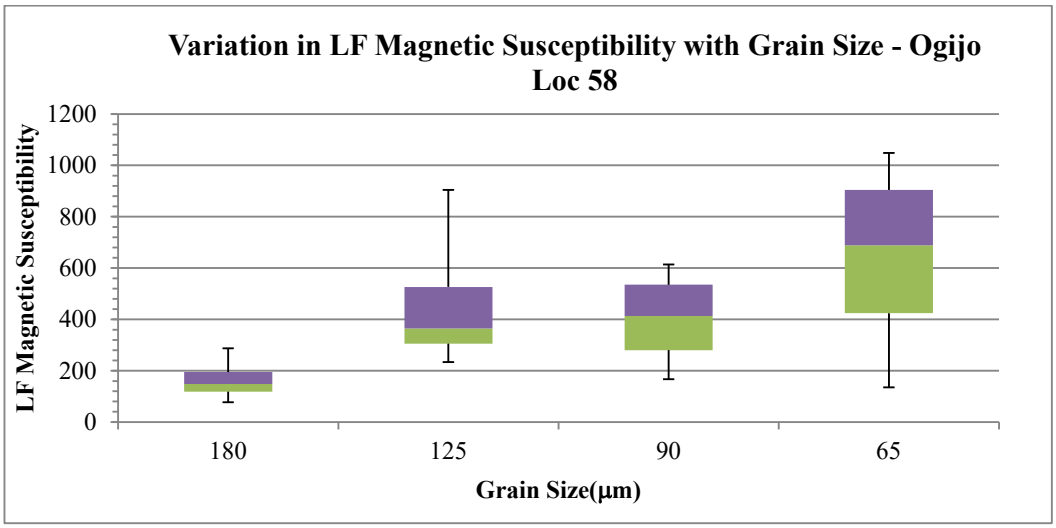
Variation in LF Magnetic Susceptibility with Grain Size - Ogijo Loc 58
LF Magnetic Susceptibility
1200
1000
800
600
400
200
0
180
125
90
65
Grain Size(µm)

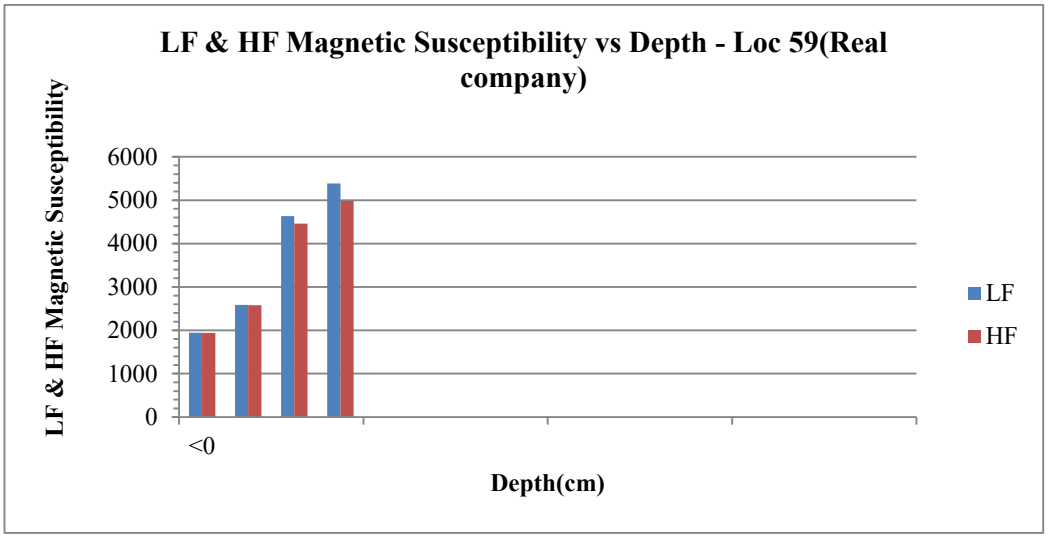
LF & HF Magnetic Susceptibility vs Depth - Loc 59(Real company)
LF & HF Magnetic Susceptibility
6000
5000
4000
3000
2000
1000
0
<0
Depth(cm)
LF
HF

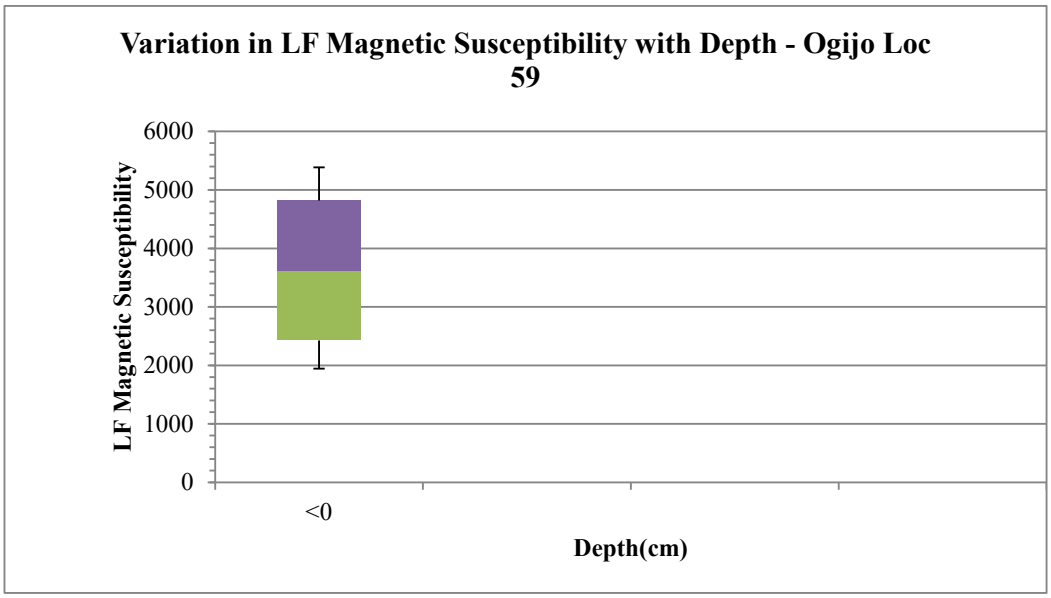
Variation in LF Magnetic Susceptibility with Depth - Ogijo Loc 59
LF Magnetic Susceptibility
6000
5000
4000
3000
2000
1000
0
<0
Depth(cm)

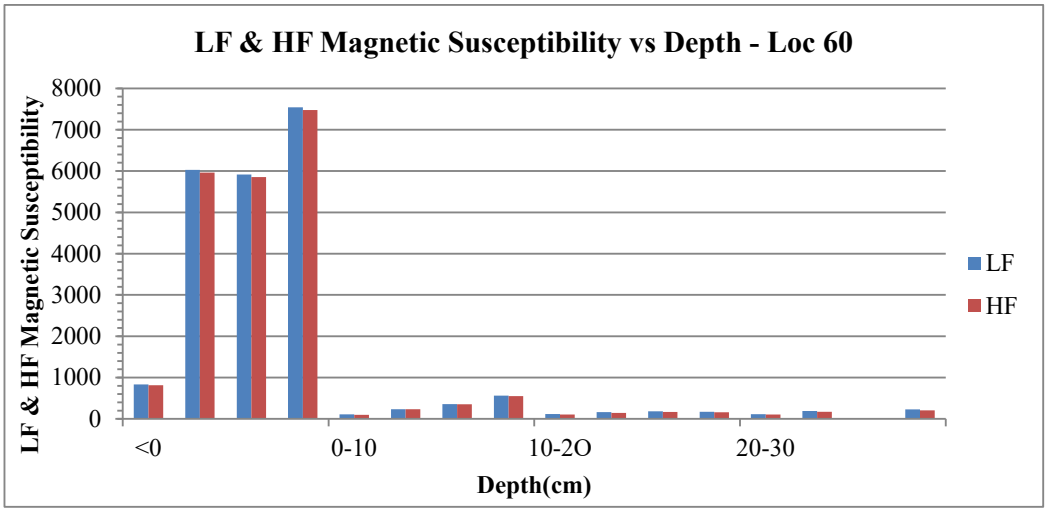
LF & HF Magnetic Susceptibility vs Depth - Loc 60
LF & HF Magnetic Susceptibility
8000
7000
6000
5000
4000
3000
2000
1000
0
<0
0-10
10-2O
20-30
Depth(cm)
LF
HF

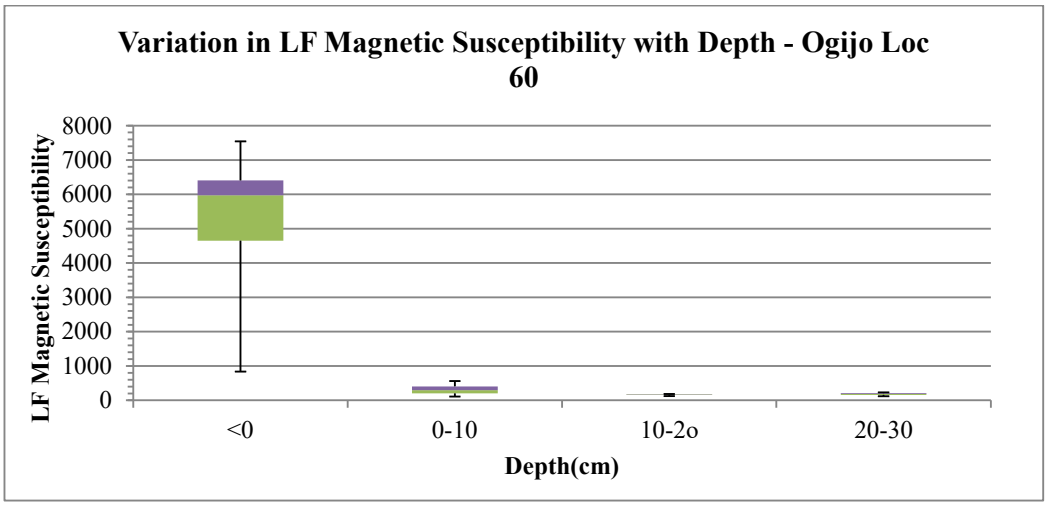
Variation in LF Magnetic Susceptibility with Depth - Ogijo Loc 60
LF Magnetic Susceptibility
8000
7000
6000
5000
4000
3000
2000
1000
0
<0
0-10
10-2o
20-30
Depth(cm)

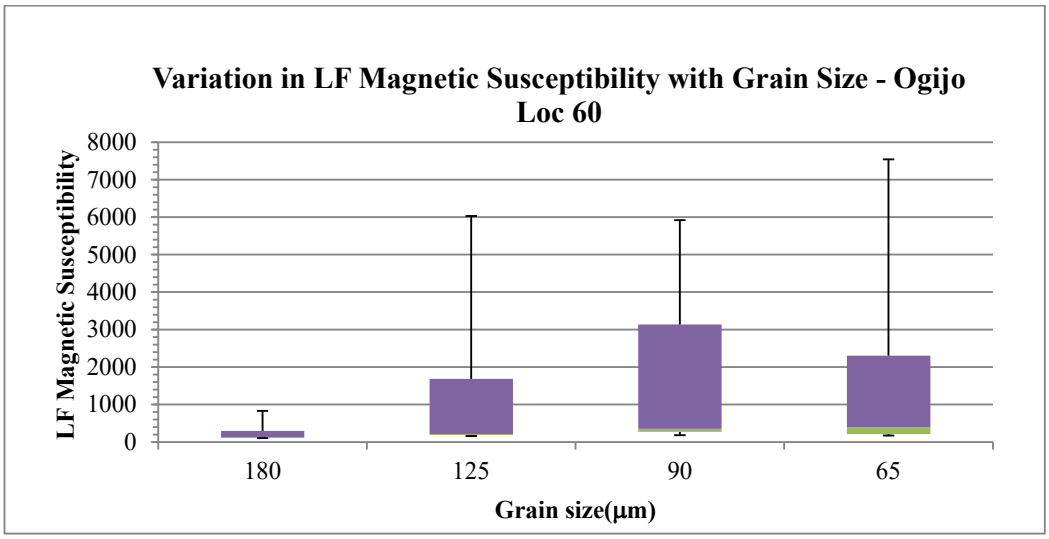
Variation in LF Magnetic Susceptibility with Grain Size - Ogijo Loc 60
LF Magnetic Susceptibility
8000
7000
6000
5000
4000
3000
2000
1000
0
180
125
90
65
Grain size(µm)

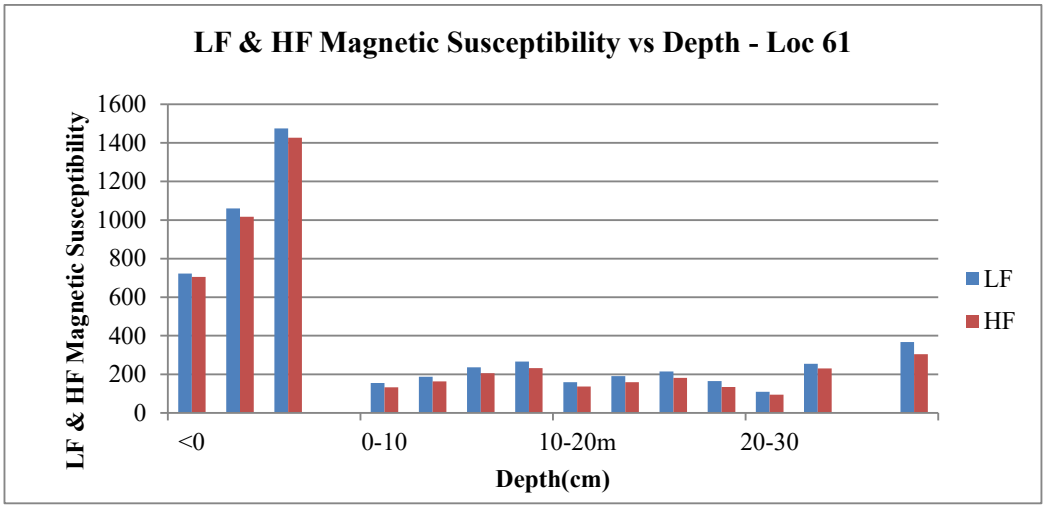
LF & HF Magnetic Susceptibility vs Depth - Loc 61
LF & HF Magnetic Susceptibility
1600
1400
1200
1000
800
600
400
200
0
<0
0-10
10-20m
20-30
Depth(cm)
LF
HF

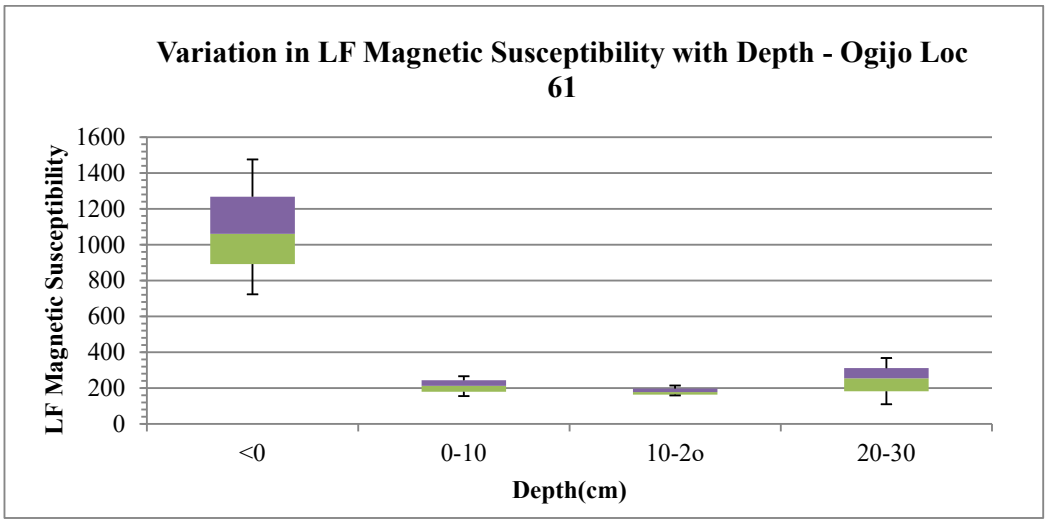
Variation in LF Magnetic Susceptibility with Depth - Ogijo Loc 61
LF Magnetic Susceptibility
1600
1400
1200
1000
800
600
400
200
0
<0
0-10
10-2o
20-30
Depth(cm)

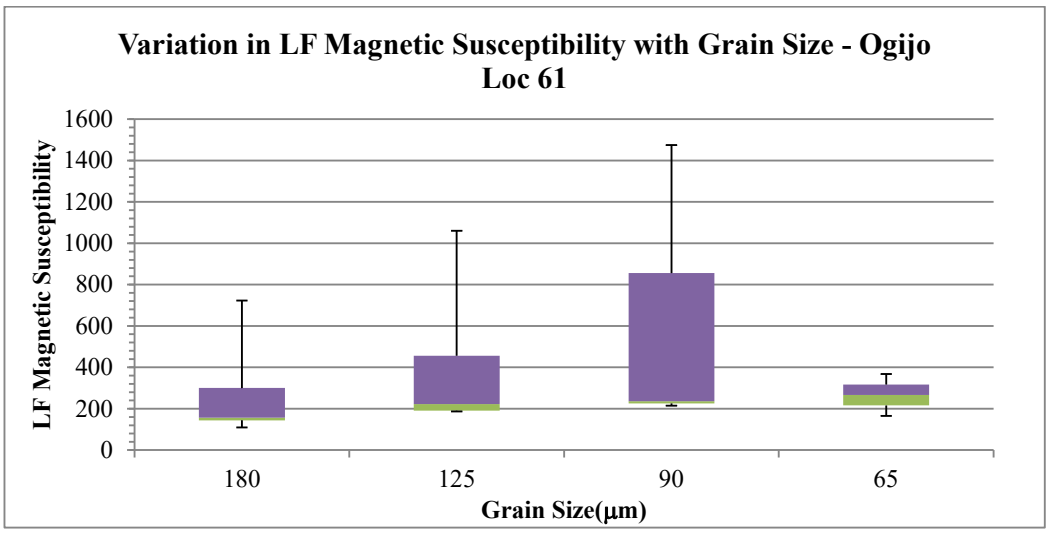
Variation in LF Magnetic Susceptibility with Grain Size - Ogijo Loc 61
LF Magnetic Susceptibility
1600
1400
1200
1000
800
600
400
200
0
180
125
90
65
Grain Size(µm)

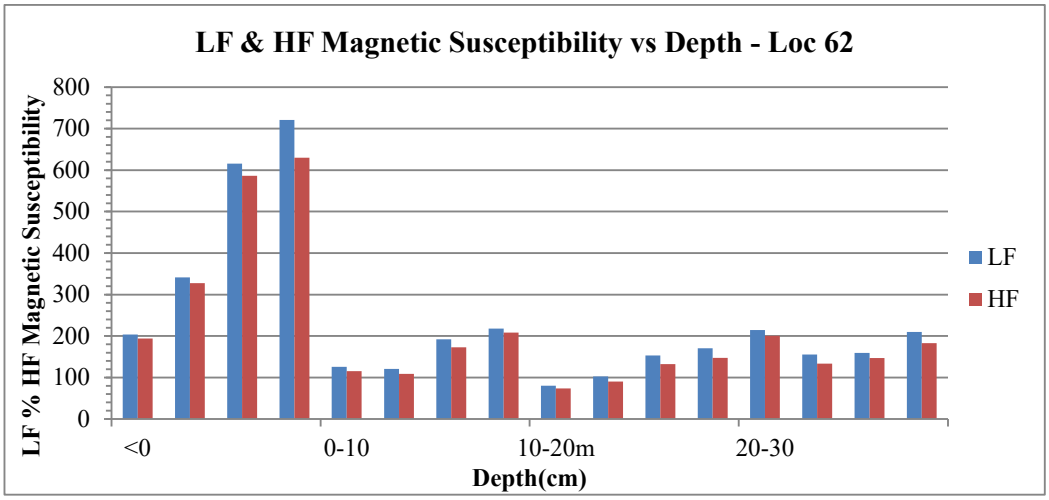
LF & HF Magnetic Susceptibility vs Depth - Loc 62
LF % HF Magnetic Susceptibility
800
700
600
500
400
300
200
100
0
<0
0-10
10-20m
20-30
Depth(cm)
LF
HF

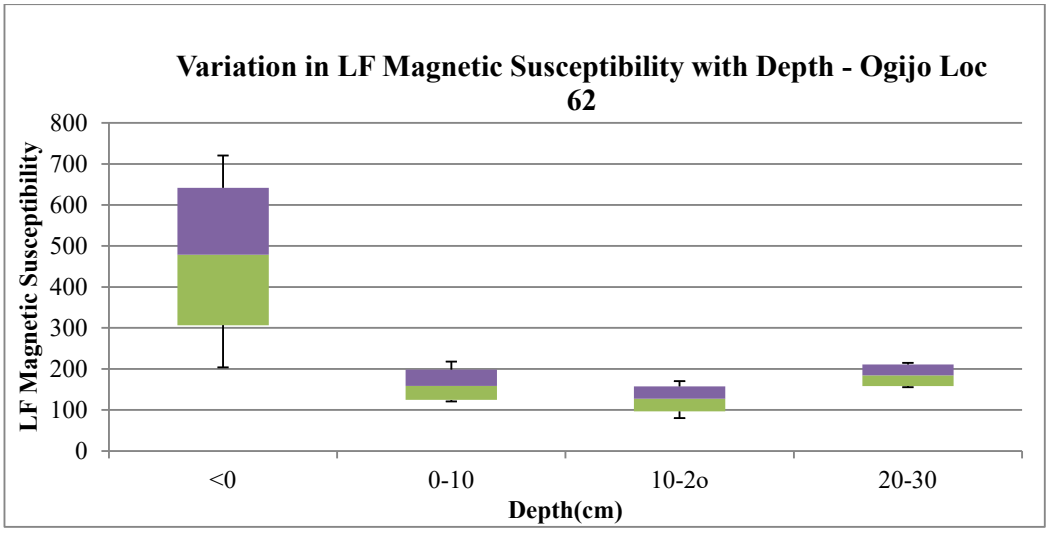
Variation in LF Magnetic Susceptibility with Depth - Ogijo Loc 62
LF Magnetic Susceptibility
800
700
600
500
400
300
200
100
0
<0
0-10
10-2o
20-30
Depth(cm)

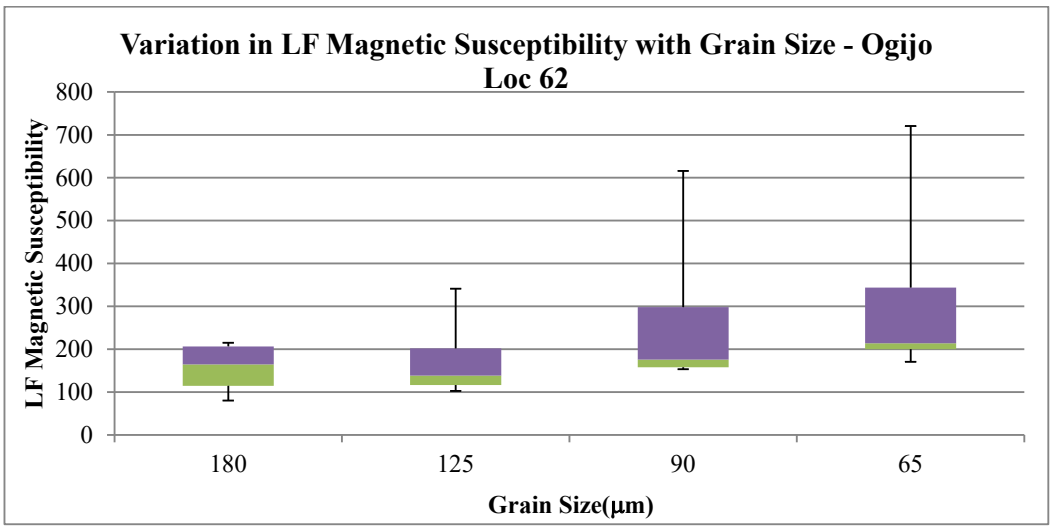
Variation in LF Magnetic Susceptibility with Grain Size - Ogijo Loc 62
LF Magnetic Susceptibility
800
700
600
500
400
300
200
100
0
180
125
90
65
Grain Size(µm)

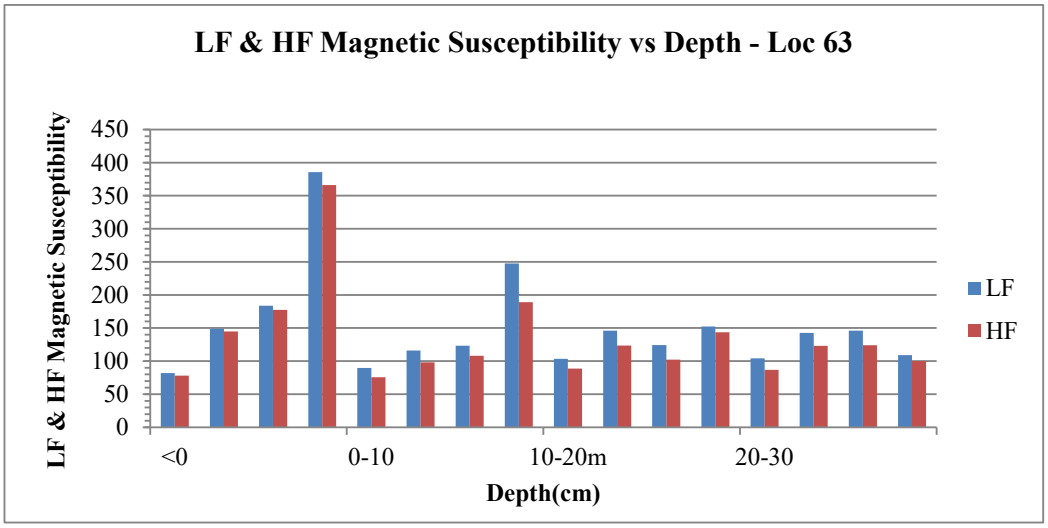
LF & HF Magnetic Susceptibility vs Depth - Loc 63
LF & HF Magnetic Susceptibility
450
400
350
300
250
200
150
100
50
0
<0
0-10
10-20m
20-30
Depth(cm)
LF
HF

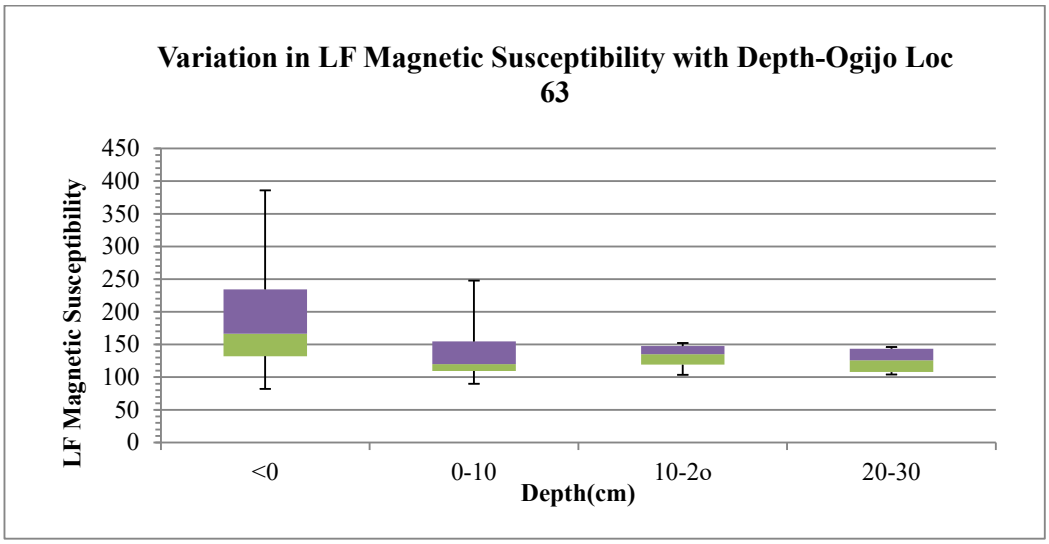
Variation in LF Magnetic Susceptibility with Depth-Ogijo Loc 63
LF Magnetic Susceptibility
450
400
350
300
250
200
150
100
50
0
<0
0-10
10-2o
20-30
Depth(cm)

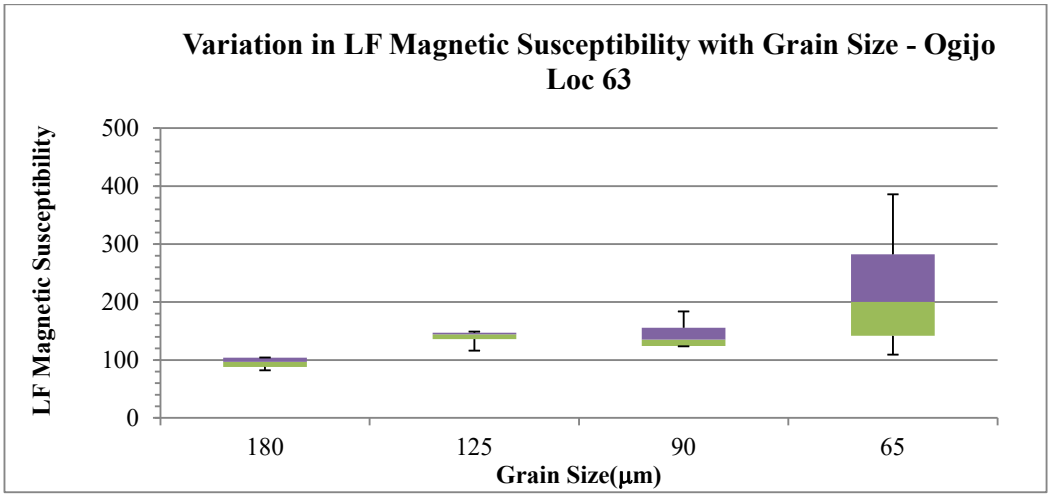
Variation in LF Magnetic Susceptibility with Grain Size - Ogijo Loc 63
LF Magnetic Susceptibility
500
400
300
200
100
0
180
125
90
65
Grain Size(µm)

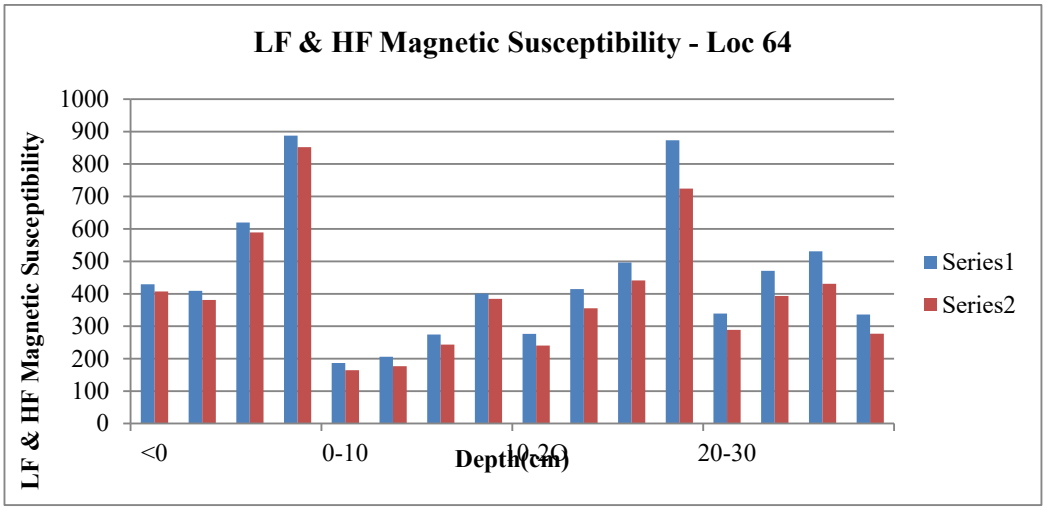
LF & HF Magnetic Susceptibility - Loc 64
LF & HF Magnetic Susceptibility
1000
900
800
700
600
500
400
300
200
100
0
<0
0-10
10-20
20-30
Depth(cm)
Series1
Series2

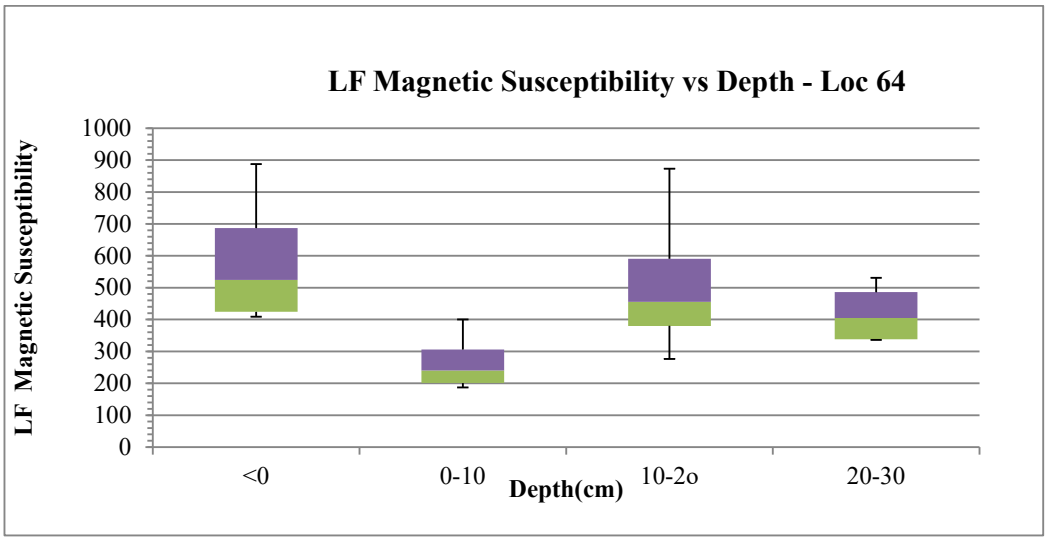
LF Magnetic Susceptibility vs Depth - Loc 64
LF Magnetic Susceptibility
1000
900
800
700
600
500
400
300
200
100
0
<0
0-10
Depth(cm)
10-2o
20-30

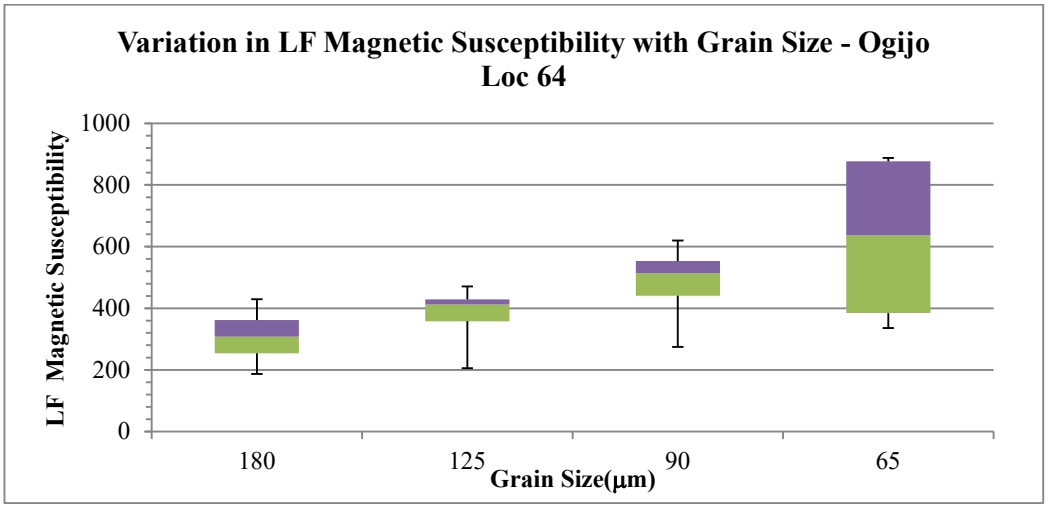
Variation in LF Magnetic Susceptibility with Grain Size - Ogijo Loc 64
LF Magnetic Susceptibility
1000
800
600
400
200
0
180
125
90
65
Grain Size(µm)

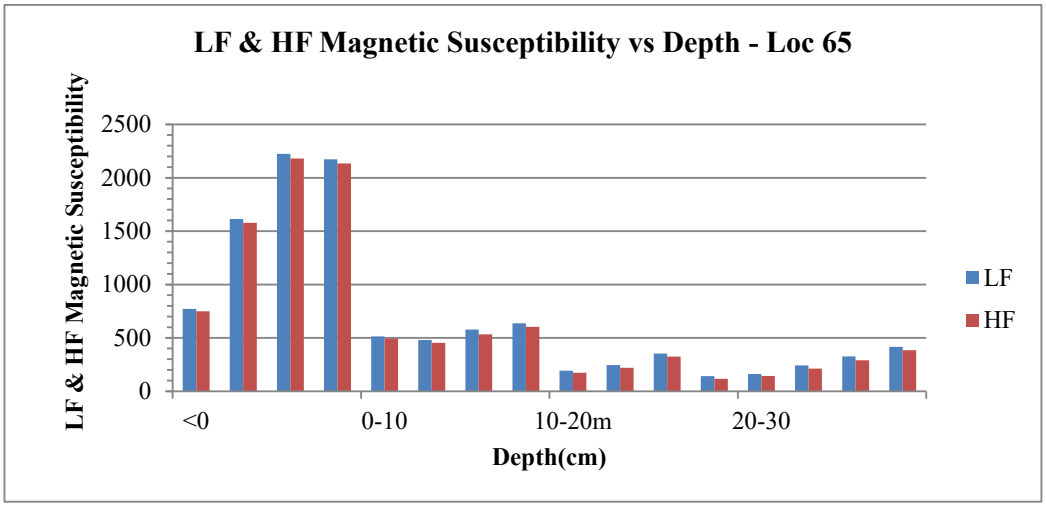
LF & HF Magnetic Susceptibility vs Depth - Loc 65
LF & HF Magnetic Susceptibility
2500
2000
1500
1000
500
0
<0
0-10
10-20m
20-30
Depth(cm)
LF
HF

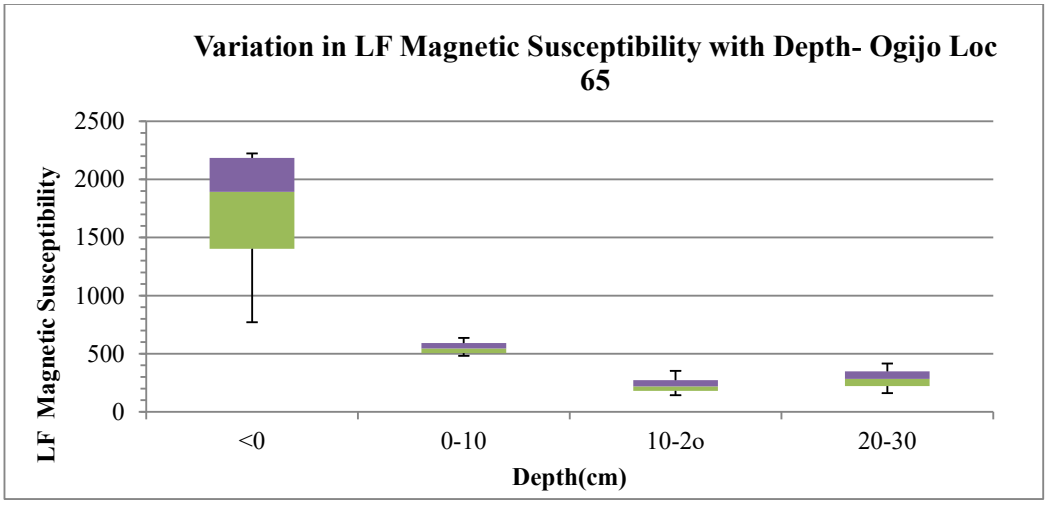
Variation in LF Magnetic Susceptibility with Depth- Ogijo Loc 65
LF Magnetic Susceptibility
2500
2000
1500
1000
500
0
<0
0-10
10-2o
20-30
Depth(cm)

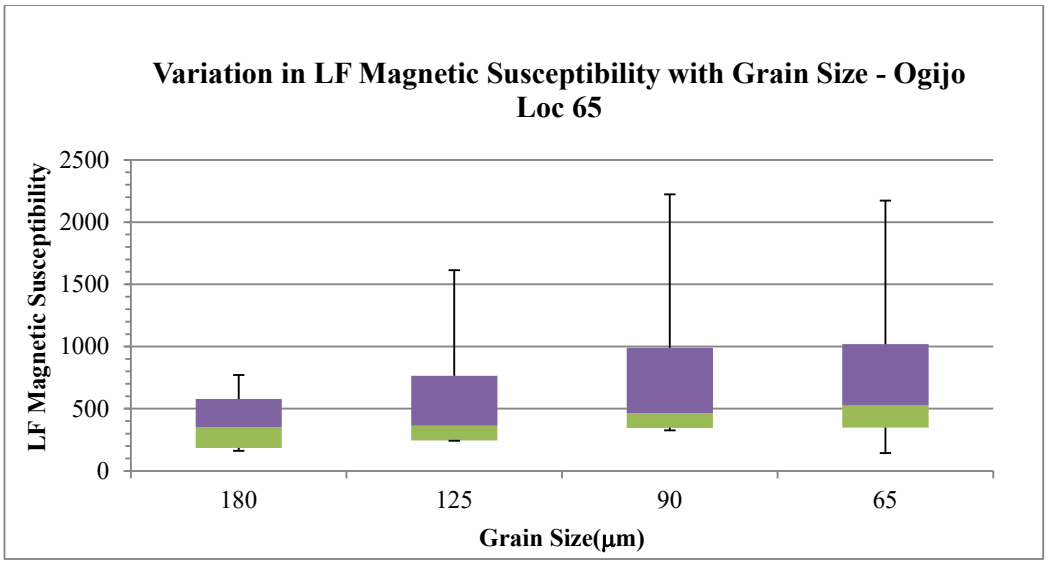
Variation in LF Magnetic Susceptibility with Grain Size - Ogijo Loc 65
LF Magnetic Susceptibility
2500
2000
1500
1000
500
0
180
125
90
65
Grain Size(µm)

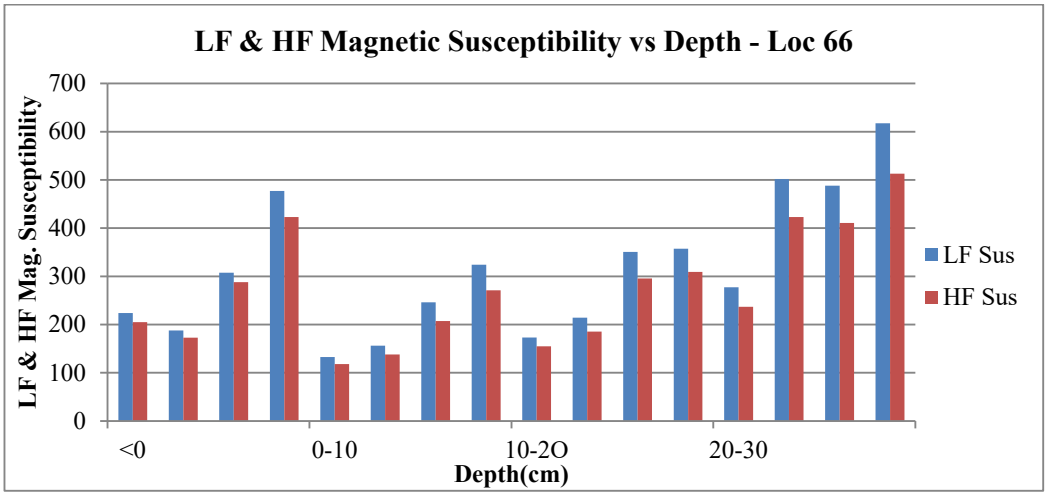
LF & HF Magnetic Susceptibility vs Depth - Loc 66
LF & HF Mag. Susceptibility
700
600
500
400
300
200
100
0
<0
0-10
10-2O
20-30
Depth(cm)
LF Sus
HF Sus

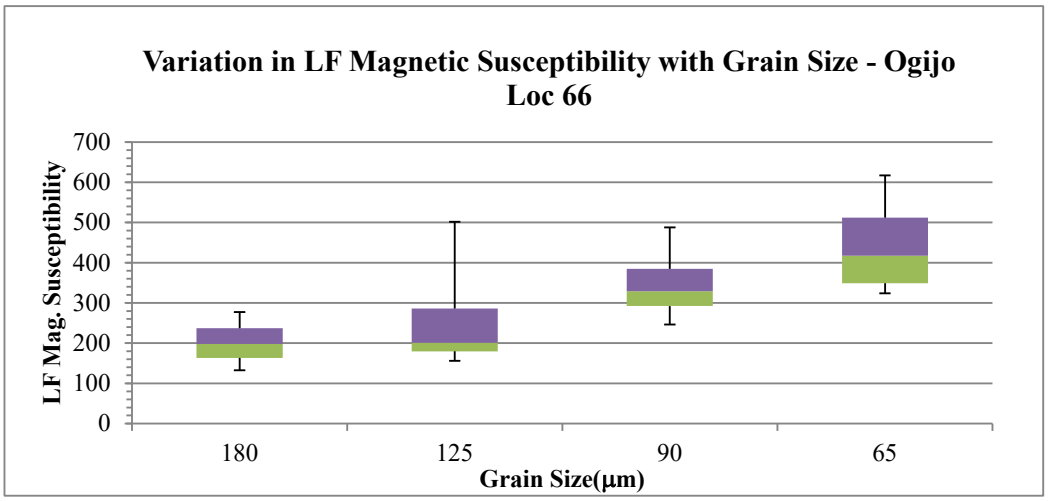
Variation in LF Magnetic Susceptibility with Grain Size - Ogijo Loc 66
LF Mag. Susceptibility
700
600
500
400
300
200
100
0
180
125
90
65
Grain Size(µm)

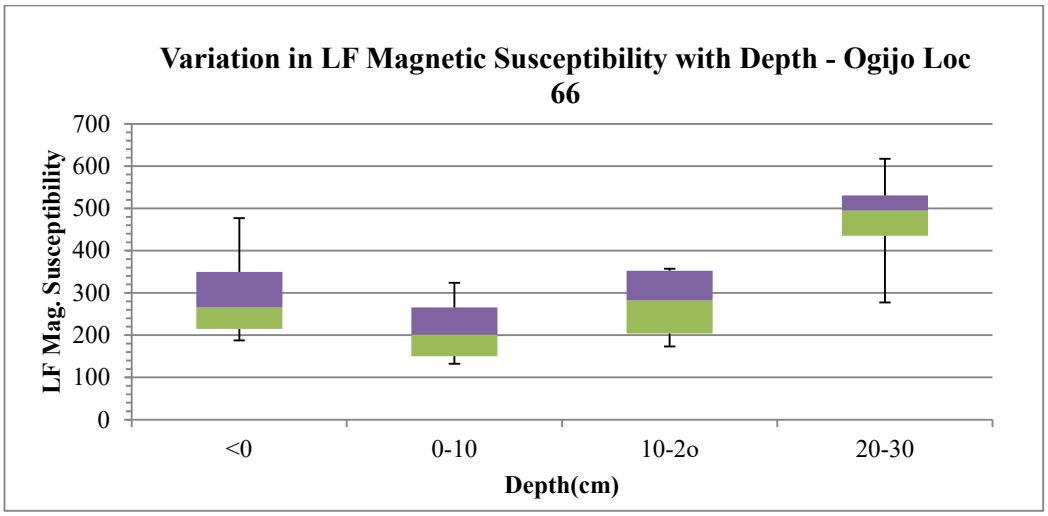
Variation in LF Magnetic Susceptibility with Depth - Ogijo Loc 66
LF Mag. Susceptibility
700
600
500
400
300
200
100
0
<0
0-10
10-2o
20-30
Depth(cm)

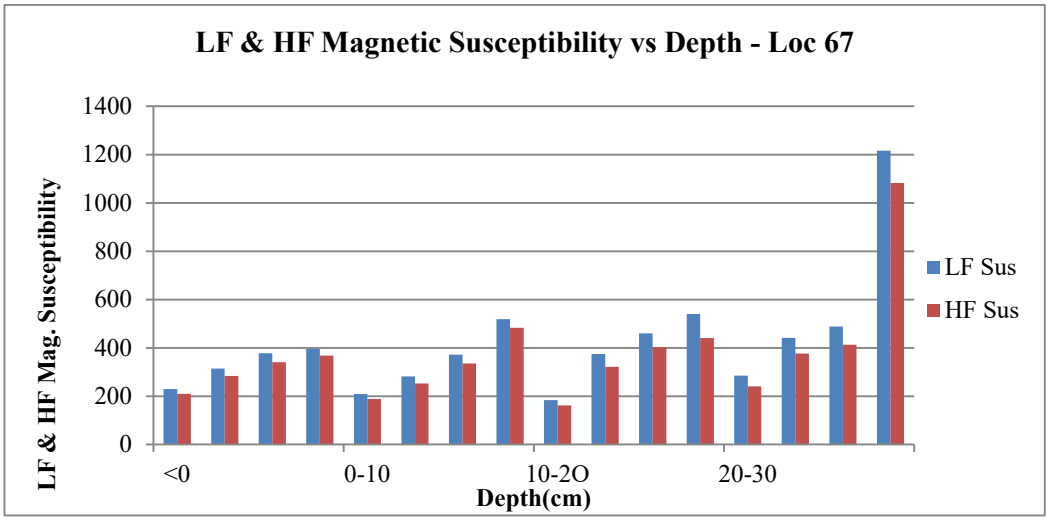
LF & HF Magnetic Susceptibility vs Depth - Loc 67
LF & HF Mag. Susceptibility
1400
1200
1000
800
600
400
200
0
<0
0-10
10-2O
20-30
Depth(cm)
LF Sus
HF Sus

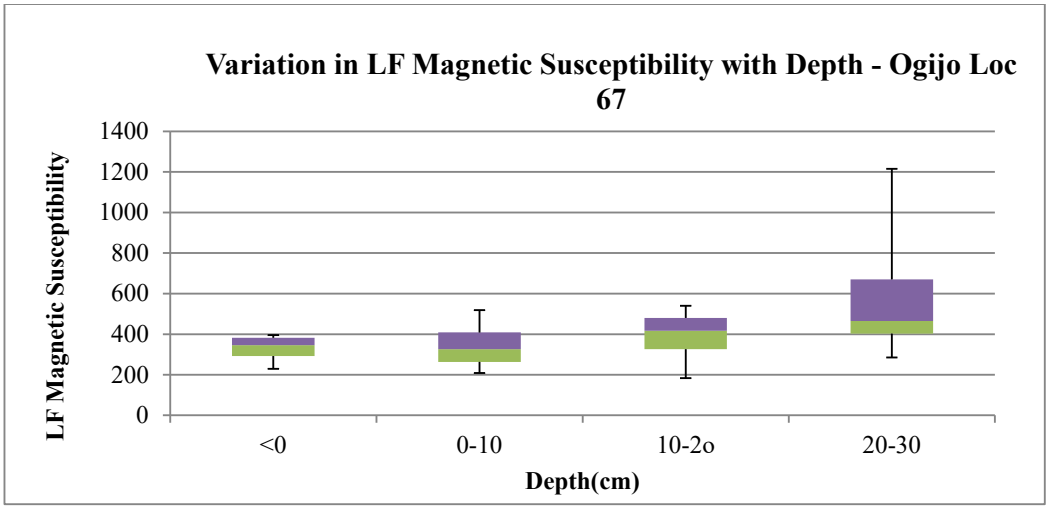
Variation in LF Magnetic Susceptibility with Depth - Ogijo Loc 67
LF Magnetic Susceptibility
1400
1200
1000
800
600
400
200
0
<0
0-10
10-2o
20-30
Depth(cm)

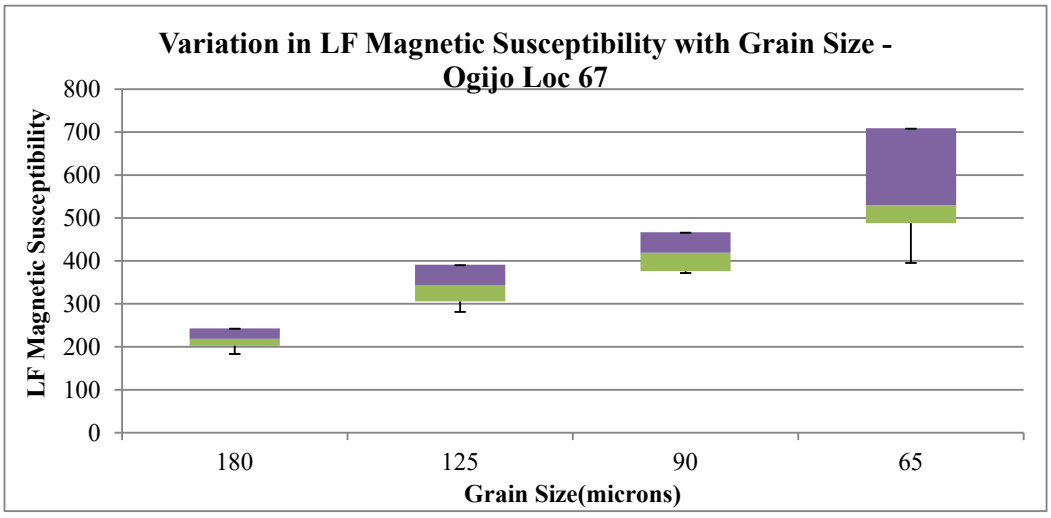
Variation in LF Magnetic Susceptibility with Grain Size - Ogijo Loc 67
LF Magnetic Susceptibility
800
700
600
500
400
300
200
100
0
180
125
90
65
Grain Size(microns)

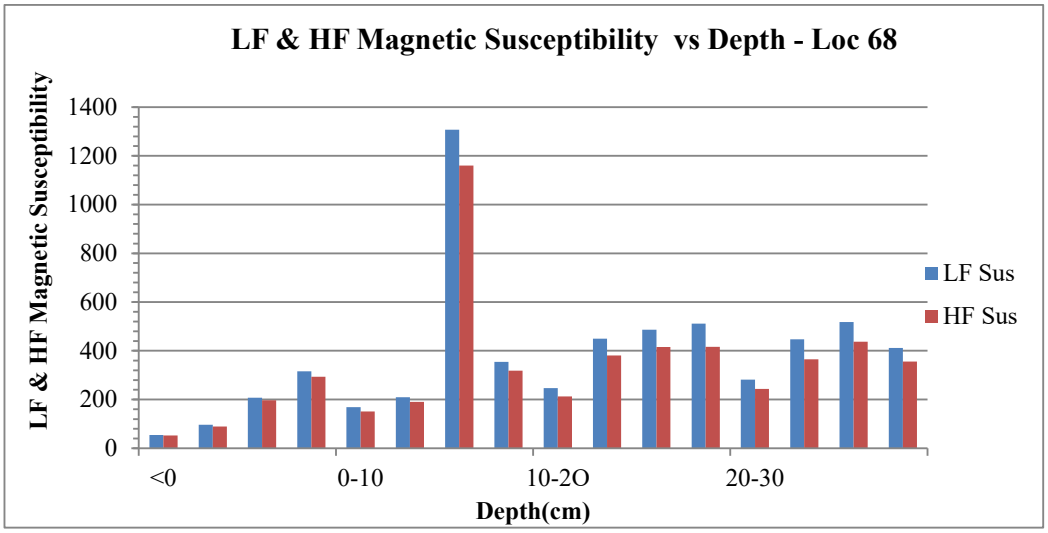
LF & HF Magnetic Susceptibility vs Depth - Loc 68
LF & HF Magnetic Susceptibility
1400
1200
1000
800
600
400
200
0
<0
0-10
10-2O
20-30
Depth(cm)
LF Sus
HF Sus

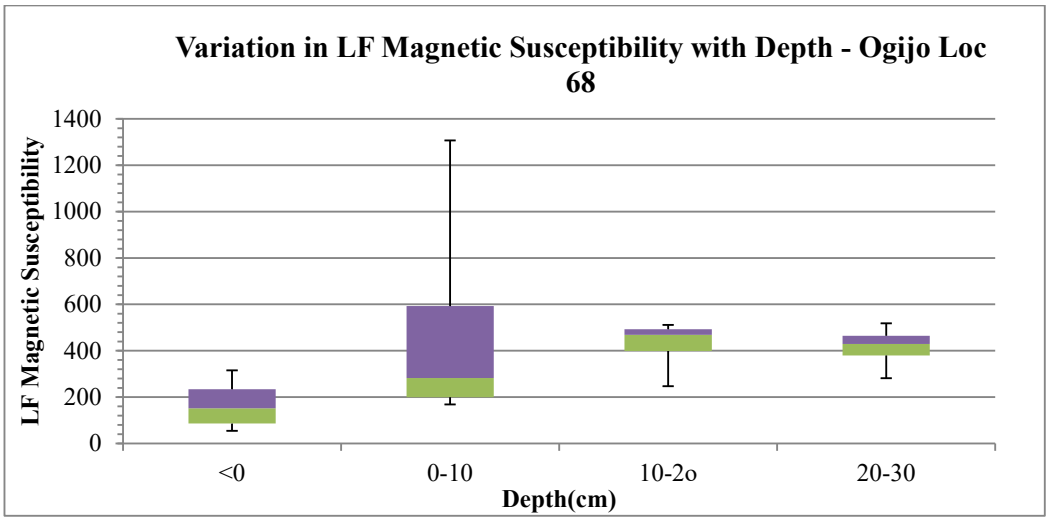
Variation in LF Magnetic Susceptibility with Depth - Ogijo Loc 68
LF Magnetic Susceptibility
1400
1200
1000
800
600
400
200
0
<0
0-10
10-2o
20-30
Depth(cm)

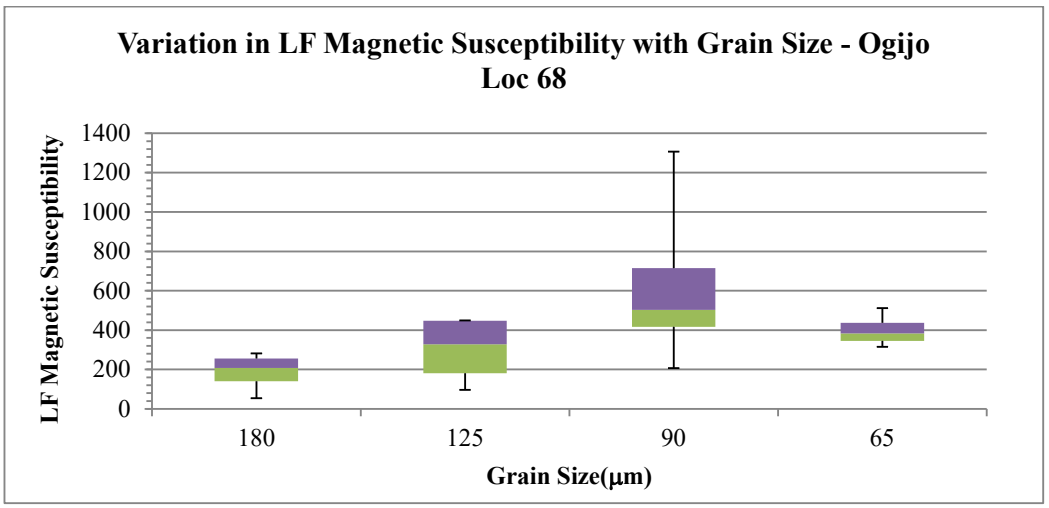
Variation in LF Magnetic Susceptibility with Grain Size - Ogijo Loc 68
LF Magnetic Susceptibility
1400
1200
1000
800
600
400
200
0
180
125
90
65
Grain Size(µm)

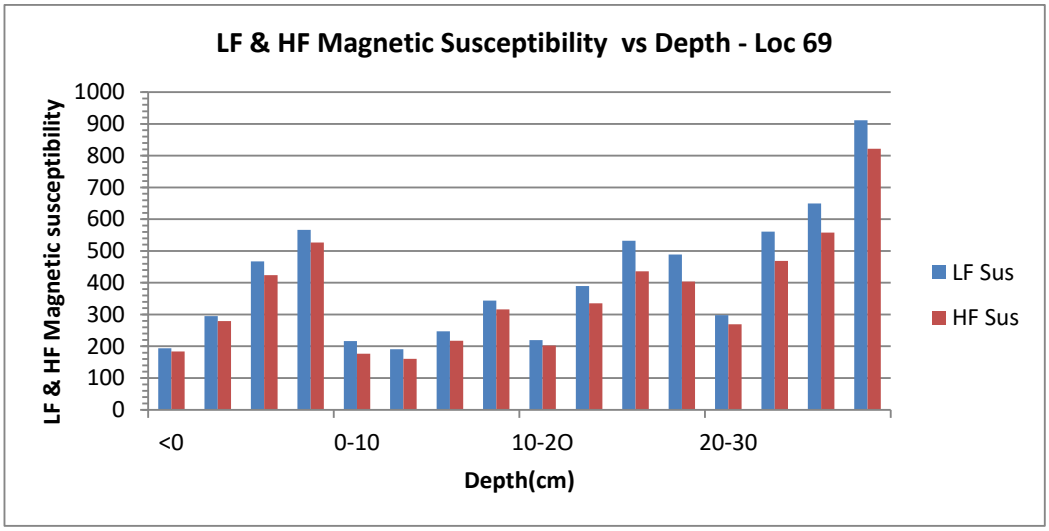
LF & HF Magnetic Susceptibility vs Depth - Loc 69
LF & HF Magnetic susceptibility
1000
900
800
700
600
500
400
300
200
100
0
<0
0-10
10-2O
20-30
Depth(cm)
LF Sus
HF Sus

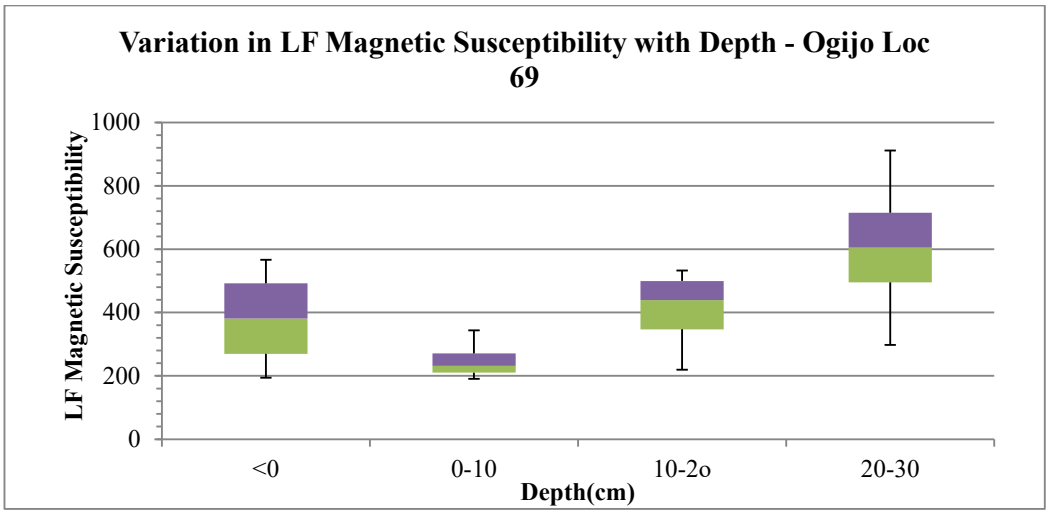
Variation in LF Magnetic Susceptibility with Depth - Ogijo Loc 69
LF Magnetic Susceptibility
1000
800
600
400
200
0
<0
0-10
10-2o
20-30
Depth(cm)

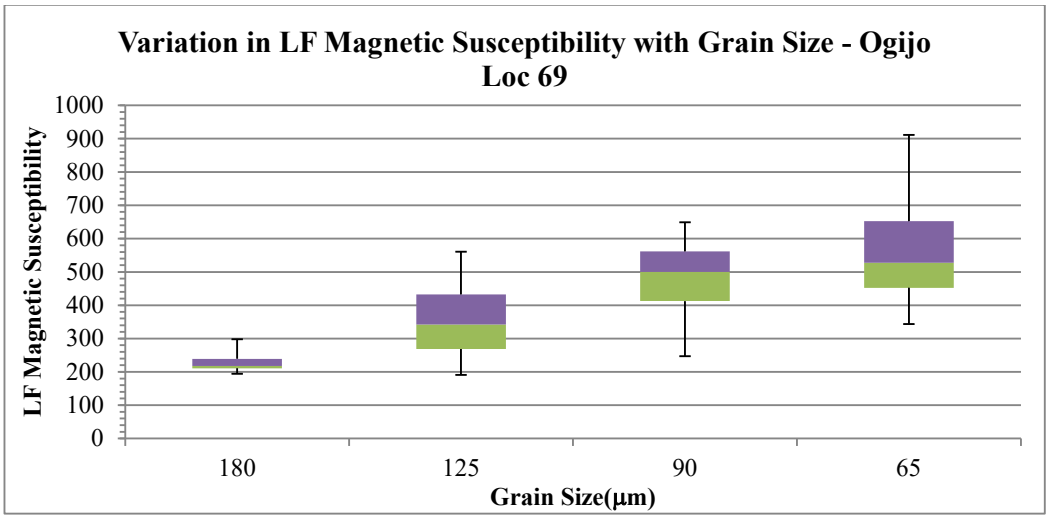
Variation in LF Magnetic Susceptibility with Grain Size - Ogijo Loc 69
LF Magnetic Susceptibility
1000
900
800
700
600
500
400
300
200
100
0
180
125
90
65
Grain Size(µm)

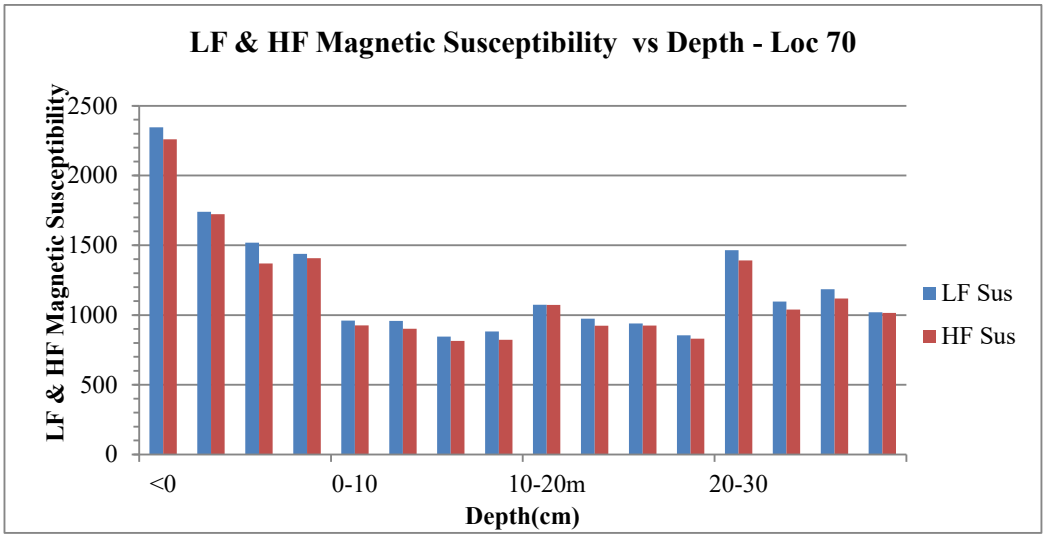
LF & HF Magnetic Susceptibility vs Depth - Loc 70
LF & HF Magnetic Susceptibility
2500
2000
1500
1000
500
0
<0
0-10
10-20m
20-30
Depth(cm)
LF Sus
HF Sus

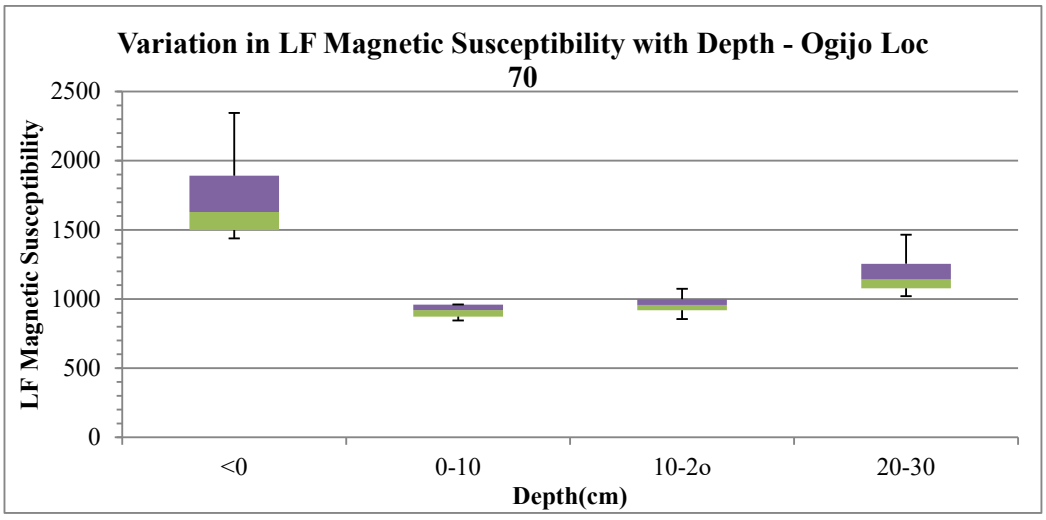
Variation in LF Magnetic Susceptibility with Depth - Ogijo Loc 70
LF Magnetic Susceptibility
2500
2000
1500
1000
500
0
<0
0-10
10-2o
20-30
Depth(cm)

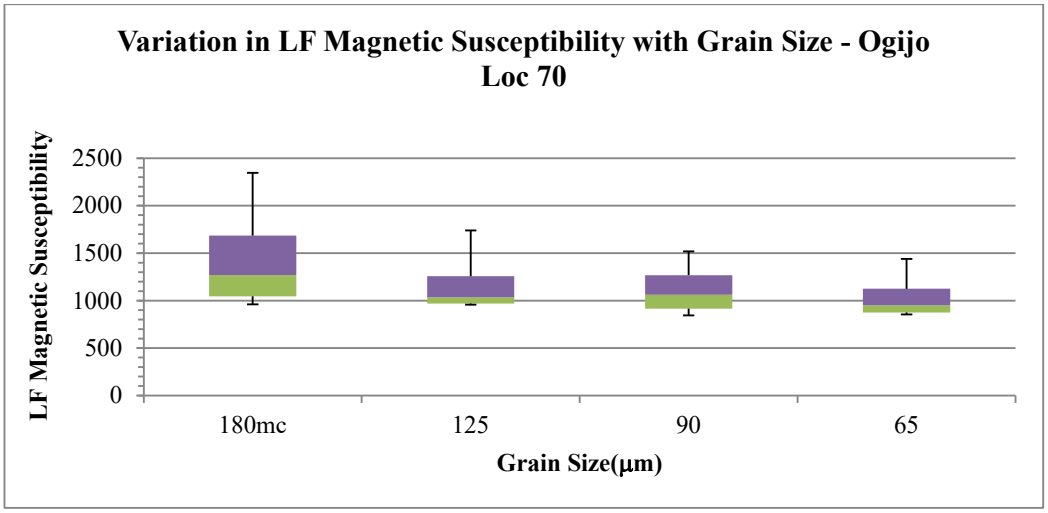
Variation in LF Magnetic Susceptibility with Grain Size - Ogijo Loc 70
LF Magnetic Susceptibility
2500
2000
1500
1000
500
0
180mc
125
90
65
Grain Size(µm)

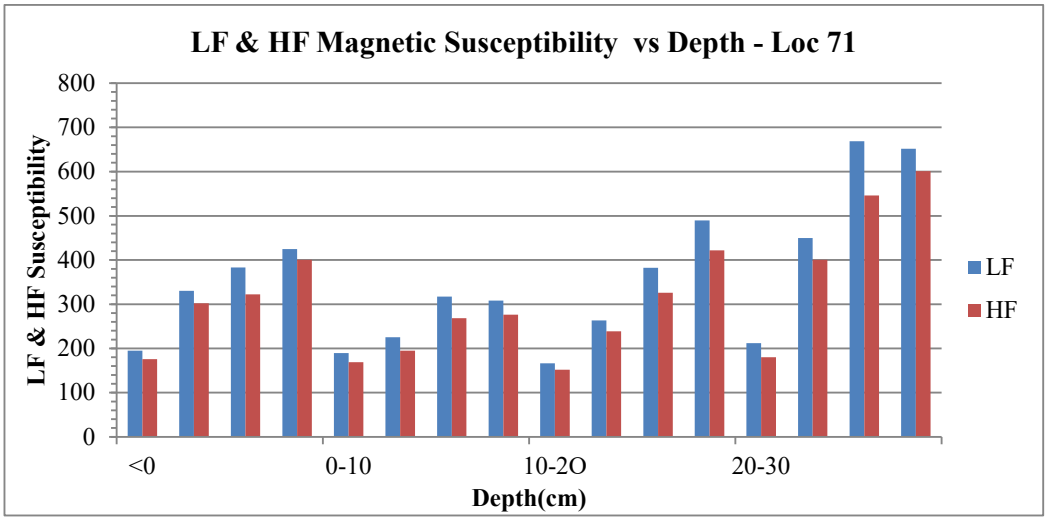
LF & HF Magnetic Susceptibility vs Depth - Loc 71
LF & HF Susceptibility
800
700
600
500
400
300
200
100
0
<0
0-10
10-2O
20-30
Depth(cm)
LF
HF

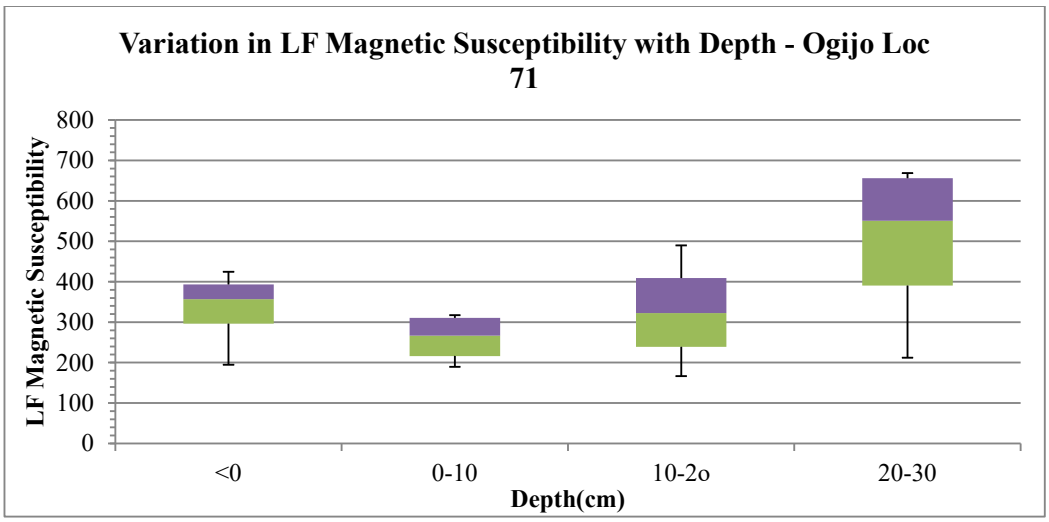
Variation in LF Magnetic Susceptibility with Depth - Ogijo Loc 71
LF Magnetic Susceptibility
800
700
600
500
400
300
200
100
0
<0
0-10
10-2o
20-30
Depth(cm)

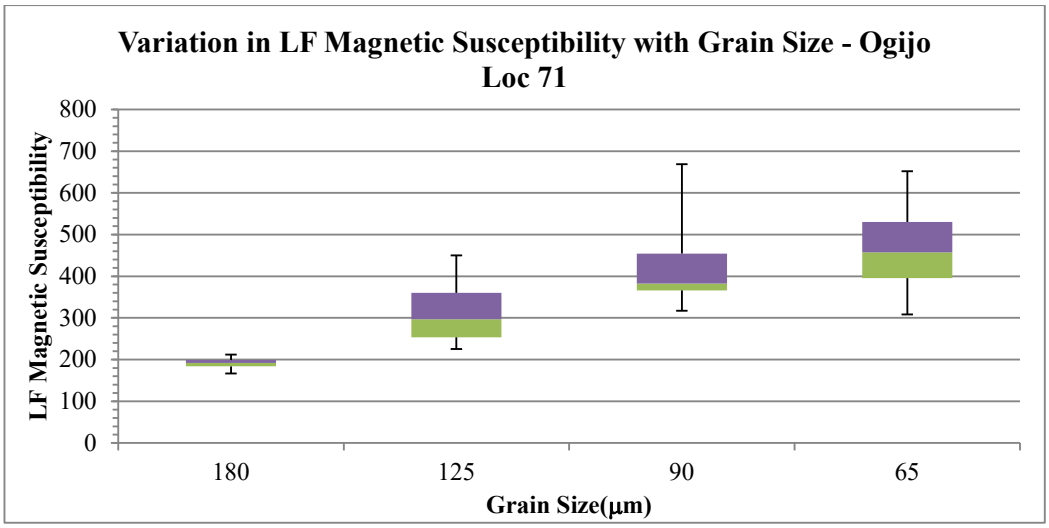
Variation in LF Magnetic Susceptibility with Grain Size - Ogijo Loc 71
LF Magnetic Susceptibility
800
700
600
500
400
300
200
100
0
180
125
90
65
Grain Size(µm)

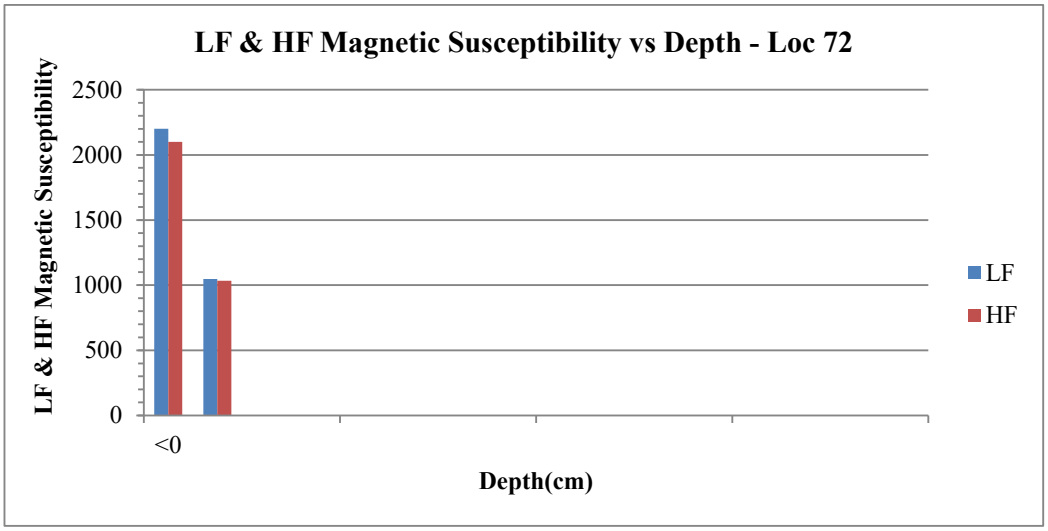
LF & HF Magnetic Susceptibility vs Depth - Loc 72
LF & HF Magnetic Susceptibility
2500
2000
1500
1000
500
0
<0
Depth(cm)
LF
HF

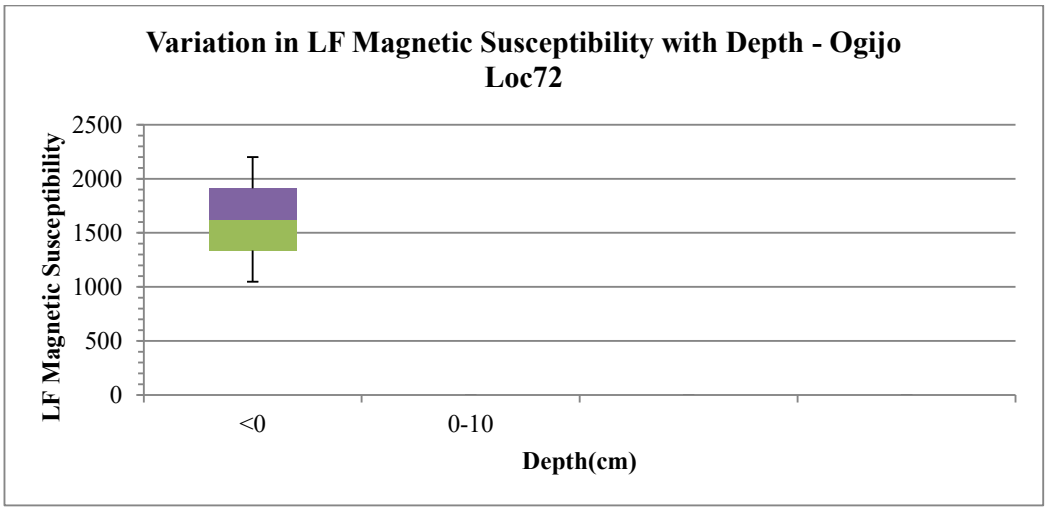
Variation in LF Magnetic Susceptibility with Depth - Ogijo Loc72
LF Magnetic Susceptibility
2500
2000
1500
1000
500
0
<0
0-10
Depth(cm)

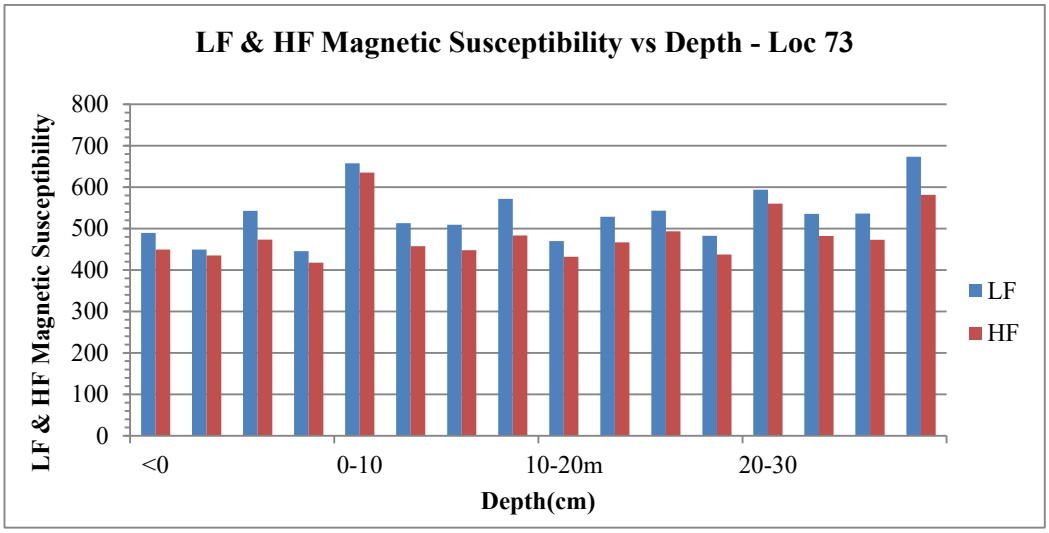
LF & HF Magnetic Susceptibility vs Depth - Loc 73
LF & HF Magnetic Susceptibility
800
700
600
500
400
300
200
100
0
<0
0-10
10-20m
20-30
Depth(cm)
LF
HF

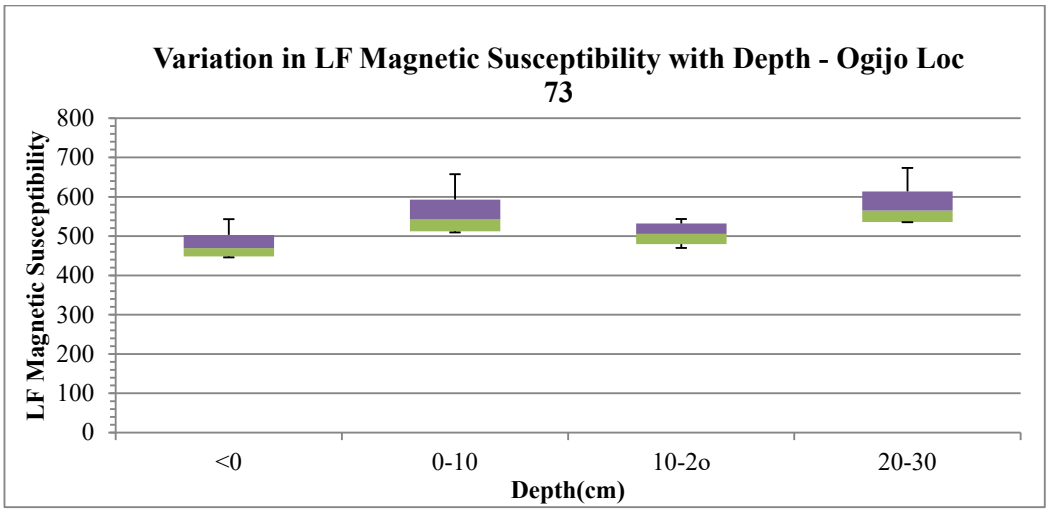
Variation in LF Magnetic Susceptibility with Depth - Ogijo Loc 73
LF Magnetic Susceptibility
800
700
600
500
400
300
200
100
0
<0
0-10
10-2o
20-30
Depth(cm)

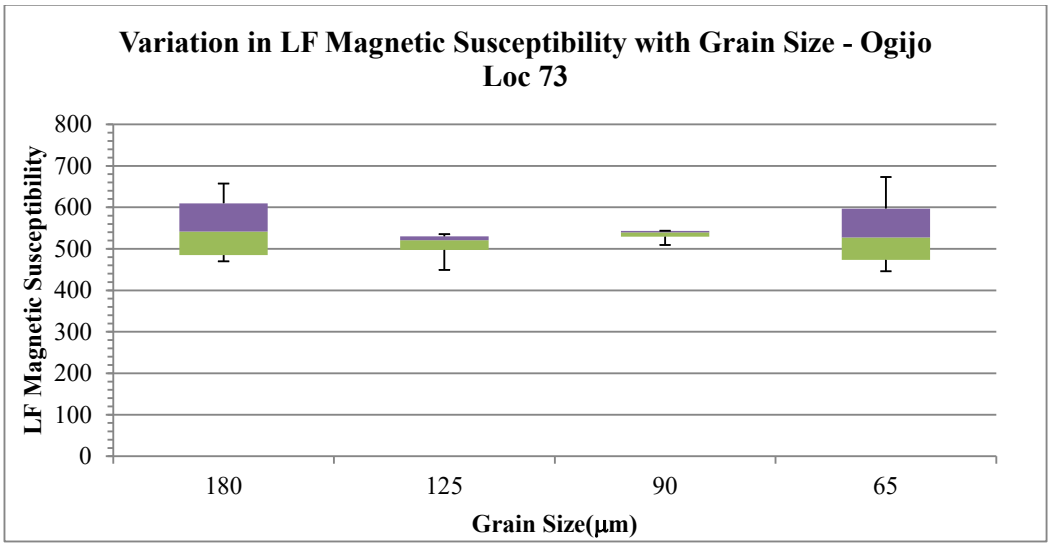
Variation in LF Magnetic Susceptibility with Grain Size - Ogijo Loc 73
LF Magnetic Susceptibility
800
700
600
500
400
300
200
100
0
180
125
90
65
Grain Size(µm)

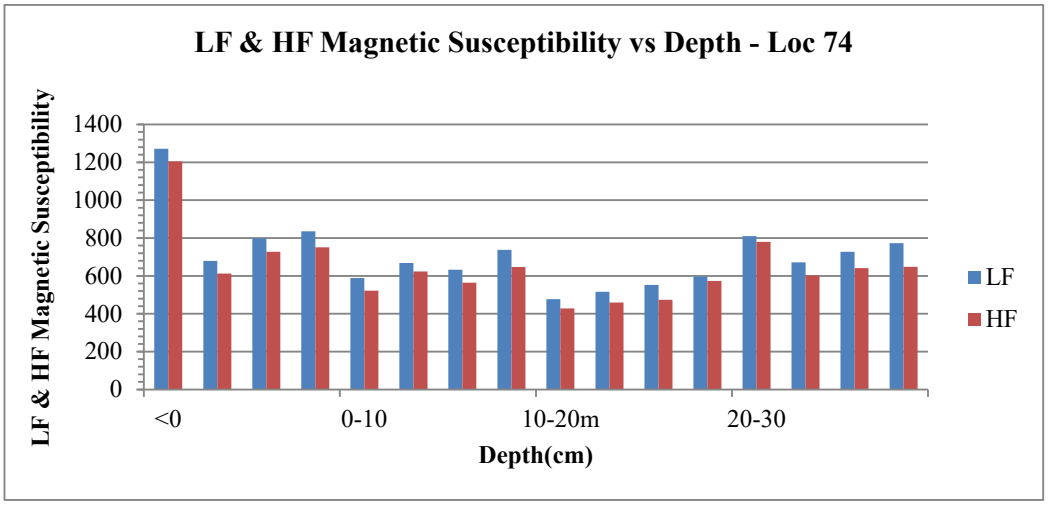
LF & HF Magnetic Susceptibility vs Depth - Loc 74
LF & HF Magnetic Susceptibility
1400
1200
1000
800
600
400
200
0
<0
0-10
10-20m
20-30
Depth(cm)
LF
HF

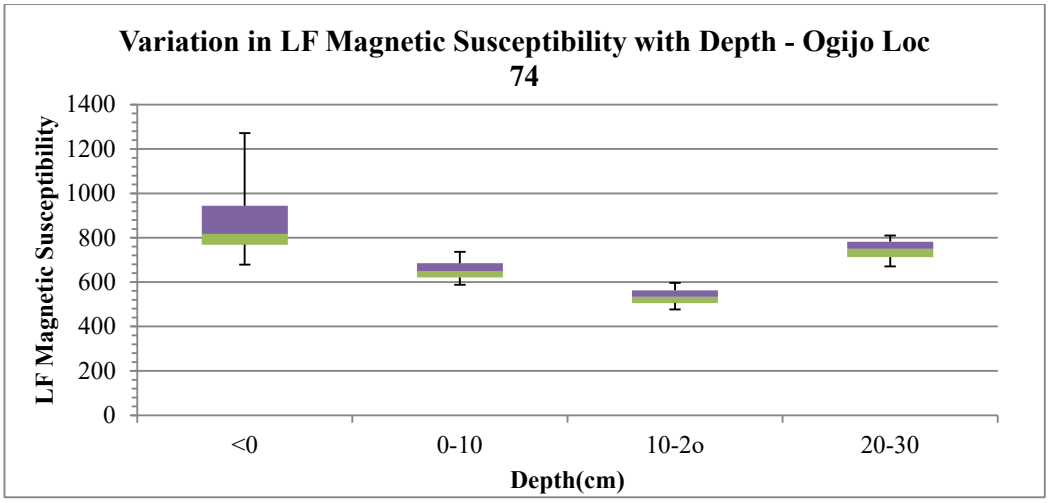
Variation in LF Magnetic Susceptibility with Depth - Ogijo Loc 74
LF Magnetic Susceptibility
1400
1200
1000
800
600
400
200
0
<0
0-10
10-2o
20-30
Depth(cm)

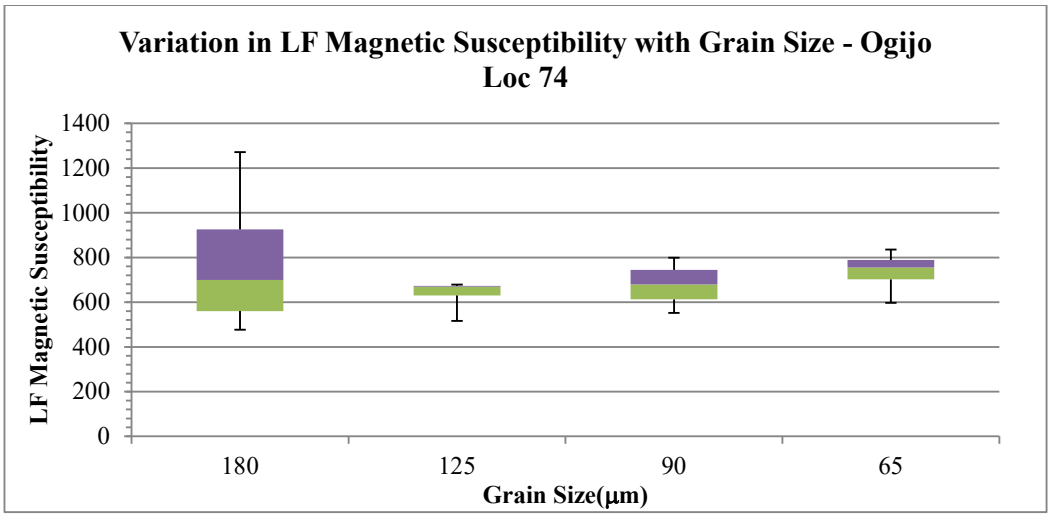
Variation in LF Magnetic Susceptibility with Grain Size - Ogijo Loc 74
LF Magnetic Susceptibility
1400
1200
1000
800
600
400
200
0
180
125
90
65
Grain Size(µm)

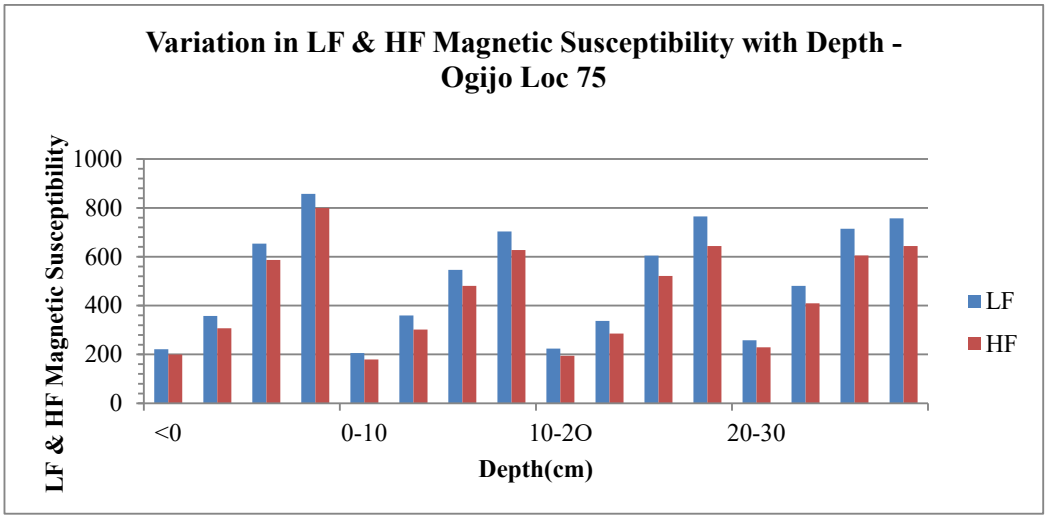
Variation in LF & HF Magnetic Susceptibility with Depth - Ogijo Loc 75
LF & HF Magnetic Susceptibility
1000
800
600
400
200
0
<0
0-10
10-2O
20-30
Depth(cm)
LF
HF

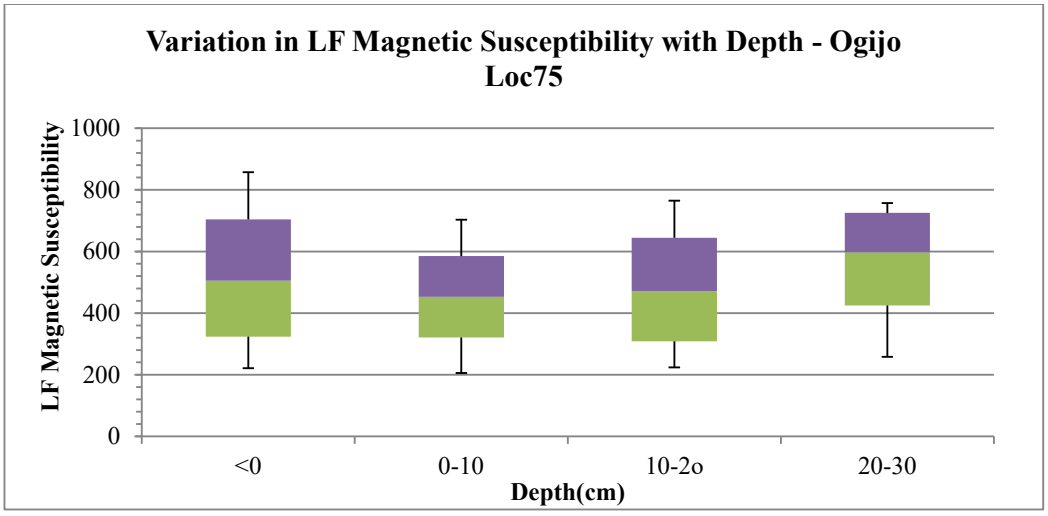
Variation in LF Magnetic Susceptibility with Depth - Ogijo Loc75
LF Magnetic Susceptibility
1000
800
600
400
200
0
<0
0-10
10-2o
20-30
Depth(cm)

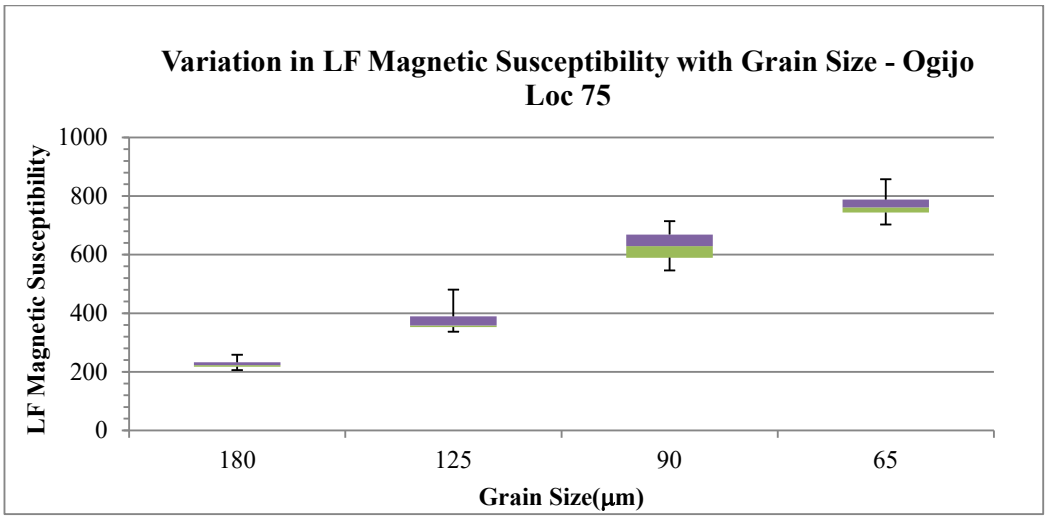
Variation in LF Magnetic Susceptibility with Grain Size - Ogijo Loc 75
LF Magnetic Susceptibility
1000
800
600
400
200
0
180
125
90
65
Grain Size(µm)

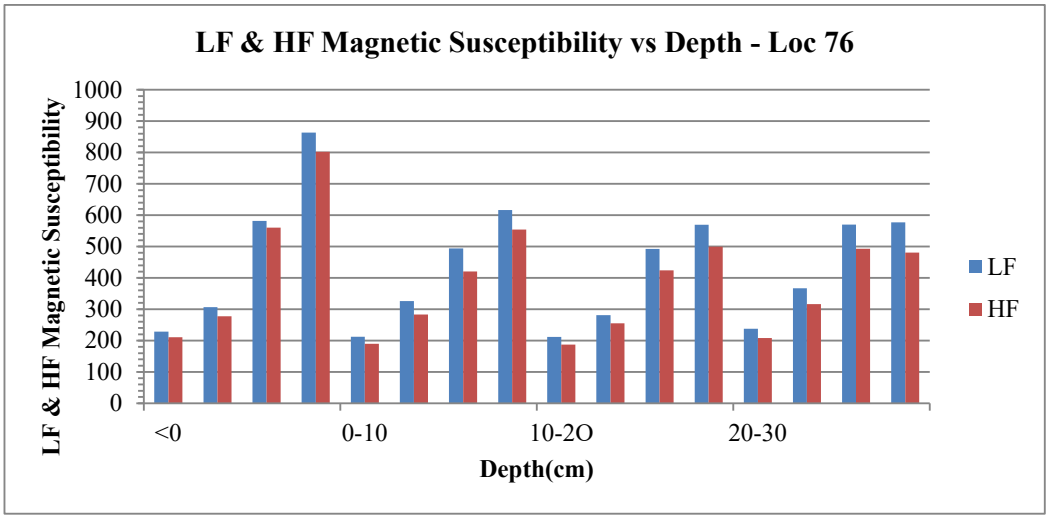
LF & HF Magnetic Susceptibility vs Depth - Loc 76
LF & HF Magnetic Susceptibility
1000
900
800
700
600
500
400
300
200
100
0
<0
0-10
10-2O
20-30
Depth(cm)
LF
HF

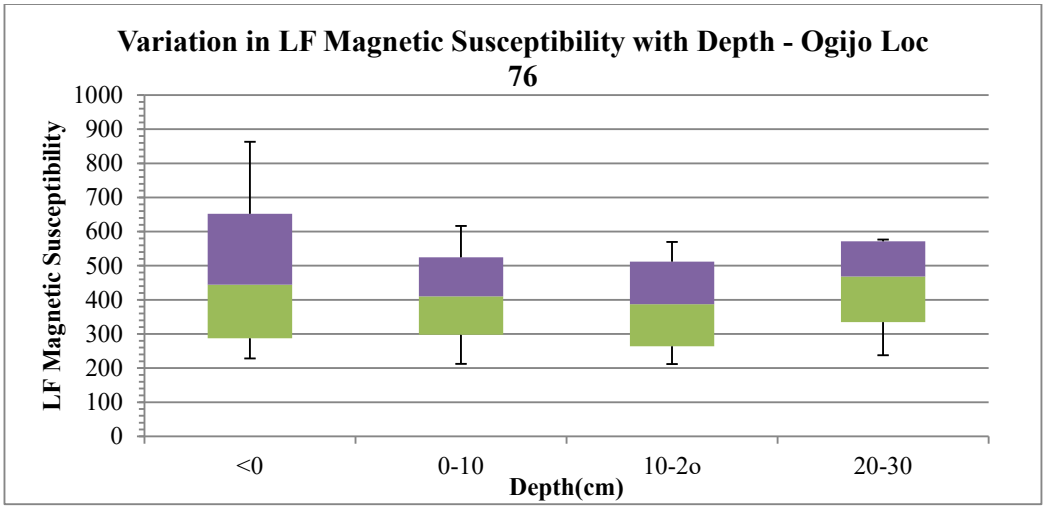
Variation in LF Magnetic Susceptibility with Depth - Ogijo Loc 76
LF Magnetic Susceptibility
1000
900
800
700
600
500
400
300
200
100
0
<0
0-10
10-2o
20-30
Depth(cm)

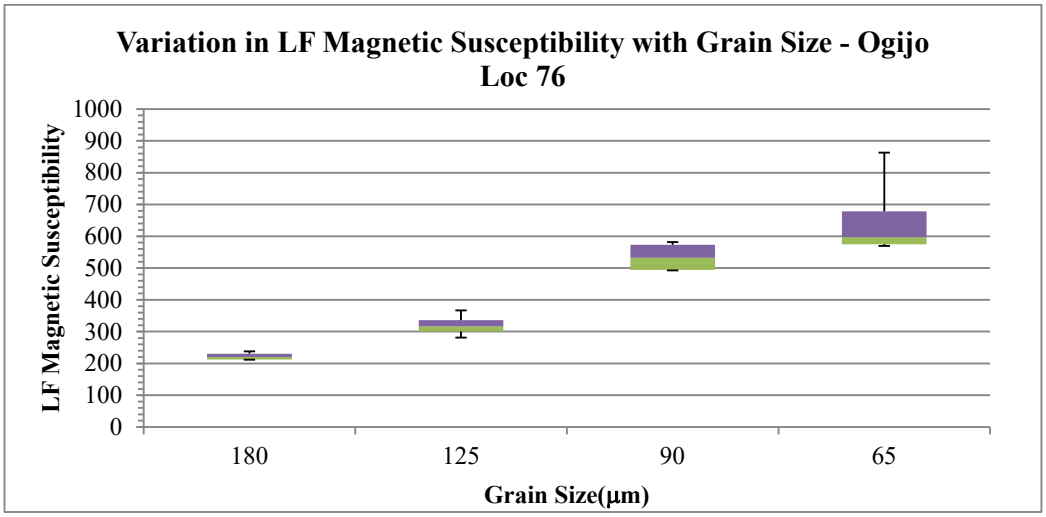
Variation in LF Magnetic Susceptibility with Grain Size - Ogijo Loc 76
LF Magnetic Susceptibility
1000
900
800
700
600
500
400
300
200
100
0
180
125
90
65
Grain Size(µm)

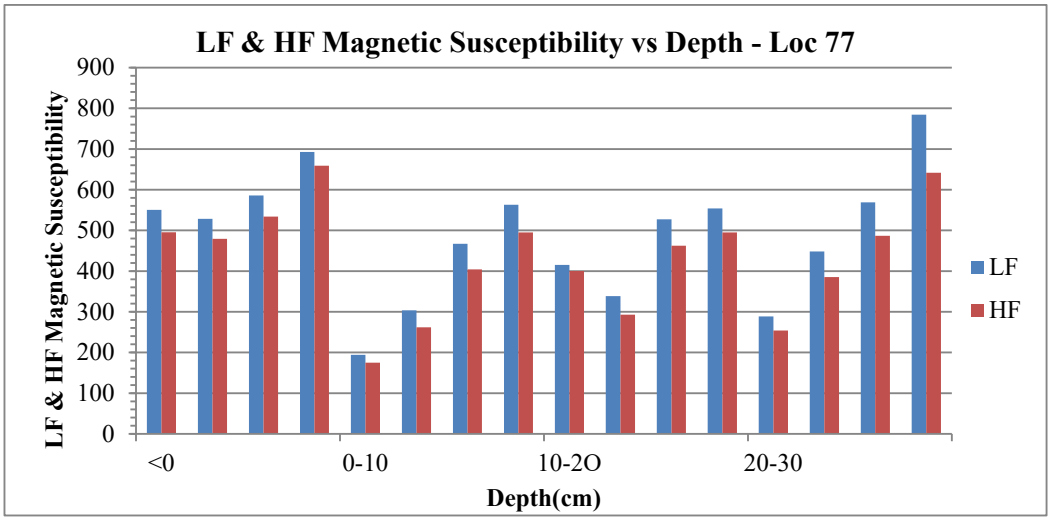
LF & HF Magnetic Susceptibility vs Depth - Loc 77
LF & HF Magnetic Susceptibility
900
800
700
600
500
400
300
200
100
0
<0
0-10
10-2O
20-30
Depth(cm)
LF
HF

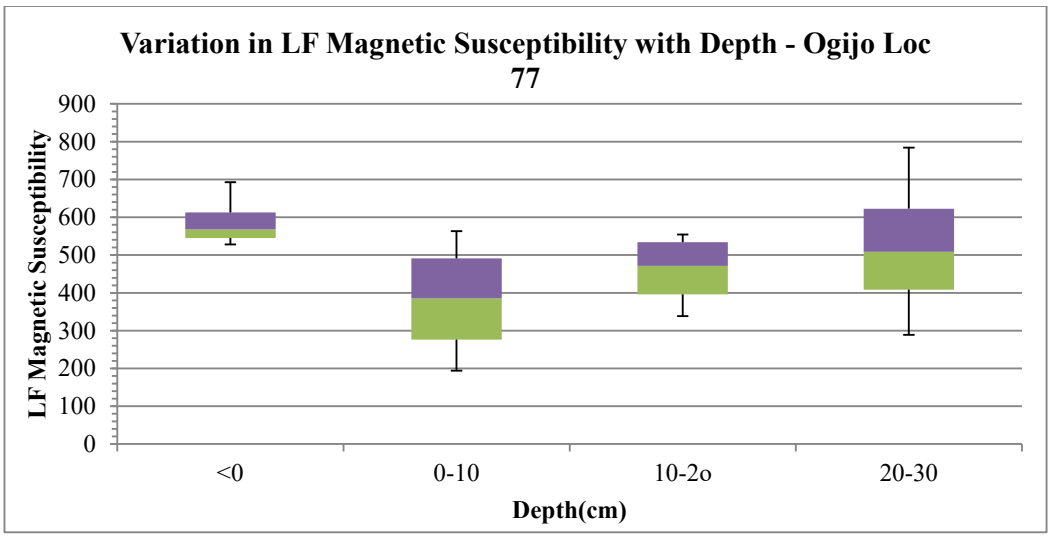
Variation in LF Magnetic Susceptibility with Depth - Ogijo Loc 77
LF Magnetic Susceptibility
900
800
700
600
500
400
300
200
100
0
<0
0-10
10-2o
20-30
Depth(cm)

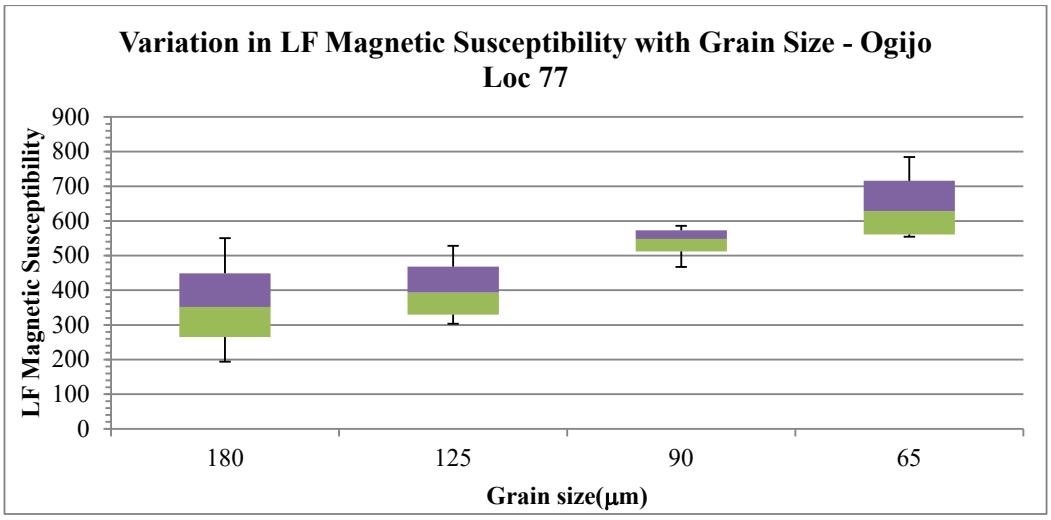
Variation in LF Magnetic Susceptibility with Grain Size - Ogijo Loc 77
LF Magnetic Susceptibility
900
800
700
600
500
400
300
200
100
0
180
125
90
65
Grain size(µm)

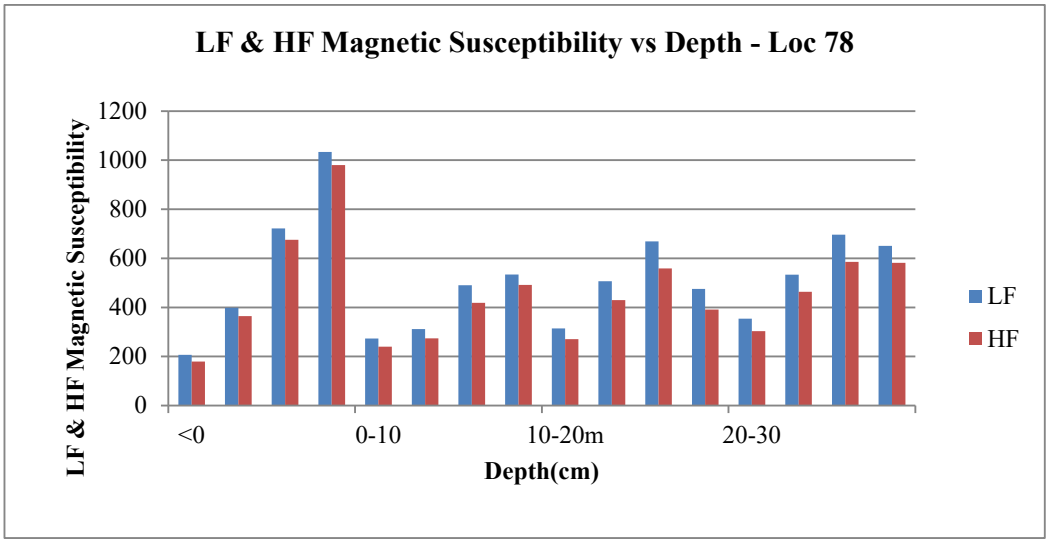
LF & HF Magnetic Susceptibility vs Depth - Loc 78
LF & HF Magnetic Susceptibility
1200
1000
800
600
400
200
0
<0
0-10
10-20m
20-30
Depth(cm)
LF
HF

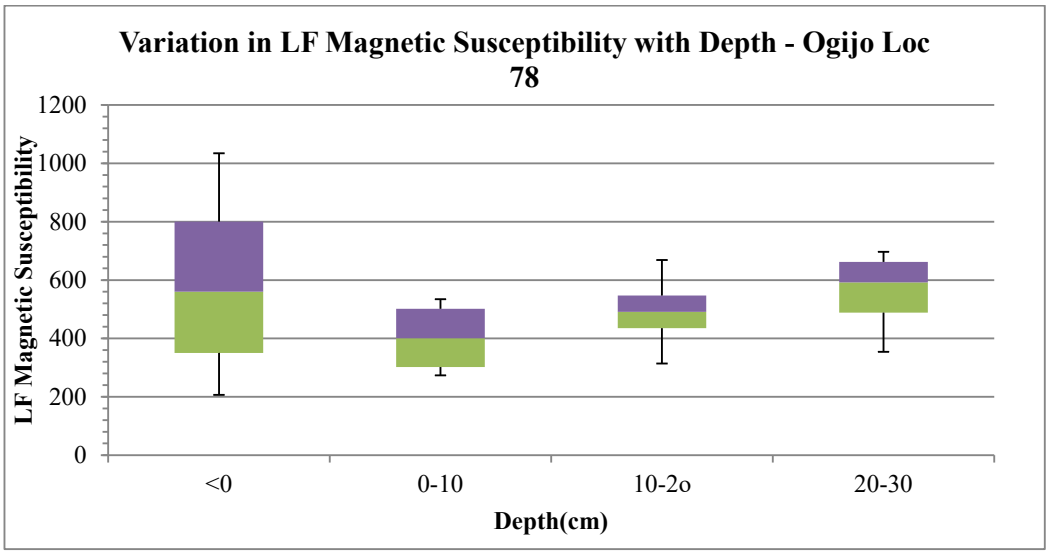
Variation in LF Magnetic Susceptibility with Depth - Ogijo Loc 78
LF Magnetic Susceptibility
1200
1000
800
600
400
200
0
<0
0-10
10-2o
20-30
Depth(cm)

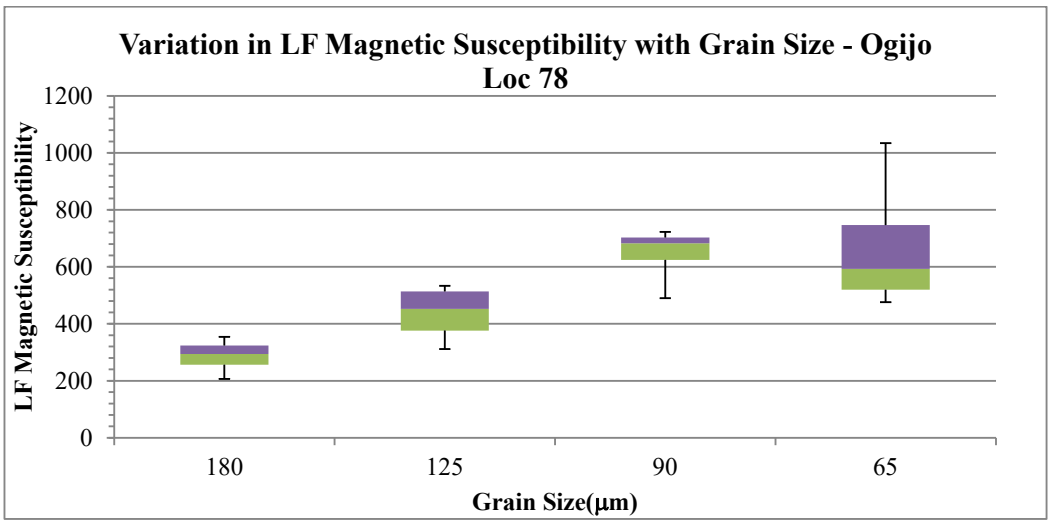
Variation in LF Magnetic Susceptibility with Grain Size - Ogijo Loc 78
LF Magnetic Susceptibility
1200
1000
800
600
400
200
0
180
125
90
65
Grain Size(µm)

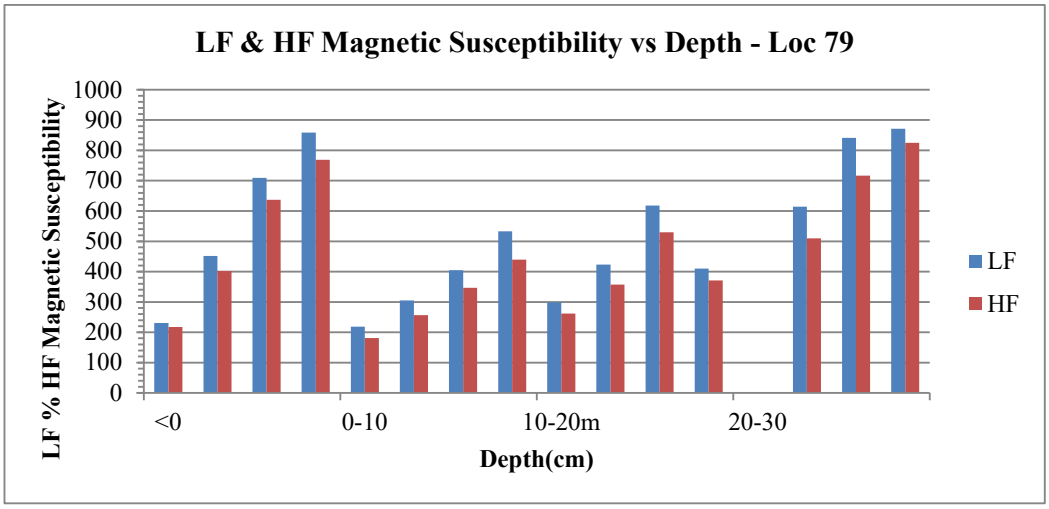
LF & HF Magnetic Susceptibility vs Depth - Loc 79
LF % HF Magnetic Susceptibility
1000
900
800
700
600
500
400
300
200
100
0
<0
0-10
10-20m
20-30
Depth(cm)
LF
HF

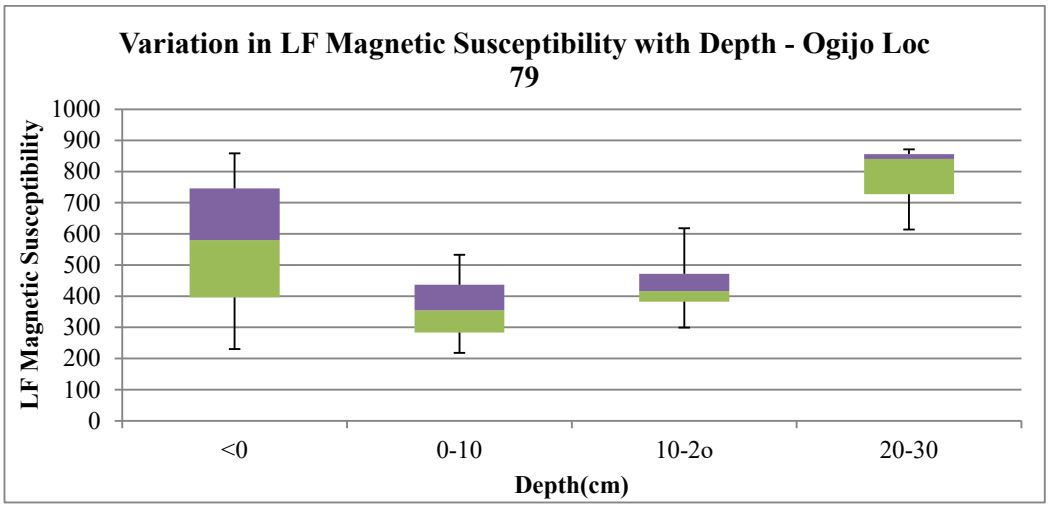
Variation in LF Magnetic Susceptibility with Depth - Ogijo Loc 79
LF Magnetic Susceptibility
1000
900
800
700
600
500
400
300
200
100
0
<0
0-10
10-2o
20-30
Depth(cm)

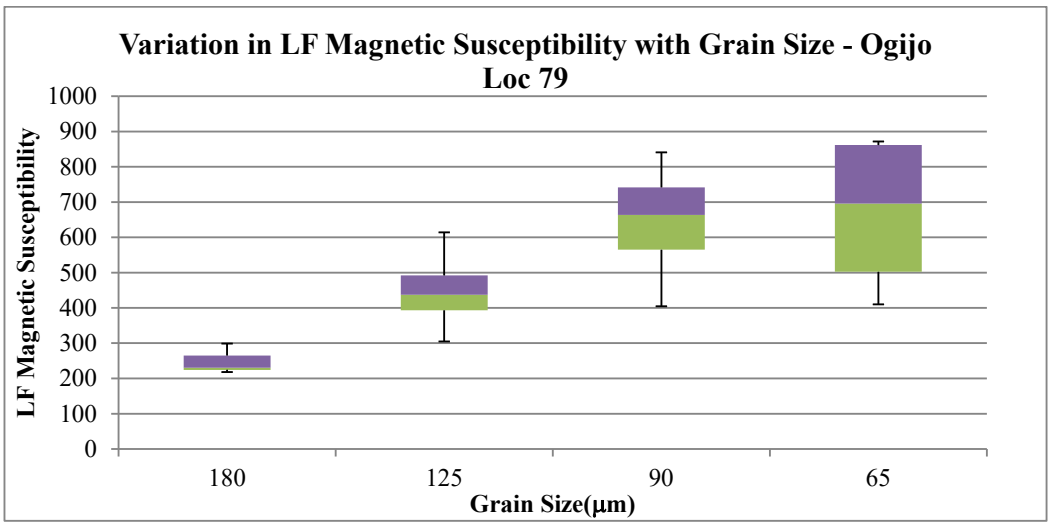
Variation in LF Magnetic Susceptibility with Grain Size - Ogijo Loc 79
LF Magnetic Susceptibility
1000
900
800
700
600
500
400
300
200
100
0
180
125
90
65
Grain Size(µm)

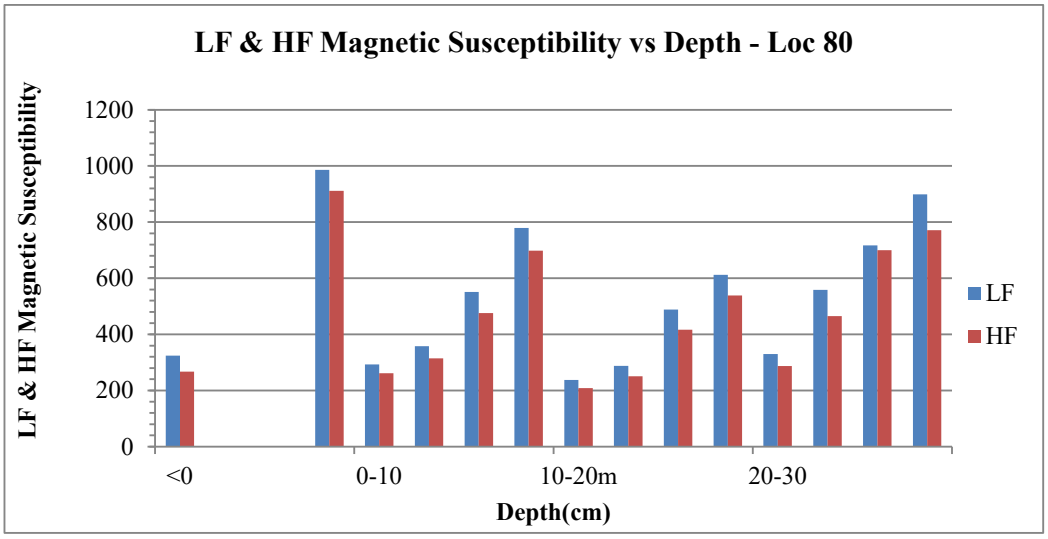
LF & HF Magnetic Susceptibility vs Depth - Loc 80
LF & HF Magnetic Susceptibility
1200
1000
800
600
400
200
0
<0
0-10
10-20m
20-30
Depth(cm)
LF
HF

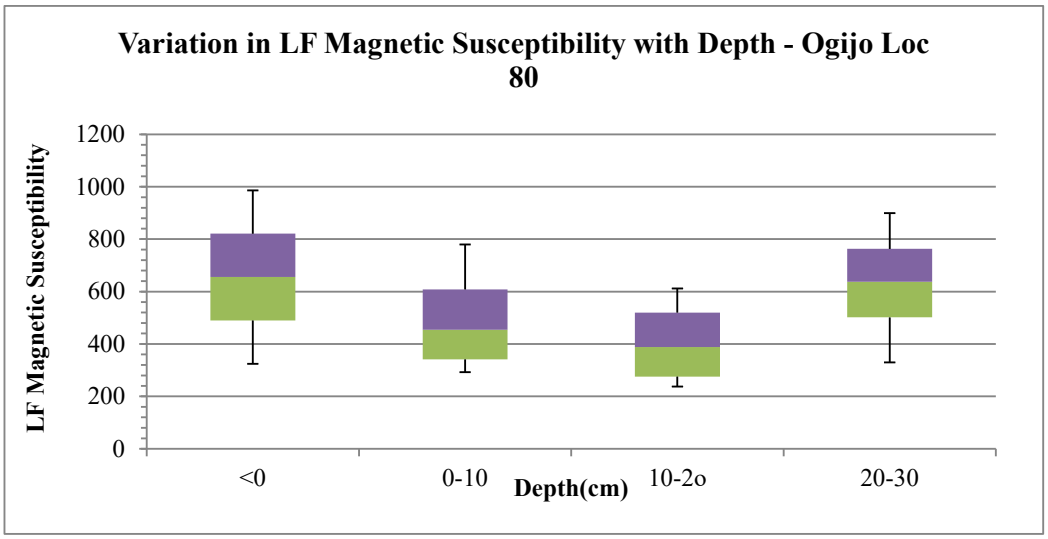
Variation in LF Magnetic Susceptibility with Depth - Ogijo Loc 80
LF Magnetic Susceptibility
1200
1000
800
600
400
200
0
<0
0-10
Depth(cm)
10-2o
20-30

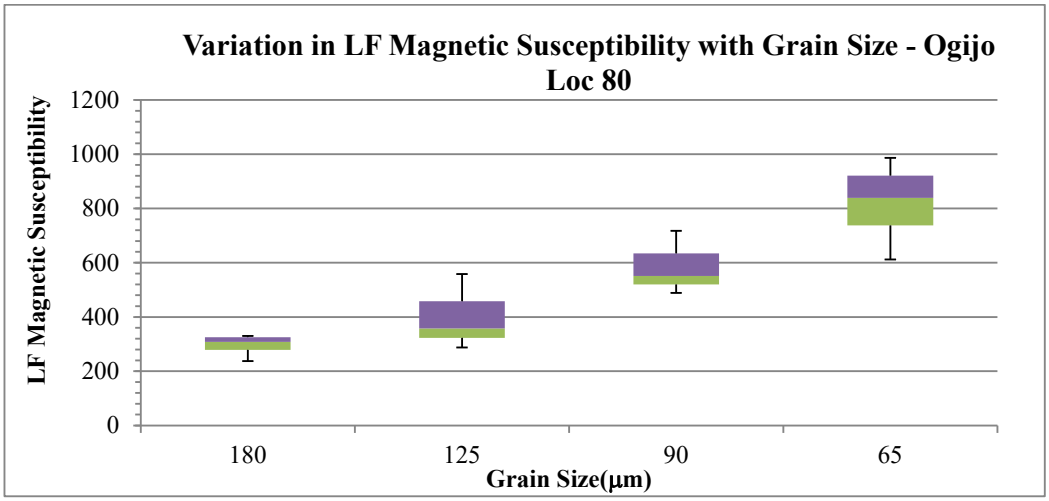
Variation in LF Magnetic Susceptibility with Grain Size - Ogijo Loc 80
LF Magnetic Susceptibility
1200
1000
800
600
400
200
0
180
125
90
65
Grain Size(µm)

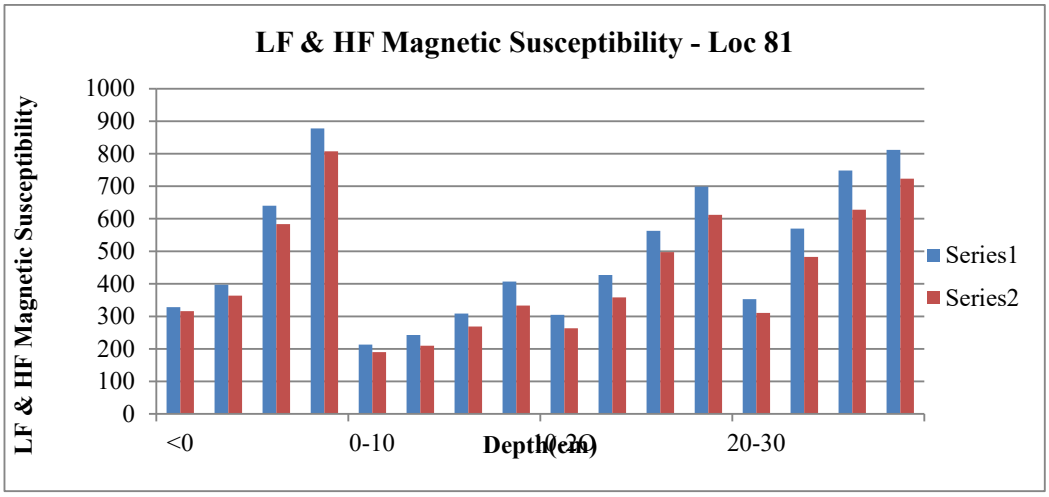
LF & HF Magnetic Susceptibility - Loc 81
LF & HF Magnetic Susceptibility
1000
900
800
700
600
500
400
300
200
100
0
<0
0-10
20-30
Depth(cm)
Series1
Series2

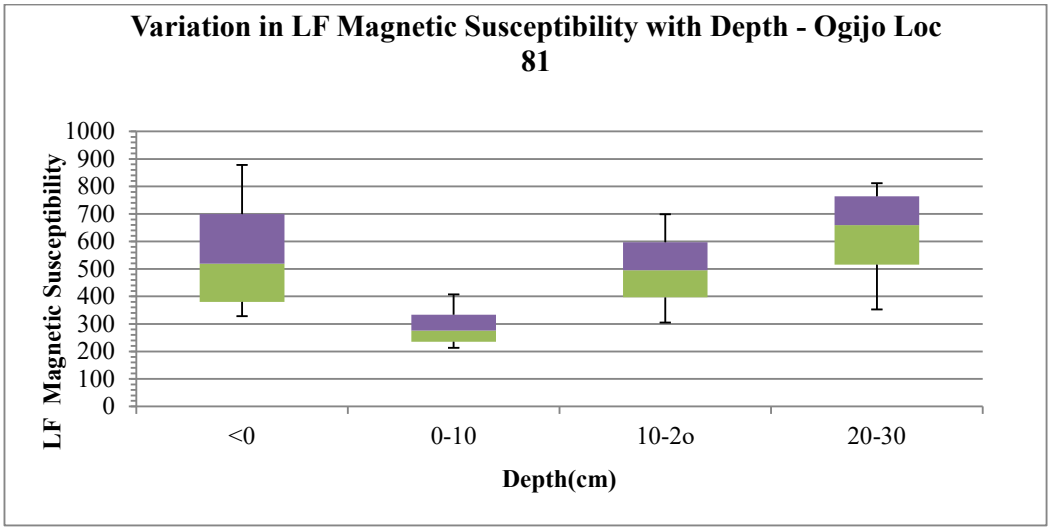
Variation in LF Magnetic Susceptibility with Depth - Ogijo Loc 81
LF Magnetic Susceptibility
1000
900
800
700
600
500
400
300
200
100
0
<0
0-10
10-2o
20-30
Depth(cm)

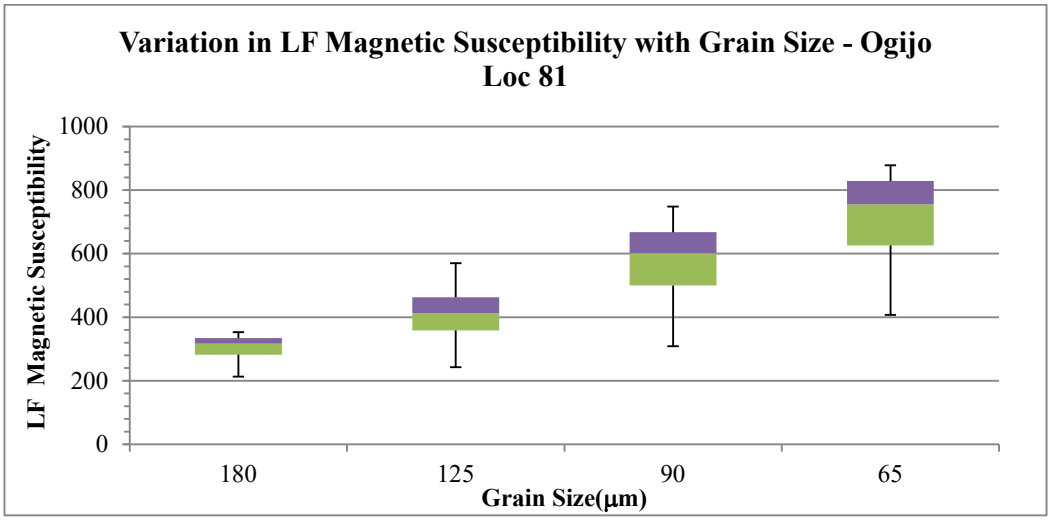
Variation in LF Magnetic Susceptibility with Grain Size - Ogijo Loc 81
LF Magnetic Susceptibility
1000
800
600
400
200
0
180
125
90
65
Grain Size(µm)

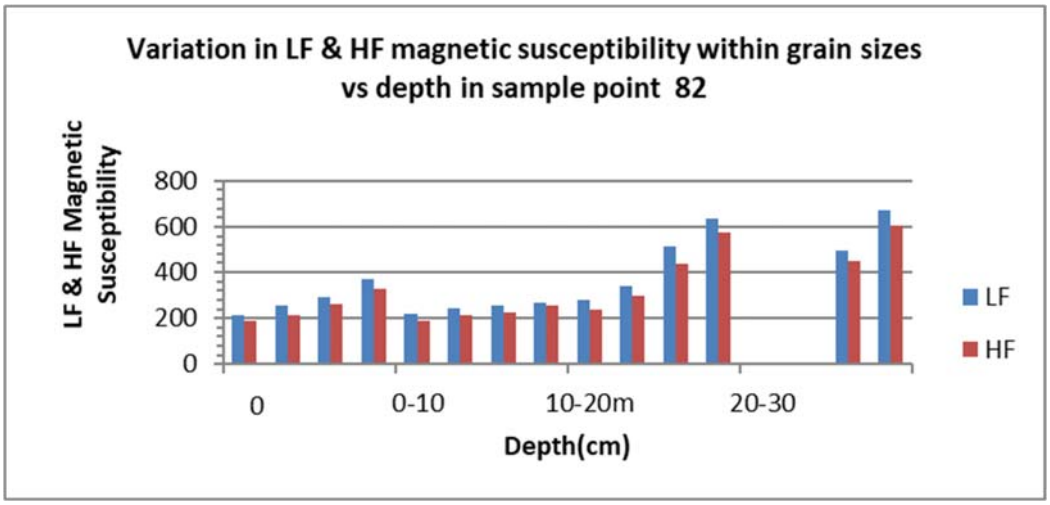
Variation in LF & HF magnetic susceptibility within grain sizes vs depth in sample point 82
LF & HF Magnetic Susceptibility
800
600
400
200
0
0
0-10
10-20m
20-30
Depth(cm)
LF
HF

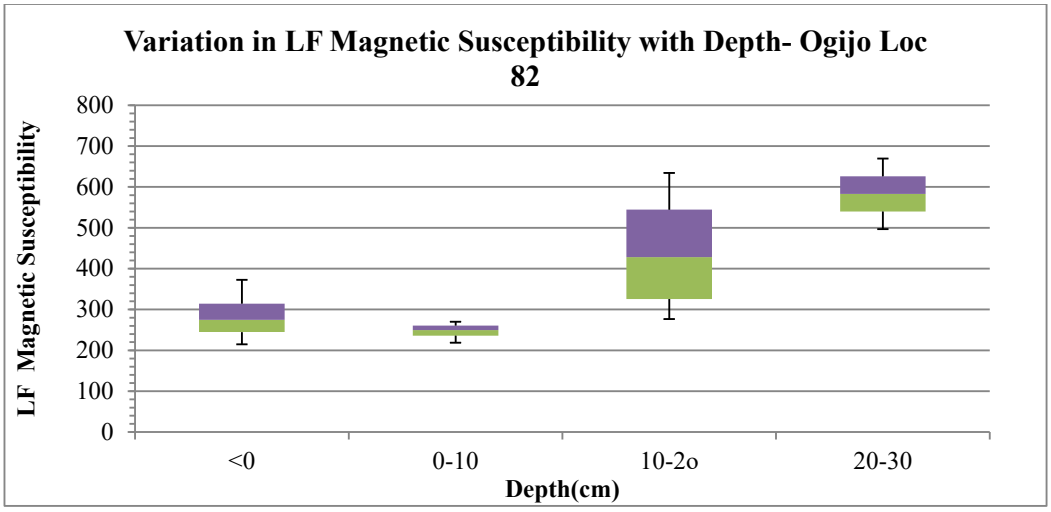
Variation in LF Magnetic Susceptibility with Depth- Ogijo Loc 82
LF Magnetic Susceptibility
800
700
600
500
400
300
200
100
0
<0
0-10
10-2o
20-30
Depth(cm)

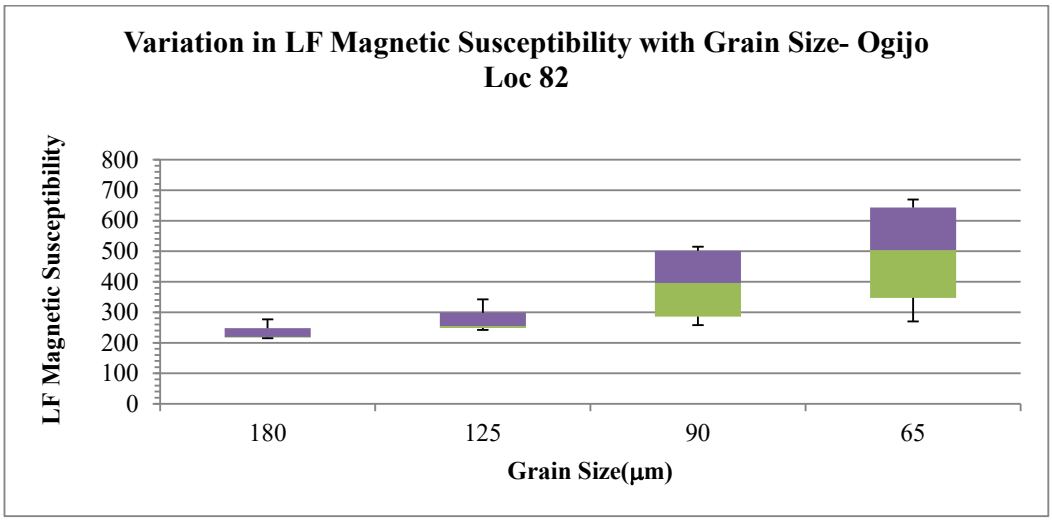
Variation in LF Magnetic Susceptibility with Grain Size- Ogijo Loc 82
LF Magnetic Susceptibility
800
700
600
500
400
300
200
100
0
180
125
90
65
Grain Size(µm)

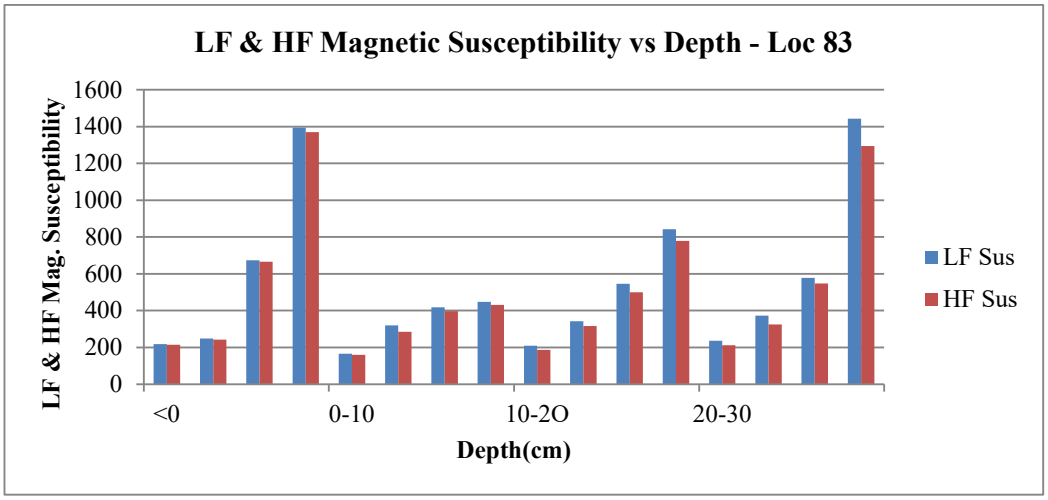
LF & HF Magnetic Susceptibility vs Depth - Loc 83
LF & HF Mag. Susceptibility
1600
1400
1200
1000
800
600
400
200
0
<0
0-10
10-2O
20-30
Depth(cm)
LF Sus
HF Sus

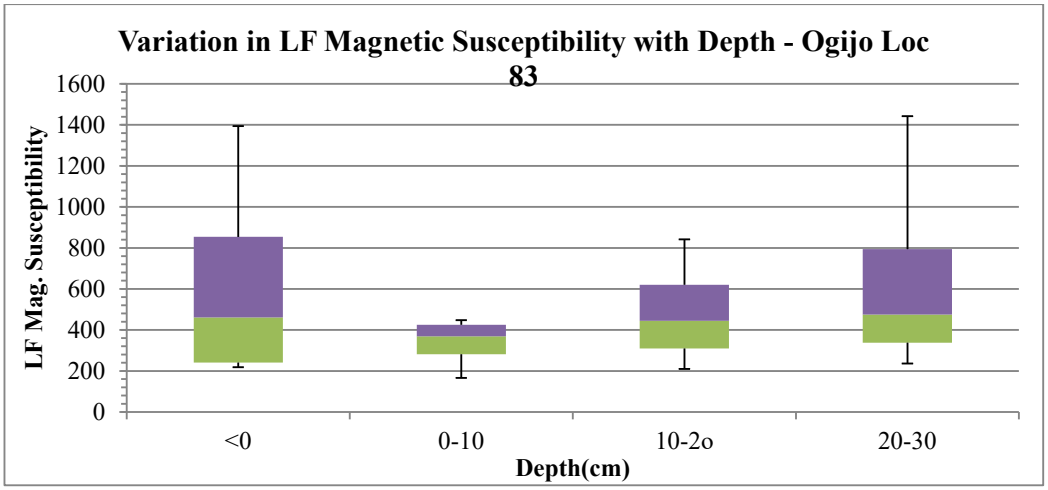
Variation in LF Magnetic Susceptibility with Depth - Ogijo Loc 83
LF Mag. Susceptibility
1600
1400
1200
1000
800
600
400
200
0
<0
0-10
10-2o
20-30
Depth(cm)

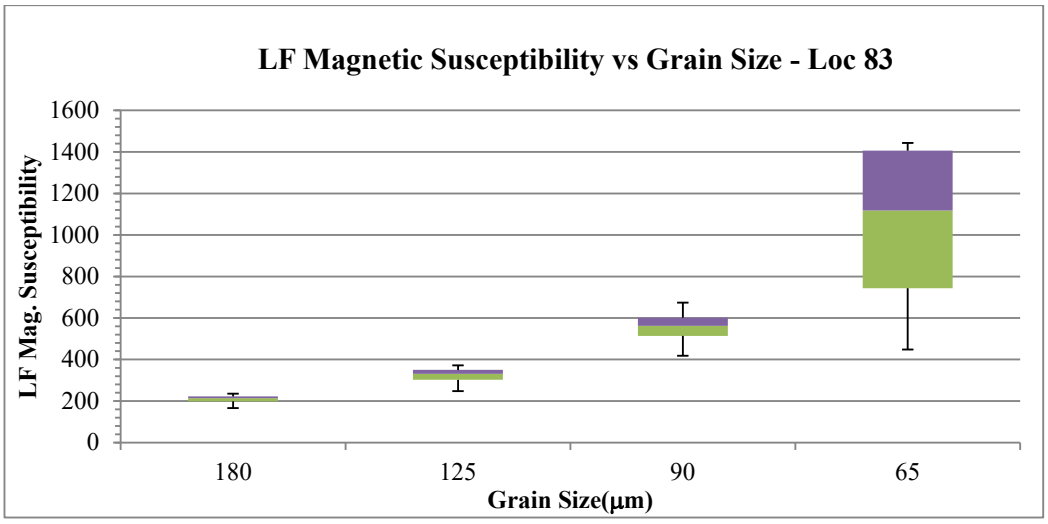
LF Magnetic Susceptibility vs Grain Size - Loc 83
LF Mag. Susceptibility
1600
1400
1200
1000
800
600
400
200
0
180
125
90
65
Grain Size(µm)

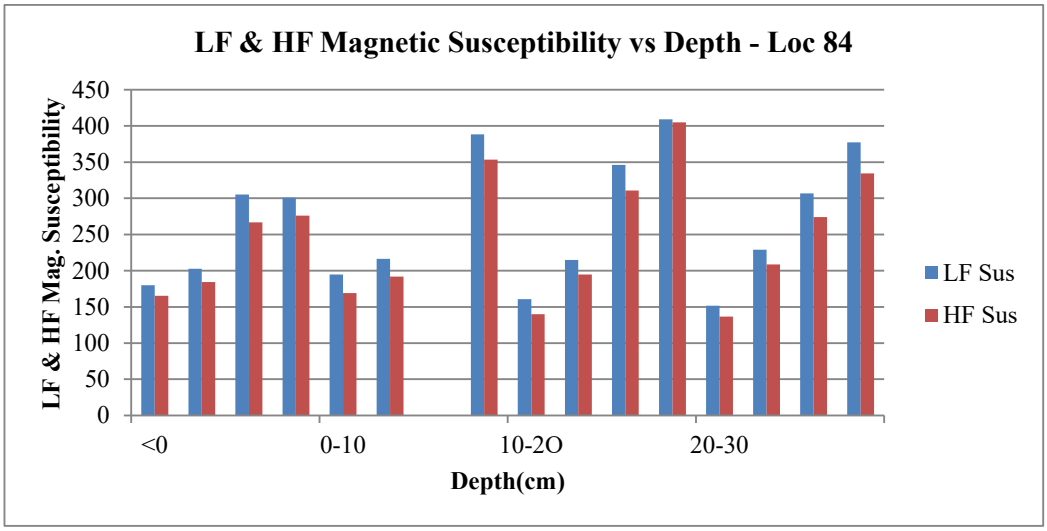
LF & HF Magnetic Susceptibility vs Depth - Loc 84
LF & HF Mag. Susceptibility
450
400
350
300
250
200
150
100
50
0
<0
0-10
10-2O
20-30
Depth(cm)
LF Sus
HF Sus

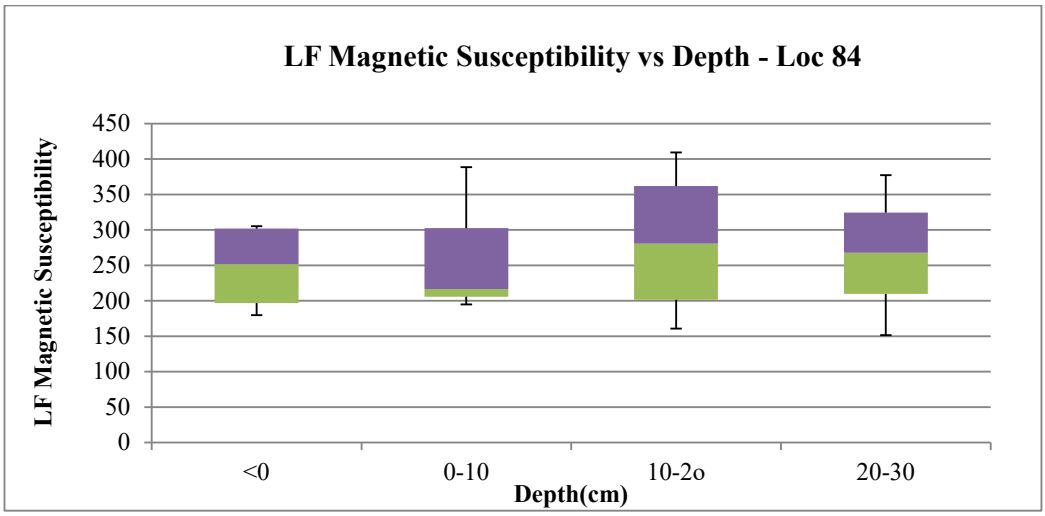
LF Magnetic Susceptibility vs Depth - Loc 84
LF Magnetic Susceptibility
450
400
350
300
250
200
150
100
50
0
<0
0-10
10-2o
20-30
Depth(cm)

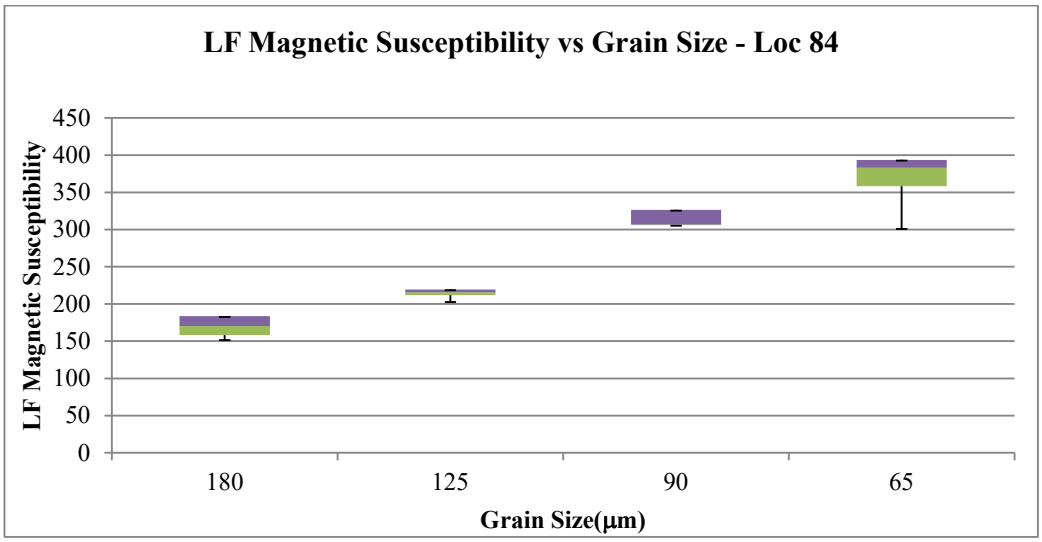
LF Magnetic Susceptibility vs Grain Size - Loc 84
LF Magnetic Susceptibility
450
400
350
300
250
200
150
100
50
0
180
125
90
65
Grain Size(µm)

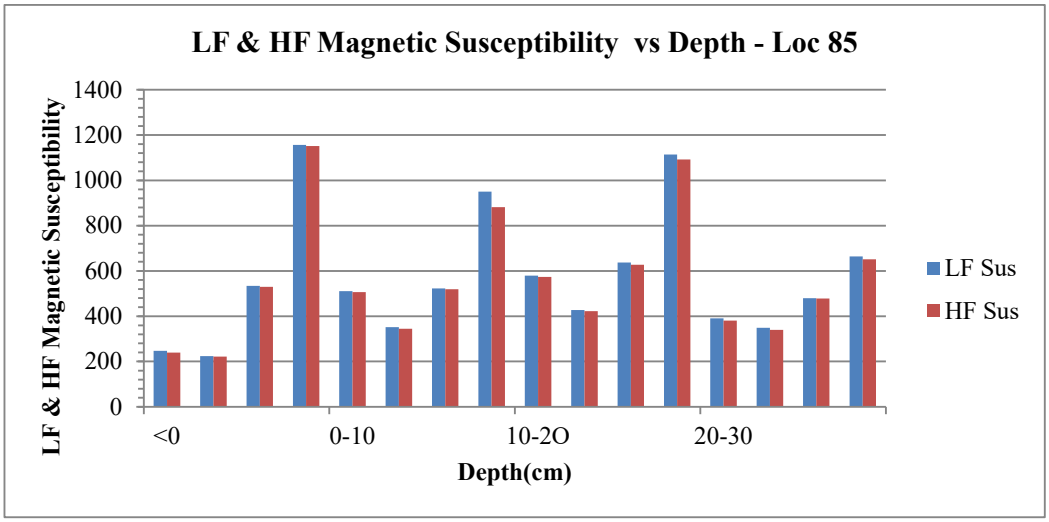
LF & HF Magnetic Susceptibility vs Depth - Loc 85
LF & HF Magnetic Susceptibility
1400
1200
1000
800
600
400
200
0
<0
0-10
10-2O
20-30
Depth(cm)
LF Sus
HF Sus

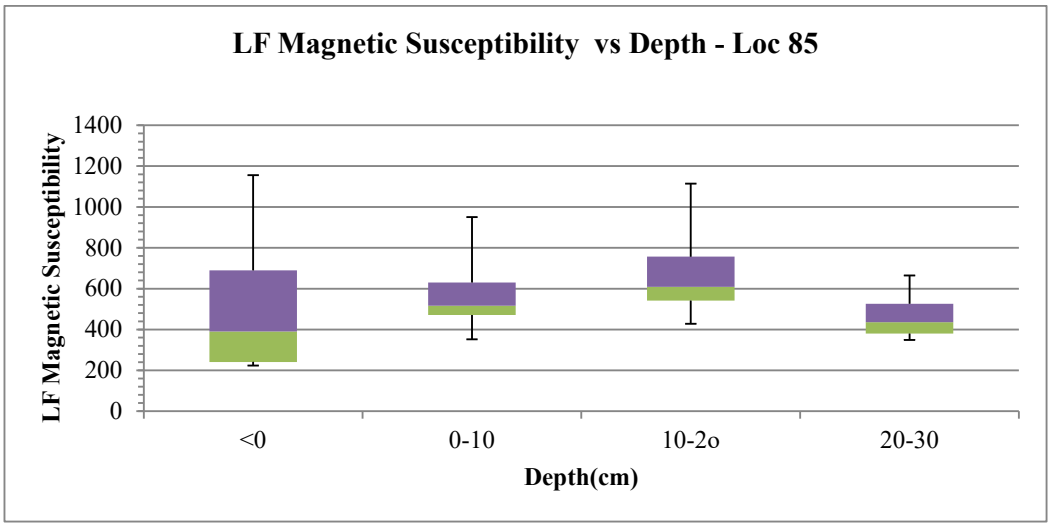
LF Magnetic Susceptibility vs Depth - Loc 85
LF Magnetic Susceptibility
1400
1200
1000
800
600
400
200
0
<0
0-10
10-2o
20-30
Depth(cm)

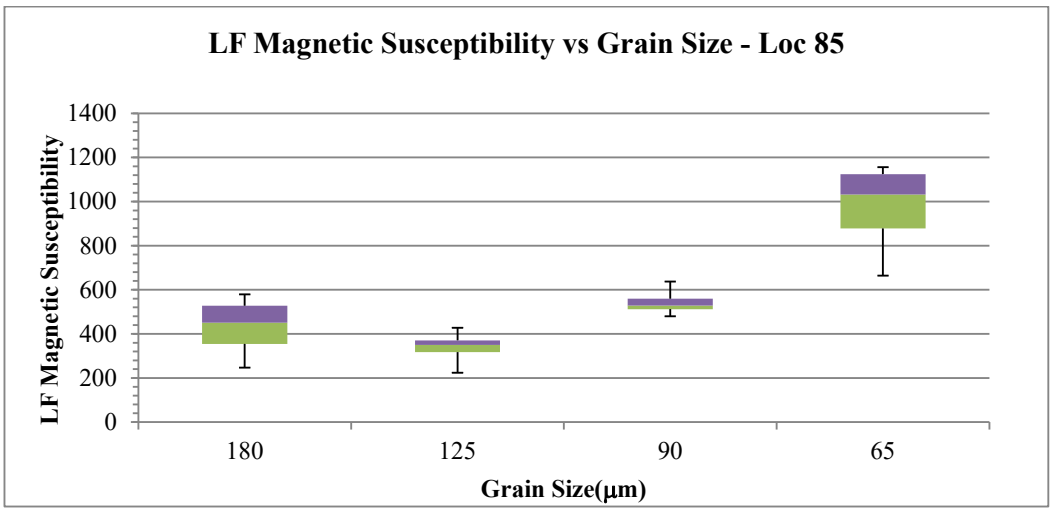
LF Magnetic Susceptibility vs Grain Size - Loc 85
LF Magnetic Susceptibility
1400
1200
1000
800
600
400
200
0
180
125
90
65
Grain Size(µm)

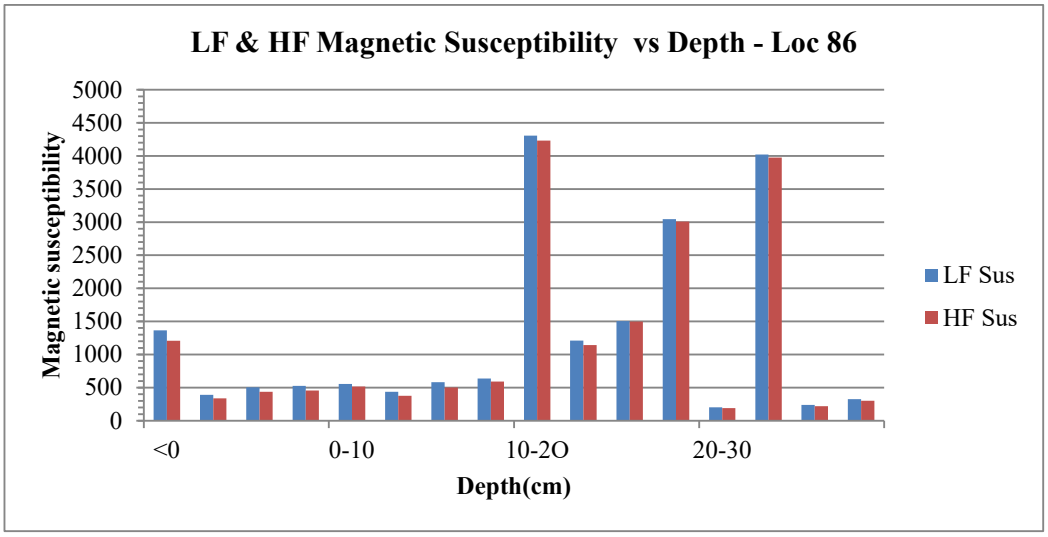
LF & HF Magnetic Susceptibility vs Depth - Loc 86
Magnetic susceptibility
5000
4500
4000
3500
3000
2500
2000
1500
1000
500
0
<0
0-10
10-2O
20-30
Depth(cm)
LF Sus
HF Sus

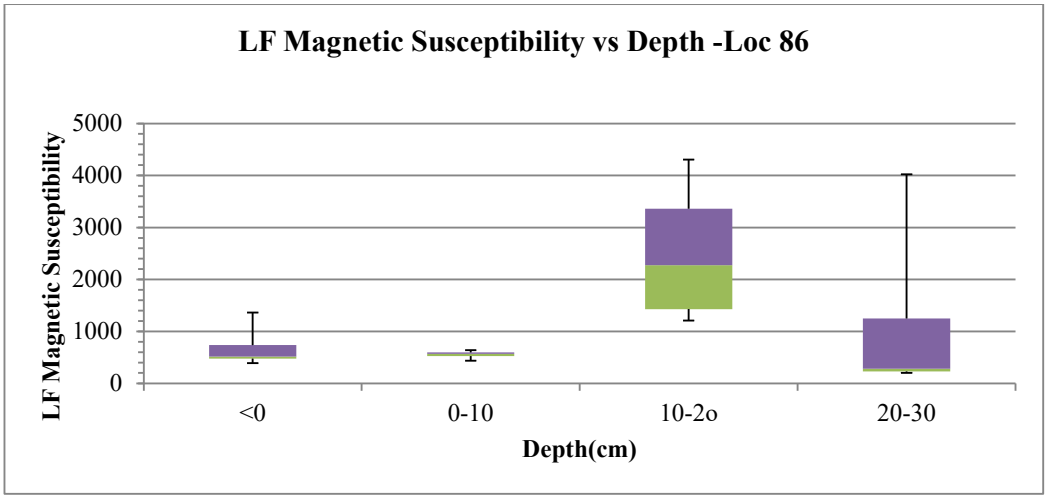
LF Magnetic Susceptibility vs Depth -Loc 86
LF Magnetic Susceptibility
5000
4000
3000
2000
1000
0
<0
0-10
10-2o
20-30
Depth(cm)

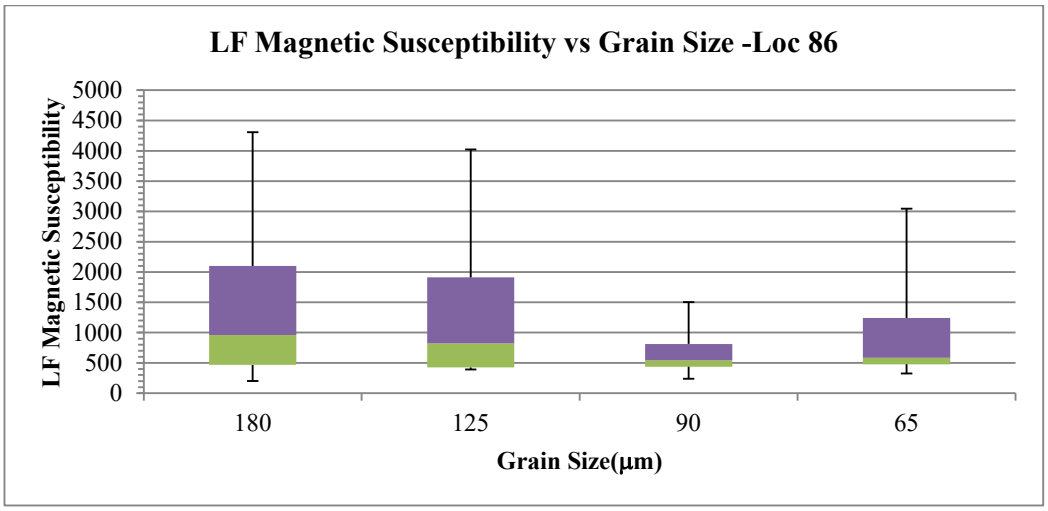
LF Magnetic Susceptibility vs Grain Size -Loc 86
LF Magnetic Susceptibility
5000
4500
4000
3500
3000
2500
2000
1500
1000
500
0
180
125
90
65
Grain Size(µm)

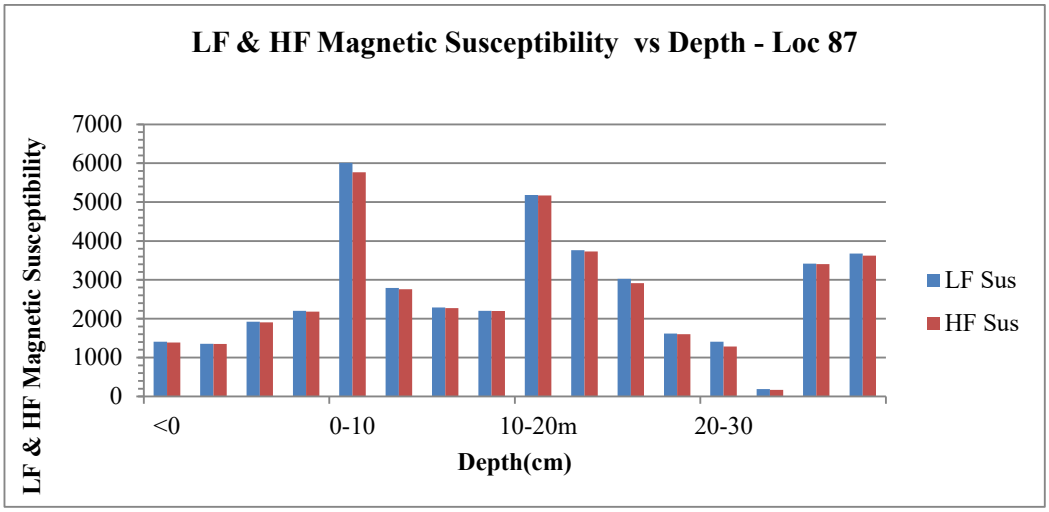
LF & HF Magnetic Susceptibility vs Depth - Loc 87
LF & HF Magnetic Susceptibility
7000
6000
5000
4000
3000
2000
1000
0
<0
0-10
10-20m
20-30
Depth(cm)
LF Sus
HF Sus

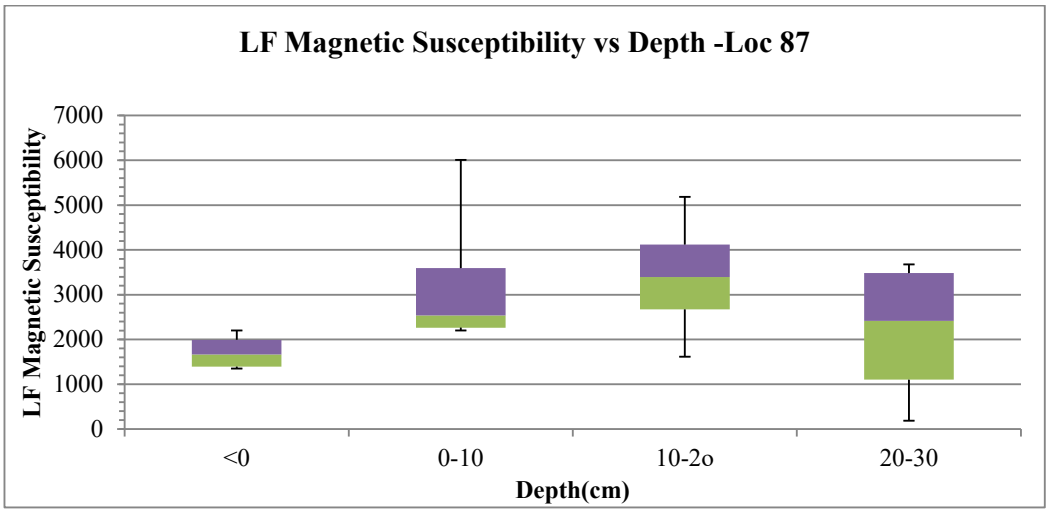
LF Magnetic Susceptibility vs Depth -Loc 87
LF Magnetic Susceptibility
7000
6000
5000
4000
3000
2000
1000
0
<0
0-10
10-2o
20-30
Depth(cm)

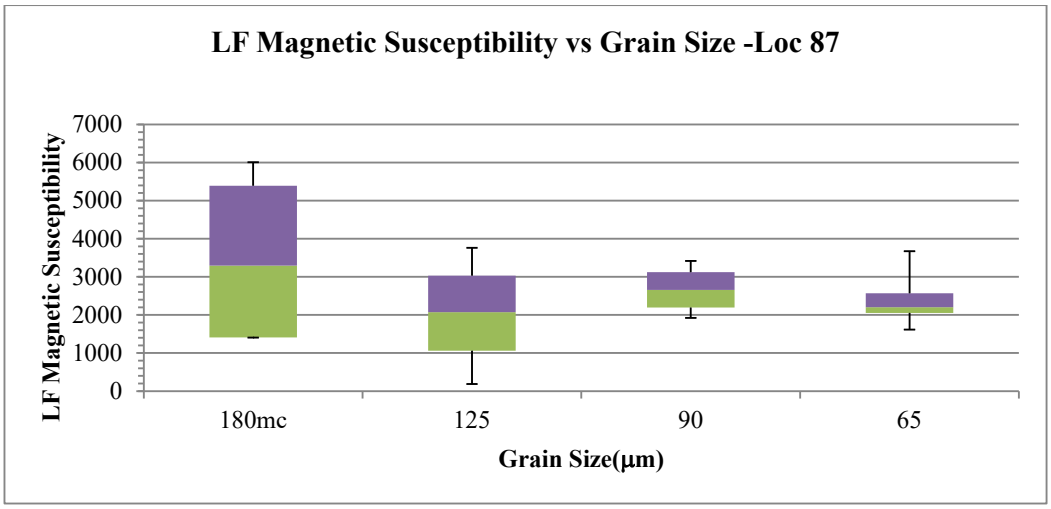
LF Magnetic Susceptibility vs Grain Size -Loc 87
LF Magnetic Susceptibility
7000
6000
5000
4000
3000
2000
1000
0
180mc
125
90
65
Grain Size(µm)

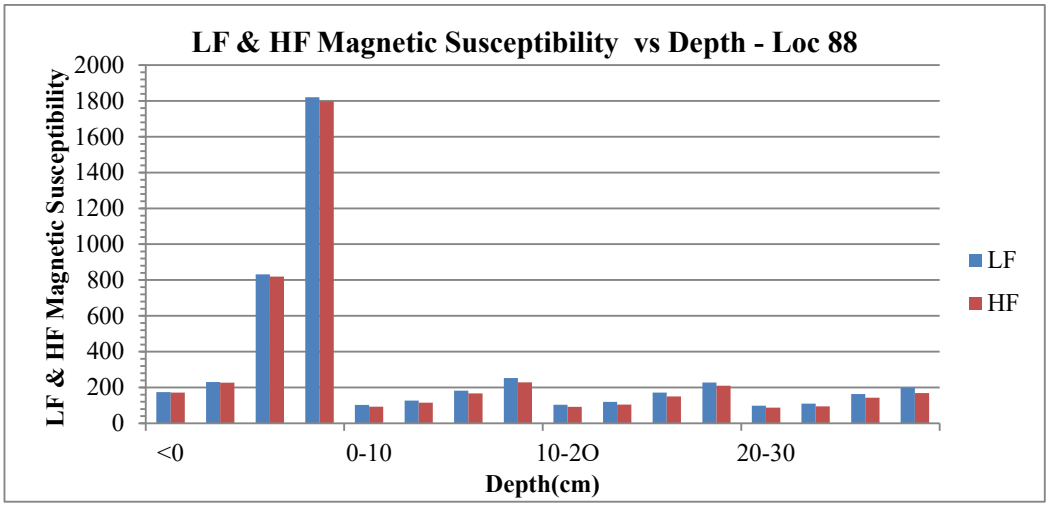
LF & HF Magnetic Susceptibility vs Depth - Loc 88
LF & HF Magnetic Susceptibility
2000
1800
1600
1400
1200
1000
800
600
400
200
0
<0
0-10
10-2O
20-30
Depth(cm)
LF
HF

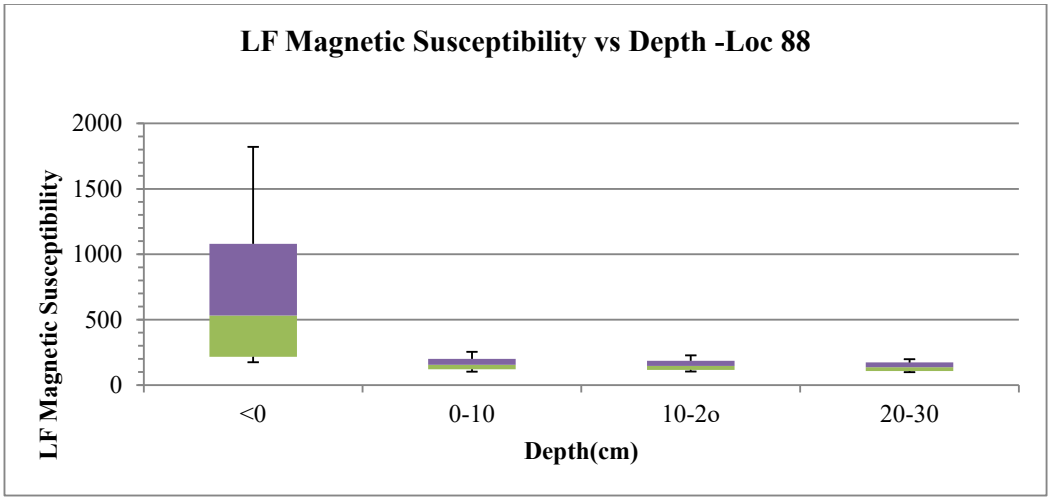
LF Magnetic Susceptibility vs Depth -Loc 88
LF Magnetic Susceptibility
2000
1500
1000
500
0
<0
0-10
10-2o
20-30
Depth(cm)

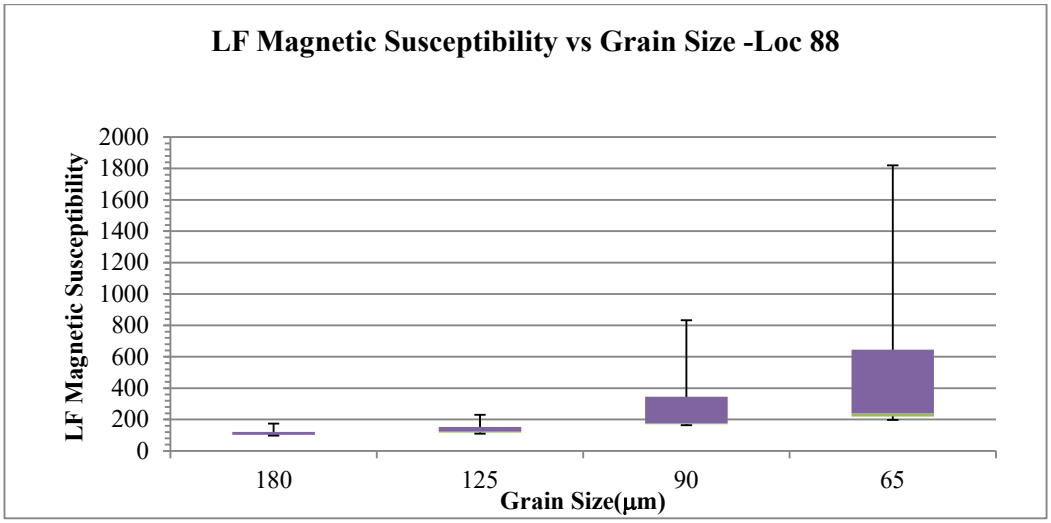
LF Magnetic Susceptibility vs Grain Size -Loc 88
LF Magnetic Susceptibility
2000
1800
1600
1400
1200
1000
800
600
400
200
0
180
125
90
65
Grain Size(µm)

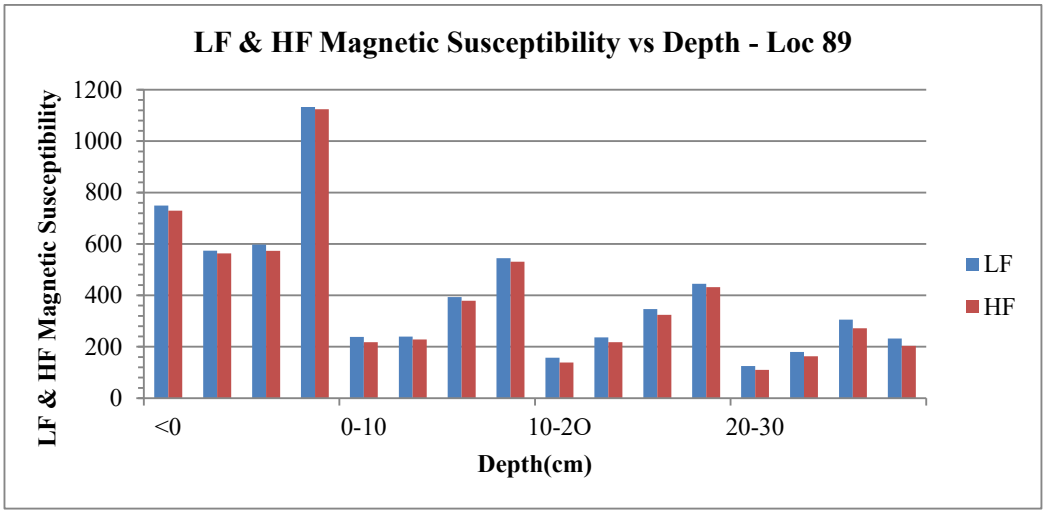
LF & HF Magnetic Susceptibility vs Depth - Loc 89
LF & HF Magnetic Susceptibility
1200
1000
800
600
400
200
0
<0
0-10
10-2O
20-30
Depth(cm)
LF
HF

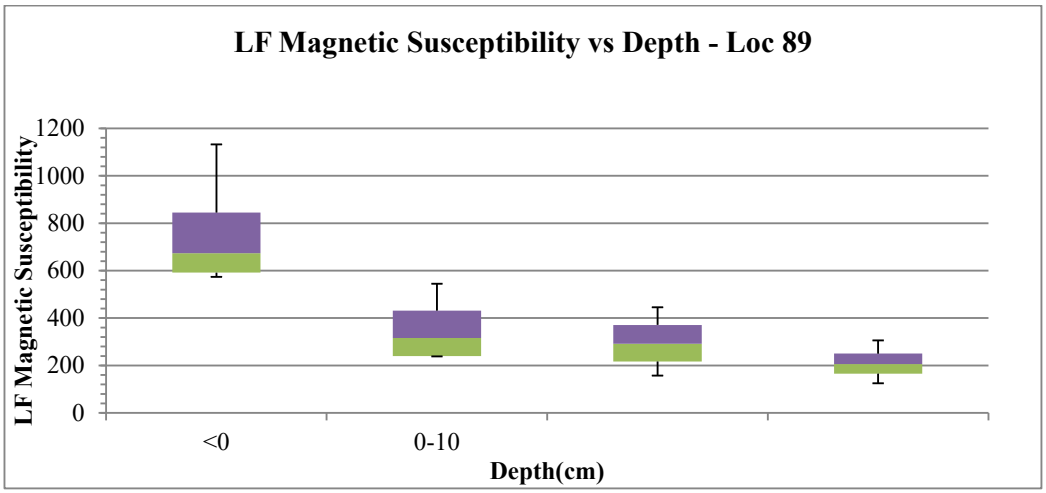
LF Magnetic Susceptibility vs Depth - Loc 89
LF Magnetic Susceptibility
1200
1000
800
600
400
200
0
<0
0-10
Depth(cm)

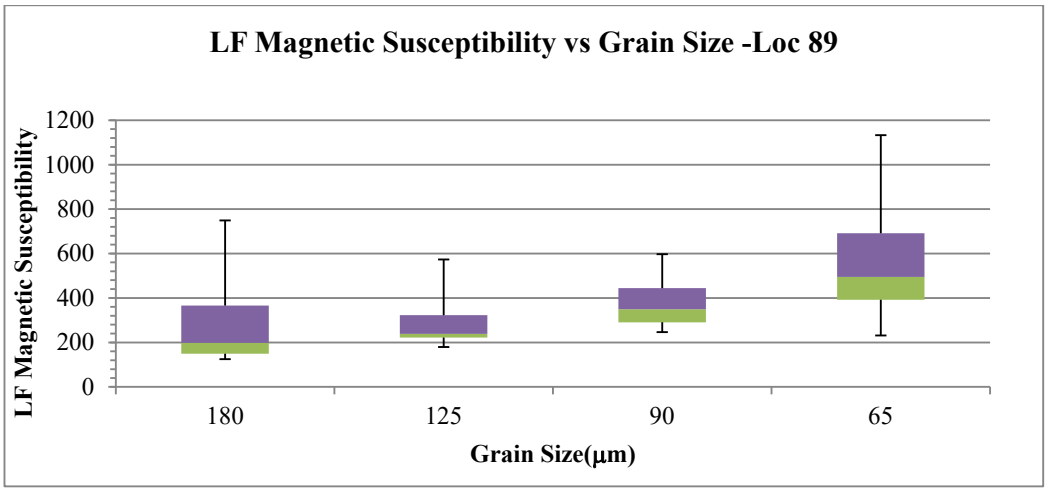
LF Magnetic Susceptibility vs Grain Size -Loc 89
LF Magnetic Susceptibility
1200
1000
800
600
400
200
0
180
125
90
65
Grain Size(µm)

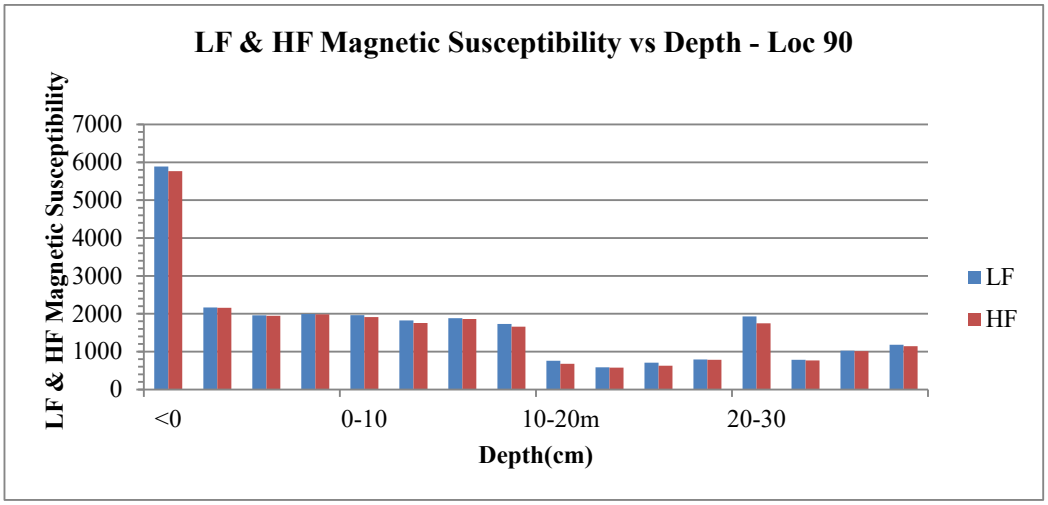
LF & HF Magnetic Susceptibility vs Depth - Loc 90
LF & HF Magnetic Susceptibility
7000
6000
5000
4000
3000
2000
1000
0
<0
0-10
10-20m
20-30
Depth(cm)
LF
HF

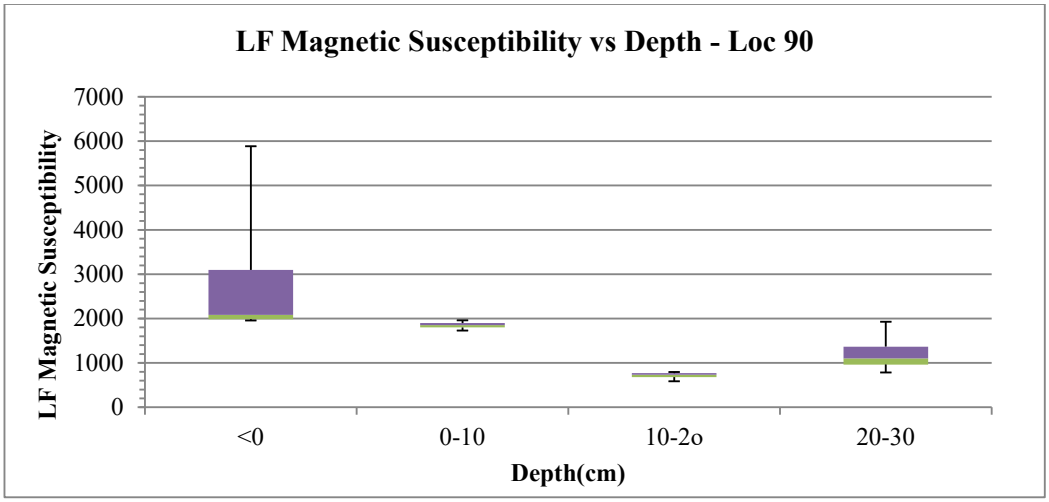
LF Magnetic Susceptibility vs Depth - Loc 90
LF Magnetic Susceptibility
7000
6000
5000
4000
3000
2000
1000
0
<0
0-10
10-2o
20-30
Depth(cm)

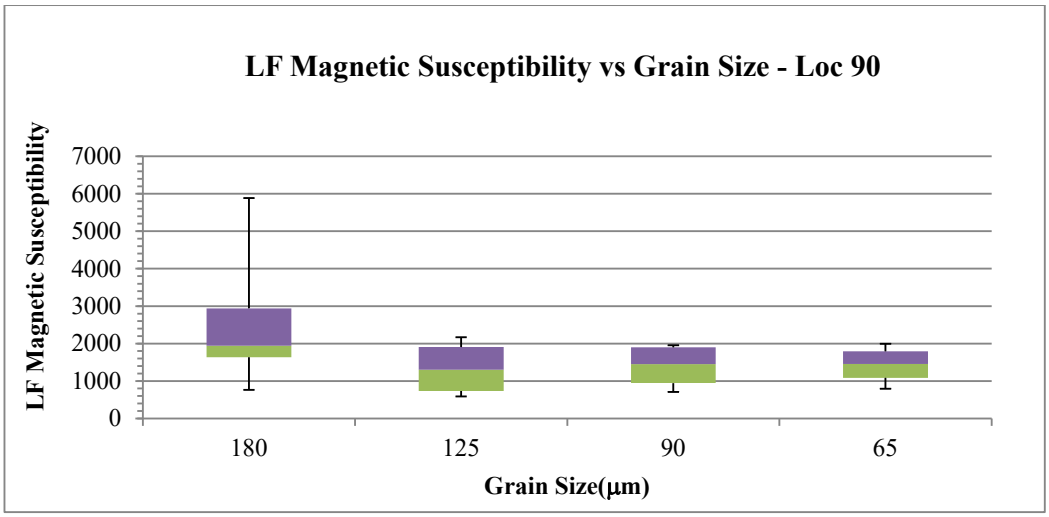
LF Magnetic Susceptibility vs Grain Size - Loc 90
LF Magnetic Susceptibility
7000
6000
5000
4000
3000
2000
1000
0
180
125
90
65
Grain Size(µm)

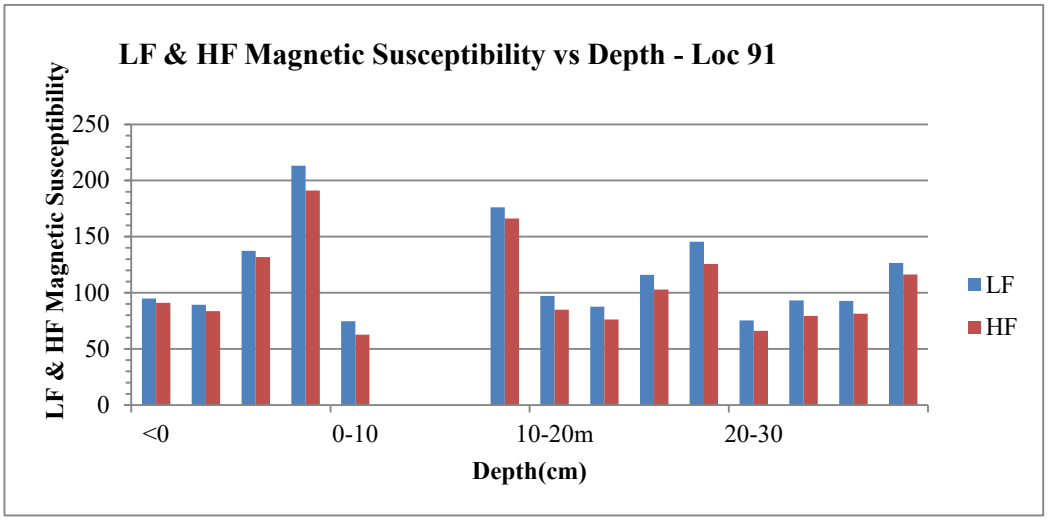
LF & HF Magnetic Susceptibility vs Depth - Loc 91
LF & HF Magnetic Susceptibility
250
200
150
100
50
0
<0
0-10
10-20m
20-30
Depth(cm)
LF
HF

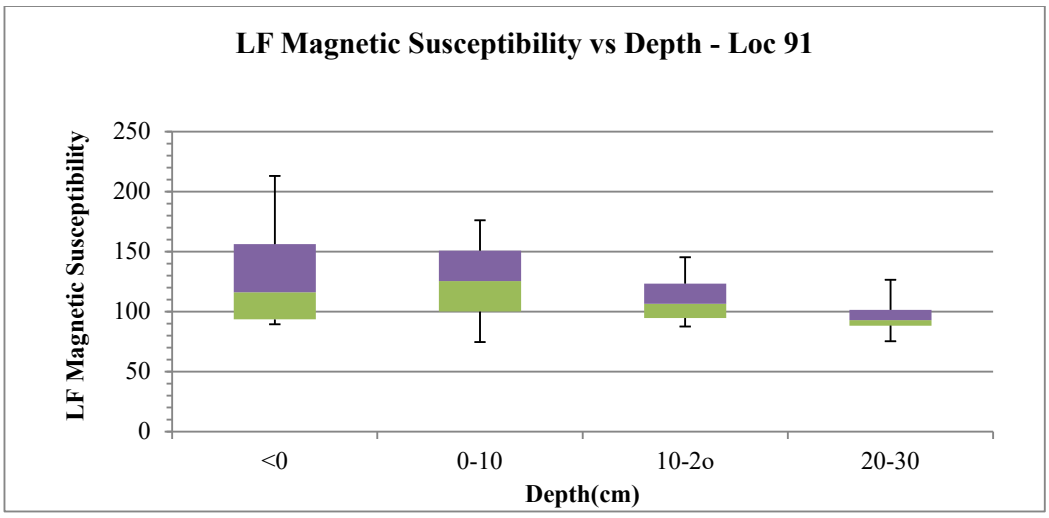
LF Magnetic Susceptibility vs Depth - Loc 91
LF Magnetic Susceptibility
250
200
150
100
50
0
<0
0-10
10-2o
20-30
Depth(cm)

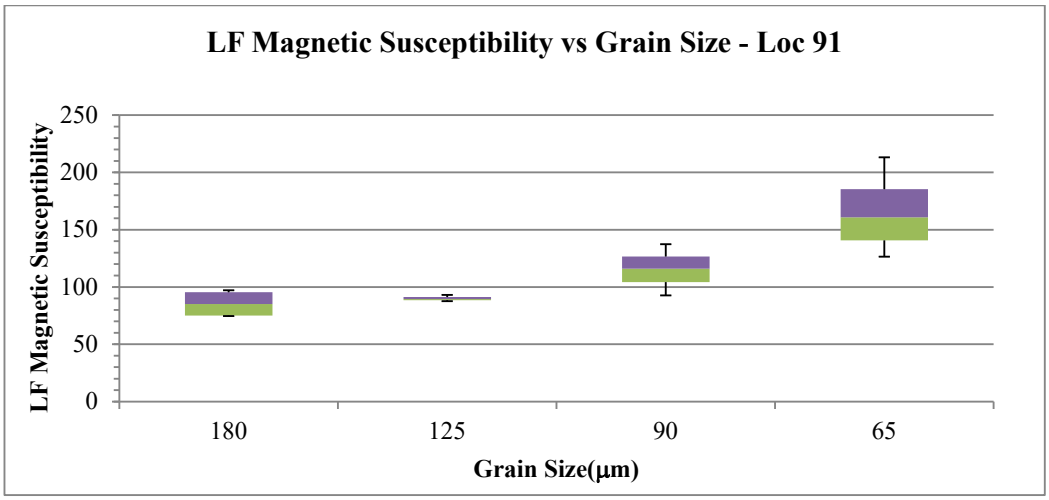
LF Magnetic Susceptibility vs Grain Size - Loc 91
LF Magnetic Susceptibility
250
200
150
100
50
0
180
125
90
65
Grain Size(µm)

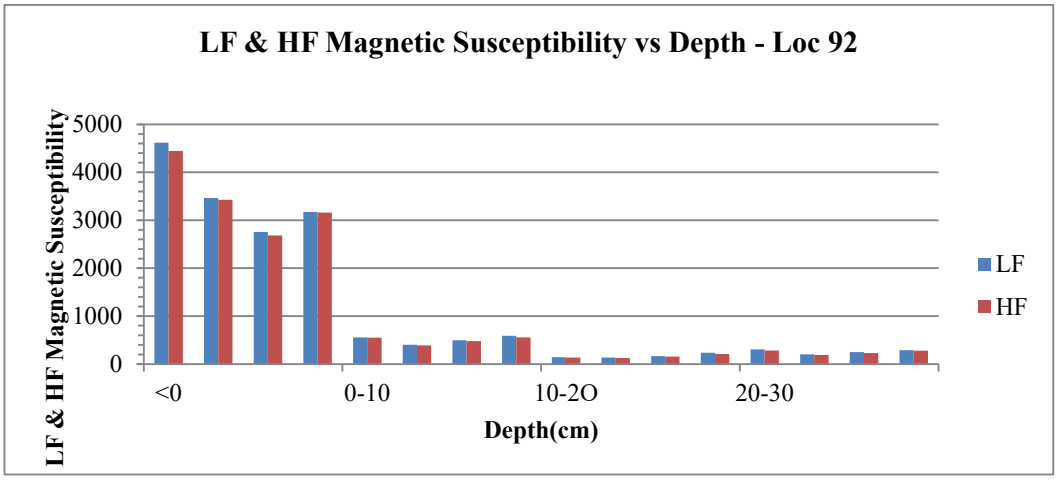
LF & HF Magnetic Susceptibility vs Depth - Loc 92
LF & HF Magnetic Susceptibility
5000
4000
3000
2000
1000
0
<0
0-10
10-2O
20-30
Depth(cm)
LF
HF

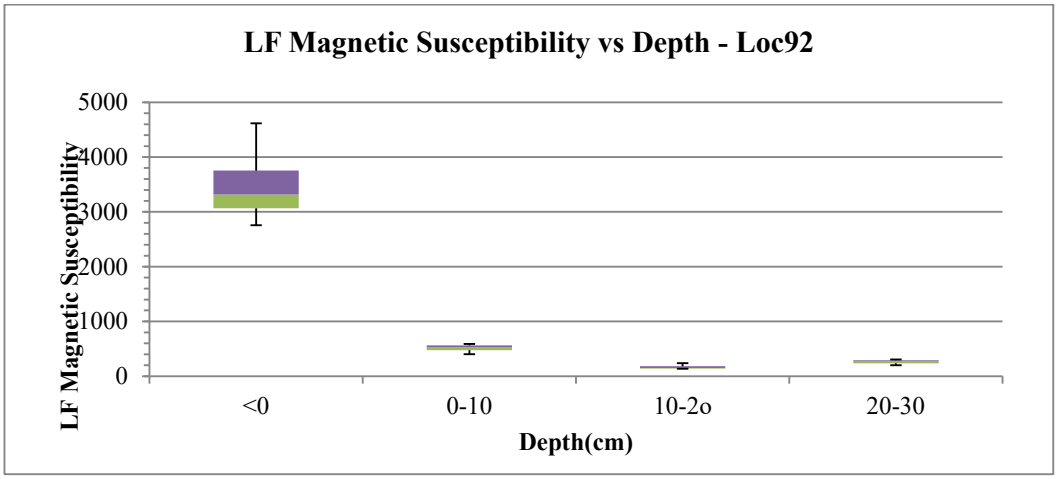
LF Magnetic Susceptibility vs Depth - Loc92
LF Magnetic Susceptibility
5000
4000
3000
2000
1000
0
<0
0-10
10-2o
20-30
Depth(cm)

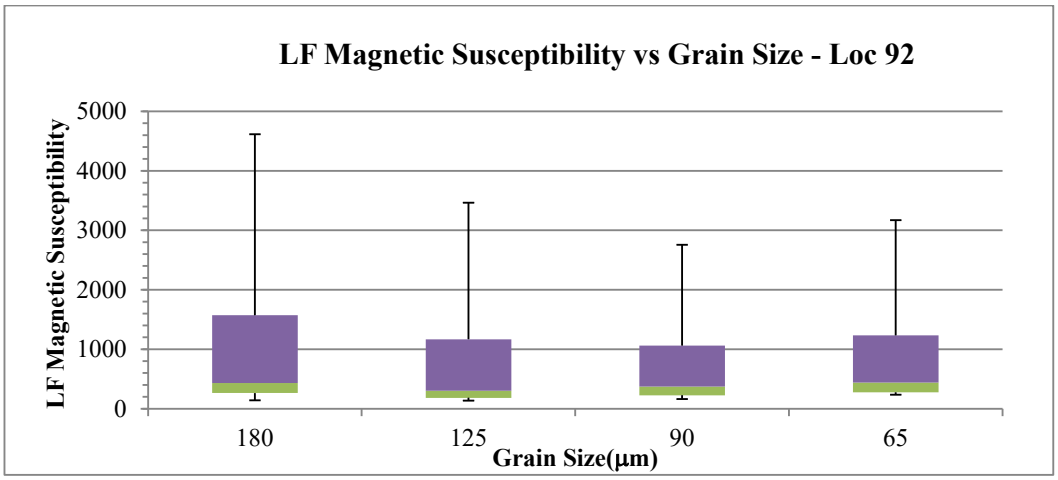
LF Magnetic Susceptibility vs Grain Size - Loc 92
LF Magnetic Susceptibility
5000
4000
3000
2000
1000
0
180
125
90
65
Grain Size(µm)

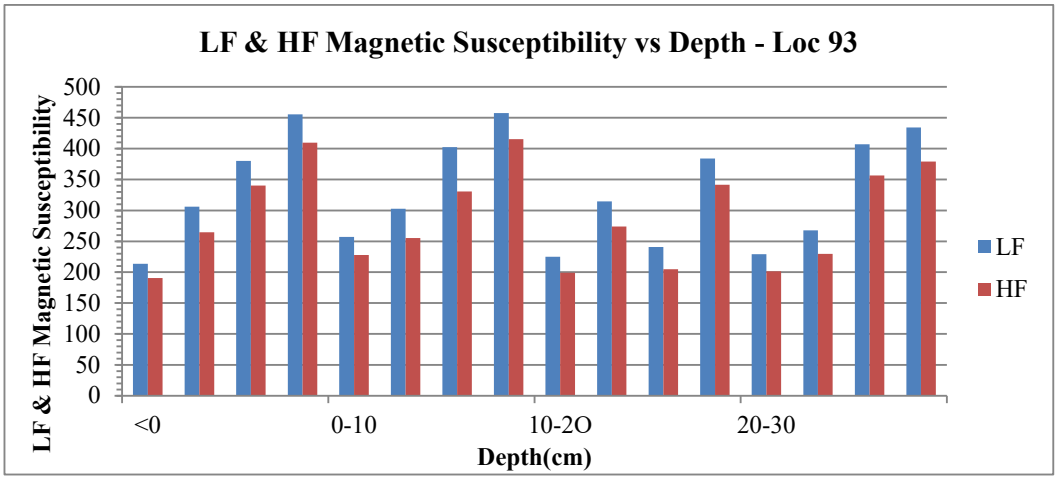
LF & HF Magnetic Susceptibility vs Depth - Loc 93
LF & HF Magnetic Susceptibility
500
450
400
350
300
250
200
150
100
50
0
<0
0-10
10-2O
20-30
Depth(cm)
LF
HF

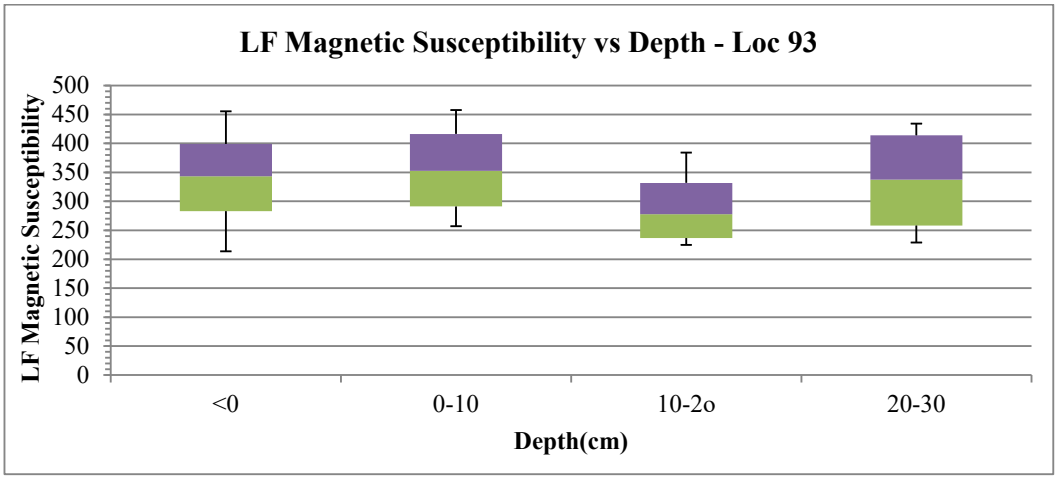
LF Magnetic Susceptibility vs Depth - Loc 93
LF Magnetic Susceptibility
500
450
400
350
300
250
200
150
100
50
0
<0
0-10
10-2o
20-30
Depth(cm)

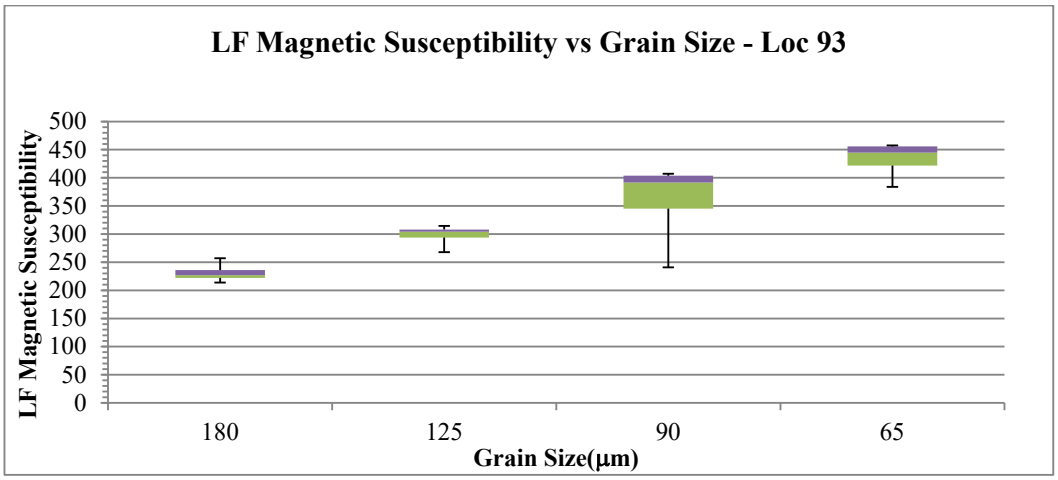
LF Magnetic Susceptibility vs Grain Size - Loc 93
LF Magnetic Susceptibility
500
450
400
350
300
250
200
150
100
50
0
180
125
90
65
Grain Size(µm)

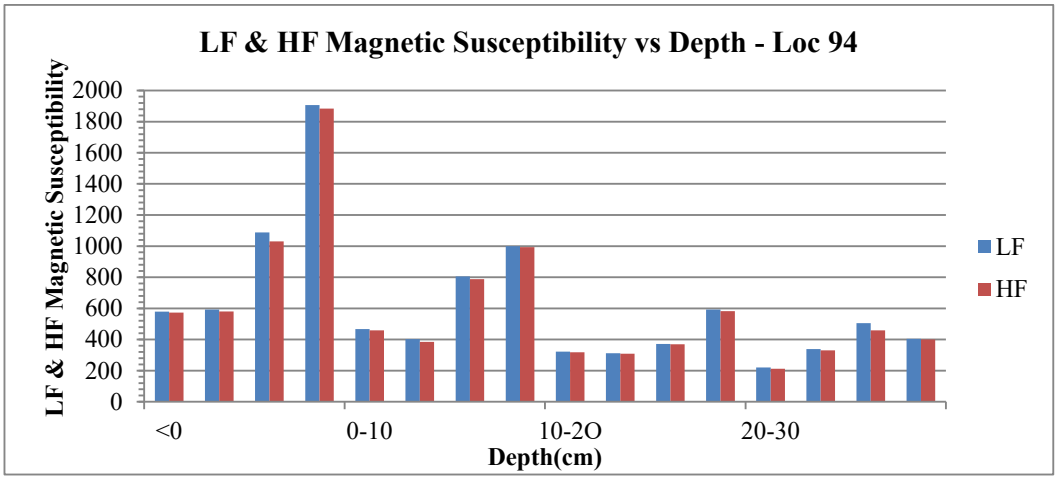
LF & HF Magnetic Susceptibility vs Depth - Loc 94
LF & HF Magnetic Susceptibility
2000
1800
1600
1400
1200
1000
800
600
400
200
0
<0
0-10
10-2O
20-30
Depth(cm)
LF
HF

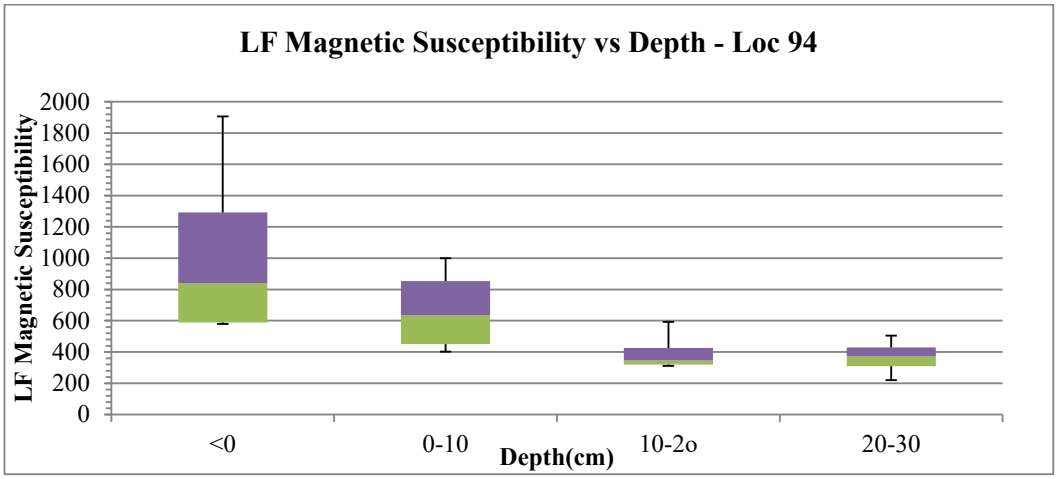
LF Magnetic Susceptibility vs Depth - Loc 94
LF Magnetic Susceptibility
2000
1800
1600
1400
1200
1000
800
600
400
200
0
<0
0-10
10-2o
20-30
Depth(cm)

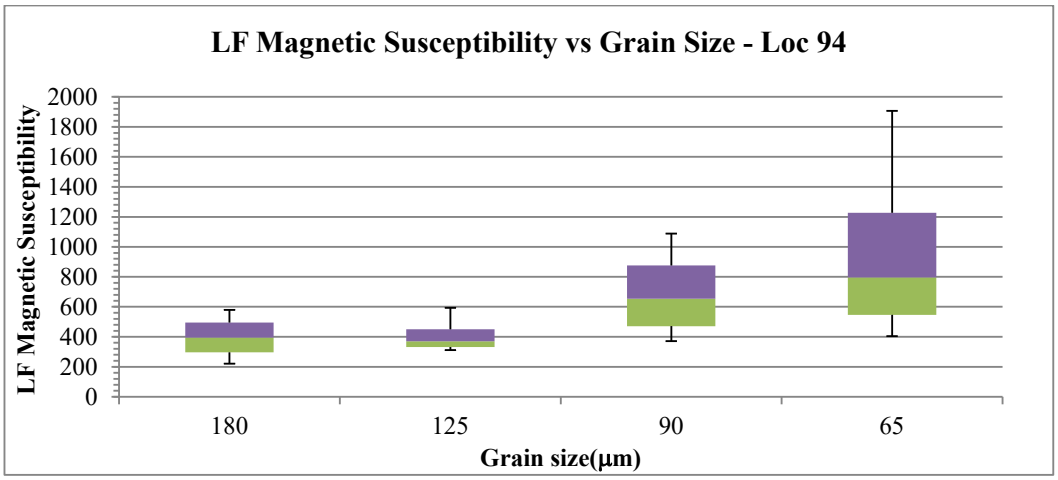
LF Magnetic Susceptibility vs Grain Size - Loc 94
LF Magnetic Susceptibility
2000
1800
1600
1400
1200
1000
800
600
400
200
0
180
125
90
65
Grain size(µm)

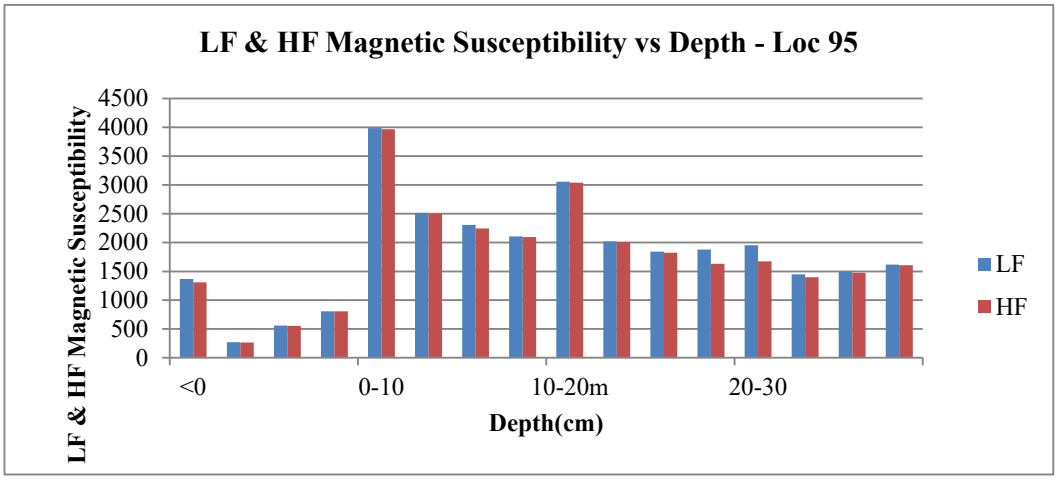
LF & HF Magnetic Susceptibility vs Depth - Loc 95
LF & HF Magnetic Susceptibility
4500
4000
3500
3000
2500
2000
1500
1000
500
0
<0
0-10
10-20m
20-30
Depth(cm)
LF
HF

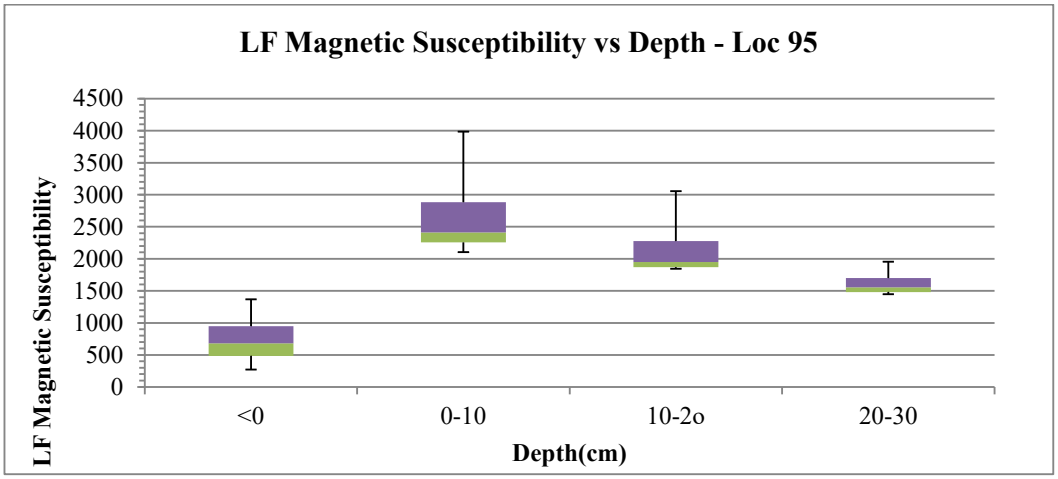
LF Magnetic Susceptibility vs Depth - Loc 95
LF Magnetic Susceptibility
4500
4000
3500
3000
2500
2000
1500
1000
500
0
<0
0-10
10-2o
20-30
Depth(cm)

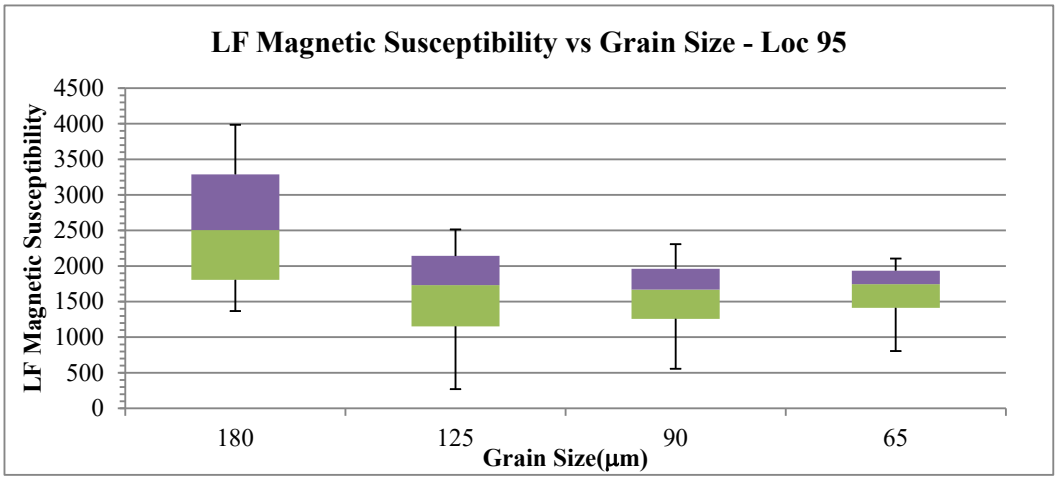
LF Magnetic Susceptibility vs Grain Size - Loc 95
LF Magnetic Susceptibility
4500
4000
3500
3000
2500
2000
1500
1000
500
0
180
125
90
65
Grain Size(µm)

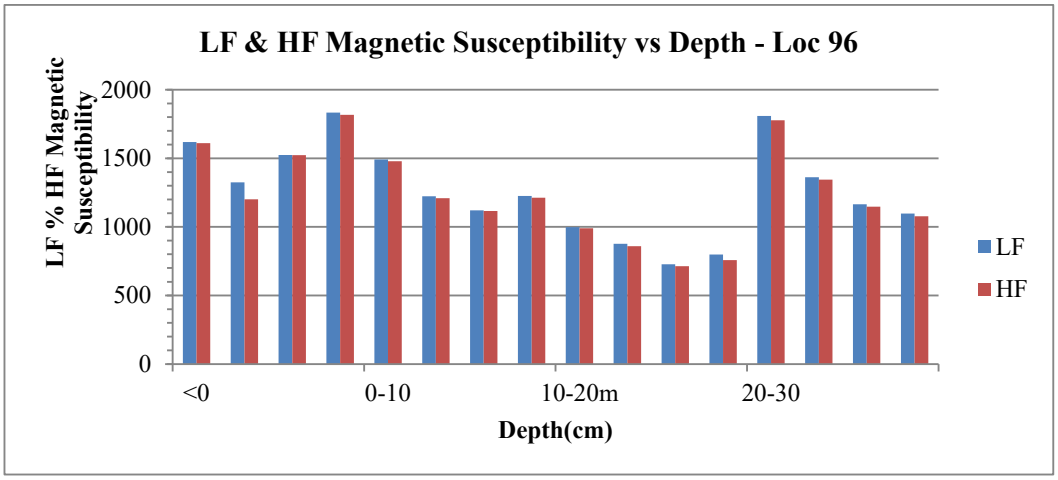
LF & HF Magnetic Susceptibility vs Depth - Loc 96
LF % HF Magnetic Susceptibility
2000
1500
1000
500
0
<0
0-10
10-20m
20-30
Depth(cm)
LF
HF

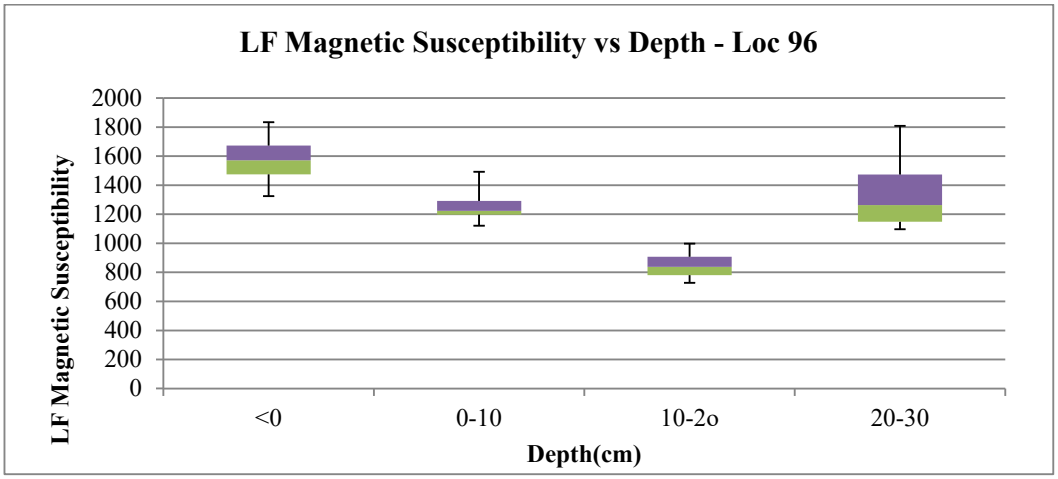
LF Magnetic Susceptibility vs Depth - Loc 96
LF Magnetic Susceptibility
2000
1800
1600
1400
1200
1000
800
600
400
200
0
<0
0-10
10-2o
20-30
Depth(cm)

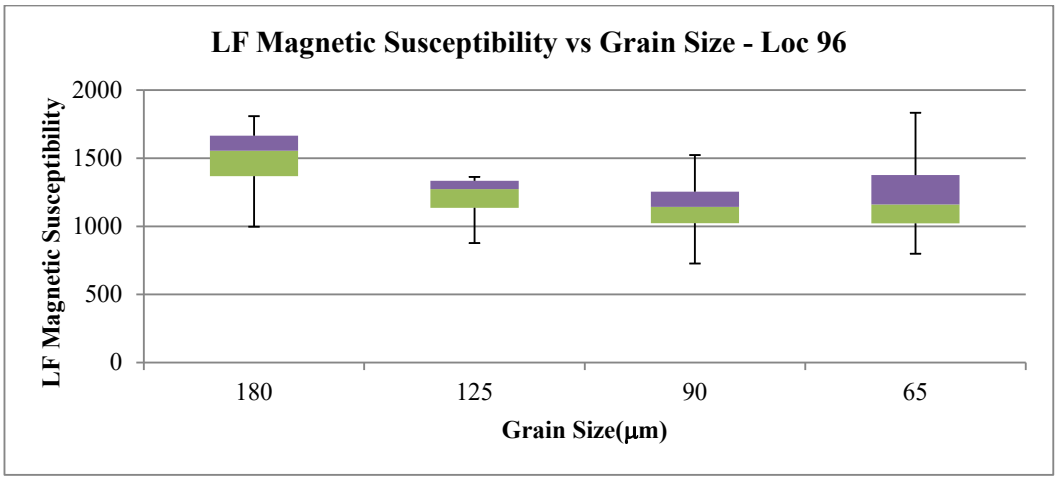
LF Magnetic Susceptibility vs Grain Size - Loc 96
LF Magnetic Susceptibility
2000
1500
1000
500
0
180
125
90
65
Grain Size(µm)

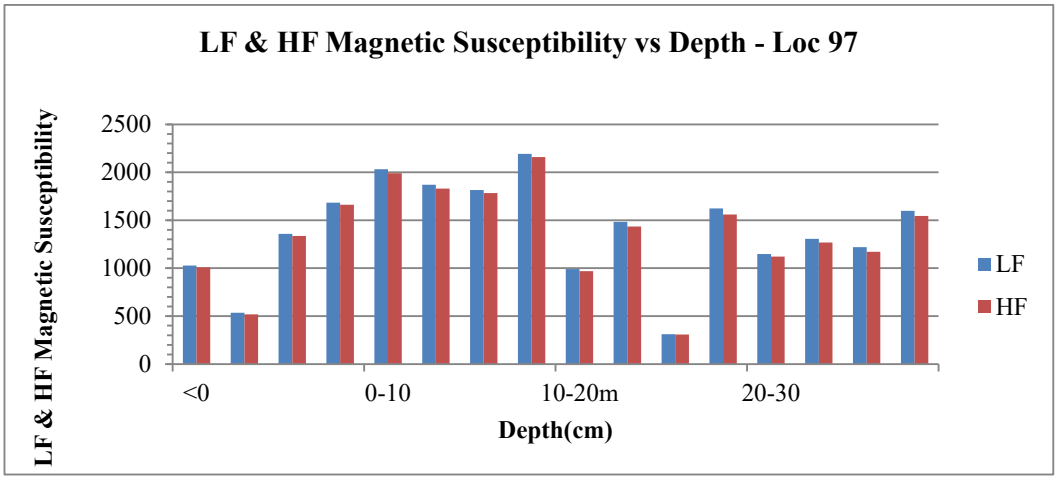
LF & HF Magnetic Susceptibility vs Depth - Loc 97
LF & HF Magnetic Susceptibility
2500
2000
1500
1000
500
0
<0
0-10
10-20m
20-30
Depth(cm)
LF
HF

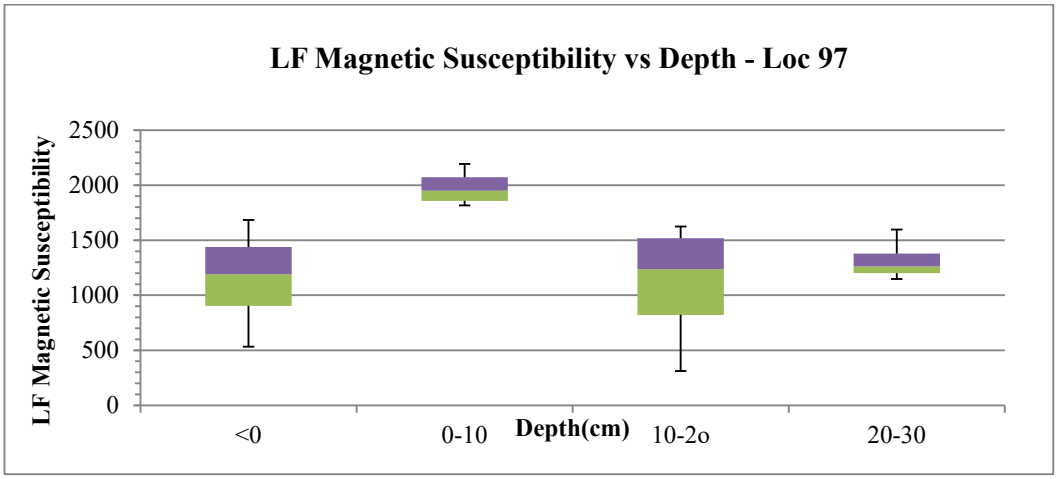
LF Magnetic Susceptibility vs Depth - Loc 97
LF Magnetic Susceptibility
2500
2000
1500
1000
500
0
<0
0-10
Depth(cm)
10-2o
20-30

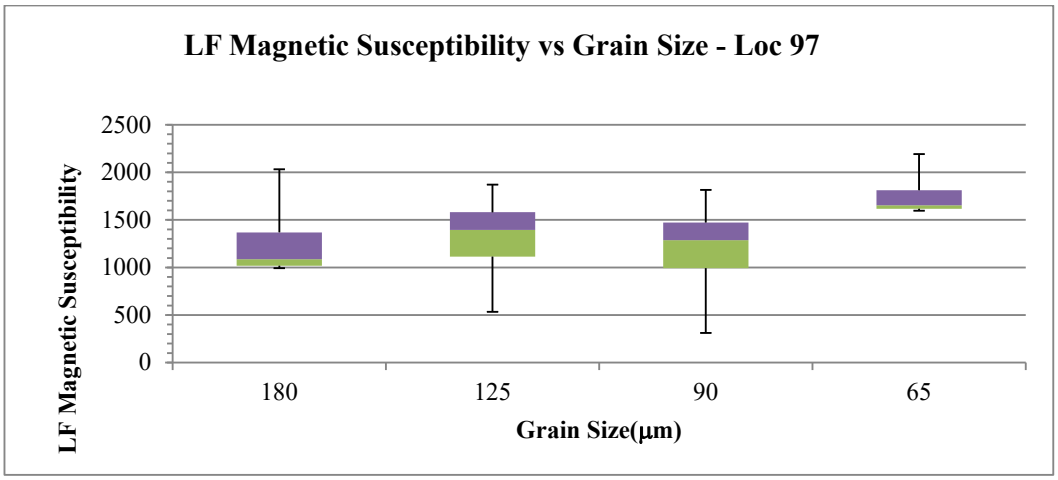
LF Magnetic Susceptibility vs Grain Size - Loc 97
LF Magnetic Susceptibility
2500
2000
1500
1000
500
0
180
125
90
65
Grain Size(µm)

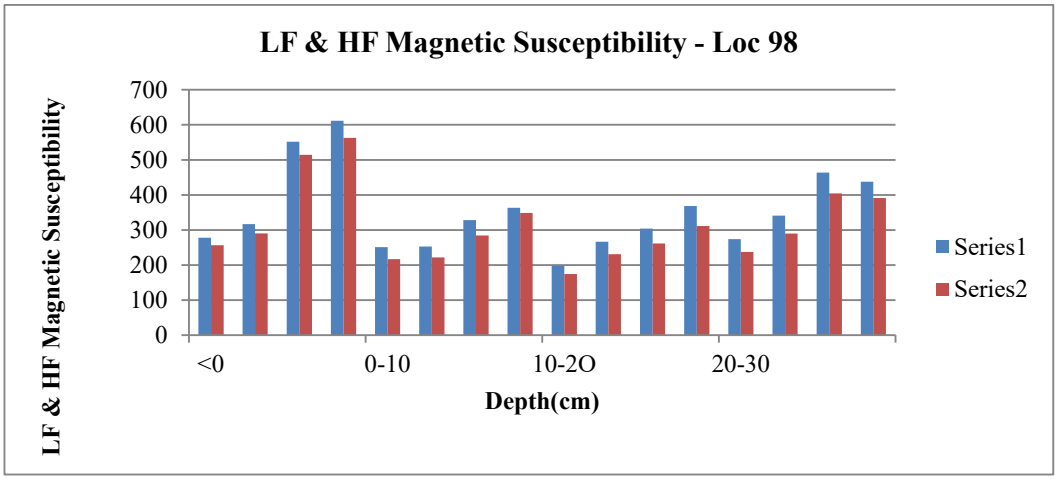
LF & HF Magnetic Susceptibility - Loc 98
LF & HF Magnetic Susceptibility
700
600
500
400
300
200
100
0
<0
0-10
10-2O
20-30
Depth(cm)
Series1
Series2

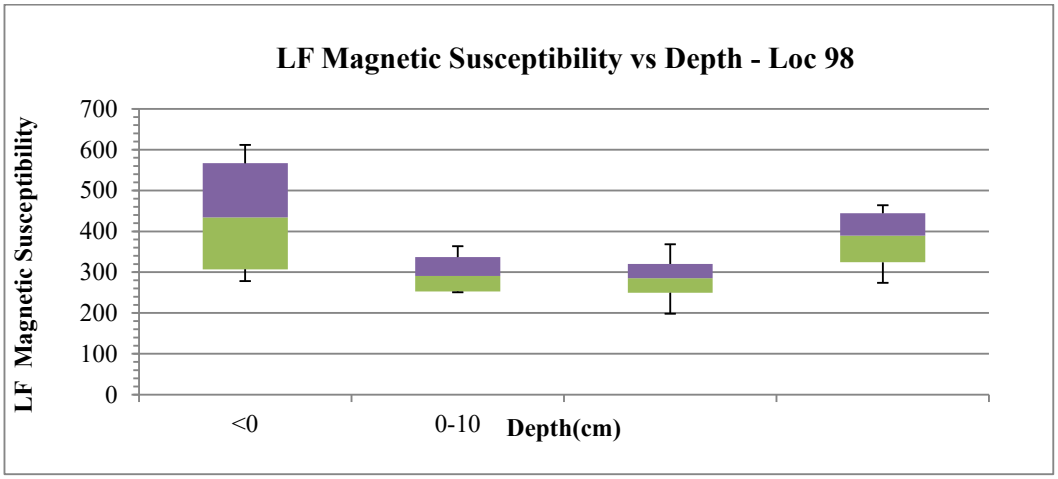
LF Magnetic Susceptibility vs Depth - Loc 98
LF Magnetic Susceptibility
700
600
500
400
300
200
100
0
<0
0-10
Depth(cm)

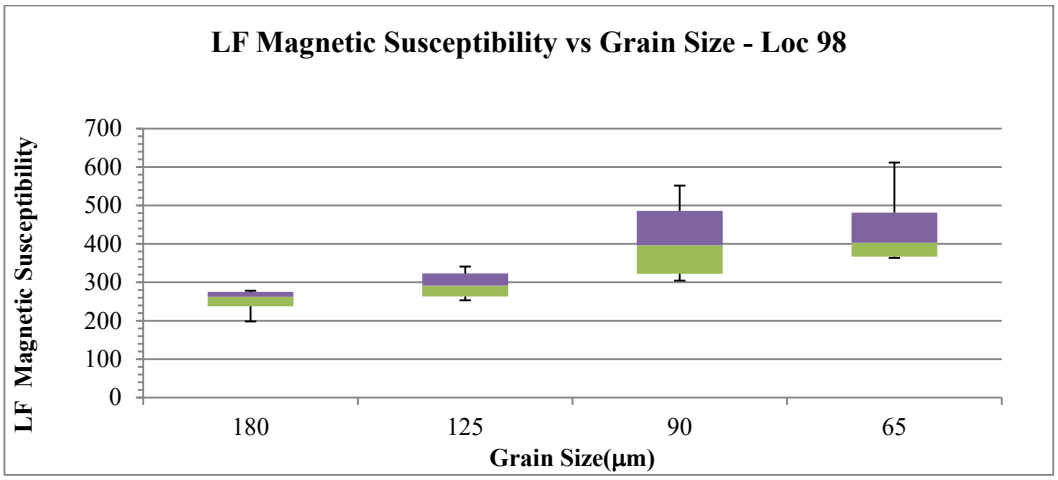
LF Magnetic Susceptibility vs Grain Size - Loc 98
LF Magnetic Susceptibility
700
600
500
400
300
200
100
0
180
125
90
65
Grain Size(µm)

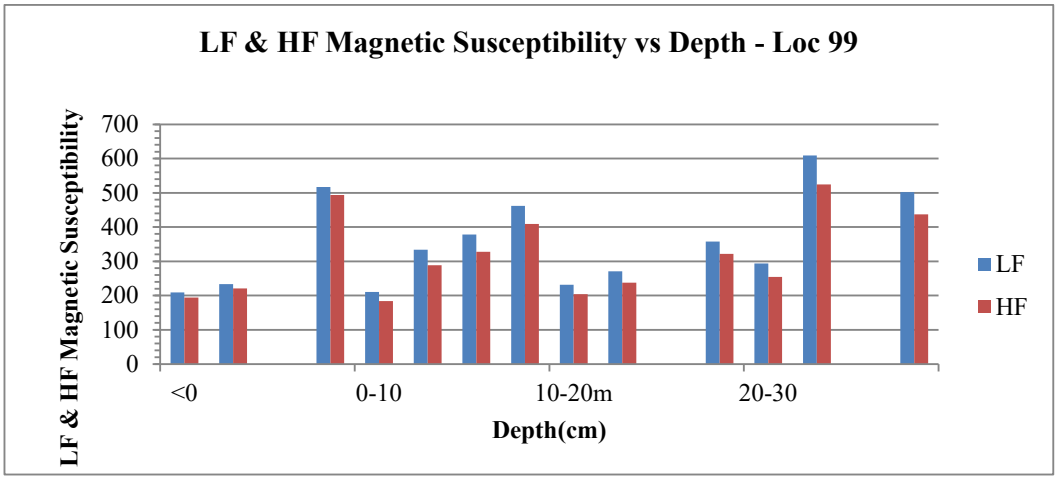
LF & HF Magnetic Susceptibility vs Depth - Loc 99
LF & HF Magnetic Susceptibility
700
600
500
400
300
200
100
0
<0
0-10
10-20m
20-30
Depth(cm)
LF
HF

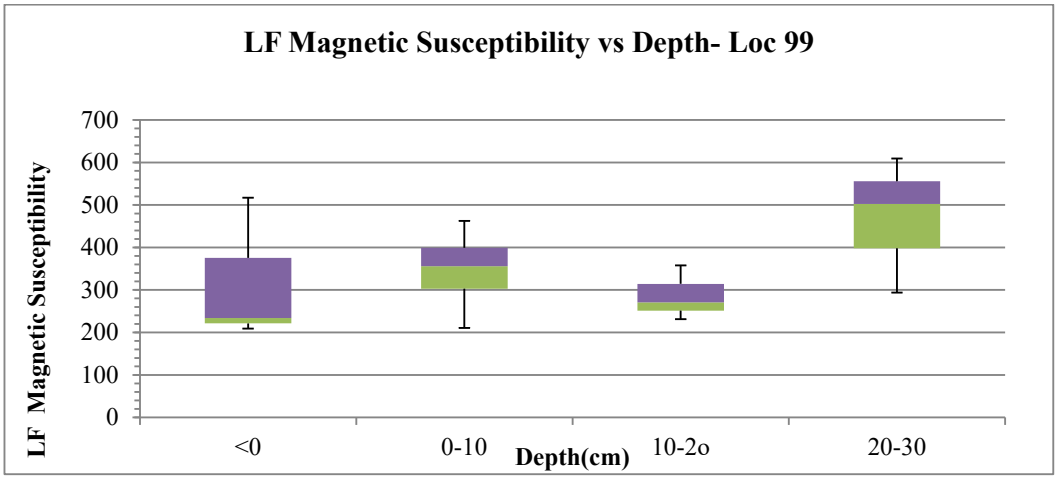
LF Magnetic Susceptibility vs Depth- Loc 99
LF Magnetic Susceptibility
700
600
500
400
300
200
100
0
<0
0-10
Depth(cm)
10-2o
20-30

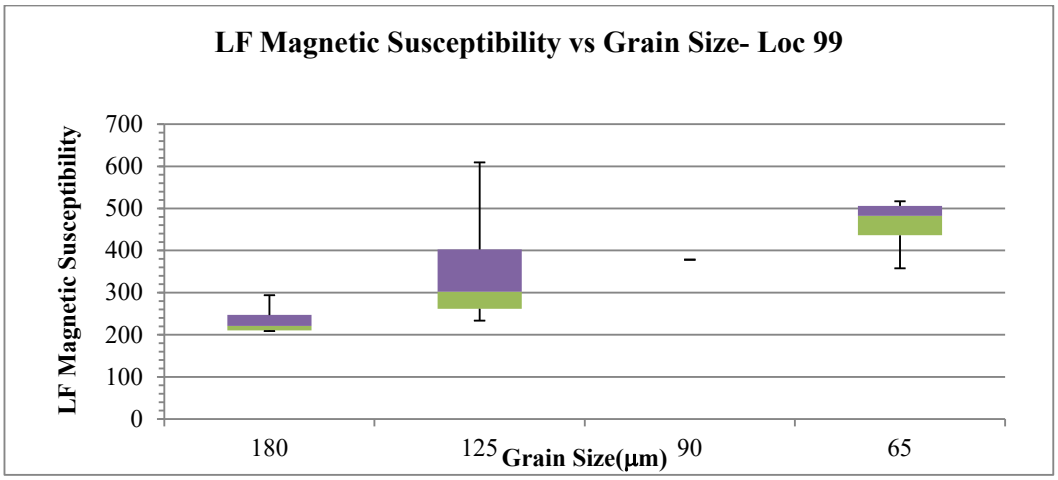
LF Magnetic Susceptibility vs Grain Size- Loc 99
LF Magnetic Susceptibility
700
600
500
400
300
200
100
0
180
125
Grain Size(µm)
90
65

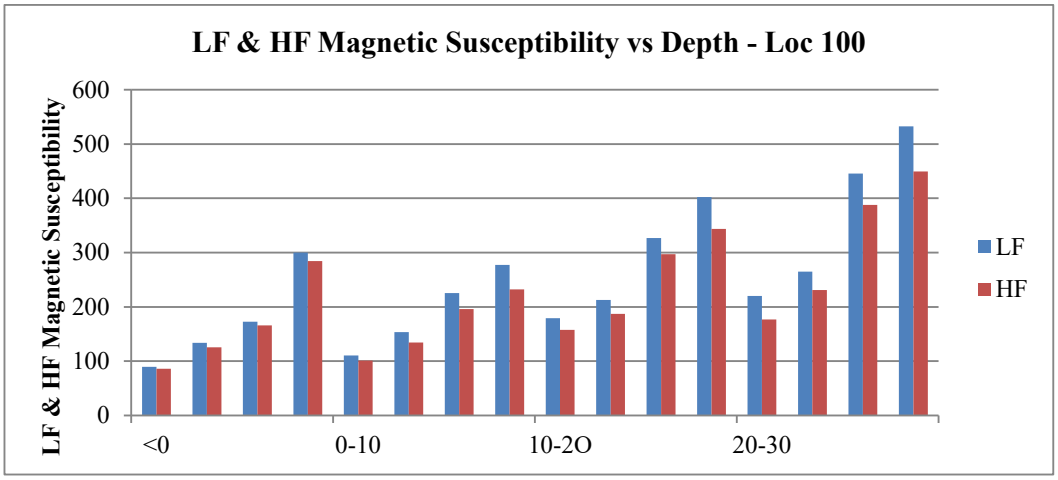
LF & HF Magnetic Susceptibility vs Depth - Loc 100
LF & HF Magnetic Susceptibility
600
500
400
300
200
100
0
<0
0-10
10-2O
20-30
LF
HF

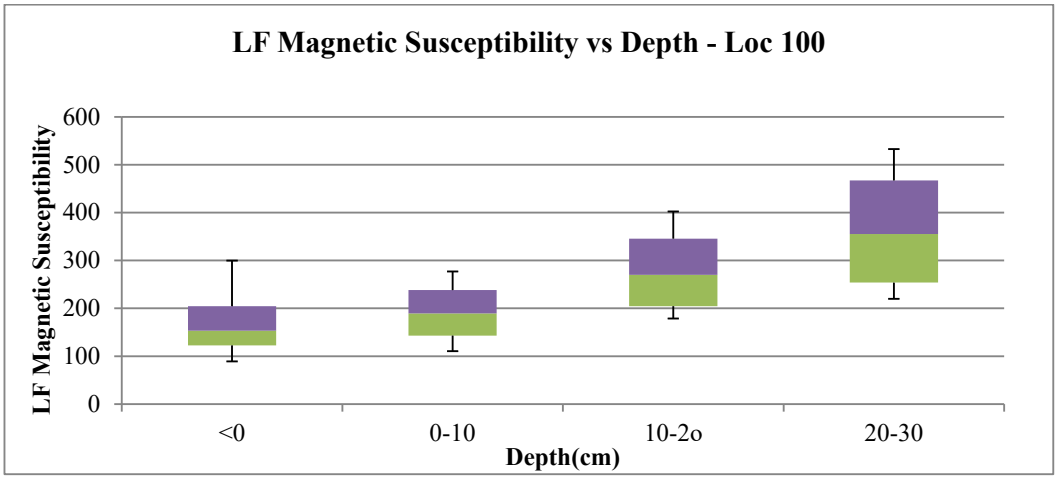
LF Magnetic Susceptibility vs Depth - Loc 100
LF Magnetic Susceptibility
600
500
400
300
200
100
0
<0
0-10
10-2o
20-30
Depth(cm)

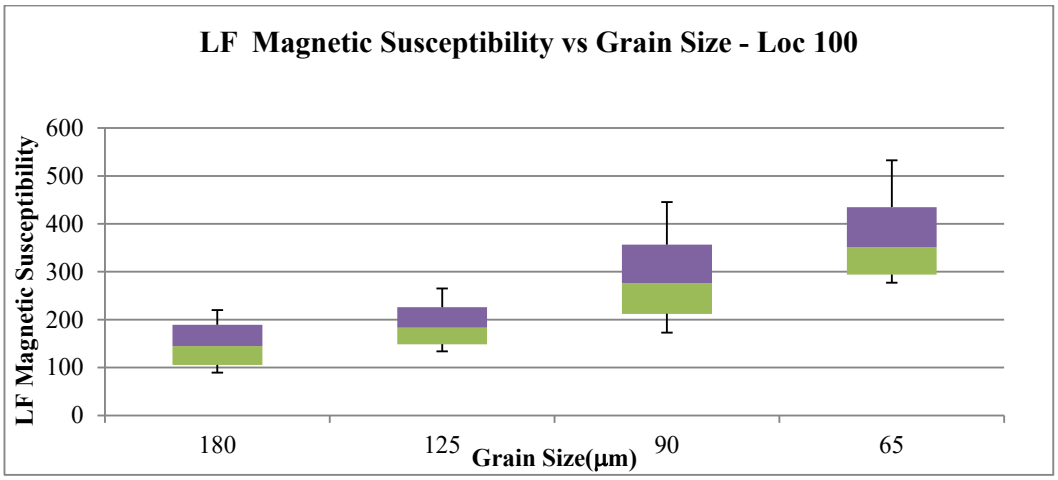
LF Magnetic Susceptibility vs Grain Size - Loc 100
LF Magnetic Susceptibility
600
500
400
300
200
100
0
180
125
90
65
Grain Size(µm)

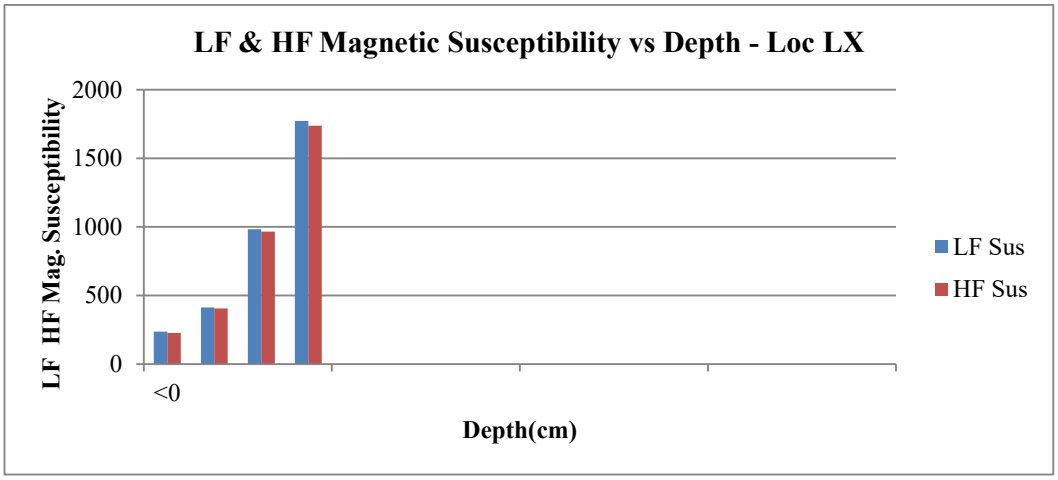
LF & HF Magnetic Susceptibility vs Depth - Loc LX
LF HF Mag. Susceptibility
2000
1500
1000
500
0
<0
Depth(cm)
LF Sus
HF Sus

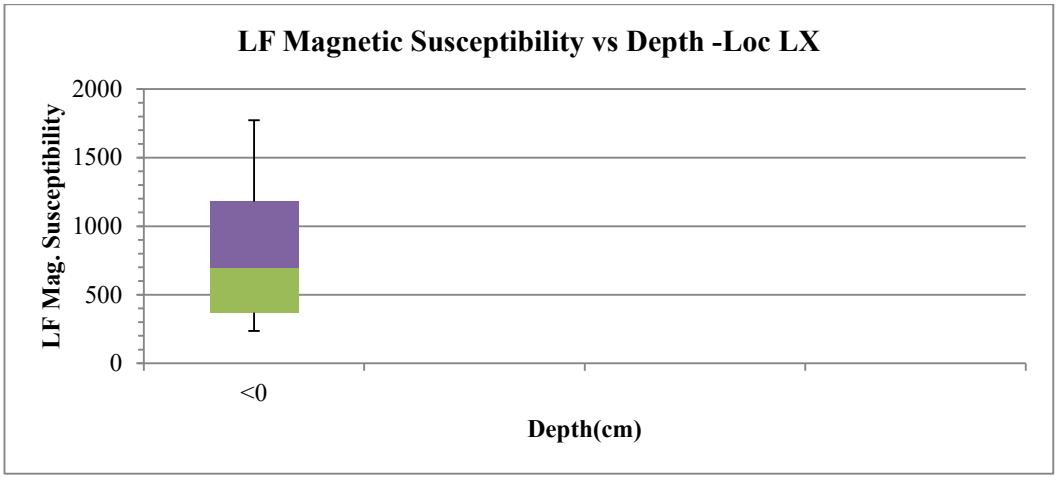
LF Magnetic Susceptibility vs Depth -Loc LX
LF Mag. Susceptibility
2000
1500
1000
500
0
<0
Depth(cm)

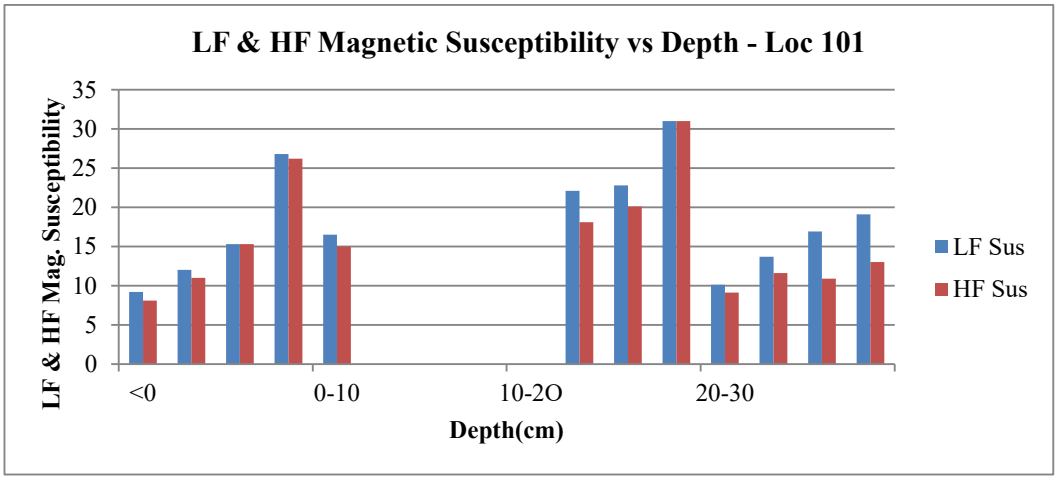
LF & HF Magnetic Susceptibility vs Depth - Loc 101
LF & HF Mag. Susceptibility
35
30
25
20
15
10
5
0
<0
0-10
10-2O
20-30
Depth(cm)
LF Sus
HF Sus

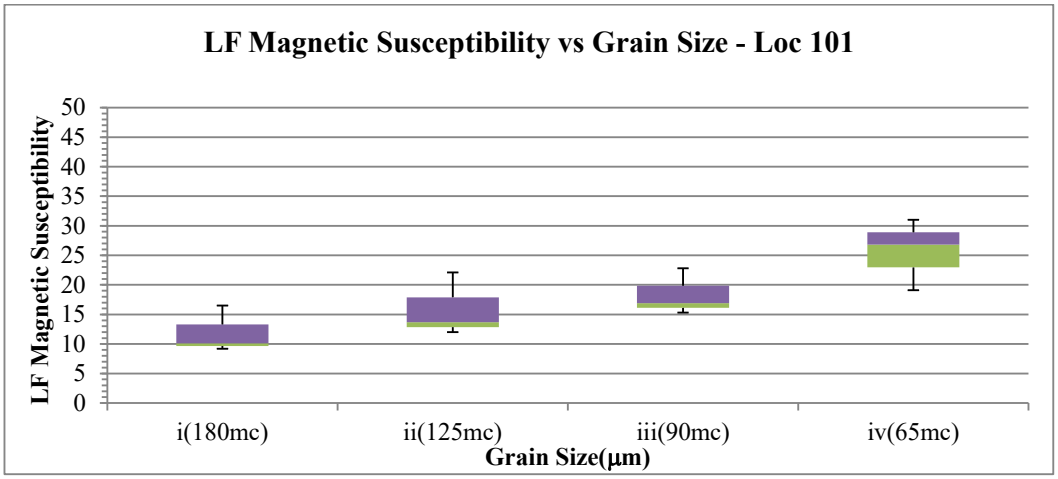
LF Magnetic Susceptibility vs Grain Size - Loc 101
LF Magnetic Susceptibility
50
45
40
35
30
25
20
15
10
5
0
i(180mc)
ii(125mc)
iii(90mc)
iv(65mc)
Grain Size(µm)

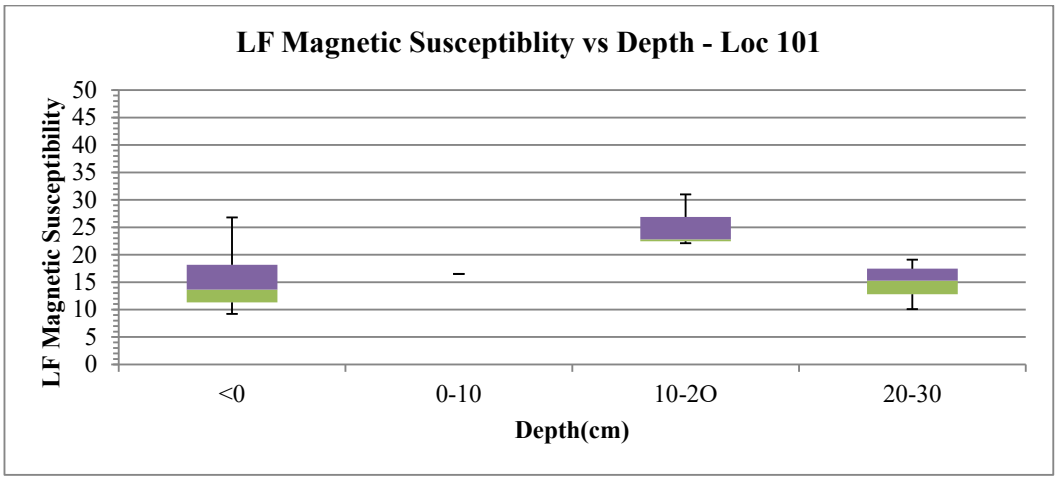
LF Magnetic Susceptiblity vs Depth - Loc 101
LF Magnetic Susceptibility
50
45
40
35
30
25
20
15
10
5
0
<0
0-10
10-2O
20-30
Depth(cm)

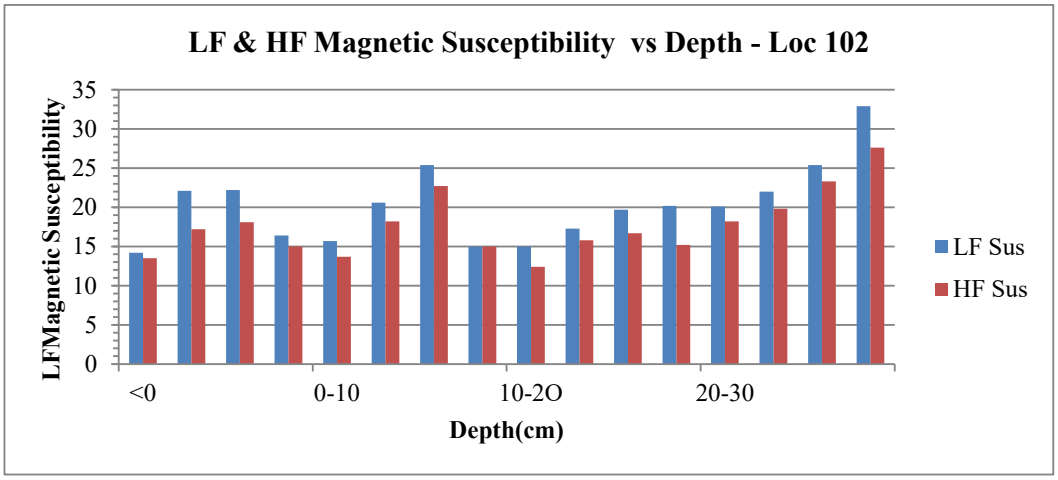
LF & HF Magnetic Susceptibility vs Depth - Loc 102
LFMagnetic Susceptibility
35
30
25
20
15
10
5
0
<0
0-10
10-2O
20-30
Depth(cm)
LF Sus
HF Sus

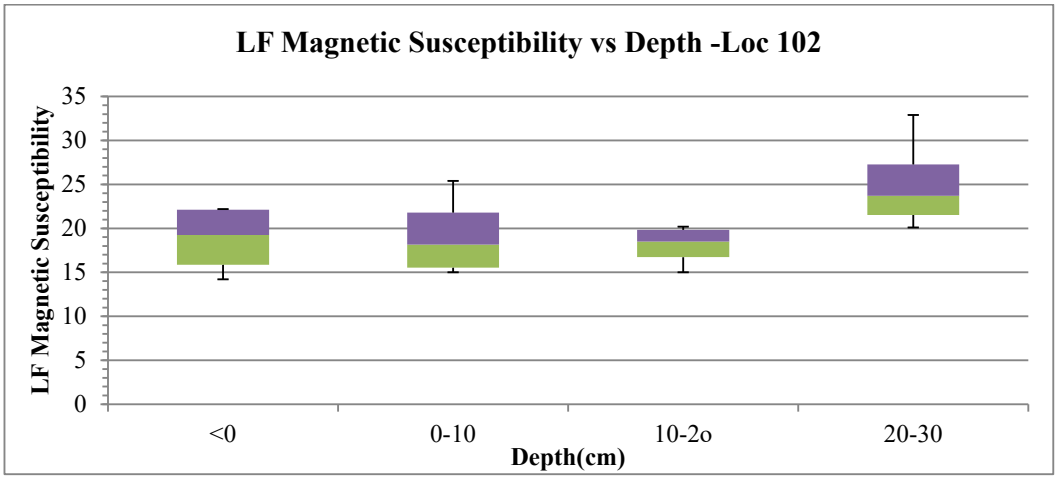
LF Magnetic Susceptibility vs Depth -Loc 102
LF Magnetic Susceptibility
35
30
25
20
15
10
5
0
<0
0-10
10-2o
20-30
Depth(cm)

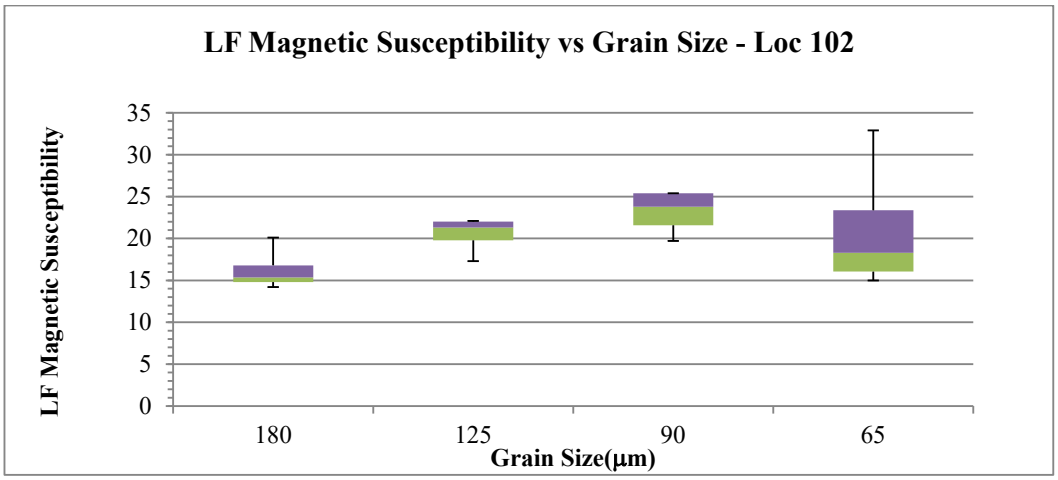
LF Magnetic Susceptibility vs Grain Size - Loc 102
LF Magnetic Susceptibility
35
30
25
20
15
10
5
0
180
125
90
65
Grain Size(µm)

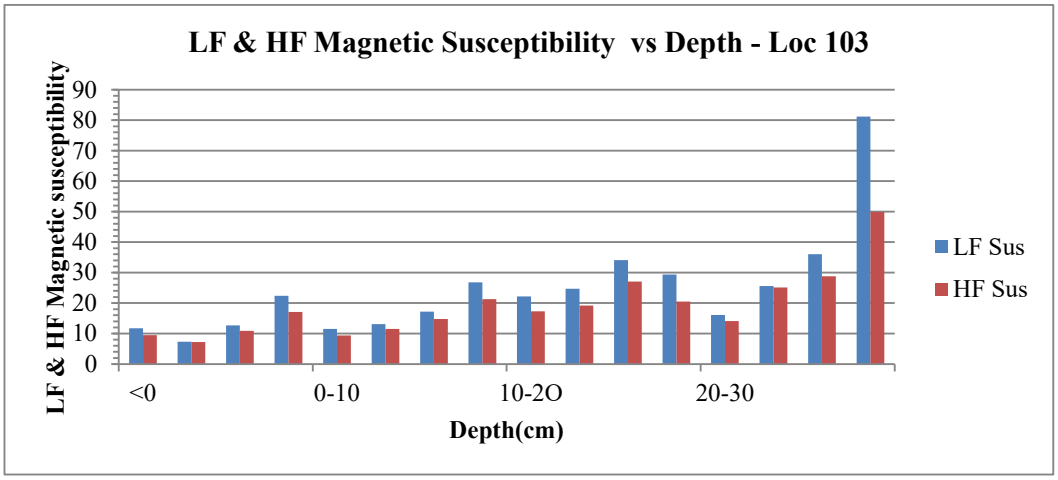
LF & HF Magnetic Susceptibility vs Depth - Loc 103
LF & HF Magnetic susceptibility
90
80
70
60
50
40
30
20
10
0
<0
0-10
10-2O
20-30
Depth(cm)
LF Sus
HF Sus

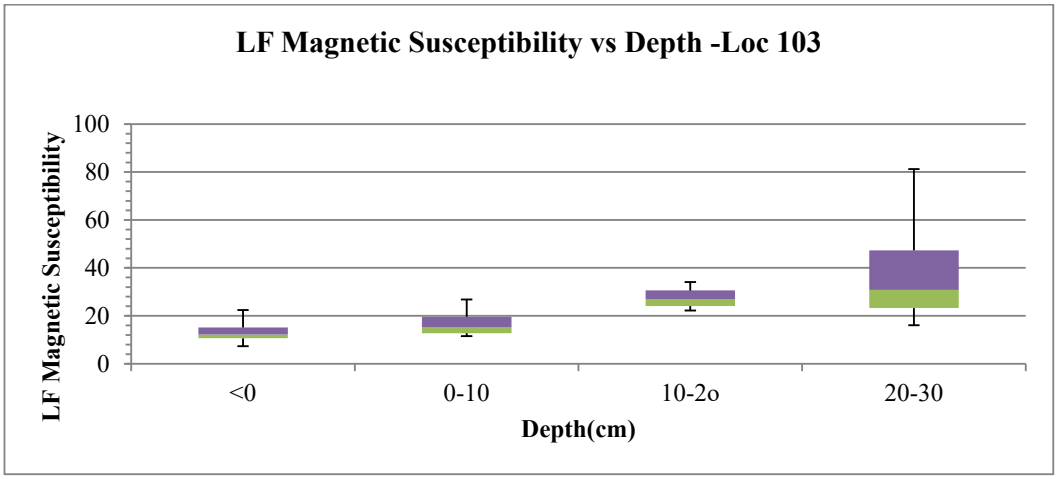
LF Magnetic Susceptibility vs Depth -Loc 103
LF Magnetic Susceptibility
100
80
60
40
20
0
<0
0-10
10-2o
20-30
Depth(cm)

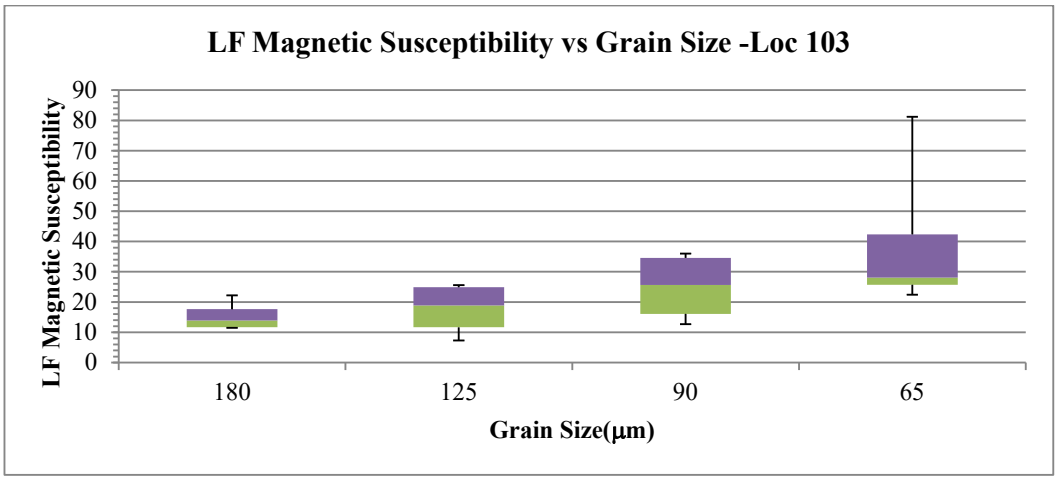
LF Magnetic Susceptibility vs Grain Size -Loc 103
LF Magnetic Susceptibility
90
80
70
60
50
40
30
20
10
0
180
125
90
65
Grain Size(µm)

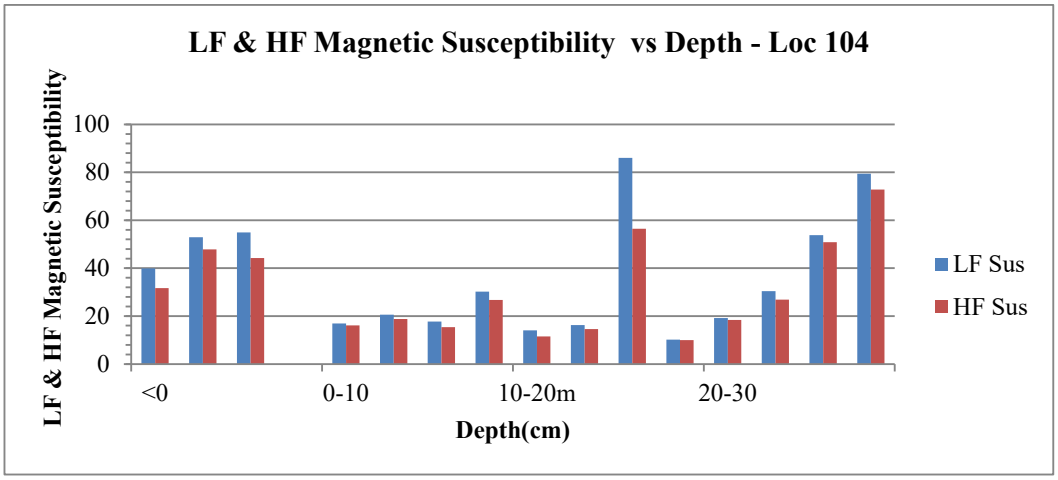
LF & HF Magnetic Susceptibility vs Depth - Loc 104
LF & HF Magnetic Susceptibility
100
80
60
40
20
0
<0
0-10
10-20m
20-30
Depth(cm)
LF Sus
HF Sus

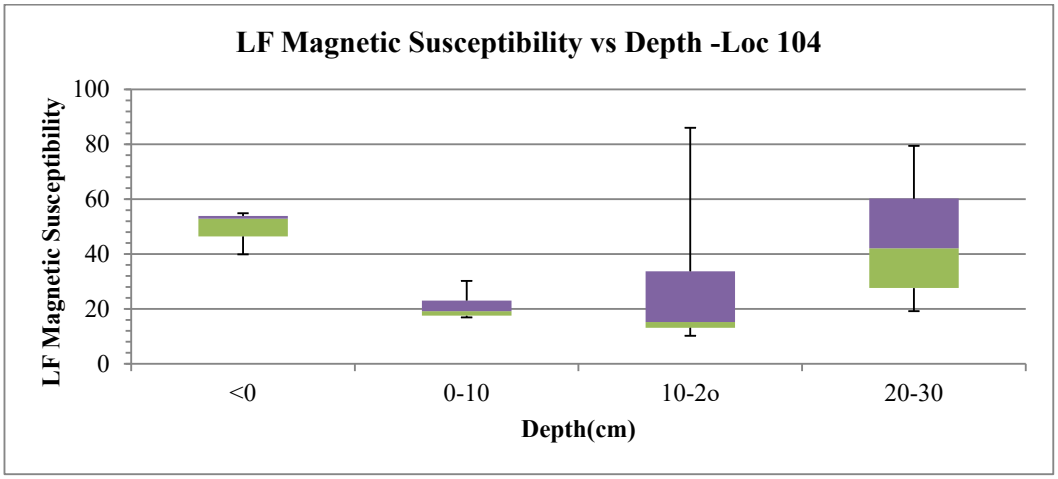
LF Magnetic Susceptibility vs Depth -Loc 104
LF Magnetic Susceptibility
100
80
60
40
20
0
<0
0-10
10-2o
20-30
Depth(cm)

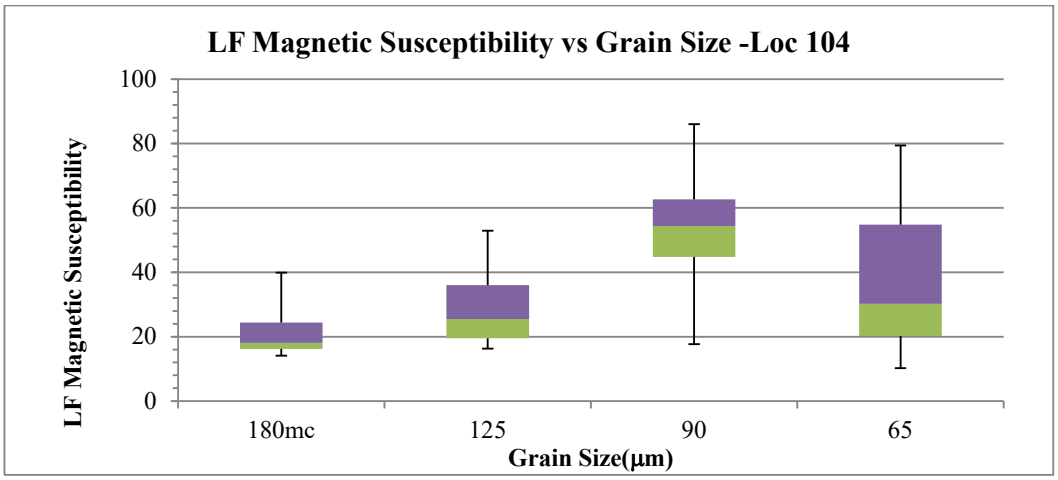
LF Magnetic Susceptibility vs Grain Size -Loc 104
LF Magnetic Susceptibility
100
80
60
40
20
0
180mc
125
90
65
Grain Size(µm)

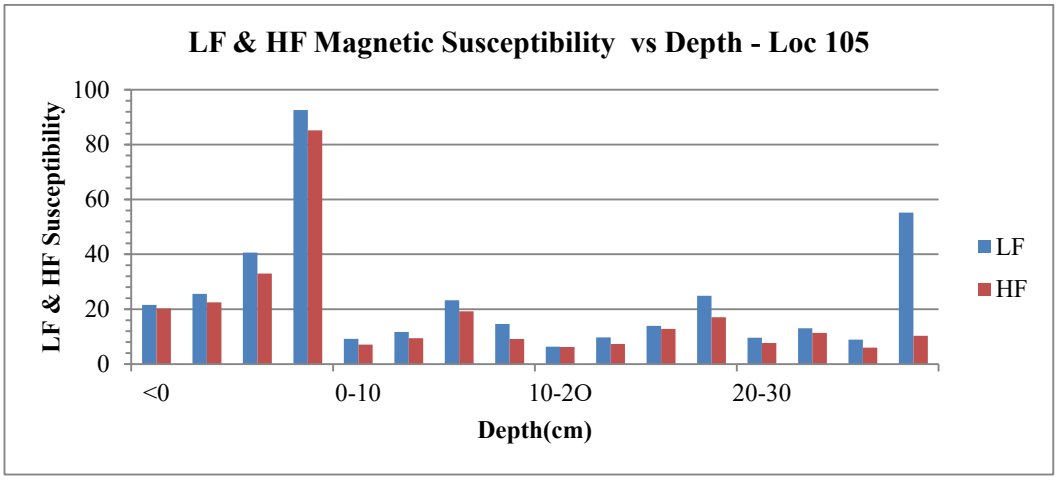
LF & HF Magnetic Susceptibility vs Depth - Loc 105
LF & HF Susceptibility
100
80
60
40
20
0
<0
0-10
10-2O
20-30
Depth(cm)
LF
HF

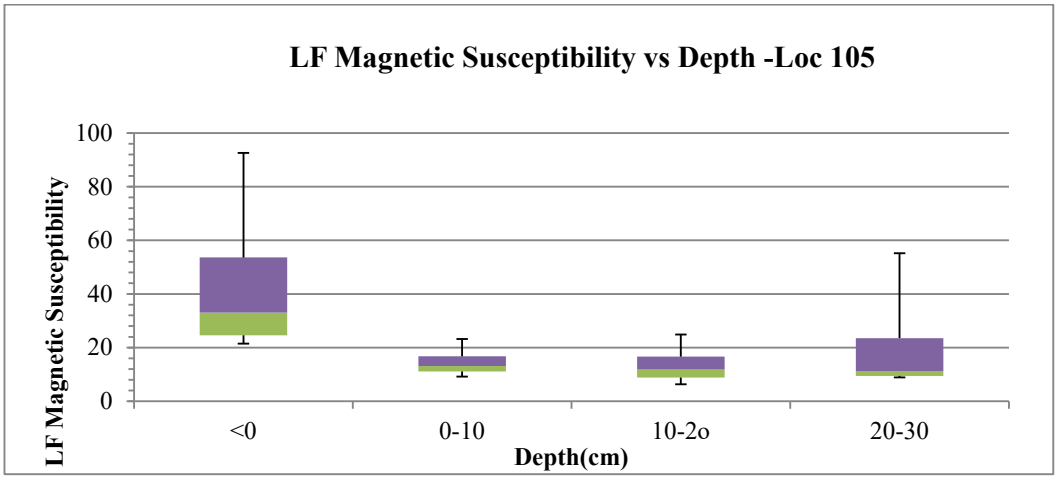
LF Magnetic Susceptibility vs Depth -Loc 105
LF Magnetic Susceptibility
100
80
60
40
20
0
<0
0-10
10-2o
20-30
Depth(cm)

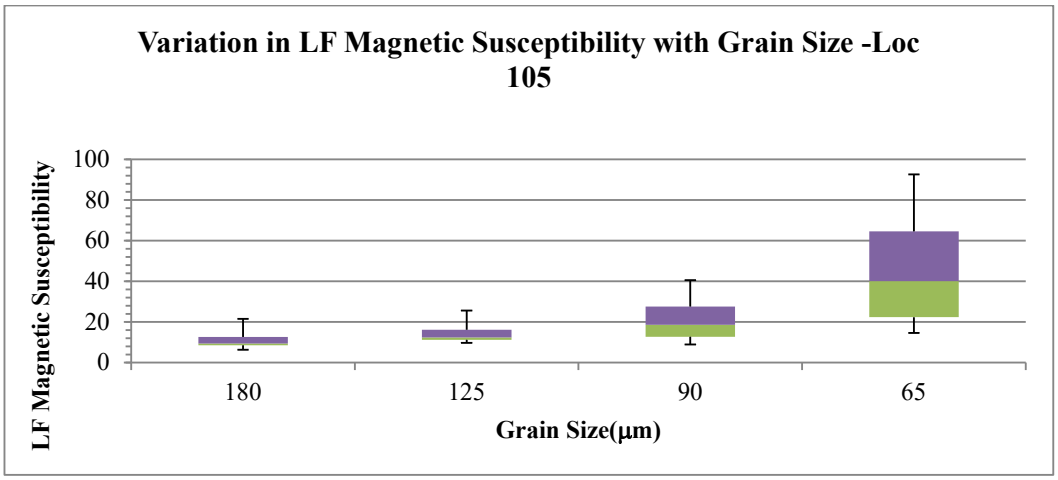
Variation in LF Magnetic Susceptibility with Grain Size -Loc 105
LF Magnetic Susceptibility
100
80
60
40
20
0
180
125
90
65
Grain Size(µm)

Appendix 4. 3: Variation in Magnetic Susceptibility Readings Within Different Grain Sizes with Depth in Ogijo Industrial Layout

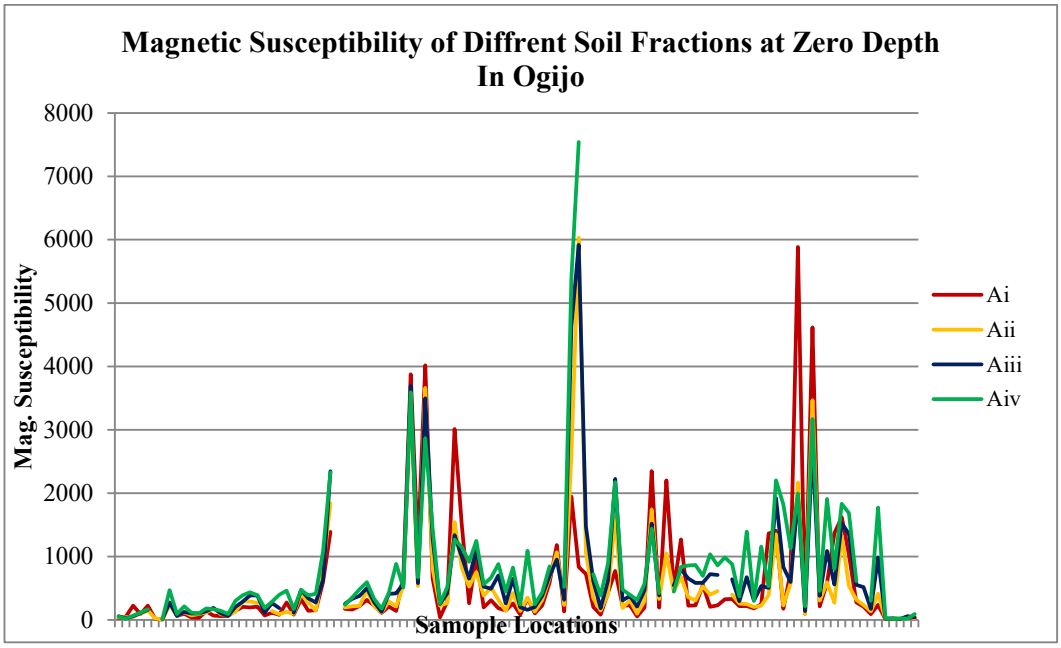

Appendix 4.3.1: Magnetic susceptibility readings within grains sizes 180 µm (Ai), 120 µm (Aii), 90 µm (Aiii), and 65µm (Aiv) from sampling depth of 0 cm across the site in Ogijo

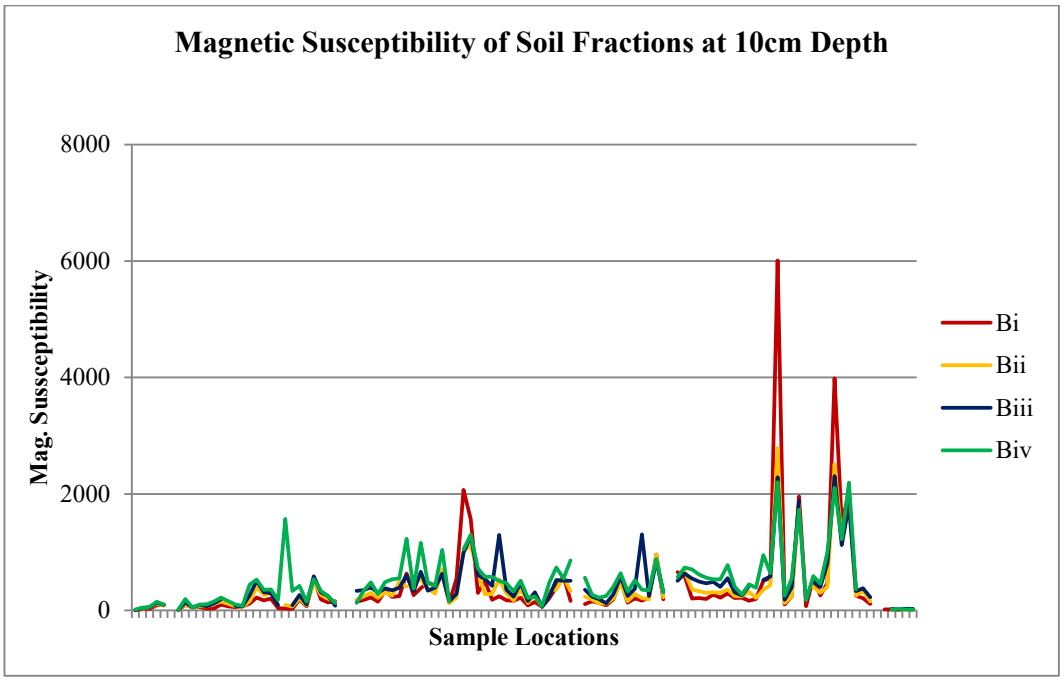

Appendix 4.3.2: Magnetic susceptibility readings within grains sizes 180 µm (Bi), 120 µm (Bii), 90 µm (Biii), and 65µm (Biv) from sampling depth of 10 cm across the site in Ogijo

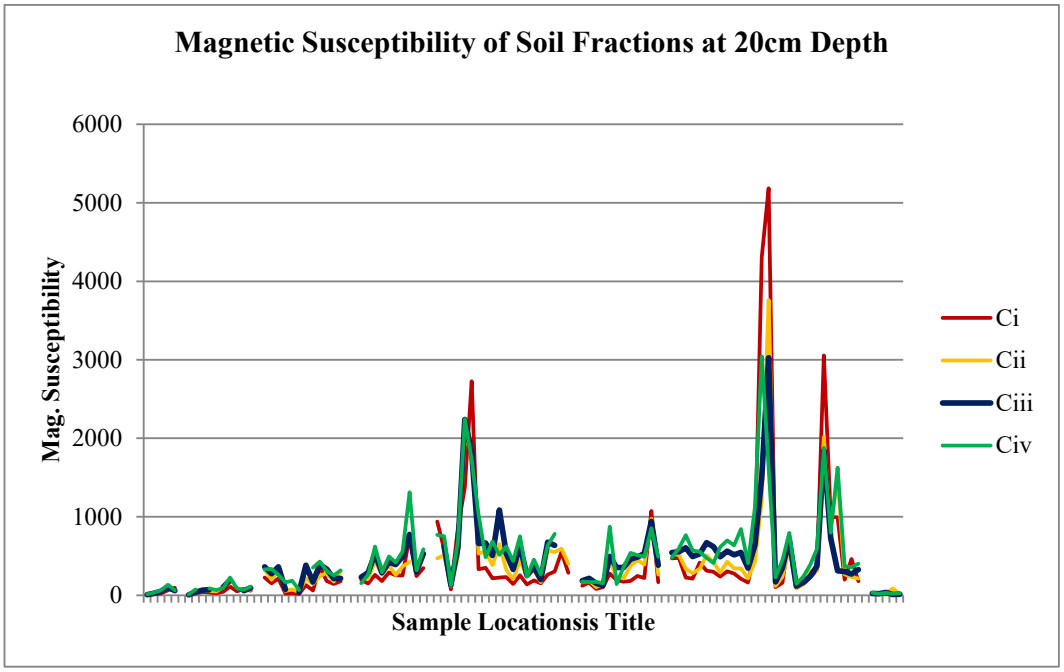

Appendix 4.3.3: Variation in magnetic susceptibility readings within grains sizes 180 µm (Ci), 120 µm (Cii), 90 µm (Ciii), and 65µm (Civ) from sampling depth of 20 cm across the site in Ogijo

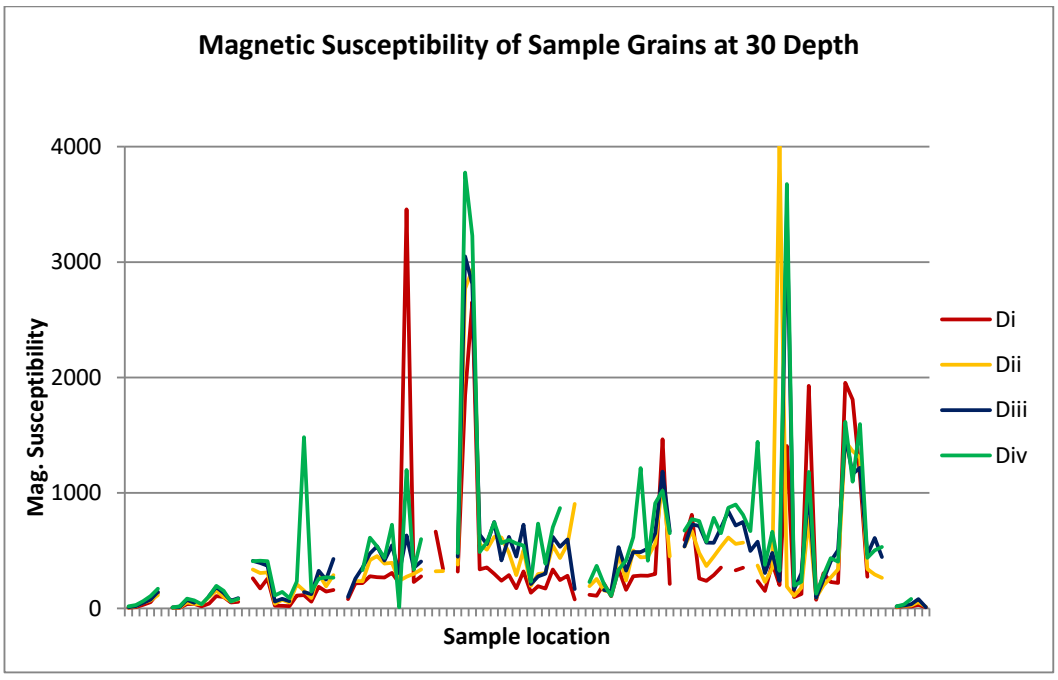

Appendix 4.3.4: Variation in magnetic susceptibility readings within grains sizes 180 µm (Di), 120 µm (Dii), 90 µm (Diii), and 65 µm (Div) from sampling depth of 30 cm across the site in Ogijo

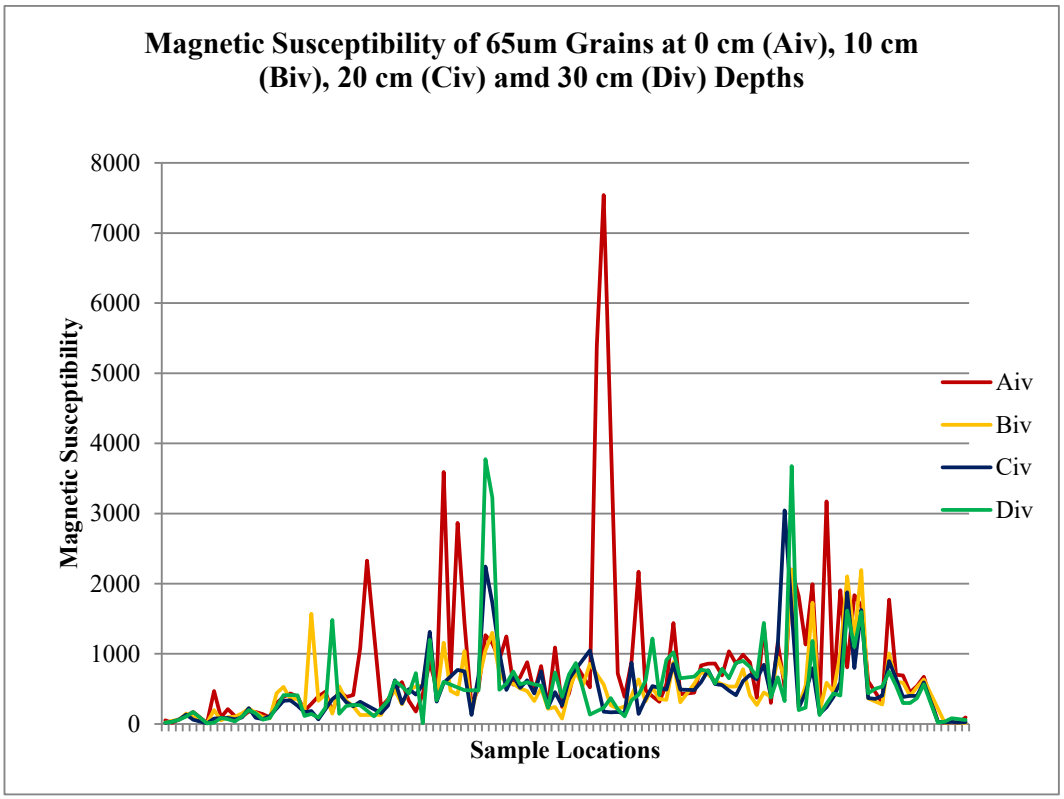

Appendix 4.3.5: Magnetic Susceptibility readings from the 65µm sample grains at different depths

Appendix 4. 4: Magnetic Susceptibility / Temperature Analysis Results of Soil Samples from Ogijo Industrial Layout

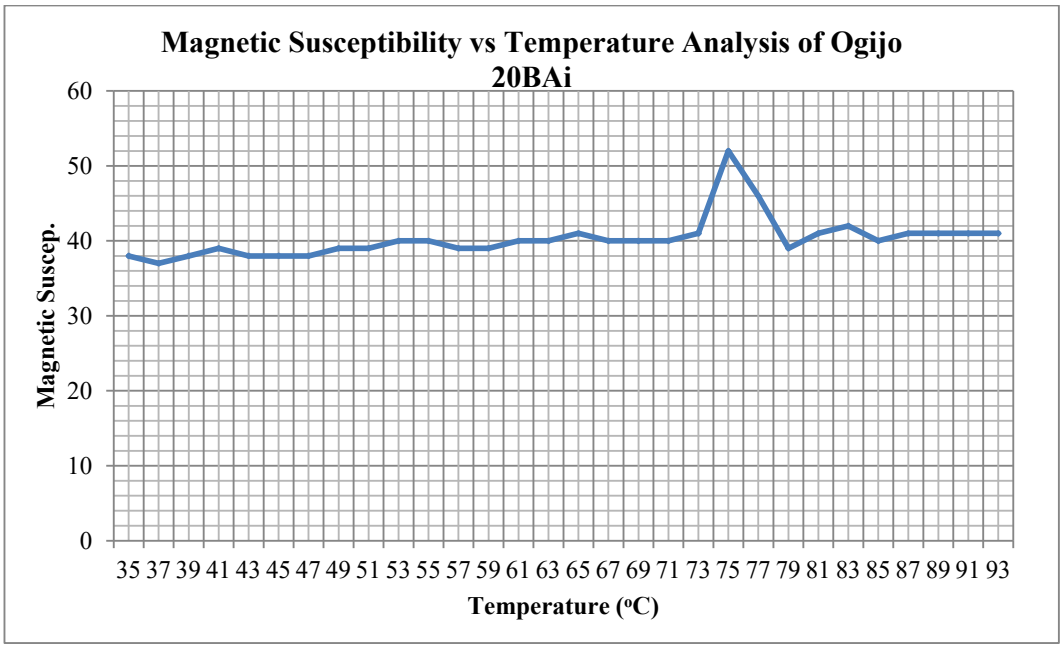

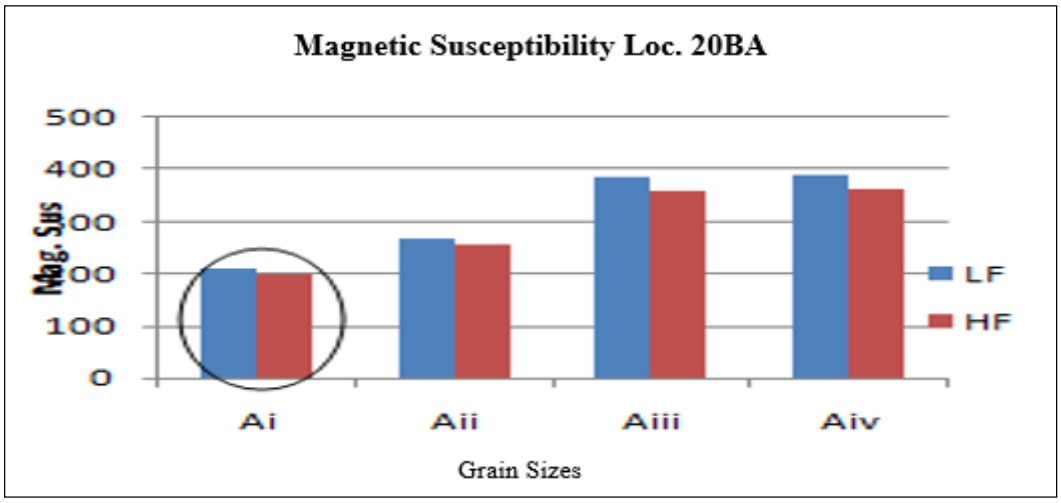

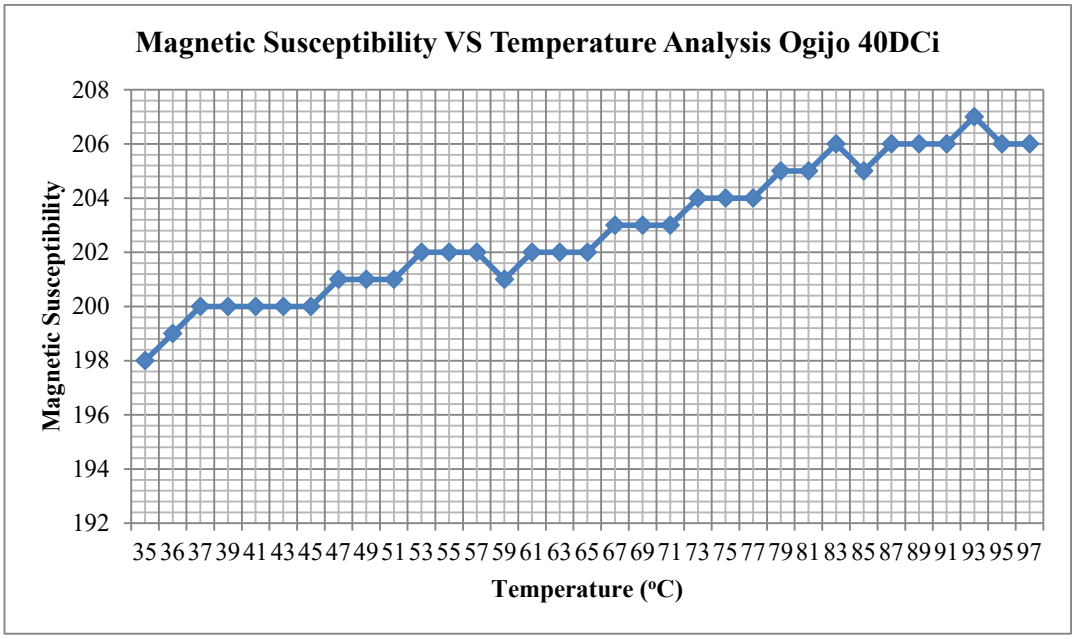
Magnetic Susceptibility VS Temperature Analysis Ogijo 40DCi
Magnetic Susceptibility
208
206
204
202
200
198
196
194
192
35 36 37 39 41 43 45 47 49 51 53 55 57 59 61 63 65 67 69 71 73 75 77 79 81 83 85 87 89 91 93 95 97
Temperature (°C)

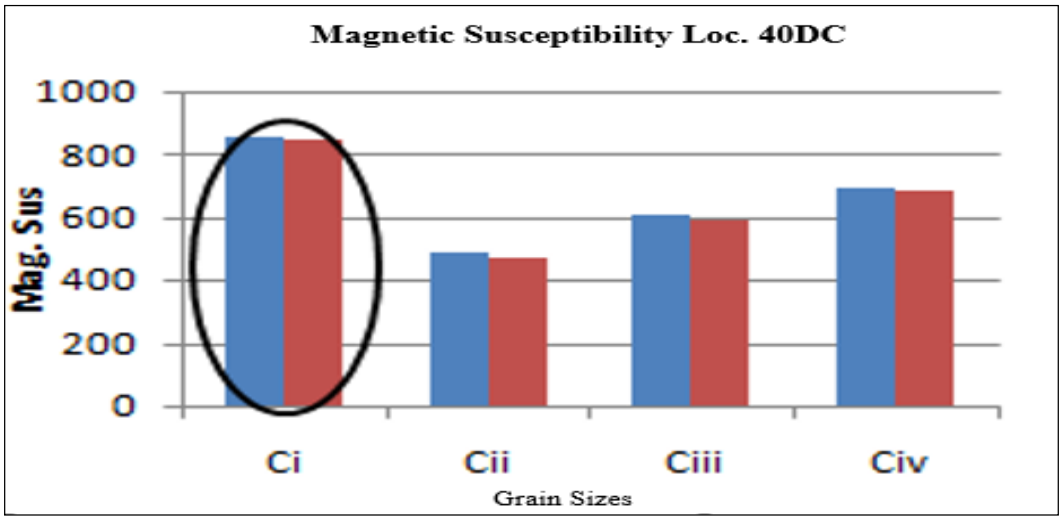
Magnetic Susceptibility Loc. 40DC
Mag. Sus
1000
800
600
400
200
0
Ci
Cii
Ciii
Civ
Grain Sizes

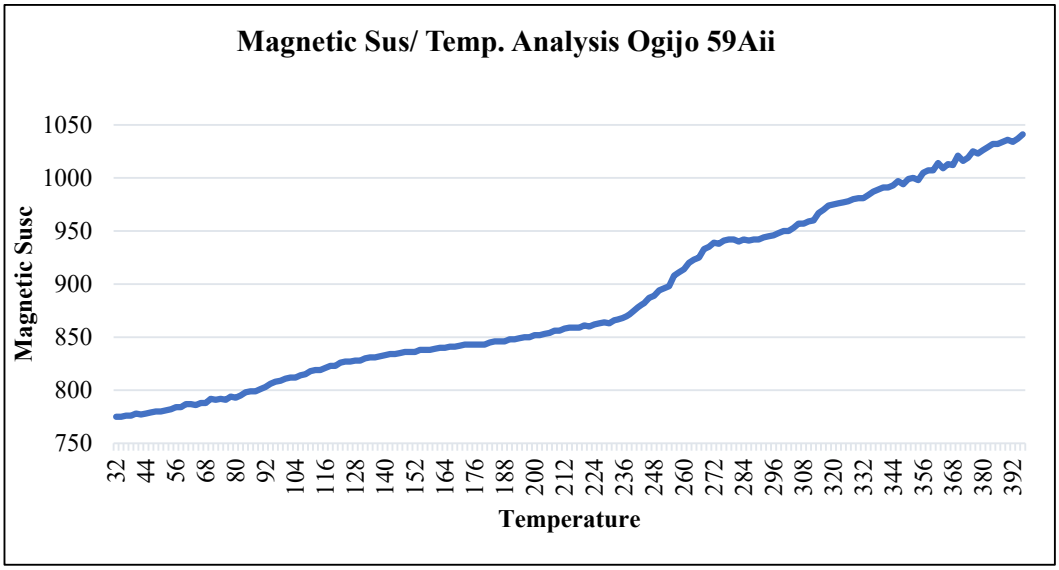
Magnetic Sus/ Temp. Analysis Ogijo 59Aii
Magnetic Susc
1050
1000
950
900
850
800
750
32 44 56 68 80 92 104 116 128 140 152 164 176 188 200 212 224 236 248 260 272 284 296 308 320 332 344 356 368 380 392
Temperature

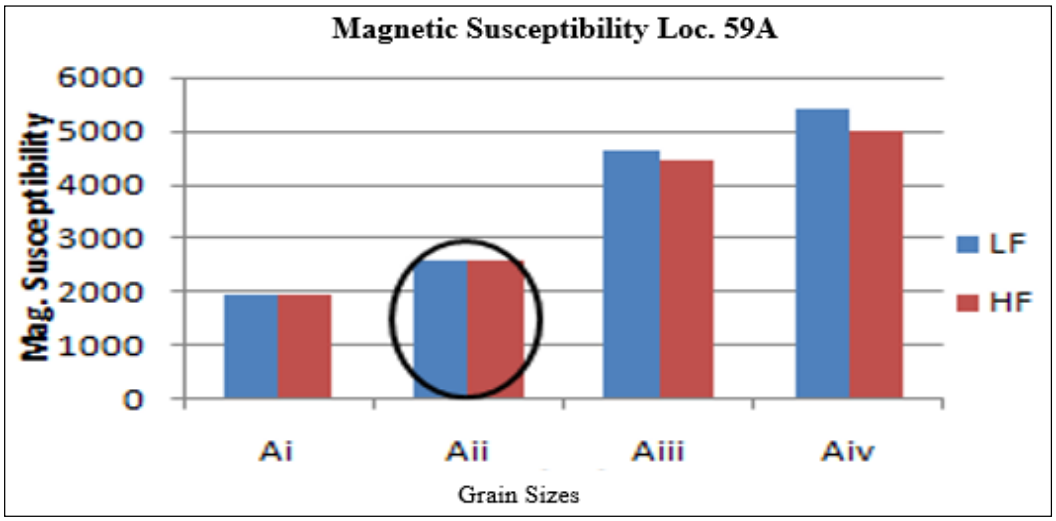
Magnetic Susceptibility Loc. 59A
Mag. Susceptibility
6000
5000
4000
3000
2000
1000
0
Ai
Aii
Aiii
Aiv
Grain Sizes
LF
HF

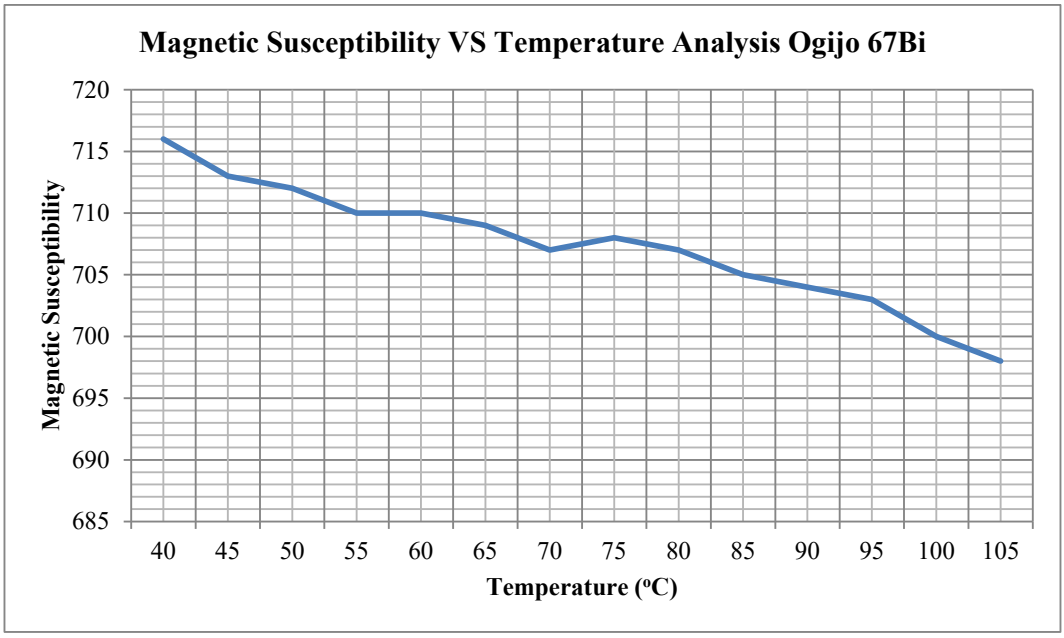
Magnetic Susceptibility VS Temperature Analysis Ogijo 67Bi
Magnetic Susceptibility
720
715
710
705
700
695
690
685
40
45
50
55
60
65
70
75
80
85
90
95
100
105
Temperature (°C)

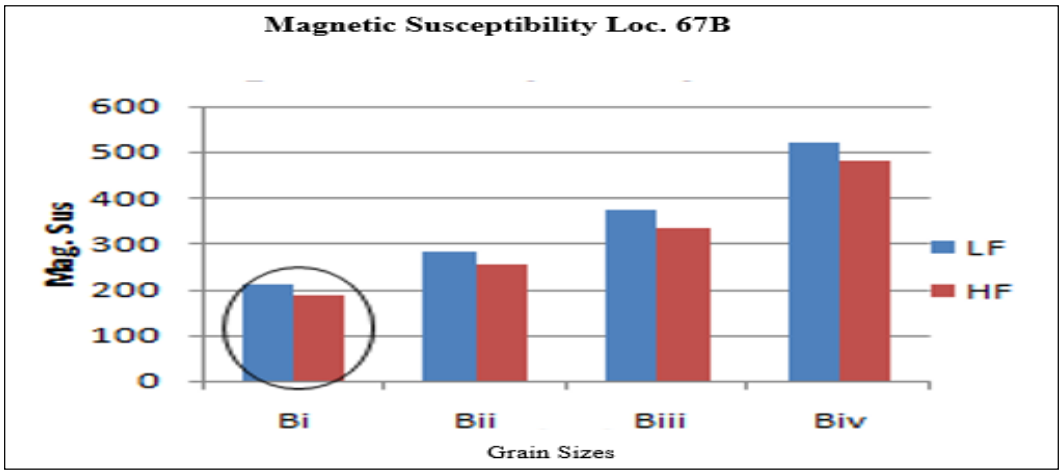
Magnetic Susceptibility Loc. 67B
Mag. Sus
600
500
400
300
200
100
0
Bi
Bii
Biii
Biv
Grain Sizes
LF
HF

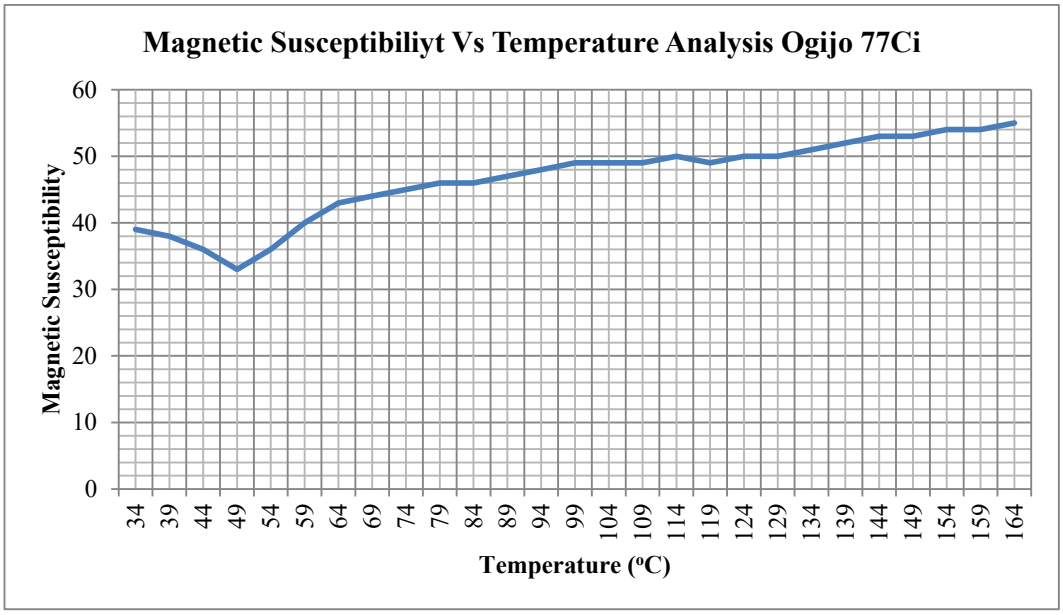
Magnetic Susceptibiliyt Vs Temperature Analysis Ogijo 77Ci
Magnetic Susceptibility
60
50
40
30
20
10
0
34 39 44 49 54 59 64 69 74 79 84 89 94 99 104 109 114 119 124 129 134 139 144 149 154 159 164
Temperature (°C)

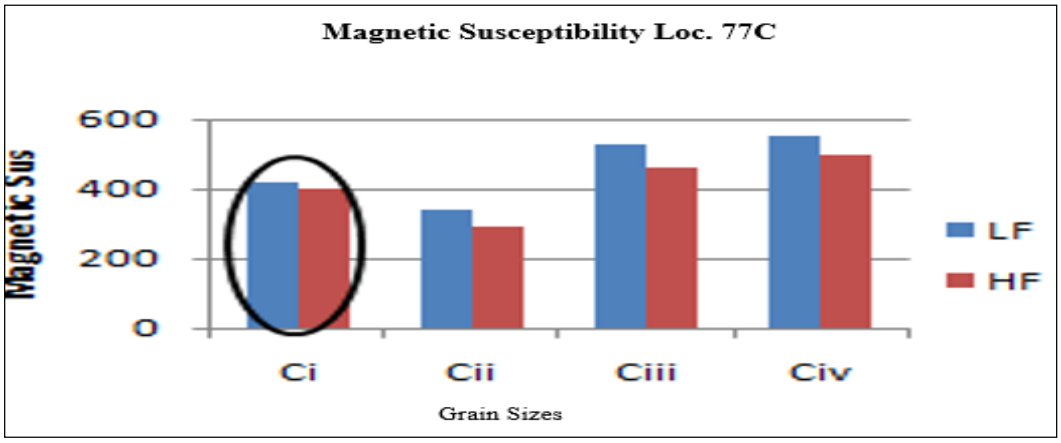
Magnetic Susceptibility Loc. 77C
Magnetic Sus
600
400
200
0
Ci
Cii
Ciii
Civ
Grain Sizes
LF
HF

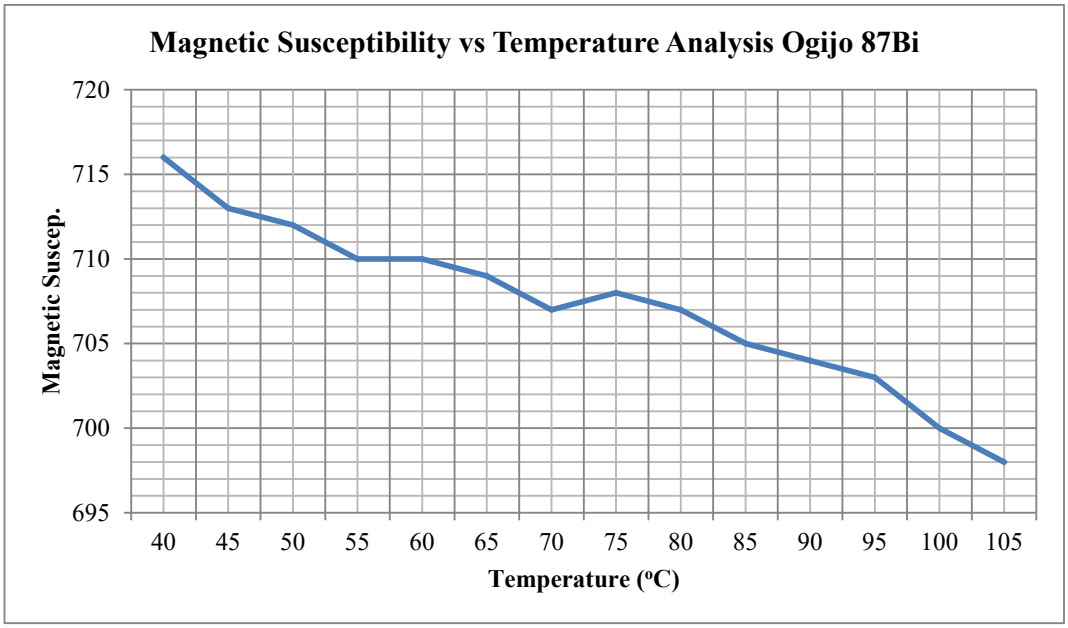
Magnetic Susceptibility vs Temperature Analysis Ogijo 87Bi
Magnetic Suscep.
720
715
710
705
700
695
40
45
50
55
60
65
70
75
80
85
90
95
100
105
Temperature (ºC)

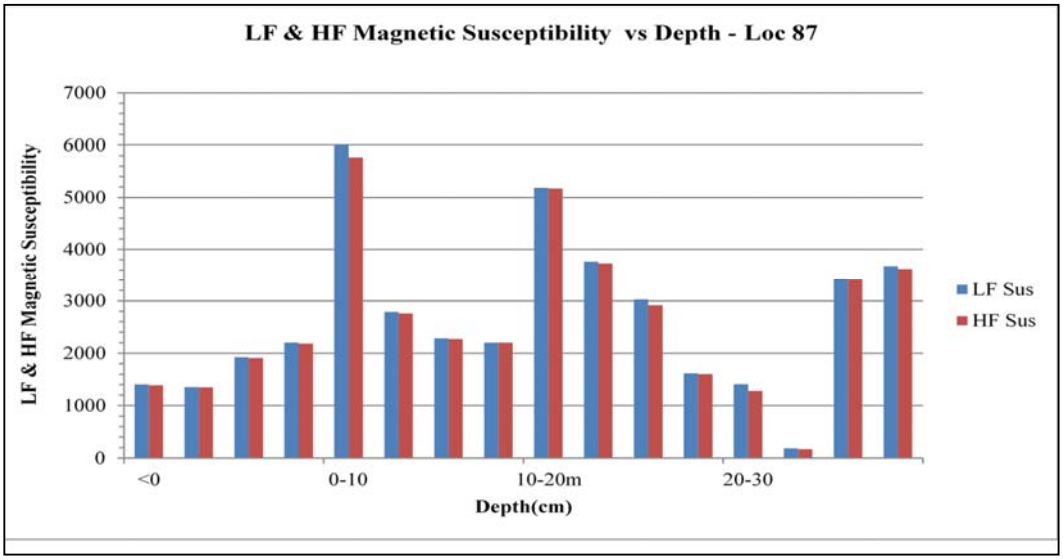
LF & HF Magnetic Susceptibility vs Depth - Loc 87
LF & HF Magnetic Susceptibility
7000
6000
5000
4000
3000
2000
1000
0
<0
0-10
10-20m
20-30
Depth(cm)
LF Sus
HF Sus

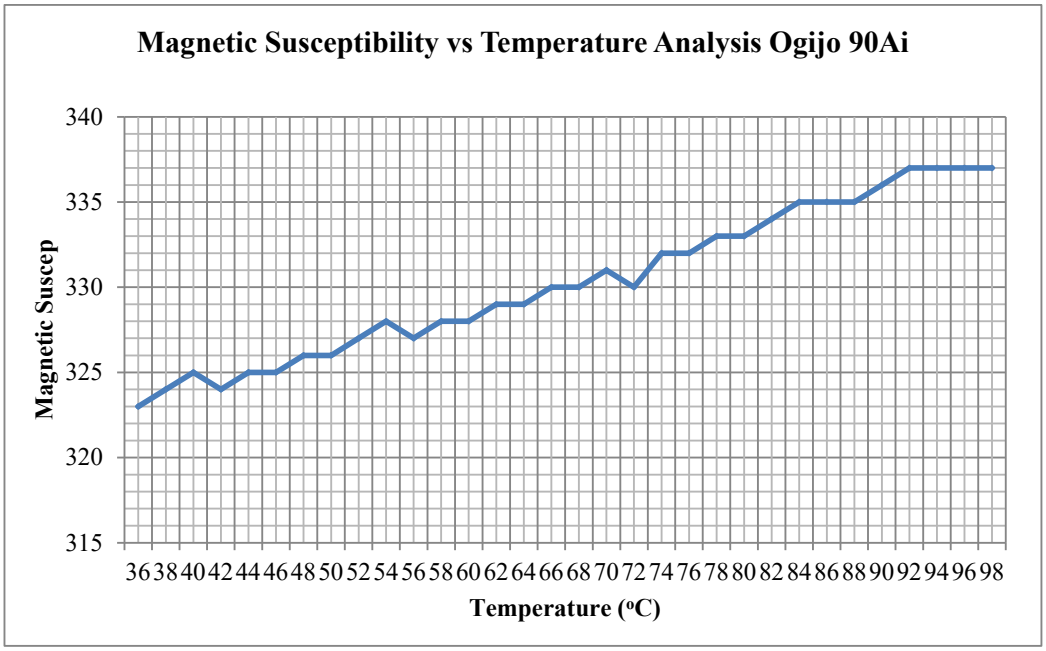
Magnetic Susceptibility vs Temperature Analysis Ogijo 90Ai
Magnetic Suscep
340
335
330
325
320
315
36 38 40 42 44 46 48 50 52 54 56 58 60 62 64 66 68 70 72 74 76 78 80 82 84 86 88 90 92 94 96 98
Temperature (°C)

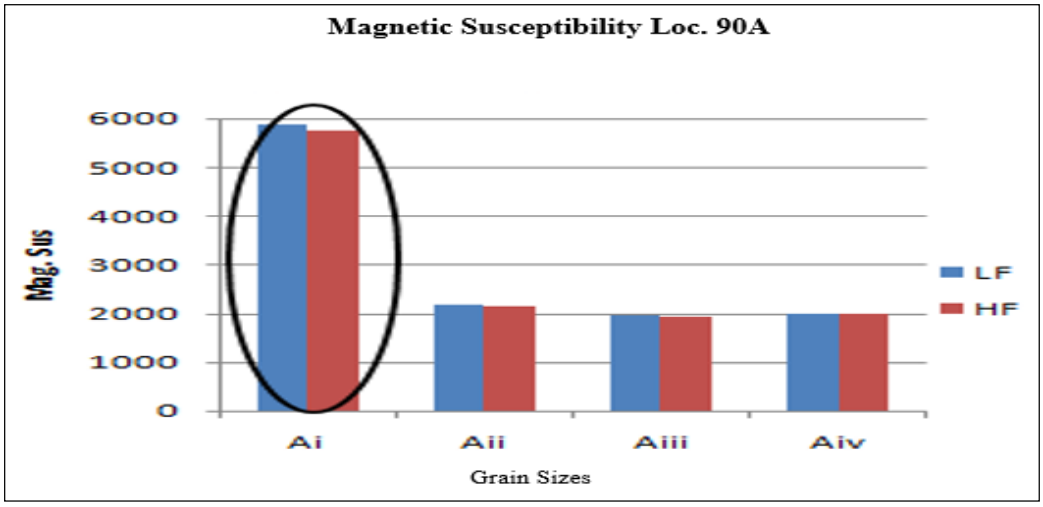
Magnetic Susceptibility Loc. 90A
Mag. Sus
6000
5000
4000
3000
2000
1000
0
Ai
Aii
Aiii
Aiv
Grain Sizes
LF
HF

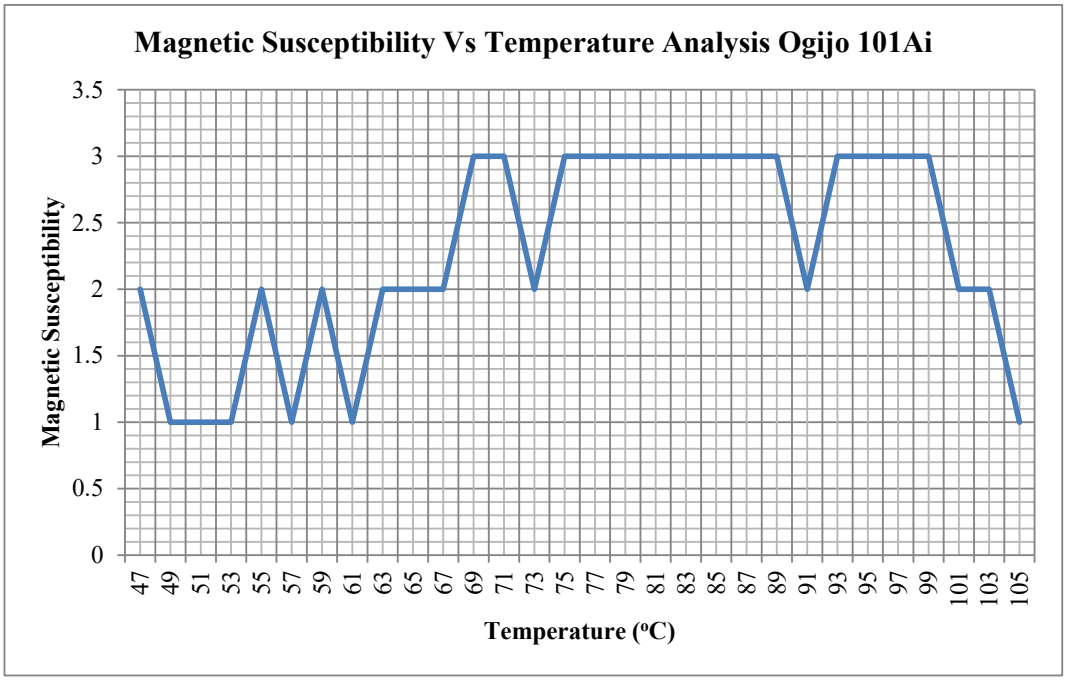
Magnetic Susceptibility Vs Temperature Analysis Ogijo 101Ai
Magnetic Susceptibility
3.5
3
2.5
2
1.5
1
0.5
0
47 49 51 53 55 57 59 61 63 65 67 69 71 73 75 77 79 81 83 85 87 89 91 93 95 97 99 101 103 105
Temperature (°C)

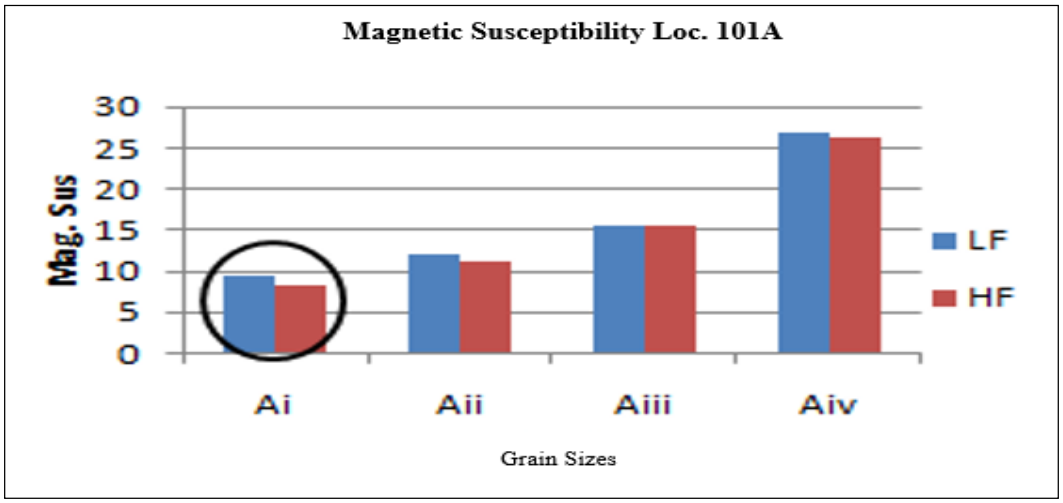
Magnetic Susceptibility Loc. 101A
Mag. Sus
30
25
20
15
10
5
0
Ai
Aii
Aiii
Aiv
LF
HF
Grain Sizes

Appendix 4. 5: Results from Aqua Regia Method of Geochemical Analysis of Some Samples from Ogijo Industrial Layout

Element	Unit	51Aii	40DCi	97Bi	86Ci	55Ai	94Ai	62Aii
Mo	PPM	<1	1	8	11	<1	3	<1
Cu	PPM	29	75	303	286	16	111	31
Pb	PPM	2381	29	306	207	158	200	66
Zn	PPM	804	332	1666	2513	249	598	625
Ag	PPM	<0.3	<0.3	<0.3	0.9	<0.3	<0.3	<0.3
Ni	PPM	10	16	48	90	6	23	9
Co	PPM	5	4	7	12	4	5	5
Mn	PPM	728	3237	10000	2322	799	1070	630
Fe	%	2.05	3.64	10.8	8.04	1.68	2.92	1.99
As	PPM	2	2	4	7	3	4	3
Th	PPM	4	3	<2	<2	4	2	3
Sr	PPM	10	40	187	89	11	22	16
Cd	PPM	0.8	<0.5	<0.5	1.6	<0.5	1.9	<0.5
Sb	PPM	8	<3	4	8	<3	7	<3
Bi	PPM	4	<3	<3	3	<3	<3	3
V	PPM	36	31	58	35	30	24	30
Ca	%	0.21	0.35	0.67	1.31	0.16	0.34	0.28
P	%	0.031	0.013	0.017	0.066	0.022	0.017	0.026
La	PPM	15	8	10	6	7	4	4
Cr	PPM	26	273	416	206	44	67	59
Mg	%	0.05	0.09	0.19	0.27	0.05	0.07	0.04
Ba	PPM	35	131	749	352	29	115	45
Ti	%	0.024	0.035	0.108	0.027	0.019	0.024	0.02
B	PPM	<20	47	334	163	<20	193	25
Al	%	1.16	0.82	1.79	1.3	0.81	0.52	0.72
Na	%	<0.01	0.02	0.1	0.04	<0.01	0.05	<0.01
K	%	0.03	0.03	0.08	0.05	0.02	0.04	0.03
W	PPM	<2	<2	2	5	<2	<2	<2

S	%	<0.05	<0.05	<0.05	0.05	<0.05	<0.05	<0.05
Hg	PPM	<1	<1	<1	<1	<1	<1	<1
Tl	PPM	<5	<5	<5	<5	<5	<5	<5
Ga	PPM	7	<5	<5	<5	<5	<5	<5
Sc	PPM	<5	<5	<5	<5	<5	<5	<5

Results from Aqua Regia Method of Geochemical Analysis of Some Samples from Ogijo Industrial Layout (Continued)

Element	Unit	23Ciii	25Biii	30CIV	29Aii	20Aiii	29Ai	27Aiii
Mo	PPM	1	11	9	18	6	9	3
Cu	PPM	39	296	190	308	198	153	106
Pb	PPM	31	720	1054	529	1824	251	1003
Zn	PPM	54	4696	4843	1428	7393	1080	1930
Ag	PPM	<0.3	1	0.6	0.4	0.6	0.3	0.3
Ni	PPM	18	86	58	102	48	51	29
Co	PPM	11	16	11	20	11	9	8
Mn	PPM	1271	1880	991	3208	905	1501	714
Fe	%	4.74	10.77	12.61	18.63	8.37	10.32	5.28
As	PPM	2	9	10	8	9	6	3
Th	PPM	15	6	10	7	8	3	9
Sr	PPM	13	25	13	17	15	13	11
Cd	PPM	<0.5	8.3	1.3	0.8	2.1	<0.5	1.5
Sb	PPM	<3	8	5	5	9	5	7
Bi	PPM	<3	7	<3	3	6	<3	<3
V	PPM	100	72	124	61	105	34	73
Ca	%	0.22	0.59	0.24	0.33	0.34	0.32	0.2
P	%	0.036	0.112	0.055	0.044	0.091	0.019	0.068
La	PPM	32	16	17	15	17	7	18
Cr	PPM	42	199	158	198	134	112	71
Mg	%	0.07	0.41	0.14	0.3	0.33	0.27	0.12
Ba	PPM	31	202	191	128	134	87	101
Ti	%	0.04	0.046	0.043	0.051	0.05	0.028	0.043

B	PPM	<20	35	<20	32	<20	27	<20
Al	%	3.58	2.74	2.38	1.06	2.9	0.8	2.33
Na	%	<0.01	0.03	<0.01	0.02	<0.01	0.01	<0.01
K	%	0.04	0.08	0.03	0.03	0.09	0.04	0.08
W	PPM	<2	6	5	2	4	<2	2
S	%	<0.05	0.13	<0.05	<0.05	0.07	<0.05	<0.05
Hg	PPM	<1	<1	<1	<1	<1	<1	<1
Tl	PPM	<5	<5	5	8	<5	8	<5
Ga	PPM	20	8	11	<5	12	<5	12
Sc	PPM	12	<5	6	<5	6	<5	6

Results from Aqua Regia Method of Geochemical Analysis of Some Samples from Ogijo Industrial Layout (Continued)

Element	Unit	39Ai	77Ai	29Aiv	30Bi	L60	48Ai	25Aii
Mo	PPM	59	1	26	<1	17	2	5
Cu	PPM	834	27	424	17	509	29	135
Pb	PPM	536	66	1024	82	792	333	1299
Zn	PPM	4180	176	2084	104	>10000	371	1379
Ag	PPM	1.3	<0.3	1.1	<0.3	1.9	<0.3	0.6
Ni	PPM	74	7	152	5	171	7	33
Co	PPM	29	2	27	2	96	2	7
Mn	PPM	1767	398	3825	299	3022	295	869
Fe	%	12.25	1.84	28.81	1.08	15.85	1.38	4.8
As	PPM	6	1	11	1	12	1	4
Th	PPM	3	3	18	<2	7	<2	4
Sr	PPM	33	8	20	19	49	7	15
Cd	PPM	1.3	<0.5	<0.5	<0.5	14.3	<0.5	2.7
Sb	PPM	16	3	7	<3	24	<3	5
Bi	PPM	3	<3	<3	5	<3	<3	4
V	PPM	23	28	85	21	62	18	33
Ca	%	0.4	0.19	0.44	1.22	0.79	0.18	0.35
P	%	0.066	0.015	0.054	0.034	0.113	0.016	0.101
La	PPM	9	5	35	5	14	3	9
Cr	PPM	83	46	288	24	242	51	91

Mg	%	0.11	0.05	0.33	0.04	0.22	0.02	0.17
Ba	PPM	425	38	200	18	444	19	89
Ti	%	0.028	0.022	0.059	0.011	0.065	0.013	0.03
B	PPM	75	34	28	<20	191	<20	<20
Al	%	0.72	0.73	1.75	0.58	2.62	0.39	1.26
Na	%	0.03	0.01	0	<0.01	0.07	<0.01	0.01
K	%	0.05	0.05	0.05	0.02	0.17	0.01	0.04
W	PPM	3	<2	3	<2	<2	<2	3
S	%	0.07	<0.05	<0.05	<0.05	0.11	<0.05	0.22
Hg	PPM	<1	<1	<1	<1	<1	<1	<1
Tl	PPM	6	<5	11	<5	<5	<5	<5
Ga	PPM	<5	<5	<5	<5	10	<5	5
Sc	PPM	<5	<5	<5	<5	5	<5	<5

Appendix 4. 6: Charts Showing Concentration (ppm) of Each Major Elements in Ogijo Industrial Layout

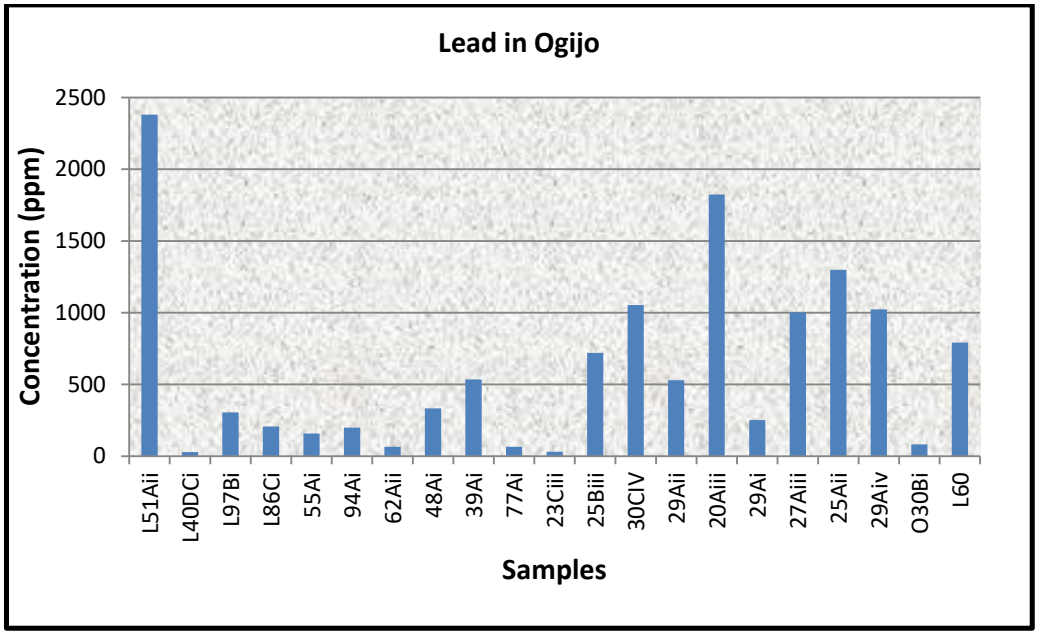

Appendix 4.6.1: Variation in concentration of Lead in the samples from Ogijo

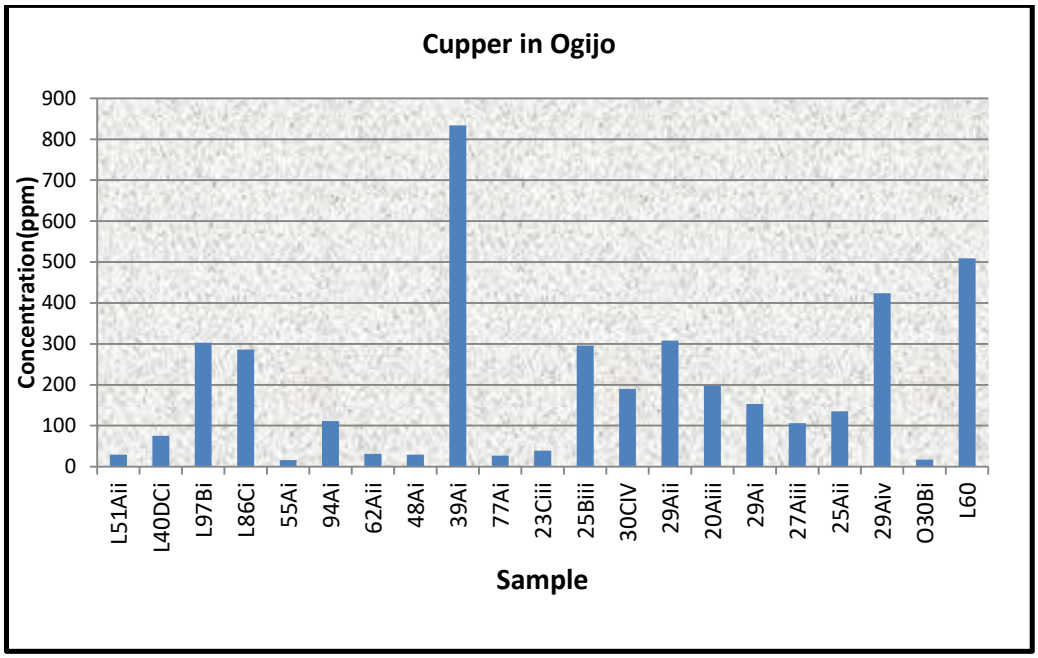

Appendix 4.6.2: Variation in concentration of Copper in the samples from Ogijo

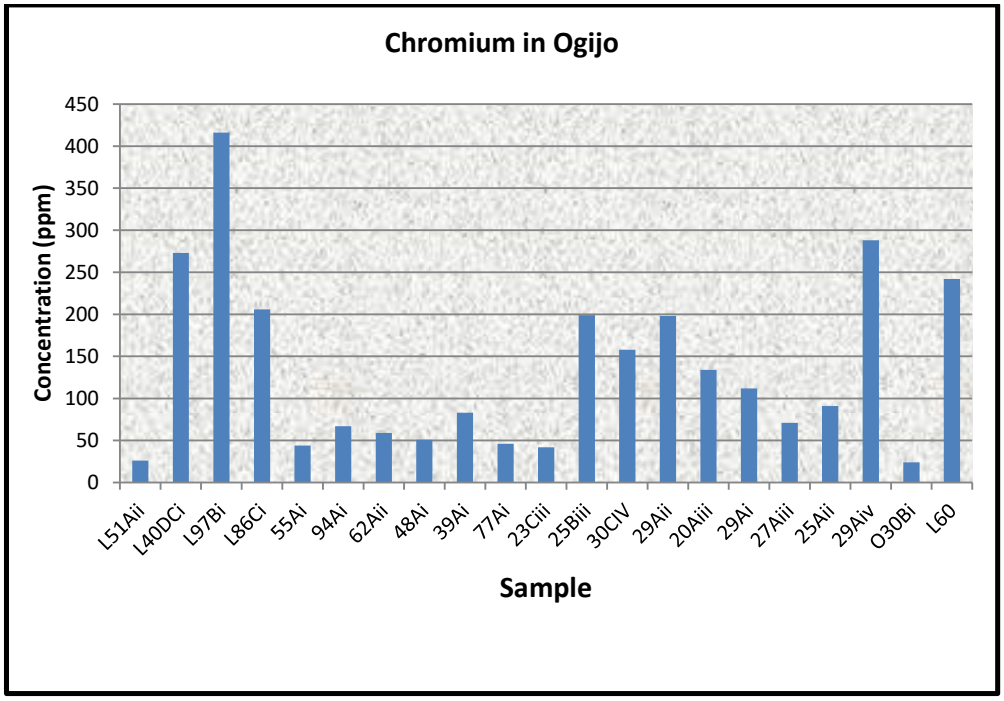

Appendix 4.6.3: Variation in concentration of Chromium in the samples from Ogijo

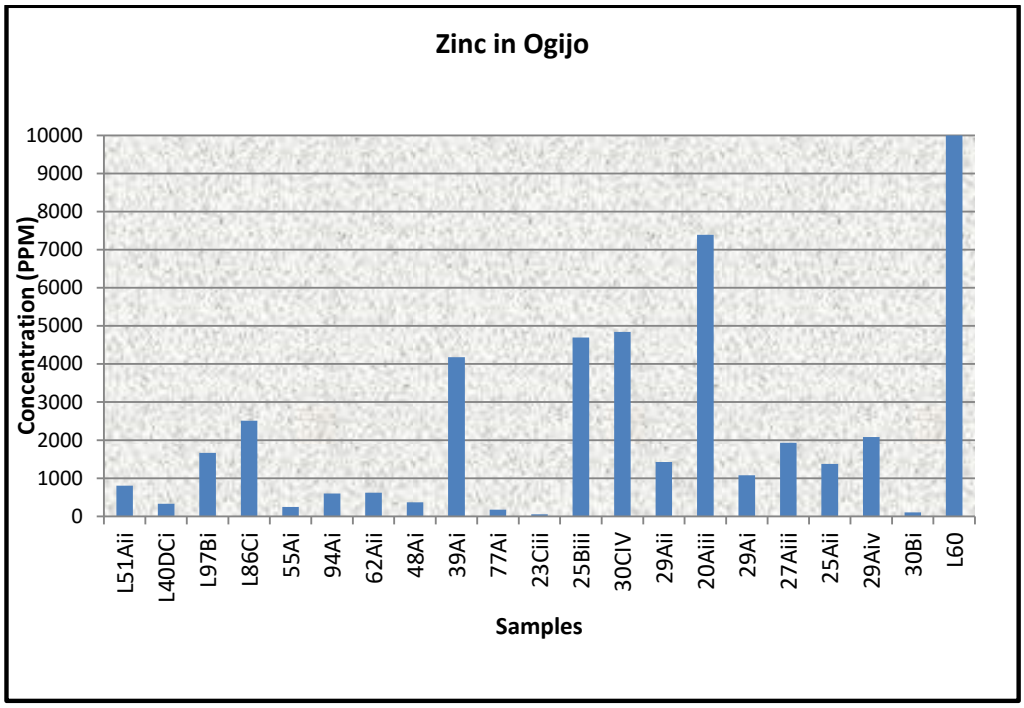

Appendix 4.6.4: Variation in concentration of Zinc in the samples from Ogijo

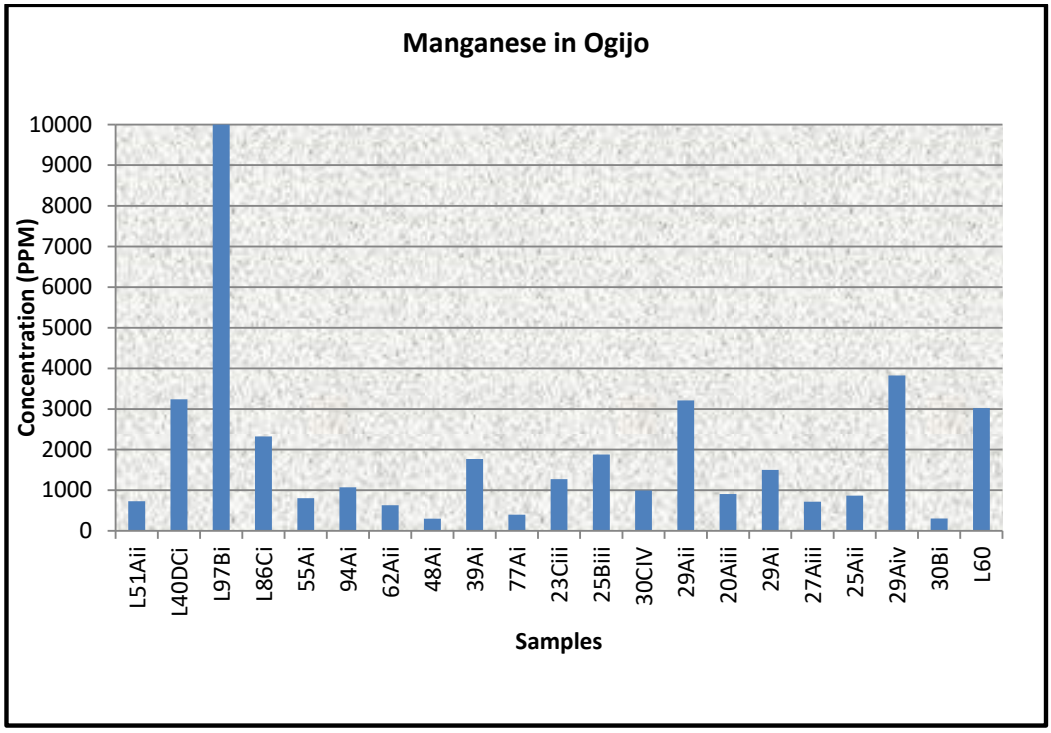

Appendix 4.6.5: Variation in concentration of Manganese in the samples from Ogijo

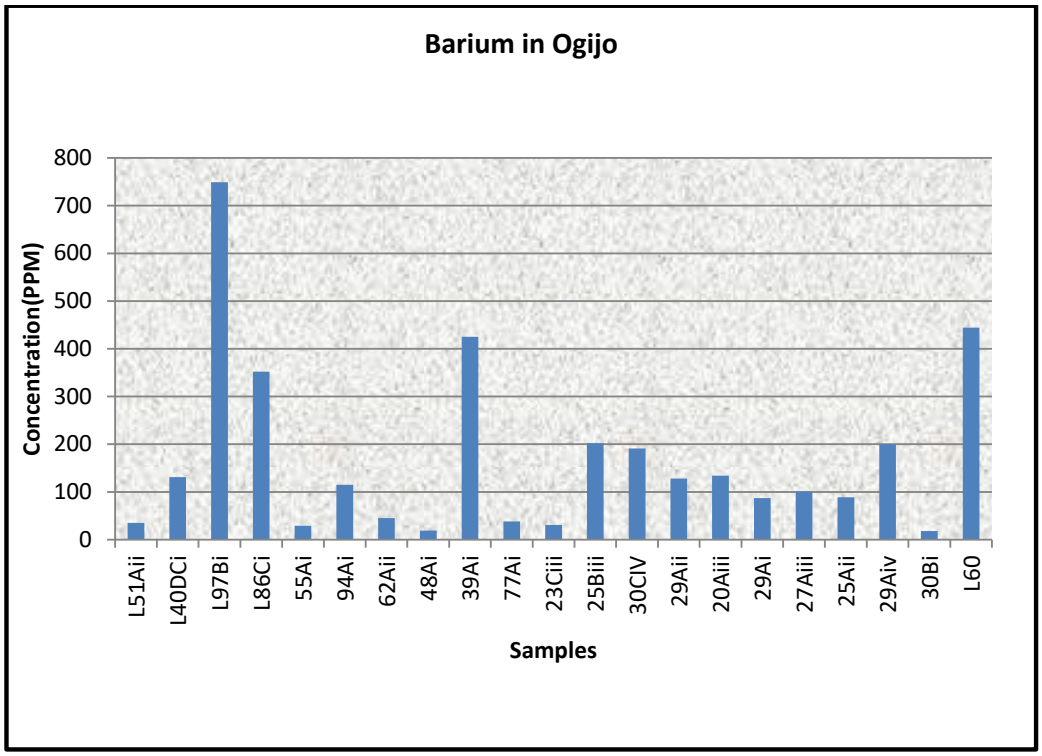

Appendix 4.6.6: Variation in concentration of Barium in the samples from Ogijo

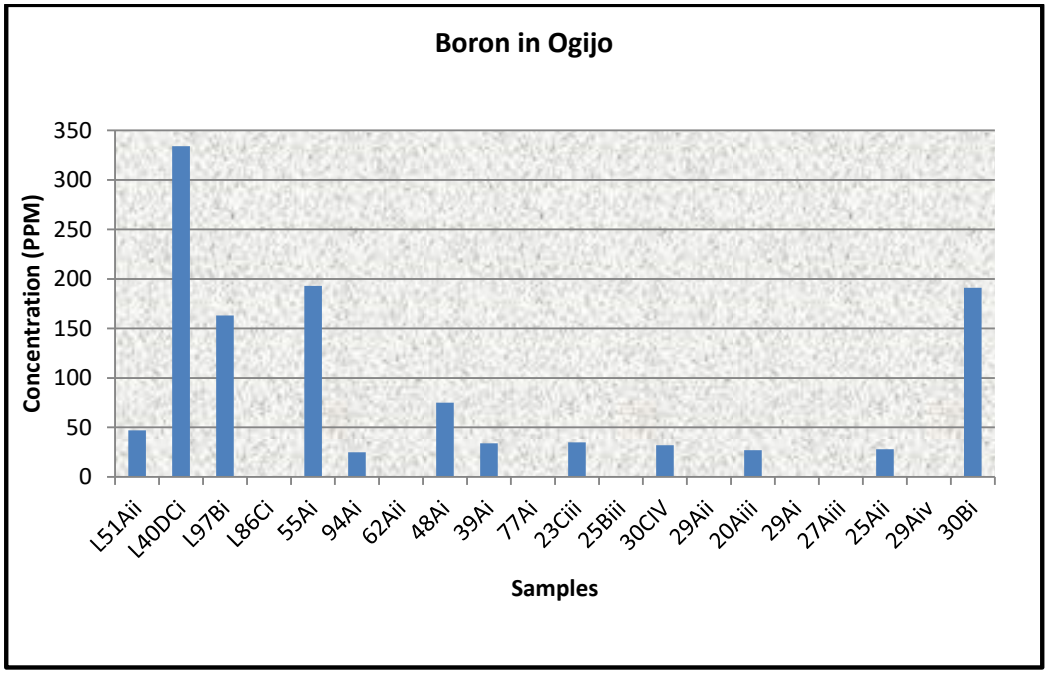

Appendix 4.6.7: Variation in concentration of Boron in the Samples from Ogijo

Appendix 4.7: Comparison Between Magnetic Susceptibility Readings and Geochemical concentration of Heavy Metals in Ogijo

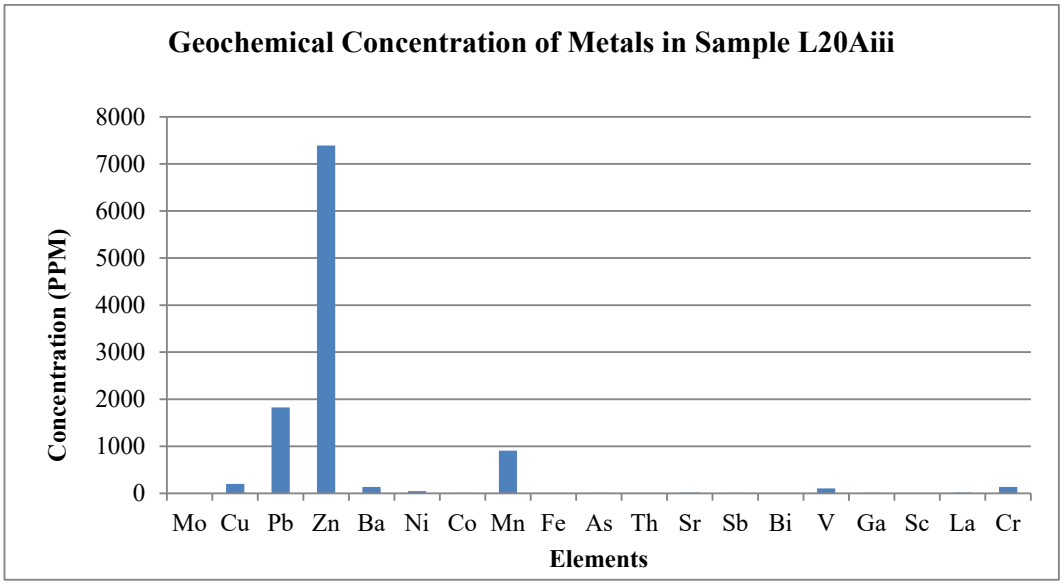

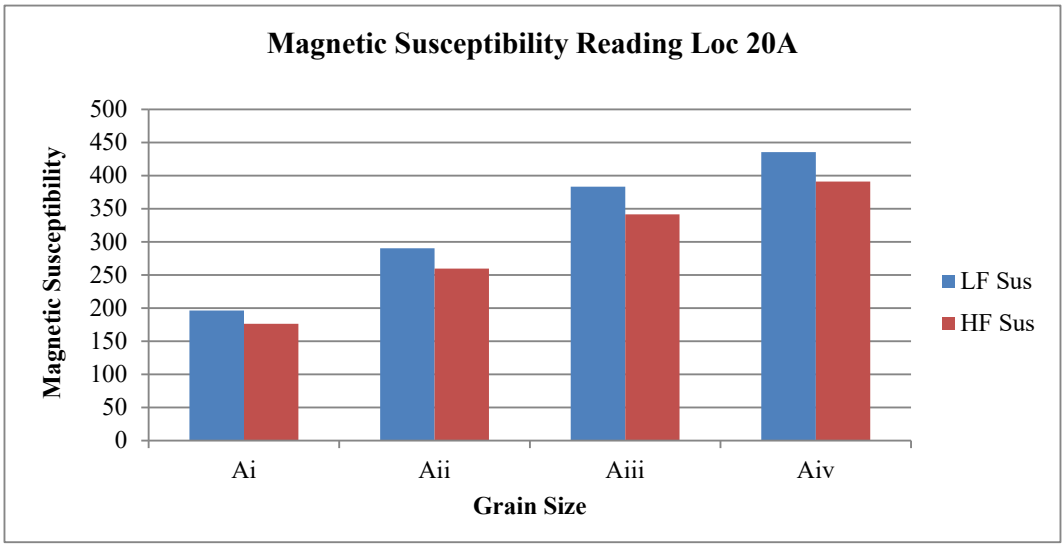

Appendix 4.7.1: 90µm (Aiii) grain at 0cm depth of location 20; with LF383.5, HF341.5 and its heavy metal contents and their concentration

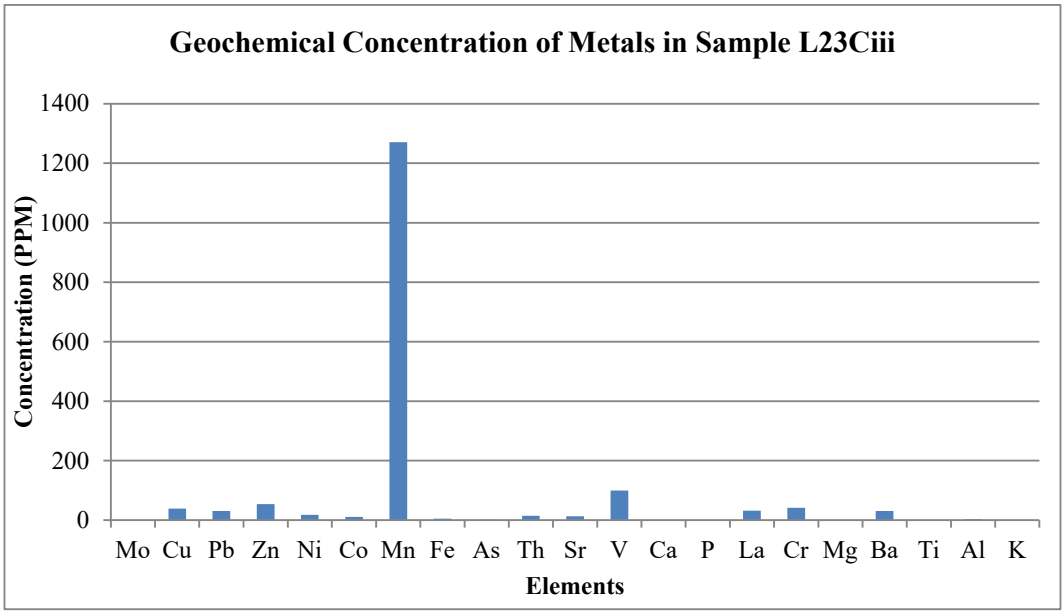

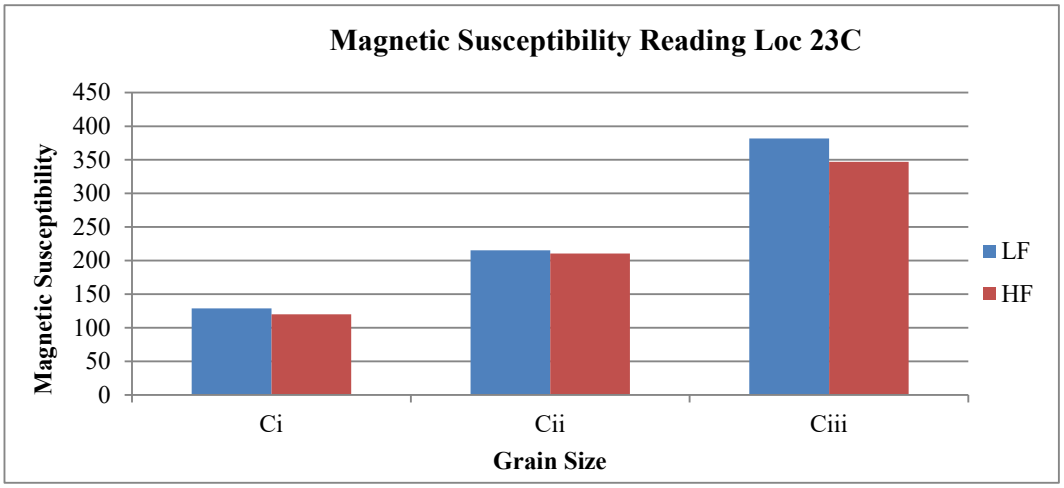

Appendix 4.7.2: 90µm(Ciii) grain at 20cm depth of location 23; with LF381.8, HF347 and its heavy metal contents and their concentration

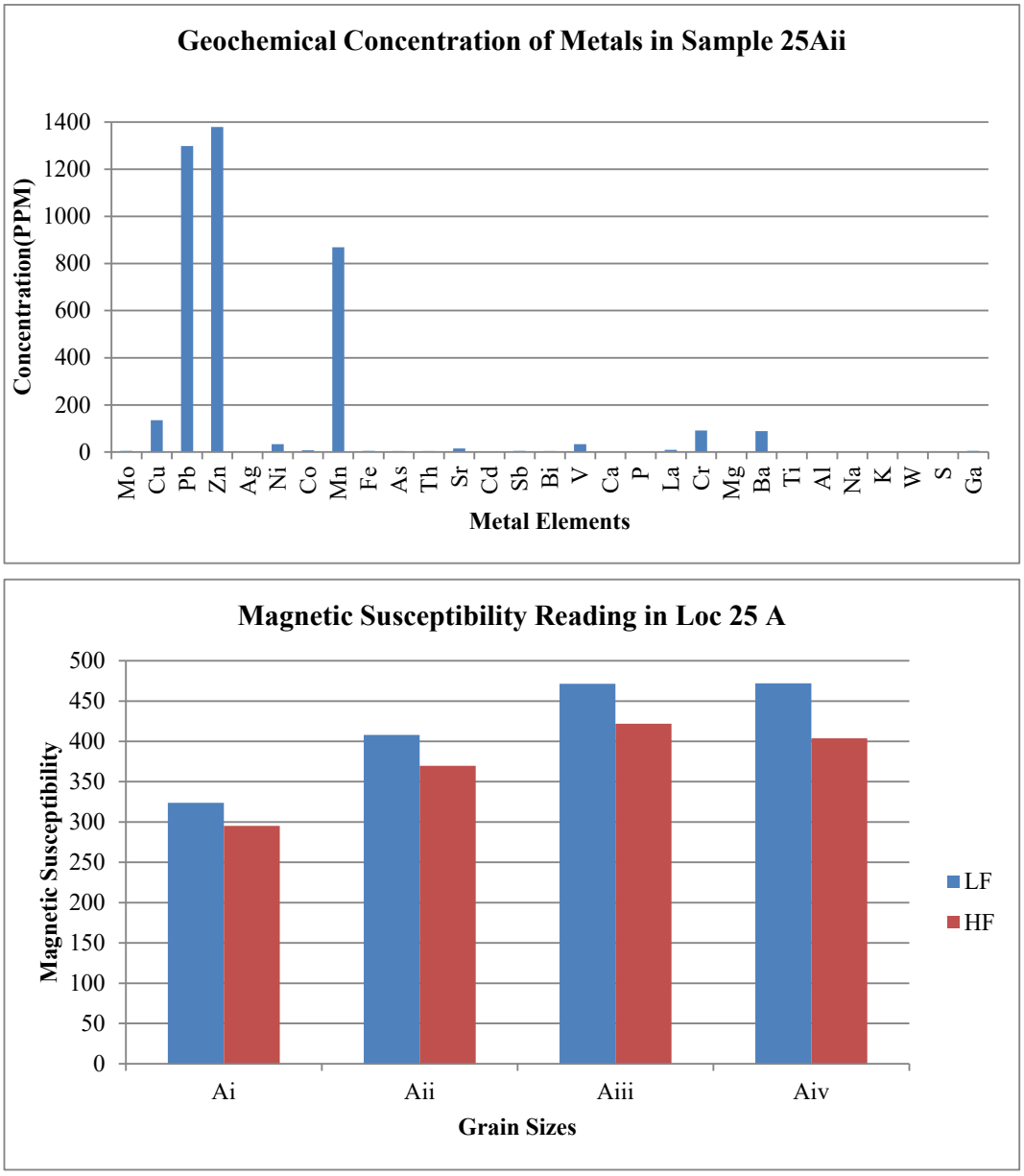

Appendix 4.7.3: 125 µm (Aii) grain at 0 cm depth of location 25; with LF408, HF369.8 and its heavy metal contents and their concentration

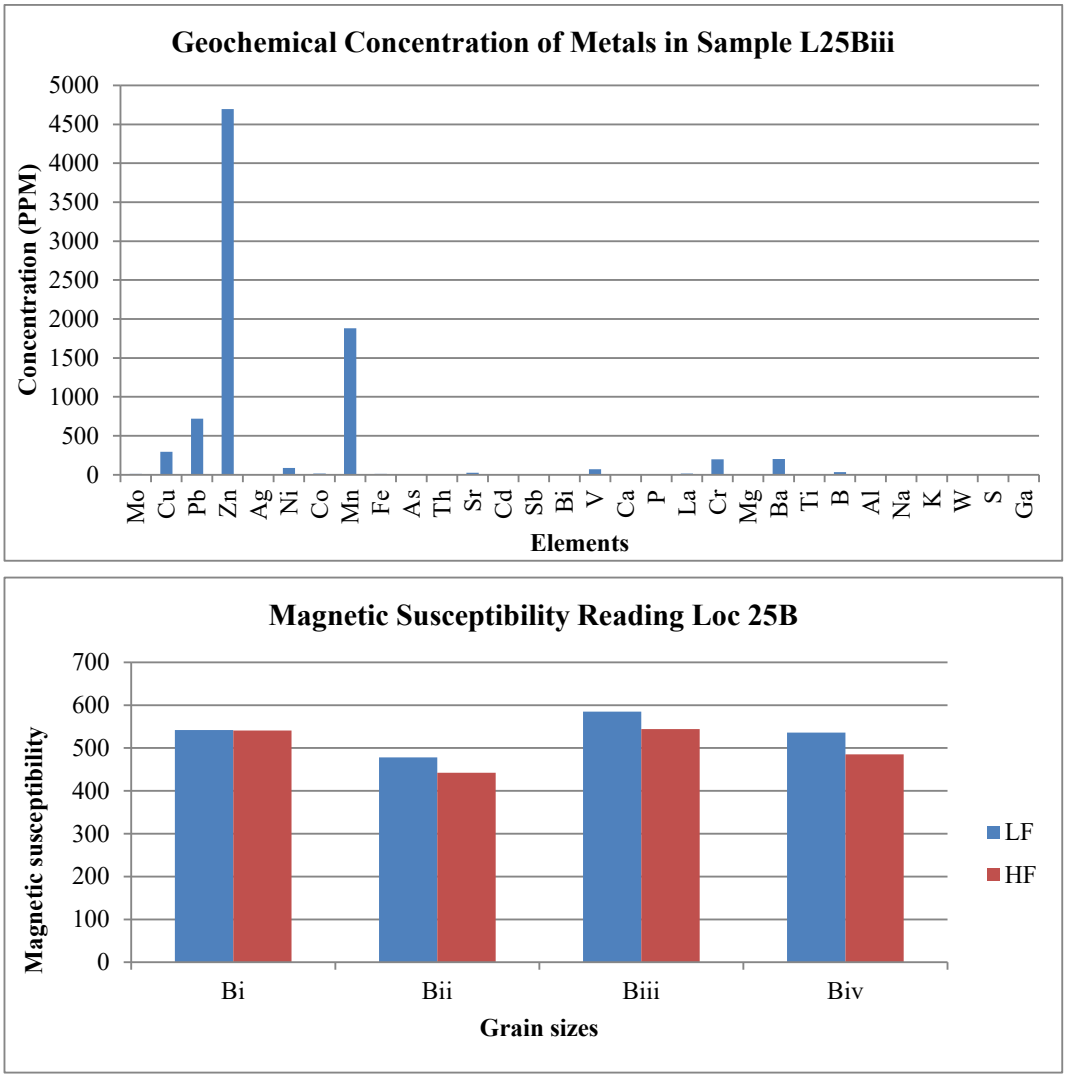

Appendix 4.7.4: 90 µm (Biii) grain at 10 cm depth of location 25; with LF585, HF544.4 and its heavy metal contents and their concentration

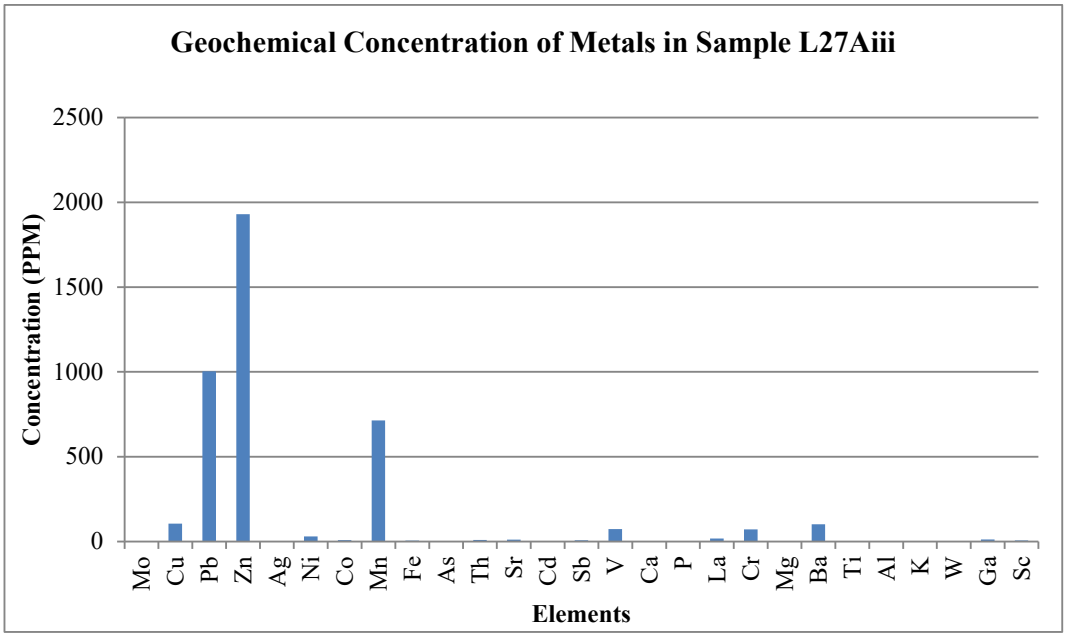

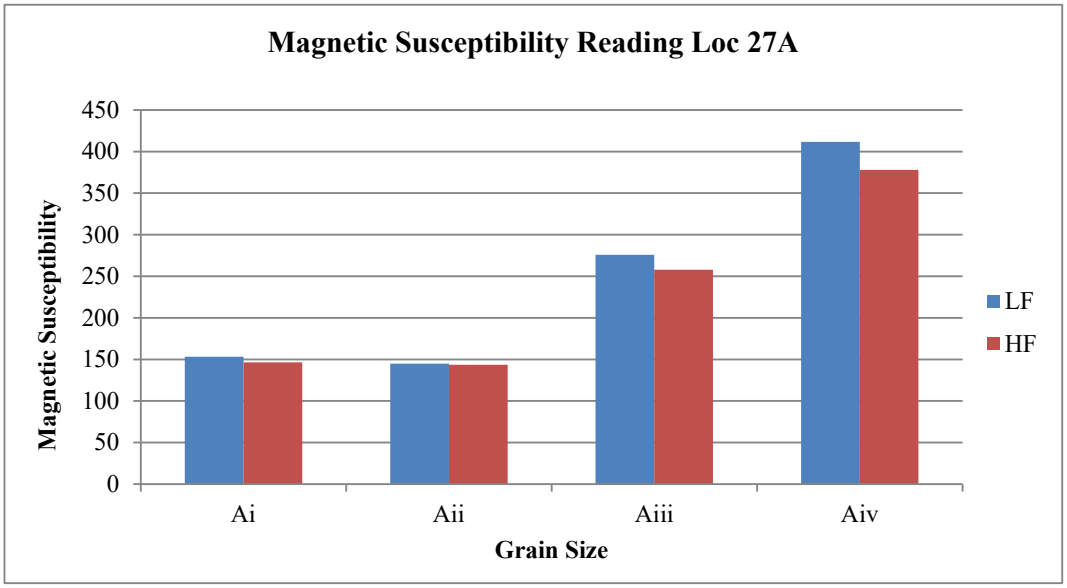

Appendix 4.7.5: 90 µm (Aiii) grain at 0 cm depth of location 27; with LF275.8, HF257.8 and its heavy metal contents and their concentration

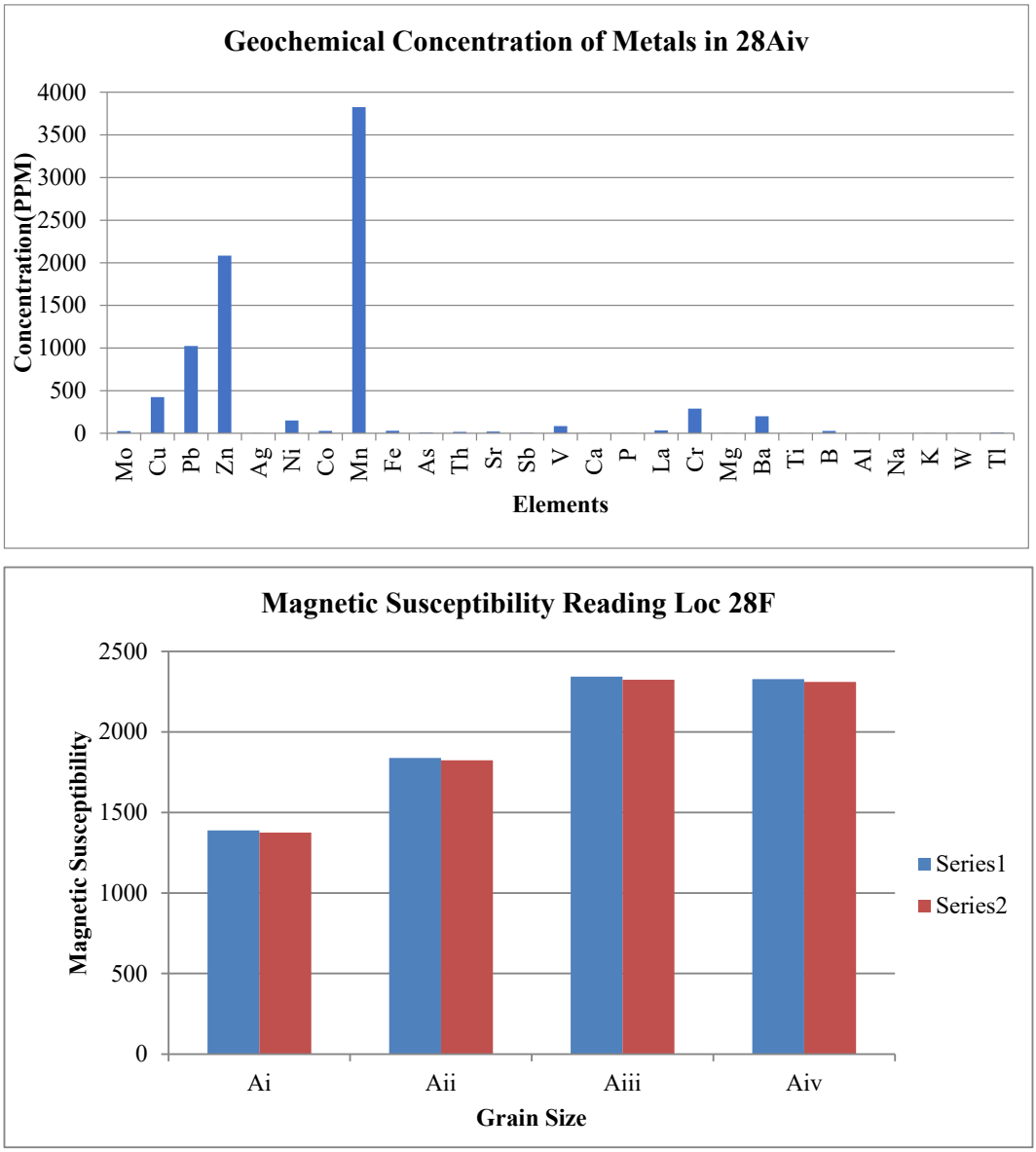

Appendix 4.7.6: 180µm (Ai) grain at 0 cm depth of location 28F; with LF1389, HF1374.7; 125µm (Aii) grain with LF1838.6, HF1824.1; 65µm (Aiv) with LF2328.4, HF2310.5 and its heavy metal contents and their concentration

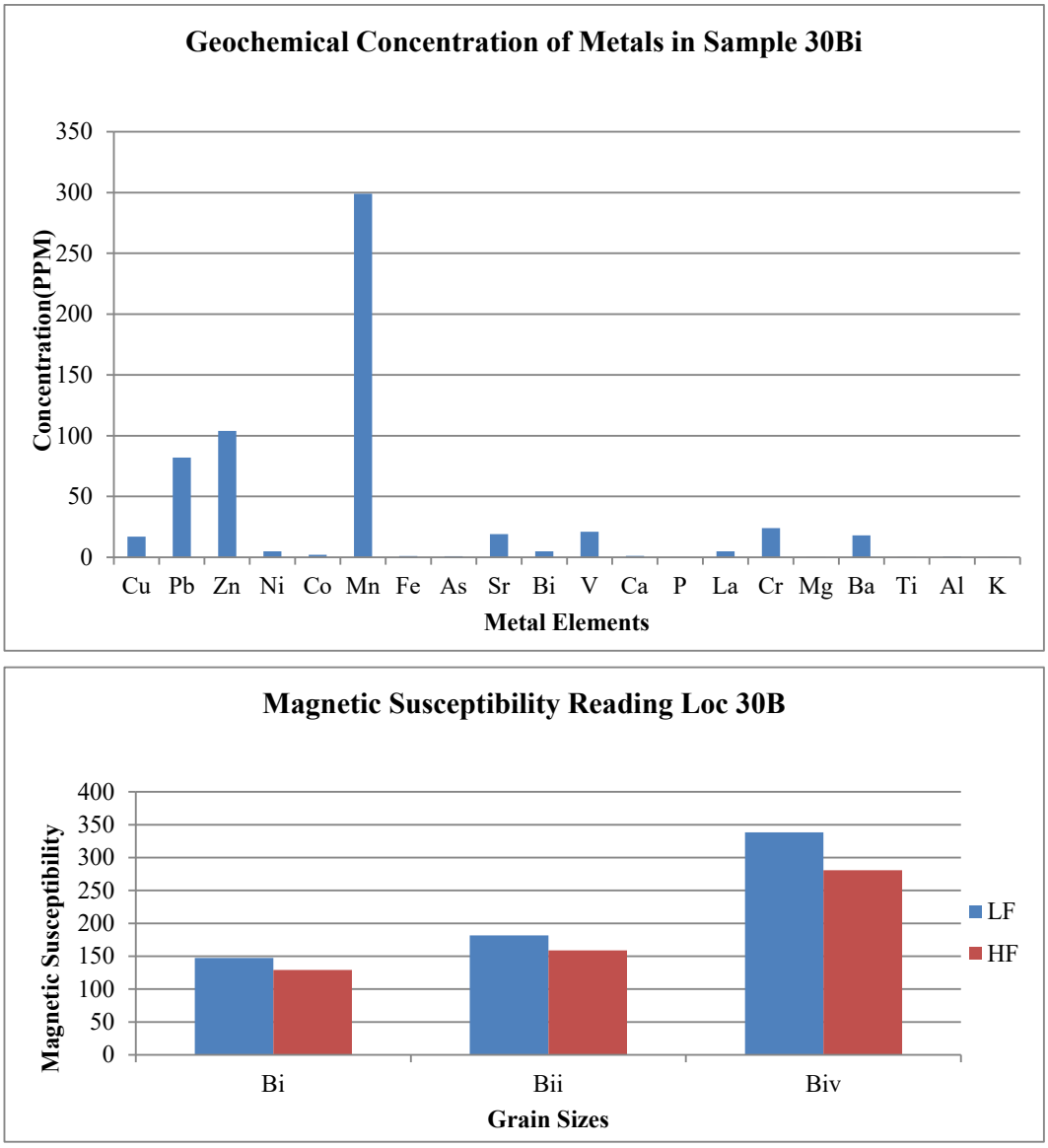

Appendix 4.7.7: 180µm (Bi) grain at 10cm depth of location 30; with LF147.2, HF129.2 and its heavy metal contents and their concentration

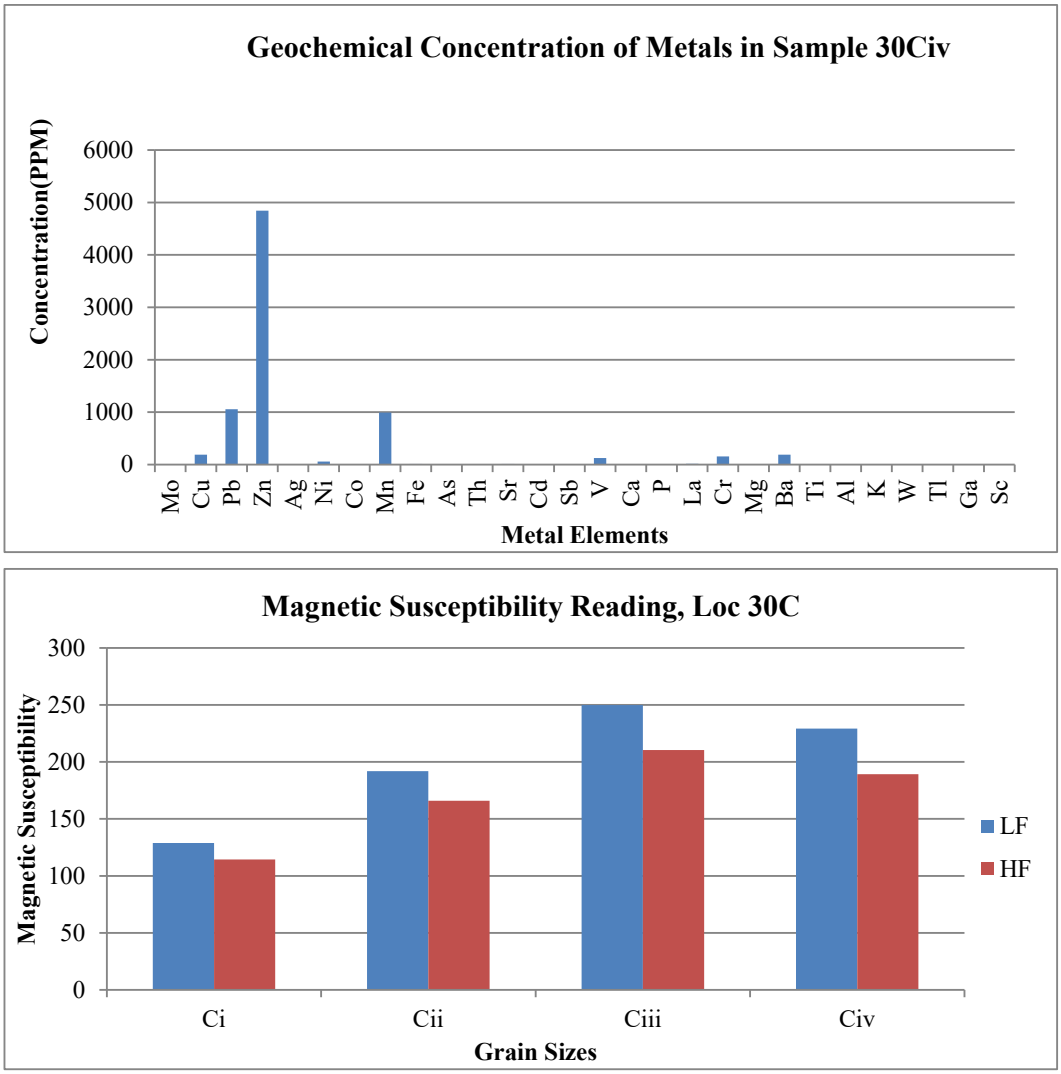

Appendix 4.7.8: 65µm (Civ) grain at 20cm depth of location 30; with LF229.2, HF189.2 and its heavy metal contents and their concentration

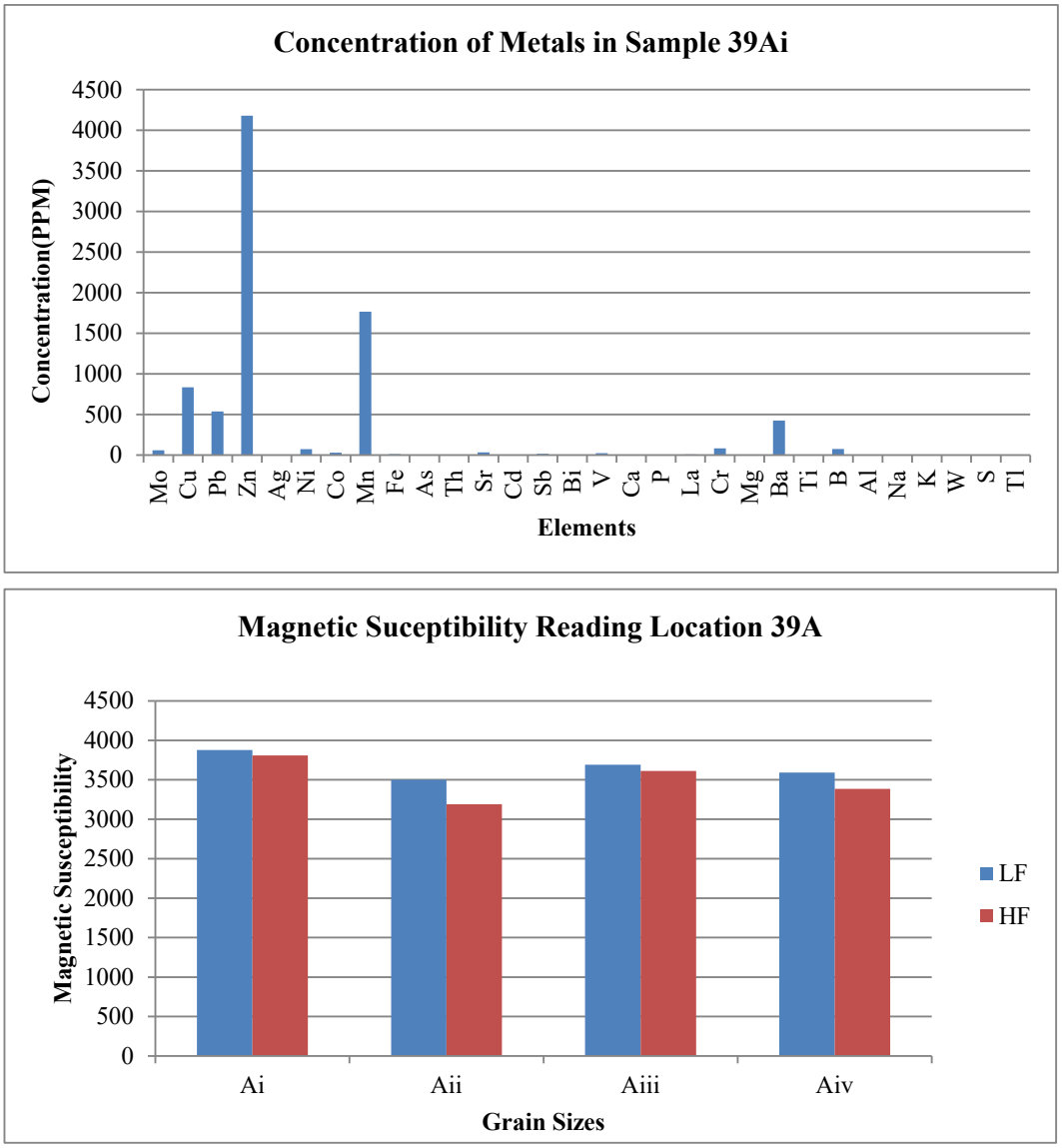

Appendix 4.7.9: 180µm (Aiii) grain at 0cm depth of location 39; with LF3877.8, HF3808.6and its heavy metal contents and their concentration

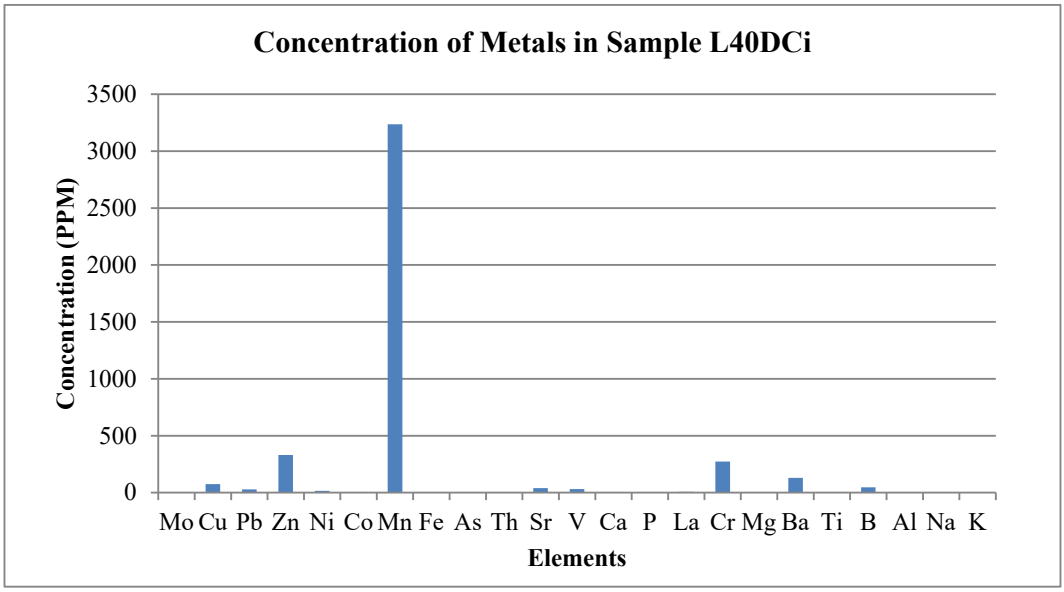

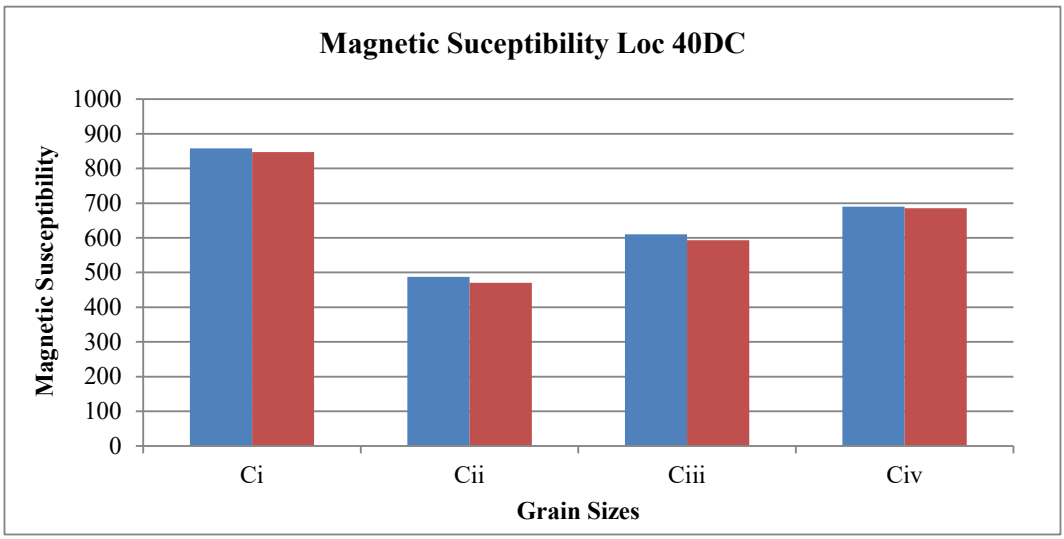

Appendix 4.7.10: 180 µm (Ci) grain at 20cm depth of location 40D; with LF857.7, HF847.3and its heavy metal contents and their concentration

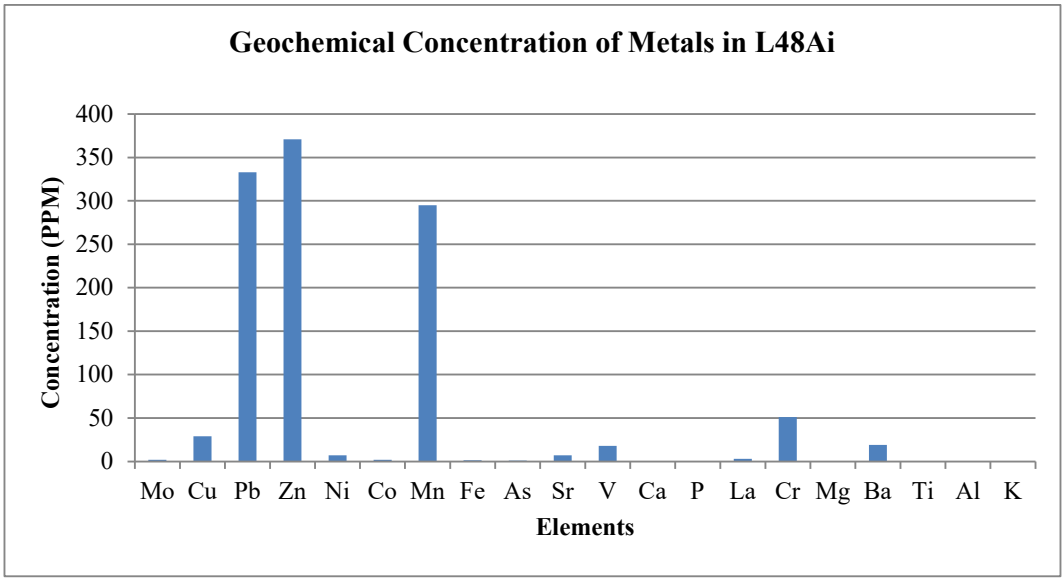

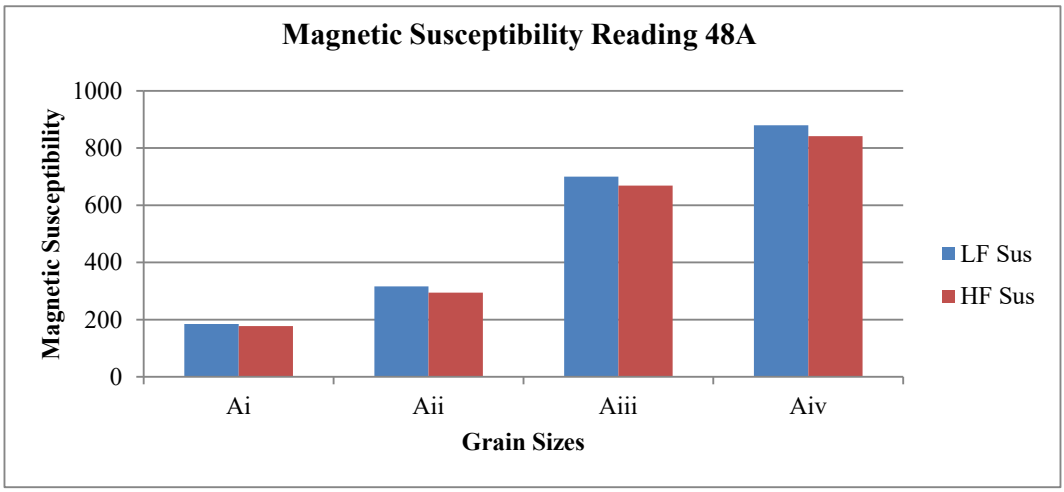

Appendix 4.7.11: 180µm (Ai) grain at 0 cm depth of location 48; with LF184.8, HF177.1 and its heavy metal contents and their concentration

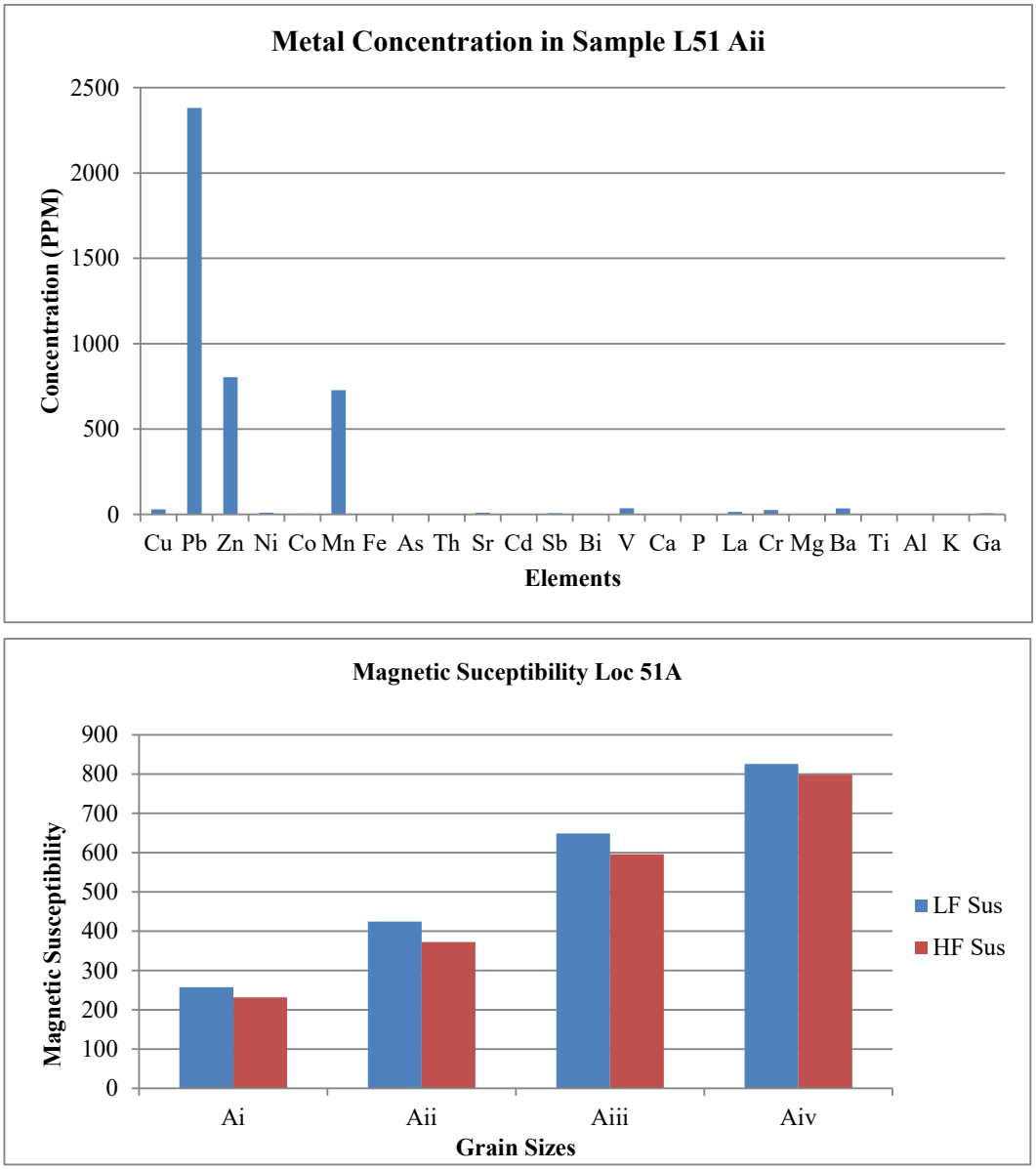

Appendix 4.7.12: 125µm(Aii) grain at 0 cm depth of location 51; with LF424.3, HF372.5 and its heavy metal contents and their concentration

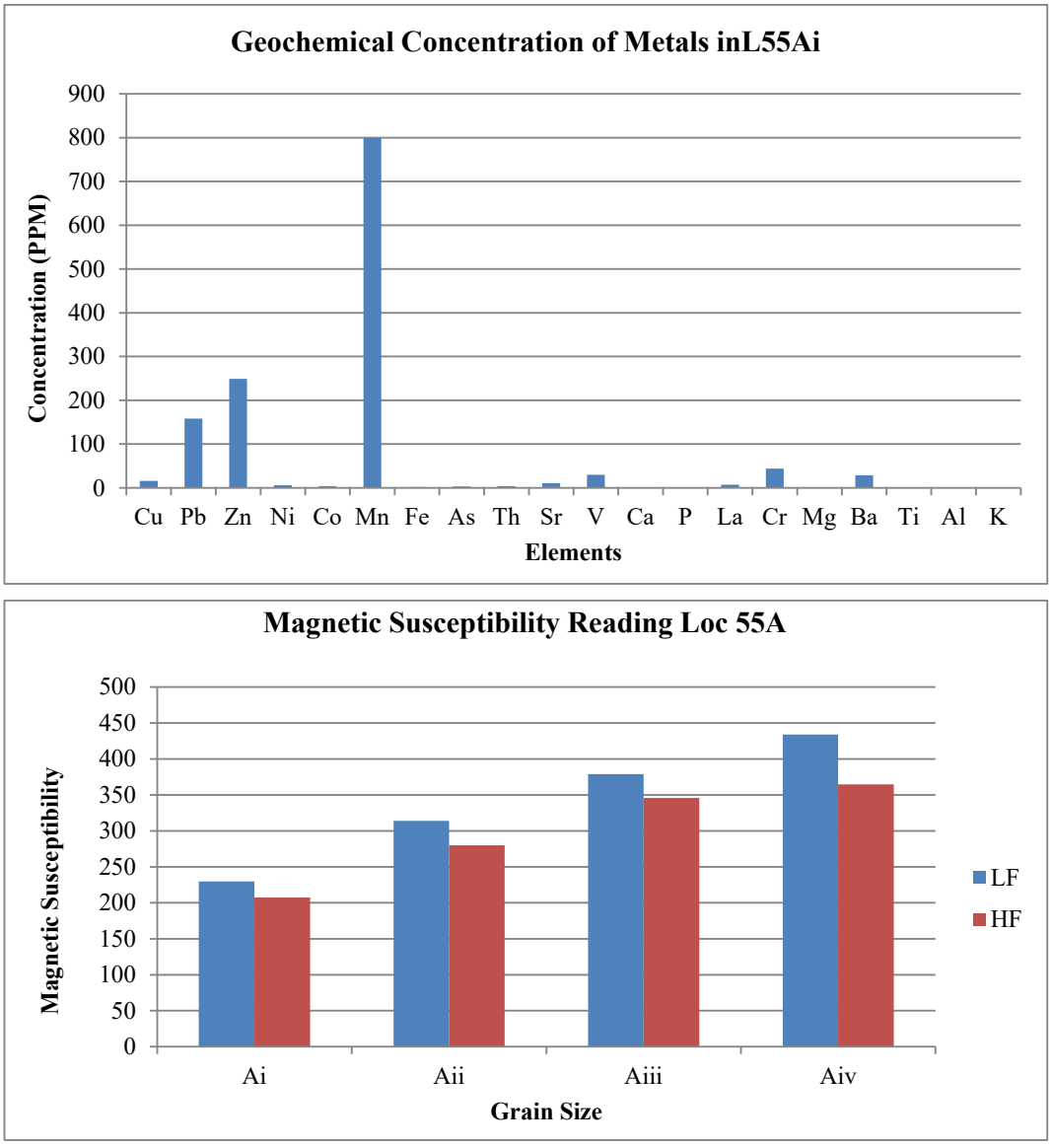

Appendix 4.7.13: 180µm(Ai) grain at 0 cm depth of location 55; with LF229.8, HF207.6 and its heavy metal contents and their concentration

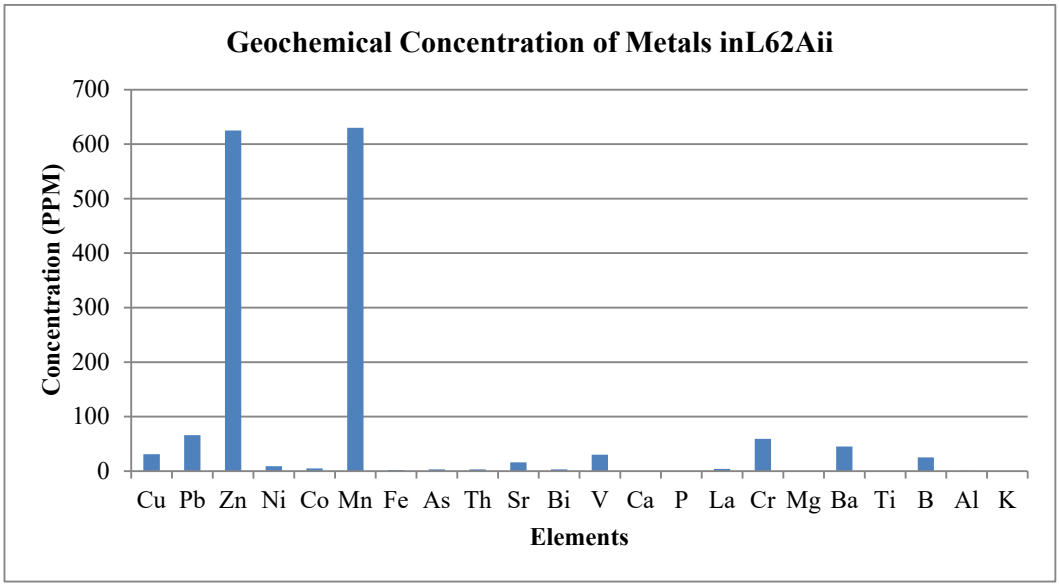

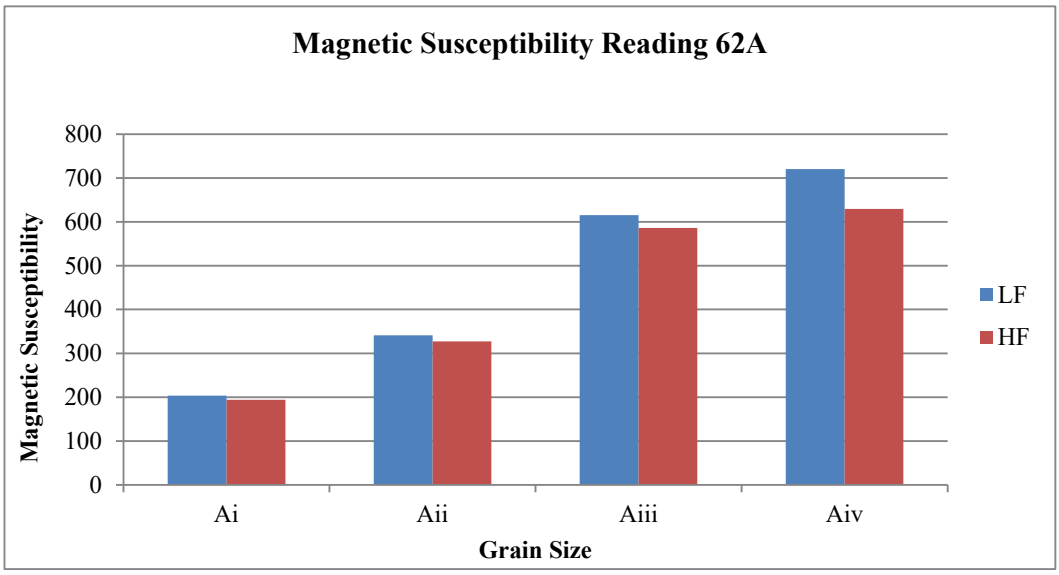

Appendix 4.7.14: 125µm (Aii) grain at 0cm depth of location 62; with LF341.1, HF327.3 and its heavy metal contents and their concentration

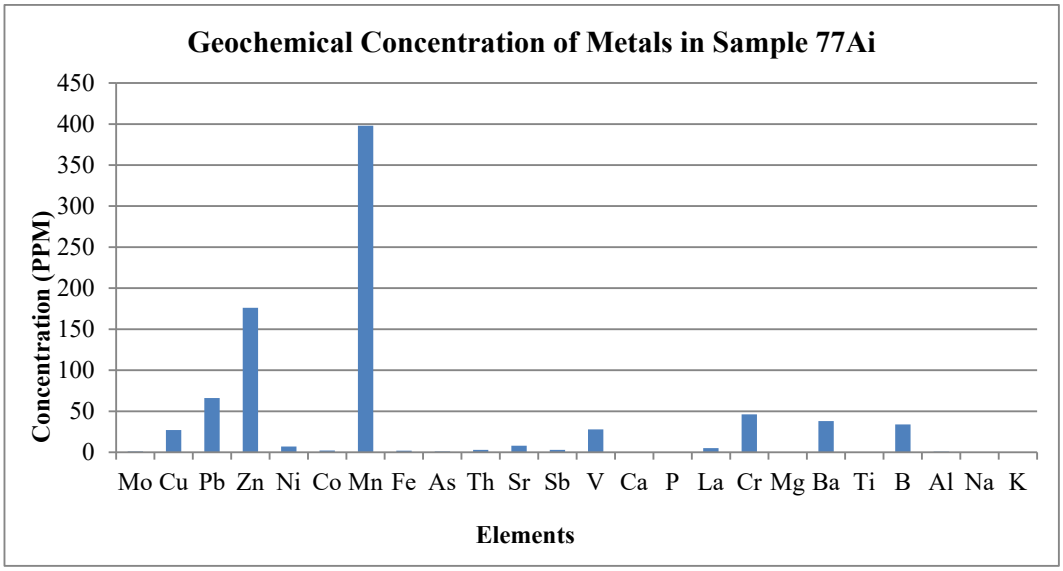

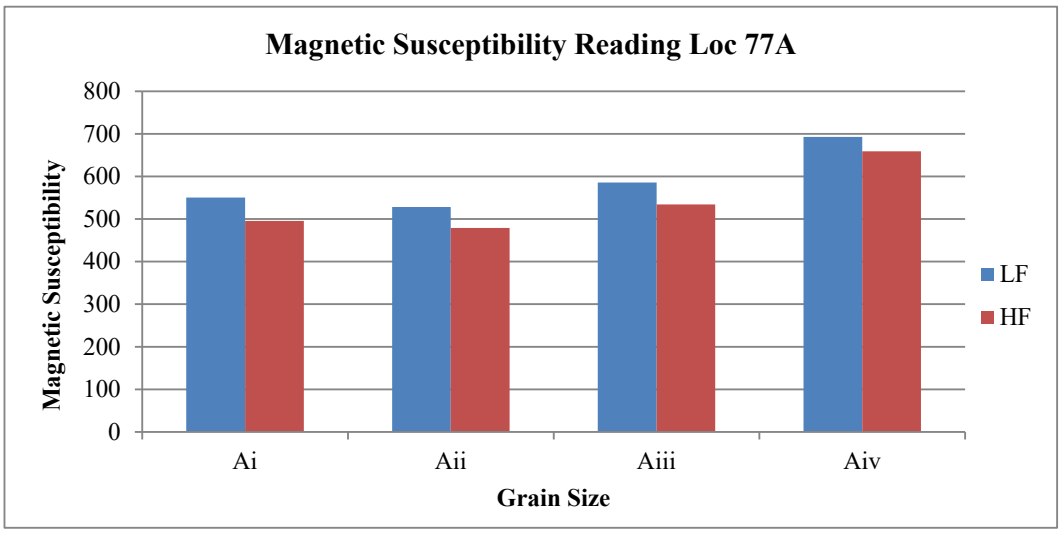

Appendix 4.7.15: 180µm (Ai) grain at 0 cm depth of location 77; with LF550.4, HF495.5 and its heavy metal contents and their concentration

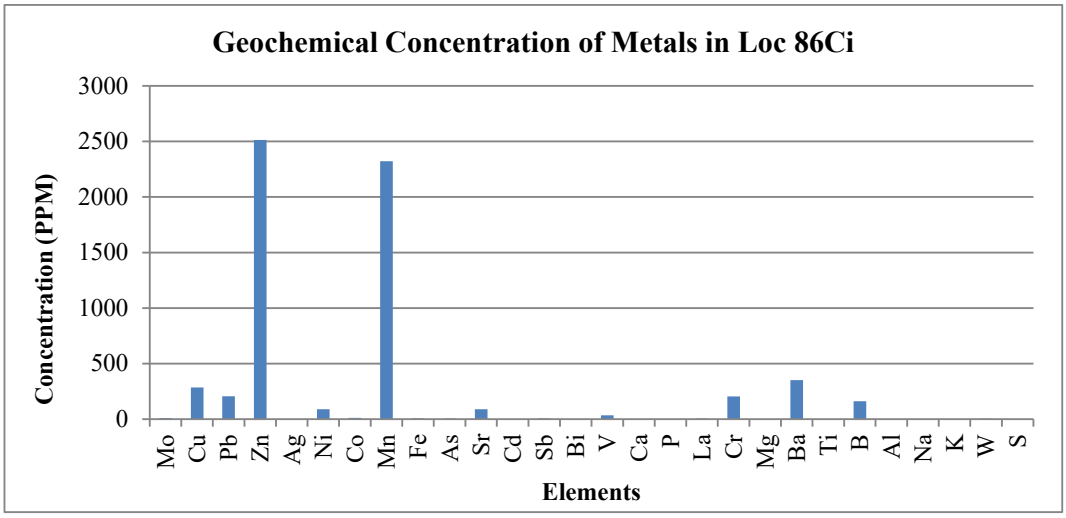

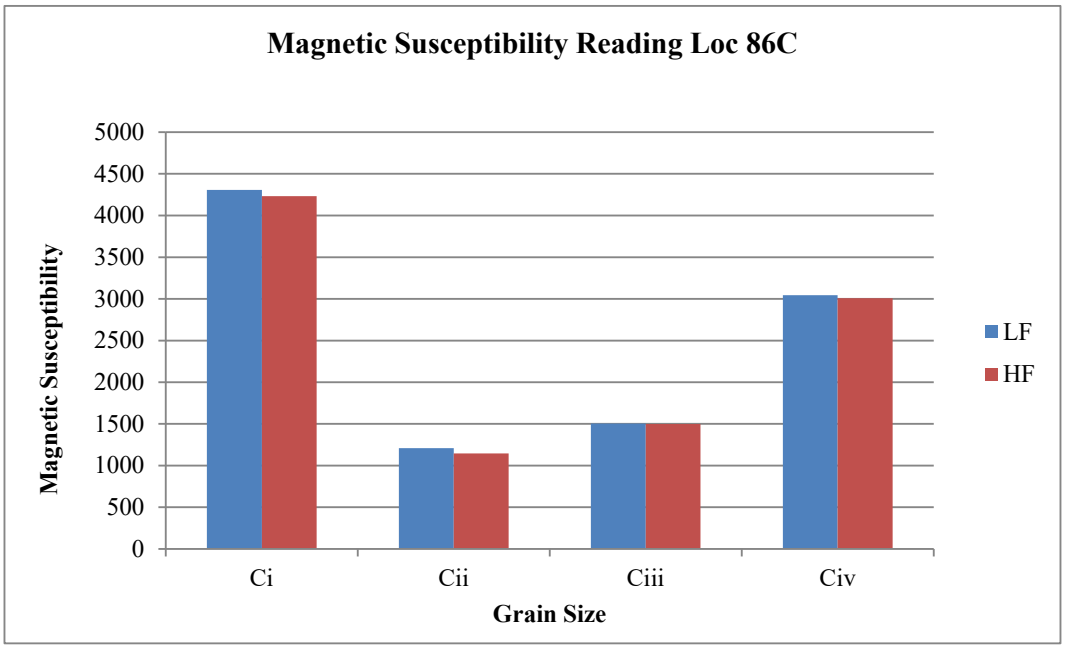

Appendix 4.7.15: 180µm (Ci) grain at 20 cm depth of location 86; with LF4306'9, HF4232 and its heavy metal contents and their concentration

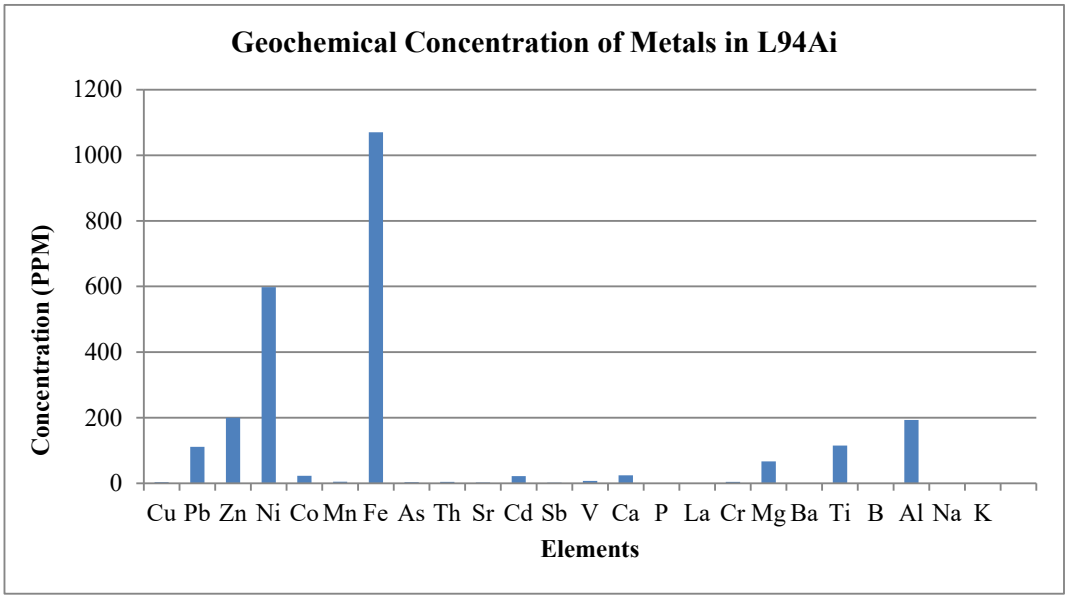

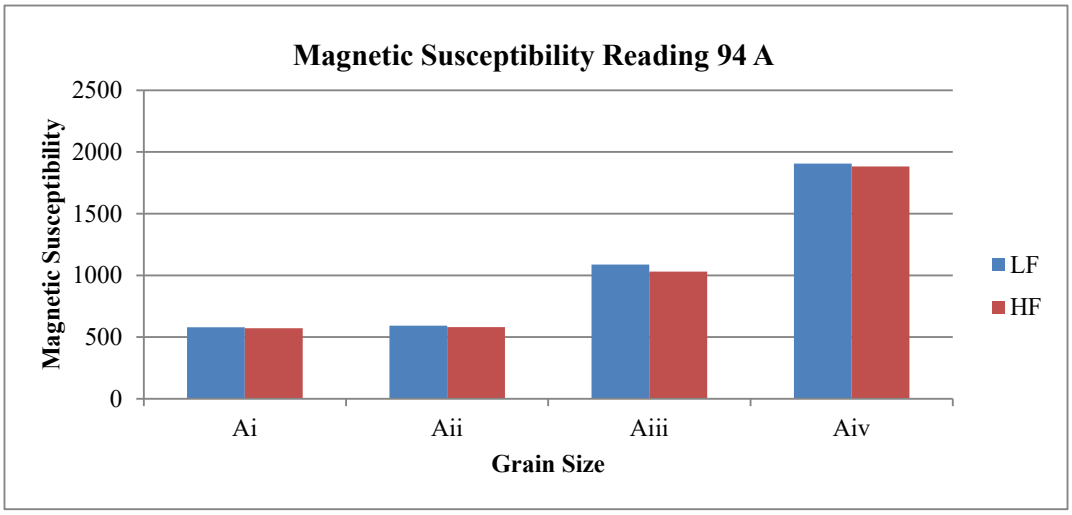

Appendix 4.7.16: 180µm (Ai) grain at 0cm depth of location 94; with LF579.4, HF572 and its heavy metal contents and their concentration

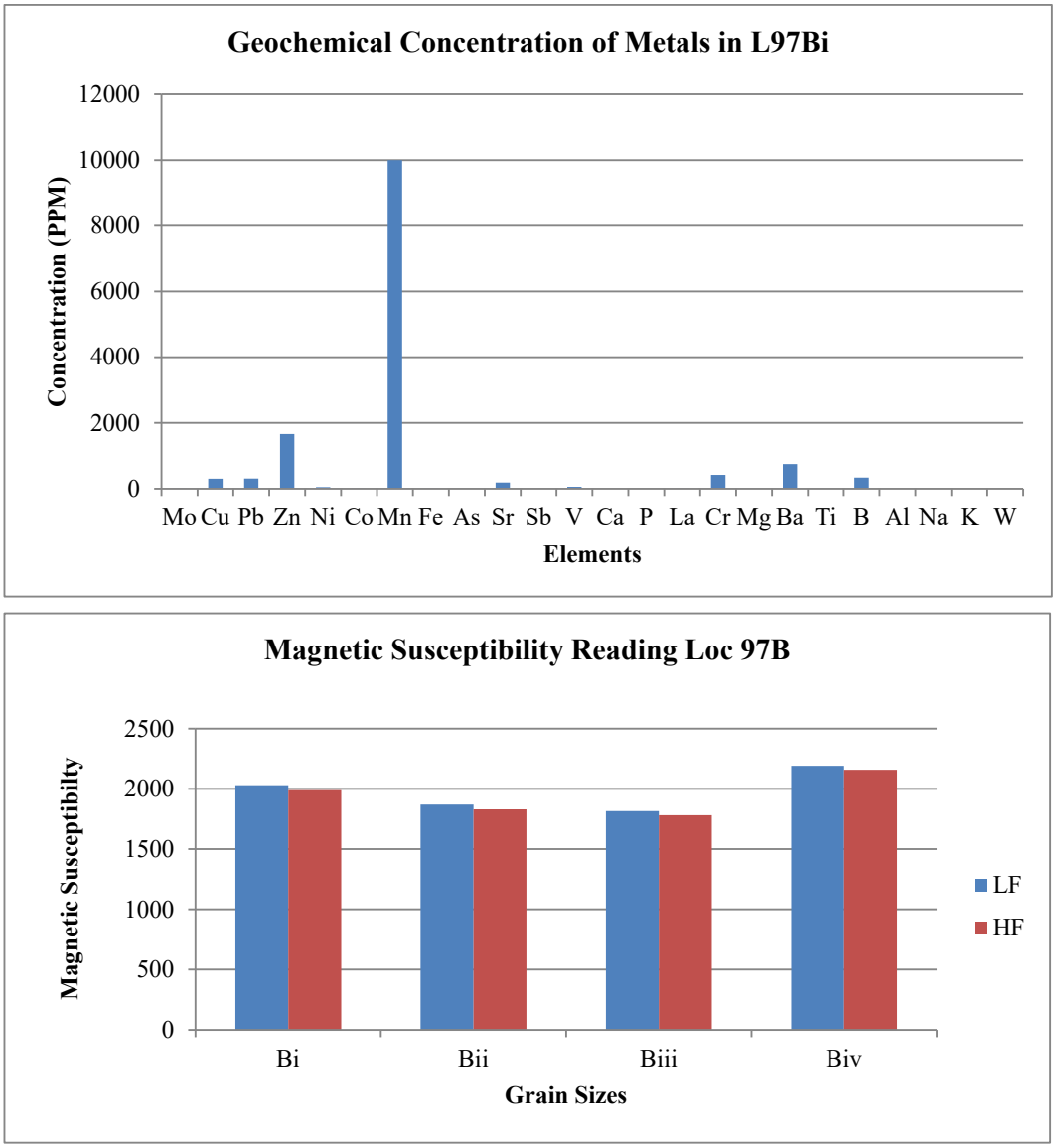

Appendix 4.7.17: 180 µm (Bi) grain at 10 cm depth of location 97; with LF2031.8, HF1990.2 and its heavy metal contents and their concentration

Appendix 4. 8: Low and High Magnetic Susceptibility Readings of Whole Samples from Ota Industrial Layout

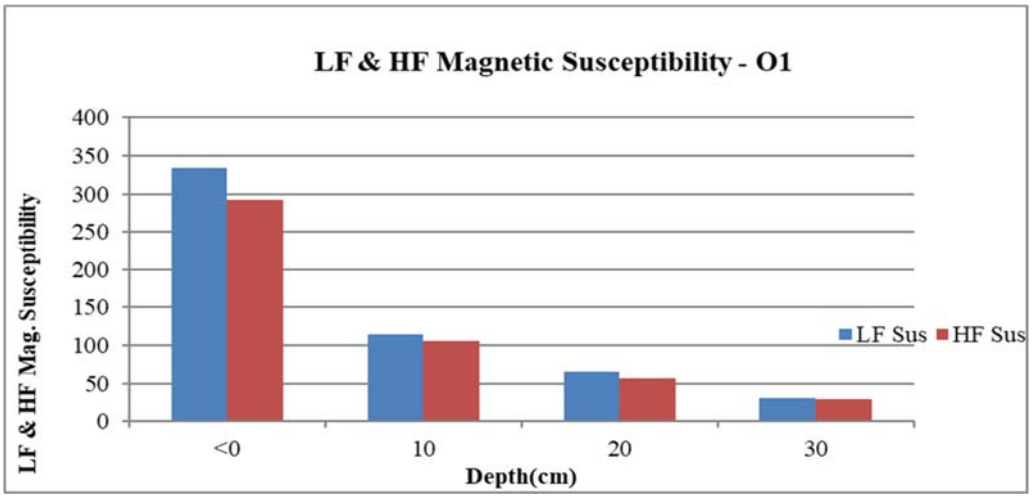

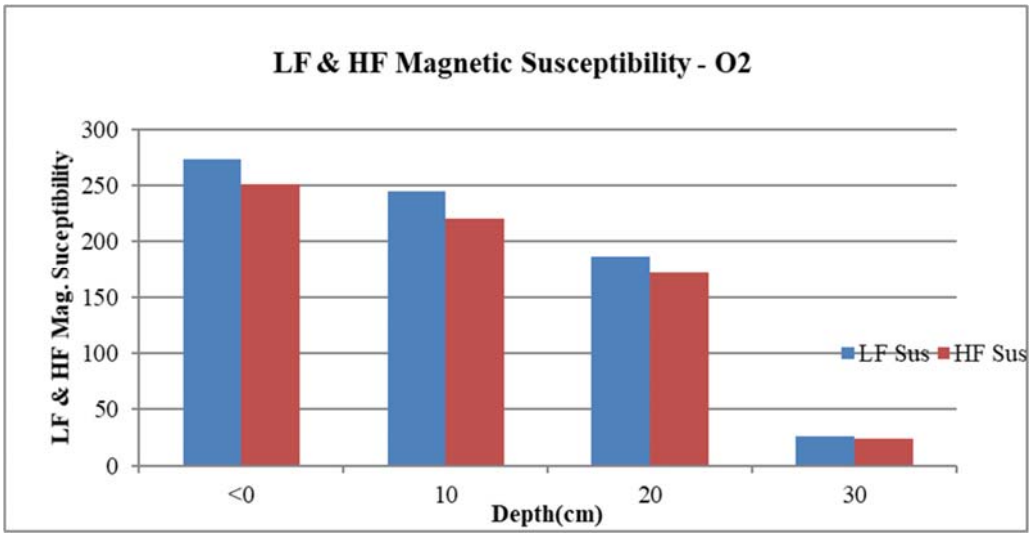

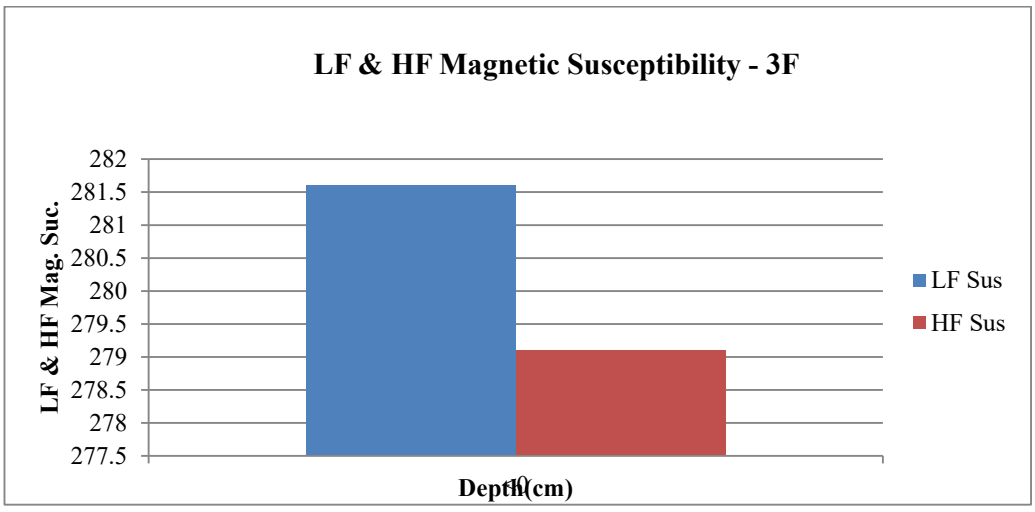

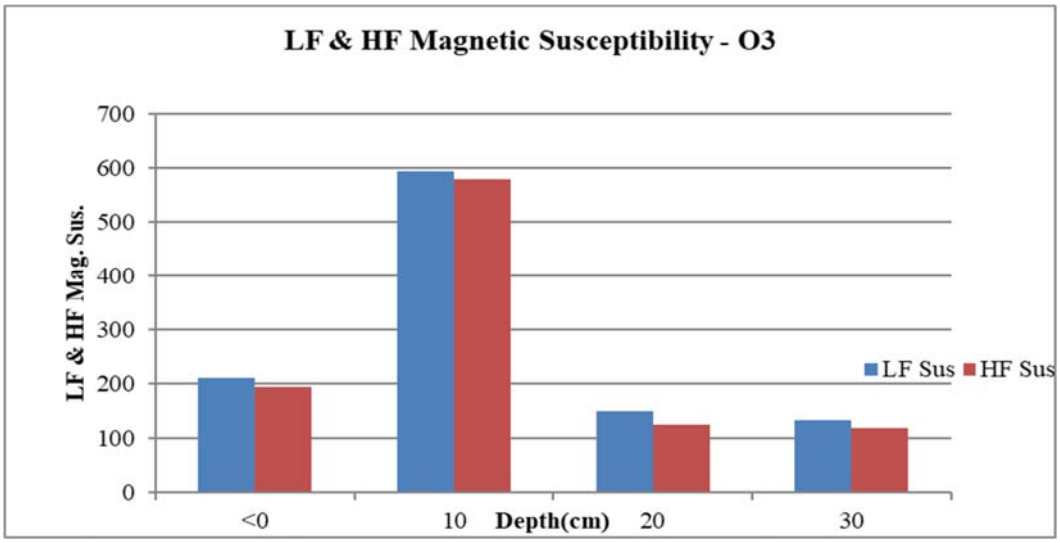
LF & HF Magnetic Susceptibility - O3
LF & HF Mag. Sus.
700
600
500
400
300
200
100
0
<0
10
20
30
Depth(cm)
LF Sus
HF Sus

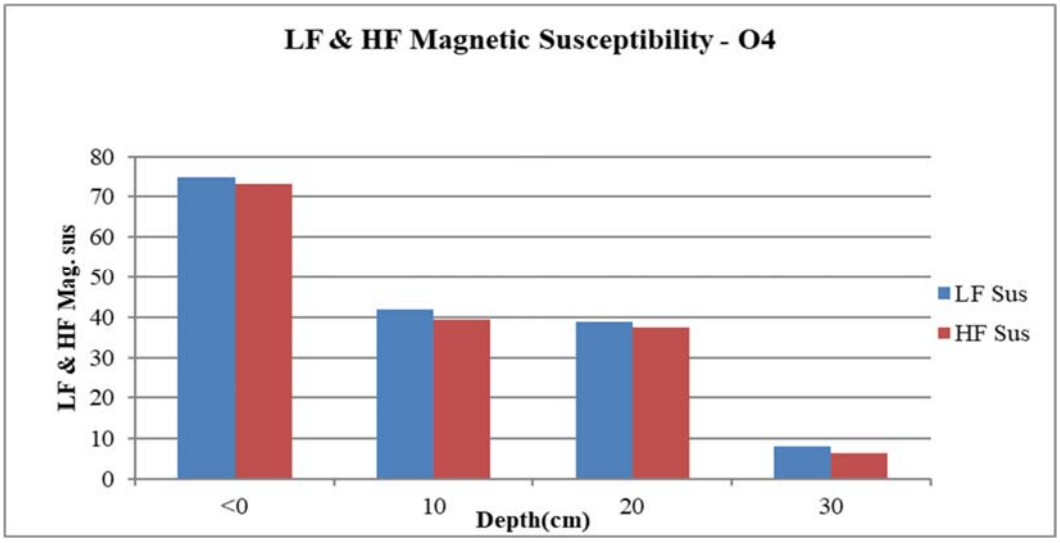
LF & HF Magnetic Susceptibility - O4
LF & HF Mag. sus
80
70
60
50
40
30
20
10
0
<0
10
20
30
Depth(cm)
LF Sus
HF Sus

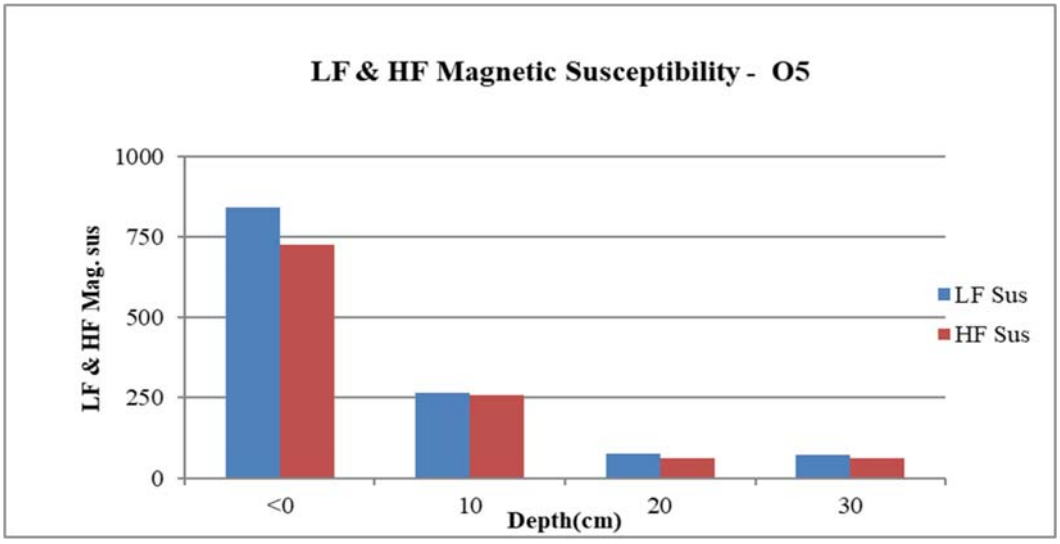
LF & HF Magnetic Susceptibility - O5
LF & HF Mag. sus
1000
750
500
250
0
<0
10
20
30
Depth(cm)
LF Sus
HF Sus

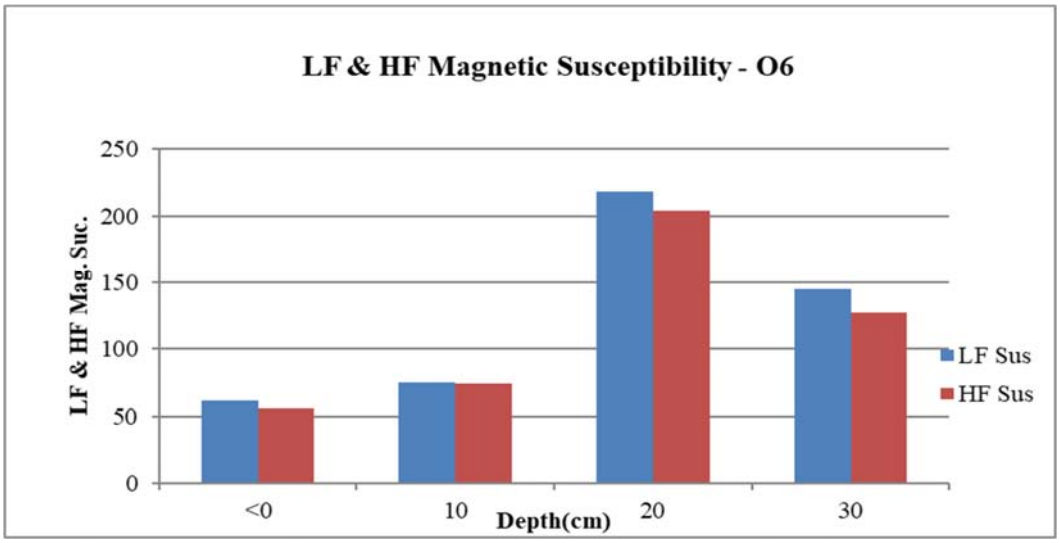
LF & HF Magnetic Susceptibility - O6
LF & HF Mag. Suc.
250
200
150
100
50
0
<0
10
20
30
Depth(cm)
LF Sus
HF Sus

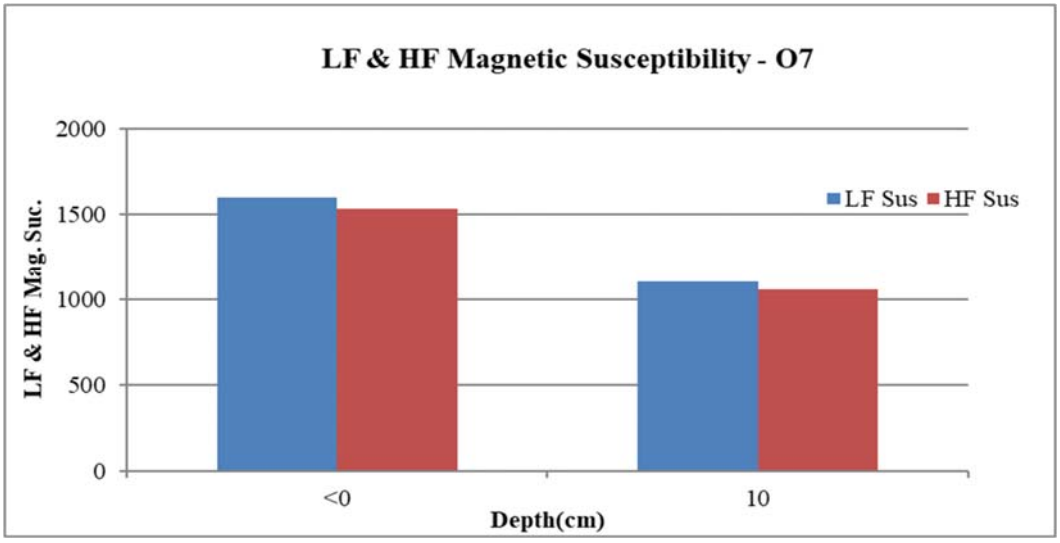
LF & HF Magnetic Susceptibility - O7
LF & HF Mag. Suc.
2000
1500
1000
500
0
<0
10
Depth(cm)
LF Sus
HF Sus

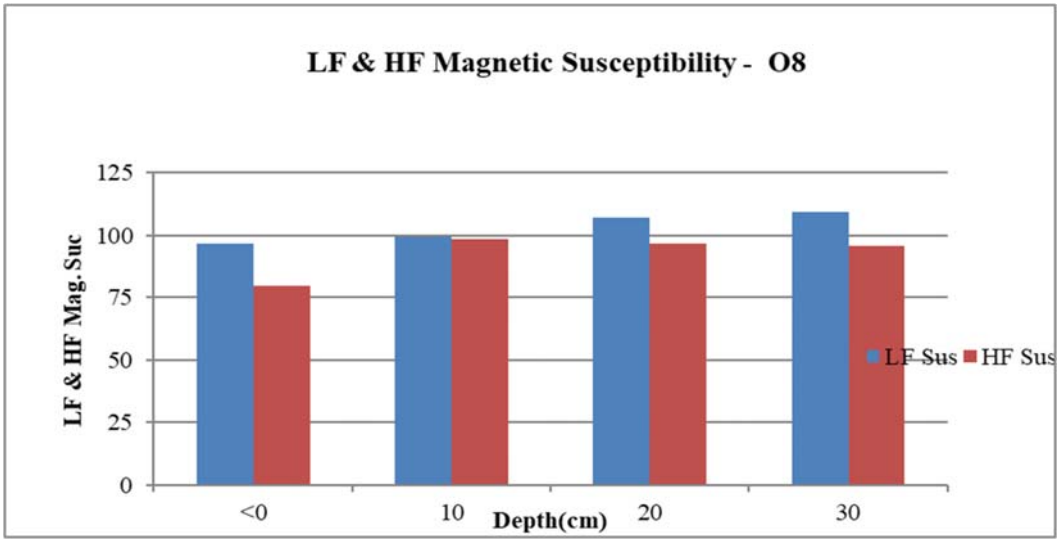
LF & HF Magnetic Susceptibility - O8
LF & HF Mag. Suc
125
100
75
50
25
0
<0
10
20
30
Depth(cm)
LF Sus
HF Sus

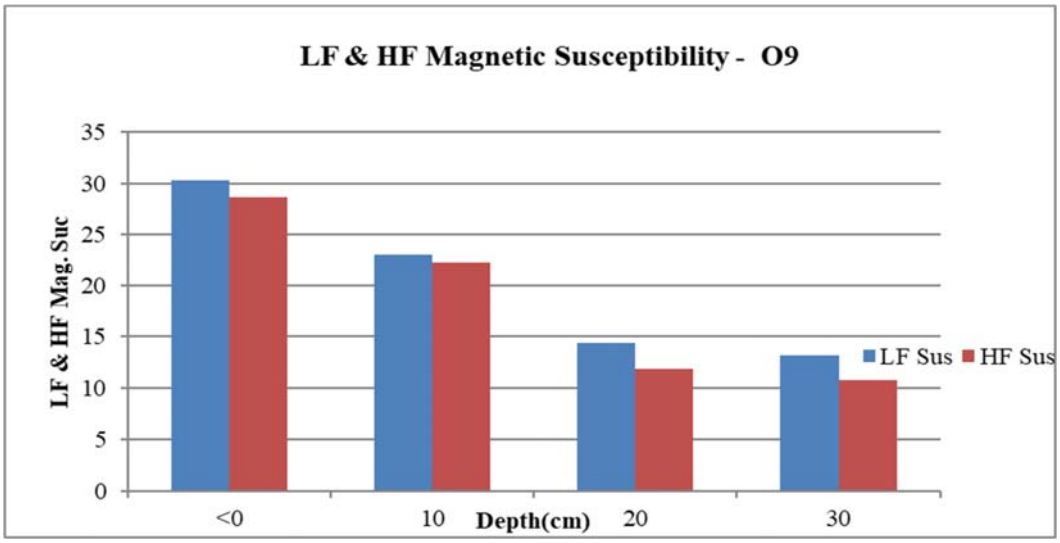
LF & HF Magnetic Susceptibility - O9
LF & HF Mag. Suc
35
30
25
20
15
10
5
0
<0
10
Depth(cm)
20
30
LF Sus
HF Sus

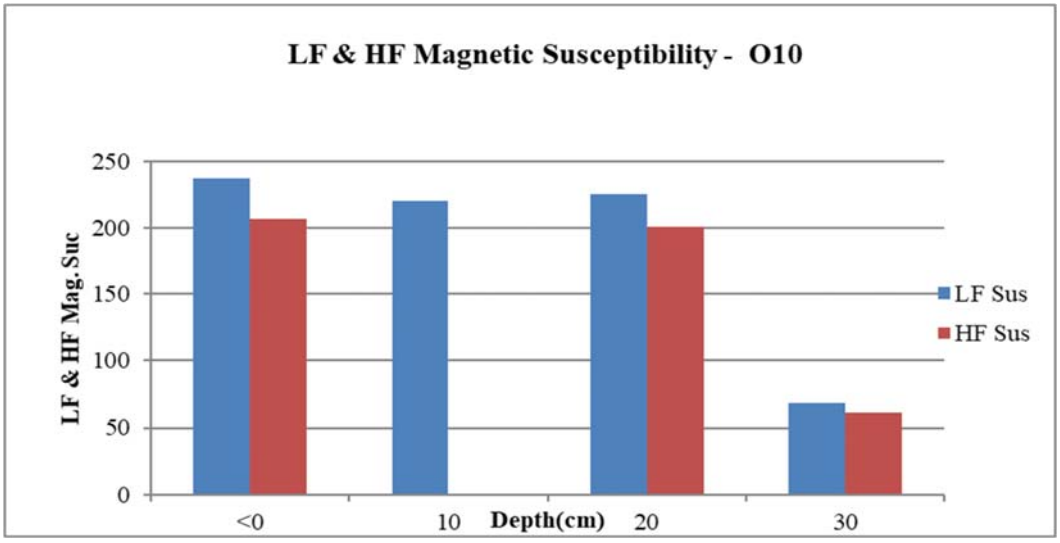
LF & HF Magnetic Susceptibility - O10
LF & HF Mag. Suc
250
200
150
100
50
0
<0
10
Depth(cm)
20
30
LF Sus
HF Sus

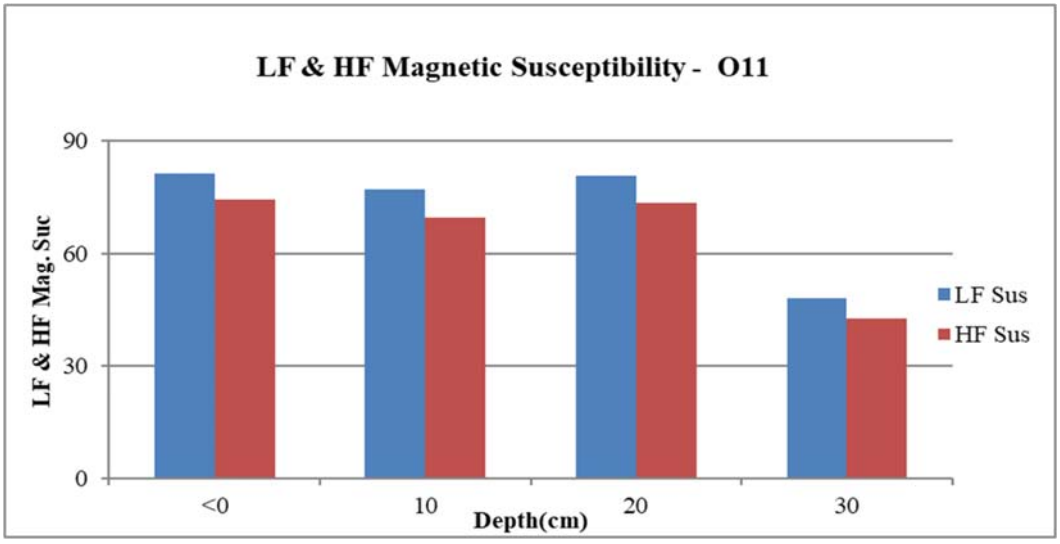
LF & HF Magnetic Susceptibility - O11
LF & HF Mag. Suc
90
60
30
0
<0
10
Depth(cm)
20
30
LF Sus
HF Sus

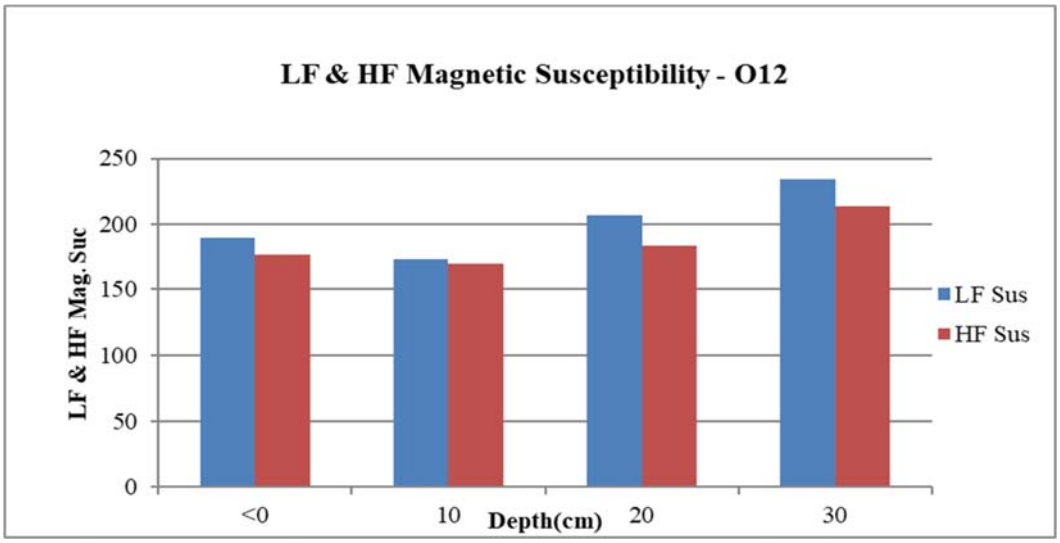
LF & HF Magnetic Susceptibility - O12
LF & HF Mag. Suc
250
200
150
100
50
0
<0
10
20
30
Depth(cm)
LF Sus
HF Sus

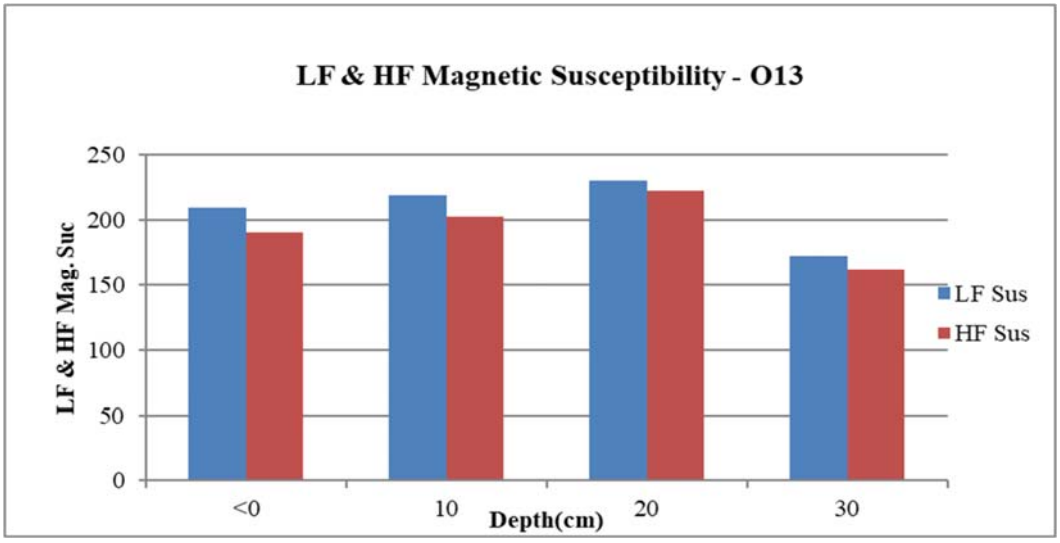
LF & HF Magnetic Susceptibility - O13
LF & HF Mag. Suc
250
200
150
100
50
0
<0
10
20
30
Depth(cm)
LF Sus
HF Sus

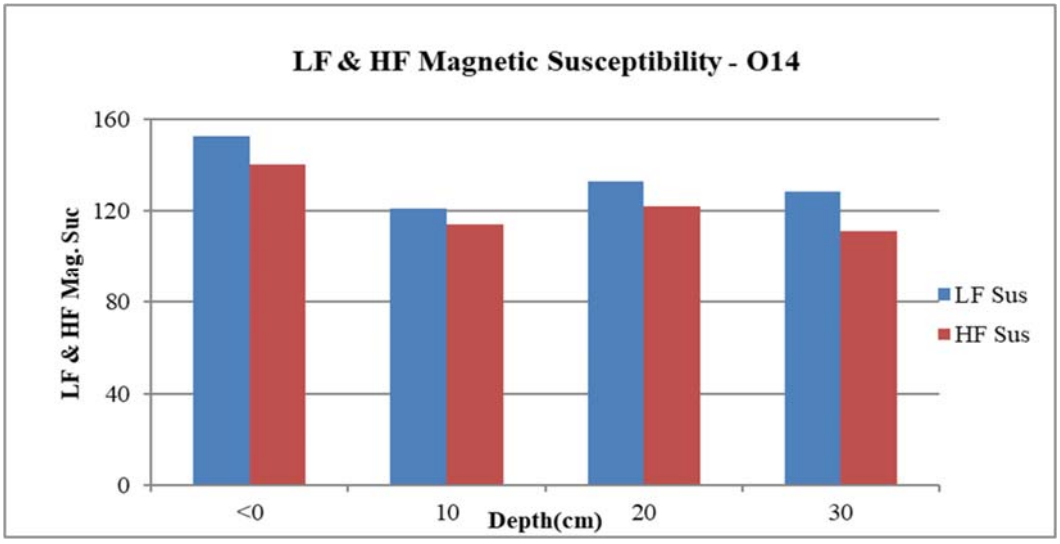
LF & HF Magnetic Susceptibility - O14
LF & HF Mag. Suc
160
120
80
40
0
<0
10
20
30
Depth(cm)
LF Sus
HF Sus

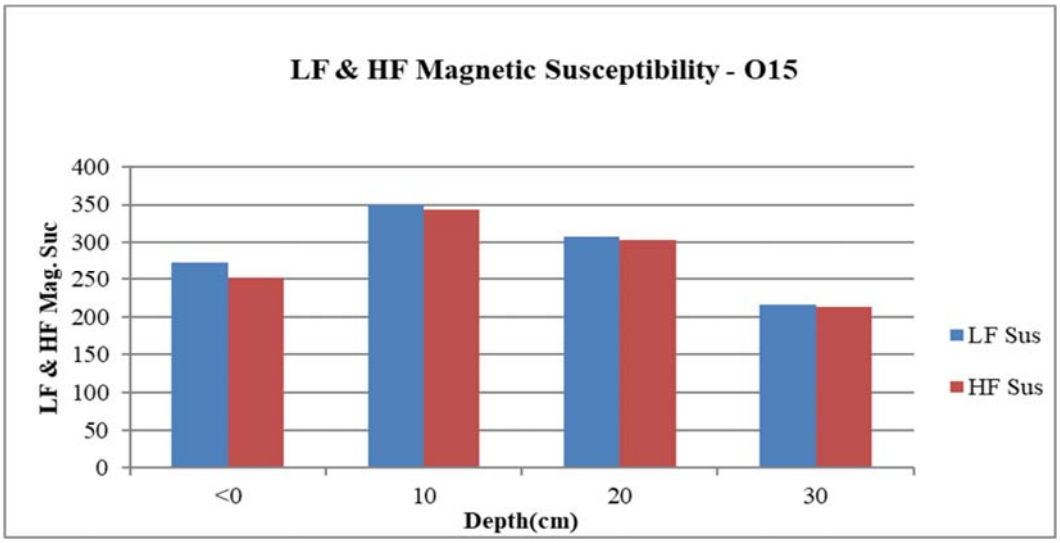
LF & HF Magnetic Susceptibility - O15
LF & HF Mag. Suc
400
350
300
250
200
150
100
50
0
<0
10
20
30
Depth(cm)
LF Sus
HF Sus

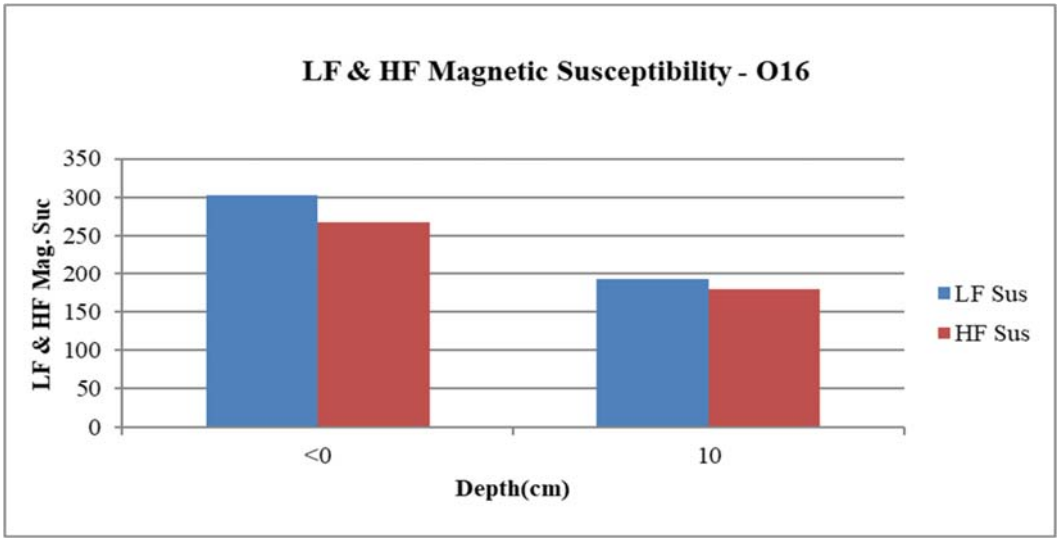
LF & HF Magnetic Susceptibility - O16
LF & HF Mag. Suc
350
300
250
200
150
100
50
0
<0
10
Depth(cm)
LF Sus
HF Sus

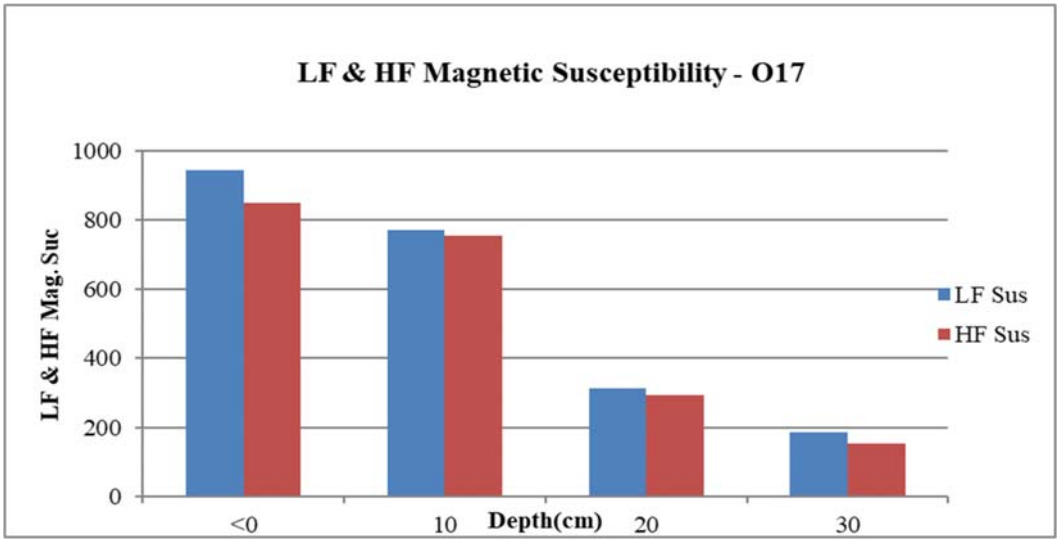
LF & HF Magnetic Susceptibility - O17
LF & HF Mag. Suc
1000
800
600
400
200
0
<0
10
Depth(cm)
20
30
LF Sus
HF Sus

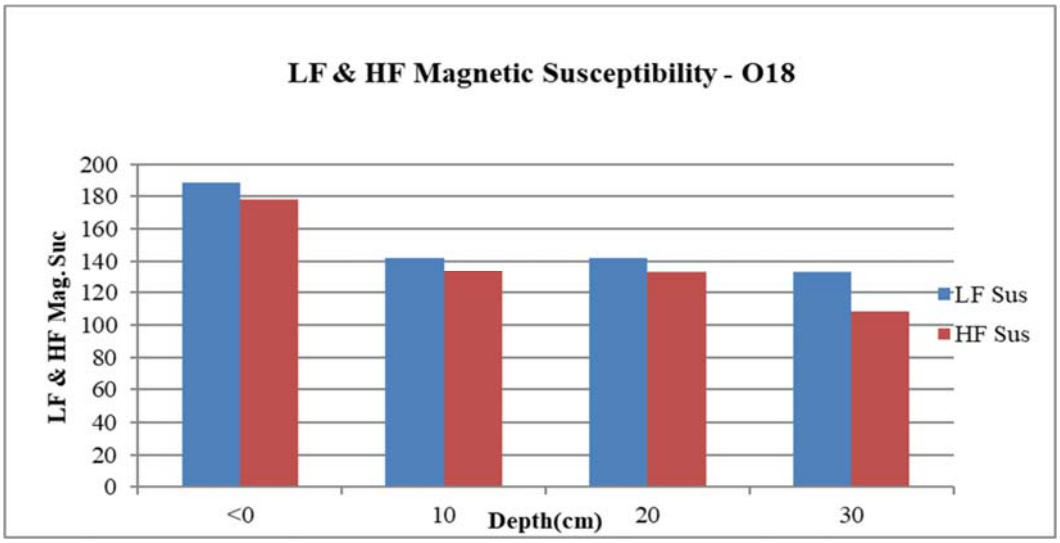
LF & HF Magnetic Susceptibility - O18
LF & HF Mag.Suc
200
180
160
140
120
100
80
60
40
20
0
<0
10
20
30
Depth(cm)
LF Sus
HF Sus

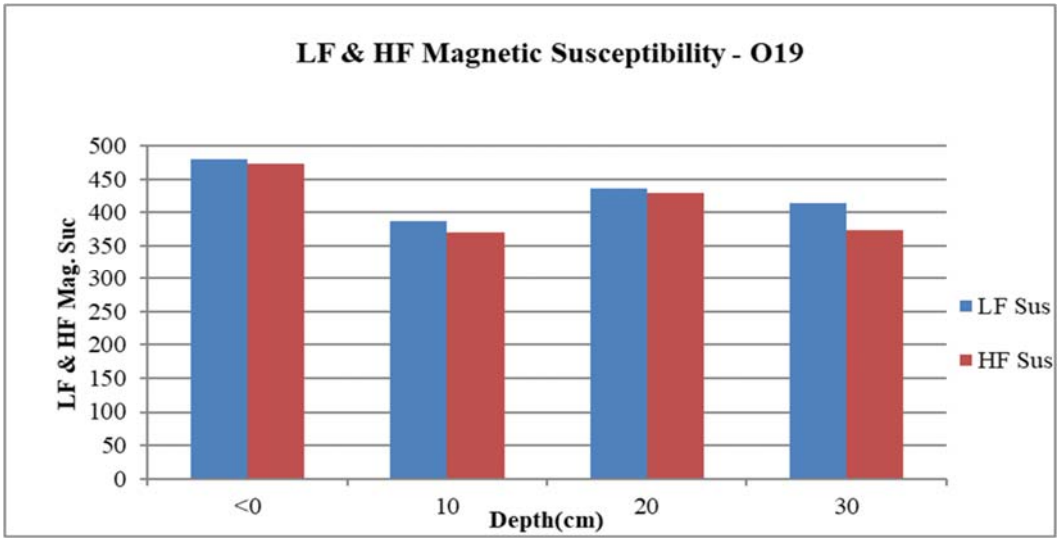
LF & HF Magnetic Susceptibility - O19
LF & HF Mag. Suc
500
450
400
350
300
250
200
150
100
50
0
<0
10
20
30
Depth(cm)
LF Sus
HF Sus

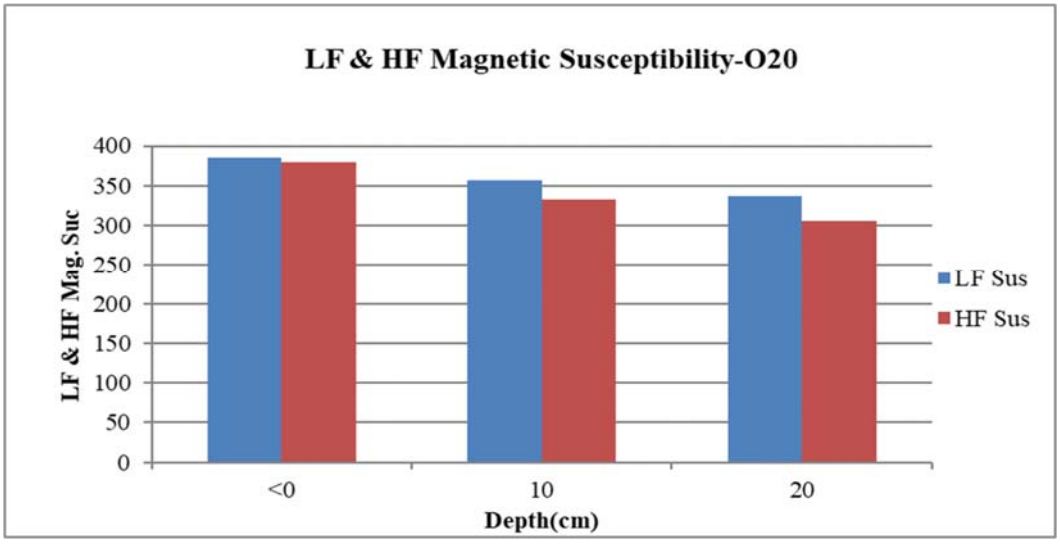
LF & HF Magnetic Susceptibility-O20
LF & HF Mag. Suc
400
350
300
250
200
150
100
50
0
<0
10
20
Depth(cm)
LF Sus
HF Sus

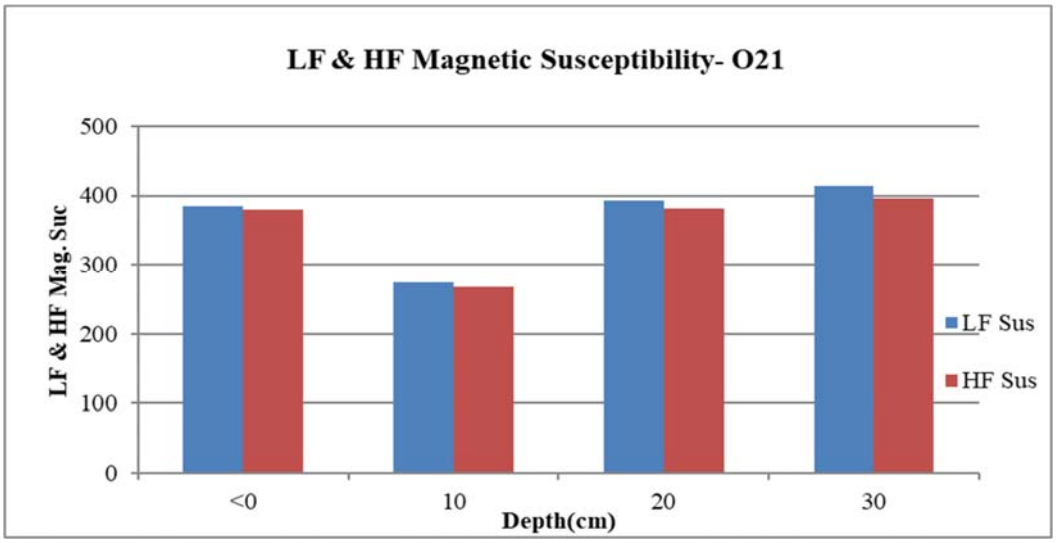
LF & HF Magnetic Susceptibility- O21
LF & HF Mag. Suc
500
400
300
200
100
0
<0
10
20
30
Depth(cm)
LF Sus
HF Sus

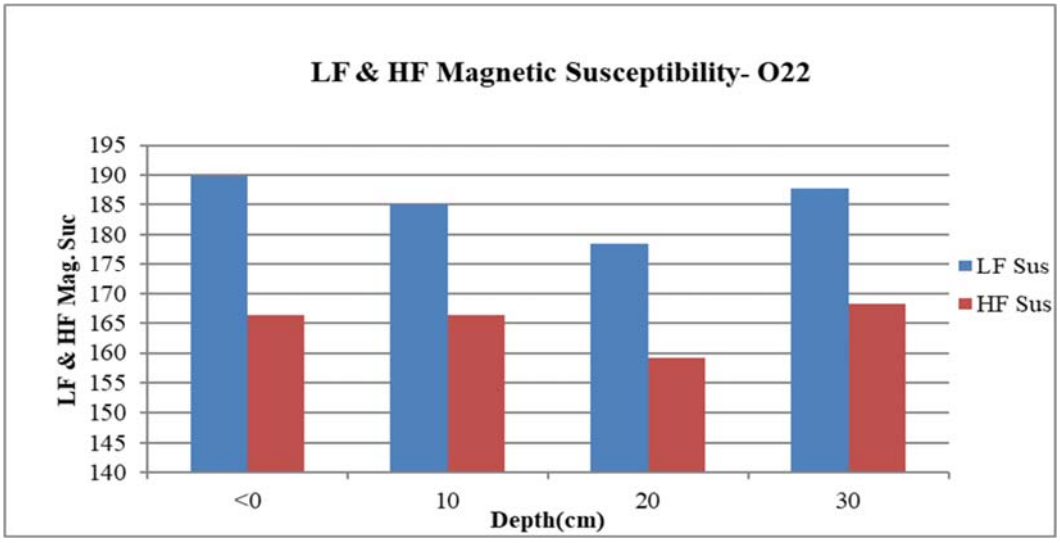
LF & HF Magnetic Susceptibility- O22
LF & HF Mag. Suc
195
190
185
180
175
170
165
160
155
150
145
140
<0
10
20
30
Depth(cm)
LF Sus
HF Sus

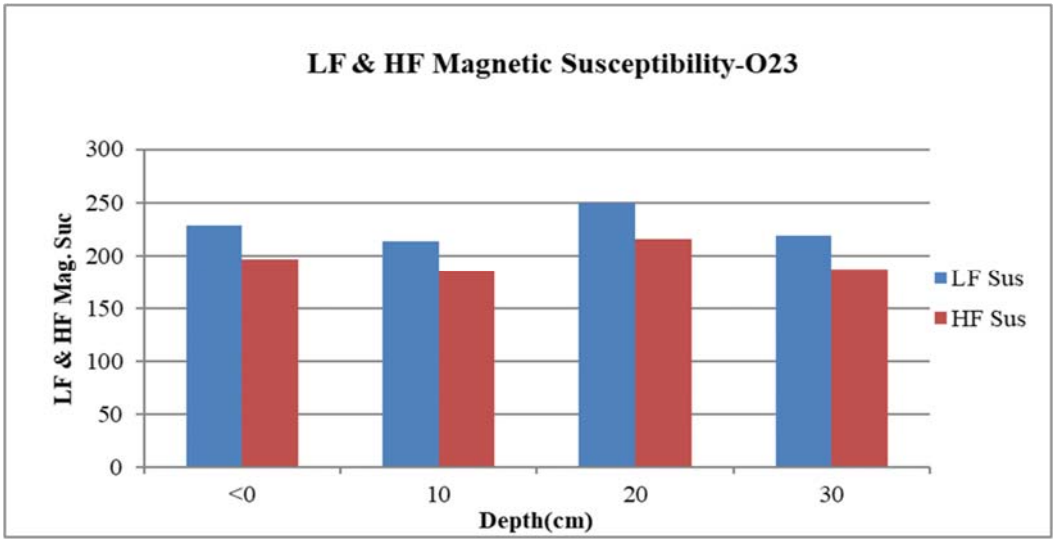
LF & HF Magnetic Susceptibility-O23
LF & HF Mag. Suc
300
250
200
150
100
50
0
<0
10
20
30
Depth(cm)
LF Sus
HF Sus

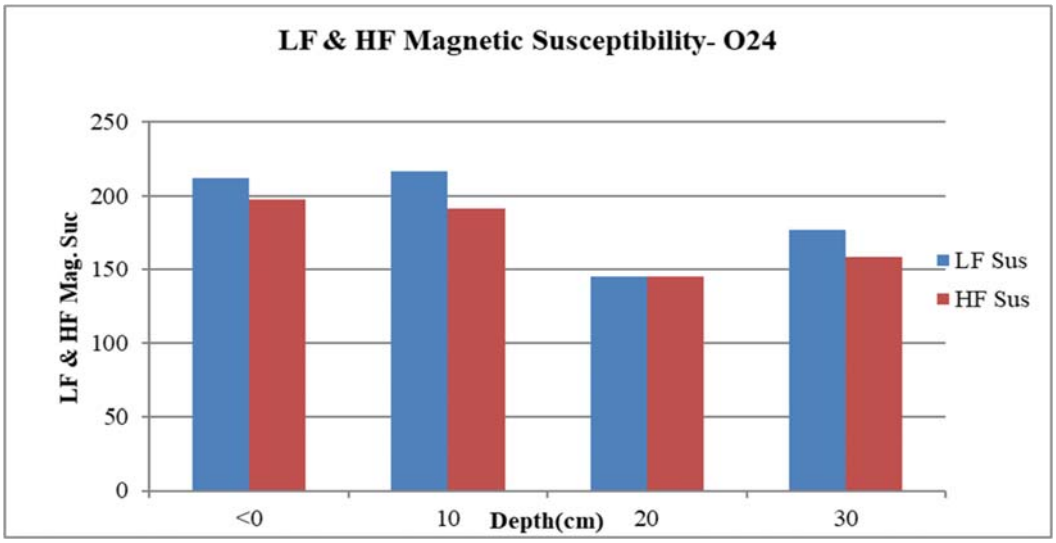
LF & HF Magnetic Susceptibility- O24
LF & HF Mag. Suc
250
200
150
100
50
0
<0
10
20
30
Depth(cm)
LF Sus
HF Sus

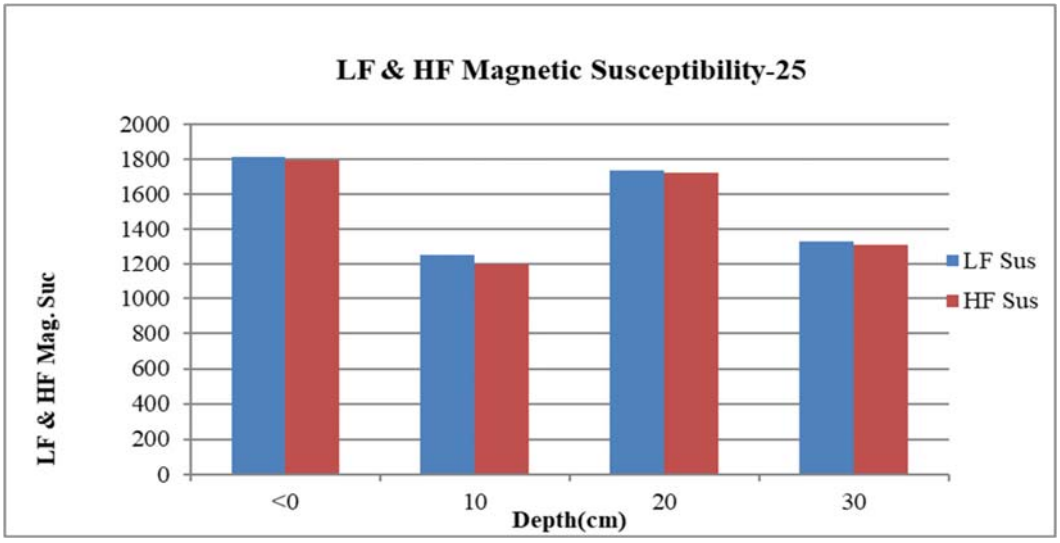
LF & HF Magnetic Susceptibility-25
LF & HF Mag. Suc
2000
1800
1600
1400
1200
1000
800
600
400
200
0
<0
10
20
30
Depth(cm)
LF Sus
HF Sus

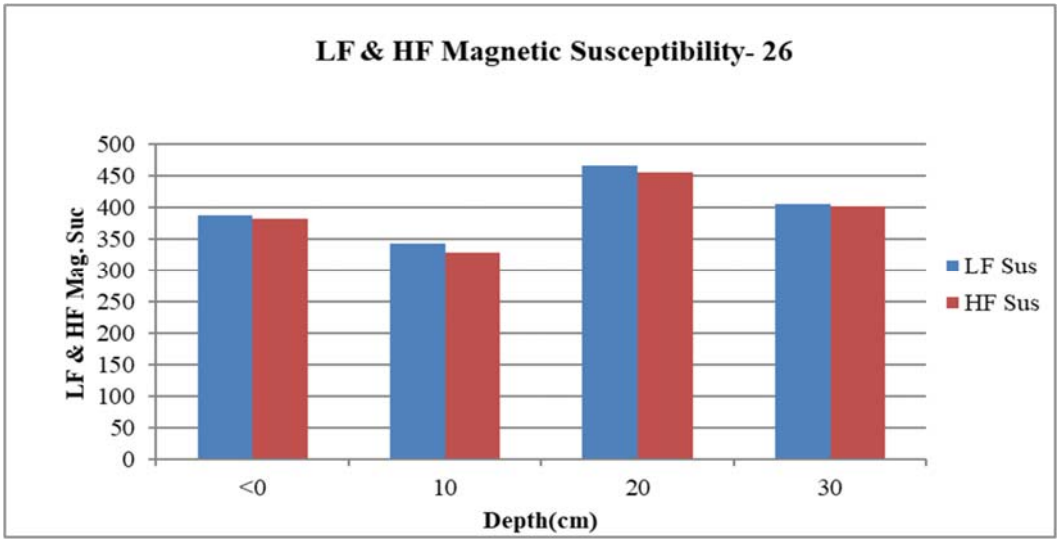
LF & HF Magnetic Susceptibility- 26
LF & HF Mag. Suc
500
450
400
350
300
250
200
150
100
50
0
<0
10
20
30
Depth(cm)
LF Sus
HF Sus

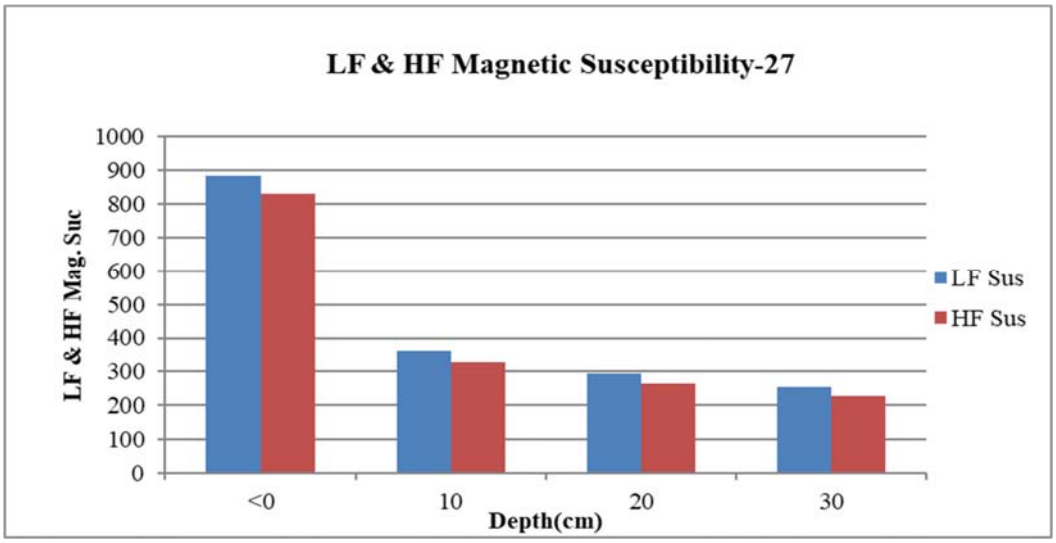
LF & HF Magnetic Susceptibility-27
LF & HF Mag. Suc
1000
900
800
700
600
500
400
300
200
100
0
<0
10
20
30
Depth(cm)
LF Sus
HF Sus

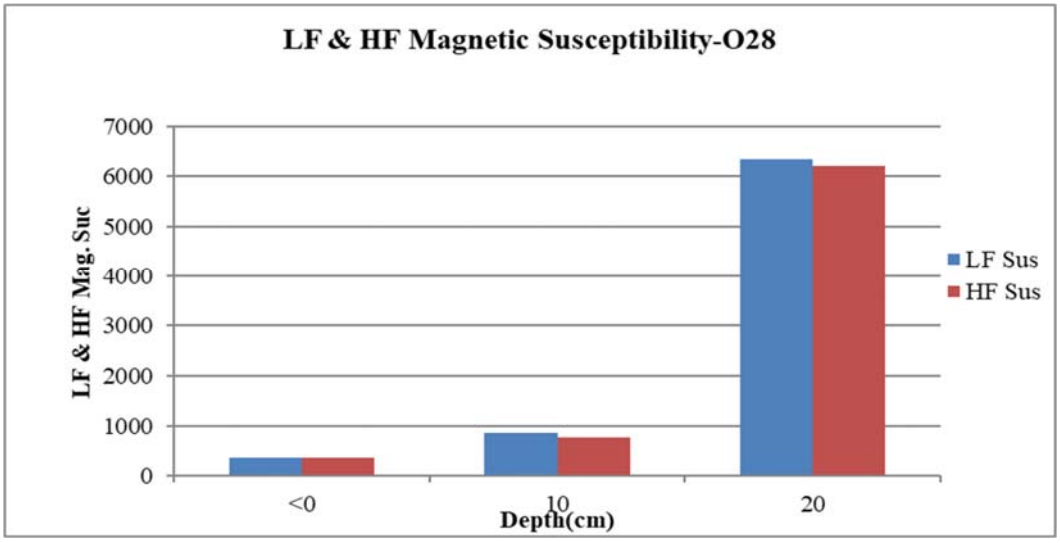
LF & HF Magnetic Susceptibility-O28
LF & HF Mag. Suc
7000
6000
5000
4000
3000
2000
1000
0
<0
10
20
Depth(cm)
LF Sus
HF Sus

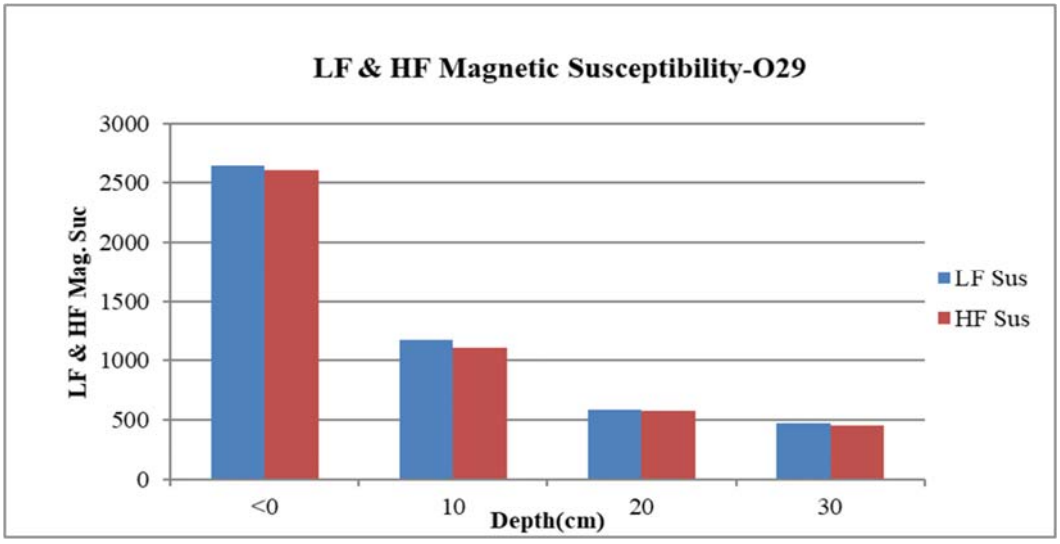
LF & HF Magnetic Susceptibility-O29
LF & HF Mag. Suc
3000
2500
2000
1500
1000
500
0
<0
10
20
30
Depth(cm)
LF Sus
HF Sus

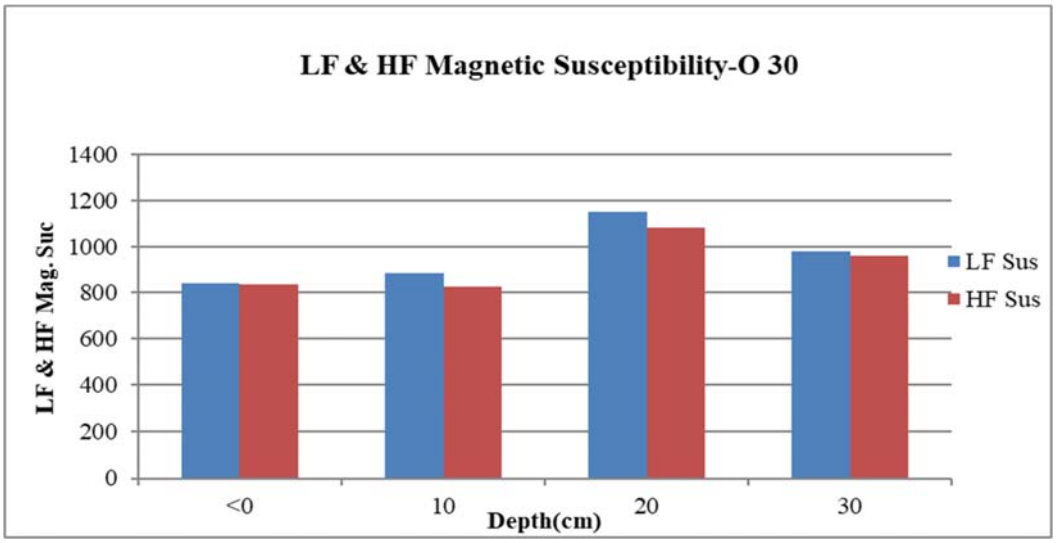
LF & HF Magnetic Susceptibility-O 30
LF & HF Mag. Suc
1400
1200
1000
800
600
400
200
0
<0
10
20
30
Depth(cm)
LF Sus
HF Sus

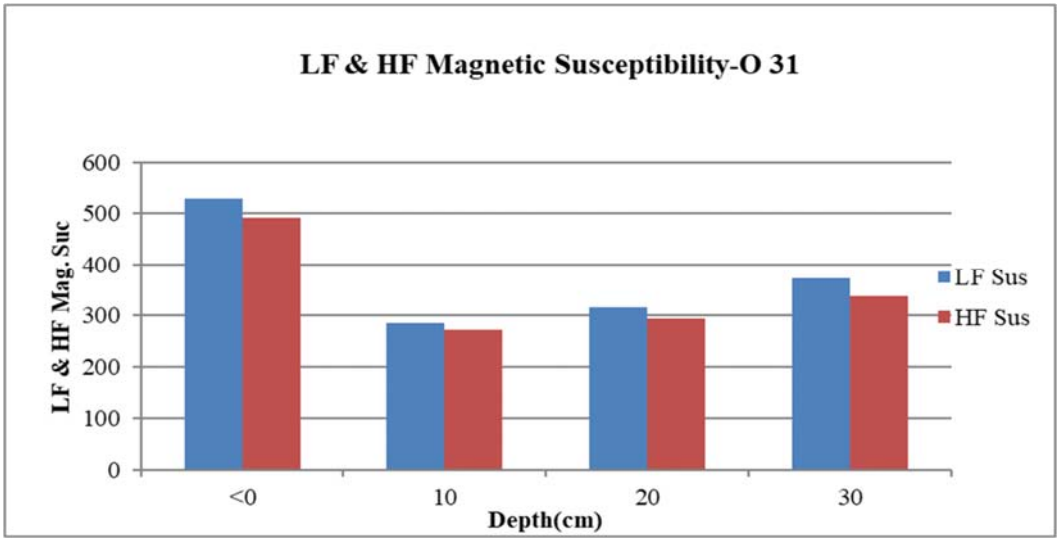
LF & HF Magnetic Susceptibility-O 31
LF & HF Mag. Suc
600
500
400
300
200
100
0
<0
10
20
30
Depth(cm)
LF Sus
HF Sus

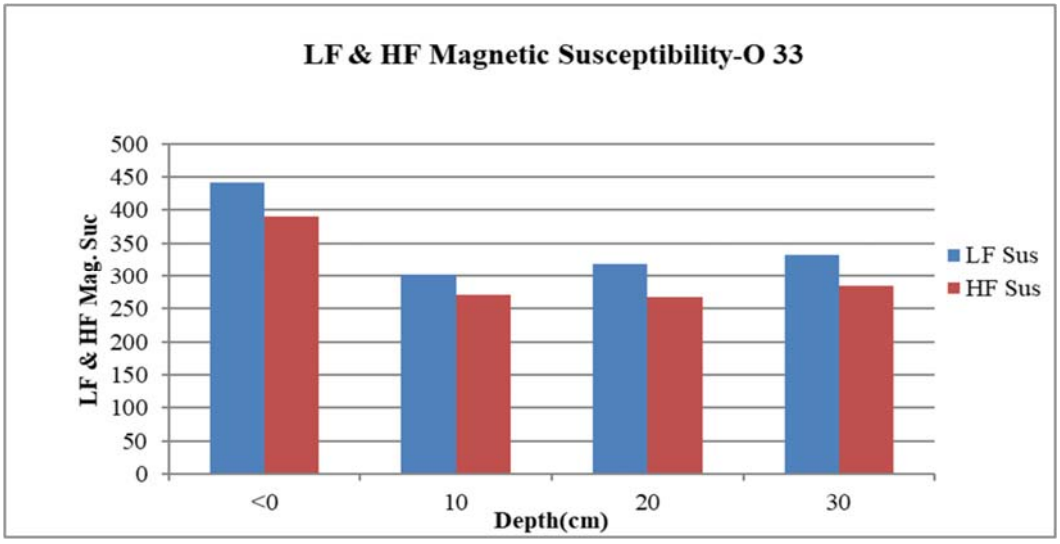
LF & HF Magnetic Susceptibility-O 33
LF & HF Mag. Suc
500
450
400
350
300
250
200
150
100
50
0
<0
10
20
30
Depth(cm)
LF Sus
HF Sus

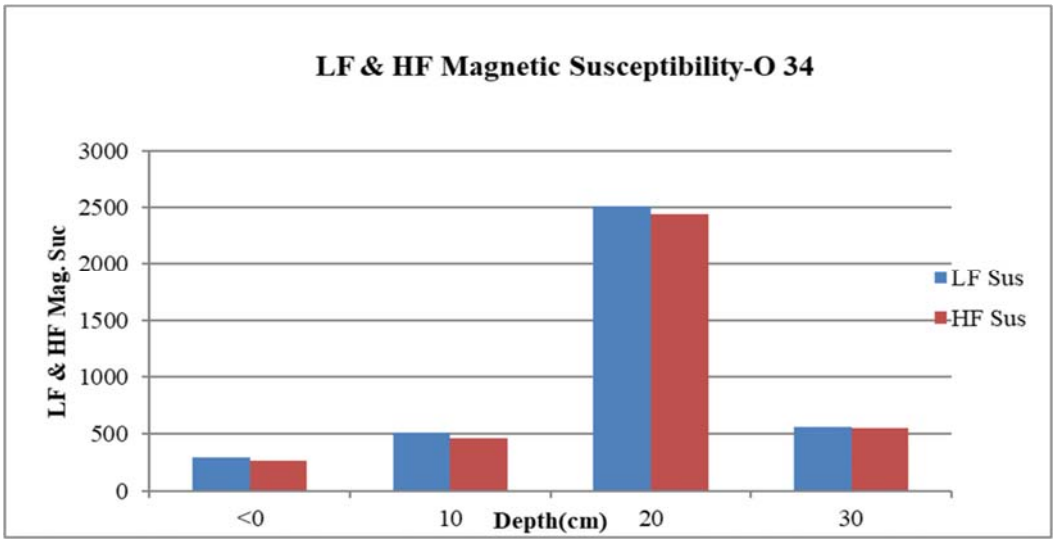
LF & HF Magnetic Susceptibility-O 34
LF & HF Mag. Suc
3000
2500
2000
1500
1000
500
0
<0
10
20
30
Depth(cm)
LF Sus
HF Sus

Appendix 4. 9: Variation in Magnetic Susceptibility Readings Recorded for Different Grain Sizes in Ota Industrial Layout

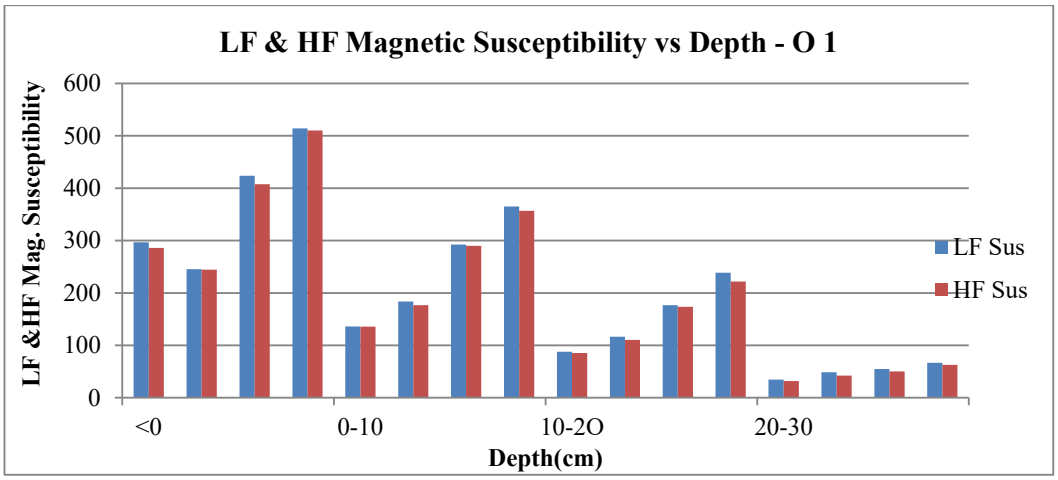

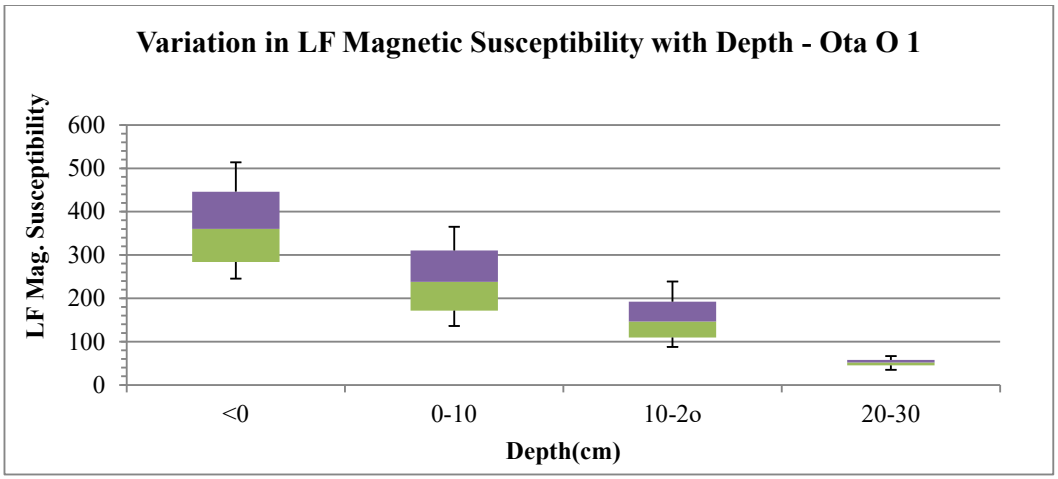

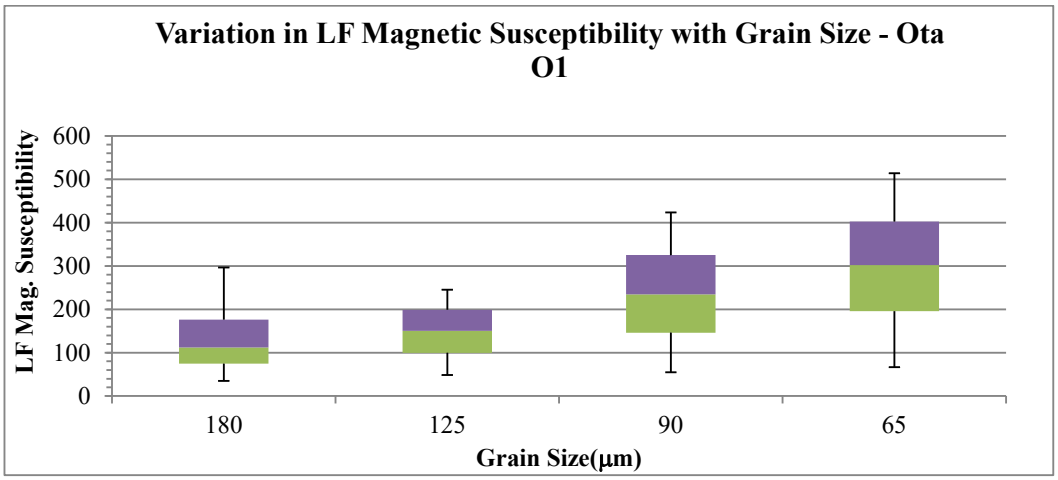

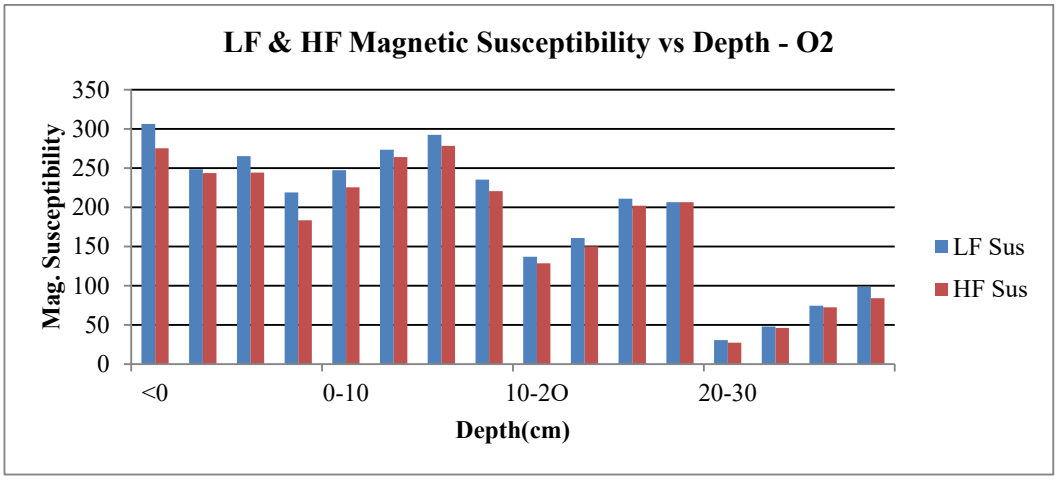
LF & HF Magnetic Susceptibility vs Depth - O2
Mag. Susceptibility
350
300
250
200
150
100
50
0
<0
0-10
10-2O
20-30
Depth(cm)
LF Sus
HF Sus

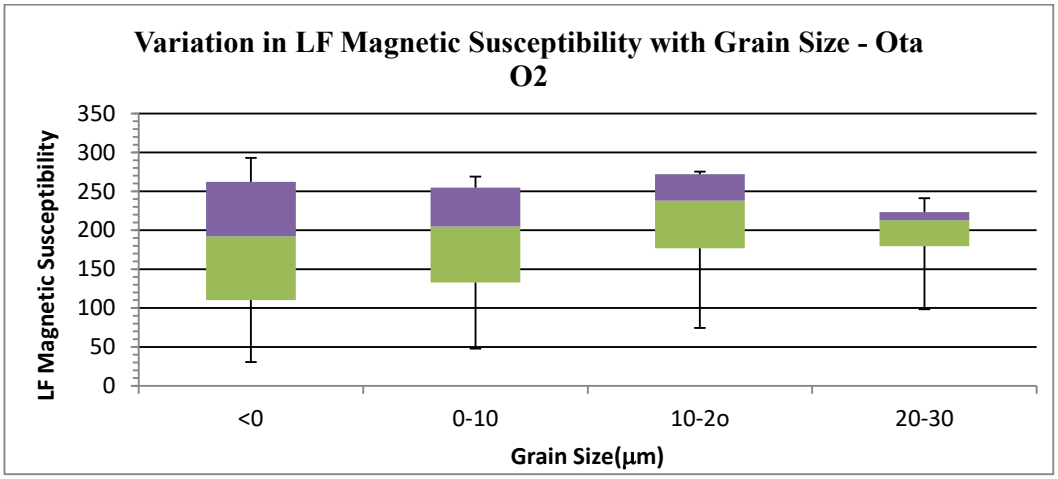
Variation in LF Magnetic Susceptibility with Grain Size - Ota O2
LF Magnetic Susceptibility
350
300
250
200
150
100
50
0
<0
0-10
10-2o
20-30
Grain Size(µm)

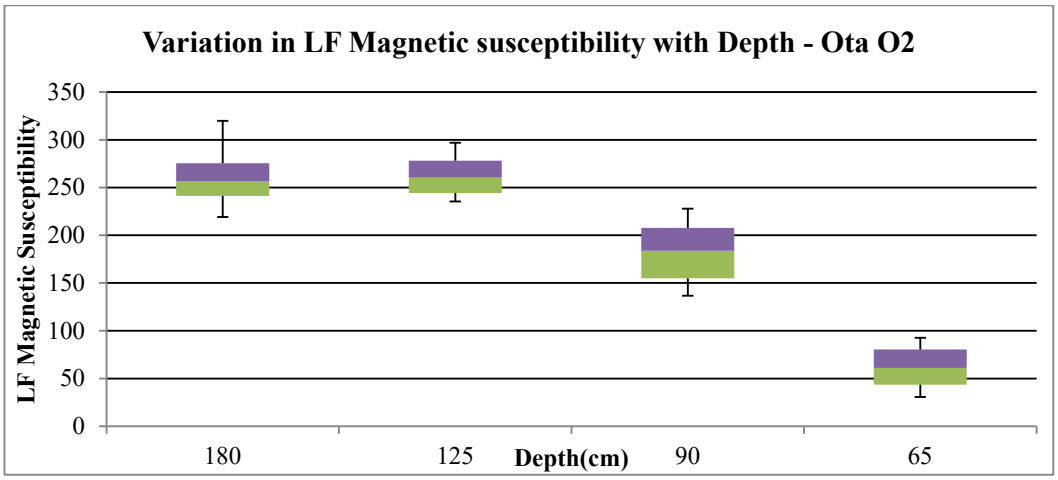
Variation in LF Magnetic susceptibility with Depth - Ota O2
LF Magnetic Susceptibility
350
300
250
200
150
100
50
0
180
125
Depth(cm)
90
65

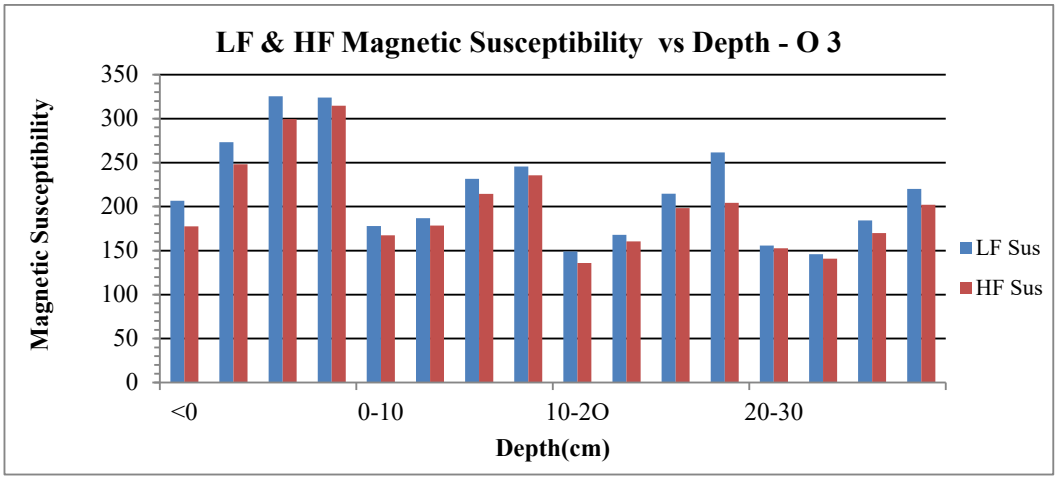
LF & HF Magnetic Susceptibility vs Depth - O 3
Magnetic Susceptibility
350
300
250
200
150
100
50
0
<0
0-10
10-2O
20-30
Depth(cm)
LF Sus
HF Sus

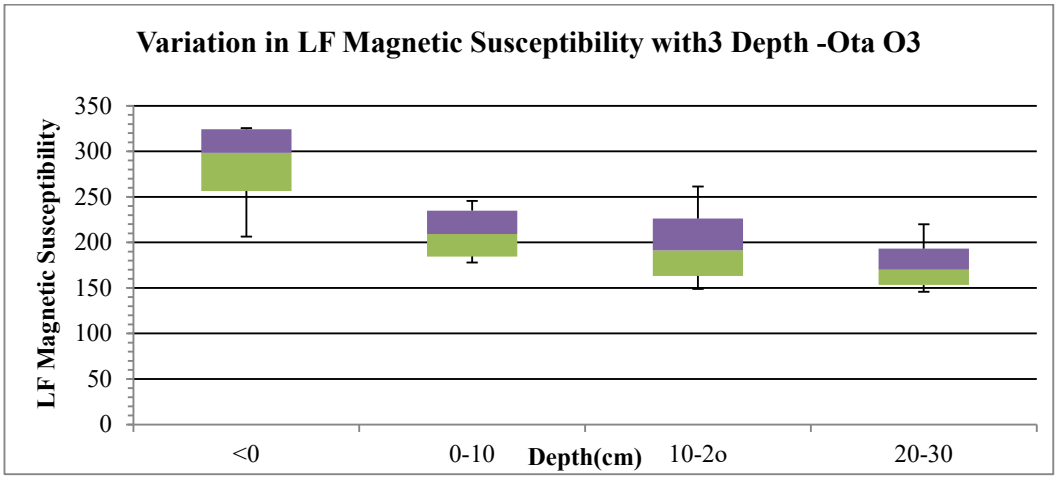
Variation in LF Magnetic Susceptibility with3 Depth -Ota O3
LF Magnetic Susceptibility
350
300
250
200
150
100
50
0
<0
0-10
Depth(cm)
10-2o
20-30

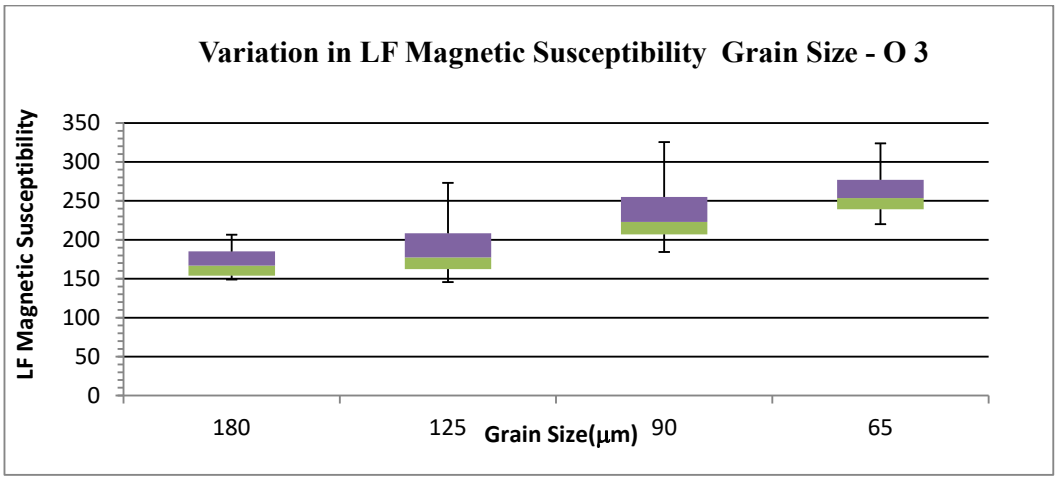
Variation in LF Magnetic Susceptibility Grain Size - O 3
LF Magnetic Susceptibility
350
300
250
200
150
100
50
0
180
125
Grain Size(µm)
90
65

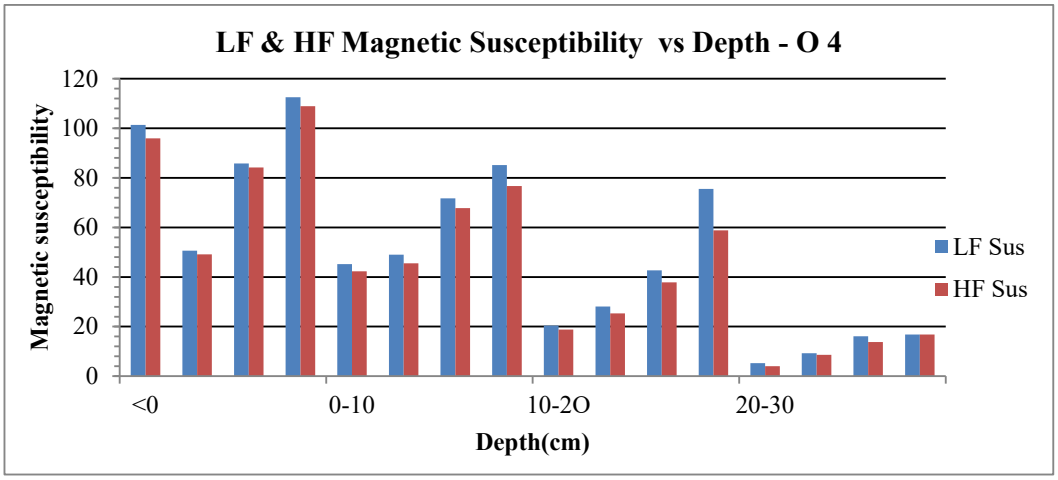
LF & HF Magnetic Susceptibility vs Depth - O 4
Magnetic susceptibility
120
100
80
60
40
20
0
<0
0-10
10-2O
20-30
Depth(cm)
LF Sus
HF Sus

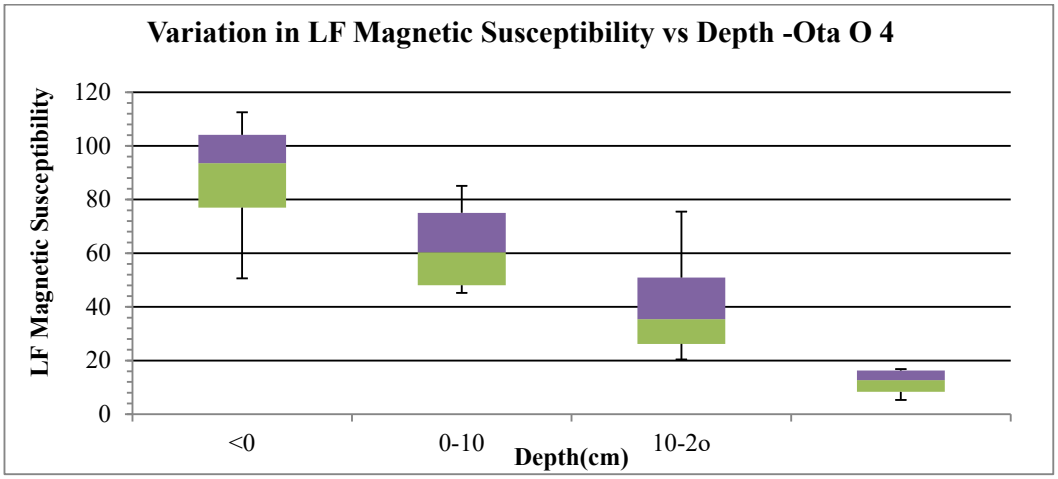
Variation in LF Magnetic Susceptibility vs Depth -Ota O 4
LF Magnetic Susceptibility
120
100
80
60
40
20
0
<0
0-10
10-2o
Depth(cm)

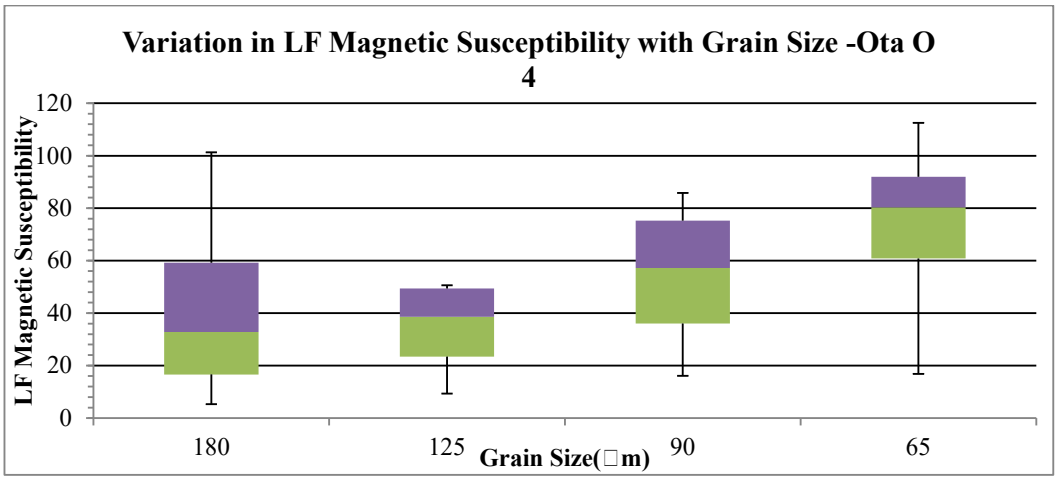
Variation in LF Magnetic Susceptibility with Grain Size -Ota O 4
LF Magnetic Susceptibility
120
100
80
60
40
20
0
180
125
90
65
Grain Size(□m)

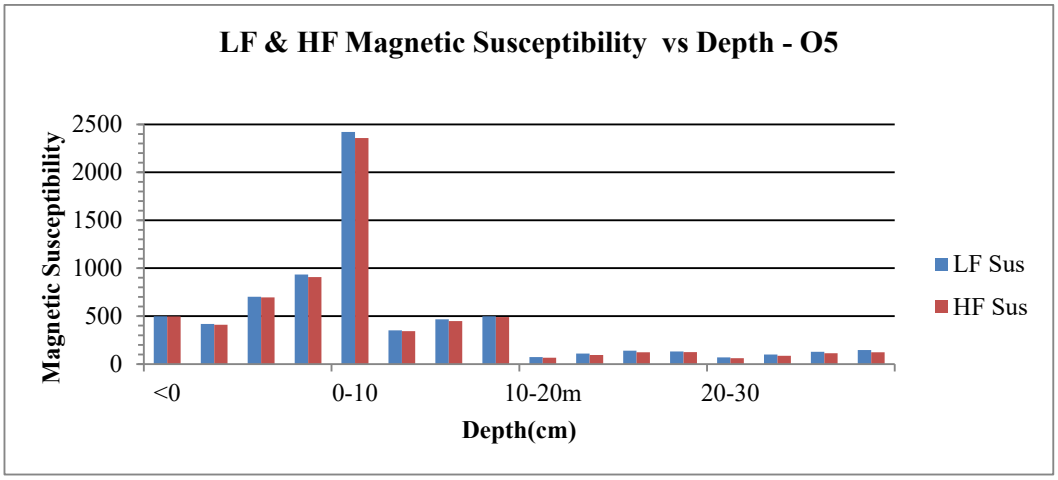
LF & HF Magnetic Susceptibility vs Depth - O5
Magnetic Susceptibility
2500
2000
1500
1000
500
0
<0
0-10
10-20m
20-30
Depth(cm)
LF Sus
HF Sus

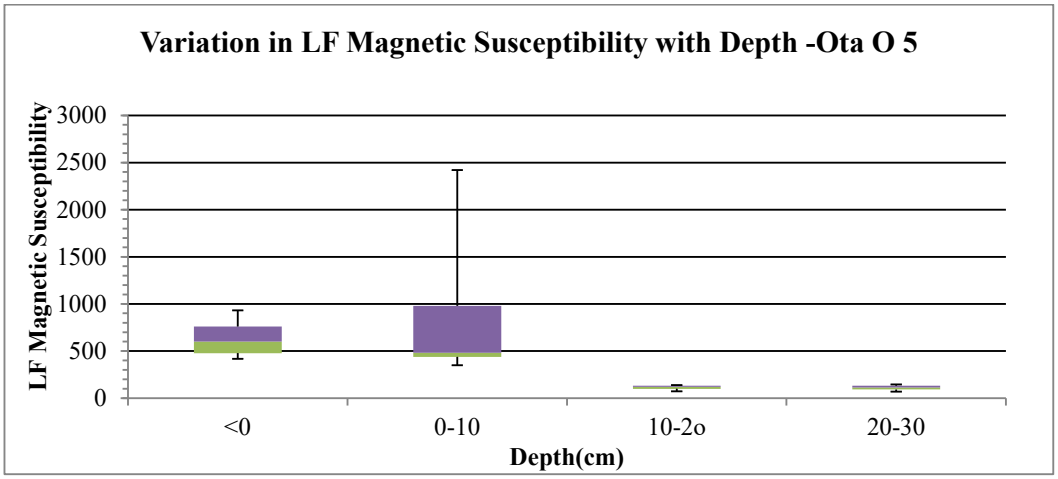
Variation in LF Magnetic Susceptibility with Depth -Ota O 5
LF Magnetic Susceptibility
3000
2500
2000
1500
1000
500
0
<0
0-10
10-2o
20-30
Depth(cm)

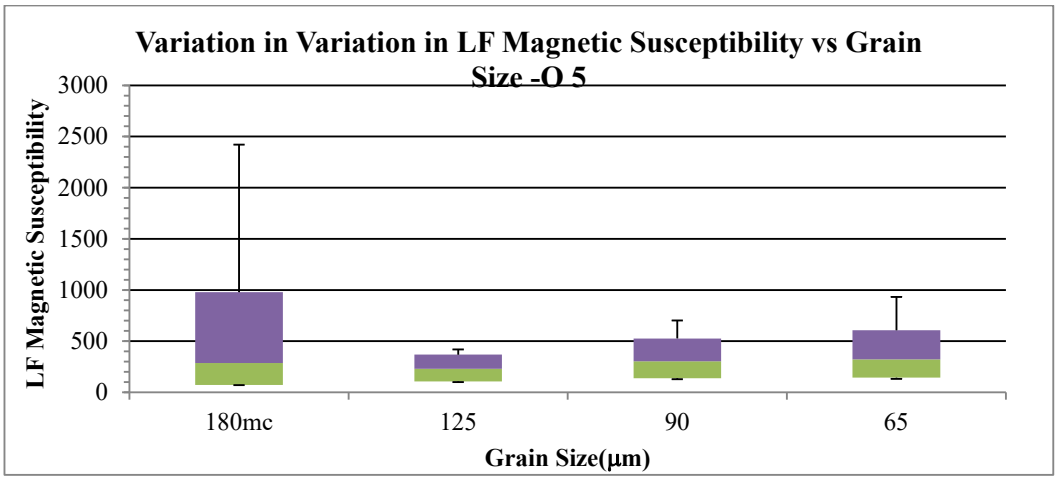
Variation in Variation in LF Magnetic Susceptibility vs Grain Size -O 5
LF Magnetic Susceptibility
3000
2500
2000
1500
1000
500
0
180mc
125
90
65
Grain Size(µm)

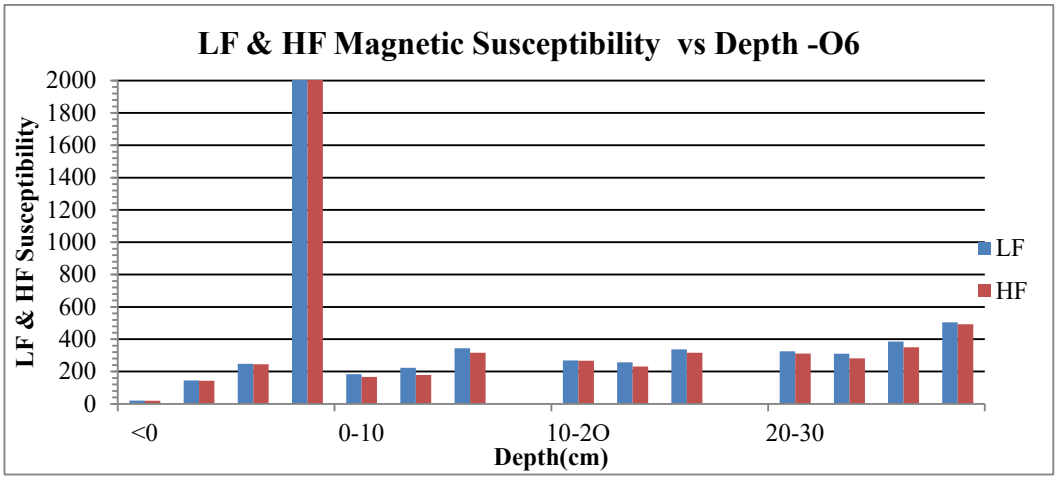
LF & HF Magnetic Susceptibility vs Depth -O6
LF & HF Susceptibility
2000
1800
1600
1400
1200
1000
800
600
400
200
0
<0
0-10
10-2O
20-30
Depth(cm)
LF
HF

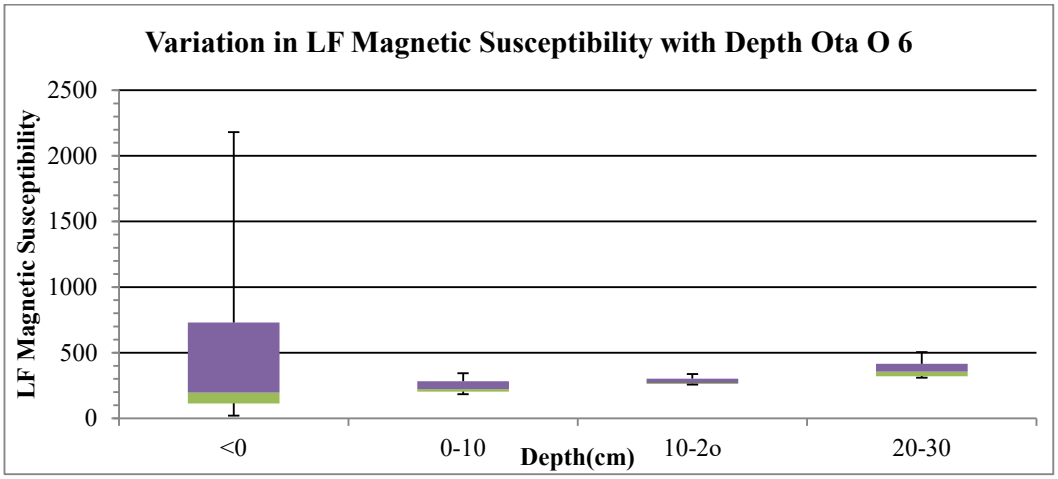
Variation in LF Magnetic Susceptibility with Depth Ota O 6
LF Magnetic Susceptibility
2500
2000
1500
1000
500
0
<0
0-10
Depth(cm)
10-2o
20-30

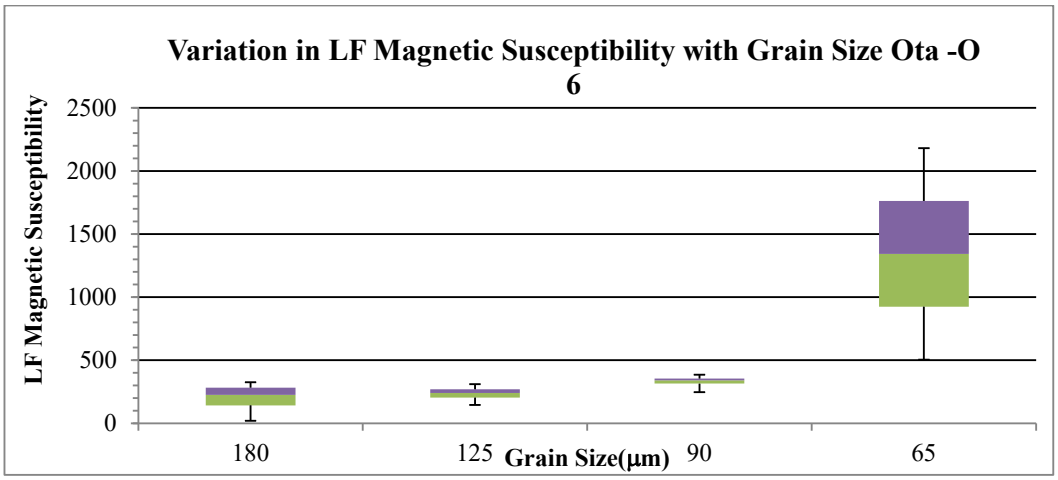
Variation in LF Magnetic Susceptibility with Grain Size Ota -O 6
LF Magnetic Susceptibility
2500
2000
1500
1000
500
0
180
125
Grain Size(µm)
90
65

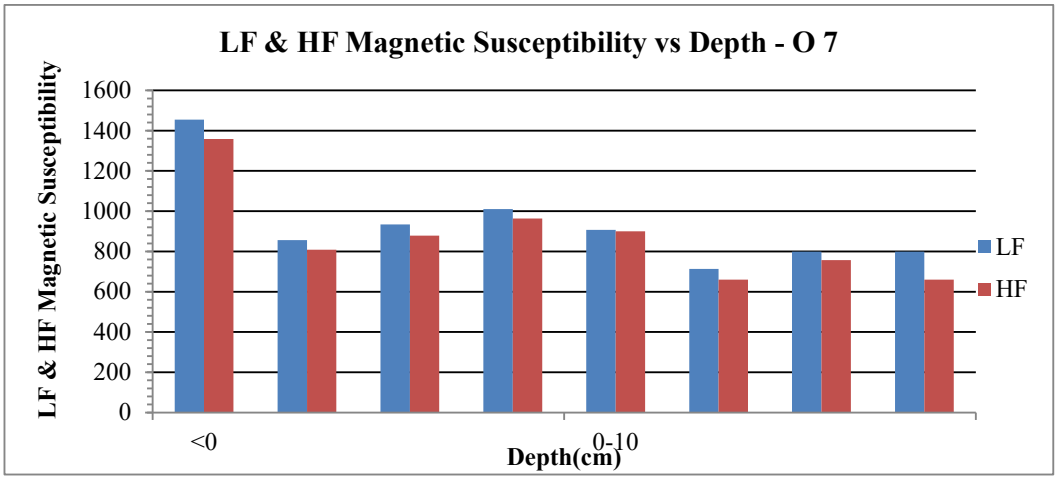
LF & HF Magnetic Susceptibility vs Depth - O 7
LF & HF Magnetic Susceptibility
1600
1400
1200
1000
800
600
400
200
0
<0
0-10
Depth(cm)
LF
HF

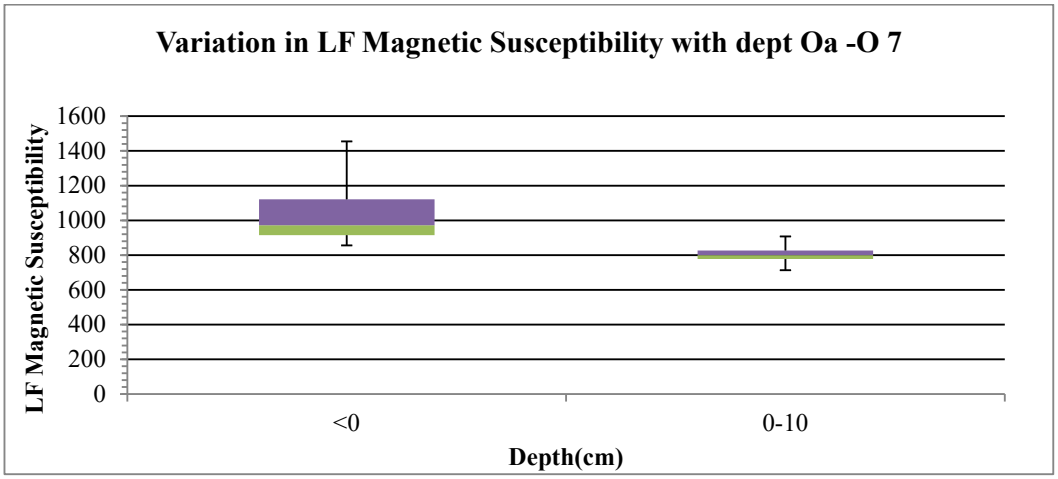
Variation in LF Magnetic Susceptibility with dept Oa -O 7
LF Magnetic Susceptibility
1600
1400
1200
1000
800
600
400
200
0
<0
0-10
Depth(cm)

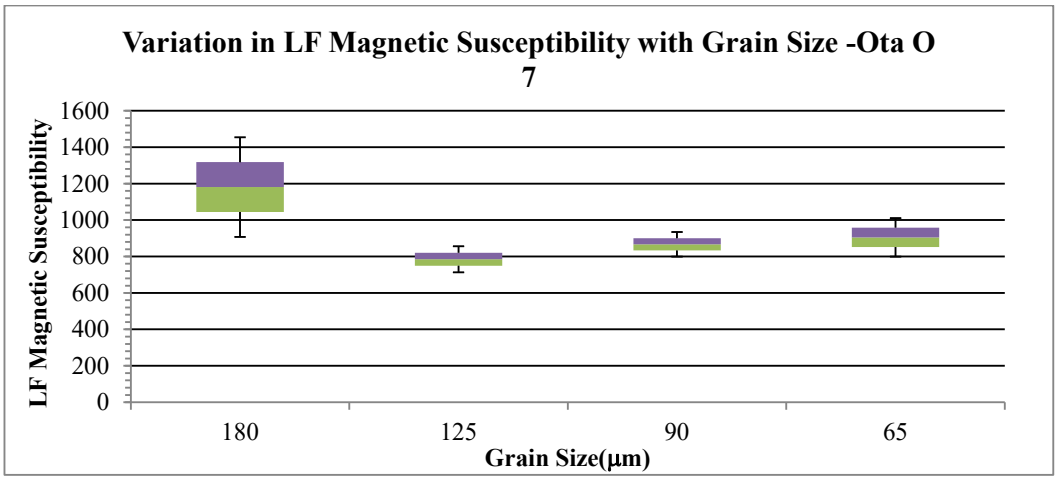
Variation in LF Magnetic Susceptibility with Grain Size -Ota O 7
LF Magnetic Susceptibility
1600
1400
1200
1000
800
600
400
200
0
180
125
90
65
Grain Size(µm)

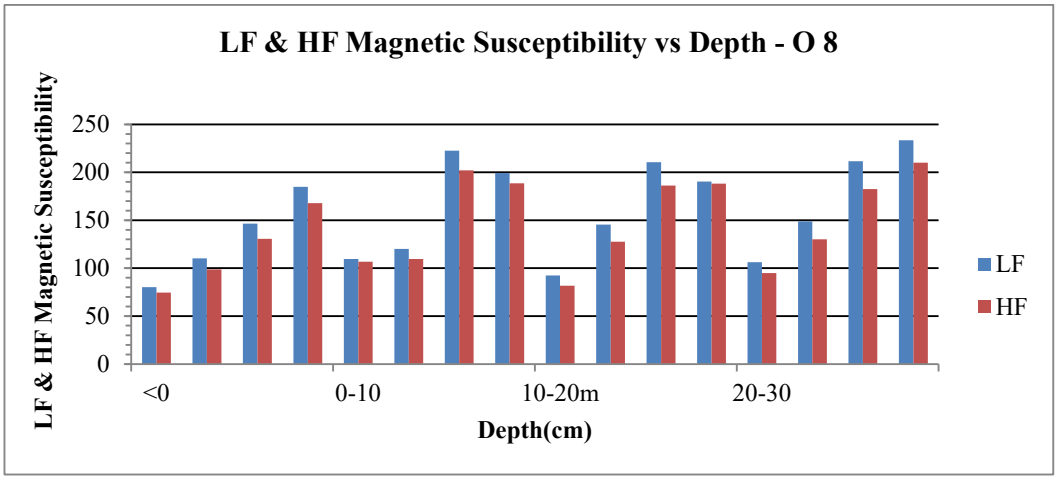
LF & HF Magnetic Susceptibility vs Depth - O 8
LF & HF Magnetic Susceptibility
250
200
150
100
50
0
<0
0-10
10-20m
20-30
Depth(cm)
LF
HF

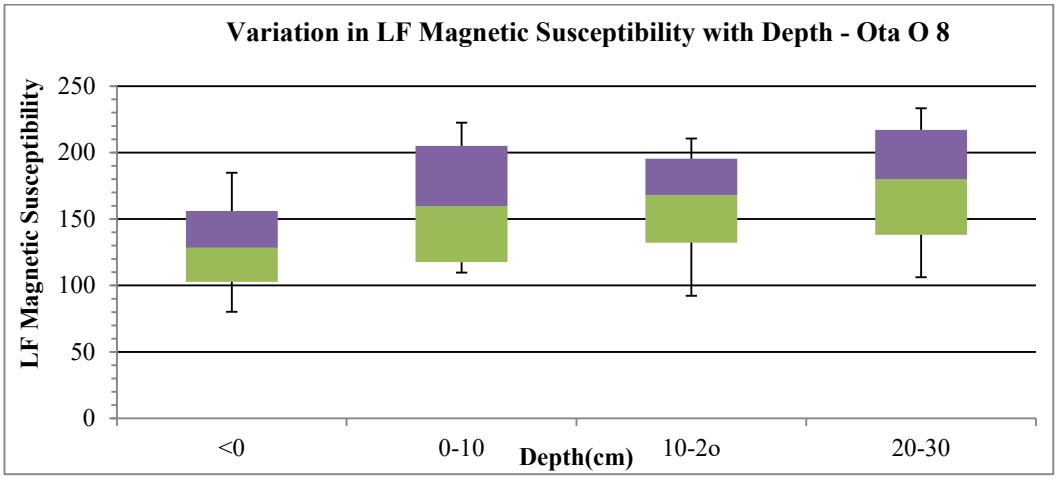
Variation in LF Magnetic Susceptibility with Depth - Ota O 8
LF Magnetic Susceptibility
250
200
150
100
50
0
<0
0-10
Depth(cm)
10-2o
20-30

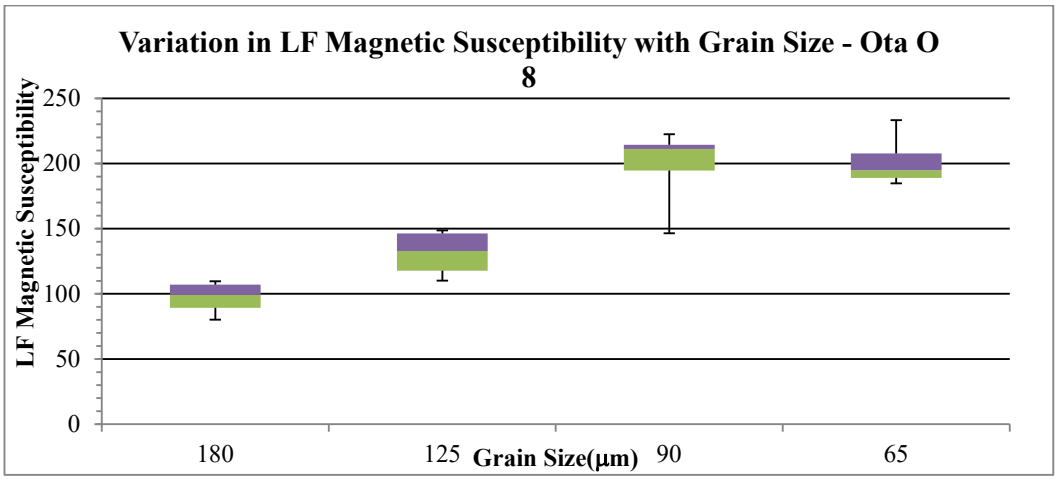
Variation in LF Magnetic Susceptibility with Grain Size - Ota O 8
LF Magnetic Susceptibility
250
200
150
100
50
0
180
125
Grain Size(µm)
90
65

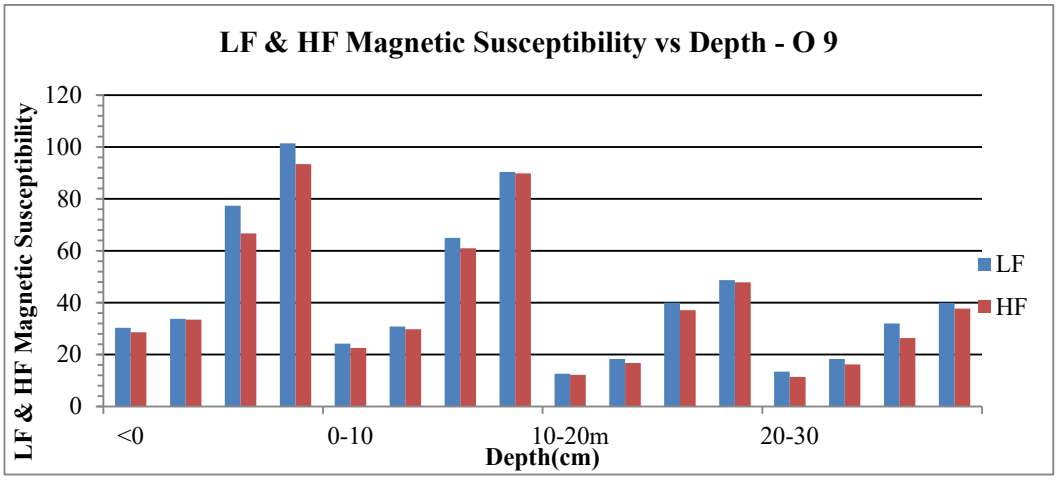
LF & HF Magnetic Susceptibility vs Depth - O 9
LF & HF Magnetic Susceptibility
120
100
80
60
40
20
0
<0
0-10
10-20m
20-30
Depth(cm)
LF
HF

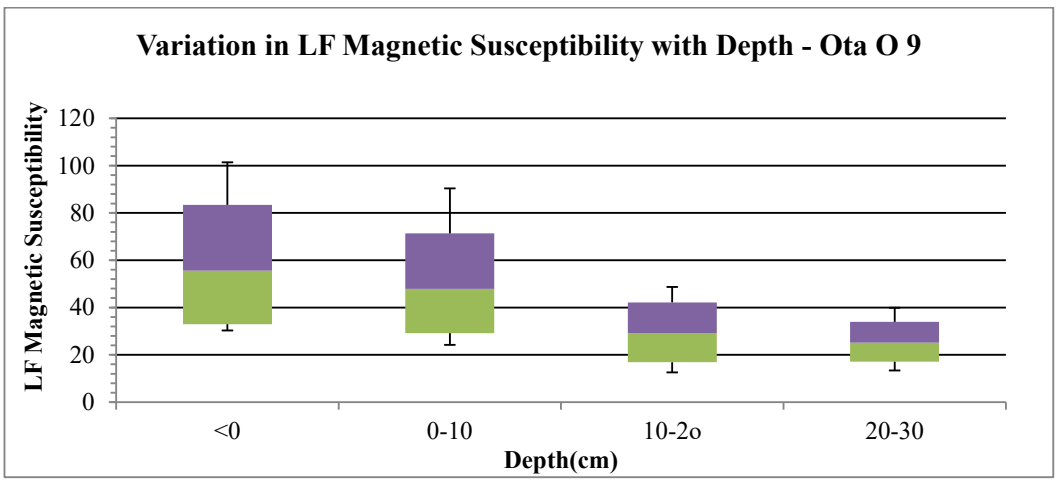
Variation in LF Magnetic Susceptibility with Depth - Ota O 9
LF Magnetic Susceptibility
120
100
80
60
40
20
0
<0
0-10
10-2o
20-30
Depth(cm)

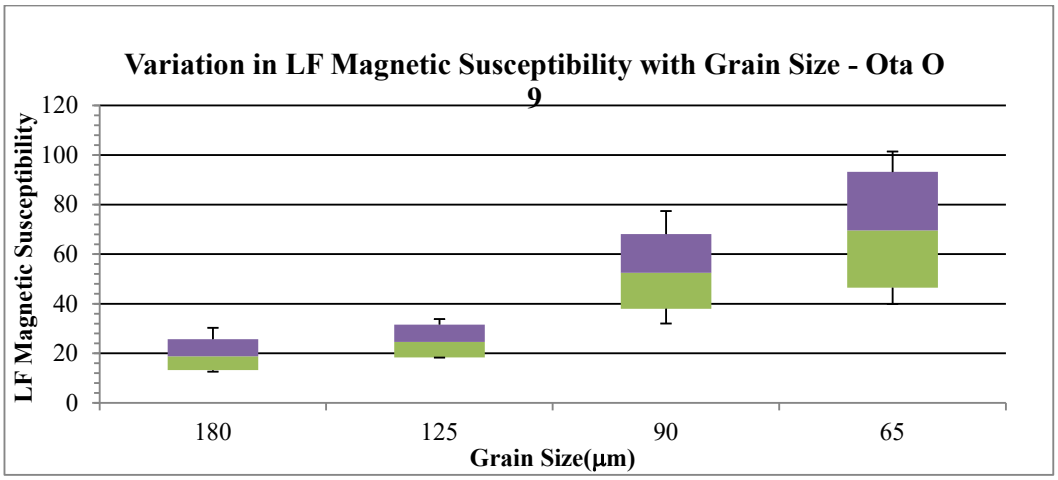
Variation in LF Magnetic Susceptibility with Grain Size - Ota O 9
LF Magnetic Susceptibility
120
100
80
60
40
20
0
180
125
90
65
Grain Size(µm)

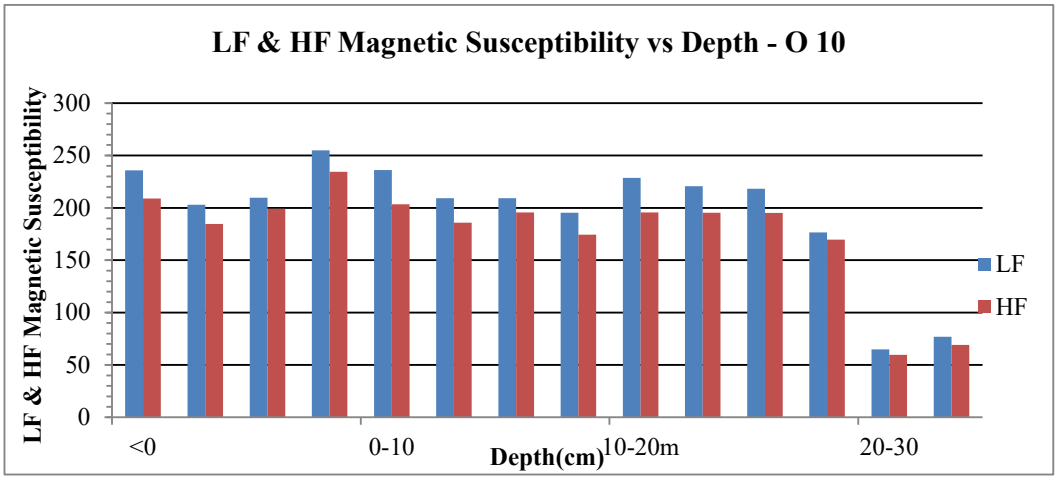
LF & HF Magnetic Susceptibility vs Depth - O 10
LF & HF Magnetic Susceptibility
300
250
200
150
100
50
0
<0
0-10
10-20m
20-30
Depth(cm)
LF
HF

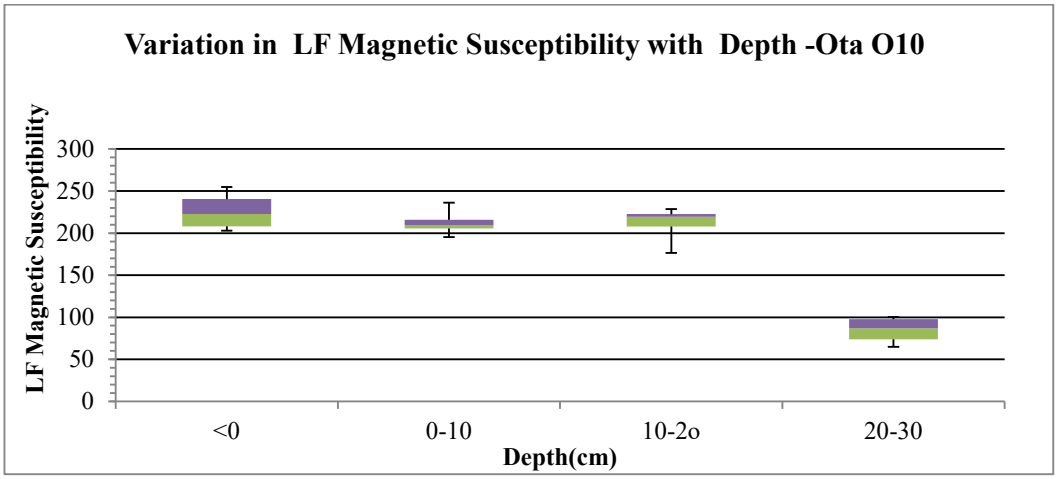
Variation in LF Magnetic Susceptibility with Depth -Ota O10
LF Magnetic Susceptibility
300
250
200
150
100
50
0
<0
0-10
10-2o
20-30
Depth(cm)

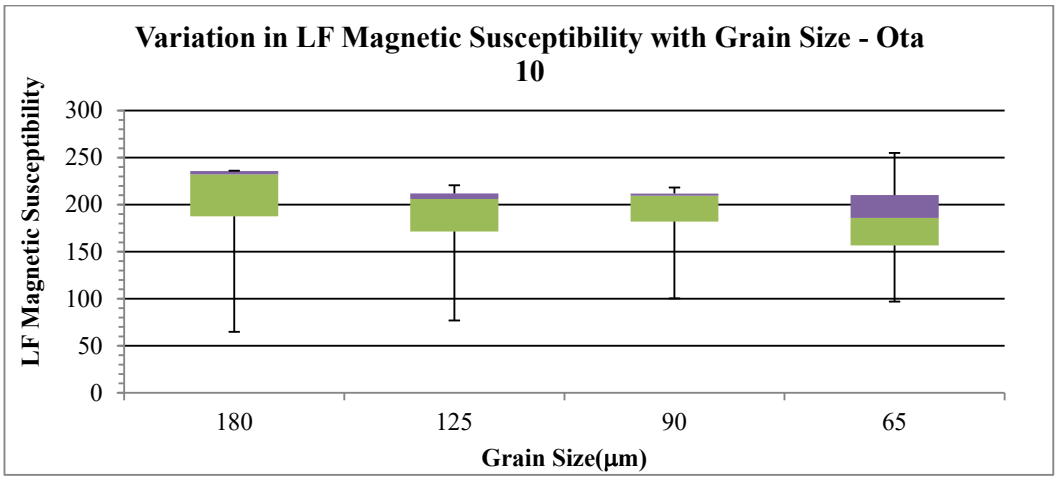
Variation in LF Magnetic Susceptibility with Grain Size - Ota 10
LF Magnetic Susceptibility
300
250
200
150
100
50
0
180
125
90
65
Grain Size(µm)

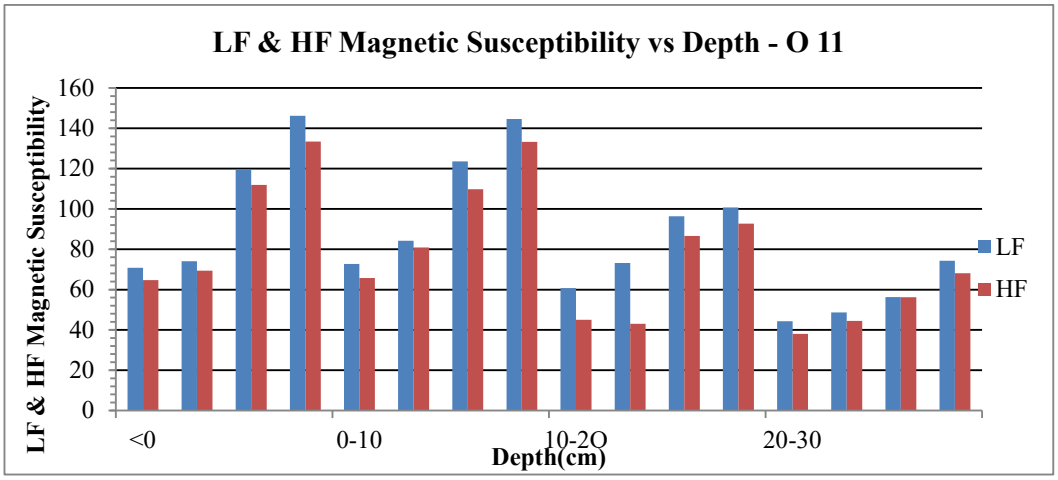
LF & HF Magnetic Susceptibility vs Depth - O 11
LF & HF Magnetic Susceptibility
160
140
120
100
80
60
40
20
0
<0
0-10
10-2O
20-30
Depth(cm)
LF
HF

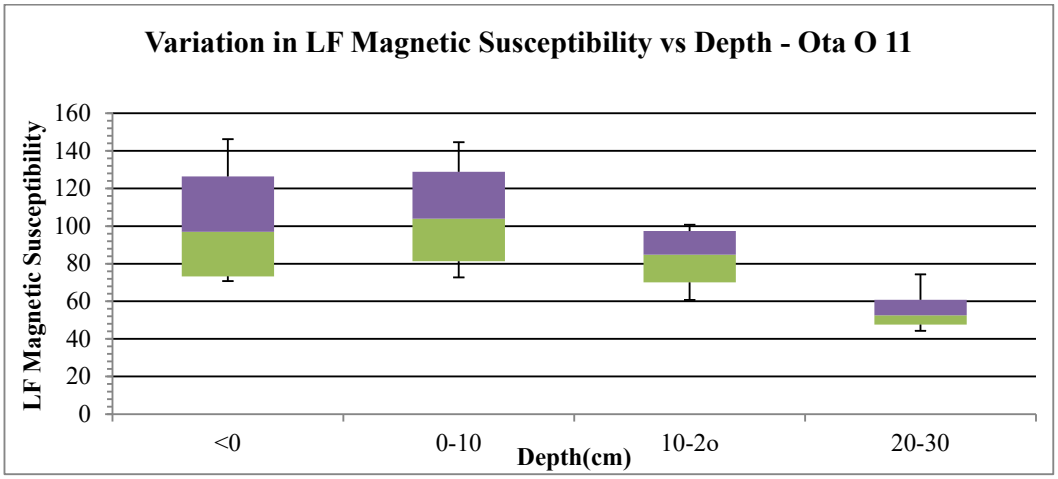
Variation in LF Magnetic Susceptibility vs Depth - Ota O 11
LF Magnetic Susceptibility
160
140
120
100
80
60
40
20
0
<0
0-10
10-2o
20-30
Depth(cm)

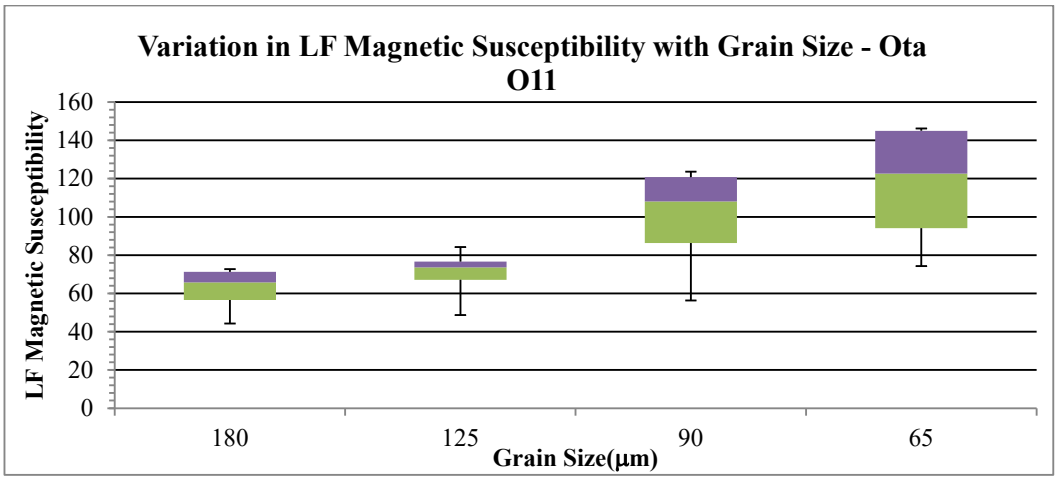
Variation in LF Magnetic Susceptibility with Grain Size - Ota O11
LF Magnetic Susceptibility
160
140
120
100
80
60
40
20
0
180
125
90
65
Grain Size(µm)

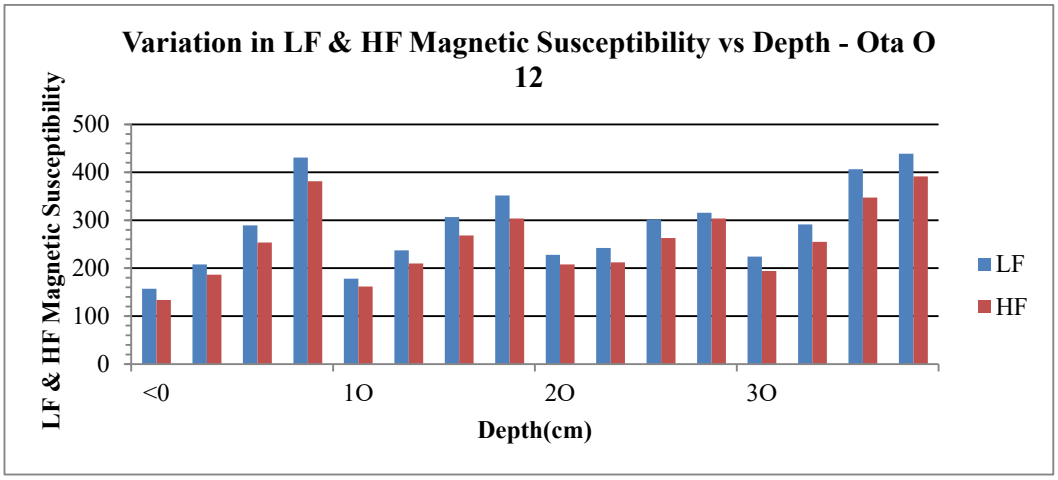
Variation in LF & HF Magnetic Susceptibility vs Depth - Ota O 12
LF & HF Magnetic Susceptibility
500
400
300
200
100
0
<0
1O
2O
3O
Depth(cm)
LF
HF

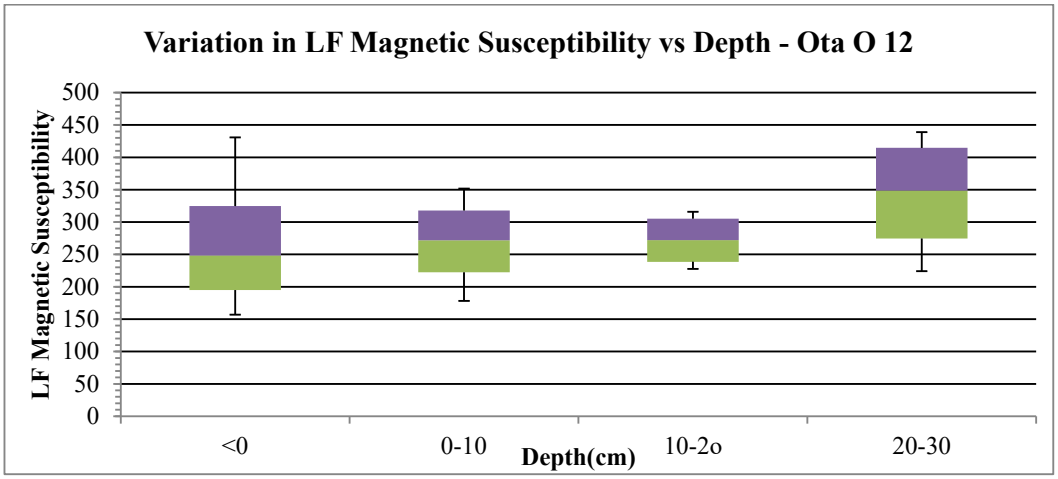
Variation in LF Magnetic Susceptibility vs Depth - Ota O 12
LF Magnetic Susceptibility
500
450
400
350
300
250
200
150
100
50
0
<0
0-10
10-2o
20-30
Depth(cm)

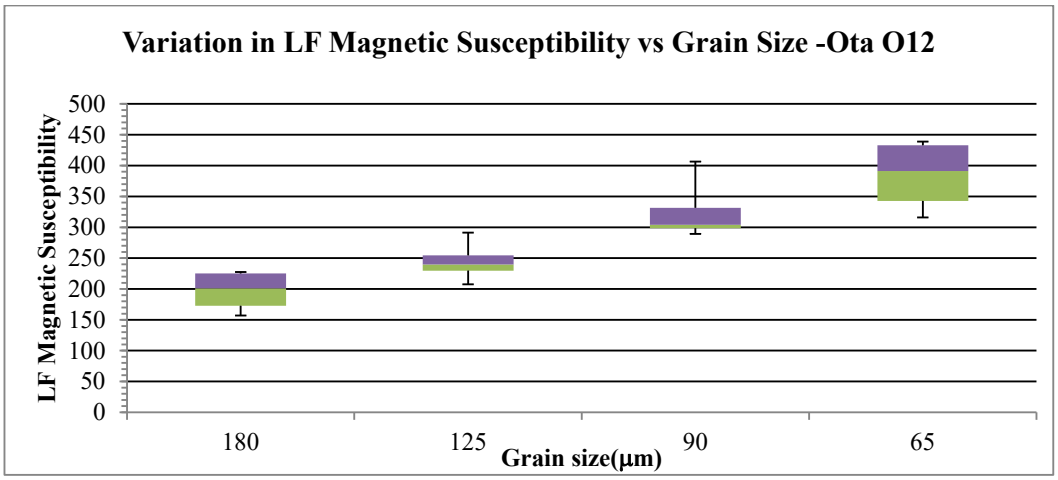
Variation in LF Magnetic Susceptibility vs Grain Size -Ota O12
LF Magnetic Susceptibility
500
450
400
350
300
250
200
150
100
50
0
180
125
90
65
Grain size(µm)

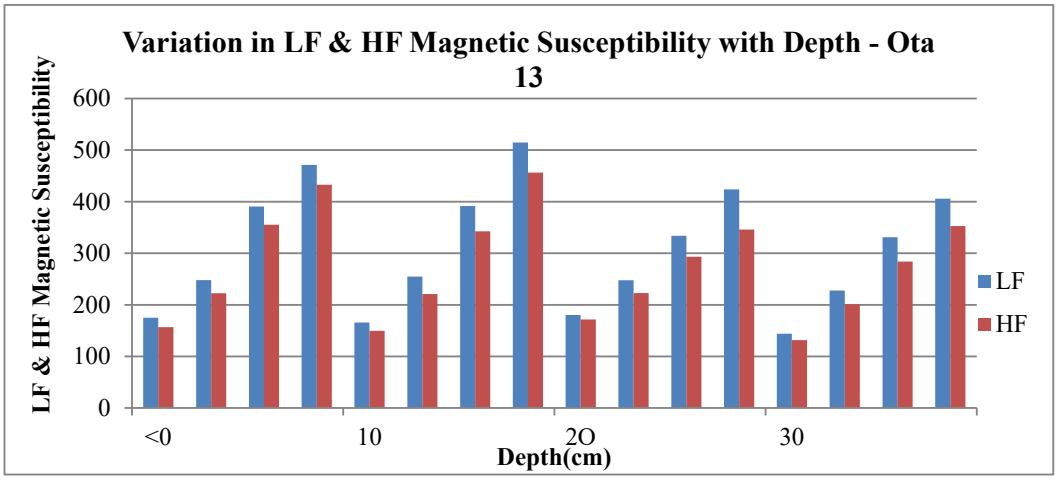
Variation in LF & HF Magnetic Susceptibility with Depth - Ota 13
LF & HF Magnetic Susceptibility
600
500
400
300
200
100
0
<0
10
2O
30
Depth(cm)
LF
HF

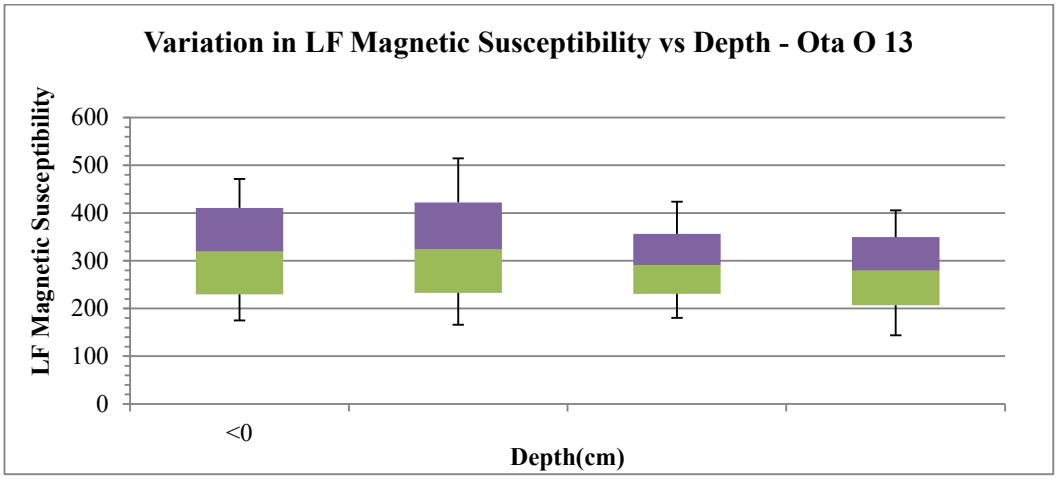
Variation in LF Magnetic Susceptibility vs Depth - Ota O 13
LF Magnetic Susceptibility
600
500
400
300
200
100
0
<0
Depth(cm)

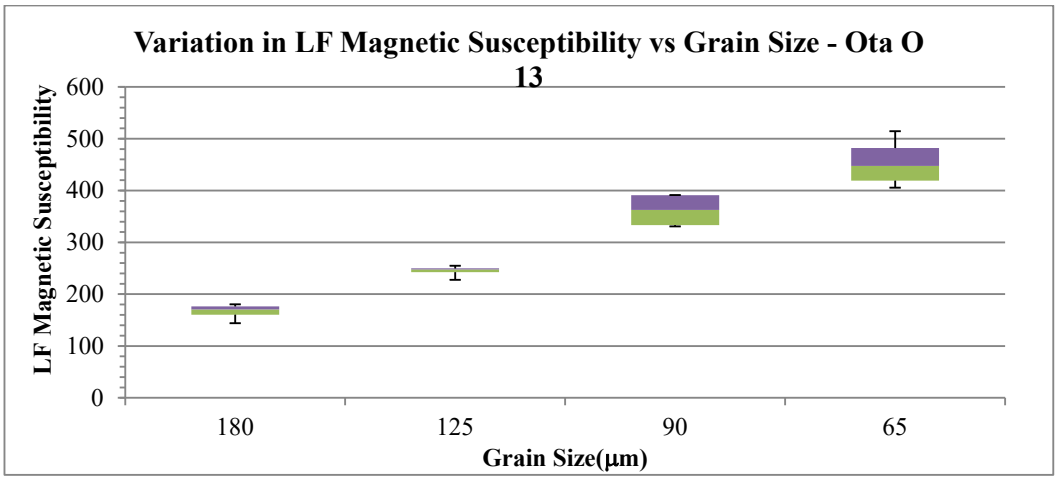
Variation in LF Magnetic Susceptibility vs Grain Size - Ota O 13
LF Magnetic Susceptibility
600
500
400
300
200
100
0
180
125
90
65
Grain Size(µm)

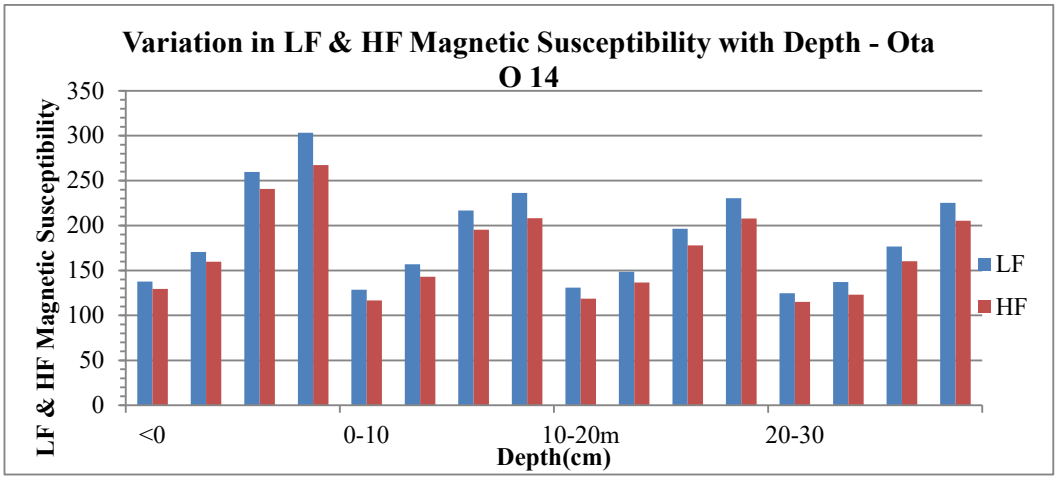
Variation in LF & HF Magnetic Susceptibility with Depth - Ota O 14
LF & HF Magnetic Susceptibility
350
300
250
200
150
100
50
0
<0
0-10
10-20m
20-30
Depth(cm)
LF
HF

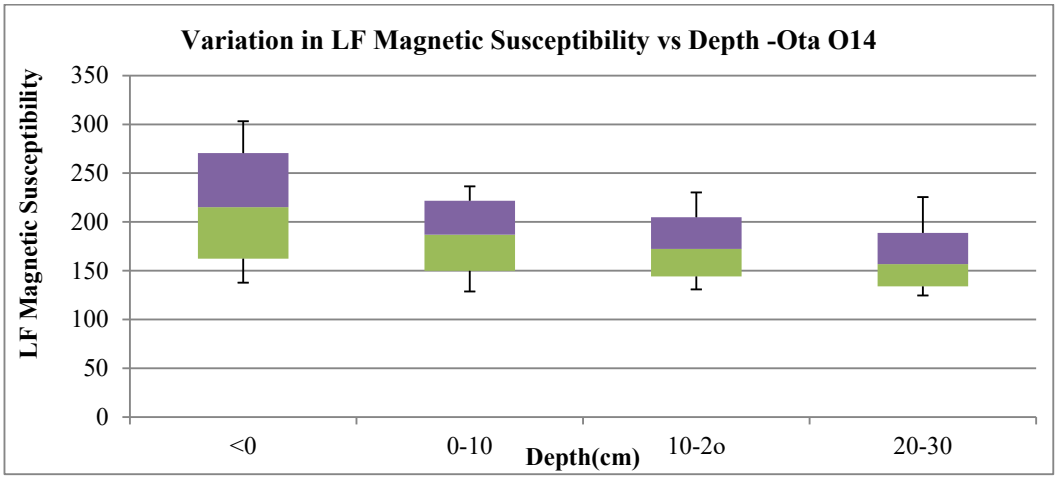
Variation in LF Magnetic Susceptibility vs Depth -Ota O14
LF Magnetic Susceptibility
350
300
250
200
150
100
50
0
<0
0-10
Depth(cm)
10-2o
20-30

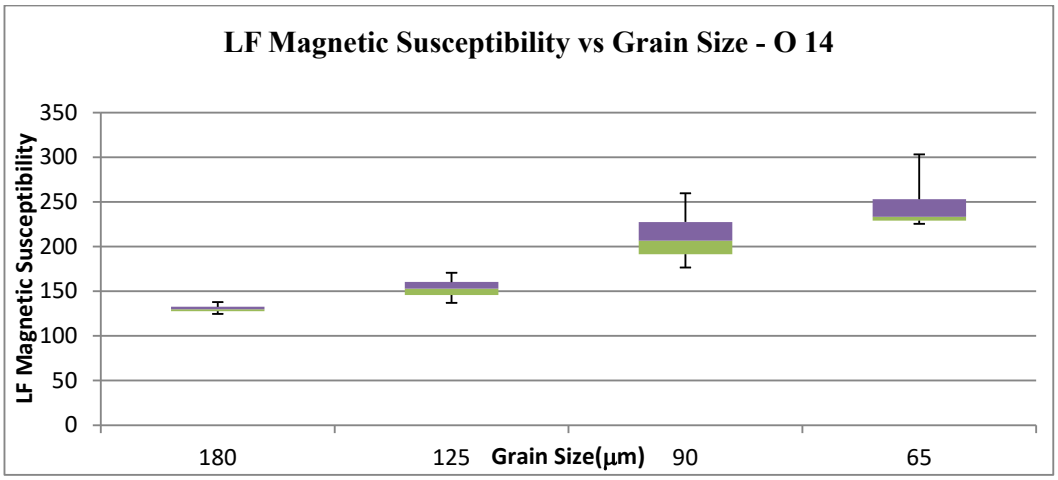
LF Magnetic Susceptibility vs Grain Size - O 14
LF Magnetic Susceptibility
350
300
250
200
150
100
50
0
180
125
Grain Size(µm)
90
65

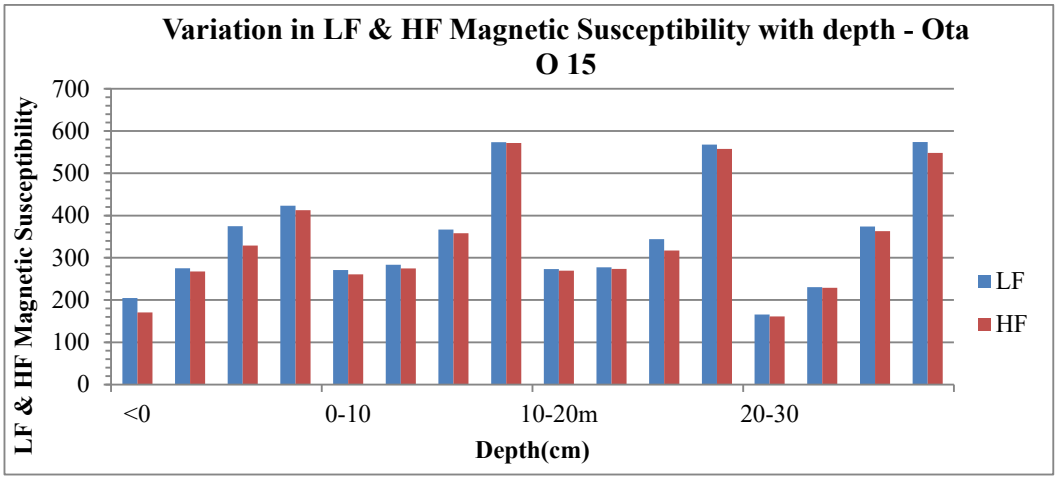
Variation in LF & HF Magnetic Susceptibility with depth - Ota O 15
LF & HF Magnetic Susceptibility
700
600
500
400
300
200
100
0
<0
0-10
10-20m
20-30
Depth(cm)
LF
HF

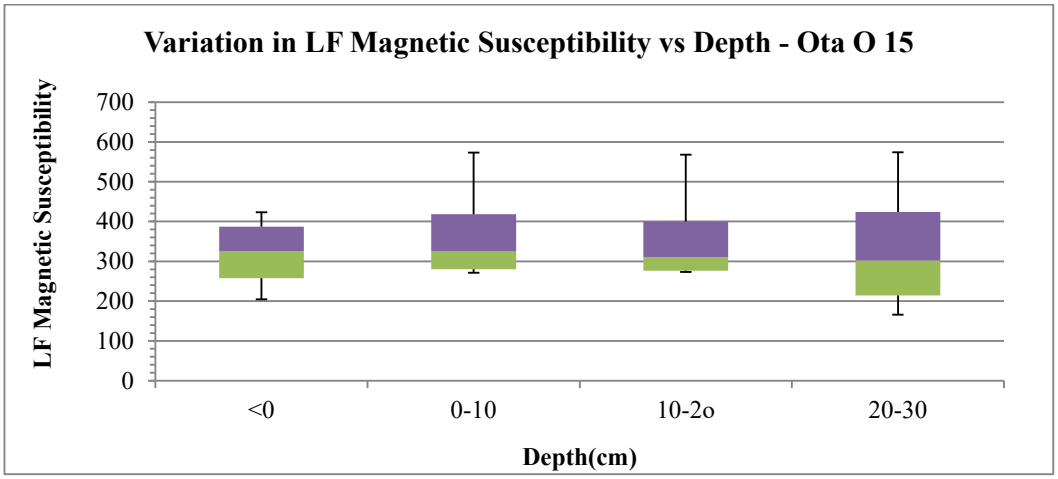
Variation in LF Magnetic Susceptibility vs Depth - Ota O 15
LF Magnetic Susceptibility
700
600
500
400
300
200
100
0
<0
0-10
10-2o
20-30
Depth(cm)

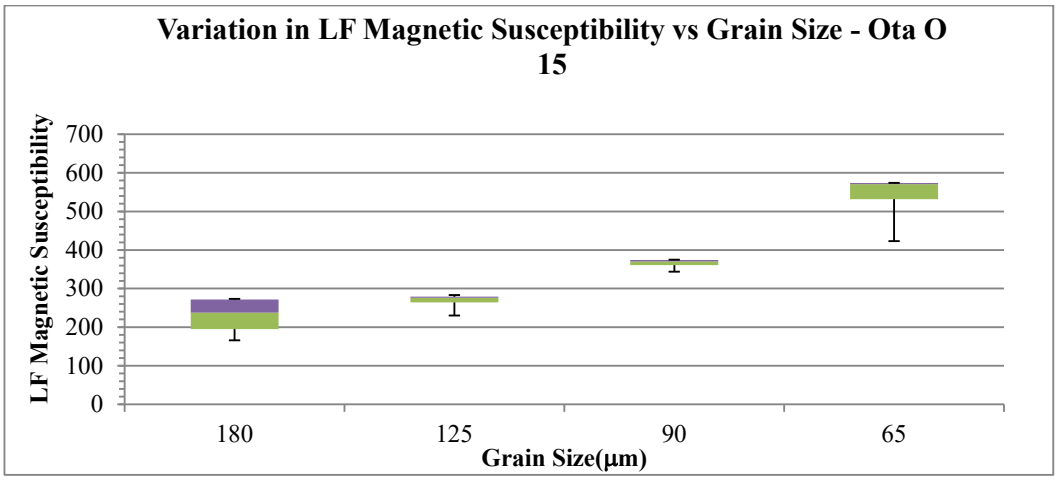
Variation in LF Magnetic Susceptibility vs Grain Size - Ota O 15
LF Magnetic Susceptibility
700
600
500
400
300
200
100
0
180
125
90
65
Grain Size(µm)

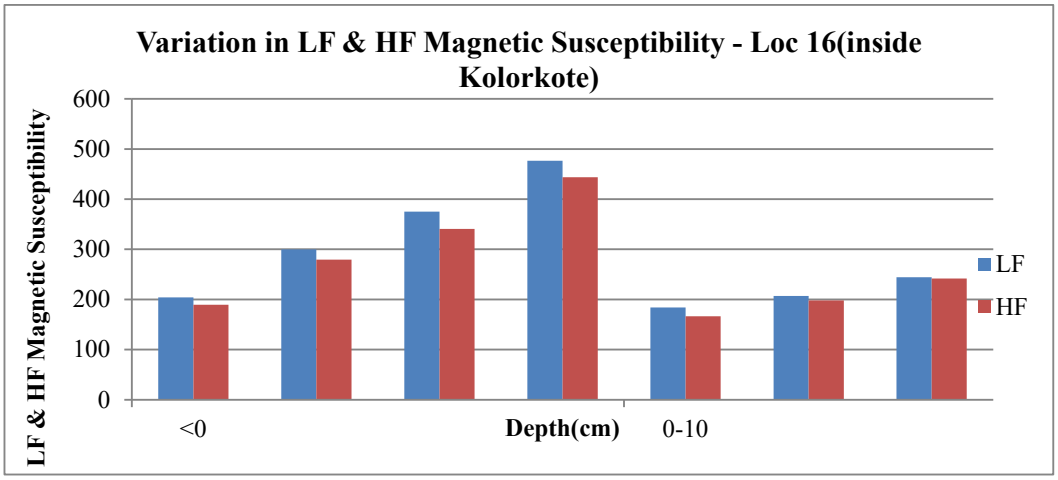
Variation in LF & HF Magnetic Susceptibility - Loc 16(inside Kolorkote)
LF & HF Magnetic Susceptibility
600
500
400
300
200
100
0
<0
Depth(cm)
0-10
LF
HF

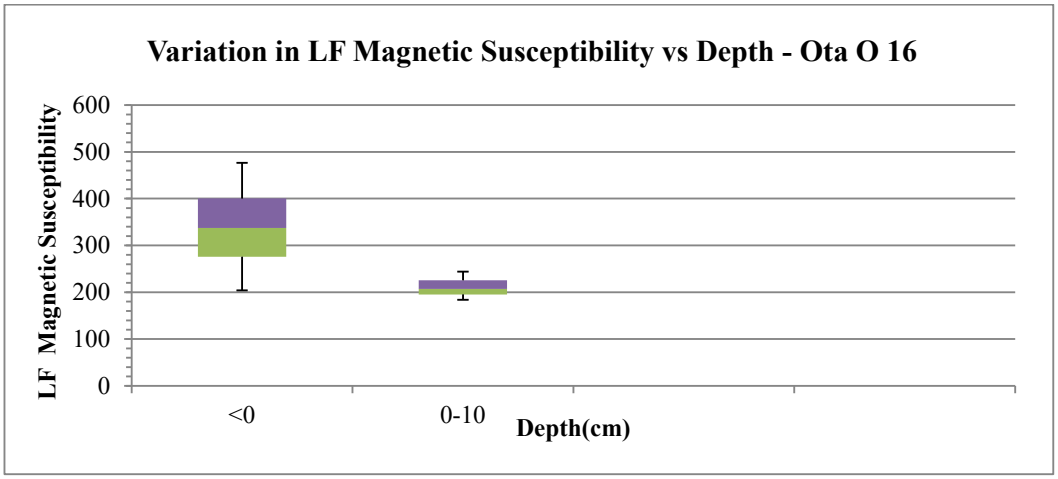
Variation in LF Magnetic Susceptibility vs Depth - Ota O 16
LF Magnetic Susceptibility
600
500
400
300
200
100
0
<0
0-10
Depth(cm)

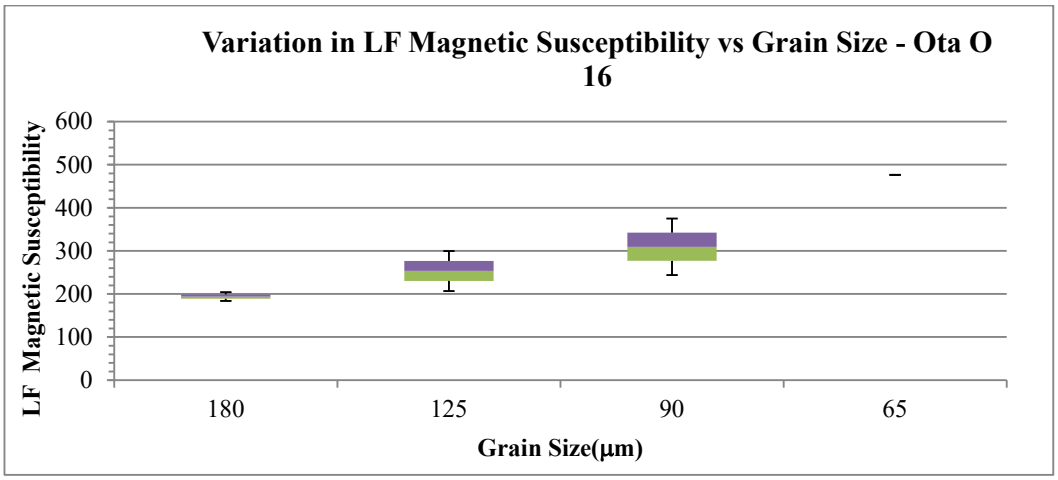
Variation in LF Magnetic Susceptibility vs Grain Size - Ota O 16
LF Magnetic Susceptibility
600
500
400
300
200
100
0
180
125
90
65
Grain Size(µm)

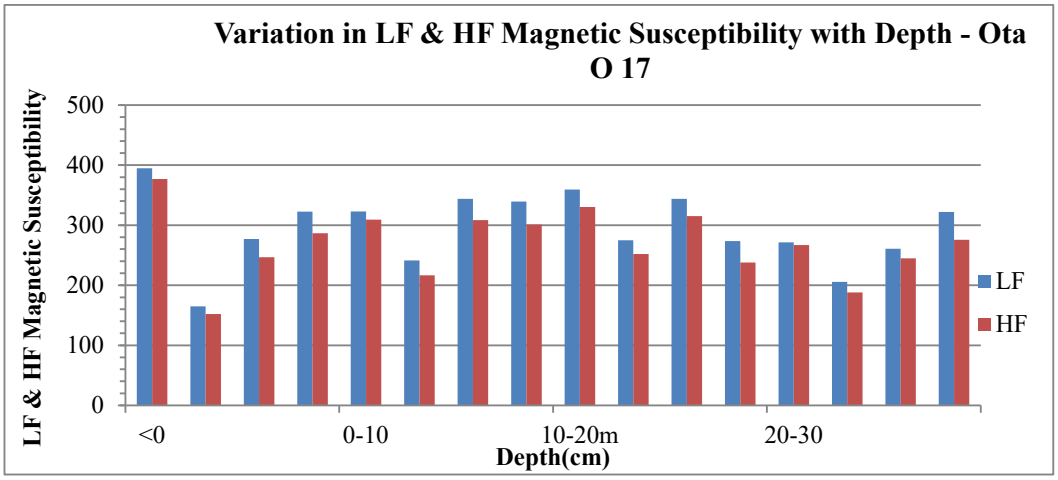
Variation in LF & HF Magnetic Susceptibility with Depth - Ota O 17
LF & HF Magnetic Susceptibility
500
400
300
200
100
0
<0
0-10
10-20m
20-30
Depth(cm)
LF
HF

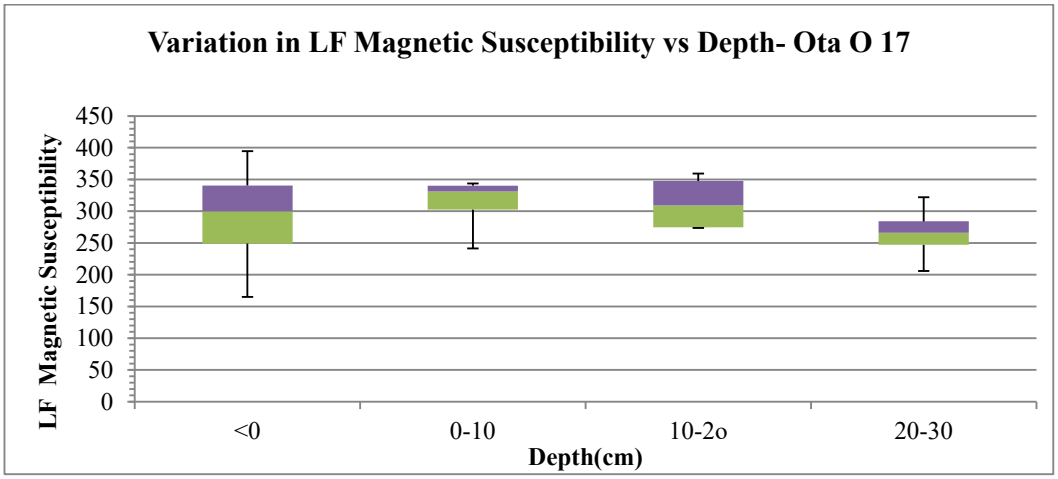
Variation in LF Magnetic Susceptibility vs Depth- Ota O 17
LF Magnetic Susceptibility
450
400
350
300
250
200
150
100
50
0
<0
0-10
10-2o
20-30
Depth(cm)

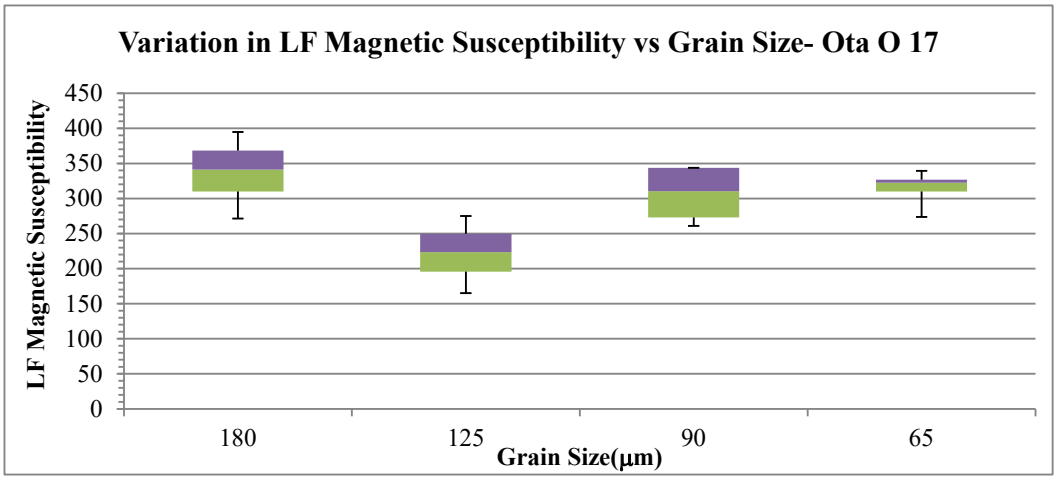
Variation in LF Magnetic Susceptibility vs Grain Size- Ota O 17
LF Magnetic Susceptibility
450
400
350
300
250
200
150
100
50
0
180
125
90
65
Grain Size(µm)

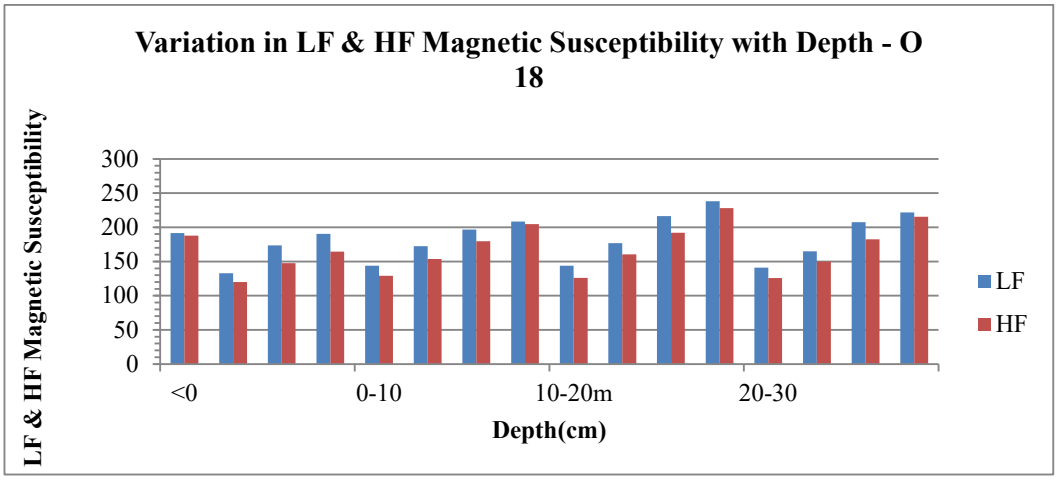
Variation in LF & HF Magnetic Susceptibility with Depth - O 18
LF & HF Magnetic Susceptibility
300
250
200
150
100
50
0
<0
0-10
10-20m
20-30
Depth(cm)
LF
HF

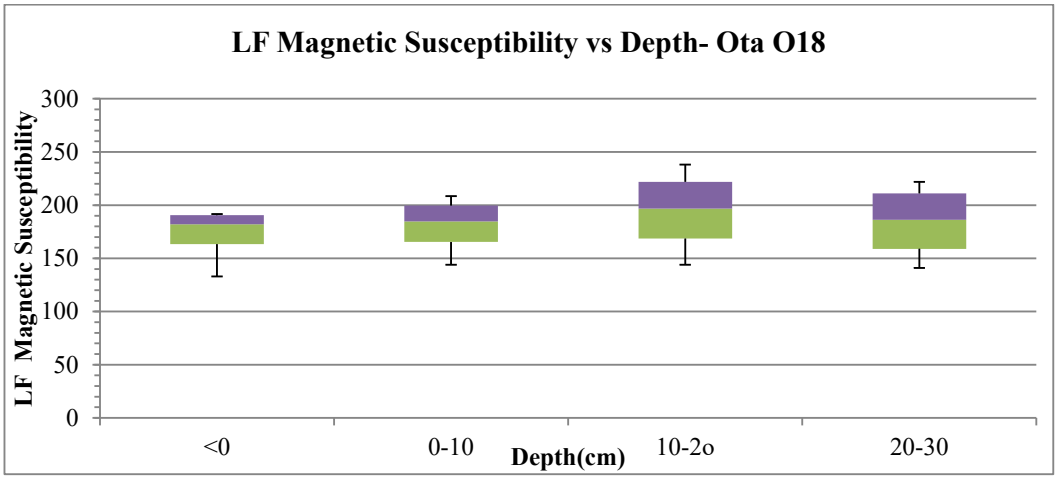
LF Magnetic Susceptibility vs Depth- Ota O18
LF Magnetic Susceptibility
300
250
200
150
100
50
0
<0
0-10
Depth(cm)
10-2o
20-30

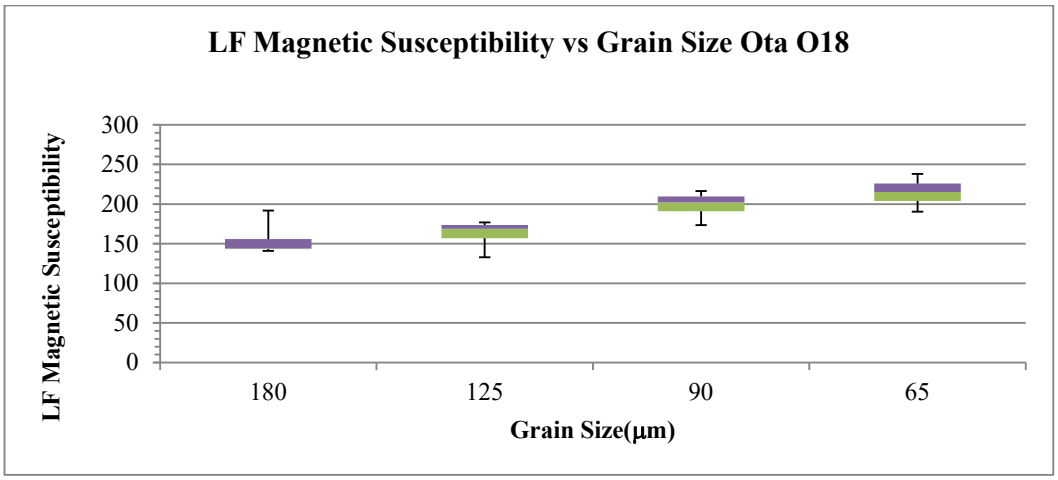
LF Magnetic Susceptibility vs Grain Size Ota O18
LF Magnetic Susceptibility
300
250
200
150
100
50
0
180
125
90
65
Grain Size(µm)

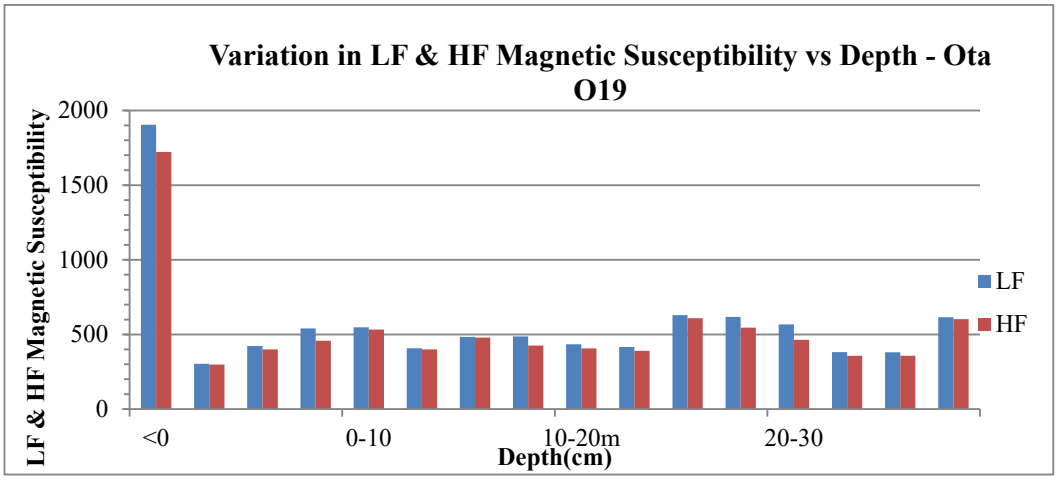
Variation in LF & HF Magnetic Susceptibility vs Depth - Ota O19
LF & HF Magnetic Susceptibility
2000
1500
1000
500
0
<0
0-10
10-20m
20-30
Depth(cm)
LF
HF

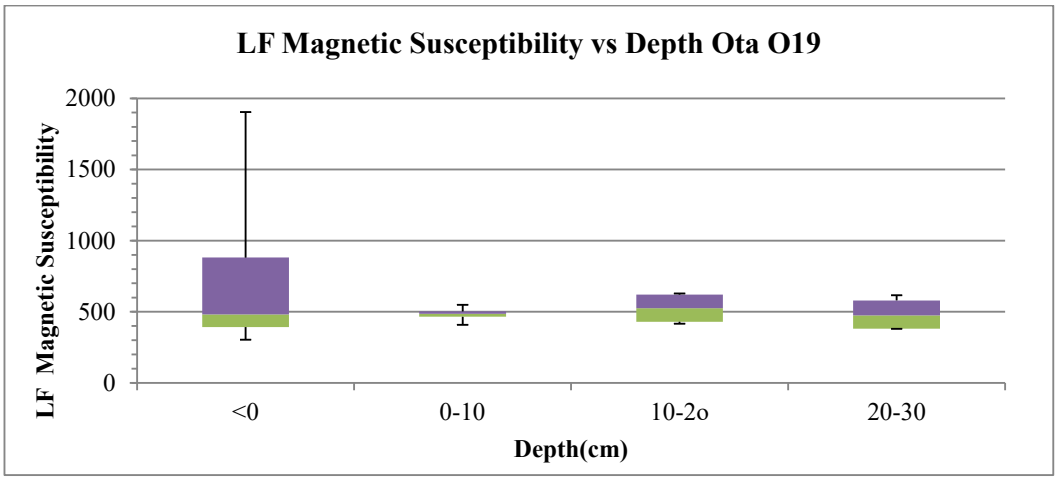
LF Magnetic Susceptibility vs Depth Ota O19
LF Magnetic Susceptibility
2000
1500
1000
500
0
<0
0-10
10-2o
20-30
Depth(cm)

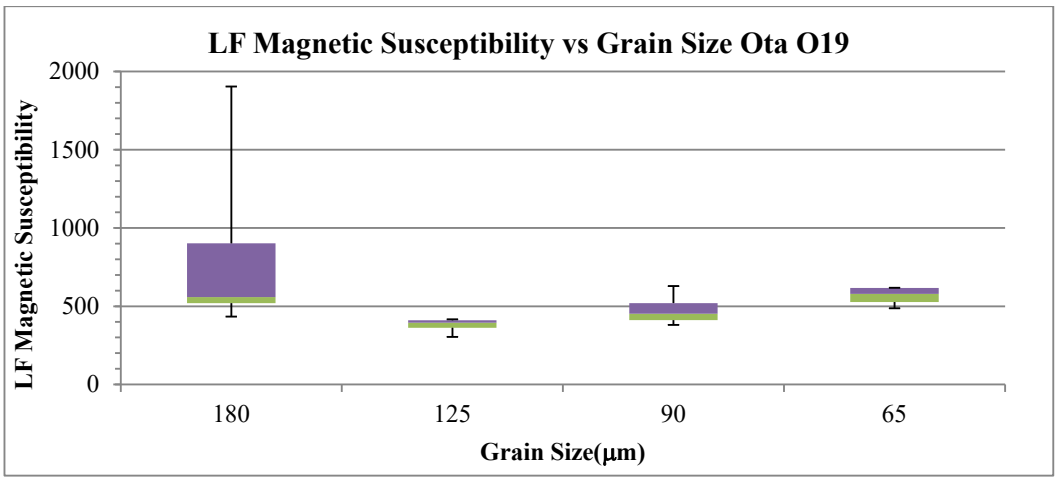
LF Magnetic Susceptibility vs Grain Size Ota O19
LF Magnetic Susceptibility
2000
1500
1000
500
0
180
125
90
65
Grain Size(µm)

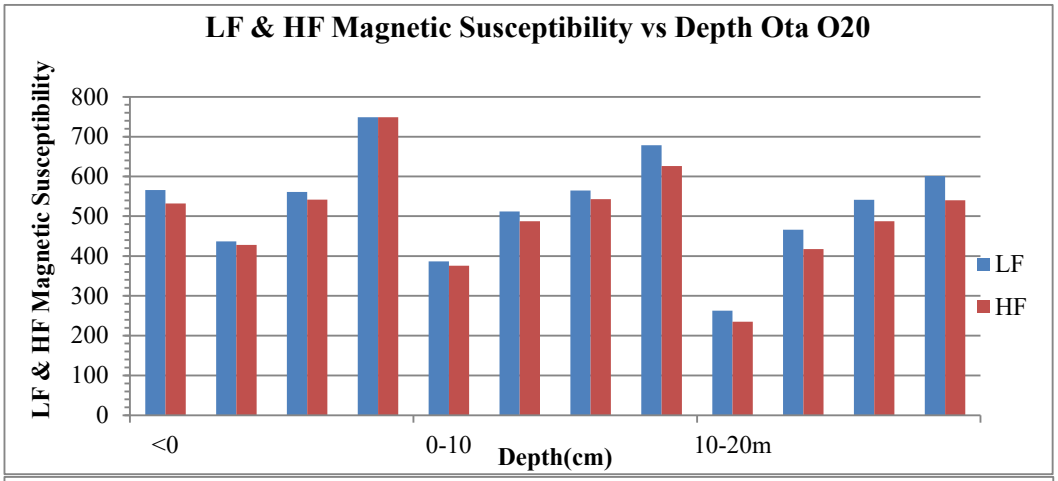
LF & HF Magnetic Susceptibility vs Depth Ota O20
LF & HF Magnetic Susceptibility
800
700
600
500
400
300
200
100
0
<0
0-10
10-20m
Depth(cm)
LF
HF

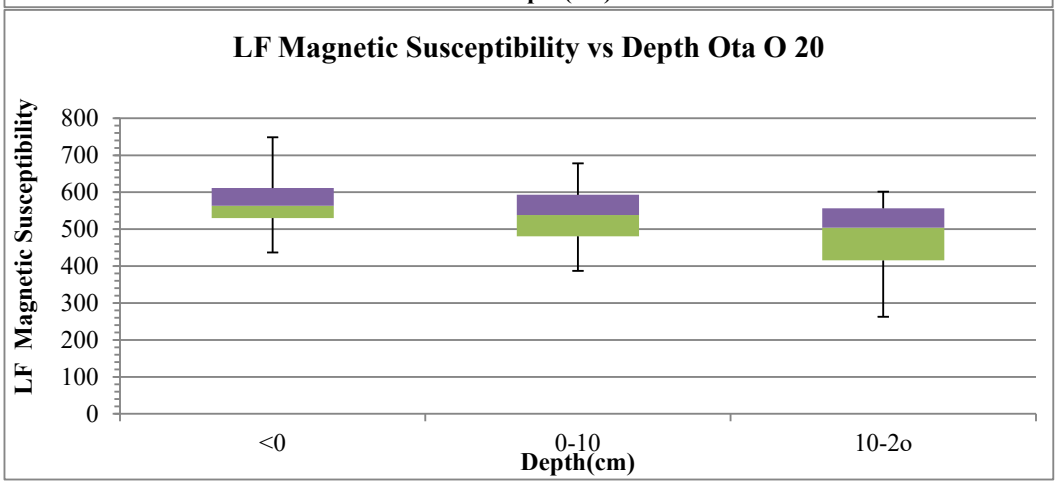
LF Magnetic Susceptibility vs Depth Ota O 20
LF Magnetic Susceptibility
800
700
600
500
400
300
200
100
0
<0
0-10
10-2o
Depth(cm)

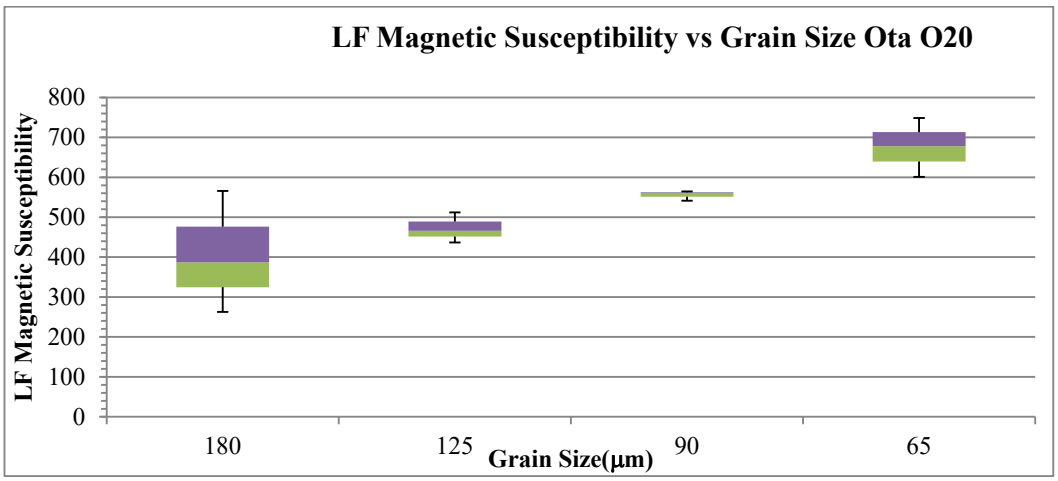
LF Magnetic Susceptibility vs Grain Size Ota O20
LF Magnetic Susceptibility
800
700
600
500
400
300
200
100
0
180
125
90
65
Grain Size(µm)

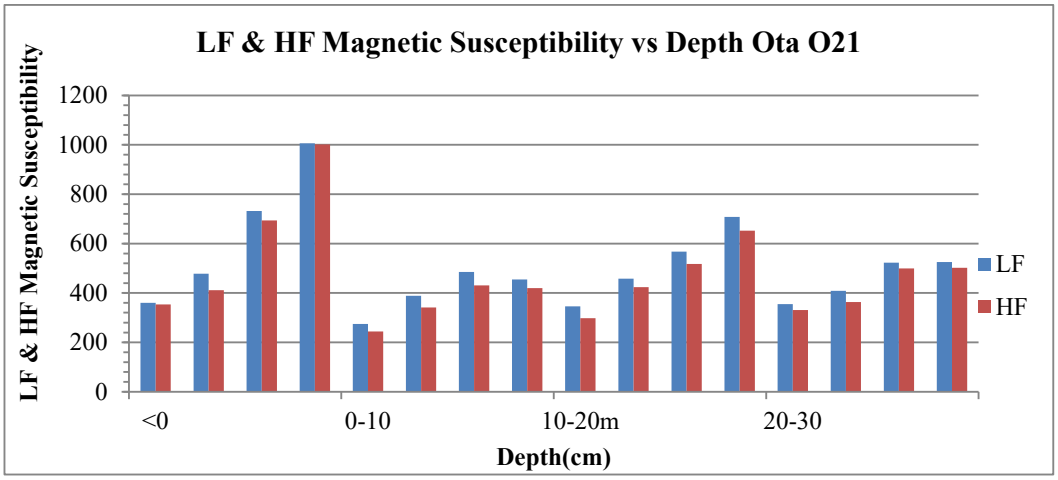
LF & HF Magnetic Susceptibility vs Depth Ota O21
LF & HF Magnetic Susceptibility
1200
1000
800
600
400
200
0
<0
0-10
10-20m
20-30
Depth(cm)
LF
HF

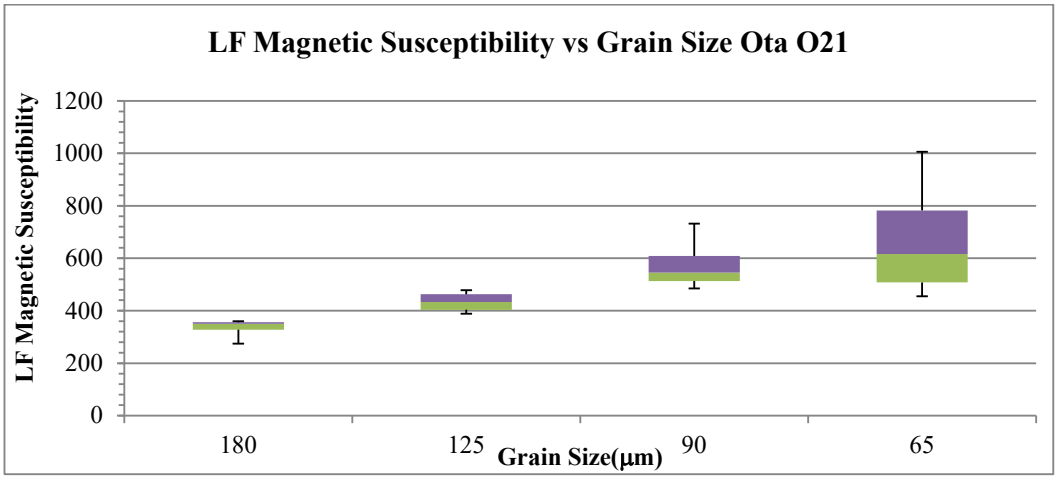
LF Magnetic Susceptibility vs Grain Size Ota O21
LF Magnetic Susceptibility
1200
1000
800
600
400
200
0
180
125
90
65
Grain Size(µm)

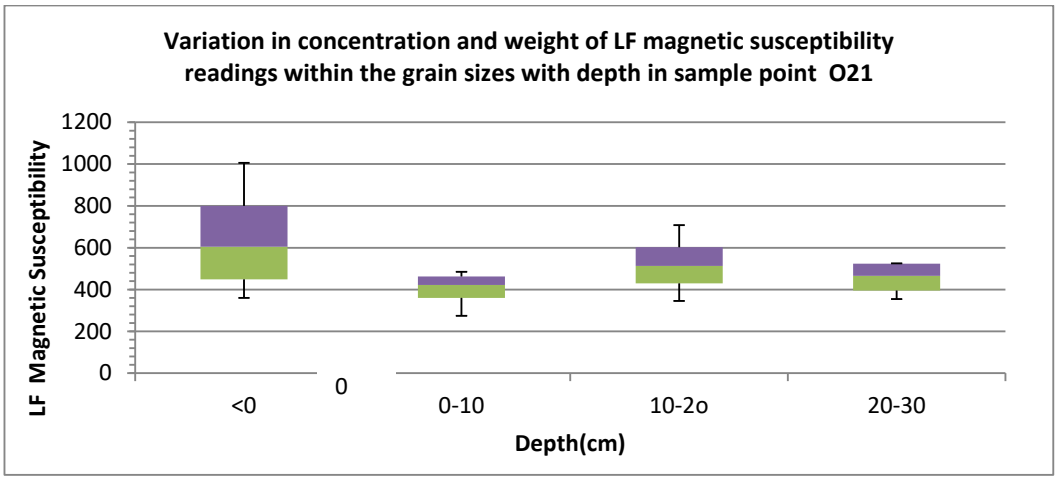
Variation in concentration and weight of LF magnetic susceptibility readings within the grain sizes with depth in sample point O21
LF Magnetic Susceptibility
1200
1000
800
600
400
200
0
0
<0
0-10
10-2o
20-30
Depth(cm)

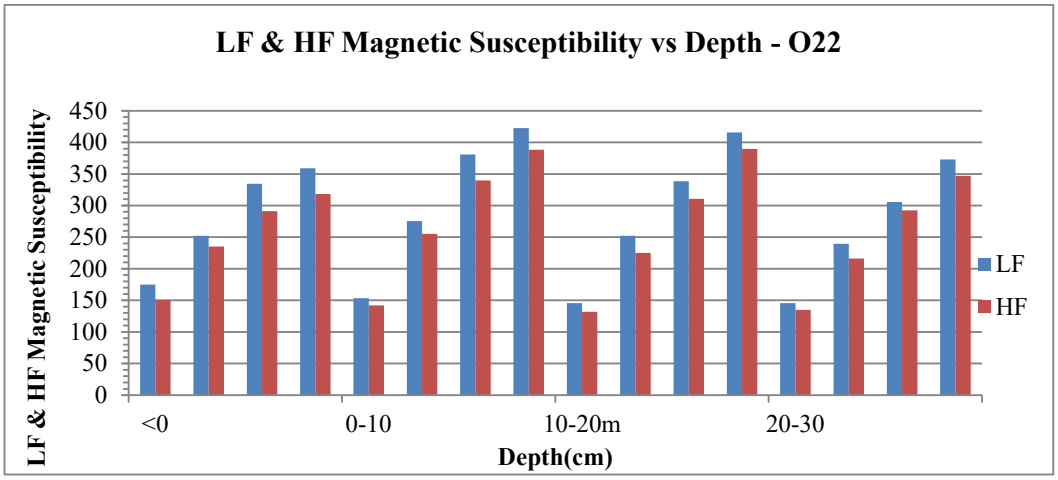
LF & HF Magnetic Susceptibility vs Depth - O22
LF & HF Magnetic Susceptibility
450
400
350
300
250
200
150
100
50
0
<0
0-10
10-20m
20-30
Depth(cm)
LF
HF

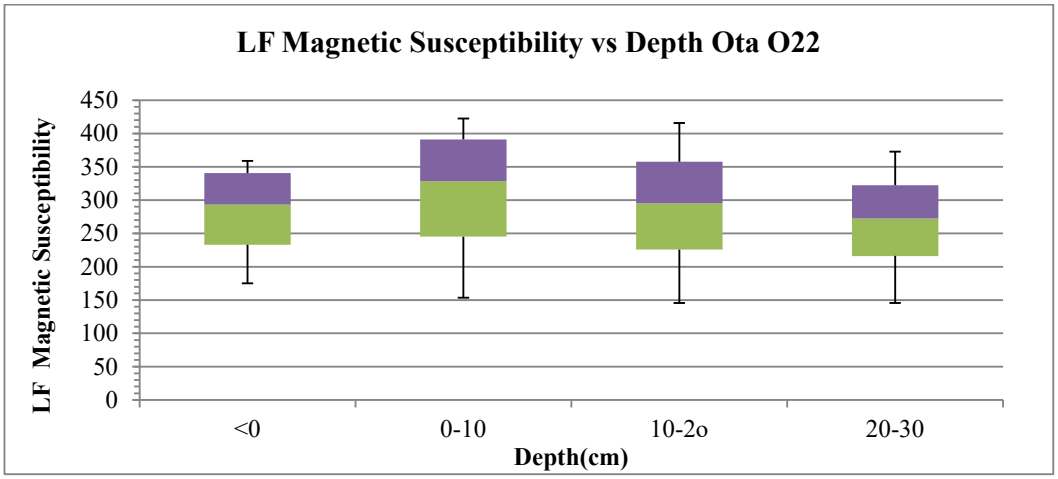
LF Magnetic Susceptibility vs Depth Ota O22
LF Magnetic Susceptibility
450
400
350
300
250
200
150
100
50
0
<0
0-10
10-2o
20-30
Depth(cm)

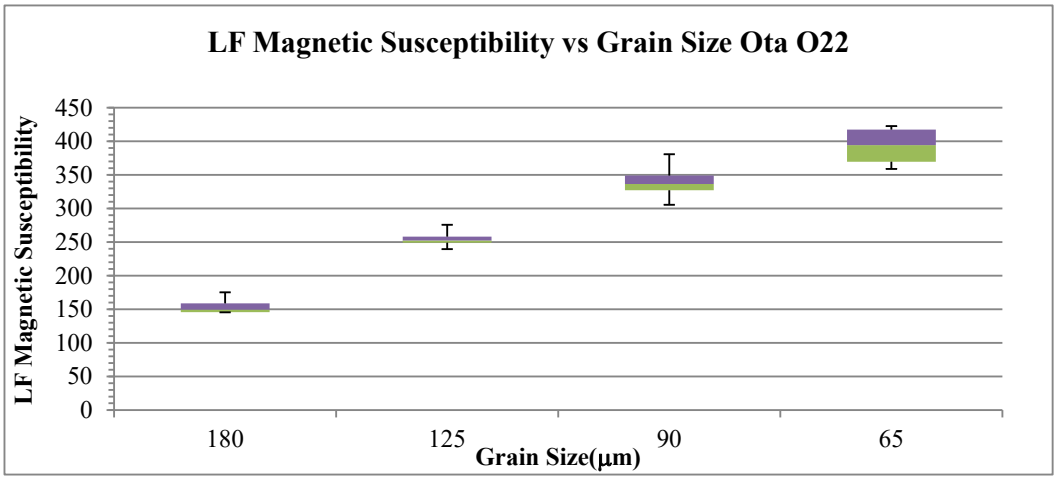
LF Magnetic Susceptibility vs Grain Size Ota O22
LF Magnetic Susceptibility
450
400
350
300
250
200
150
100
50
0
180
125
90
65
Grain Size(µm)

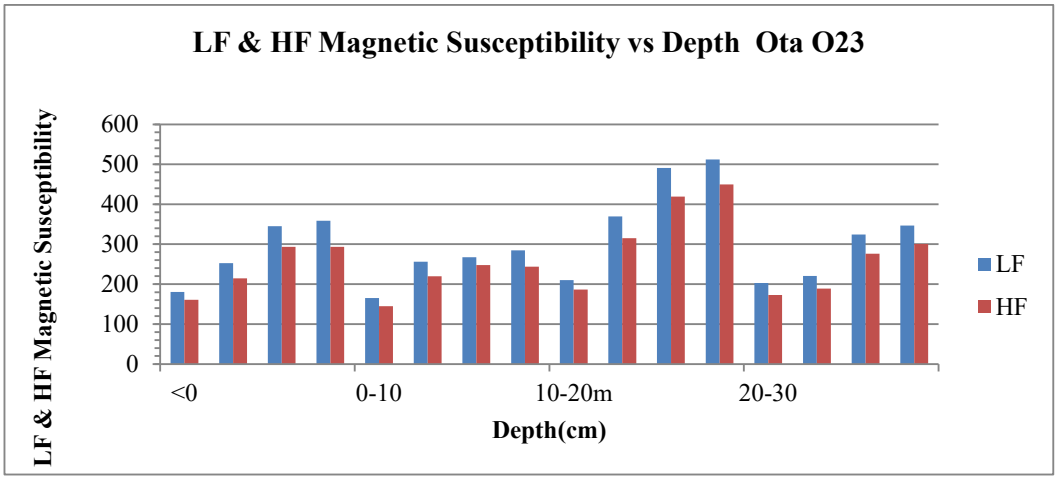
LF & HF Magnetic Susceptibility vs Depth Ota O23
LF & HF Magnetic Susceptibility
600
500
400
300
200
100
0
<0
0-10
10-20m
20-30
Depth(cm)
LF
HF

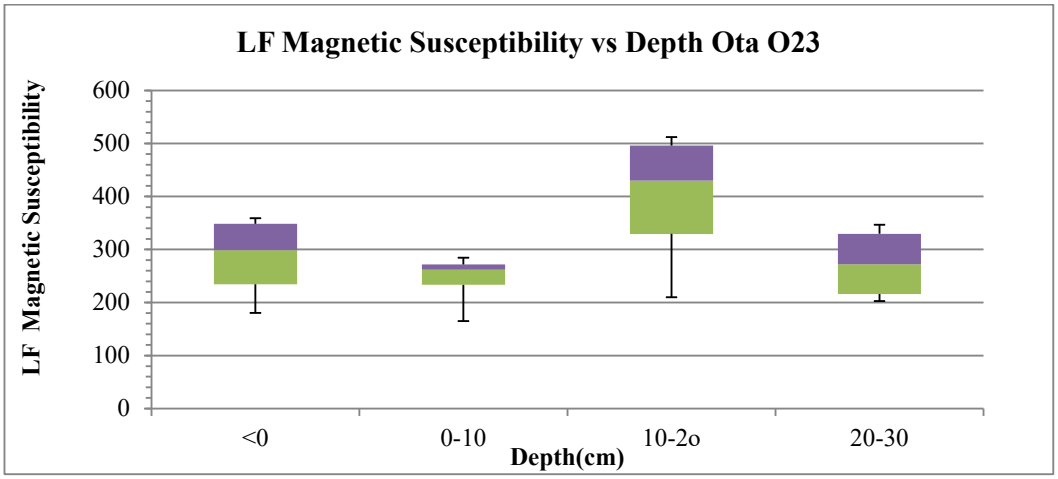
LF Magnetic Susceptibility vs Depth Ota O23
LF Magnetic Susceptibility
600
500
400
300
200
100
0
<0
0-10
10-2o
20-30
Depth(cm)

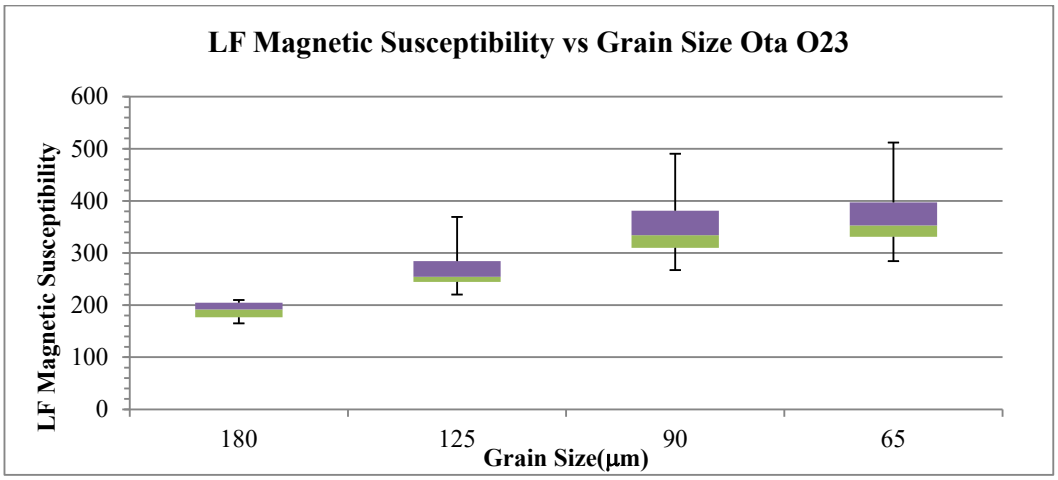
LF Magnetic Susceptibility vs Grain Size Ota O23
LF Magnetic Susceptibility
600
500
400
300
200
100
0
180
125
90
65
Grain Size(µm)

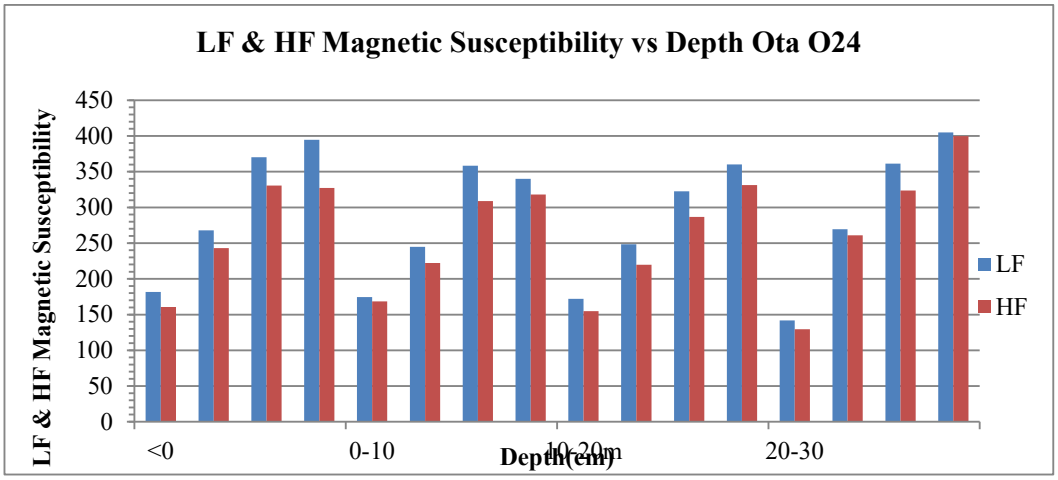
LF & HF Magnetic Susceptibility vs Depth Ota O24
LF & HF Magnetic Susceptibility
450
400
350
300
250
200
150
100
50
0
<0
0-10
10-20m
20-30
Depth(cm)
LF
HF

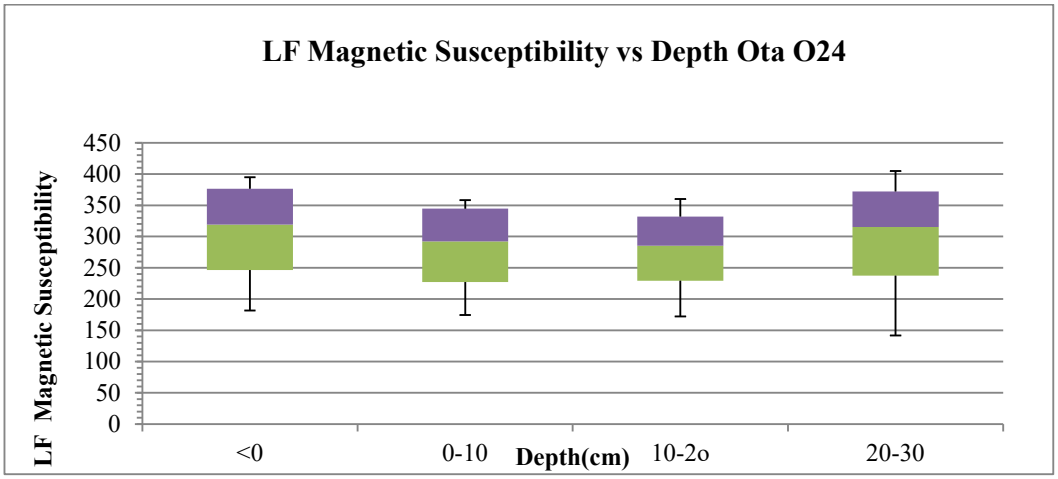
LF Magnetic Susceptibility vs Depth Ota O24
LF Magnetic Susceptibility
450
400
350
300
250
200
150
100
50
0
<0
0-10
Depth(cm)
10-2o
20-30

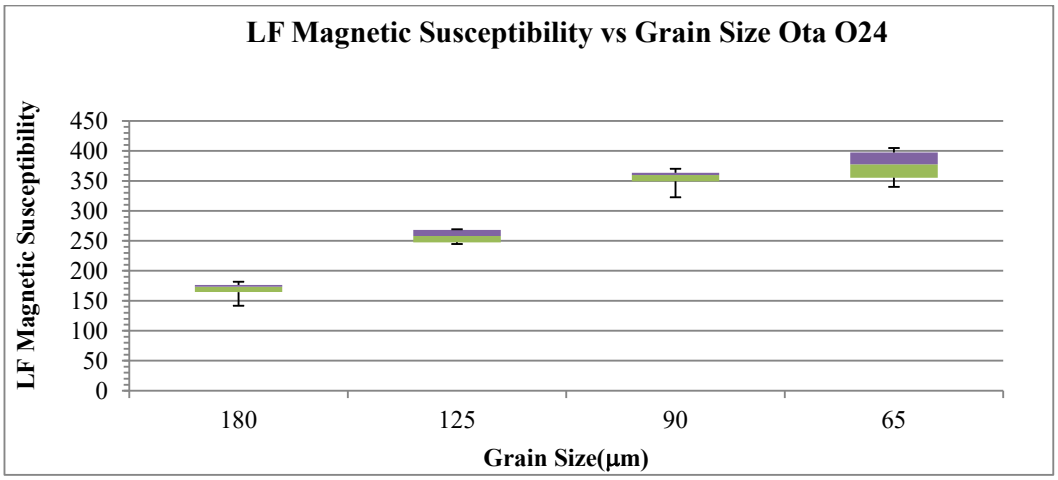
LF Magnetic Susceptibility vs Grain Size Ota O24
LF Magnetic Susceptibility
450
400
350
300
250
200
150
100
50
0
180
125
90
65
Grain Size(µm)

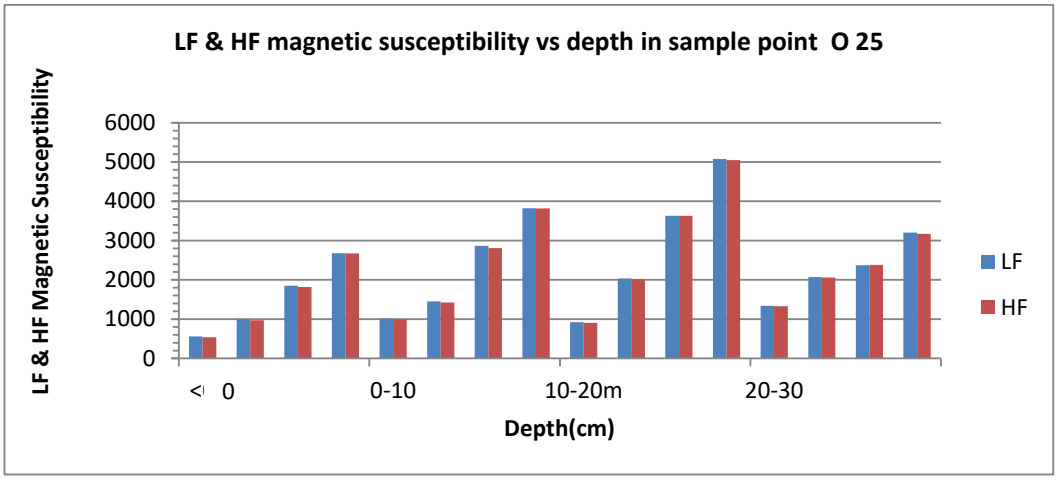
LF & HF magnetic susceptibility vs depth in sample point O 25
LF & HF Magnetic Susceptibility
6000
5000
4000
3000
2000
1000
0
< 0
0-10
10-20m
20-30
Depth(cm)
LF
HF

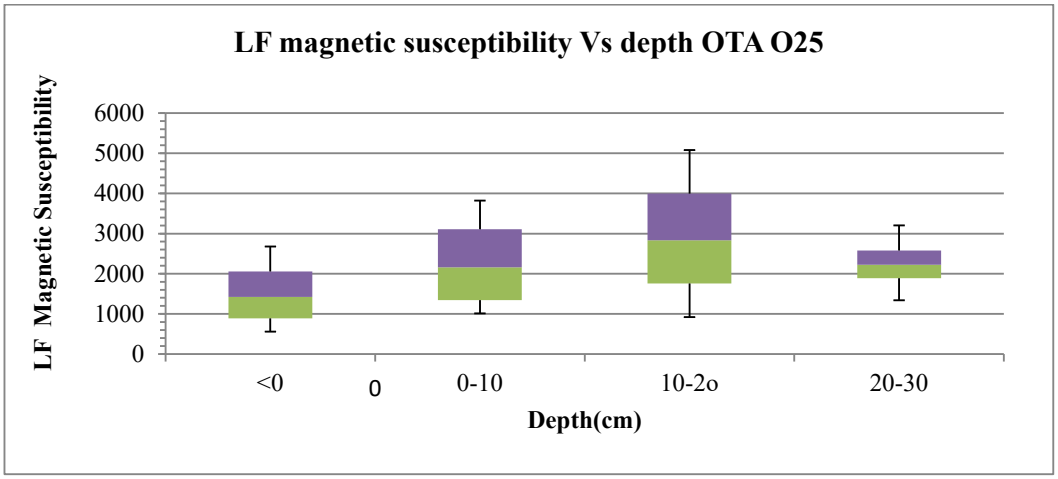
LF magnetic susceptibility Vs depth OTA O25
LF Magnetic Susceptibility
6000
5000
4000
3000
2000
1000
0
<0
0
0-10
10-2o
20-30
Depth(cm)

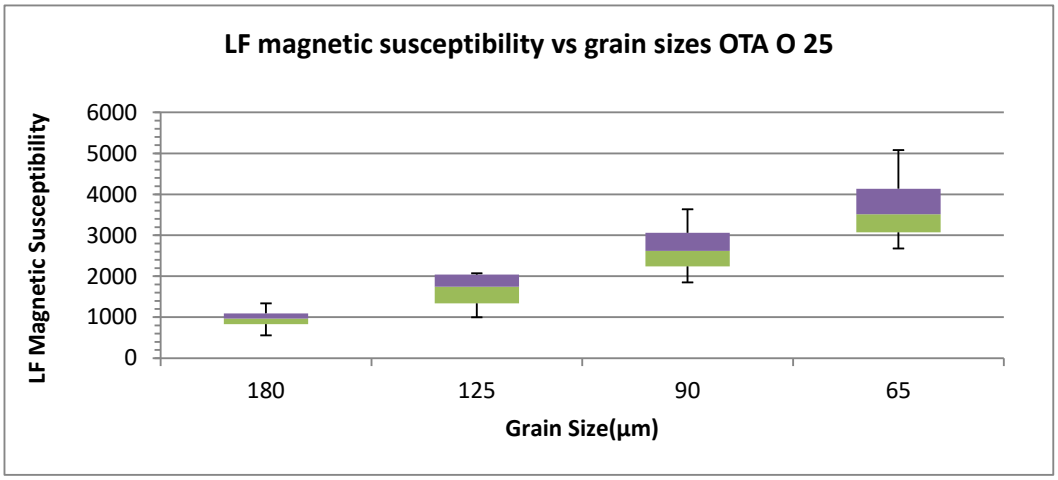
LF magnetic susceptibility vs grain sizes OTA O 25
LF Magnetic Susceptibility
6000
5000
4000
3000
2000
1000
0
180
125
90
65
Grain Size(µm)

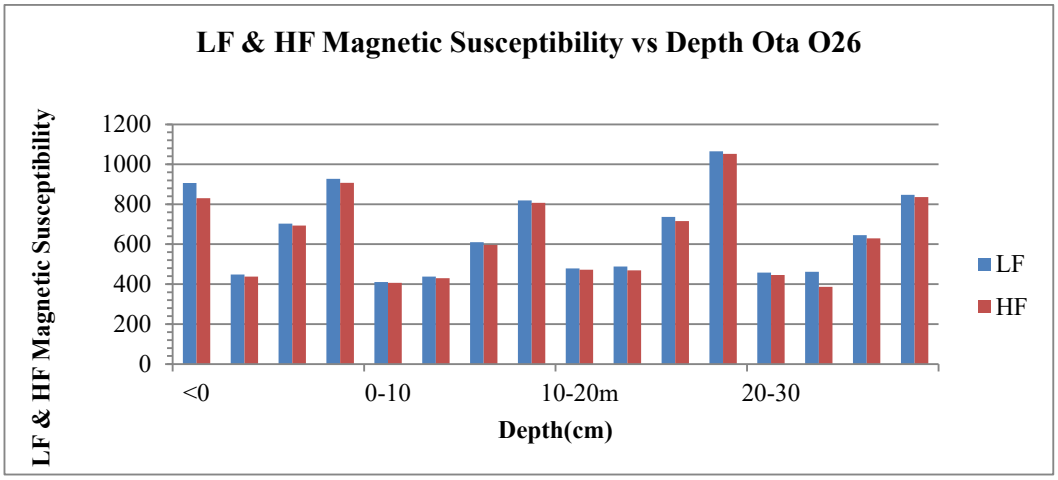
LF & HF Magnetic Susceptibility vs Depth Ota O26
LF & HF Magnetic Susceptibility
1200
1000
800
600
400
200
0
<0
0-10
10-20m
20-30
Depth(cm)
LF
HF

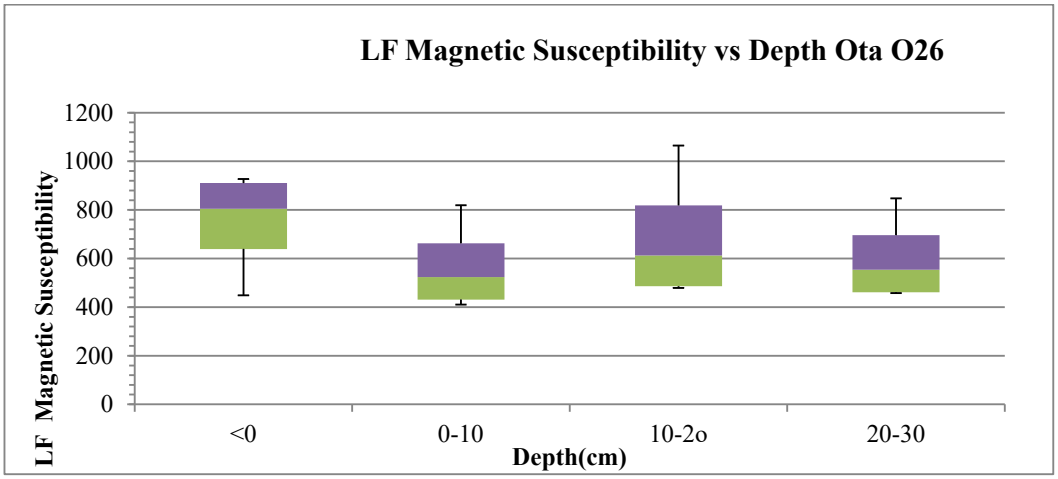
LF Magnetic Susceptibility vs Depth Ota O26
LF Magnetic Susceptibility
1200
1000
800
600
400
200
0
<0
0-10
10-2o
20-30
Depth(cm)

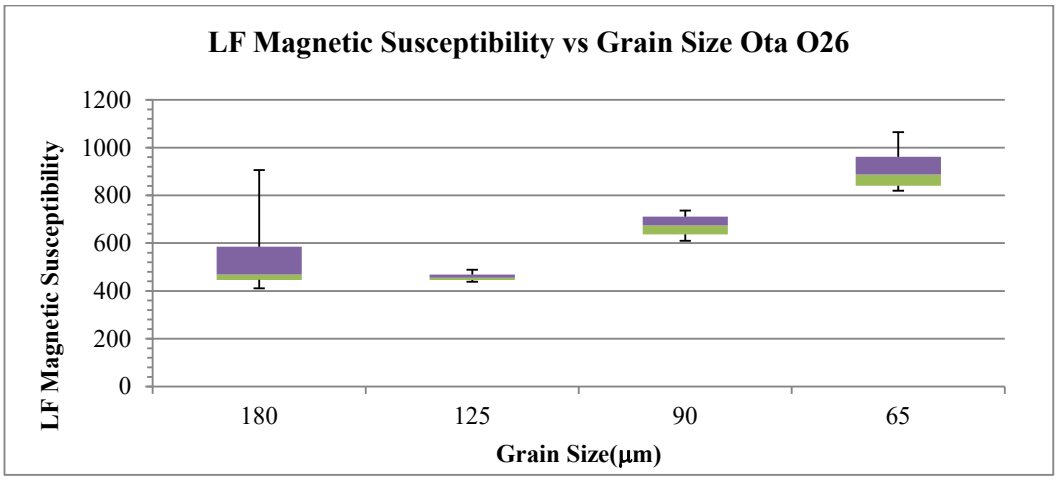
LF Magnetic Susceptibility vs Grain Size Ota O26
LF Magnetic Susceptibility
1200
1000
800
600
400
200
0
180
125
90
65
Grain Size(µm)

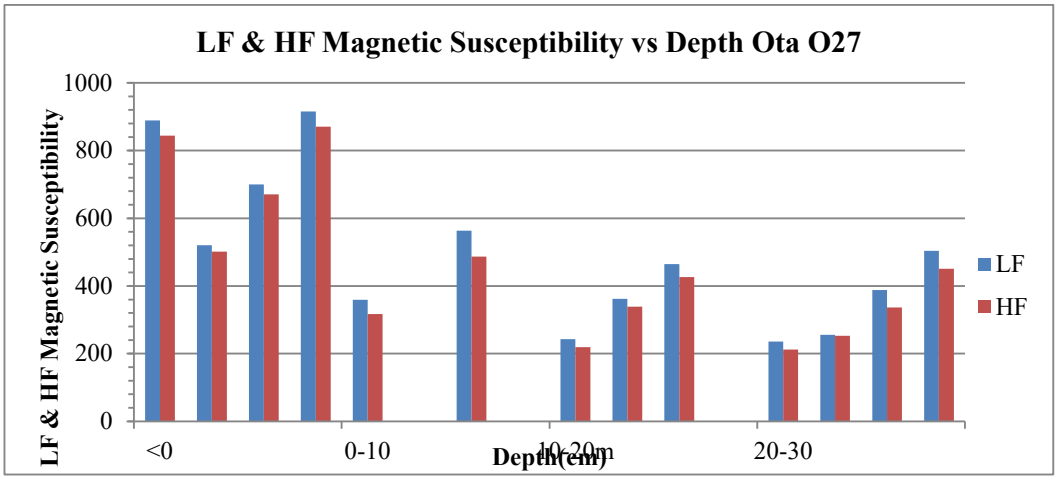
LF & HF Magnetic Susceptibility vs Depth Ota O27
LF & HF Magnetic Susceptibility
1000
800
600
400
200
0
<0
0-10
10-20m
20-30
Depth(cm)
LF
HF

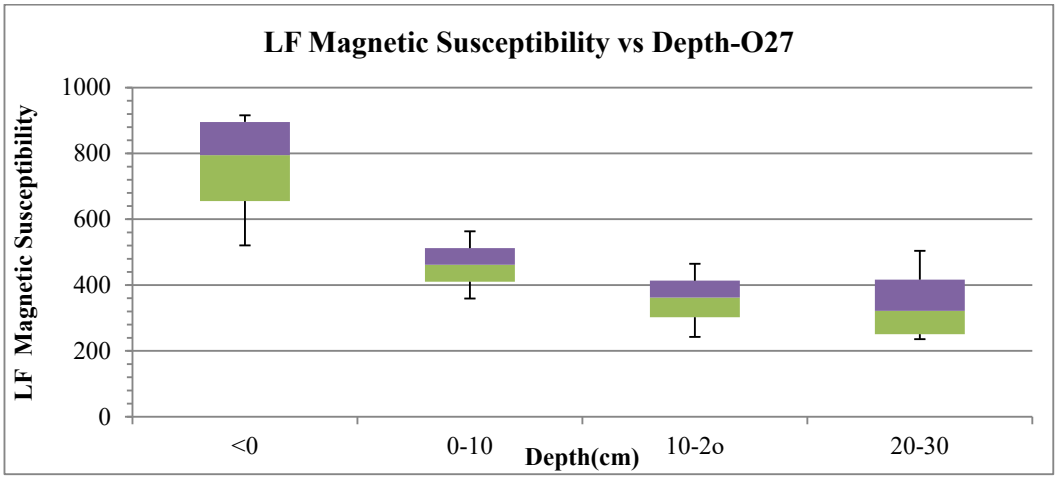
LF Magnetic Susceptibility vs Depth-O27
LF Magnetic Susceptibility
1000
800
600
400
200
0
<0
0-10
Depth(cm)
10-2o
20-30

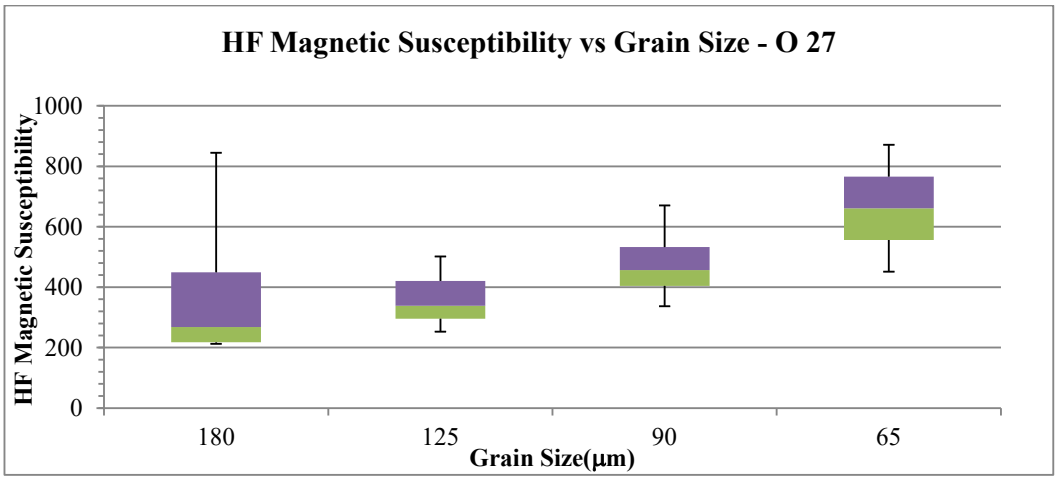
HF Magnetic Susceptibility vs Grain Size - O 27
HF Magnetic Susceptibility
1000
800
600
400
200
0
180
125
90
65
Grain Size(µm)

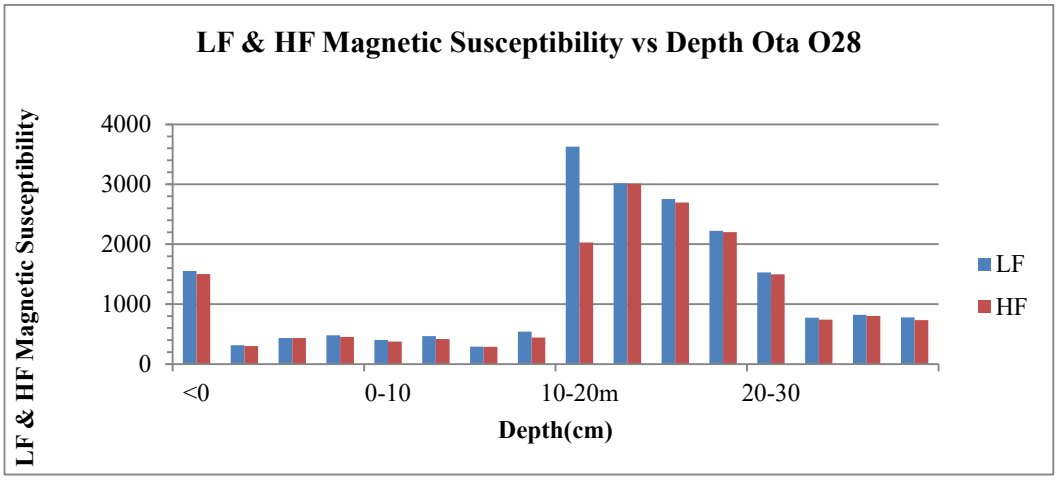
LF & HF Magnetic Susceptibility vs Depth Ota O28
LF & HF Magnetic Susceptibility
4000
3000
2000
1000
0
<0
0-10
10-20m
20-30
Depth(cm)
LF
HF

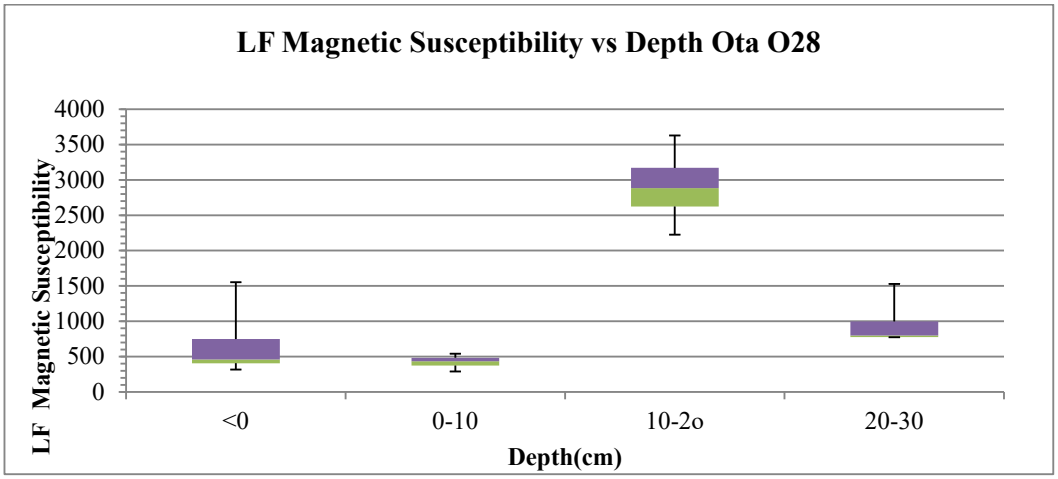
LF Magnetic Susceptibility vs Depth Ota O28
LF Magnetic Susceptibility
4000
3500
3000
2500
2000
1500
1000
500
0
<0
0-10
10-2o
20-30
Depth(cm)

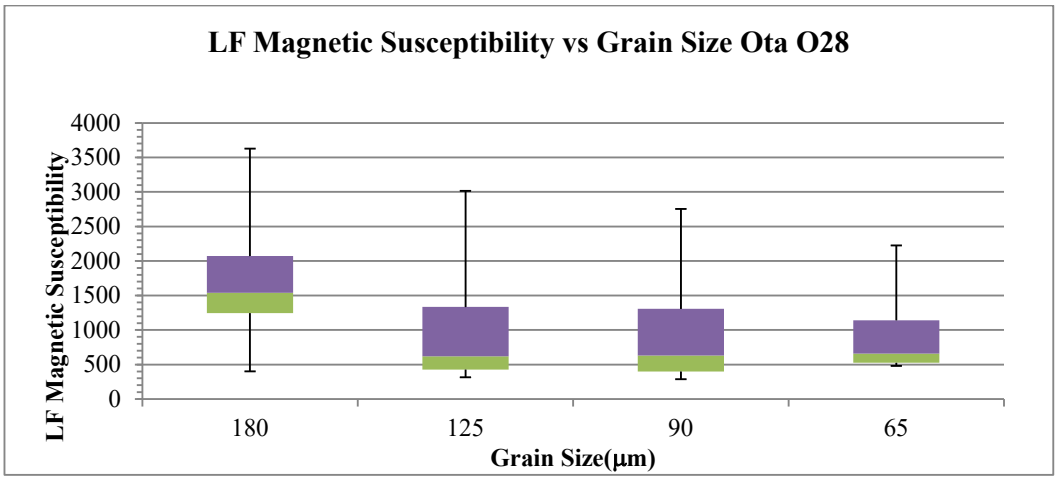
LF Magnetic Susceptibility vs Grain Size Ota O28
LF Magnetic Susceptibility
4000
3500
3000
2500
2000
1500
1000
500
0
180
125
90
65
Grain Size(µm)

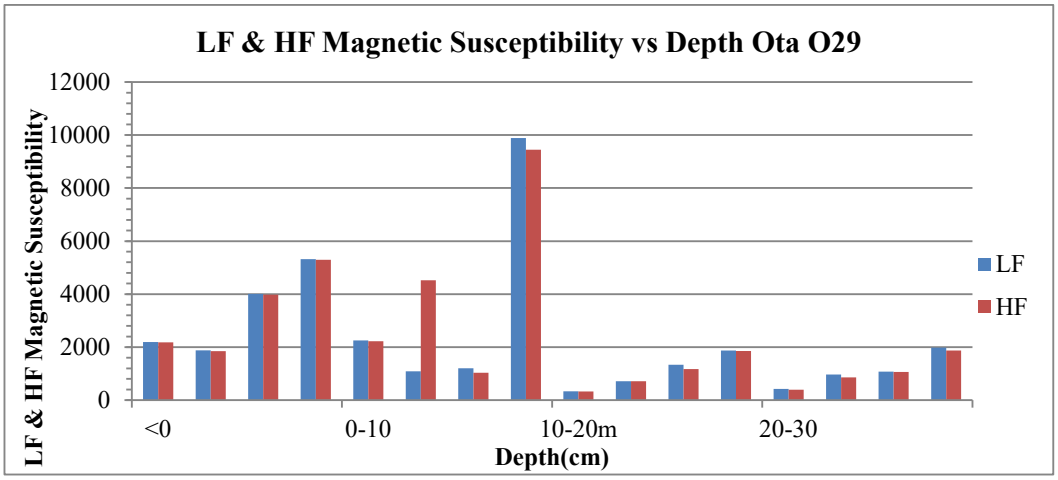
LF & HF Magnetic Susceptibility vs Depth Ota O29
LF & HF Magnetic Susceptibility
12000
10000
8000
6000
4000
2000
0
<0
0-10
10-20m
20-30
Depth(cm)
LF
HF

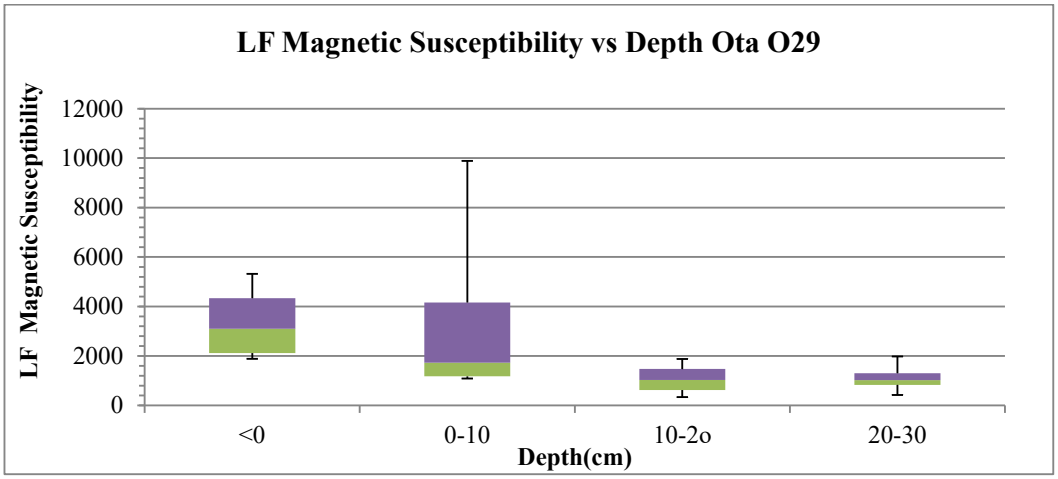
LF Magnetic Susceptibility vs Depth Ota O29
LF Magnetic Susceptibility
12000
10000
8000
6000
4000
2000
0
<0
0-10
10-2o
20-30
Depth(cm)

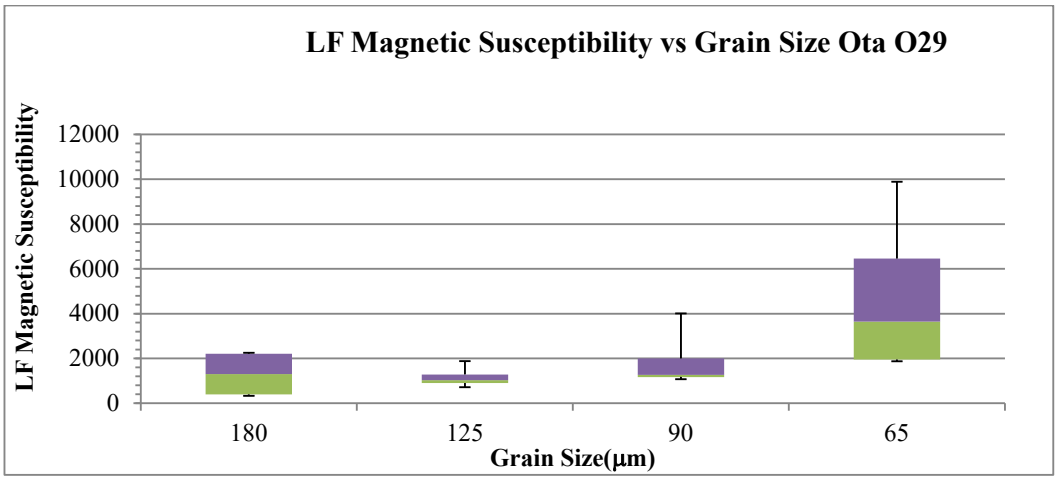
LF Magnetic Susceptibility vs Grain Size Ota O29
LF Magnetic Susceptibility
12000
10000
8000
6000
4000
2000
0
180
125
90
65
Grain Size(µm)

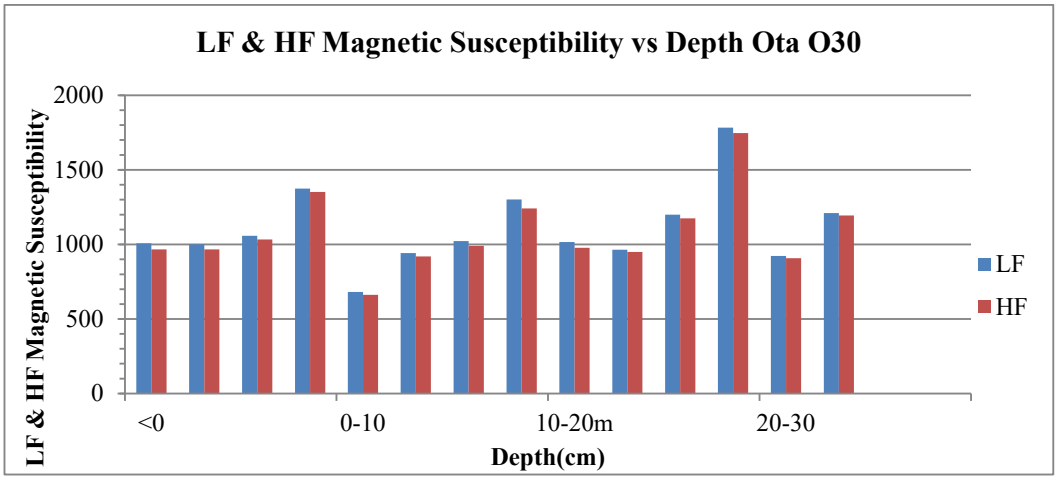
LF & HF Magnetic Susceptibility vs Depth Ota O30
LF & HF Magnetic Susceptibility
2000
1500
1000
500
0
<0
0-10
10-20m
20-30
Depth(cm)
LF
HF

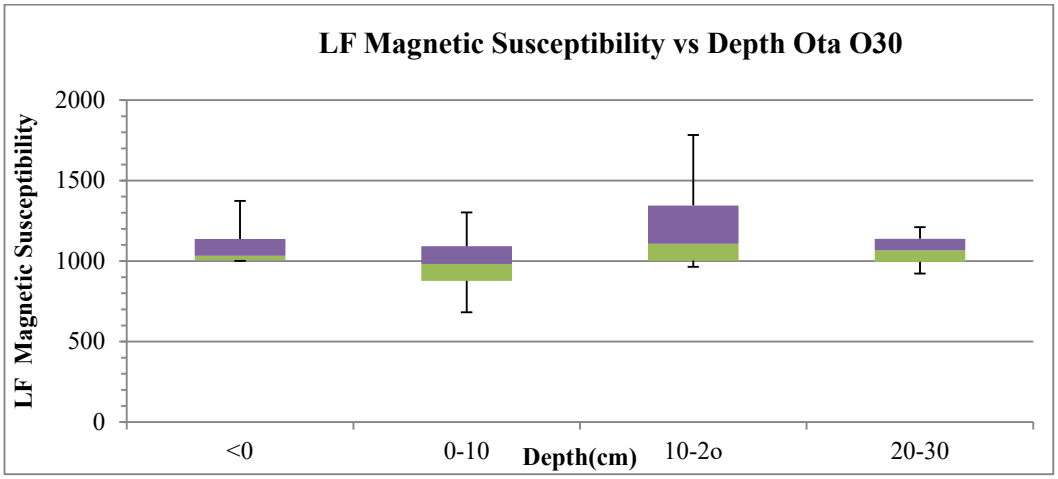
LF Magnetic Susceptibility vs Depth Ota O30
LF Magnetic Susceptibility
2000
1500
1000
500
0
<0
0-10
Depth(cm)
10-2o
20-30

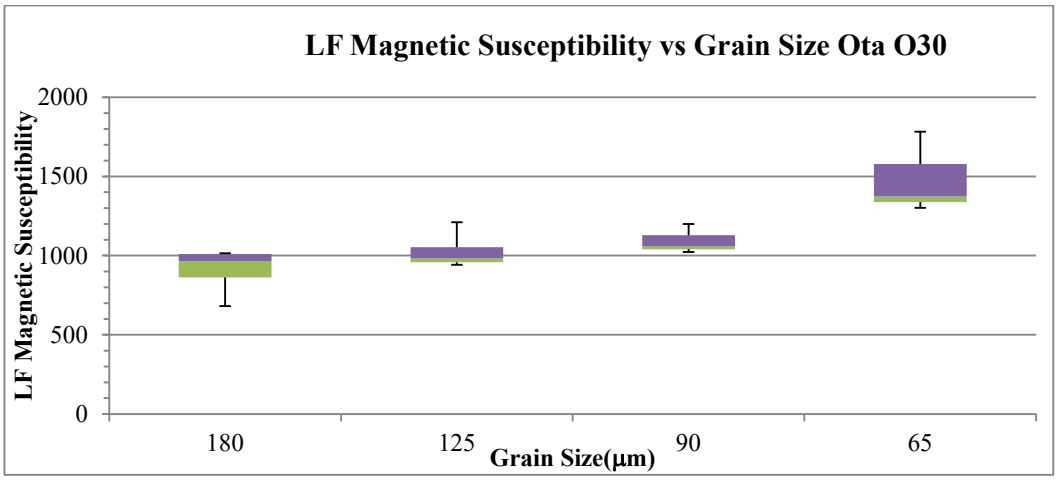
LF Magnetic Susceptibility vs Grain Size Ota O30
LF Magnetic Susceptibility
2000
1500
1000
500
0
180
125
90
65
Grain Size(µm)

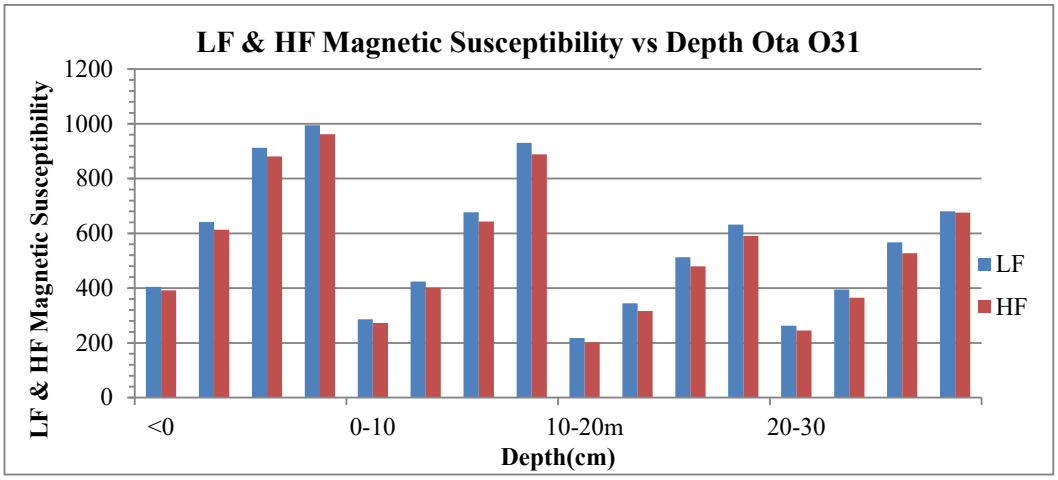
LF & HF Magnetic Susceptibility vs Depth Ota O31
LF & HF Magnetic Susceptibility
1200
1000
800
600
400
200
0
<0
0-10
10-20m
20-30
Depth(cm)
LF
HF

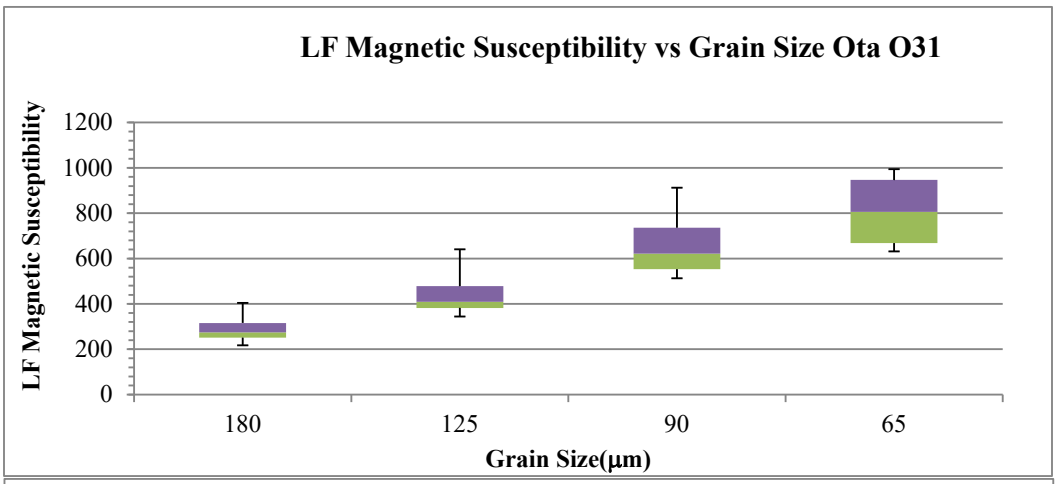
LF Magnetic Susceptibility vs Grain Size Ota O31
LF Magnetic Susceptibility
1200
1000
800
600
400
200
0
180
125
90
65
Grain Size(µm)

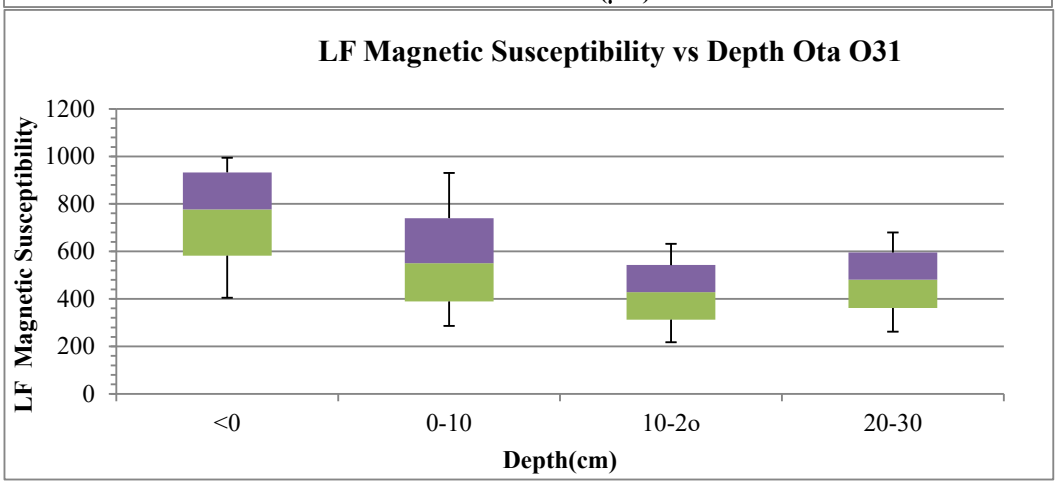
LF Magnetic Susceptibility vs Depth Ota O31
LF Magnetic Susceptibility
1200
1000
800
600
400
200
0
<0
0-10
10-2o
20-30
Depth(cm)

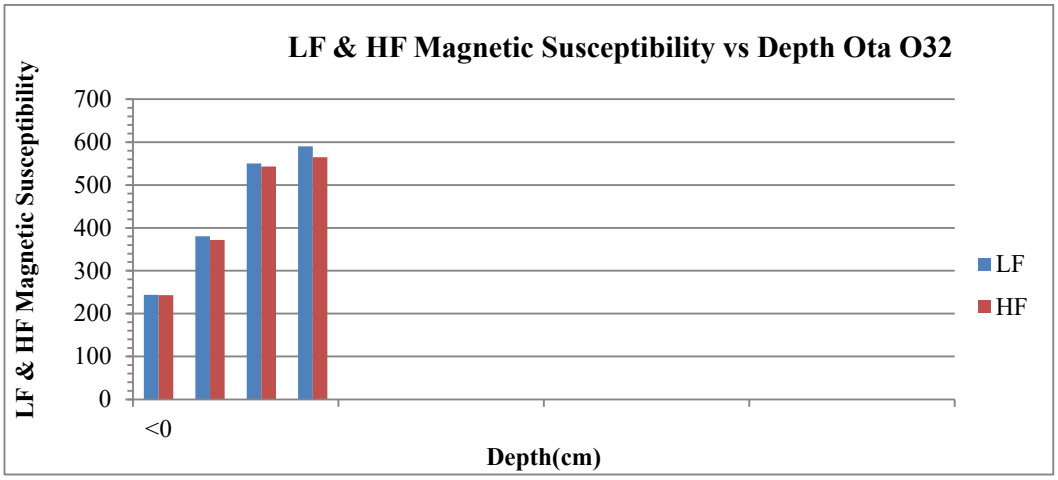
LF & HF Magnetic Susceptibility vs Depth Ota O32
LF & HF Magnetic Susceptibility
700
600
500
400
300
200
100
0
<0
Depth(cm)
LF
HF

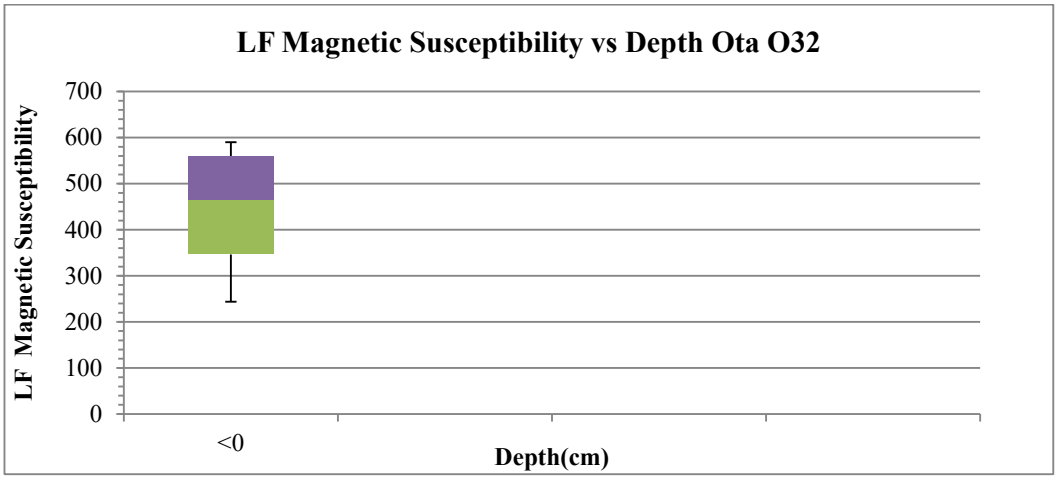
LF Magnetic Susceptibility vs Depth Ota O32
LF Magnetic Susceptibility
700
600
500
400
300
200
100
0
<0
Depth(cm)

Appendix 4. 10: Variation in Magnetic Susceptibility Readings of Different Grain Sizes from Surface Samples Across Ota Industrial Layout

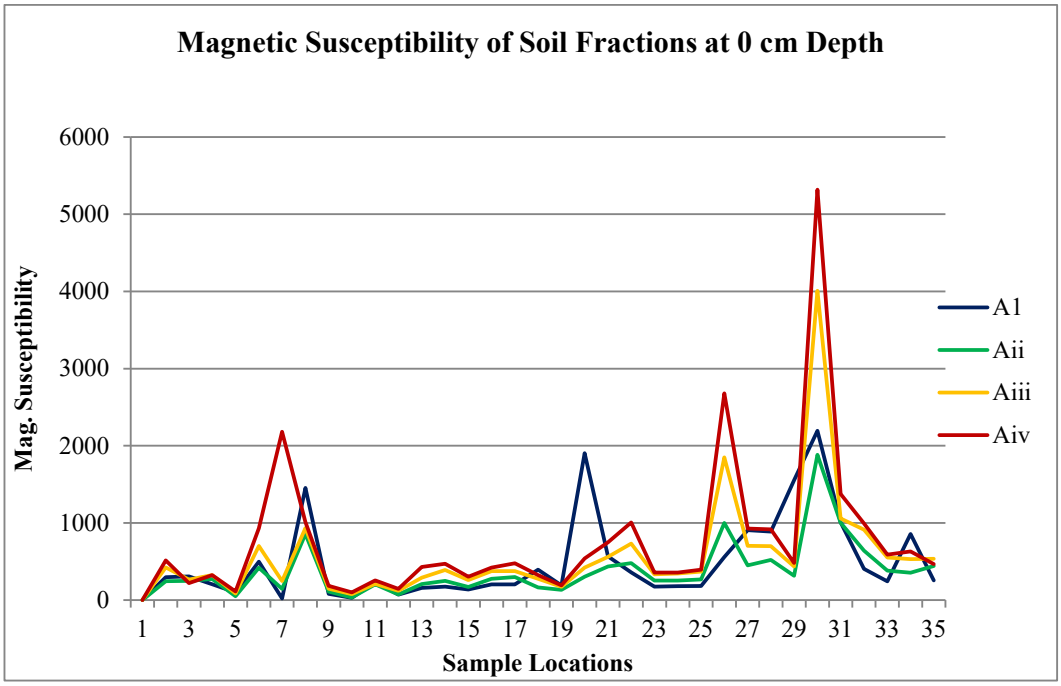

Appendix 4.10.1: Variation in magnetic susceptibility readings within grains sizes 180 µm (Ai), 125 µm (Aii), 90 µm (Aiii), and 65µm (Aiv) from surface samples across the site in Ota

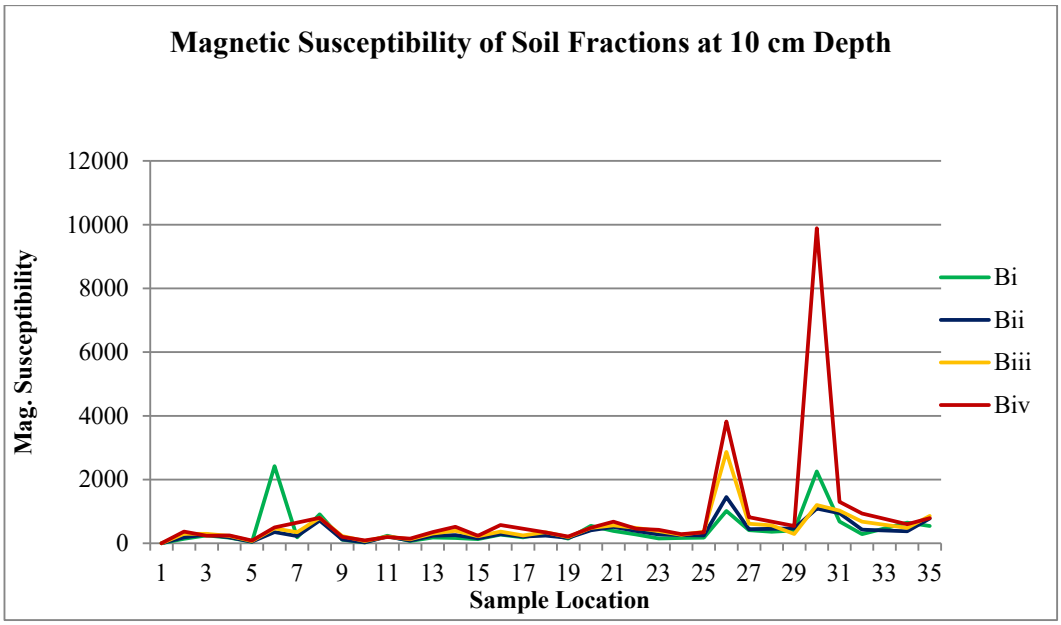

Appendix 4.10.1: Magnetic susceptibility readings within grains sizes 180µm (Bi),

120µm (Bii), 90µm (Biii), and 65µm (Biv) from sampling depth of 10cm across the site in Ota

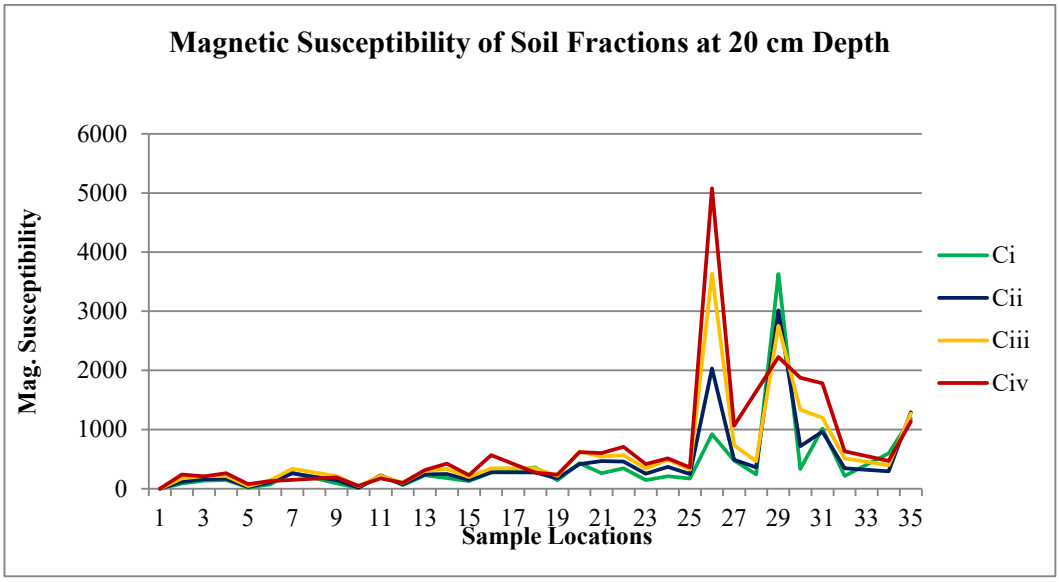

Appendix 4.10.1: Variation in magnetic susceptibility readings within grains sizes 180µm (Ci), 120µm (Cii), 90µm (Ciii), and 65µm (Civ) from sampling depth of 20cm across the site in Ota

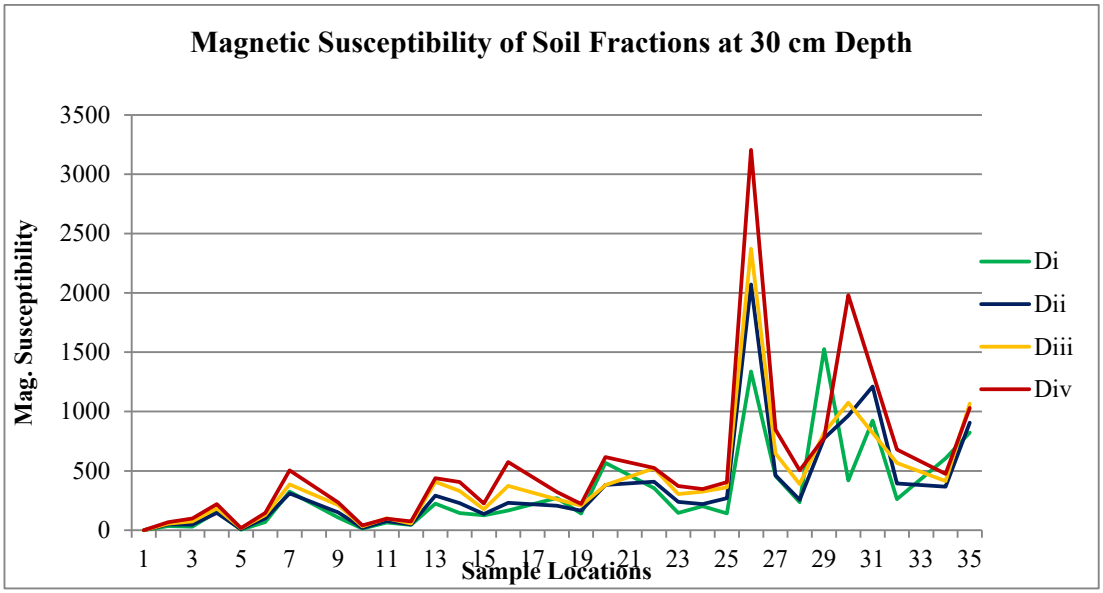

Appendix 4.10.1: Variation in magnetic susceptibility readings within grains sizes 180 µm (Di), 120 µm (Dii), 90 µm (Diii), and 65 µm (Div) from sampling depth of 30 cm across the site in Ota

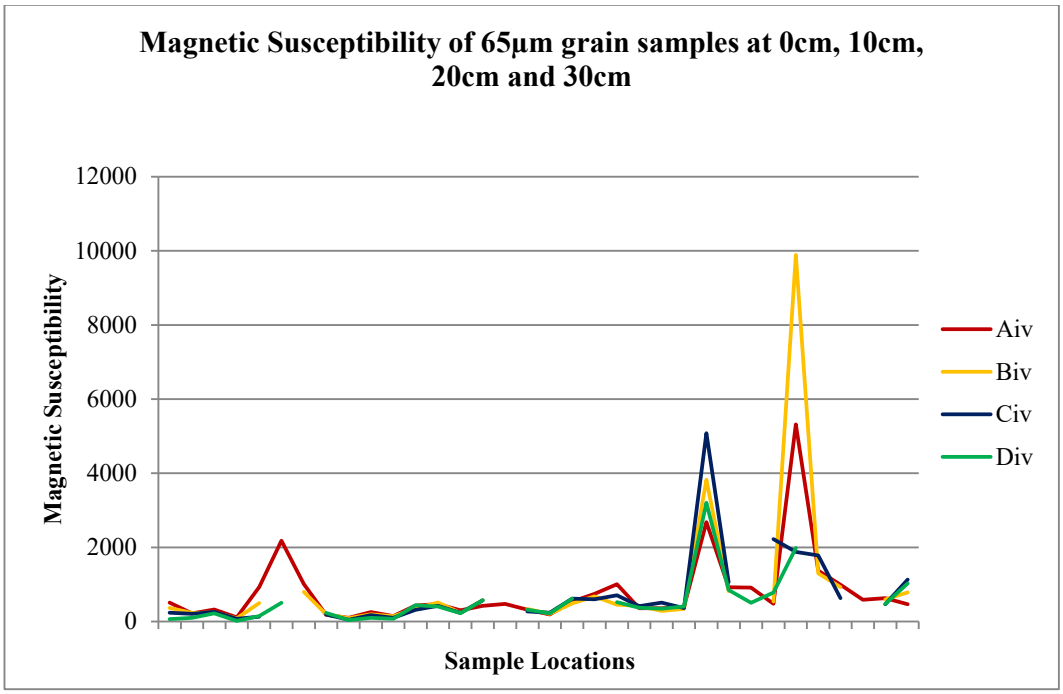

Appendix 4.10.1: Variation in magnetic susceptibility reading from 65µm grain samples at 0cm, 10cm, 20cm and 30cm depths in Ota industrial layout

Appendix 4. 11: Magnetic Susceptibility / Temperature Analysis Results of Soil Samples from Ota Industrial Layout

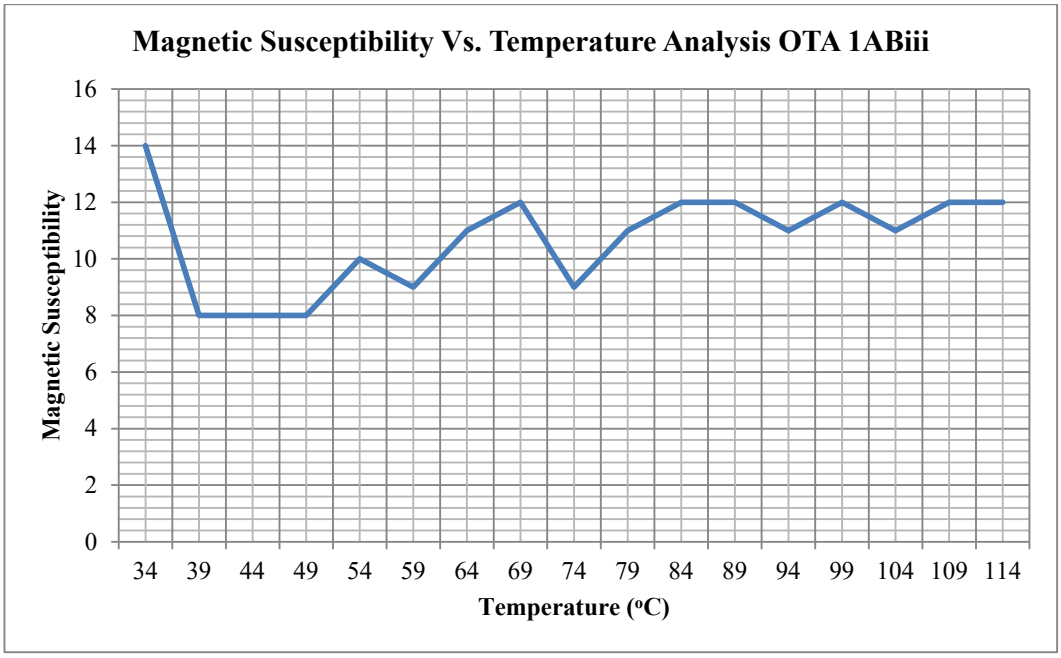

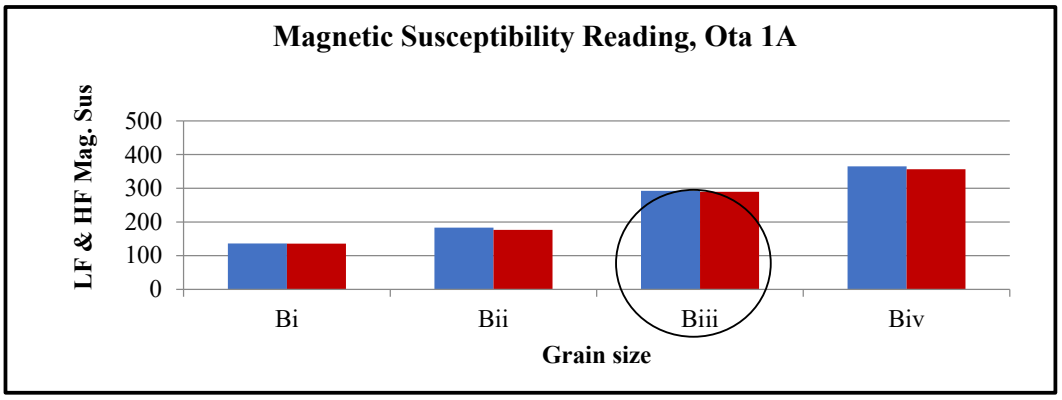

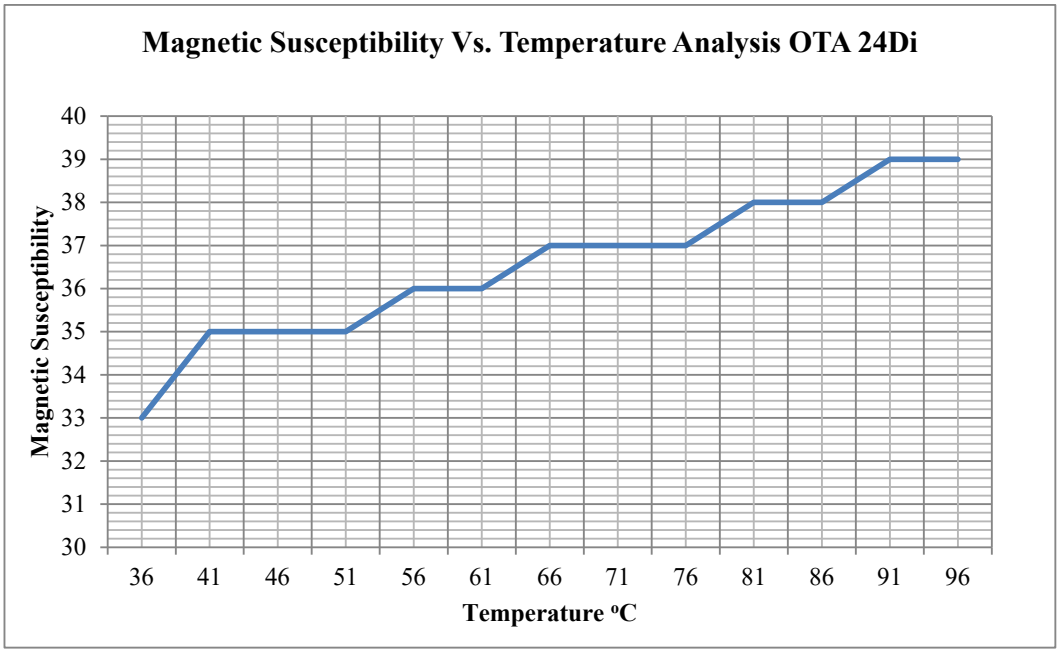
Magnetic Susceptibility Vs. Temperature Analysis OTA 24Di
Magnetic Susceptibility
40
39
38
37
36
35
34
33
32
31
30
36
41
46
51
56
61
66
71
76
81
86
91
96
Temperature ºC

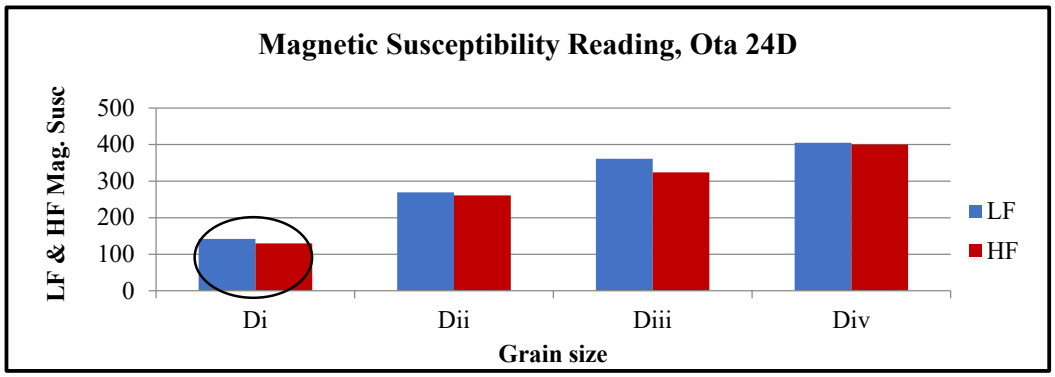
Magnetic Susceptibility Reading, Ota 24D
LF & HF Mag. Susc
500
400
300
200
100
0
Di
Dii
Diii
Div
Grain size
LF
HF

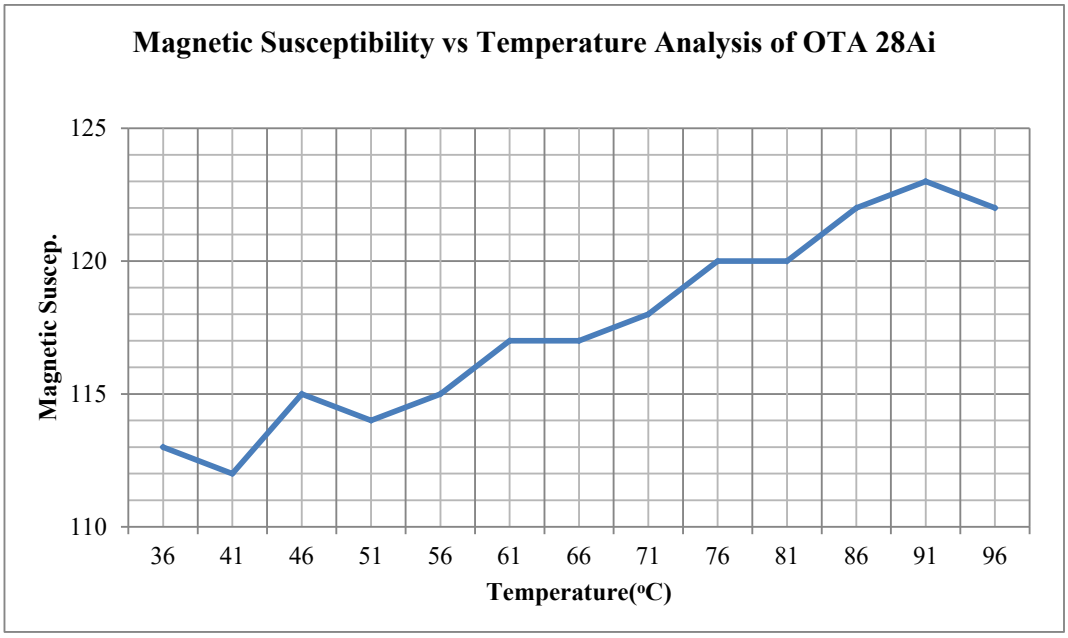
Magnetic Susceptibility vs Temperature Analysis of OTA 28Ai
Magnetic Suscep.
125
120
115
110
36
41
46
51
56
61
66
71
76
81
86
91
96
Temperature(°C)

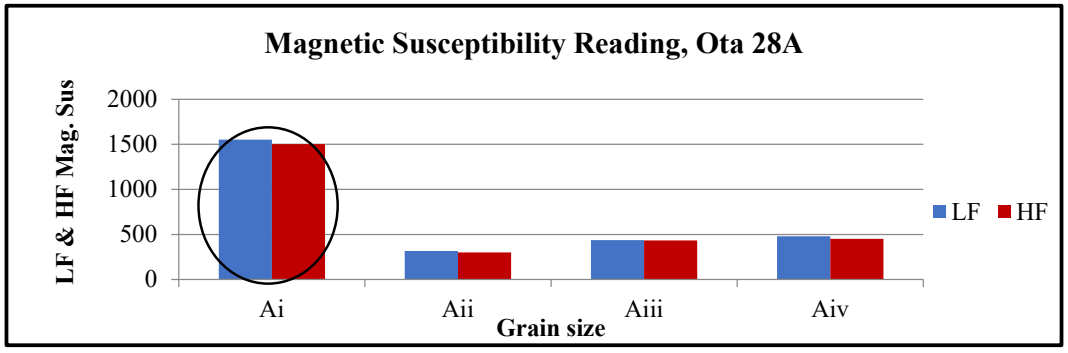
Magnetic Susceptibility Reading, Ota 28A
LF & HF Mag. Sus
2000
1500
1000
500
0
Ai
Aii
Aiii
Aiv
Grain size
LF
HF

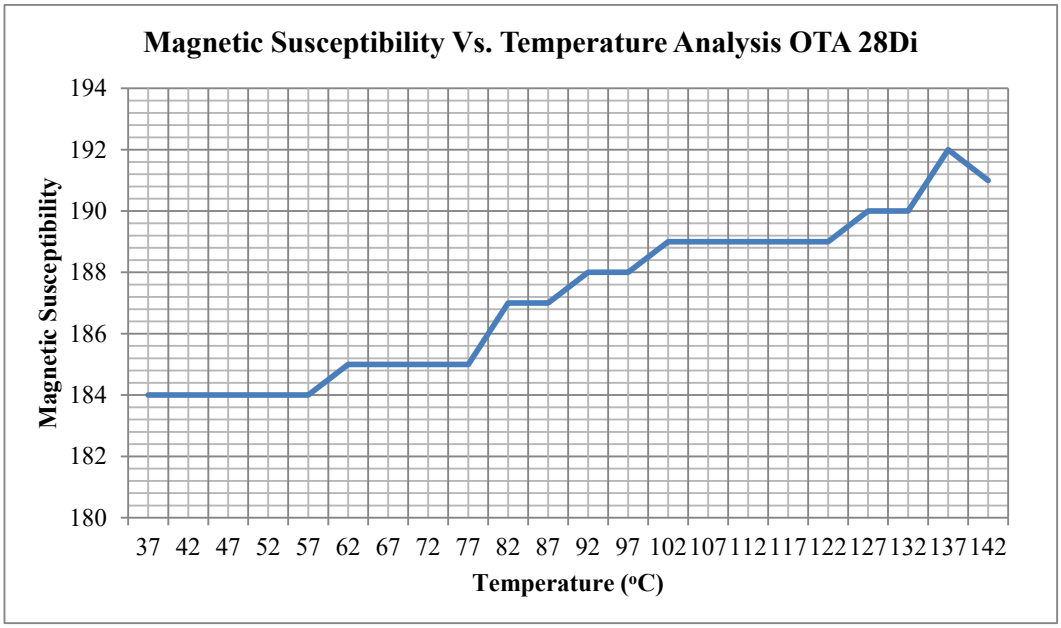
Magnetic Susceptibility Vs. Temperature Analysis OTA 28Di
Magnetic Susceptibility
194
192
190
188
186
184
182
180
37 42 47 52 57 62 67 72 77 82 87 92 97 102 107 112 117 122 127 132 137 142
Temperature (°C)

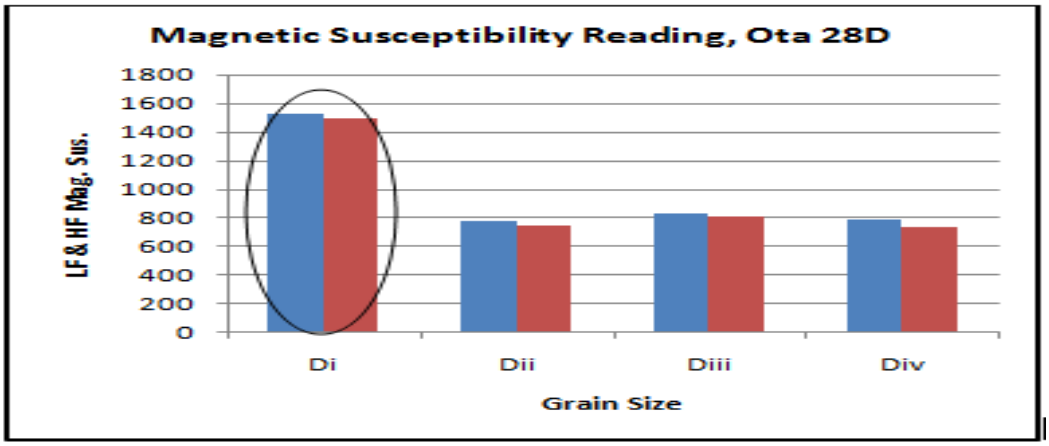
Magnetic Susceptibility Reading, Ota 28D
LF & HF Mag. Sus.
1800
1600
1400
1200
1000
800
600
400
200
0
Di
Dii
Diii
Div
Grain Size

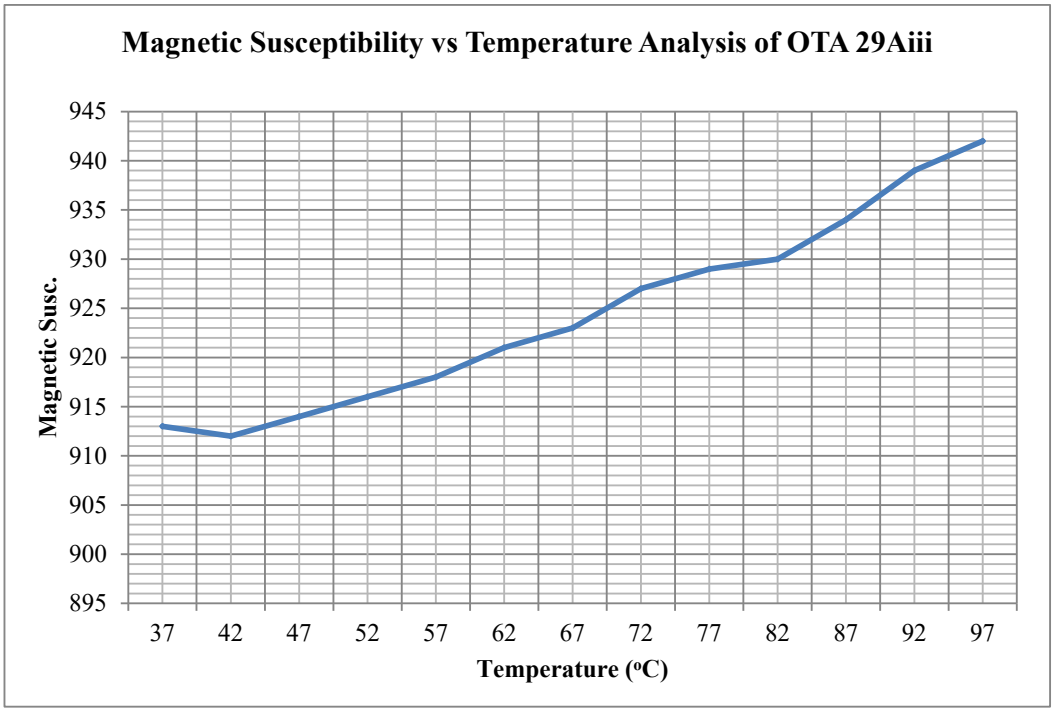
Magnetic Susceptibility vs Temperature Analysis of OTA 29Aiii
Magnetic Susc.
945
940
935
930
925
920
915
910
905
900
895
37
42
47
52
57
62
67
72
77
82
87
92
97
Temperature (°C)

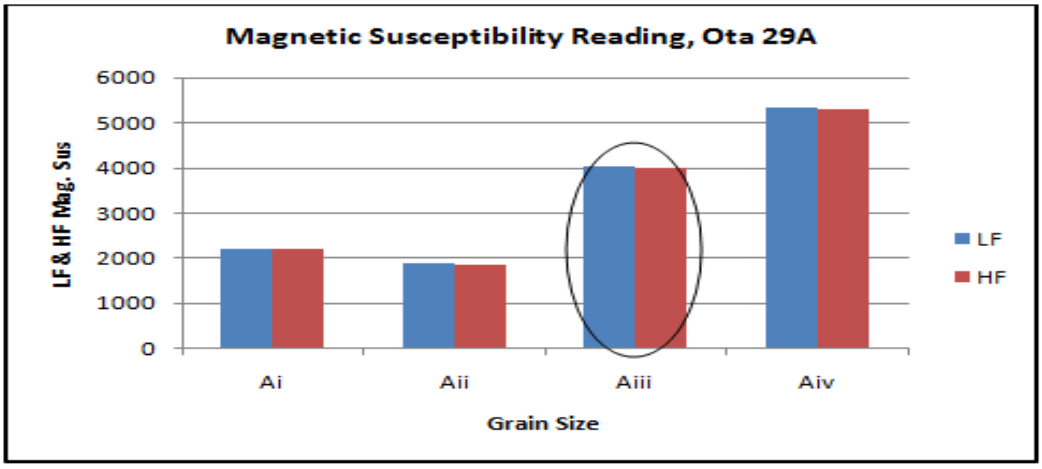
Magnetic Susceptibility Reading, Ota 29A
LF & HF Mag. Sus
6000
5000
4000
3000
2000
1000
0
Ai
Aii
Aiii
Aiv
Grain Size
LF
HF

Appendix 4. 12: Charts Showing Concentration (ppm) of Each Major Elements in Ota Industrial Layout

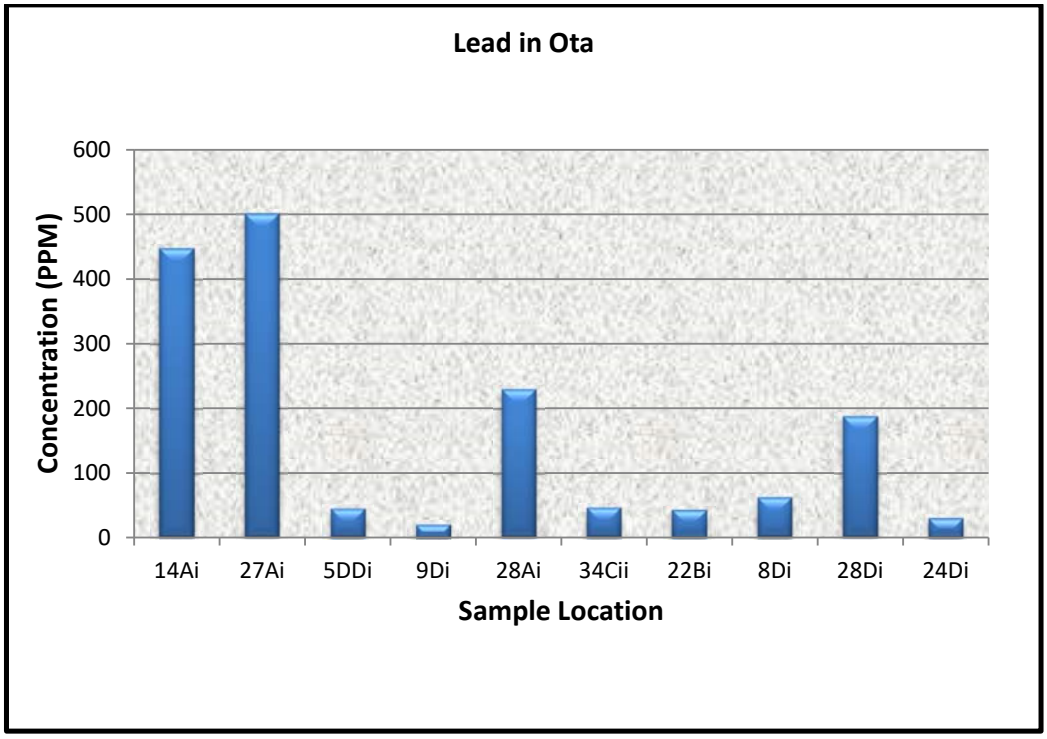

Appendix 4.12.1: Variation in concentration of Lead in the samples from Ota

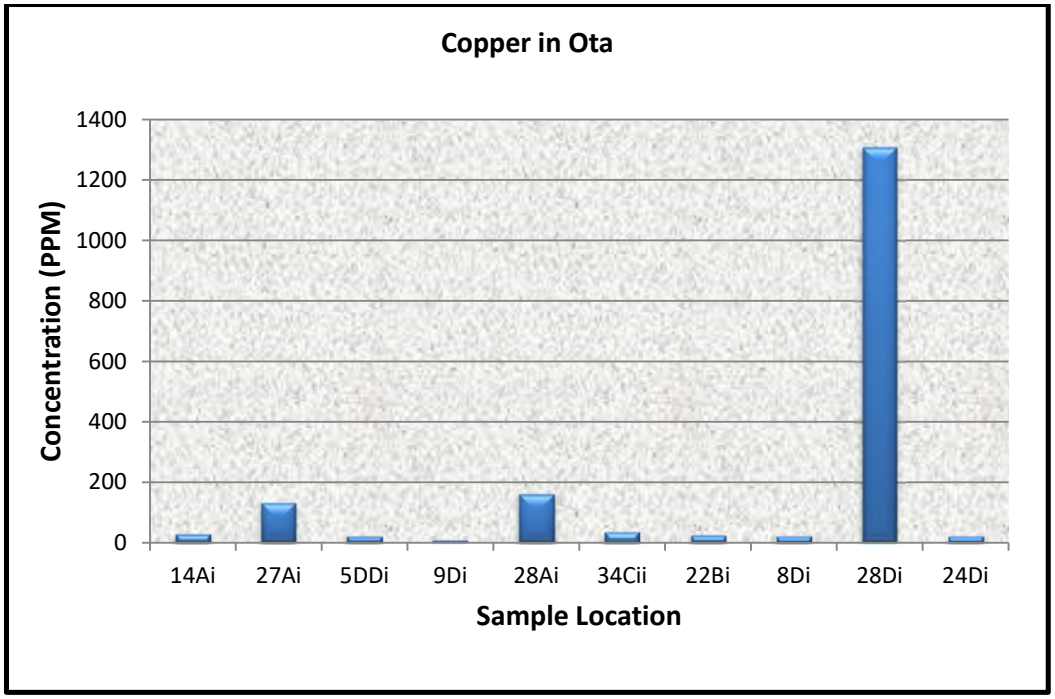

Appendix 4.12.2: Variation in concentration of Copper in the samples from Ota

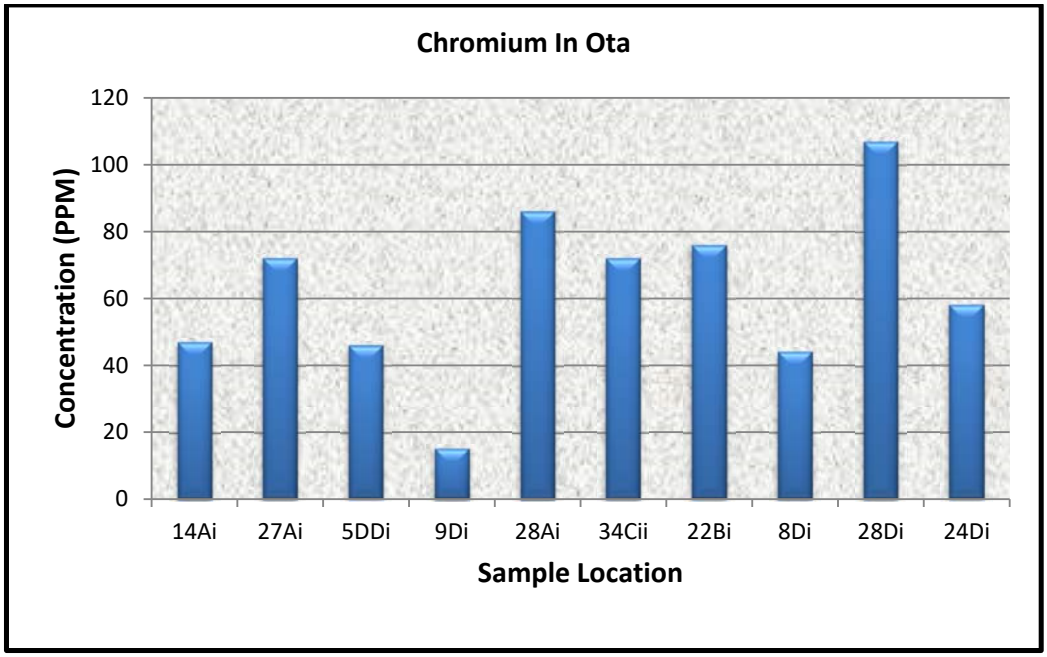

Appendix 4.12.3: Variation in concentration of Chromium in the samples from Ota

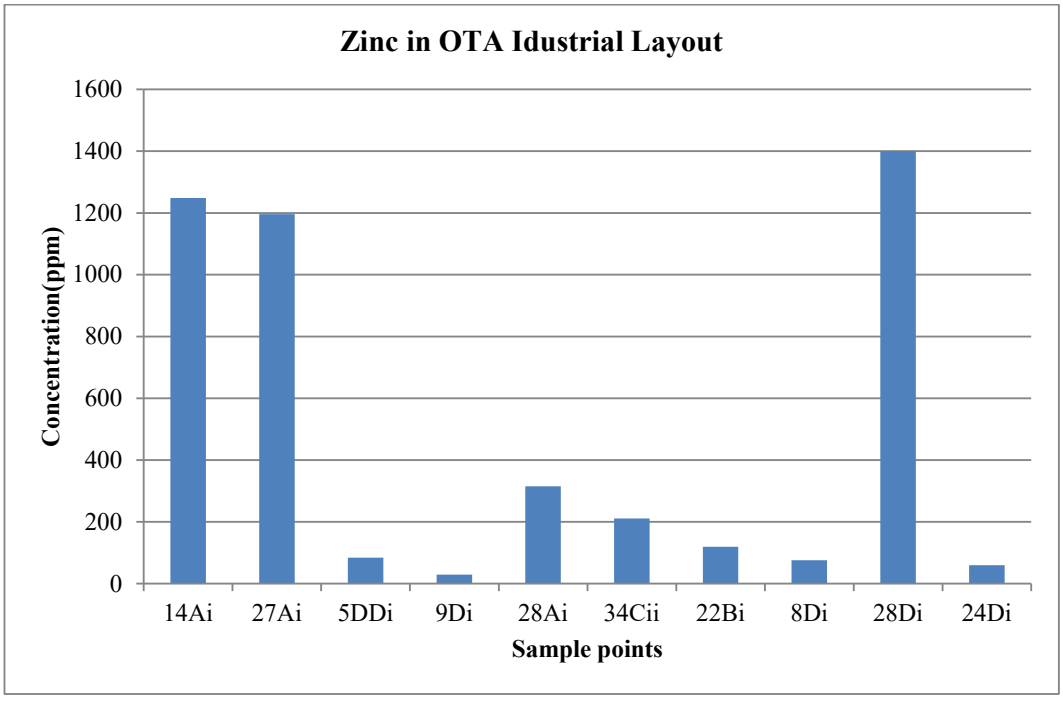

Appendix 4.12.4: Variation in concentration of Zinc in the samples from Ota

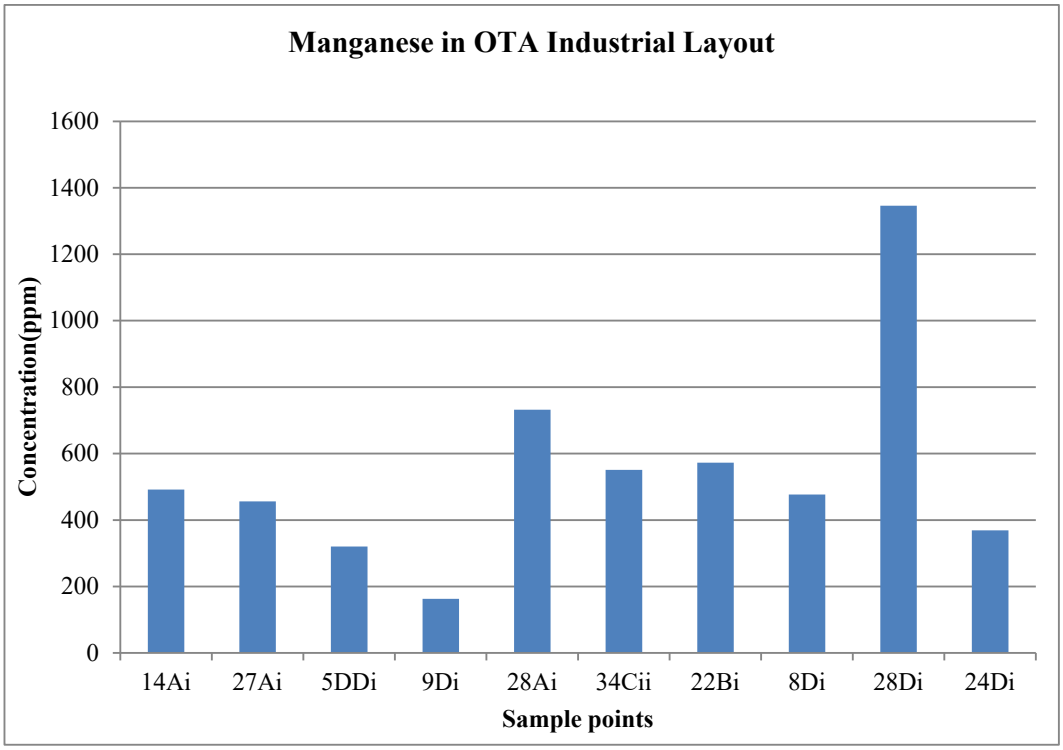

Appendix 4.12.5: Variation in concentration of Manganese in the samples from Ota

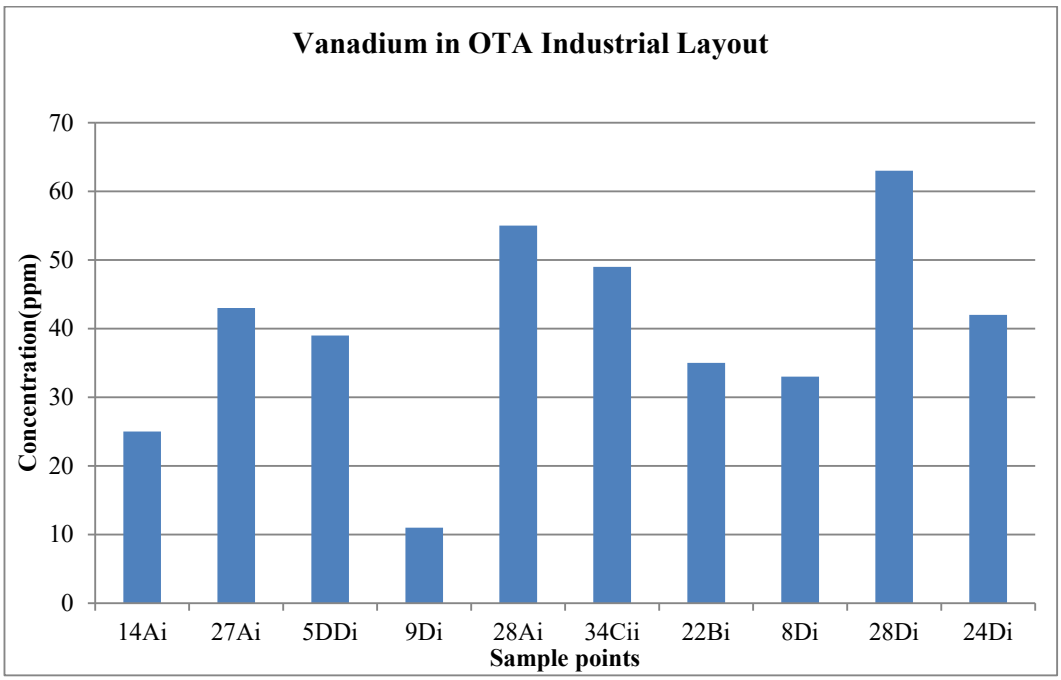

Appendix 4.12.6: Variation in concentration of Vanadium in the samples from Ota

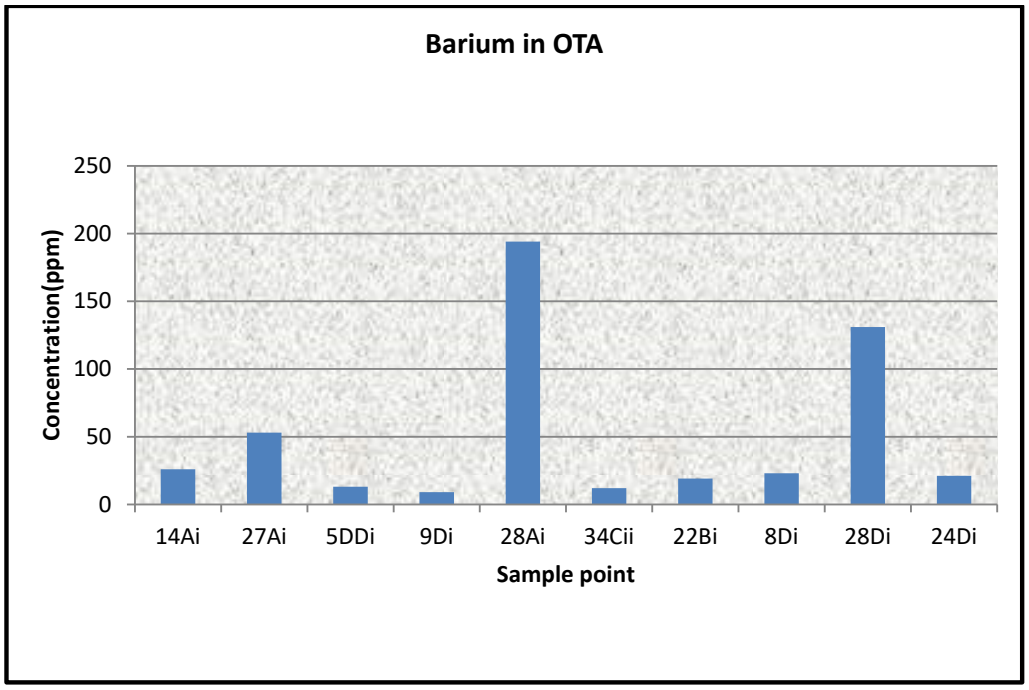

Appendix 4.12.7: Variation in concentration of Barium in the samples from Ota

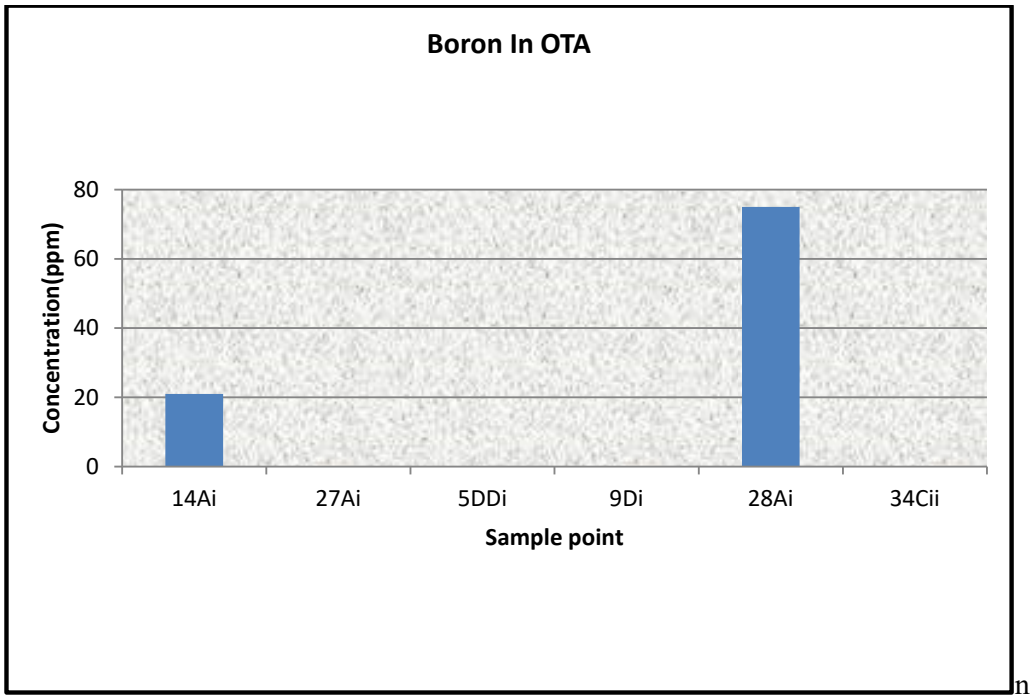

Appendix 4.12.8: Variation in concentration of Boron in the Samples from Ota

Appendix 4. 13: Charts Showing Magnetic Susceptibility Values for Specific Grain Sizes and their Corresponding Elemental Concentration in Ota Industrial Layout

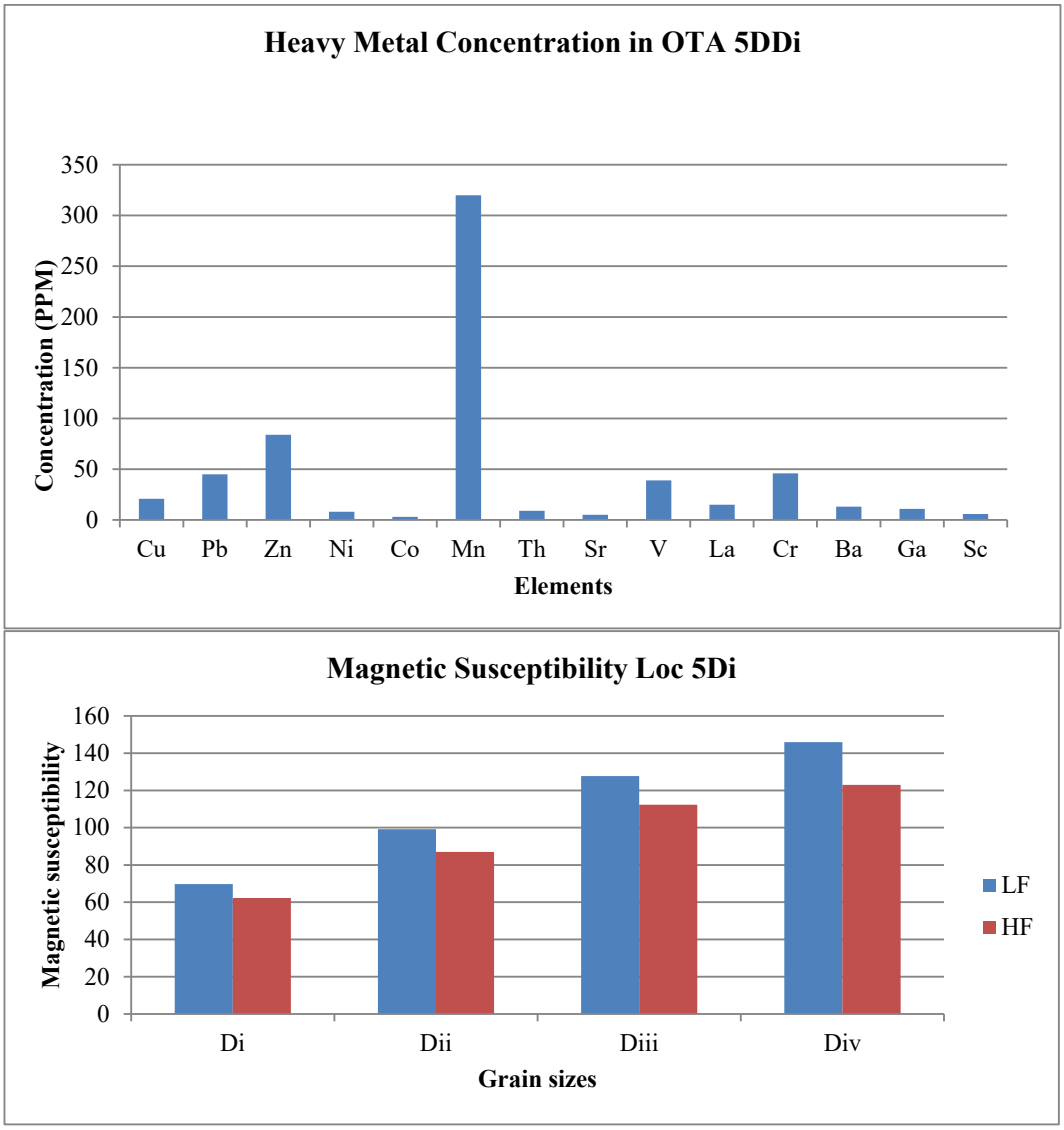

Appendix 4.13.1: 180 µm (Di) grain at 30cm depth of location 5D; with LF69.7, HF62.3 and its heavy metal contents and their concentration.

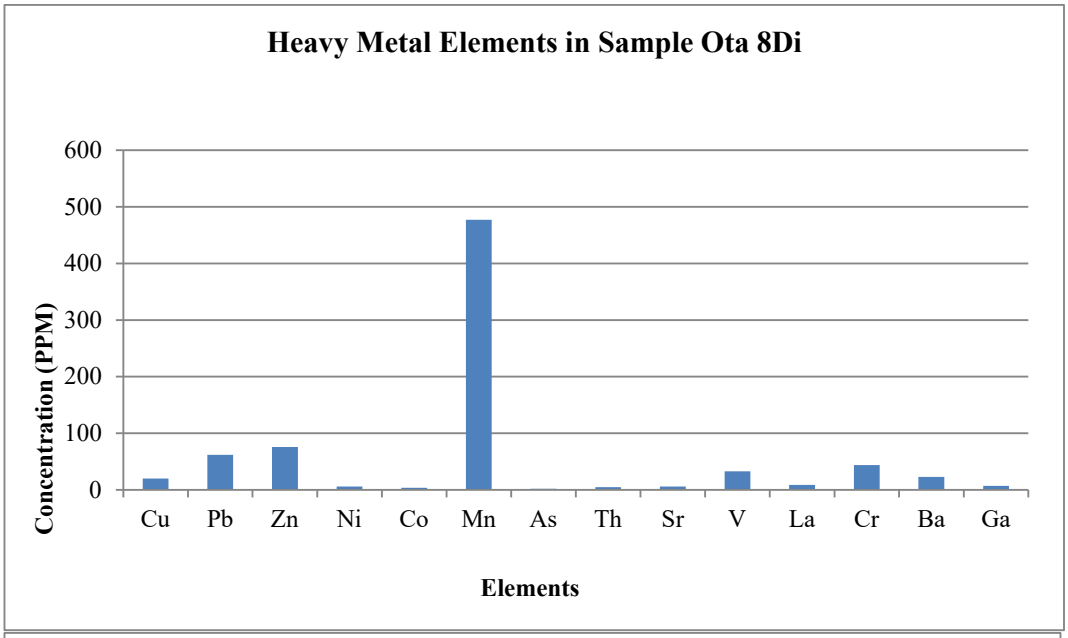

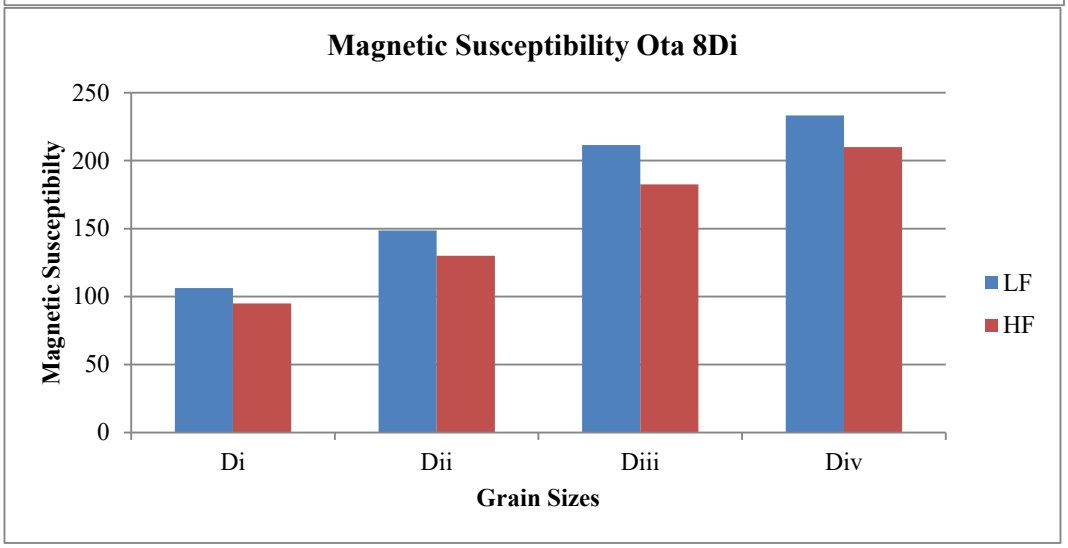

Appendix 4.13.2: 180 µm (Di) grain at 30cm depth of location 8; with LF106.2, HF94.9 and its heavy metal contents and their concentration.

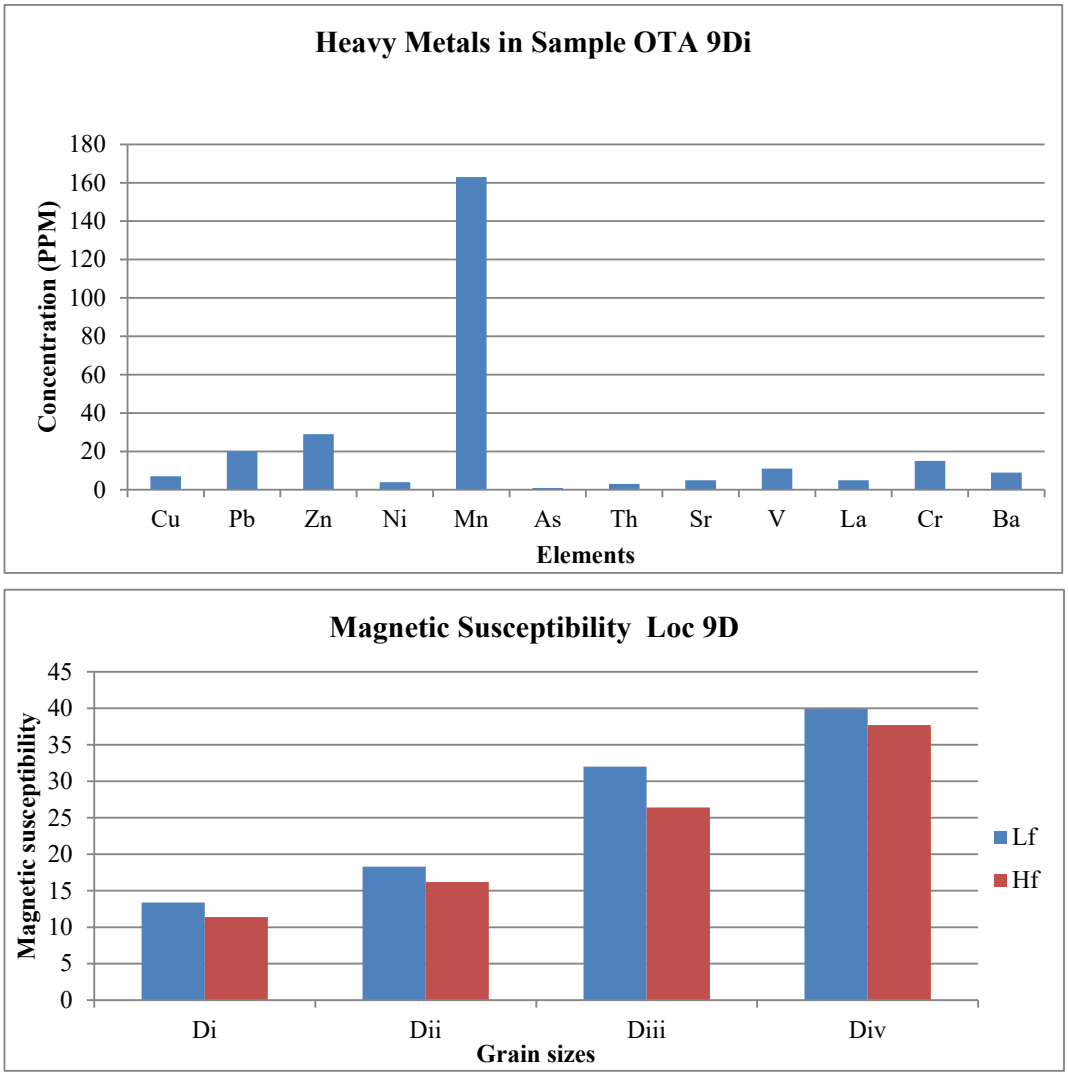

Appendix 4.13.3: 180µm (Di) grain at 30cm depth of location 9; with LF13.4, HF11.4 and its heavy metal contents and their concentration

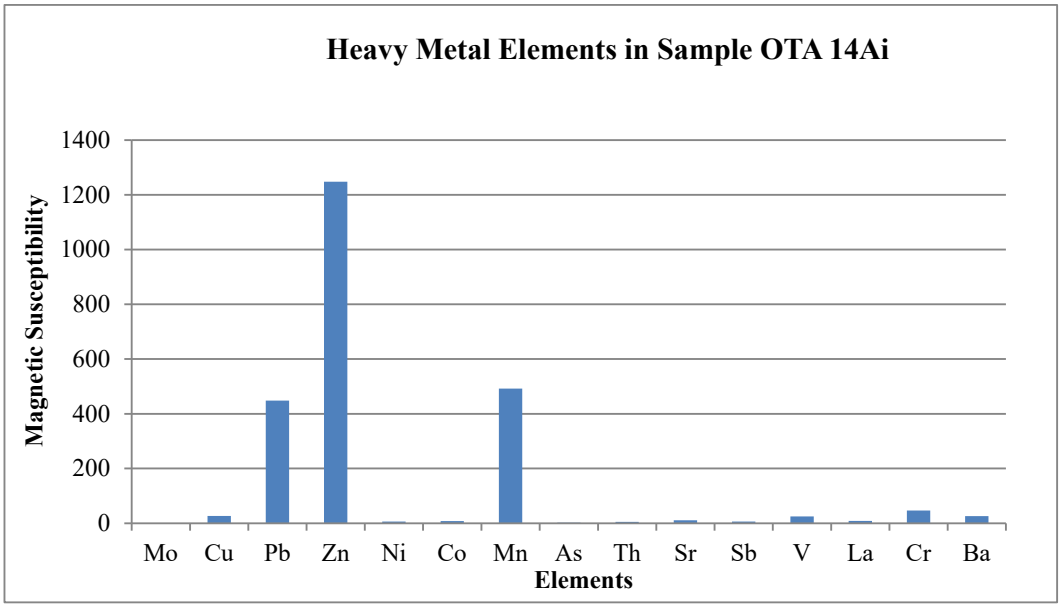

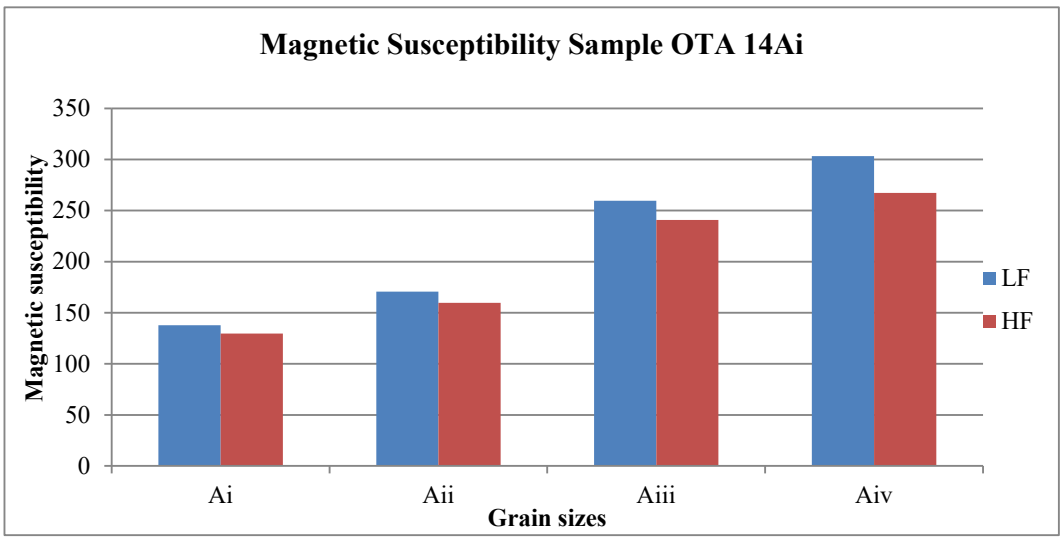

Appendix 4.13.4: 180 µm (Ai) grain at 0cm depth of location 14; with LF137.8, HF129.6 and its heavy metal contents and their concentration

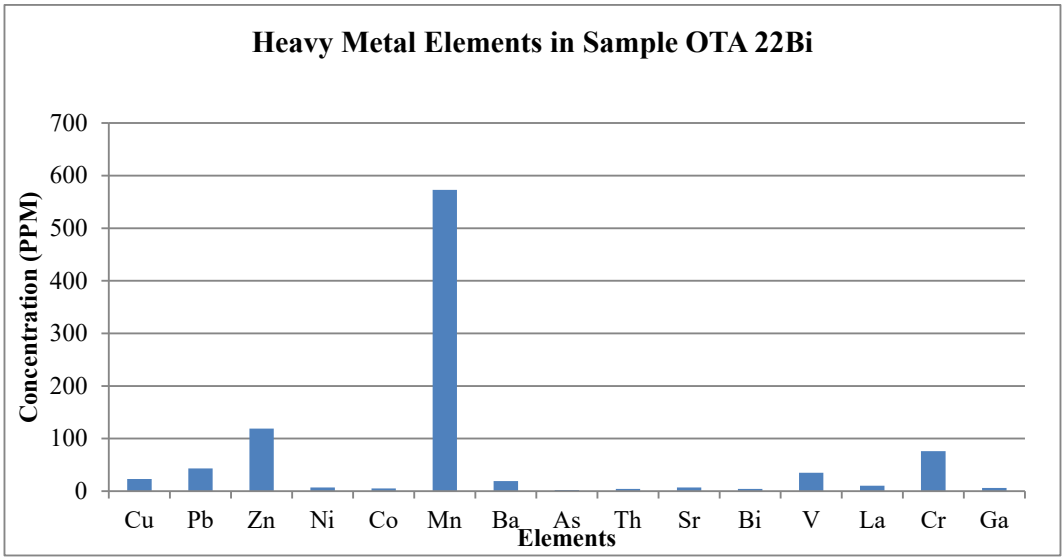

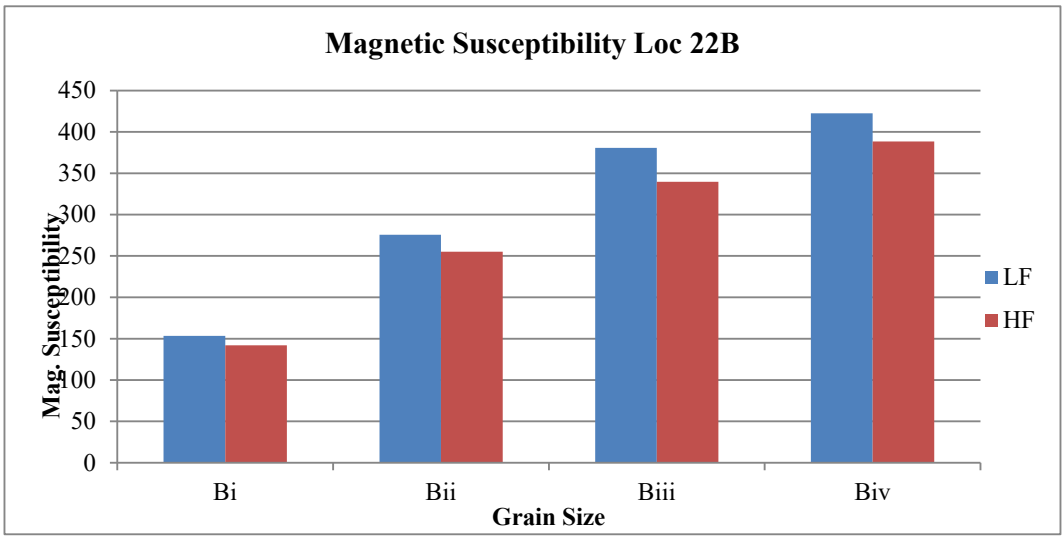

Appendix 4.13.5: 180 µm (Bi) grain at 10cm depth of location 22; with LF153.4, HF142 and its heavy metal contents and their concentration

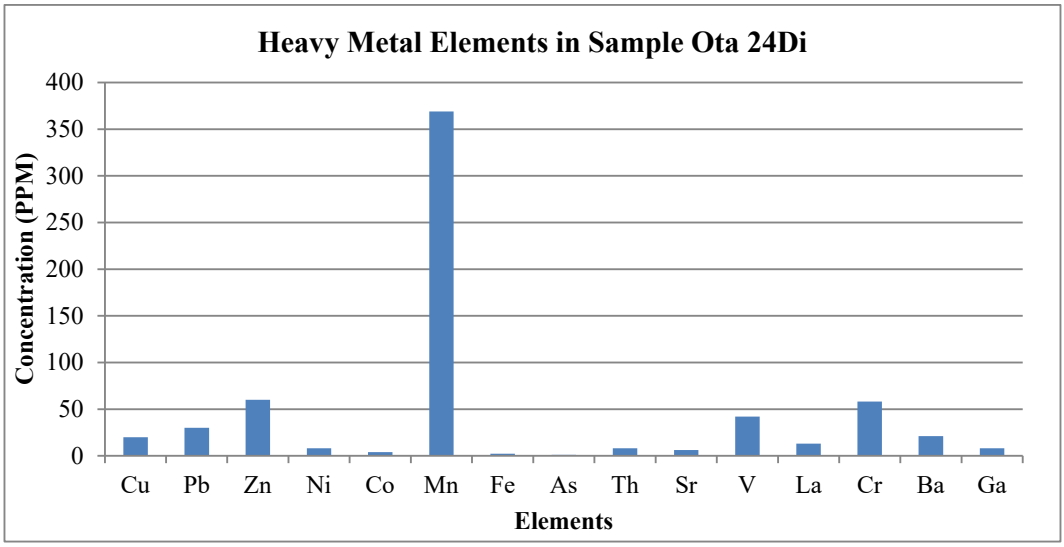

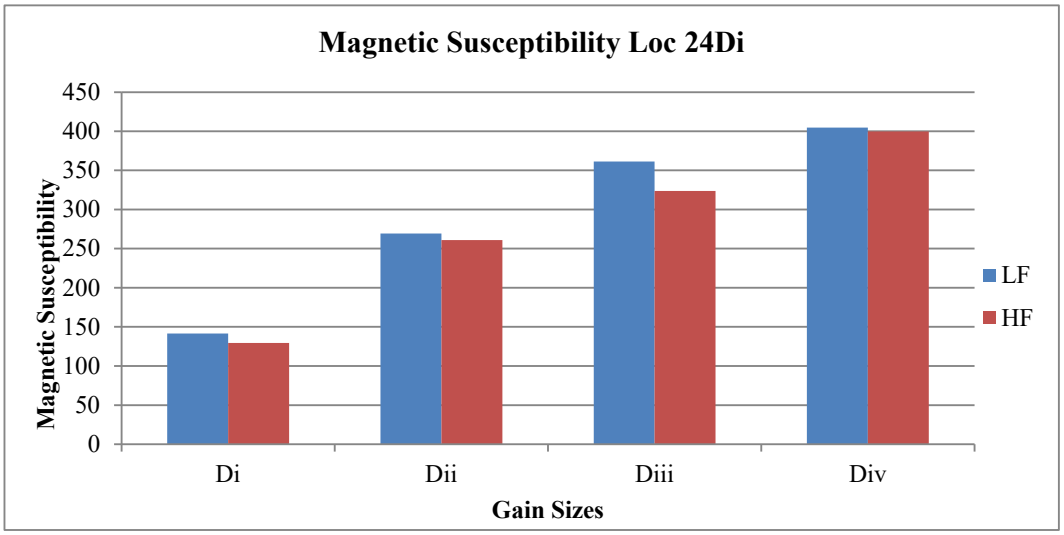

Appendix 4.13.6: 180µm (Di) grain at 30 cm depth of location 24; with LF141.6, HF129.4 and its heavy metal contents and their concentration

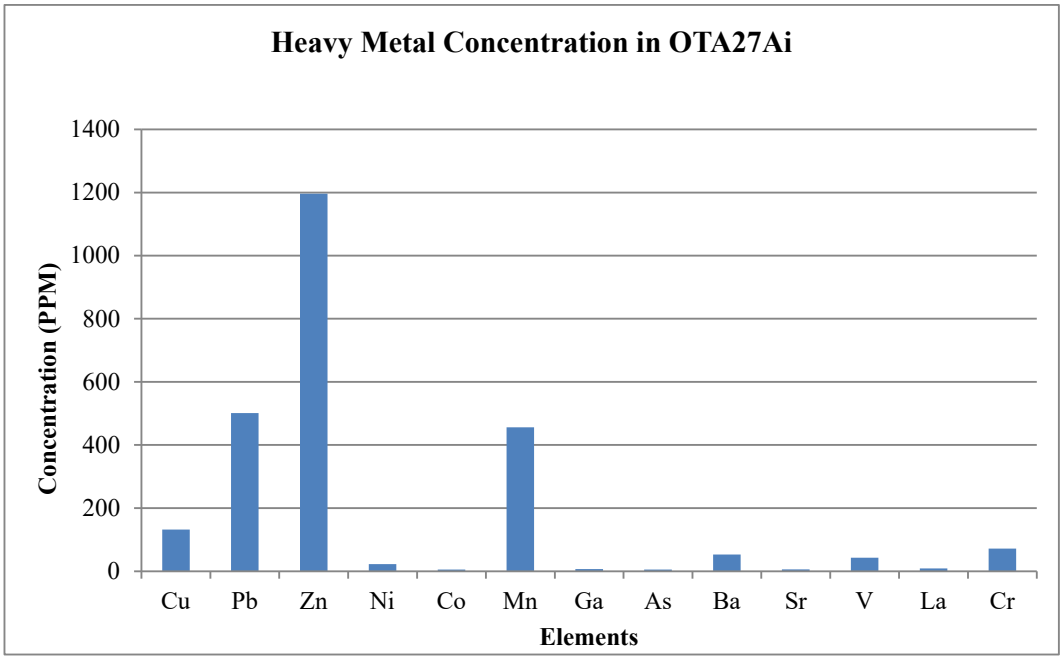

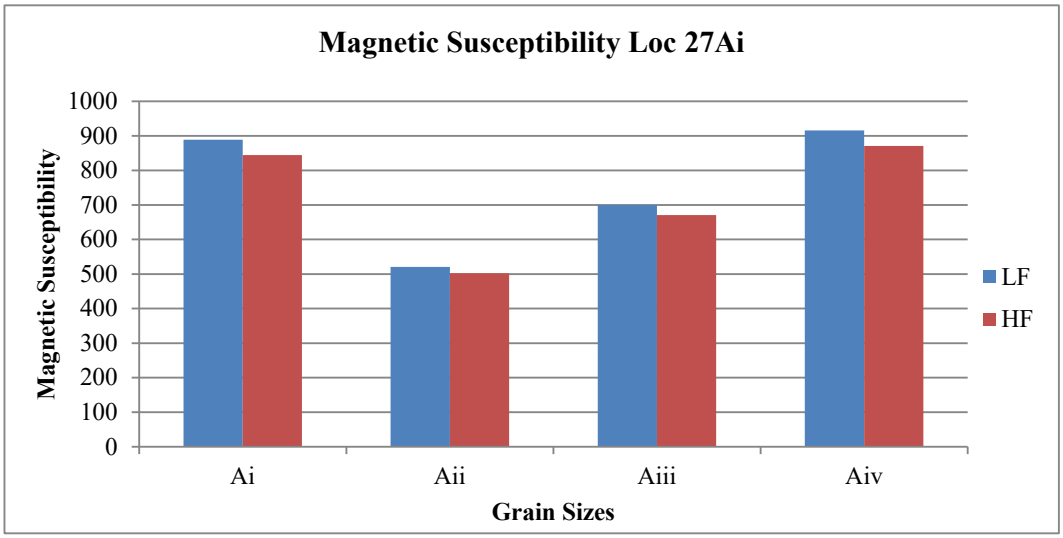

Appendix 4.13.7: 180µm (Ai) grain at 0 cm depth of location 27; with LF889.1, HF844.3 and its heavy metal contents and their concentration

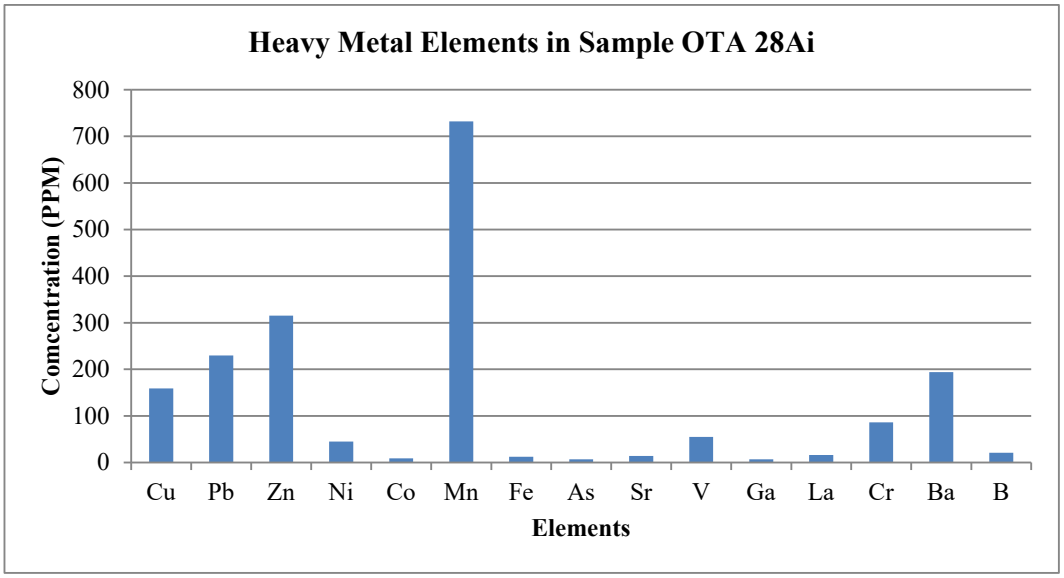

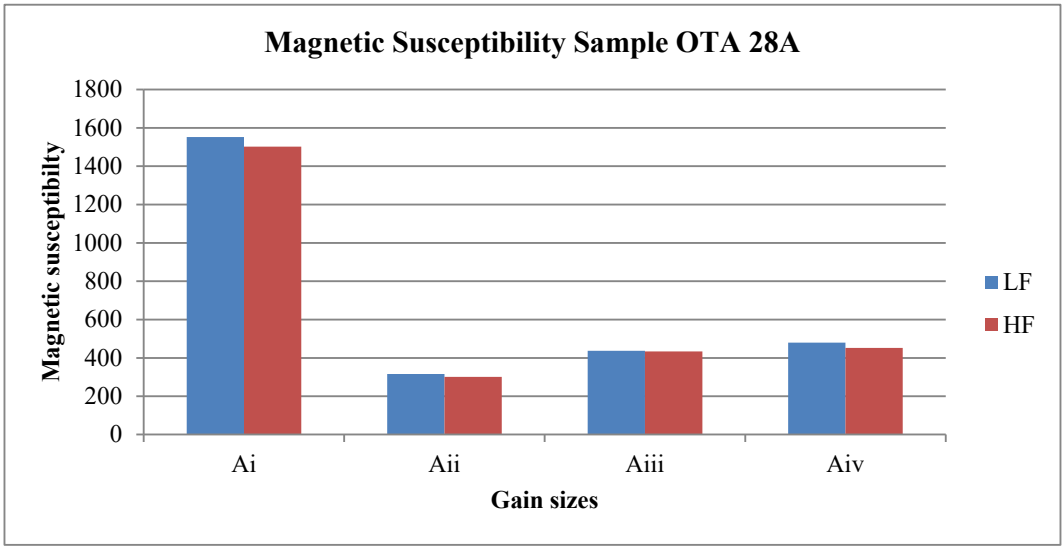

Appendix 4.13.8: 180 µm (Ai) grain at 0 cm depth of location 28; with LF1553, HF1502.2 and its heavy metal contents and their concentration

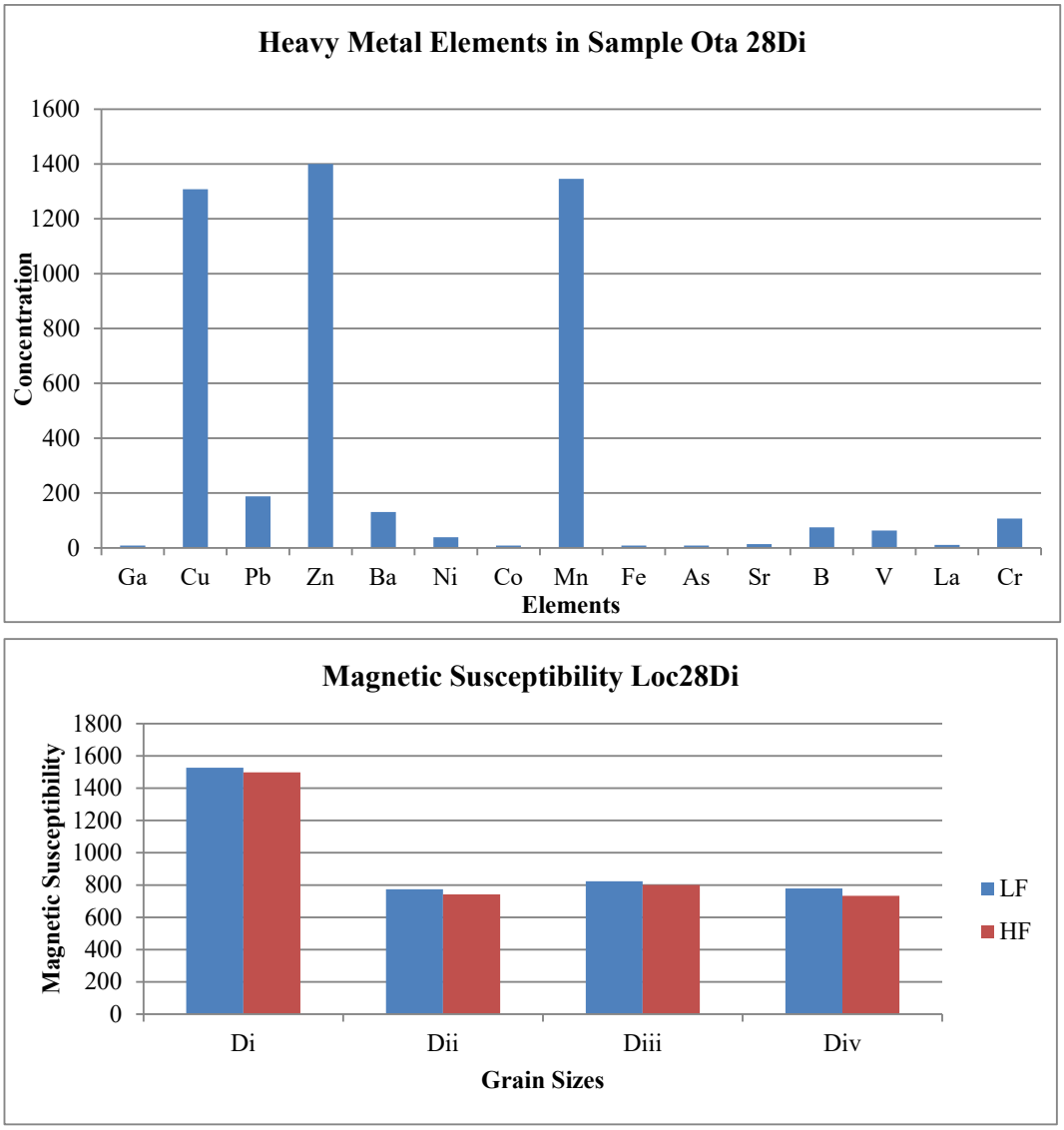

Appendix 4.13.9: 180 µm (Di) grain at 30 cm depth of location 28; with LF1527, HF1498.1 and its heavy metal contents and their concentration

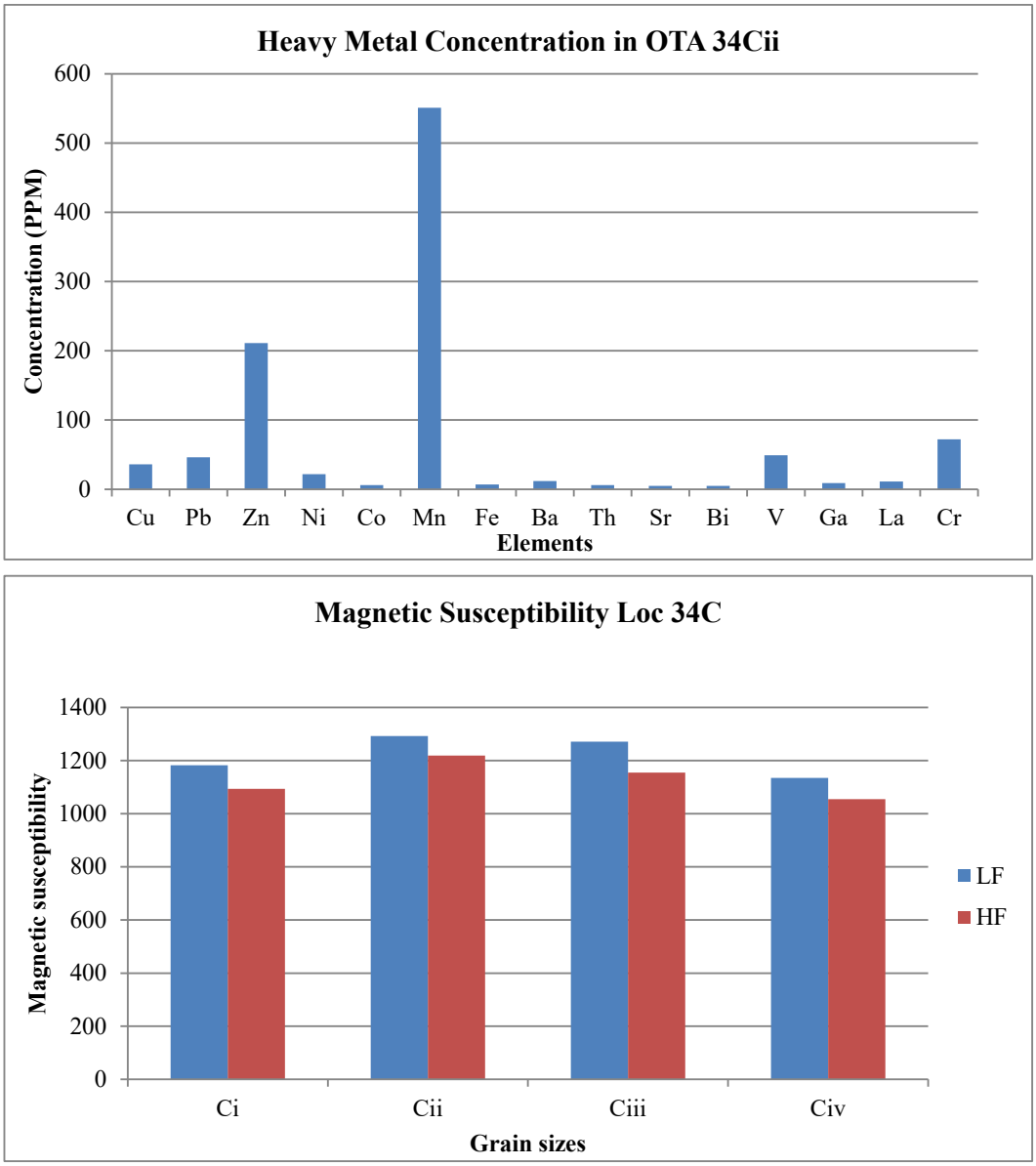

Appendix 4.13.10: 125 µm (Cii) grain at 20 cm depth of location 34; with LF1292.5, HF1218.6 and its heavy metal contents and their concentration